QUANTIFYING AND MANAGING AGRICULTURAL NITROGEN AND PHOSPHORUS POLLUTION FROM FIELD TO CATCHMENT SCALE

MICHAEL VAN DER LAAN, LINUS FRANKE

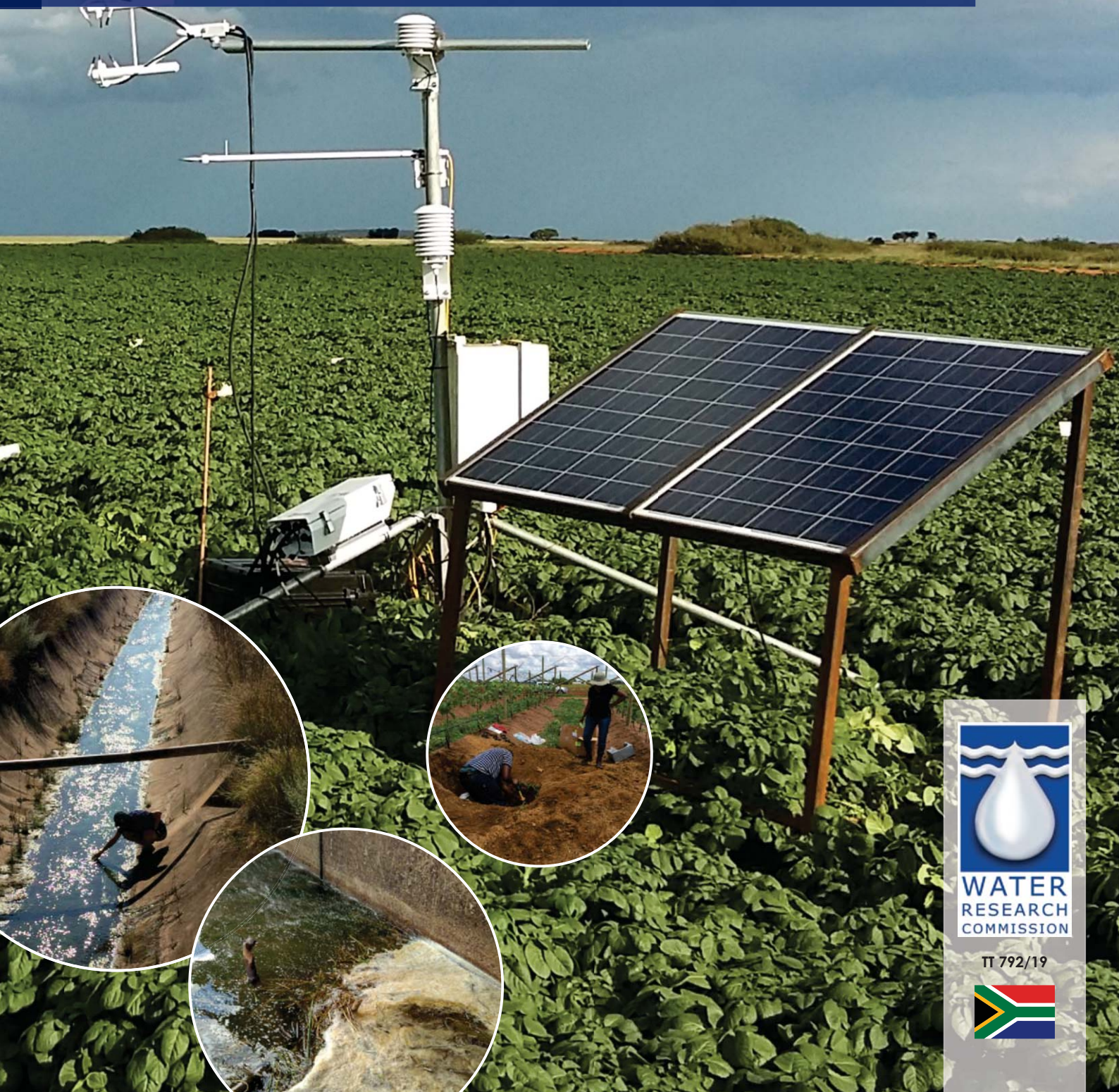

WATER RESEARCH COMMISSION

TT 792/19

Quantifying and Managing Agricultural Nitrogen and Phosphorus Pollution from Field to Catchment Scale

Report to the
WATER RESEARCH COMMISSION

by

MICHAEL VAN DER LAAN[1], LINUS FRANKE[2] (Editors)
[1]Department of Plant and Soil Sciences, University of Pretoria
[2]Department of Soil, Crop and Climate Sciences, University of the Free State

WRC Report No. TT 792/19
ISBN 978-0-6392-0055-2

June 2019

Obtainable from
Water Research Commission
Private Bag X03
Gezina 0031
South Africa

orders@wrc.org.za or download from www.wrc.org.za

EXECUTIVE SUMMARY

Overview

Background to the project

The WRC-funded project entitled 'Quantifying and managing agricultural nitrogen and phosphorus pollution from field to catchment scale' ran from April 2015 to April 2019, and was a collaboration between the University of Pretoria and the University of the Free State. Elevated nitrogen (N) and phosphorus (P) concentrations in surface and sub-surface waters leading to eutrophication of water ways is a major problem in South Africa and agricultural non-point source pollution has been identified as an important contributor to eutrophication. Agricultural N and P pollution is extremely difficult to quantify because of challenges in measuring nutrient losses via runoff and drainage at the plot scale, and the complications to upscale field measurements to a catchment scale. Agricultural N and P pollution is also difficult to mitigate because of the diffuse nature of the pollution and the essential role that N and P fertilisation plays in enhancing agricultural productivity. Reducing N and P fertilisation rates can lead to reduced yields, so management practices that lead to a higher N and P use efficiency by the crop are needed to reduce N and P pollution without impacting yields and profitability. The current project was therefore initiated to improve our understanding of N and P dynamics in arable fields and provide data for model testing, to determine the pollution potential of different cropping systems in South Africa, to identify mitigation measures, and to refine upscaling techniques to improve the quantification of pollution at catchment level.

Scoping study

A scoping study was conducted to assess potential 'hotspots' where irrigated agriculture may be contributing to surface water eutrophication and enriched groundwater nitrate levels via non-point source N and P pollution. A number of sites were identified and have been listed for further investigation. Based on the study, the Lower Vaal and Middle Olifants Catchments were selected for more detailed research in this project.

Model comparisons

Hydrus, APSIM and SWAT are models that are commonly used internationally to investigate non-point source pollution from agriculture. A brief description of each of these models has been provided, as well as a table comparing the different relevant processes simulated and input parameters required. Hydrus is recommended for investigation of complex hydrological systems, APSIM is recommended to explore in-field best management practices to reduce N and P pollution, while SWAT is best applied at the sub-catchment to basin scale. Despite its ability to simulate large areas, SWAT includes many relevant and detailed processes often not considered by plot scale models.

Simulation of soil water solute concentrations

Data from a large drainage lysimeter trial in which soil water potential and chloride (conservative tracer) and nitrate concentrations were measured was compared with output from the Hydrus model. Despite simulating a wide range of bypass (mobile/immobile water) flow conditions, measured values from suction cups and wetting front detectors were in most cases much lower than modelled values. This reaffirms the bias of such samplers to larger soil pores and the measurement of the respective solute concentrations in these pores only. We also caution that the history of the wetting and solute addition pattern will influence concentrations sampled by such devices relative to the average concentration across all pore volumes. Based on these results suction cups were used to a lesser extent in subsequent studies than originally envisaged.

Wheat nitrogen leaching trial

The purpose of this study was to evaluate different techniques used to quantify N leaching from the rootzone and determine fertiliser N use efficiency (FNUE). Lysimeter and field trial sites were planted with wheat (*Triticum aestivum*) (PAN3400 cultivar) at the University of Pretoria's Hillcrest Campus Experimental Farm. A drain gauge was installed adjacent two drainage lysimeters already at the site. Water content sensors and suction cups (SCs) were installed at 0.15, 0.3, 0.5 and 0.7 m depths in the weighing lysimeters and also in close proximity to the drain gauge, while SCs, wetting front detectors (WFDs) and water content sensors were installed at 0.25 and 0.5 m in the field trial site. The crop was fertilised with 200 kg N ha^{-1}, but no fertiliser was applied on unfertilised control plots. High density drip irrigation was used, and bromide (Br^-) was applied to all field plots at 0.020 kg m^{-2}. Water was sampled from the SCs, WFDs and the bottom of weighing lysimeters and drain gauge to determine soil water NO_3-N and Br^- concentrations. Soil samples collected before and after the trial, and plant samples taken at tillering, flowering and physiological maturity were analysed for plant N% and stable ^{15}N natural abundance using a mass spectrometer. The APSIM model was then validated using data from the field trial. The drain gauge drained more frequently and in greater amounts than the weighing lysimeters, and NO_3^- was observed in drainage water from the drain gauge, but was undetectable from the weighing lysimeters' drainage, possibly because of saturated bottom layer that promoted denitrification. Based on stable ^{15}N natural abundance, the FNUE was 68%, so the fertilised crop did not use 32% of the applied fertiliser. Good correlation was noted between the flag leaf and total plant N% at physiological maturity, indicating that the flag leaf can be used to determine the FNUE without requiring whole plant analysis. Potential NO_3-N leaching determined using a Br^- conservative tracer was 51.5 kg ha^{-1} $season^{-1}$. In fertilised plots, the calibrated model predicted NO_3-N leaching of 22.7 kg ha^{-1} $season^{-1}$, which was slightly lower than the drain gauge measured NO_3-N leaching 24.9 kg ha^{-1} season. Therefore, the drain gauge shows excellent promise in quantifying N leaching but will require further testing under a range of cropping systems. This confirms that the APSIM model can be applied to

investigate wheat cropping systems to improve N management decisions. The model confirmed that proper timing of N applications can reduce leaching losses, but further tests are required in several wheat growing agro-ecological zones to explore N management options that minimise N leaching losses. Even without additional measurements and/or modelling of N losses and crop uptake, results of this study for wheat indicate that the ^{15}N stable isotopes can be used on its own to estimate FNUE.

Modelling runoff at the plot scale using the APSIM crop model

Surface runoff is one of the main processes by which P, one of the major drivers of eutrophication, is transported to surface waters. A previous study evaluated P losses via surface runoff in sugarcane fields in Mauritius by using simulated rainfall events (50, 100 and 150 mm) and three slope classes (flat, gently sloping and sloping). The volume of runoff as well as the fractions of the different forms of P were measured. The results of this study were used to test the runoff subroutines in APSIM. A sensitivity analysis revealed that the most sensitive calibration parameters were curve number and initial water content. The accuracy of the model's prediction of surface runoff was also linked to soil type and soil texture. The soil type that showed a good correlation between simulated and observed runoff was a Humic Ferruginous Latosol, however, accuracy decreased with increasing clay content. The APSIM model does not mechanistically quantify P losses in surface runoff, but the developers recommend using a simple enrichment factor approach to estimate who much soluble and sediment-bound P is lost with the simulated runoff. These data can help inform the parameterisation of such enrichment factors.

Nutrient use efficiencies and leaching potentials of irrigated potato-maize systems in central South Africa

Field trials were conducted on potato-maize rotations in three intensively managed fields differing in soil texture (sandy loam and loamy sand soils) at a farm nearby Christiana in the western Free State for three seasons (2016-2018). Field measurements of water use efficiency (WUE) (rainfall + irrigation) ranged from 1.0 to 3.7 g potato l^{-1} water with 406 to 939 mm received, nitrogen use efficiency (NUE) ranged from 32 to 63 g potato g^{-1} N with 214 to 325 kg N applied, phosphorous use efficiency (PUE) ranged from 63 to 128 g potato g^{-1} P with 145 to 154 kg P applied and potassium use efficiency (KUE) ranged from 37 to 81 g potato g^{-1} K with 217 to 325 kg K applied as inorganic fertilizer. For the subsequent maize crop, 1.3 and 1.7 g grain l^{-1} water as WUE, 88 and 93 g grain g^{-1} N as NUE, 517 and 575 g grain g^{-1} P as PUE and, 798 and 861 g grain g^{-1} K as KUE were measured with 516 to 770 mm water applied and 103 kg N, 17 kg P and 11 kg K applied as inorganic fertilizer.

The fieldwork in the Lower Vaal Catchment has indicated that N losses through leaching from intensively fertilized, irrigated sandy soils can be as high as 173 kg N ha^{-1}. Also the high N levels observed in borehole water (higher than the concentrations in the Vaal River) indicate

that agriculture definitely contributes to N pollution of the Vaal River. High drainage and N leaching events were observed after heavy rainfall. In dry periods, farmers can reduce nutrient leaching if appropriate irrigation scheduling tools were used. Measured P leaching in deep drainage was low (at most 2 kg P ha^{-1}) despite high P fertilization levels. In this region, in case substantial P losses from arable fields occur, it is likely through runoff or wind erosion and not through deep drainage.

Phosphorus concentrations in deep drainage water in irrigated fields measured using a drainage gauge were observed to be low, even on sandy soils receiving a high P fertiliser rate, presumably due to immobilisation of soluble P by soil particles. A maximum of 2 kg P ha^{-1} was observed in the deep drainage over a cropping season. These results suggest that leaching of P from cropping fields is unlikely to form a major contribution to P pollution of surface waters in South Africa.

Using Climate Forecast System Reanalysis data as weather input to SWAT in a data poor catchment

Hydrological modelling remains one of the main tools for efficient and effective water resource assessment and management. A challenge facing this type of modelling in many developing countries is the scarcity of good quality weather data. This is largely because of gaps in weather records and uneven spatial and temporal distribution of weather stations. Satellite-based weather estimates are spatially and temporally continuous data that seamlessly capture weather variability across the globe. Accuracy, however, differs per area due to variability in hydro-climatic conditions. The utility of Climate Forecast System Reanalysis (CFSR) data for streamflow simulation in parts of the Lower Vaal River Catchment was assessed in this study. We setup two SWAT 'models', first with conventional gauge weather data obtained from the South African Weather Services (SAWS) and the Agricultural Research Council (ARC), second with CFSR data. The conventional gauge weather data had eight stations and CFSR weather data had 33 stations. The performance of the two models was compared against the observed flow at five stream gauge locations. The results indicated that gauge weather stations data remain the most important dataset to drive the SWAT model, whereas CFSR data could be a valuable alternative weather data source in areas lacking observed data. We found that CFSR data was also very useful to patch gaps and missing values in gauge weather data due to its ability to provide a complete set of climatic record at a high space-time resolution. But while the use of CFSR data as an alternative to gauge weather data in SWAT model looks promising, no satisfactory quantitative relation was obtained between the CFSR and gauge rainfall data, although there was comparable model performance between the two datasets.

Modelling nutrient loads from irrigated agriculture at a sub-catchment scale in the lower Vaal River system

SWAT was applied to estimate N and P loads in part of the Lower Vaal River Catchment, covering an area of approximately 1 343 km^2. The model was manually calibrated for streamflow, ammonium (NH_4), total-P and total-N loads. SWAT performed satisfactorily for flow, based on the R^2, whereas other statistical measures performed poorly. Nutrient load calibration is ongoing at this stage to enable full application of this set-up to investigate NPS pollution in the region. Nonetheless, irrigated cropping systems in the Lower Vaal River Catchment have been identified as a significant source of NPS pollution. The problem may worsen in the region in future due to the intensification of irrigated agricultural practices in terms of new land development and changing crop production practices.

Understanding the contribution of irrigated agriculture to nitrogen and phosphorous concentrations in the Middle Olifants

Nitrate-N (NO_3-N) and phosphate-P (PO_4-P) concentrations were monitored over a 20-month period at selected sites in the Middle Olifants Catchment, which contains the second largest irrigation scheme in South Africa making it an intensively irrigated watershed. Water quality in the irrigation canals did not always reflect the water quality of the source (Loskop Dam), indicating that contamination potentially comes from surface runoff into the canals, seepage through the canals and/or a concentrating effect following evaporation. The drainage canals (which export water from irrigated fields directly into the nearest freshwater bodies) and rivers themselves showed relatively high PO_4-P concentrations for most of the sampling period. The concentrations peaked in the summer rainfall months and to a lesser extent (but still above the eutrophication threshold value), after winter crop fertilization. The Flag Boshielo Dam (at the bottom of the catchment) PO_4-P concentration was consistently higher than Loskop Dam, indicating that activities in the Middle Olifants may result in impaired water quality for users downstream. Comparison with DWS data showed that we measured higher PO_4-P concentrations than DWS data, with the opposite being observed for NO_3-N. There was also a closer match between our measured values and those measured by commercial laboratories than DWS laboratories. Low flow in the drainage canals prevented load calculation, but the elevated P levels do warrant further investigation to better quantify the contribution from this source. It is acknowledged that point sources, such as poorly functioning wastewater treatment works, most likely contribute the bulk of the nutrient pollution in the catchment.

Contribution of irrigated agriculture to river N and P loads in the Middle Olifants

The SWAT model was also used to model the hydrology and water quality, in particular P losses from agricultural activity, of the Middle Olifants Catchment. The SWAT-CUP program was used for automatic calibration. Global sensitivity analysis revealed that the most sensitive parameters for calibration are soil saturated hydraulic conductivity, the baseflow alpha factor for bank

storage, the moist soil bulk density and the baseflow alpha factor. Streamflow was often over-estimated by the model, and work is still underway to better represent the irrigation systems within the catchment to improve streamflow simulation. Highest P pollution loads were estimated to come from sub-basins with intensive horticulture, but relatively low exports were predicted for irrigated agriculture, ranging from 0.004 to 0.013 kg P ha^{-1}.

Main findings and recommendations

Field-scale mitigation measures

Even a in a very carefully managed winter wheat trial with scientific irrigation and nutrient scheduling, only 68% of the applied fertiliser was taken up by the crop. This still represents a significant improvement from the 50% efficiency often reported in the literature. Careful application of best management practices, the use of suitable crop rotations including catch crops, and adoption of new technological advances, such as decision support systems and precision agriculture can assist farmers with improving the efficiencies of applied fertilisers.

In the Lower Vaal study, observed N concentrations in deep drainage water were substantial and higher than that of river water and borehole water in the region. It is therefore likely that N leaching from irrigated cropped fields forms a considerable contribution to N pollution of sub-surface and surface waters. Nitrogen leaching is associated with the high fertilizer input rates used in intensive potato production systems. These N leaching risks in potato-based rotations may be minimized by rotating shallow-rooted potato with a deep-rooted crop with a high N demand such as maize, which can partly recover some of the nutrients lost in drainage to deeper soil layers. Other shallow rooted crops like onion are also rotated with potato and further studies should evaluate leaching potential of a potato-onion system as it is expected to perform differently.

In dry climates, farmers in South Africa using appropriate irrigation scheduling tools may have limited deep drainage and associated nutrient losses in crops, even in soils with relatively low water holding capacity. Heavy rainfall events, however, disturb the balance between water input and evapotranspiration and can lead to substantial drainage. This type of drainage cannot be avoided through improved irrigation management, and ultimately it comes down to whether fertiliser nutrient supply is well match with crop demand over the longer-term.

The APSIM model, parameterised and validated with local data, was found to be an appropriate tool for simulating yield, and water and N dynamics, and to identify pollution mitigation measures at plots scale. In the Lower Vaal, the cropping sequence was found to have a major impact on nutrient leaching. A shallow-rooting, intensively-fertilised crop such as potato has a high leaching potential, but if the crop is followed by a maize crop that is modestly fertilised, the deep-rooting crop can recover a fair amount of the nutrients lost by the potato crop. Furthermore, irrigation scheduling was found to have a major impact on N leaching. The

mobility of water and N are closely linked and irrigation beyond the crop demand leads to deep drainage and N leaching. Heavy rainfall also causes leaching obviously, but farmers have little control over leaching induced by heavy showers. Under-irrigation reduces crop yield and the N use efficiency of the crop, leaving more N behind in the soil that can be leached, and is therefore not recommendable either. Split applications of N fertiliser is even more practical through fertigation in irrigated systems. This can greatly improve N use efficiency and reduce leaching, especially in sandy soils with a low water and nutrient holding capacity.

Upscaling to catchment scale

The upscaling of results from plot or field scale to a watershed level was found challenging. Quality weather data from functional weather stations was a limitation in the parameterisation of SWAT. Using weather data from the Climate Forecast System Reanalysis (CFSR) for streamflow simulation was very useful to patch gaps and missing values in rain gauge weather data, but could not serve as an alternative to measured data from weather stations. Despite the poor statistical performance of SWAT for nutrient loads simulation at catchment scale, the identification of some measured peak nutrient loading events suggest that SWAT is an appropriate tool for water quality investigations at the catchment scale.

Future research

Catchment scale modelling

The calibration, refinement and application of the SWAT model to simulate nutrient loads for the Lower Vaal and Middle Olifant Catchments is on-going. Future work will focus on the auto-calibration and validation of sub-catchment scale models. The plan is to use a higher resolution DEM (5 m), improve the soil data using profile description from land type data, improve land use mapping with remote sensing data (Sentinel, Google data and SPOT 6), and represent more accurate on-farm management operations of the study area. We would also like to upscale the sub-catchment scale model to a larger Lower Vaal River catchment and perform scenarios analysis in terms of the implications of land use and climate change on water quality. This will enable us to assess the impact of land use changes and crop management changes on nutrients loads in the river from agriculture. Ideally, a platform is created with all the necessary GIS layers for the whole of South Africa so that new users can get the model up and running for their catchment faster.

Quantifying other sources of nutrient pollution

Wind erosion is a major threat to the long-term sustainability of crop production, especially in central South Africa, and likely contributes to the eutrophication of surface waters, especially through P additions. No studies have quantified the contribution of dust deposits in dams to the eutrophication of surface waters in central South Africa. It is recommended to research this in

more detail, as it is potentially a major, though poorly quantified source of water pollution. Runoff remains poorly understood and modelled, and further studies are need validate N and P losses from agricultural fields through runoff even as our catchment scale modelling capabilities improve.

Wastewater treatments works represent another major contributor to N and P loads in surface waters. There is a dire need to better quantify the contributions of wastewater treatment works to river N and P loads and reduce this source.

Development and policy implications

Communication with stakeholders

The implications of N and P export from cropping systems to downstream water bodies must be widely communicated. At the same time, unavoidable inefficiencies in fertiliser use must be recognised, and agriculture must not be unduly blamed. Some impact on the environment is the price we pay for our food, even under optimal management practices. Mitigating impacts will sometimes come at the cost of short-term farm profitability. In such cases, incentives for farmers will be required to ensure reliability of food supply. Ultimately society will need to pay for this, so do we pay more for our food so farmers look after the environment better, or do we pay higher taxes so government can pay farmers for their stewardship of landscapes on behalf of society? Better ways engage various stakeholders on NPS pollution and potential mitigation measures within catchments (the proposed unit of management) should be investigated, including through social media.

Data availability

Besides the above-mentioned need for a platform with GIS-referenced data to facilitate spatial modelling, a key problem with the parameterisation of catchment flow and other weather-based models in South Africa is the lack of complete long-term weather datasets from weather stations. While SAWS and the ARC both run an extensive network of weather stations throughout the country, the accessibility of the data and the large gaps that these datasets often have makes the availability of reliable long-term weather data a key limiting factor in the improvement of models. While satellite-based weather data can somewhat compensate for sub-optimal ground data, it does not replace the need for reliable long-term datasets from weather stations, as shown in this project.

Towards a policy to reduce agricultural NPS nutrient pollution

In certain parts of the world, for instance in the European Union (EU), fertiliser use and leaching loads are carefully monitored and highly regulated. This may be through pre-defined ceilings for fertiliser application rates, and through management tools such as the obligatory cultivation of nutrient catch crops in periods when no crop is in the field means the risk of leaching is high. In South Africa, regulations regarding fertiliser use by farmers is minimal and monitoring of nutrient losses from cropped fields non-existent. Commercial farmers often depend on representatives of fertiliser companies for advice on fertilizer application rates. These companies do not necessarily have an interest in reducing fertiliser application rates. Due to a lack of reliable decision support systems for nutrient use, farmers generally rather apply a bit too much fertilizer rather than running the risk of under-supplying nutrients and harming yield. This is especially true for high-value crops such as potato, onions and other vegetable crops. To reduce NPS nutrient pollution from cropped farming, South Africa needs to begin to implement the monitoring of fertiliser use and prevention of over-use.

ACKNOWLEDGEMENTS

The research team is very thankful to the Reference Group (RG) members for their guidance and support throughout the project. The RG members were:

Dr S Mpandeli	Water Research Commission (Chairman)
Dr G Backeberg	Water Research Commission
Dr HG Snyman	Golder Associates
Dr AD Manson	KwaZulu-Natal Department of Agriculture
Dr S Jooste	Department of Water and Sanitation
Mr HM du Plessis	University of Pretoria
Prof CC du Preez	University of the Free State

We would like to thank Omnia Fertilizer for assisting with soil analyses, and Miss Stephanie Roberts for all her assistance with the University of Pretoria field trials.

We are grateful to Netafim for sponsoring the drip irrigation system for the trial conducted on the University of Pretoria Experimental Farm and also for providing technical support.

Wesgrow is thanked for facilitating the field trials conducted on commercial farms.

We thank the South African Sugarcane Research Institute for sharing data from their long-term trial (BT1) with the project team.

We are very thankful to the Loskop Irrigation Board for assistance with our monitoring programme in the Middle Olifants, especially Mr Leon de Waal and Mr Pieter Pretorius. We also like to thank Ms Coleen Fourie from the Loskop ARC Experimental Farm who helped us with access to storage dams and drainage canals for sampling purposes.

We are grateful to Mr Keketso Mokhothu and Mr Richard Hay for assistance with monitoring, Miss Monica Oberholster for assisting with formatting the technical report, and Mrs Joey Herman for assisting with administration of the project.

While sections of this report are author-specific, contributing authors included:
M van der Laan[1], AC Franke[2], N Mararakanye[2,3], L Mudaly[1], ATB Machakaire[2,4], TE Mangwende[1], S Maseko[1], LR Fredericks[2], JJ le Roux[2], JM Dabrowski[5], JG Annandale[1], GM Ceronio[2], J.H. Barnard[2] and G Hall[1]

[1]Department of Plant and Soil Sciences, University of Pretoria
[2]Department of Soil, Crop and Climate Sciences, University of the Free State
[3]Department of Agriculture, Forestry and Fisheries
[4]McCain Foods
[5]Confluent

TABLE OF CONTENTS

LIST OF FIGURES

LIST OF TABLES

LIST OF ABBREVIATIONS

APSIM	Agricultural Production Systems Simulator
APSRU	Agricultural Productions Systems Research Unit
ARC	Agricultural Research Council
ARC ISCW	Agricultural Research Council's Institute for Soil, Climate and Water
AWS	Automatic Weather Station
BD	Bulk Density
CD	Chief Directorate
CEC	Cation Exchange Capacity
CFSR	Climate Forecast System Reanalysis
CLL	Crop Lower Limit
CMORPH	Climate Prediction Centre Morphing Technique
CN	Curve Number
CS	Capacitance Sensor
D	Index of Agreement
DAFF	Department of Agriculture, Forestry and Fisheries
DAP	Days After Planting
DCT	Divergence Control Tube
DEA	Department of Environmental Affairs
DEM	Digital Elevation Model
DRDLR	Department of Rural Development and Land Reform
DSSAT	Decision Support System for Agrotechnology Transfer
DSVI	DRASTIC Specific Vulnerability Index
DUL	Drained Upper Limit
DWAF	Department of Water Affairs and Forestry
DWS	Department of Water and Sanitation
EC	Electrical Conductivity
ECV	Eddie Covariance
ET	Evapotranspiration
FAO	Food and Agriculture Organization
FNUE	Fertiliser N Use Efficiency
G	Heat Flux
GDD	Growing Degree Days
GFS	Global Forecasts System
GHG	Greenhouse Gas
GIS	Geographic Information System
GLUE	Generalized Likelihood Uncertainty Estimation
H	Sensible Heat
HRU	Hydrological Response Unit
HSG	Hydrologic Soil Group

K_c	Crop Factor
LAI	Leaf Area Index
LE	Latent Energy
MAE	Mean Absolute Error
MAR	Mean Annual Runoff
MCMC	Markov Chain Monte Carlo
NCEP	National Centres for Environmental Prediction
Ndff	N derived from fertiliser
NGI	National Geospatial Information
NOAA	National Oceanic and Atmospheric Administration
NORAD	The Norwegian Agency for Development Cooperation
NPS	Non-Point Sources
NSE	Nash-Sutcliffe Efficiency
NUE	Nitrogen Use Efficiency
OM	Organic Matter
PAR	Photosynthetic Active Radiation
ParaSol	Parameter Solution
PBIAS	Percent Bias
PSO	Particle Swarm Optimization
RMSE	Root Mean Square Error
Rn	Net Radiation
RSR	Standard Deviation Ratio
RUE	Radiation Use Efficiency
RZWQM	Root Zone Water Quality Model
R^2	Coefficient of Determination
SANBI	South African National Biodiversity Institute
SAT	Saturation
SAWS	South African Weather Service
SC	Suction Cup
SCS	Soil Conservation Service
SOC	Soil Organic Carbon
SOM	Soil Organic Matter
SPAW	Soil-Plant-Air-Water
SRTM	Shuttle Radar Topographic Mission
SUFI-2	Sequential Uncertainty Fitting ver.2
SWAT	Soil and Water Assessment Tool
SWAT- CUP	SWAT Calibration Uncertainties Program
SWB	Soil Water Balance
SWIM	Soil Water Infiltration and Movement
TAV	Annual Average Temperature

TDM	Total Aboveground Dry Matter
TRMM-TMPA	Tropical Rainfall Measuring Mission-Multisatellite Precipitation Analysis
UP	University of Pretoria
UFC	University of Free State
USDA	United States Department of Agriculture
USGS	United States Geological Survey
VIS	Vaalharts Irrigation Scheme
VPD	Vapour Pressure Deficit
VWC	Volumetric Water Content
WFD	Wetting Front Detector
WMA	Water Management Area
WRB	World Reference Base for Soil Resources
WRC	Water Research Commission
WUE	Water Use Efficiency

1 INTRODUCTION

1.1 Background to crop production in South Africa

Producing food is the most important use of our natural resources. Since World War II, intensive, mechanised agriculture has been evolving, so many of the fields we continue to cultivate today have produced food under intensifying practices for more than 70 years. In 2005, 90% of all food calories and 80% of all food protein and fats were derived from croplands (Kastner et al., 2012). Unfortunately, these practices have resulted in salinization of irrigated fields, depletion of freshwater aquifers, degradation of ecosystems due to the export of harmful agrochemicals, soil profile acidification, soil organic matter (SOM) decline, and a general loss of soil quality and fertility.

South Africa cultivates around 12-13% of its total area of 122 million ha. Just over 14 million ha is under commercial agriculture (approximately 40 000 farming units), a well-developed sector relying on a high degree of mechanisation and synthetic agrochemical use. There are around 1.3 million smallholder farmers in former homelands, with around 2.9 million households engaging primarily in agriculture at the subsistence level (DAFF, 2012), generally characterised by low input – low production systems. Approximately 1.3 million ha of South Africa (1% of total 13% of cultivated land) is under irrigation (DAFF, 2012), compared to the national average of irrigation covering 21% of arable land (http://www.fao.org/nr/water). Food insecurity remains widespread throughout South Africa at 25% of the population (Labadarios et al., 2011), and this in the context of a population that is expected to increase from the current 50 million to over 80 million people by 2035 (Goldblatt, Undated). This population is also becoming more affluent, placing ever greater pressures on the natural environment.

Supplying a projected global population of 9 billion with the present diet and agricultural technology of northern America would mean that current cropland may need to double (Kastner et al., 2012). If no new land is to be brought into cultivation, this translates into a 2.4% yield increase per hectare per year for maize, rice, wheat and soybean (Ray et al., 2013). But yields for these crops are only increasing at 1.6%, 1.0%, 0.9% and 1.3% per year, respectively (Ray et al., 2013). More land will, therefore, inevitably need to be converted to cropping unless circumstances change and there is radical increase in intensification or dietary preferences. As we are already using the better agricultural land in most cases, conversion of poorer quality land will require greater input and management costs.

Climate change is an additional major new challenge affecting various climate-sensitive sectors across the globe. Counter-intuitively, the ratio of food energy outputs to energy inputs for our production systems has decreased greatly since the birth of mechanised agriculture and its reliance on fossil fuels. As an emitter of greenhouse gases (GHGs) and one of the sectors expected to be burdened most with the impacts of changing weather patterns, the agricultural

South African irrigated agriculture uses around 60% of the 13×10^9 m^3 runoff per annum used by all sectors, or just under 40% of the estimated 20×10^9 m^3 exploitable runoff (DWAF, 2004). Despite only 1% of the country's surface area being under irrigation, it is responsible for 30% of agricultural

production by value (Nieuwoudt et al., 2004). As a result of increasing demands for water there is pressure on irrigation to divert more water to the industrial and domestic sectors. It is estimated that freshwater demand will exceed supply nationally by 2025 (Musvoto et al., 2014), less than a decade from now.

1.2 Eutrophication

Eutrophication is a major problem in many agricultural regions around the world. In the United States, 70% of nitrogen (N) and phosphorus (P) delivered by the Mississippi River into the Gulf of Mexico is derived from agriculture (Alexander et al., 2008). Isermann (1990) calculated that agriculture was responsible for about 60% of the N and 25% of the P emissions into the North Sea. Agricultural runoff is also largely blamed for the degradation of the Great Barrier Reef in Australia (Brodie et al., 2011).

According to Van Ginkel (2011), eutrophication is a major concern in a number of South African catchments. De Villiers and Thiart (2007) observed alarming and statistically significant increasing concentrations of dissolved phosphate at or nearing critical levels in approximately 60% of the major South African river catchments studied (1970-2005 data). The authors noted that the seasonal nature of river nutrient levels indicates that both point and non-point sources (NPS) are major contributors and that these nutrient fluxes equate to significant loss of fertiliser-equivalent nutrients. Phosphorus levels are generally low in South African groundwater, but certain regions do contain groundwater that is nitrate (NO_3^-) enriched (Annandale and Du Preez, 2005).

Due to the diffuse nature of agricultural nutrient pollution it is extremely difficult to quantify. Despite the work that has been undertaken so far (Görgens, 2012), NPS pollution remains a major problem and needs much greater investment in research and incentives to improve farmer water and nutrient management. The ineffective management of sewerage in South Africa means that untreated or partially treated sewerage is often returned to waterways, and this is frequently the dominant source of N and P pollution. Informal settlements that do not have sanitation infrastructure can also contribute significant amounts of N and P to watercourses.

Accurate quantification of agriculture's contribution to surface and subsurface water N and P levels is, however, hindered by (i) the quality of models available and issues with upscaling from plot to catchment scale, (ii) the lack of adequate data for model parameterisation, initialisation and calibration, and (iii) the lack of adequate, independent datasets for model testing and verification (Berry, 2011; Dressing et al., 2016).

1.3 Nitrogen and phosphorus use in South Africa

In intensive crop production, N fertilizer is often applied in excess of crop requirements to reduce the risk of N deficiencies occurring during the growing season. This, and a failure to account for N contributions made available through the mineralization of SOM, irrigation water and N biofixation leads to fertiliser N use efficiencies in the region of only 30 to 50% being commonly reported in the literature (Smil, 1999). Galloway et al. (2004) estimated that 20% of N fertiliser ends up in aquatic ecosystems.

In less-intensive systems, such as dryland crop production, fertiliser N is frequently under-applied, resulting in a net 'mining' of soil N (Annandale and Du Preez, 2005). As irrigated systems are often characterized by higher nutrient application rates and excess irrigation, these systems are 'leakier' than dryland cropping systems. From field scale nutrient balances, Annandale and Du Preez (2005) concluded that dryland crop production in South Africa generally has a limited impact on freshwater NO_3^- levels, especially when cropping takes place on deep soils. In addition to N losses via runoff and deep drainage, NH_3 volatilisation also leads to the eutrophication of ecosystems due to subsequent deposition of N, and N losses can be high when urea is applied, especially if surface applied.

Once in soil, inorganic P is relatively immobile as it adsorbs strongly to soil particles and organic matter. It is, therefore, generally accepted that the main pathway of P from cultivated fields to waterways is via surface runoff as soluble phosphate or attached to sediment. In addition to soil slope and surface conditions, runoff losses are influenced by timing and method of application, form of fertiliser used and tillage practice.

Since the early 1960s, there appears to have been a dramatic decline in N use efficiency (Figure 1). This may in part be as a result of increased cropping frequency giving less time for N mineralisation, and/or a general decline in N mineralisation as a result of SOM rundown. It is notable that South Africa has followed the same trend as the World average. The World figure has stabilised at approximately 23 tonnes of cereal per tonne of inorganic N fertiliser applied. If we assume a grain N content of 3%, this indicates an efficiency of around 70%, which is higher than often reported (Cameron et al., 2013). Put differently, we would expect to produce at least 33 tonnes grain per tonne of N applied, so the value of 23 tonnes grain per tonne of N applied represents very inefficient systems. Of course it must be remembered that some of the N is applied to crops other than cereal crops and that organic fertilisers and N fixed by legumes are also used as a source of N for cereal crops, and these are not accounted for in the data in Figure 1. Offsetting this in turn, not all grain produced is marketed through formal channels, and is therefore not included in yield estimates.

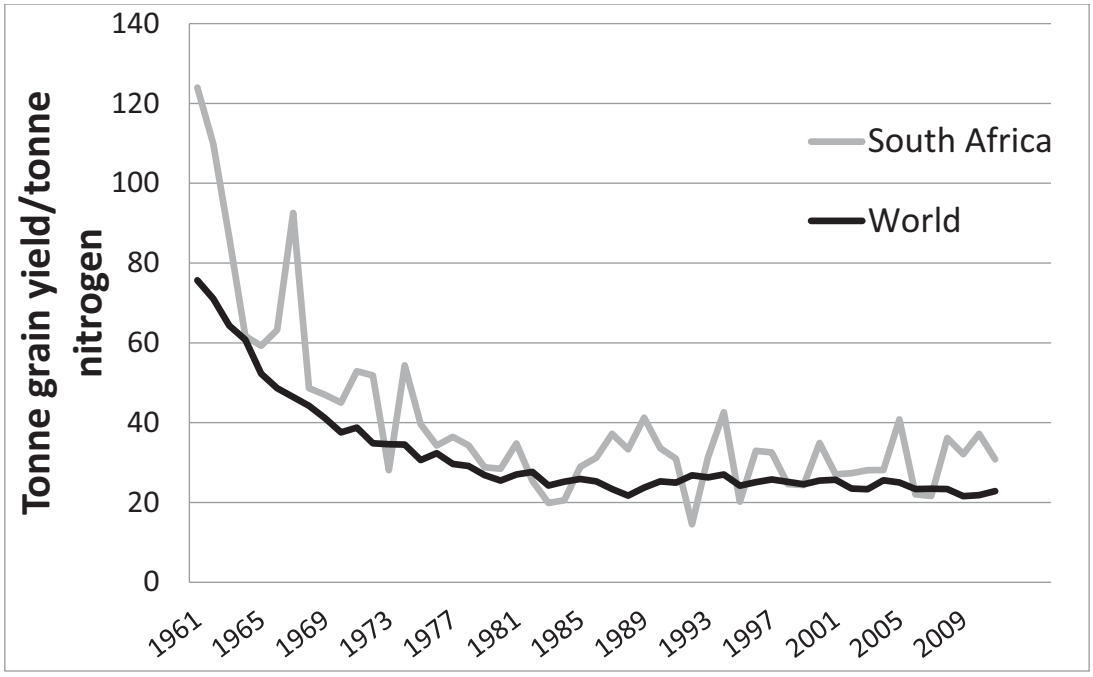

Figure 1: Cereal yield divided by nitrogen fertiliser consumption for South Africa and the world (http://faostat3.fao.org. http://www.fssa.org.za/Statistics.html, accessed 10 October 2015)

A decline and levelling off of P fertiliser consumption potentially indicates increased crop use efficiency (Figure 2). Phosphorus fertiliser may in many cases have been over-applied in the past when energy costs were low. In the future, increased demand for water and resultant abstraction from rivers, along with increasing N and stabilised P fertiliser may result in ever-increasing N and P concentrations in our waters and saturation of our ecosystems with these nutrients unless new approaches and technologies drastically improve crop N and P fertiliser use efficiencies. Eutrophication also leads to the clogging of irrigation equipment, so upstream irrigators can have a direct negative effect on irrigators downstream.

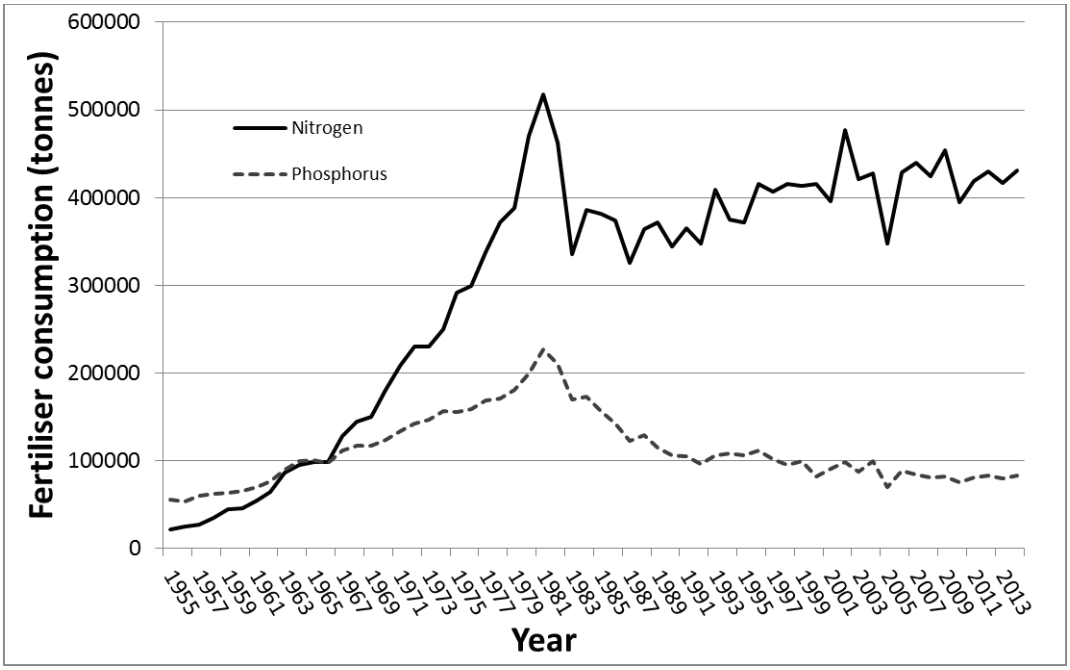

Figure 2: Nitrogen and phosphorus fertiliser consumption in South Africa between 1995 and 2014 (http:www.fssa.org.za/Statistics.html, accessed 10 May 2015)

1.4 Aims of the project

This project builds on work done in previous WRC research (Görgens, 2012; Van der Laan, Annandale et al., 2012) to quantify and mitigate non-point source N and P pollution from South African cropping systems. During the proposal writing phase, it was recognised that a plot to catchment scale approach was essential in dealing with this type of pollution, as in-field management practices can have an important impact on the amount of nutrient export, but also that the larger issue often needs to be tackled at the catchment scale to understand issues such as land use influences and the ultimate fate of nutrients in the landscape in response to structures such as reservoirs and wetlands.

Non-point source pollution by its very nature is extremely difficult to measure or estimate. It was therefore also recognised that an approach incorporating historical data, newly measured data, as well as modelling would be essential in extrapolating results and developing capacity in tools that can be applied in addressing this problem.

Teams from the University of Pretoria and the University of Free State collaborated on this project, in geographically distinct regions but employing similar methodologies. Technical support across teams was shared as required. Following a literature review, a scoping study was done to identify eutrophication hotspots in South Africa that may be linked with agriculture. From this scoping study, two case study catchments were selected, namely the Lower Vaal River (managed by the UFS team) and Middle Olifants River (managed by the UP team) catchments. Field trials were conducted in potato-maize cropping systems in the Christiana area of the western Free State that is near the Vaal River, and with maize and wheat on the UP Hillcrest Campus Experimental Farm, and additional monitoring was done in the Middle Olifants. Additional model testing of specific processes that are essential in

estimating NPS N and P pollution were tested using historical datasets. The final conclusions section is a synthesis of the variety of research done, addressed mitigation measures that may be adopted to reduce this type of pollution, and makes recommendations for future research.

1.5 References

ANNANDALE, J. and DU PREEZ, C. (2005) Nutrients – Agricultural Contribution Management and Modelling. Knowledge review of modelling non-point source pollution in agriculture from field to catchment scale. WRC report (1467/1), 05.

BRODIE, J., DEVLIN, M., HAYNES, D. and WATERHOUSE, J. (2011) Assessment of the eutrophication status of the Great Barrier Reef lagoon (Australia). Biogeochemistry 106(2), 281-302.

DE VILLIERS, S. and THIART, C. (2007) The nutrient status of South African rivers: concentrations, trends and fluxes from the 1970s to 2005. South African Journal of Science 103(7-8), 343-349.

GALLOWAY, J.N., DENTENER, F.J., CAPONE, D.G., BOYER, E.W., HOWARTH, R.W., SEITZINGER, S.P., ASNER, G.P., CLEVELAND, C., GREEN, P. and HOLLAND, E. (2004) Nitrogen cycles: past, present, and future. Biogeochemistry 70(2), 153-226.

LABADARIOS, D., MCHIZA, Z. J. R., STEYN, N. P., GERICKE, G., MAUNDER, E. M. W., DAVIDS, Y. D., & PARKER, W. A. (2011) Food security in South Africa: a review of national surveys. *Bulletin of the World Health Organization*, *89*, 891-899.

MACKAY, H., ROUX, D., ASHTON, P., VAN VLIET, H. & JOOSTE, S. (1995) The development of South African water quality guidelines for the natural aquatic environment. Water Science and Technology 32(5), 293-299.

MATTHEWS, M.W. (2014) Eutrophication and cyanobacterial blooms in South African inland waters: 10years of MERIS observations. Remote Sensing of Environment 155, 161-177.

MUSEKIWA, C. & MAJOLA, K. (2014) Groundwater vulnerability map for South Africa. South African Journal of Geomatics 2(2), 152-162.

VAN DER LAAN, M., VAN ANTWERPEN, R. & BRISTOW, K.L. (2012) River water quality in the northern sugarcane-producing regions of South Africa and implications for irrigation: A scoping study. Water SA 38(1), 87-96.

SMIL, V. (1999) Nitrogen in crop production: An account of global flows. Global Biogeochemical Cycles 13(2), 647-662.

VAN GINKEL, C. (2011) Eutrophication: Present reality and future challenges for South Africa. Water SA 37(5), 693-701.

WALMSLEY, R. (2000) Perspectives on Eutrophication of Surface Waters: Policy/research Needs in South Africa: a Review and Discussion Document, Water Research Commission.

2 IDENTIFICATION OF EUTROPHICATION HOTSPOTS IN SOUTH AFRICA POTENTIALLY CONTRIBUTED TO BY AGRICULTURE

M. van der Laan and L. Mudaly
Department of Plant and Soil Sciences, University of Pretoria, Pretoria 0002, South Africa

2.1 Introduction

In a source-directed approach to manage eutrophication, the South African government has set effluent discharge standards (Walmsley, 2000), and depending on the level of enrichment, water bodies can be classified as oligotrophic (low nutrient levels and no quality problems), mesotrophic (intermediate nutrient levels with emerging signs of quality problems), eutrophic (high nutrient levels and frequent quality problems) or hypertrophic (excessive nutrient levels and almost continuous quality problems) (Table 1). Nitrogen concentrations of 0.4-1.0 mg ℓ^{-1} are generally considered low enough to limit eutrophication, but this is dependent on site-specific conditions (MacKay et al., 1995). As prokaryotic blue-green algae (cyanobacteria) are able to fix atmospheric N, however, it may be inappropriate to set a guideline value on eutrophication (ANZECC, 1992). The reduction of P is therefore recognised as the only practical way to limit eutrophication (Walmsley, 2000).

Table 1: South African effluent discharge standards and phosphorus levels for trophic status classification (DWAF, 1996)

	Effluent discharge standard*	Oligotrophic#	Mesotrophic#	Eutrophic#	Hyper-eutrophic#
Nitrogen (mg l^{-1})	< 10	-	-	-	-
Phosphorus (mg l^{-1})	< 1	0.004-0.010	0.010-0.035	0.035-0.100	>0.100

Matthews (2014) used remote sensing with satellite imagery to establish a time series of chlorophyll-a, cyanobacteria and surface scum status for the 50 largest standing water bodies in South Africa (Table 2). Worryingly, 62% of the water bodies were observed to be hypertrophic (mean chl-a > 30 mg m^{-3}), and 46% had intermediate to extensive cyanobacteria coverage. Interestingly spikes in Chl-a coincide with the summer crop planting and fertilisation dates for most regions in South Africa.

Table 2: Reservoir Chlorophyll-a (Chl-a) levels derived from 10 years of MERIS observations (Matthews, 2014)

Reservoir name	Area (km^2)	Lat.	Lon.	Alt. (masl)	N (number)	Chl-a (mg m^{-3})
Gariep	346.6	-30.69	25.71	1260	650	137.2
Vaal	251.4	-26.90	28.14	1490	756	99.6
Bloemhof	186.5	-27.67	25.65	1235	521	142.8
Pongolapoort	113.4	-27.37	31.95	140	625	3.8
Vanderkloof	113.1	-30.15	24.88	1170	628	55.3
Sterkfontein	60.8	-28.43	29.02	1702	566	3.3
Lake Sibhayi	54.7	-27.37	32.69	20	647	10.8
Darlington	52.2	-33.15	25.15	239	412	120.5
Theewaterskloof	50.8	-34.03	19.20	307	176	43.1
Heyshope	48.8	-27.03	30.50	1308	727	23.7
Kalkfontein	42.0	-29.52	25.26	1241	548	117.3
Grootdraai	32.7	-26.93	29.33	1549	731	81.8
Spitskop	31.7	-28.09	24.55	1045	525	163.4
Erfenis	29.9	-28.55	26.84	1331	534	351.4
Kuhlange (Kosi Lake)	28.3	-26.98	32.84	2	629	8.3
Allemanskraal	26.4	-28.30	27.21	1371	573	248.0
Woodstock	26.1	-28.72	29.21	1180	584	14.3
Loskop	23.0	-25.43	29.32	1006	863	58.1
Albert Falls	21.8	-29.44	30.41	658	514	8.4
Brandvlei	18.7	-33.71	19.43	203	214	6.4
Ntshingwayo	18.7	-27.99	29.91	1248	566	314.2
Tzaneen	16.8	-23.79	30.15	728	592	39.9
Hartbeespoort	15.6	-25.75	27.86	1165	775	92.6

Reservoir name	Area (km^2)	Lat.	Lon.	Alt. (masl)	N (number)	Chl-a (mg m^{-3})
Krugersdrift	15.3	-28.87	26.00	1252	538	317.9
Umtata (Mthatha)	15.2	-31.54	28.73	695	598	478.3
Voëlvlei	14.5	-33.36	19.04	75	242	114.7
Midmar	14.3	-29.51	30.19	1046	533	4.4
Xonxa	14.0	-31.82	27.14	939	625	65.6
Spioenkop	13.9	-28.69	29.49	1091	583	67.5
Ncora	12.8	-31.78	27.65	1038	627	380.5
Barberspan	12.7	-26.58	25.59	1354	637	42.0
Klipvoor	12.6	-25.15	27.82	994	777	145.7
Grassridge	12.5	-31.77	25.47	1055	648	176.7
Koppies	11.4	-27.23	27.69	1424	670	133.0
Zaaihoek	10.9	-27.43	30.09	1737	707	14.3
Lubisi	10.7	-31.79	27.41	1020	669	82.8
Lake Chrissiesmeer	10.4	-26.33	30.22	1676	723	116.8
Flag Boshielo	10.4	-24.83	29.44	821	862	42.6
Goedertrou	10.1	-28.77	31.44	228	541	20.1
Rustfontein	10.1	-29.30	26.63	1374	557	115.6
Fairview	9.8	-26.16	31.66	297	693	33.3
Vaalkop	9.7	-25.31	27.47	987	752	108.5
Kwena	9.6	-25.37	30.37	1185	746	30.2
Roodekoppies	8.9	-25.41	27.59	1018	750	147.0
Witbank	8.7	-25.90	29.31	1507	745	117.5
Lake Msingazi	8.7	-28.76	32.10	5	553	5.6
Bronkhorstspruit	7.7	-25.90	28.69	1435	747	105.9
Jericho	7.7	-26.64	30.48	1470	696	18.7

Reservoir name	Area (km^2)	Lat.	Lon.	Alt. (masl)	N (number)	Chl-a (mg m^{-3})
Mokolo	7.3	-23.98	27.75	912	708	31.4
Inanda	6.7	-29.69	30.87	151	510	27.3

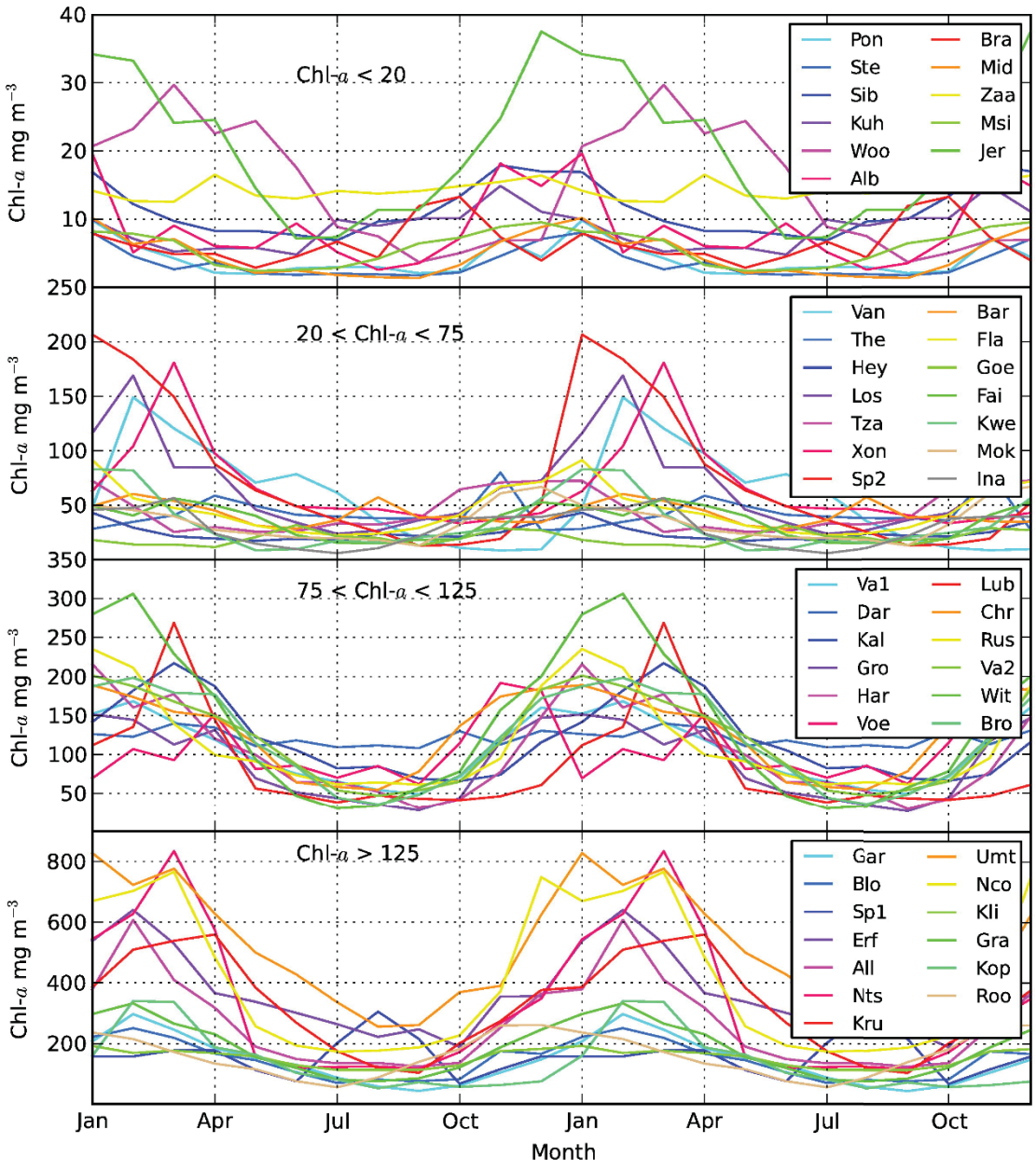

Figure 3: Seasonal cycle of chlorophyll-a (Chl-a) for 50 South African water bodies. Reservoir names abbreviated with first three letters except for Vaal = Va1, Vaalkop = Va2, Spioenkop = Sp1 and Spitskop = Sp2 (Matthews, 2014).

Quantifying the contribution of agriculture to N and P pollution

As irrigated systems are often characterized by higher nutrient application rates and are 'wetter systems', it may be expected that these systems are 'leakier' relative to dryland production. From field scale nutrient balances, Annandale and Du Preez (2005) concluded that dryland crop production in South Africa generally has a limited impact on freshwater NO_3^- levels, especially on deeper soils. In addition to N losses via runoff and deep drainage, NH_3 volatilisation also leads to the eutrophication of ecosystems due to subsequent deposition of this N, and losses can be high when urea is applied, especially if surface applied.

Despite intensive agricultural activities along the Crocodile River, including sugarcane and horticultural crops, Van der Laan et al. (2012) observed that PO_4-P concentrations were reduced downstream. Inorganic N concentrations for the period studied (1999-2009) have also decreased from a previous study period (1983-1993). This is interesting as irrigation activities have intensified in the region, and may indicate more efficient management practices, in-stream biochemical processes leading to the decline, or different analytical techniques being used. River inorganic N and PO_4-P concentrations were also found to be generally low in the Komati-Lomati River and Pongola River catchments except for some seasons where PO_4-P concentrations were high enough to cause eutrophication (Van der Laan et al., 2012). The sources of P were not established as part of the study, however. For agriculture, pollution from fields to waterways is most commonly via surface runoff as soluble PO_4^{3-} or attached to sediment. In addition to soil slope and surface conditions, runoff losses are influenced by timing and method of application, form of fertiliser used and tillage practice.

2.2 Surface water N and P concentrations: Analysis of Department of Water and Sanitation water quality monitoring data

2.2.1 Identification of eutrophication 'hotspots' in irrigation regions

An eutrophication assessment website of the Department of Water and Sanitation was used to identify meso- and eutrophication water bodies in agricultural regions which could represent 'hotspots'. Long-term water quality monitoring data was obtained from: http://www.waterscience.co.za/waterchemistry/data.html. It was noted that the map produced by the Department of Water and Sanitation based on actual water quality monitoring closely matched the map produced by Matthews (2014) (Figure 5). The full list and status of points monitored is presented in the Appendix. Google Earth was then painstakingly used in conjunction with these data to identify eutrophic or mesotrophic water bodies located in close proximity to intensively irrigated regions. Due to the high population density in the Gauteng Province, many of these points were discarded as it was assumed that inadequately treated sludge and other point sources may contribute significantly to water nutrient loads.

Statistic	Unit	Current trophic status:			
Median annual chlorophyll a	µg ℓ^{-1}	0<x≤10	10<x≤20	20<x≤30	>30
		Oligotrophic (low)	Mesotrophic (moderate)	Eutrophic (significant)	**Hypertrophic (serious)**
		Potential for algal and plant productivity:			
Median annual total phosphorus	mg ℓ^{-1}	x≤0.015	0.015<x≤0.047	0.047<x≤0.130	>0.130
		negligible	moderate	significant	**serious**

Table 3: Simplified method for classifying trophic status classes used on www.dwaf.gov.za

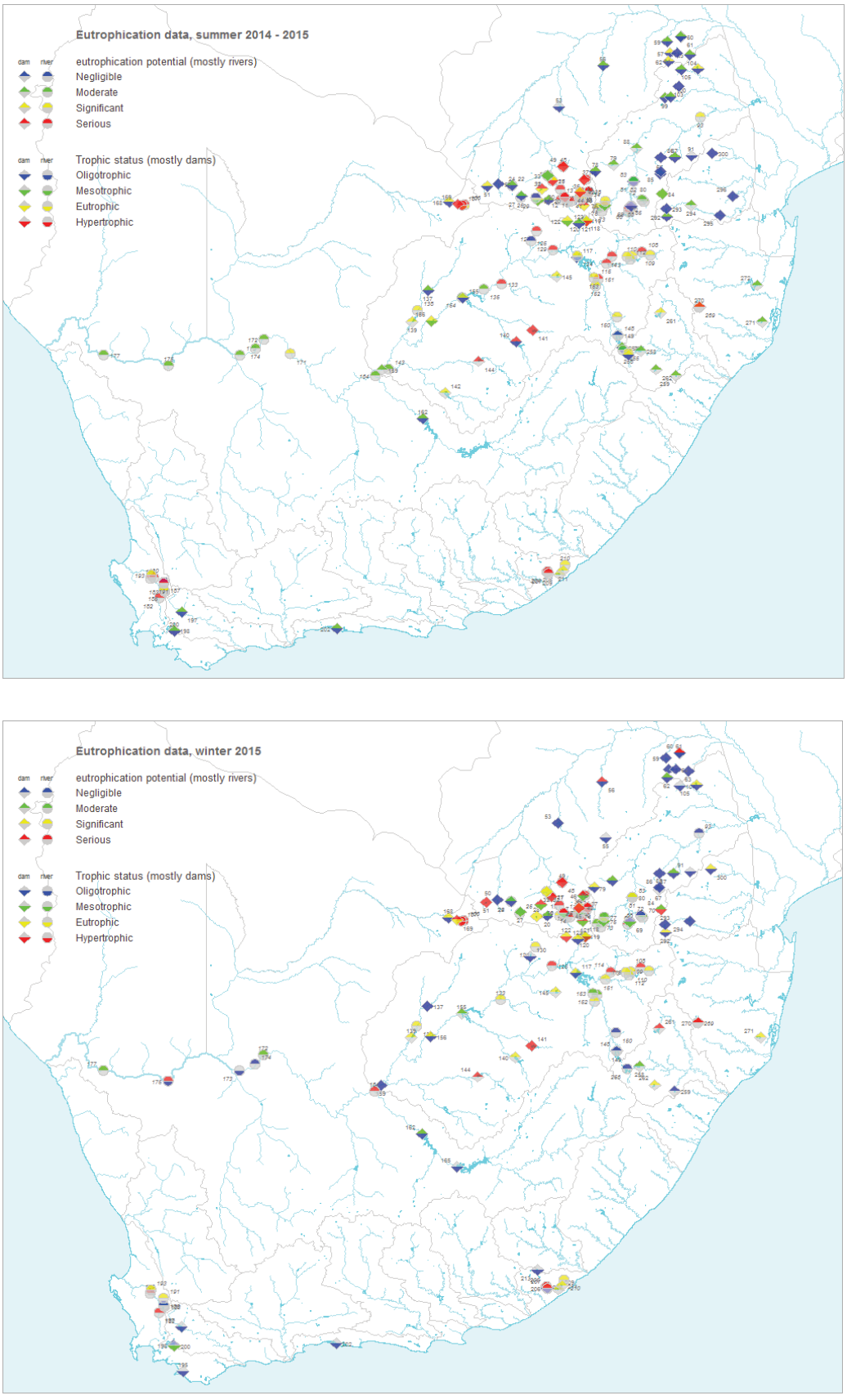

Figure 4: Department of Water and Sanitation eutrophication maps for summer (top) and winter (bottom) 2014/2015 (www.dwaf.gov.za)

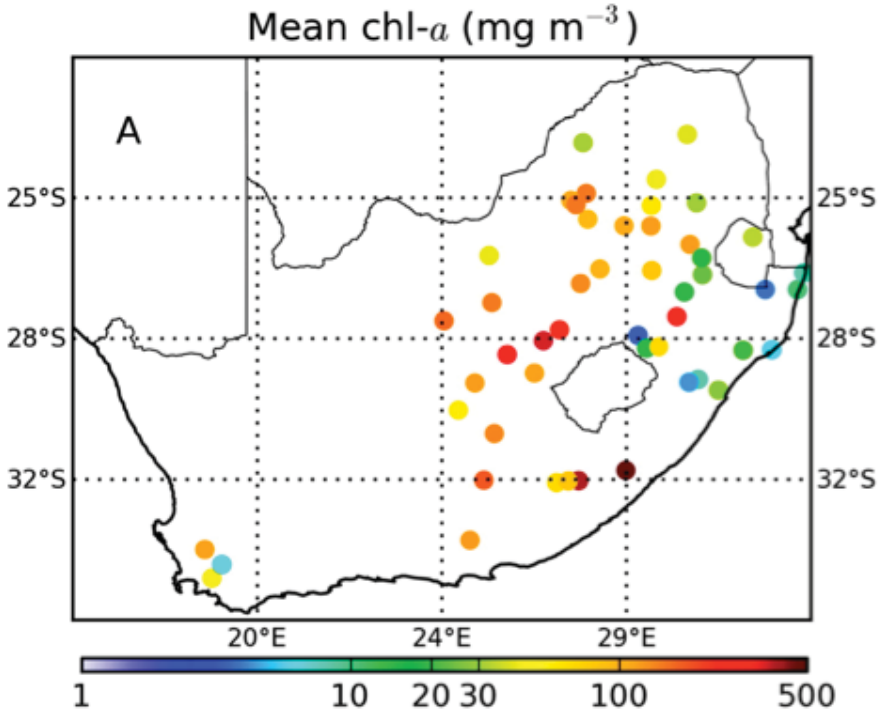

Figure 5: Status of eutrophication in 50 South African water bodies (expressed as mean chlorophyll-a) (Matthews, 2014)

The Google Earth map developed in the current study below highlights the eutrophic (green) or hypertrophic (red) points identified from www.dwaf.gov.za/iwqs/eutrophication/NEMP/ that fall in agricultural regions. A list of these potential 'hotspots' is provided in Table 4. The percentage of a pixel area equipped for irrigation for the year 2000 is also shown (http://www.fao.org/nr/water/aquastat/irrigationmap/zaf/index.stm). While this map as presented here is not very clear, its value lies in that it is an interactive map that can be viewed in Google Earth. Different layers can be switched off and on to improve clarity, and areas of interest can be zoomed in on to investigate specific regions more closely. A .kmz file containing all this information which can be opened in Google Earth can be found at: https://www.dropbox.com/s/u0zty3csx0ut1a7/NPS%20Hotspot%20exercise.kmz?dl=0.

Table 4: Potential agricultural eutrophication 'hotspots' for South Africa (green = eutrophic, red = hypertrophic)

№	Median Chl a µg/L	n	Median TP mg/L	n	Code/Name
1	60.4	12	0.115	11	A2R015Q01 Roodekopjes 203 JQ - Roodekopjes Dam on Krokodilrivier: near Dam Wall
2			0.056	13	A2H111Q01 Vaalkop Dam on Elands River: downstream Weir
3	7.2	4	0.071	8	A3R002 Klein-Maricopoort Dam at Kalkdam 241 JP near Dam Wall
4			0.060	4	B7H007Q01 at Oxford on Olifants River
5	5.0	8	0.082	4	B8R009 Nsami at Nsami Dam near Dam Wall
6					B8R005Q01 Tzaneen Dam on Groot Letaba: near dam wall
7			0.102	12	C1H005 Welbedacht 382 IS on Leeuspruit
8	6.6	12	0.078	14	C1R001Q01 Vaalbank 476 IR - Vaal Dam on Vaalrivier: near Dam Wall
9			0.108	12	C3R002Q01 Farm 92 - Spitskop Dam on Hartsrivier: near Dam Wall
10	0.3	2	0.174	3	C4R002Q01 Corannakraal 87 - Erfenis Dam on Vet River near Dam Wall
11	66.2	2	0.489	10	C4R001Q01 Willem Pretorius Wildtuin - Allemanskraaldam on Sandrivier: near Dam Wall
12			0.076	16	C5R002Q01 Kalkfontein Nature Reserve - Kalkfontein Dam on Rietrivier: near Dam Wall
13			0.147	11	C5R004Q01 Uitvlugt West 2810 - Krugersdrifdam on Modderrivier: near Dam Wall
14			0.097	6	C7R001Q01 Fischer 58 - Koppies Dam on Renosterrivier: near Dam Wall
15			0.109	7	C8H023Q01 at the Willows on Meul River
16	4.7	2	0.057	3	C9R002Q01 Bloemhofdam Nature Reserve - Bloemhofdam on Vaalrivier: near Dam Wall
17			0.083	1	Volgraafsig B See Hartswater Irrigation scheme
18			0.048	2	G1H066 Gouda Nieuwkloof - on Inlet Canal from Klein Berg River to Voelvlei Dam
19			0.136	6	G1H059Q01 Canal (Right) from Leeu River at de Hoek Estates
20			0.107	6	G1H031Q01 at Misverstand Die Brug on Berg River
21			0.094	5	R2R003Q01 Bridle Dam Nature Reserve - Bridle Drift Dam on Buffalo River: near Dam Wal
22	chem	-	0.069	3	R3H001Q01 Gqunube River at Outspan
23			0.083	3	R3R001Q01 Farm 305 - Nahoon Dam on Nahoon River: near Dam Wall
24			0.196	2	W2R001Q01 Klipfontein Dam on White Mfolozi River: near Dam

2.2.2 Consideration of long term river N and P concentrations for specific important irrigation regions in South Africa

As part of this scoping study, historical DWS data river N and P concentrations were plotted for specific important irrigation regions in South Africa, ideally at points upstream and downstream of major irrigation activities if available. This exercise was also used to determine whether any long-term trends could be observed.

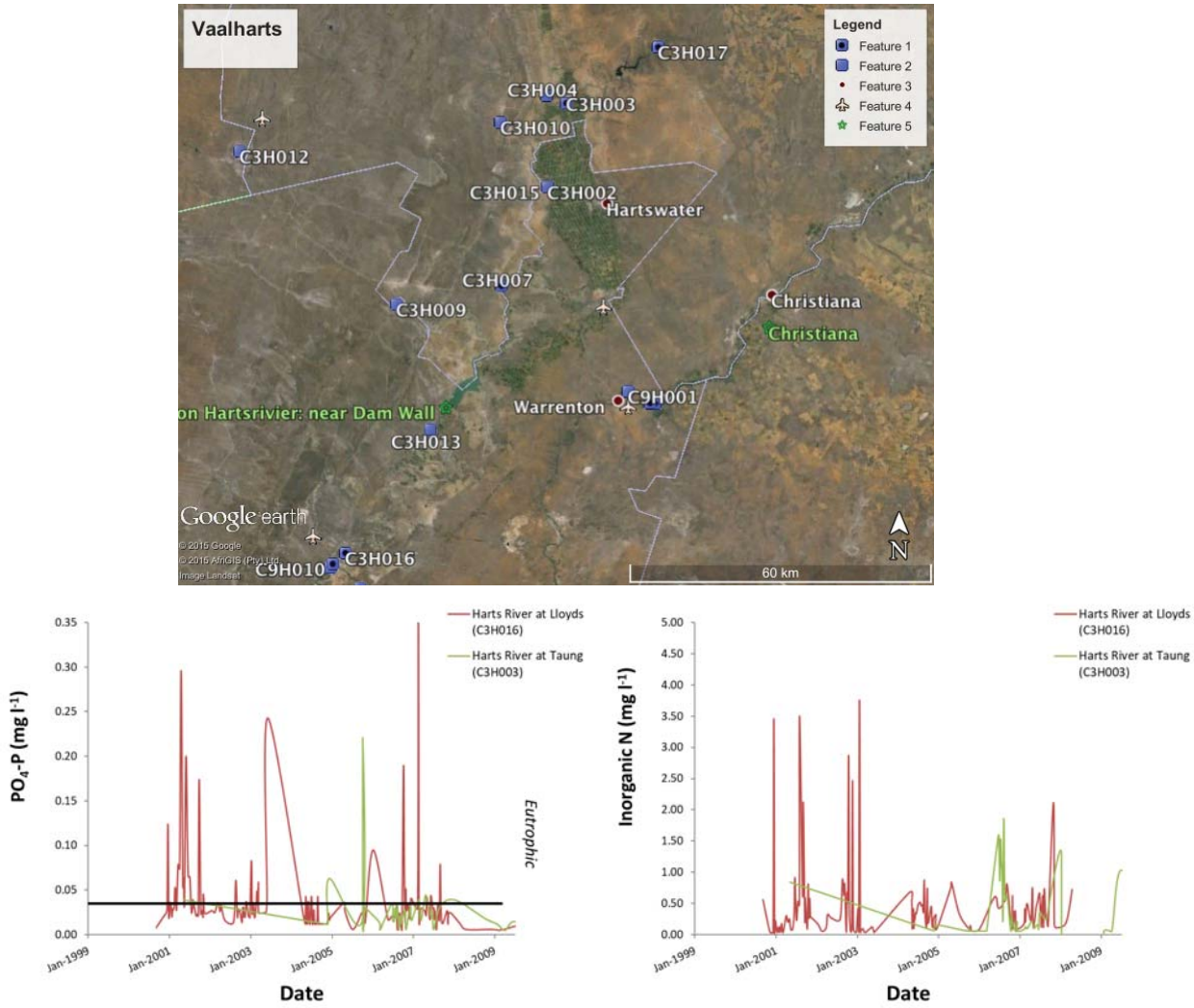

Figure 6: Google Earth image of the Vaalharts region and long-term phosphate-phosphorus (PO_4-P) and inorganic nitrogen (N)

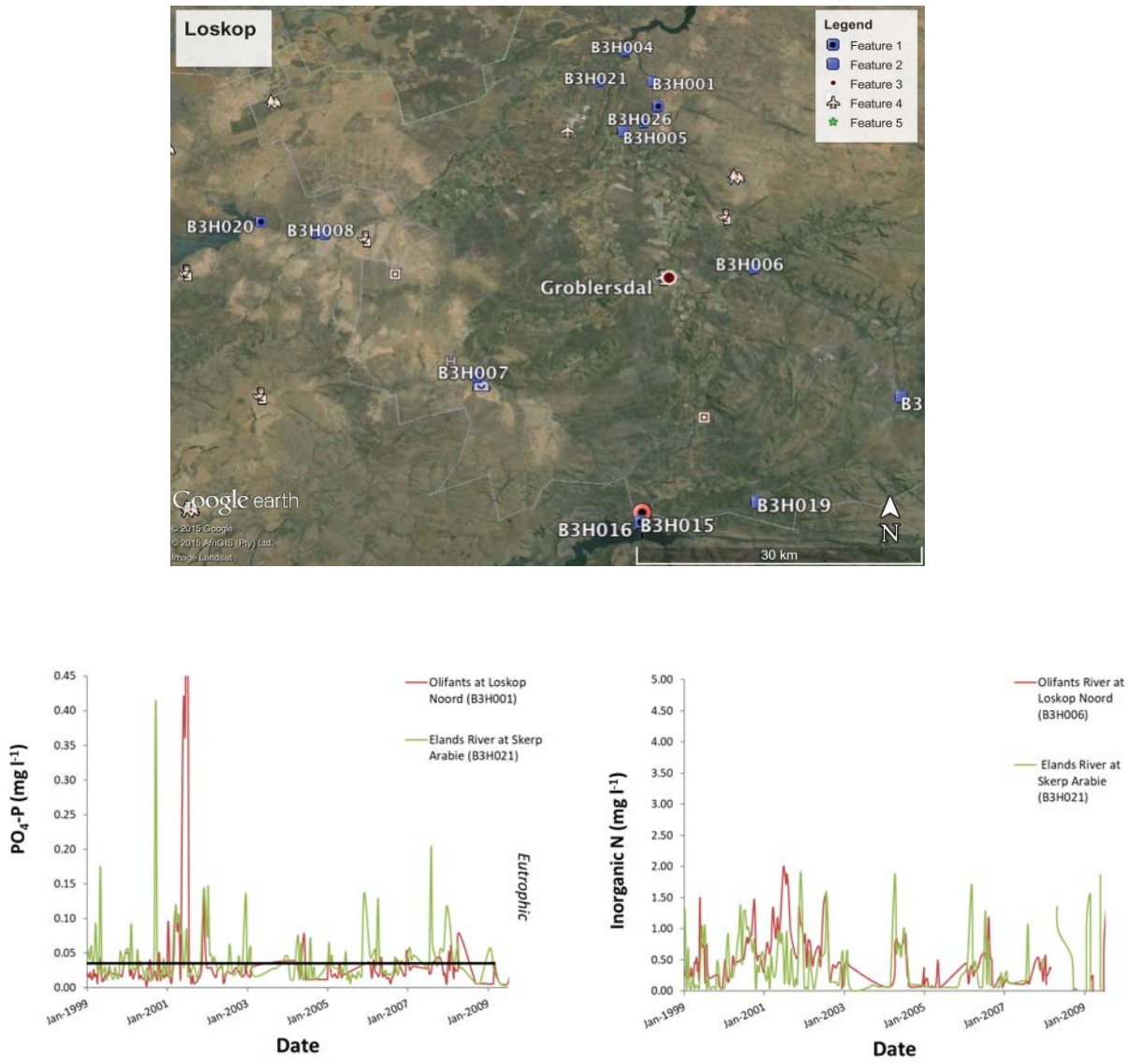

Figure 7: Google Earth image of the Loskop region and long-term phosphate-phosphorus (PO_4-P) and inorganic nitrogen (N)

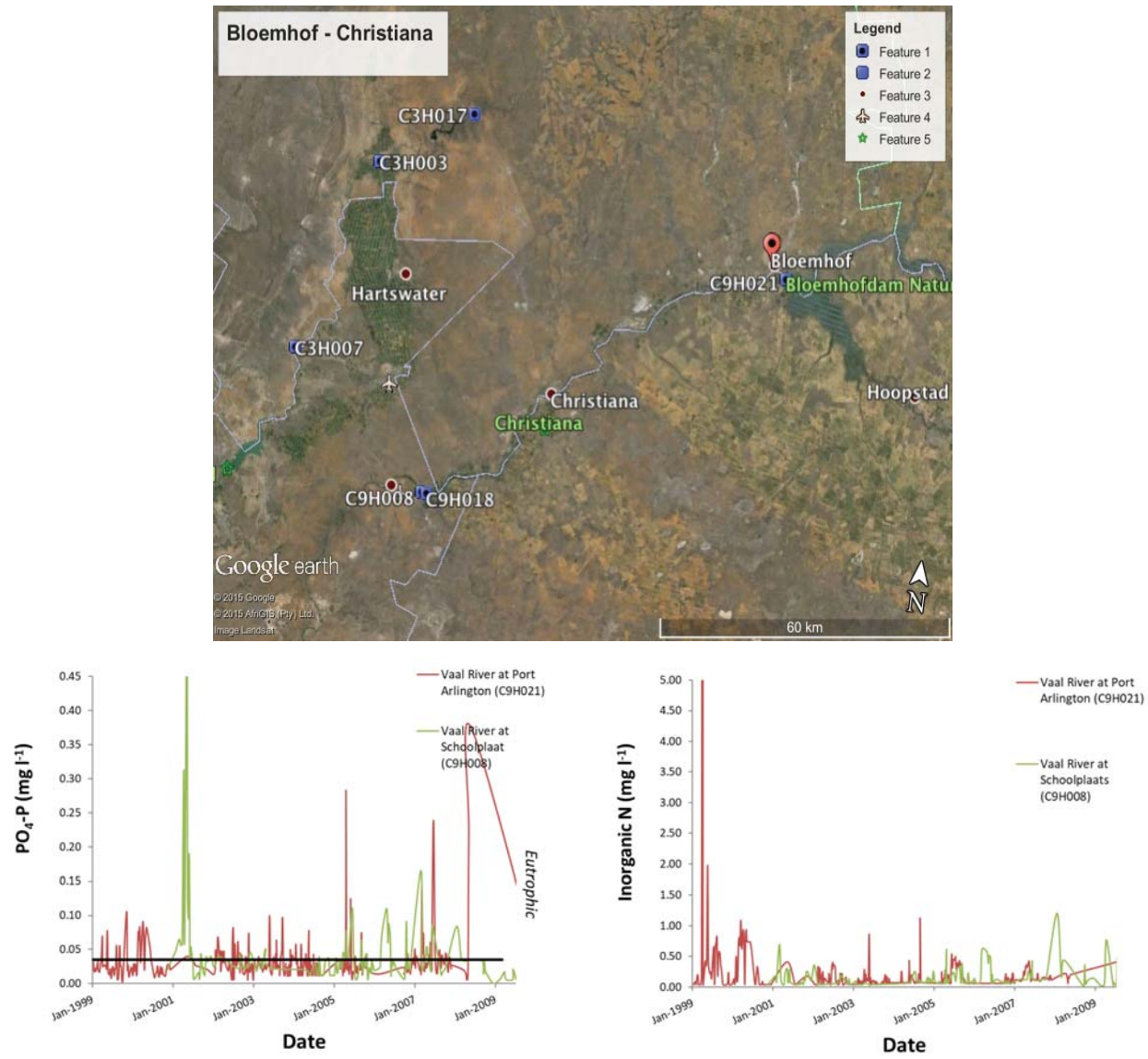

Figure 8: Google Earth image of the Bloemhof-Christiana region and long-term phosphate-phosphorus (PO_4-P) and inorganic nitrogen (N)

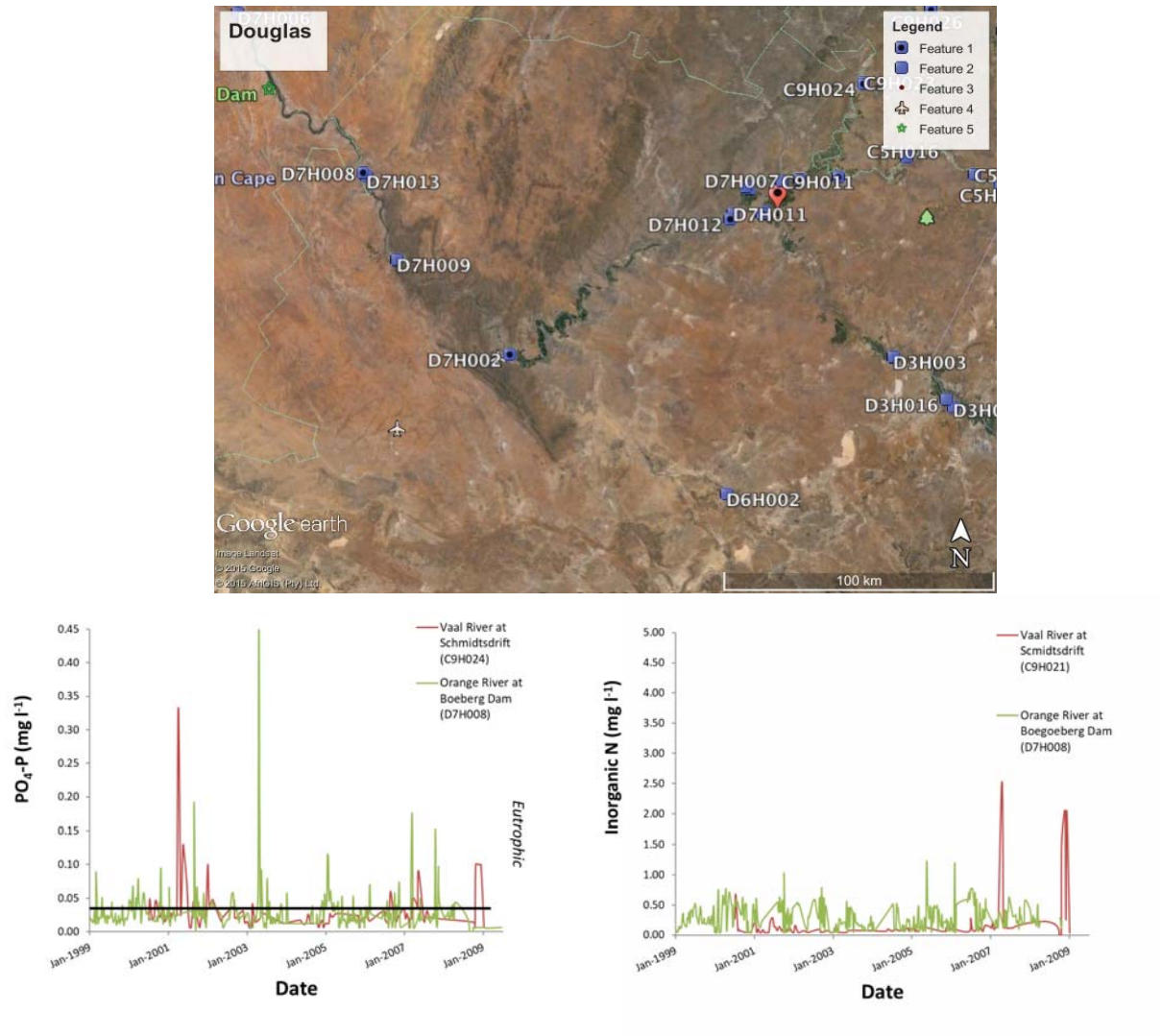

Figure 9: Google Earth image of the Douglas region and long-term phosphate-phosphorus (PO_4-P) and inorganic nitrogen (N)

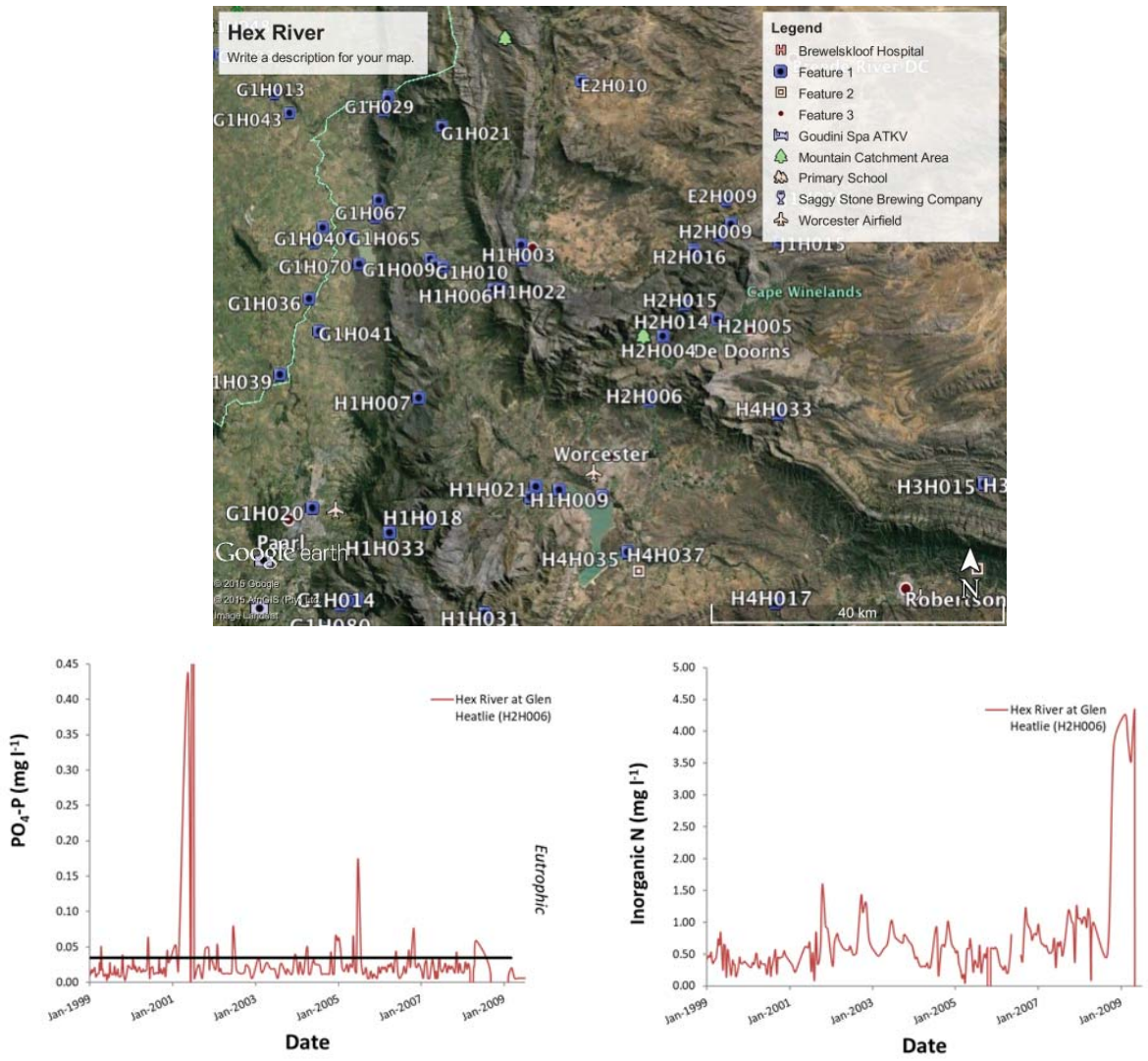

Figure 10: Google Earth image of the Hex River (Breede WMA) region and long-term phosphate-phosphorus (PO_4-P) and inorganic nitrogen (N)

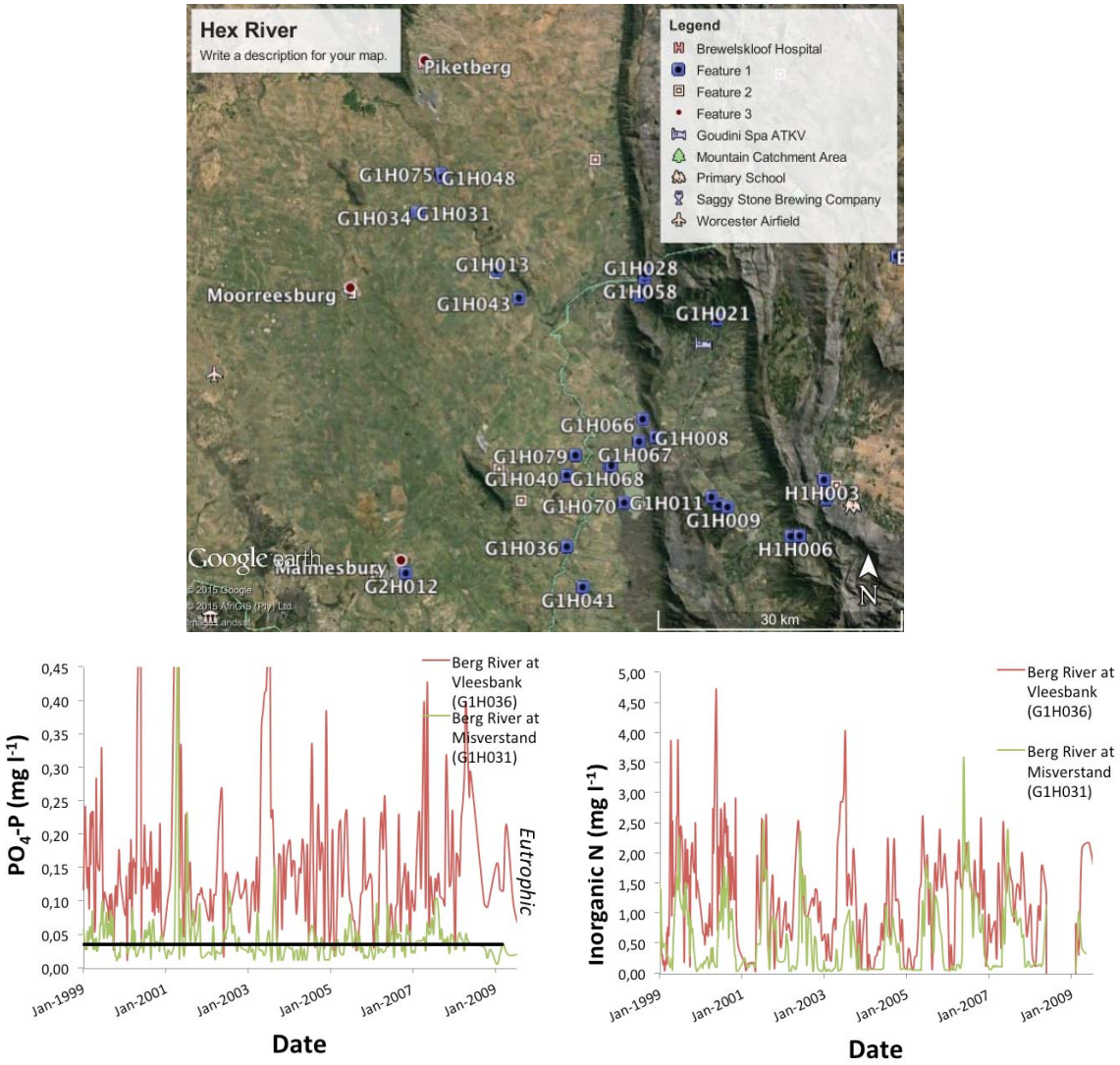

Figure 11: Google Earth image of the Berg River (Berg WMA) region and long-term phosphate-phosphorus (PO_4-P) and inorganic nitrogen (N)

2.2.3 Synthesis

Most of the monitoring points investigated have PO_4-P concentrations at levels which can cause eutrophication for at least part of the year. Elevated nutrient levels for Loskop and for the Bloemhof-Christian stretch of the Vaal River will be investigated more closely in this project to carefully quantify the contribution of irrigated agriculture, including through the use of the catchment scale model SWAT. Mitigation measures will also be investigated, and it is hoped that these will be relevant for a number of regions around South Africa.

Certainly, the most concerning monitoring point considered is for the Hex/Berg Rivers in the Berg WMA. This region has intensive horticultural production under irrigation which could be contributing significantly to elevated nutrient levels in the rivers. A number of groups are currently focussing on how to improve water quality in this region, but efforts may need to be intensified in the region.

2.3 Potential groundwater N and P pollution from agriculture

Musekiwa and Majola (2014) produced a groundwater vulnerability map for South Africa, based on the DRASTIC Specific Vulnerability Index (DSVI) using rated and weighted parameters that included: depth to groundwater (Figure 12), potential recharge rate, aquifer types, soil types, topography, vadose zone characteristics, hydraulic conductivity and land use. This vulnerability map (Figure 13) can be used to identify agricultural regions that are especially susceptible to NO_3^- leaching through the soil profile. Ultimately, however, NO_3^- leaching will be most closely related to whether N fertiliser is applied in excess of crop demand, and farmers need to be made clearly aware of this issue.

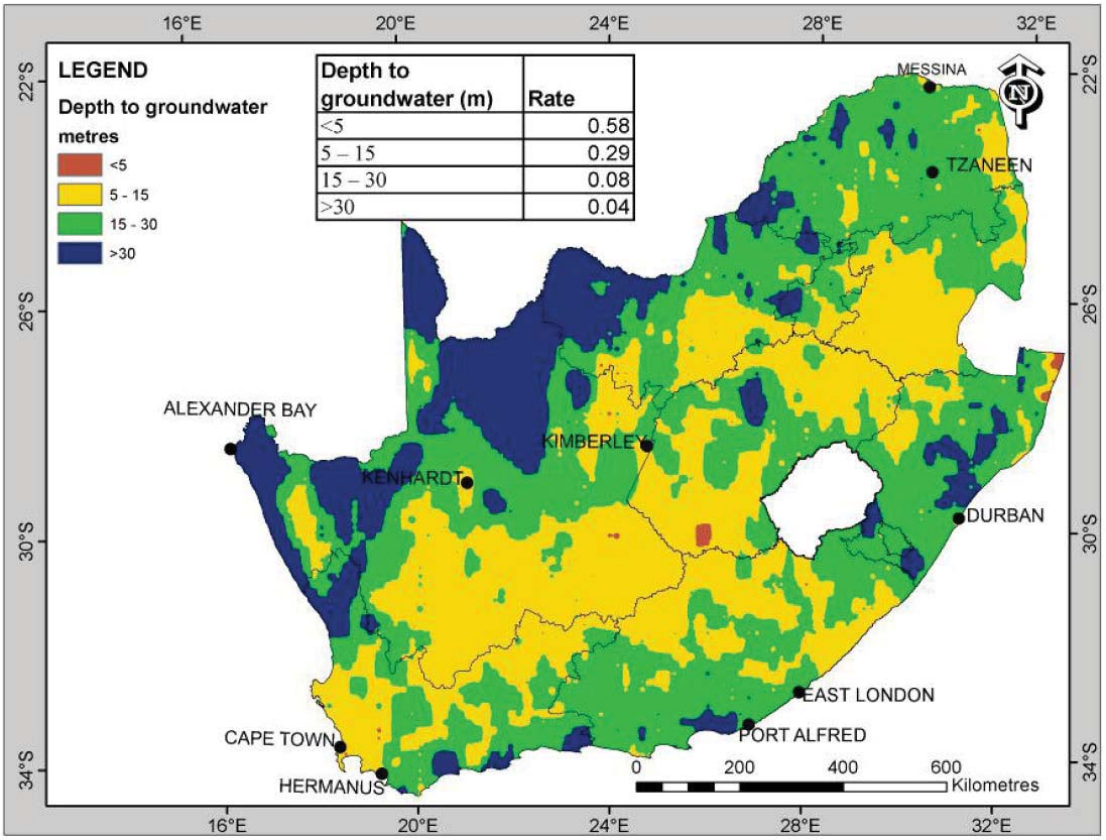

Figure 12: Depth to groundwater map (Musekiwa and Majola, 2013)

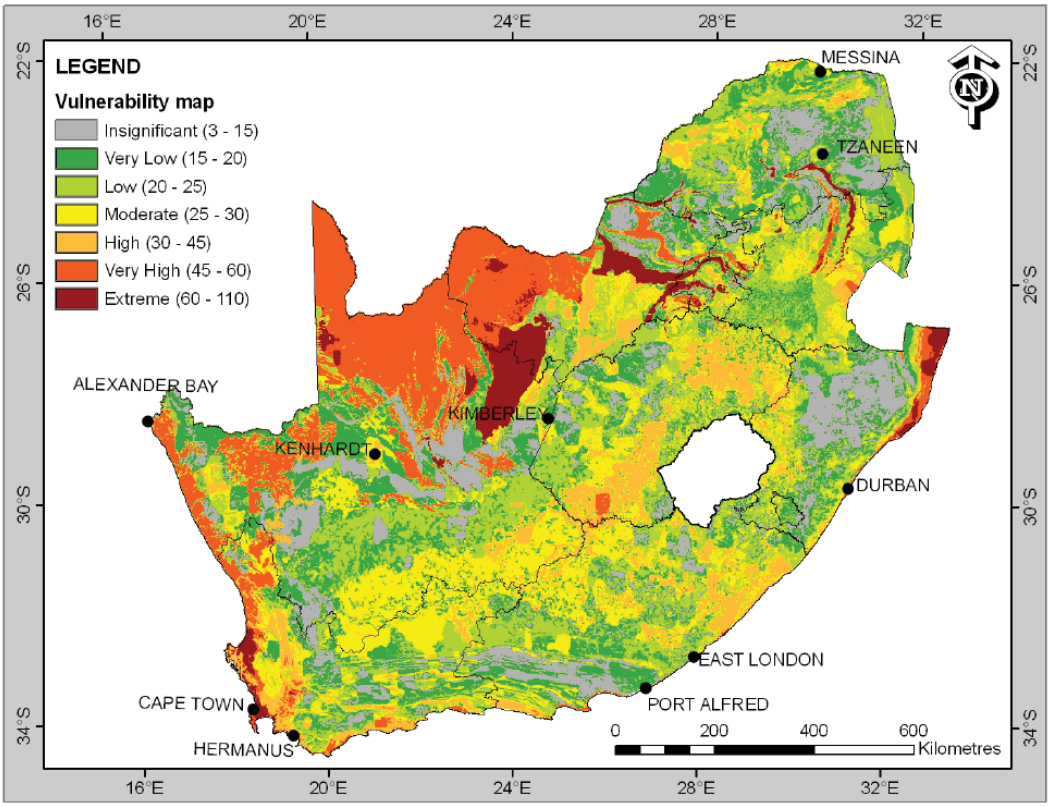

Figure 13: Groundwater vulnerability map of South Africa (Musekiwa and Majola, 2013)

The Norwegian Agency for Development Cooperation (NORAD)-Assisted Programme for the 'Sustainable Development of Groundwater Sources' under the 'Community Water and Sanitation Programme' in South Africa was managed by the Department of Water Affairs and Forestry (DWAF) between 2000 and 2004, and produced the groundwater NO_3^- map in Figure 14 (Musekiwa and Majola, 2014). Many of the zones indicated to have high groundwater NO_3^- concentrations are located in very dry regions, for example, the arid north western and northern parts of the country where limited agriculture is practiced. One region of definite concern, however, is the Overberg Region east of Hermanus which reportedly has very high groundwater NO_3^- concentrations and is under intensive agriculture (Figure 15). The role of irrigated agriculture north of Kimberley, and extensive agriculture north east of Kimberley should also be more closely investigated due to the elevated groundwater NO_3^- concentrations in these areas.

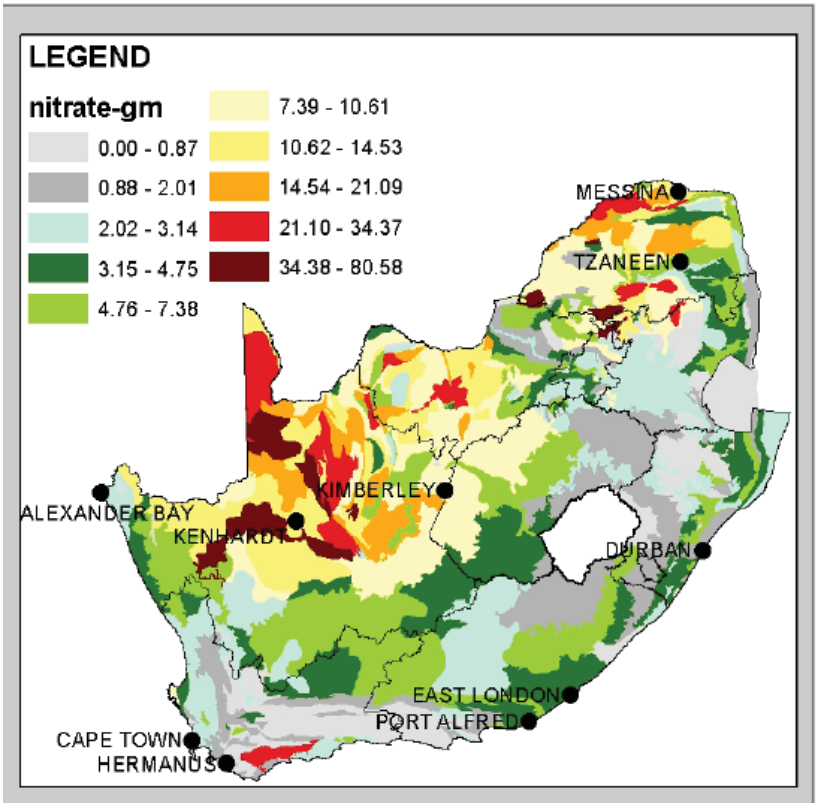

Figure 14: Groundwater nitrate map produced by Norad (Musekiwa and Majola, 2013)

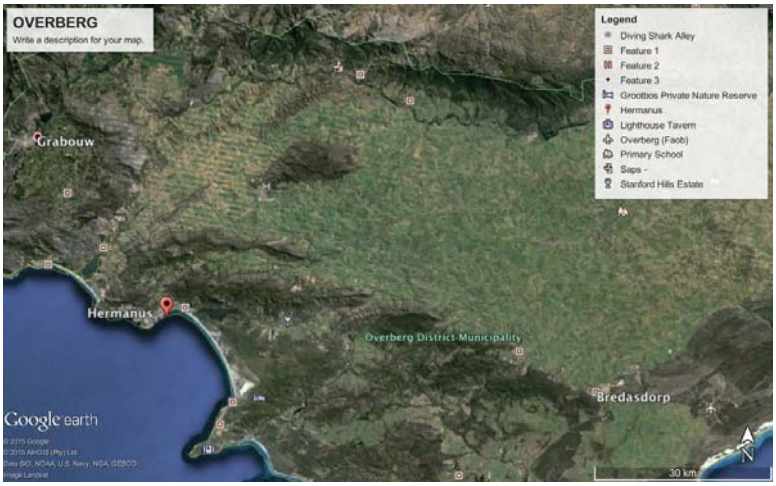

Figure 15: Google Earth image of Overberg Region with very high groundwater nitrate concentrations

2.4 Conclusions

Following this scoping study, a number of potential 'hotspots' where irrigated agriculture could be playing an important role in N and/or P pollution have been identified. A Google Earth .kmz file has been produced with shape data, including P-enriched surface water hotspots falling in agricultural regions and irrigated areas that can be used to investigate these sites in more detail. Deeper investigations will involve fertiliser mass balances for the specific region, and more mechanistic, catchment-scale modelling, for example, with the SWAT model.

The following steps are recommended to more accurately identify these hotspots and quantify agriculture's contribution:

- Spatially map irrigated regions as determined by a newly completed WRC project (Van Niekerk et al., 2018), together with river, reservoir and groundwater N and P concentrations monitored by DWS for each WMA. Quantify the area of land under cultivation upstream and correlate to downstream N and P concentrations.
- Distribute questionnaires to WMA officials and wastewater treatment works managers to quantify the N and P loads from these plants, especially dysfunctional ones. Amount of discharge (m^3) and N and P concentrations can be used to calculate pollution loads. Use mass balance and other approaches to determine the relative contribution of agriculture.
- Set-up catchment scale models for the most important 'hotspots' to investigate mitigation measures, such as land use changes, inclusion of buffer zones and better agronomic management practices.
- Make farmers fully aware of the problems associated with N and P pollution and provide information on best management practices to reduce this type of pollution. This can be done at farmer's days, local conferences and through the popular media, including social media.

This exercise has shown that acquiring data on water quality and water flow can be cumbersome, despite the owners of these data being willing to share it in most cases. More effort should go into making data, including both standard monitoring datasets that have been processed as well as published research and data more easily available to other users via the internet. This will ensure that maximum benefit is obtained from these data. Who will host these data needs to be carefully thought through, but should probably be the Department of Water and Sanitation.

While hotspots or points of interest have now been identified, it should be noted that this is a work in progress. As more data becomes available, and through capacity building in GIS, further refinements to identify key 'hotspots' in South African and potential mitigation measures can be achieved.

2.5 References

ANZECC (1992) *Australian and New Zealand Guidelines for Fresh and Marine Water Quality.* Australian and New Zealand Environment and Conservation Council, Australia and New Zealand.

ANNANDALE, J. & DU PREEZ, C. (2005) Nutrients – Agricultural Contribution Management and Modelling, Water Research Commission, Pretoria, South Africa.

MACKAY, H., ROUX, D., ASHTON, P., VAN VLIET, H. & JOOSTE, S. (1995) The development of South African water quality guidelines for the natural aquatic environment. Water Science and Technology 32(5), 293-299.

MATTHEWS, M.W. (2014) Eutrophication and cyanobacterial blooms in South African inland waters: 10years of MERIS observations. Remote Sensing of Environment 155, 161-177.

MUSEKIWA, C. & MAJOLA, K. (2014) Groundwater vulnerability map for South Africa. South African Journal of Geomatics 2(2), 152-162.

VAN DER LAAN, M., VAN ANTWERPEN, R. & BRISTOW, K.L. (2012) River water quality in the northern sugarcane-producing regions of South Africa and implications for irrigation: A scoping study. Water SA 38(1), 87-96.

VAN NIEKERK, A., JARMAIN, C., GOUDRIAAN, G., MULLER, S., FERREIRA, F., MÜNCH, Z., PAUW, T., STEPHENSON, G. & GIBSON, L. (2018) An earth observation approach towards mapping irrigated area and quantifying water use by irrigated crops in South Africa.

WALMSLEY, R. (2000) Perspectives on Eutrophication of Surface Waters: Policy/research Needs in South Africa: a Review and Discussion Document, Water Research Commission.

3 MODELLING RUNOFF AT THE PLOT SCALE USING THE AGRICULTURAL PRODUCTION SYSTEMS SIMULATOR (APSIM) CROP MODEL

L. Mudaly and M. van der Laan
Department of Plant and Soil Sciences, University of Pretoria, Pretoria 0002, South Africa

3.1 Introduction

Agricultural activities are important non-point sources of water contamination with phosphorous being one of the nutrients most commonly associated with the poor water quality resulting from such contamination (Ng Kee Kwong et al., 2002). Erosion and surface runoff are the main processes by which P is exported from agricultural lands in Mauritius (Mardamootoo, 2015). A study evaluated the extent of phosphorous losses that occurred from erosion and surface runoff from sugarcane fields in Mauritius when subjected to simulated rainfall events (Mardamootoo et al., 2015). The study was conducted on different soil groups and various slope categories. Runoff was collected and different P fractions were determined. Total P, total dissolved P and orthophosphate P were determined in the samples.

The data from the study was provided by the student conducting the research. The APSIM (Agricultural Production Systems Simulator) model was used to determine how closely the model predicted values correspond to the actual measured values from the study. This was carried out in order to provide insight into how useful the model can be in predicting P in runoff from agricultural fields. Agricultural systems models are important tools to help understand complex system interactions and provide useful information to achieve environmental goals (Archontoulis, 2014).

3.1.1 APSIM (Agricultural Production Systems Simulator)

The Agricultural Production Systems Simulator (APSIM) was developed by the Agricultural Productions Systems Research Unit (APSRU), which is a collaborative group from CSIRO and Queensland State Government agencies (Keating et al., 2003). The modelling framework was designed to combine accurate yield estimation in response to management while predicting the long-term impact of agricultural practices (Keating et al., 2003) by simulating the response of a crop or cropping system in response to climate and soil conditions (Wang et al., 2002). It allows the prediction of crop production in relation to climate, genotype, soil, and management factors while also looking at long-term resource management problems in farming systems (Keating et al., 2003) thereby improving risk management in agricultural production (Wang et al., 2002). The APSIM model also has the capability to simulate soil water, carbon (C), nitrogen (N) and phosphorous (P) dynamics, as well as their interaction within the management systems, driven by daily climate data (Gaydon, 2014). The use of APSIM allows the evaluation of management intervention through tillage, irrigation, or fertilization as well as the choice, timing and sequencing of crops (Wang et al., 2002). The APSIM model is widely used in Australia as well as many African countries, such as Kenya, Malawi and Zimbabwe in addition to South Africa (Gaydon, 2014).

Agricultural Production Systems Simulator is a daily time-step model that simulates cropping systems by combining biophysical and management modules in a central engine (Gaydon, 2014). The APSIM modelling framework is made up of the following (Keating et al., 2003):

i. A set of biophysical modules that simulate biological and physical processes in farming systems.
ii. A set of management modules for the user to specify intended management rules and characterize the scenario being simulated.
iii. Modules that facilitate data input and output from the simulation.
iv. A simulation engine that drives simulation processes and controls messages between independent modules.

3.1.2 Runoff and runoff curve numbers:

In APSIM runoff is calculated using a modified USDA curve number approach, which includes the effects of soil water content, crop cover (from crop and crop residue) and the effects of roughness produced by tillage (Keating et al., 2003). Runoff from rainfall is calculated using the curve number technique, which was developed by the USDA – Soil Conservation Service (SCS) (APSIM documentation, SoilWat). SCS curve numbers are used to estimate the amount of rainfall that becomes runoff and the amount that infiltrates the soil. If the moisture of layer 2 is below 60% of field capacity, the equation to calculate curve number (CN) is (USDA/SCS curve number method for estimating daily runoff, 2004):

CN = 0.39*CN*EXP(0.009*CN)
If the moisture level of layer 2 is above 60% then the equation becomes:
CN = 1.95*CN*EXP(-0.00663*CN)

The equation to calculate runoff is:

Runoff = (Precipitation – 0.2S)^2 / (Precipitation + 0.8S)
Where S = (1000/CN) – 10

If (Precipitation – 0.2S) is negative, then runoff = 0 (USDA/SCS curve number method for estimating daily runoff, 2004). The procedure estimates runoff using rainfall from an event(s) during a day. Rainfall intensity is not taken into account (APSIM documentation, SoilWat). Runoff curve number can be estimated from the hydrologic soil group (HSG) to which the soil belongs (USDA/SCS curve number method for estimating daily runoff, 2004).

Soils are classified into HSG's to indicate the minimum rate of infiltration obtained for bare soil after a long period of wetting. The four groups (A, B, C and D) are used to determine runoff curve numbers. The soil texture of the groups are as follows (USDA, 1986):

Group A: Sand, loamy sand or sandy loam
Group B: Silt loam or loam

Group C: Sandy clay loam
Group D: Clay loam, silty clay loam, sandy clay, silty clay, clay

Group A soils have a low runoff potential and high infiltration rates. They are generally deep, well-drained gravels. Group B soils have moderate infiltration rates. They are generally deep, well-drained fine to moderately coarse textured soils. Group C soils have low infiltration rates. They may have a layer that impedes downward water movement. The soil texture is fine to moderately fine. Group D soils have a high runoff potential and low infiltration rates. These soils include clay soils with a high swelling capacity, soils with a permanent high water table, soils with a clay layer close to the surface and shallow soils (USDA, 1986).

In the SoilWater module in APSIM, runoff response curves (which represents runoff as a function of total daily runoff) are specified by numbers 0 to 100. A value of 0 indicates no runoff and 100 indicates all runoff. A curve number (CN2Bare) is supplied as input for average antecedent rainfall conditions. From this value, two extremes are calculated. These are the wet (high runoff potential) response curve and the dry (low runoff potential) response curve. The SoilWater module then uses a family of curves between these two extremes to calculate runoff depending on the daily moisture of the soil.

3.1.3 SoilWat Source Code

The following source code provides an understanding into how the family of curve numbers and runoff is calculated in APSIM.

3.1.3.1 Curve numbers

cn2_bare = curve number input used to calculate daily runoff
cn2_new = cn2_bare (cn_red * cover_fract)
cn1 = divide (cn2_new, (2.334 – 0.01334 * cn2_new), 0.01)
cn3 = divide (cn2_new, (0.4036 + 0.005964 * cn2_new), 0.0)
cnpd = cnpd + divide (sw_dep(layer) – ll15_dep(layer), dul_dep(layer) – ll15_dep(layer), 0.0) * runoff_wf(layer)
cn = cn1 + (cn3 – cn1) * cnpd

cn_bare: curve number input used to calculate
cn_red: maximum reduction in cn2_bare due to cover
cover_fract: proportion of maximum cover effect on runoff
cnpd: fraction of available soil water weighted over the hydraulic effective depth
sw_dep: soil water content of layer
ll15_dep: 15 bar lower limit of extractable soil water for each soil layer
dul_dep: drained upper limit soil water content for each soil layer
runoff_wf: weighting factor for depth for each layer (runoff depth factor).

Runoff:

S = 254.0 * (divide (100.0, cn, 1000000) – 1.0)

xpb = (rain + runon – interception) – 0.2 * s

xpb = 1_bound(xpb, 0.0)

runoff = divide (xpb * xpb, (rain + runon – interception + 0.8 * s), 0.0)

3.2 Method

A study evaluated the extent of phosphorous losses that occurred from erosion and surface runoff from sugarcane fields in Mauritius when subjected to simulated rainfall events (Mardamootoo et al., 2015). The study was carried out just after planting since this is the time of the sugarcane crop cycle of 7-8 years when plant cover is absent and soil movement as a result of intense rainfall is most probable. The study was conducted on different soil groups and at three different slope categories. Slope class I represented a slope of 0-8%, slope class II represented a slope of 8-13% and slope class III represented a slope of 13-20%. The soils were subjected to a 30 minute simulated rainfall event at three different intensities. The rainfall intensities simulated were 50 $mm.hr^{-1}$, 100 $mm.hr^{-1}$ and 150 $mm.hr^{-1}$. The first two rainfall intensities (50 and 100 $mm.hr^{-1}$) are representative of what is typically experienced on the island while 150 $mm.hr^{-1}$ is occurs periodically during cyclones. Runoff was then collected from the runoff plots (2.1 x 0.7 m) and different P fractions were determined. The fractions analysed were total P, total dissolved P and orthophosphate P (Mardamootoo, 2015).

The data from the results of the study was provided by the student conducting the research. The APSIM model was used to determine how closely the model predicted values corresponded to the actual measured values from the study. Certain values that were required as inputs were not provided from the study and therefore the SPAW (Soil-Plant-Air-Water) computer model was used to obtain necessary values. This model simulates daily hydrologic water budgets (Saxton et al., 2006) The required values that were generated by this model included wilting point, field capacity, saturation, saturated hydraulic conductivity and bulk density.

Climate data for the sites in Mauritius could not be obtained therefore, data was obtained from CLIMWAT. This is a climatic database with agroclimatic data for over 5000 weather stations worldwide. It is generally used in conjunction with CROPWAT, which is a decision support tool for the calculation of the correct amount of water needed for the irrigation of crop fields.

3.3 Results and Discussion

The soils used for the simulation in APSIM were selected according to a full set of data that had measured values for runoff and analysed phosphorous at all rainfall intensities. The first simulation was done using a slope class of II as there was little to no runoff at slope class I. The soils selected along with their properties (as determined by the PhD student) are shown in Table 5.

Table 5: Selected soils with their accompanying chemical and physical characteristics

Soil	Soil Type (WRB Classification)	Depth	pH	OM	Clay	Silt	Sand	Ca	Mg	K	Na	CEC
		cm		%				$cmol^+ kg^{-1}$ soil				
Valetta	Humic Ferruginous Latosol	0-15	6.6	4.8	33.9	34.1	32	13.21	1.34	0.56	0.32	15.4
		15-30	6.6	4.4	33.7	35.1	31.3	11.82	1.28	0.52	0.28	13.9
Highlands	Low Humic Latosol	0-15	5.3	4.2	24.3	26.2	8.1	3.4	0.73	0.68	0.31	5.1
		15-30	5	3.8	49.8	24	26.2	2.75	0.71	0.46	0.24	4.2
Pierre Fonds (site 1)	Latosolic Reddish Prairie	0-15	6.7	4.8	44.2	19	36.8	10.14	4.48	1.11	0.78	16.5
		15-30	6.7	4.5	46.9	20.5	32.7	10.49	4.34	1.18	0.77	16.8
La Mecque	Low Humic Latosol	0-15	7	3.4	53.5	23.6	22.9	14.84	5.84	7.48	0.61	28.8
		15-30	7	3	56.1	23.3	20.6	14.24	6.15	5.12	0.55	26.1
Etoile	Humic Latosol	0-15	5.5	4.3	33.9	32.4	33.7	3.51	0.77	0.57	0.27	4.8
		15-30	5.5	4	51.5	23.6	24.9	2.29	0.74	0.16	0.2	3.4
Henrietta	Low Humic Latosol	0-15	6.9	4.3	34.2	32.2	33.6	11.06	1.09	0.58	0.23	13
		15-30	6.6	3.9	39.6	27.8	32.6	7.96	0.65	0.66	0.26	9.5
St Pierre	Humic Latosol	0-15	6	4.6	34.4	31	34.6	6.29	0.92	0.31	0.3	7.8
		15-30	5.8	4.2	32.4	34.5	33.1	5.95	0.89	0.38	0.21	7.4
Riche en Eau (site 1)	Humic Ferruginous Latosol	0-15	5.8	4.8	31.5	36.4	32.1	3.24	0.71	0.38	0.27	4.6
		15-30	5.3	3.9	25.5	33.9	40.6	1	0.39	0.06	0.13	1.6

Selected soil properties that were provided in table 1 were used as input into the SPAW model. The values generated in SPAW that were used as input for APSIM are seen in Table 6. The parameters that APSIM required that were provided from using SPAW were wilting point (representing lower limit below 15 bar), field capacity (representing drained upper limit), saturation, saturated hydraulic conductivity and bulk density.

Table 6: SPAW generated values to be used as input in APSIM

Soil	Depth (cm)	Texture	Wilting point ($m^3 m^{-3}$)	Field capacity ($m^3 m^{-3}$)	Saturation (%)	Saturated hydraulic conductivity ($mm\ day^{-1}$)	Bulk density ($g\ cm^{-3}$)
Valetta	0-15	Clay loam	0.221	0.364	0.513	195	1.29
	15-30	Clay loam	0.219	0.363	0.508	183	1.30
Highlands	0-15	Clay	0.295	0.415	0.505	42.7	1.31
	15-30	Clay	0.299	0.418	0.502	36.6	1.32

Soil	Depth (cm)	Texture	Wilting point ($m^3 m^{-3}$)	Field capacity ($m^3 m^{-3}$)	Saturation (%)	Saturated hydraulic conductivity (mm day^{-1})	Bulk density (g cm^{-3})
Pierre Fonds (site 1)	0-15	Clay	0.274	0.395	0.487	42.7	1.36
	15-30	Clay	0.287	0.407	0.491	36.6	1.35
La Mecque	0-15	Clay	0.314	0.429	0.508	30.5	1.30
	15-30	Clay	0.329	0.441	0.514	24.4	1.29
Etoile	0-15	Clay loam	0.220	0.361	0.502	171	1.32
	15-30	Clay	0.304	0.421	0.505	36.6	1.31
Henrietta	0-15	Clay loam	0.220	0.359	0.50	165	1.32
	15-30	Clay	0.249	0.381	0.494	85.3	1.34
St Pierre	0-15	Clay loam	0.221	0.360	0.503	177	1.32
	15-30	Clay loam	0.209	0.353	0.503	201	1.32
Riche en Eau (site 1)	0-15	Clay loam	0.211	0.358	0.516	238	1.28
	15-30	Loam	0.172	0.313	0.489	335	1.35

3.3.1 Runoff results at a rainfall intensity of 50m m

Slope class II was used because it is representative of sloping and runoff is expected. Slope class I is relatively flat and therefore not much runoff was expected. Slope class II has a slope range of 8-13%. An average value of 11% was therefore used as input for APSIM. At first, a curve number of 94 was used as this is the runoff curve number for Group D (clay) fallow bare soils according to the USDS HSG classification. All of the predicted values were much higher than the actual values when this curve number was used. It was then decided to calibrate the model with the values from the 50 mm rainfall event by calculating the curve number and using this value in the model. The idea was to then use the calibrated curve number to validate the model for the 100 mm and 150 mm rainfall events.

The curve number was derived from the runoff equation and resulted in the following equation:

$CN = 1000/[5 (sqrt (5PQ + 4Q^2) + P + 2Q)] + 10$

The results, however, yielded very low curve numbers (below 5) and therefore the values obtained for runoff were much lower than the measured values.

The model is therefore sensitive to curve number and this was one of the parameters that was adjusted when simulating runoff. The slope was also adjusted in order to determine if APSIM was sensitive to this parameter as well as curve number. Several extremes were used and this made no difference to

the predicted runoff values simulated by the model. It was therefore determined that APSIM is not sensitive to slope in predicting runoff.

Before the study, from which the results were obtained, was conducted, the soils were watered to field capacity. The antecedent water content of the soils was not measured, however since field capacity was obtained, it was assumed that the initial water of the soil was 100% and this was therefore used as input into the model. Again, the values obtained were inconsistent with the measured values for runoff. It was now determined that not only was the model sensitive to curve number, but to initial water as well. This parameter was therefore also adjusted during the runoff simulations.

The 50 mm rainfall event was then simulated in order to obtain predicted runoff values in APSIM. The curve numbers and initial water values were adjusted to determine what best fit the model to get the predicted values closest to the measured values. The results obtained suggested that the different soils needed different curve numbers and initial water values in order to get the predicted runoff close to the actual measured values. There was therefore no consistent curve number and initial water values that could be used. The results for the closest predicted values obtained are in Table 7.

Table 7: Results for runoff from APSIM using the 50 mm rainfall event

Soil	Actual value (mm)	Predicted Value (mm)
Valetta	6.31	6.68
Highlands	0	0
La Mecque	1.36	4.9
Etoile	26.3	24.3
Henrietta	5.75	6.67
St Pierre	1.49	2.43
Riche en Eau	7.65	6.68
Pierre Fonds	19.2	24.3

An interesting observation that was made during the simulation was that the use of the same curve number and initial water value yielded the same predicted value for several soils. For example, when a curve number of 60 and initial water of 100 was used, all the soils, apart from La Mecque and Etoile, had a predicted runoff value of 6.68 mm. Table 7, which indicates the best results, shows that Valetta, Henrietta and Riche en Eau all have the same predicted value, while Etoile and Pierre Fonds also share the same predicted value. The model therefore could not be used for the 50 mm rainfall event to accurately predict runoff.

3.3.2 Runoff results at a rainfall intensity of 100 mm

The best results when simulating runoff for the 100 mm rainfall event can be seen in Table 8. Similar to the 50 mm rainfall event, no consistent curve number and initial water value could be used to get the predicted values close to the measured values for runoff. An observation that was made for the 100 mm rainfall that did not occur for the 50 mm rainfall event was that for certain soils, changing the curve number did not influence the predicted runoff value. The soils that demonstrated this phenomenon were Highlands, La Mecque, Etoile and Pierre Fonds. It was thought that soil type influenced this. Highlands, La Mecque and Etoile are humic soils and therefore it is possible that humic soils are difficult to simulate due to their high organic carbon content. According to the WRB (World Reference Base for Soil Resources) definition, humic soils have an organic carbon percentage of 5% or more in the first 50 cm of the soil surface (Food and Agriculture Organization, 2015). Similar to the 50 mm runoff results, the model was not sensitive to slope in simulating runoff. It was determined that at the 100 mm rainfall event, runoff could not be successfully simulated because no consistent curve number and initial water could be found.

Table 8: Results for runoff from APSIM using the 100 mm rainfall event

Soil	Actual value (mm)	Predicted Value (mm)
Valetta	15.8	17.1
Highlands	10.6	42.3
La Mecque	9.25	54.9
Etoile	4.12	37.7
Henrietta	52.5	54.3
St Pierre	29.0	28.2
Riche en Eau	2.41	3.85
Pierre Fonds	14.4	51.2

3.3.3 Runoff results at a rainfall intensity of 150 mm

The table representing the best results from the simulation of runoff using APSIM is provided in Table 9. There were two soils (Valetta and Riche en Eau) that had the same classification, same curve number and initial water value and had predicted runoff values that were similar to the measured values.

Table 9: Results for runoff from APSIM using the 150 mm rainfall event

Soil	Actual value (mm)	Predicted Value (mm)
Valetta	22.0	27.0
Highlands	65.2	92.3
La Mecque	27.5	105
Etoile	19.3	87.7
Henrietta	58.3	53.8
St Pierre	54.0	53.8
Riche en Eau	25.7	27.4
Pierre Fonds	63.7	101

Valetta and Riche en Eau are classified as Humic Ferruginous Latosols. There were three other soils classified as Humic Ferruginous Latasols and these also had measured data for runoff for the 150 mm rainfall event. These soils were then added to the simulation with the same curve number (45) and initial water (80) as Valetta and Riche en Eau. Table 10 shows that the results obtained for the predicted runoff values were very close to the measured values.

Table 10: Results for runoff from APSIM for the Humic Ferruginous Latosols

Soil	Actual value (mm)	Predicted Value (mm)
Valetta	22.0	27.0
Riche en Eau (site 1)	25.7	27.4
Rose Belle	25.2	27.0
Riche en Eau (site 2)	34.2	32.6
Cent Gaulettes	20.9	40.0

The only soil that had a predicted value that was not close to the measured value was Cent Gaulettes. The difference between this soil and the others is that that the soil texture at 15-30 cm depth was clay whereas the texture for all the other soils form 0-30 cm was clay loam or loam. It is expected that clay soils would be difficult to model due to the increase in clay minerals and associated increase in chemical reactivity. In the case of runoff it could be the change in water holding capacity with an increased clay content. When this value is removed as an outlier, however, Figure 16 clearly shows the strong

correlation between the predicted runoff values and the measured values for this soil group. A larger dataset of similar soils would be valuable to further validate the strength of this relationship.

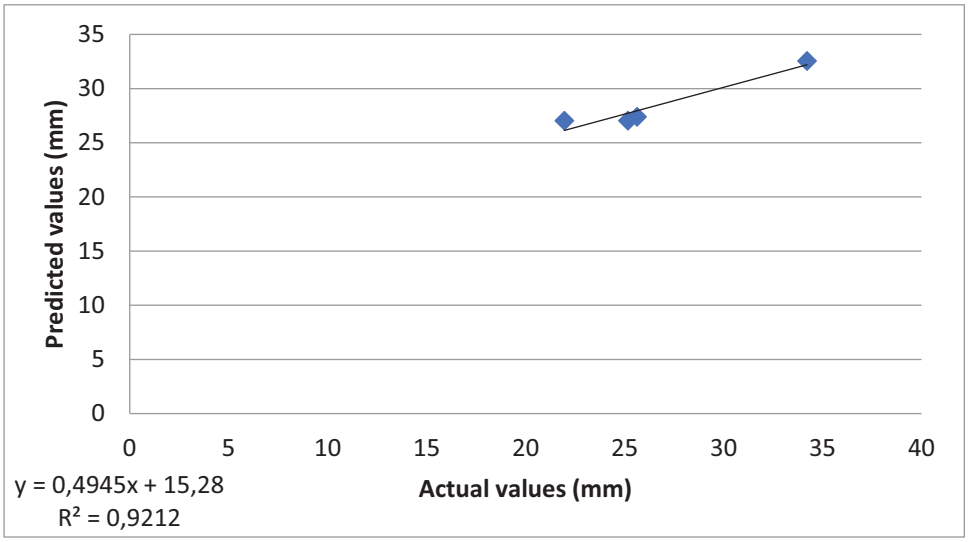

Figure 16: Graph of predicted runoff values after a 150 mm rainfall event vs. measured values

An interesting observation made for the 150 mm rainfall event was that the Henrietta and St Pierre soils both had a curve number of 60 and initial water value of 80 and these soils had predicted values close to that of the measured runoff. Although their soil types differ slightly, they are both humic soils and this result is contrary to what was observed for the 100 mm rainfall event. At the latter rainfall, predicting runoff was unsuccessful and it was thought that organic matter or humic content played a role, however this does not appear to be the case for the 150 mm rainfall event. It was observed, however, that the simulated runoff value for both of these soils was the same.

3.3.4 Simulating phosphorous in the predicted runoff using APSIM

It was attempted to use APSIM to simulate phosphorus in the surface runoff. This attempt was unsuccessful. Discussions with the APSIM support team revealed that APSIM does not have this capability. The module included in APSIM for phosphorous is SoilP, which describes P transformations in the soil (Keating et al., 2003). The SoilP module represents the availability of phosphorous in soil for crop uptake. A recommendation for future research would be to incorporate a routine in APSIM to quantify P in surface runoff.

3.4 Conclusions

From the work done to date, it appears that APSIM cannot be used to accurately predict runoff after a rainfall event on bare soil under all rainfall events. The model only appears to be sensitive to changes in curve number and initial water content and does not seem to account for slope when simulating runoff. The model did, however, generate predicted runoff values that were very close to the measured

values for a certain soil groups (Humic Ferruginous Latosols). The only outlier in this group had an increased clay content in the subsoil and this may be the reason for the difference with this soil. The results therefore indicate that getting accurate results for surface runoff is largely dependent on soil type, more specifically soil texture. The APSIM model is unable to predict phosphorous in runoff, however there may be a way to incorporate this functionality into the model with the help of the APSIM support and development team. Further work is still to be conducted to further refine modelling P losses from surface runoff with APSIM.

3.5 References

ARCHONTOULIS, S.V., MIGUEZ, F.E. and MOORE, K.J. (2014) Evaluating APSIM maize, soil water, soil nitrogen, manure and soil temperature modules in the Midwestern United States. *Agronomy Journal* 106 (3): 1025-1040.

KEATING, BA., CARBERRY, P.S., HAMMER, G.L., PROBERT, M.E., ROBERTSON, M.J., HOLZWORTH, D., HUTH, N.I., HARGREAVES, J.N.G., MEINKE, H., HOCHMAN, Z., McLEAN, G., VERBURG, K., SNOW, V., DIMES, J.P., SILBURN, M., WANG, E., BROWN, S., BRISTOW, K.L., ASSENG, S., CHAPMAN, S., McCOWAN, R.L., FREEBAIRN, D.M. and SMITH, C.J. (2003) An overview of APSIM, a model designed for farming systems simulation. *European Journal of Agronomy* 18: 267-288.

GAYDON, D.S. (2014) Chapter 2: The APSIM Model – An Overview, The SAARC-Australia Project – developing capacity in cropping systems modelling for South Asia, SAARC Agriculture Centre Monograph, SAARC Agriculture Centre (SAC), BARC Campus, Farm Gate, Dhaka-1215, Bangladesh, ISBN: 978-984-33-7469-1.

WANG, E., ROBERTSON, M.J., HAMMER, G.L., CARBERRY, P.S., HOLZWORTH, D., MEINKE, H., CHAPMAN, S.C., HARGREAVES, J.N.G., HUTH, N.I. and McLEAN, G. (2002) Development of a generic crop model template in the cropping system model APSIM. *European Journal of Agronomy* 18: 121-140.

NG KEE KWONG, K.F., BHOLAH, A., VOLCY, L. and PYNEE, K. (2002) Nitrogen and phosphorous transport by surface runoff from a silty clay loam soil under sugarcane in the humid tropical environment of Mauritius. *Agriculture, Ecosystems and Environment* 91: 147-157.

MARDAMOOTOO, T. (2015) Developing an index for phosphorous loss from sugarcane soils in Mauritius. PhD thesis, University of the Free State, South Africa.

MARDAMOOTOO, T., DU PREEZ, C.C. and SHARPLEY, A.N. (2015) Phosphorous mobilization from sugarcane soils in the tropical environment of Mauritius under simulated rainfall. *Nutrient Cycling in Agroecosystems* 103: 29-43.

APSIM documentation, SoilWat. URL: http://www.apsim.info/Documentation/Model,CropandSoil/SoilModulesDocumentation/SoilWat.aspx (Accessed 1 October 2016)

USDA/SCS curve number method for estimating daily runoff (2004). URL: https://hrsl.ba.ars.usda.gov/SPAW/Appendices/AppendixI.htm (Accessed 28 October 2016).

USDA (1986). Urban hydrology for small watersheds. Appendix A.

SAXTON, K.E., WILLEY, P.W. and RAWLS, W.J. (2006) Field and pond hydrologic analyses with the SPAW model. In: *ASABE Annual International Meeting*, 9-12 July 2006, Portland, Oregon.

FOOD AND AGRICULTURE ORGANIZATION (2015) World reference base for soil resources 2014. International soil classification system for naming soils and creating legends for soil maps. Food and Agriculture Organization of the United Nations, Rome, Italy.

4 COMPARISON OF DIFFERENT MODELS TO ESTIMATE NITROGEN AND PHOSPHORUS EXPORT FROM AGRICULTURE: THE HYDRUS, APSIM AND SWAT MODELS

M. van der Laan and L. Mudaly
Department of Plant and Soil Sciences, University of Pretoria, Pretoria 0002, South Africa

4.1 Introduction

Non-point source (NPS) nutrient pollution from agriculture occurs at different inter-linked scales. Many models have been developed worldwide to simulate NPS nitrogen (N), and to a lesser extent phosphorus (P) pollution. Some models have gained prominence as a result of factors such as robustness, user-friendliness and widespread application (e.g. EPIC, SWAT, DSSAT, APSIM, Hydrus), while others are mostly used and developed 'in-house' at a specific institution, with a key advantage in such a situation being the complete control over model development and functionality. As these models have all been developed with different objectives, they have evolved along different paths based on user needs, and vary with regards to mathematical complexity and computational requirements, so it is not always clear which model to apply for a specific application.

The objective of this chapter was to more closely scrutinise the models that can be applied to investigate NPS nutrient pollution from agriculture in South Africa. Some of the models most commonly used so far were selected, including Hydrus 1-D, SWB-Sci, APSIM and SWAT, and it is acknowledged that other models such as DSSAT and ACRU have also been applied for such purposes. The selection of the aforementioned models for comparison was primarily due to their differences in simulation of hydrological processes in the unsaturated zone and the scale at which they are most often applied. As stated by Gandolfi, Facchi et al. (2006), '…water transfer through the unsaturated zone is one of the most important [hydrological processes], as it controls evapotranspiration rates and water stress of vegetation and crops on one side, and recharge to the aquifer system on the other'. Input parameters and processes simulated in the key models are reported, and recommendations are made for the application of these models based on specific needs.

4.1.1 Model descriptions

4.1.1.1 Hydrus

Hydrus 1-D is a very mechanistic simulation package widely used to simulate solute leaching. It can take into account non-equilibrium flow and transport processes through physical non-equilibrium models (Mobile Immobile Water Model, Dual-Porosity Model, Dual-Permeability Model, and the Dual-Permeability Model with Immobile Water), chemical non-equilibrium models (One Kinetic Site Model, the Two Site model and the Two Kinetic Sites Model), and physical and chemical non-equilibrium transport models (Dual-Porosity Model with One Kinetic Site and the Dual-Permeability Model with Two-Site Sorption) (Šimůnek and Van Genuchten, 2008). As stated by the developers of the software, 'the many different models that have been developed over the years for non-equilibrium flow and transport reflect the multitude of often simultaneous processes that govern non-equilibrium and preferential flow

at the field scale' (Šimůnek and Van Genuchten, 2008). Hydrus 1-D is not a crop model cannot mechanistically simulate crop growth including biomass production in response to different stresses such as water and N deficiencies in a way that a model such as ASPIM can. Instead, evapotranspiration (ET) must be entered as an input, although weather data can also be used from which it can estimate soil water use with a crop factor type approach. There is not a sophisticated feedback mechanism between water/solute stress and physiological canopy development, and yield is not estimated, as is the case with a model such as APSIM.

The strength of Hydrus is therefore in the extent to which it can be parameterised to represent a vast array of scenarios and flow and solute mixing processes. There is a Hydrus 2D/3D version which can consider runoff, but it is complex to parameterize, for example, to study a single hill slope, and for purposes of this comparison it is not considered.

4.1.1.2 APSIM

During the course of project it was recognized that while the SWB-Sci model has key advantages in the form that the team has complete control over the source code and much calibration work has been done for South African conditions, crop models such as APSIM and DSSAT are far advanced in terms of the development and testing they have undergone. As a result they have greater functionality, for example, the ability to simulate a mulch residue and the associated nutrient cycling that takes place, simulating runoff according to the USDA curve number approach. As a result, it was decided to use APSIM to a greater extent than originally envisaged.

APSIM (**A**gricultural **P**roduction **S**ystems s**IM**ulator) is a crop model developed in Australia to assist on-farm decision making. It is possible to use two different models for the soil water and solute balance – SoilWat and SWIM3 (Huth et al., 2012). SoilWat is a cascading model while SWIM3 (Soil Water Infiltration and Movement) is based on numerical solutions to the Richards' water flow equation. The description below was obtained from Verburg (1996): during saturated water flow, solute movement is simulated using a 'mixing' algorithm in SoilWat in which all water and solute entering a layer is fully mixed with what is already there, following which an 'efficiency factor' is used to calculate the amount of solute leaving the layer. SoilWat also considers unsaturated upward and downward flows driven by water content gradients, and a second user-specified efficiency factor is used to influence the amount of solute which moves with the water from one layer to another as a result of unsaturated flow. An advection-dispersion equation is used to simulate solute movement in SWIM3.

In APSIM, runoff is estimated using the USDA Soil Conservation Service approach commonly referred to as the curve number technique. The description below is based on information provided at https://www.apsim.info/Documentation/Model,CropandSoil/SoilModulesDocumentation/SoilWat.aspx. Runoff from rainfall is calculated using the USDA-Soil Conservation Service procedure known as the curve number technique. The estimation is made at a daily time-step so storm intensity is not considered. A curve number for average antecedent rainfall conditions is a soil parameter provided by the user. The model uses this value to estimate a wet (high runoff potential) to dry (low runoff potential) range of response curves from this value, which are then used in the runoff calculation (Figure 17). For

antecedent soil moisture influences, a user-specified 'hydraulic depth' is used to give extra weighting to layers closer to the surface.

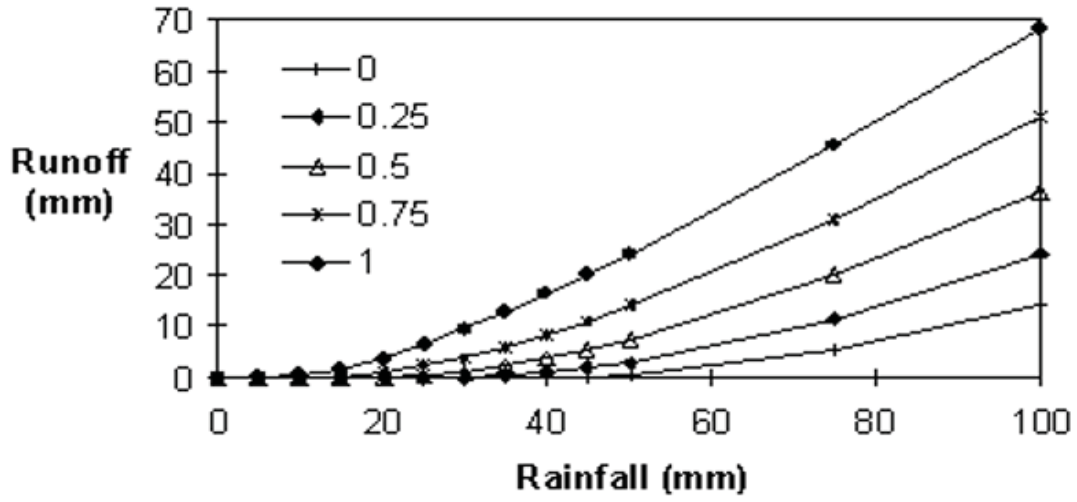

Figure 17: Runoff response curves for average antecedent rainfall condition curve number of 75 for a range of soil moisture levels [0 (dry)-1 (wet)] https://www.apsim.info/Documentation/Model,CropandSoil/SoilModulesDocumentation/SoilWat.aspx

Crop residues on the soil surface are simulated to reduce runoff via reducing the bare soil curve number. A threshold cover % leads to no further reductions in the curve number (Figure 18). For tillage events, the user is also able to reduce estimated runoff by supplying a reduced curve number (CN_red) and the rainfall amount required to remove the 'tillage roughness'. The CN number is linearly reduced with cumulative rainfall until the user-defined threshold is reached, and the CN for each day can be viewed by checking the variable CN2_new.

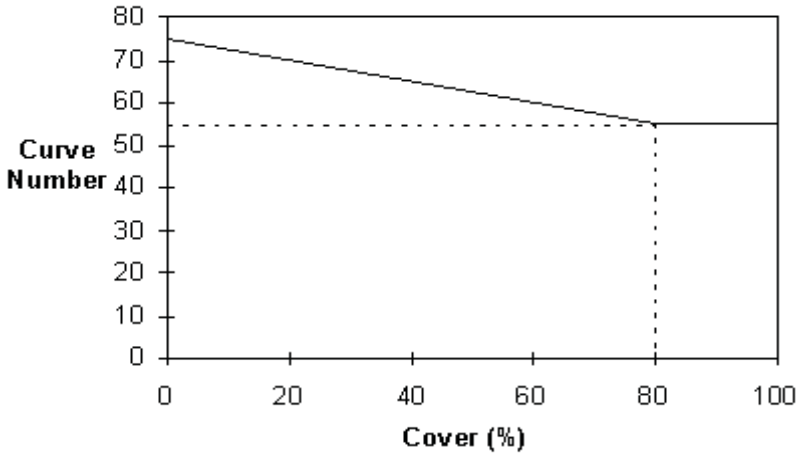

Figure 18: Increased residue cover results in a reduced runoff curve number, for example, a curve number of 75 for bare soil becomes 20 at 80% residue cover https://www.apsim.info/Documentation/Model,CropandSoil/SoilModulesDocumentation/SoilWat.aspx

4.1.1.3 SWAT model

SWAT is a physical-based, distributed-parameter model primarily 'developed to predict the impact of land management practices on water, sediment and agricultural chemical yields in large complex watersheds with varying soils, land use and management conditions over long periods of time' (Neitsch, Arnold et al., 2002). SWAT uses land use, digital elevation and soil maps together with weather data to discretise catchments into hydrological response units (HRUs) according to unique combinations of land use, soil and slope. It is a long-term yield model and not designed to simulate single event flood routing (Neitsch, Arnold et al., 2002).

SWAT uses a cascading soil water balance approach, and lateral flow between soil layers is also possible. Either the SCS-curve number of Green-Ampt infiltration method can be used to predict runoff. Being a basin scale hydrological model, it can also simulate base flow, river flow routing, sediment yield and sediment channel routing.

For N leaching, a 'mobile soil water NO_3^- concentration' is firstly estimated using the following equation:

$$conc_{NO3,mobile} = \frac{NO3_{ly} \cdot \left(1 - \exp\left[\frac{-w_{mobile}}{(1-\theta_e)\cdot SAT_{ly}}\right]\right)}{w_{mobile}}$$

Where $conc_{NO3,\ mobile}$ = concentration of nitrate in mobile water (kg N/mm)

NO3ly = amount of nitrate in the layer (kg N/ha)

ωmobile = amount of mobile water in the layer (mm)

SATly = saturated water content (mm)

Θe = fraction of porosity from which anions are excluded

It is based on the theory that anions are excluded from the areas immediately adjacent to mineral surfaces as cations are preferentially attracted to these sites, and this area is also where the slowest moving portion of the soil water volume occurs (SWAT 2009). So, bypass flow (or a shorter pathway) occurs in the case of anion transport (SWAT 2009).

Nitrate loss via runoff only occur from the top 10 mm of the soil and is estimated using the following equation

$NO3_{surf} = \beta_{NO3} \times conc_{NO3,mobile} \times Q_{surf}$

Where Q_{surf} = volume of surface runoff (mm)

β_{NO3} = nitrate percolation coefficient

According to the 2009 SWAT manual, β_{NO3} allows 'the user to set the concentration of NO_3^- in surface runoff to a fraction of the concentration in the percolate'. The input variable is called NPERCO. Lateral flow is considered in the same way as Equation X, except that $Q_{lat,ly}$ is used instead of Q_{surf}.

Sediment-bound organic N losses via surface runoff is also considered in SWAT. A loading function developed by McElroy (1976) and modified by William and Hann (1978) is used to estimate the amount of organic N transported with sediment as follows:

$$OrgN_{surf} = 0.001 \times conc_{orgN} \times \frac{sed}{area_{hru}} \times \varepsilon_{N:sed}$$

Where OrgNsurf = amount of organic N transported to the main channel in surface runoff

$conc_{orgn}$ = concentration of organic N in the top 10 mm (g N/Mg soil)

sed = sediment yield (Mg)

$area_{hru}$ = hydrological response unit area (ha)

$\varepsilon_{N:sed}$ = nitrogen enrichment ratio [small, clay particles are more easily transported, and organic N is primarily attached to the colloidal (clay) particles]

The enrichment ratio is defined as 'the ratio of the concentration of organic N transported with the sediment to the concentration in the soil surface layer' (SWAT 2009 manual). It can be calculated by the model per storm event or can be user defined. The relationship described by Menzel (1980) in which the enrichment ratio is logarithmically related to sediment concentration, as follows:

$\varepsilon_{N:sed} = 0.78 \times (conc_{sed,\ surq})^{-0.2468}$

The concentration of sediment in surface runoff is calculated as follows:

$$conc_{sed,surq} = \frac{sed}{10 \times\ area_{hru} \times\ Q_{surf}}$$

Where Q_{surf} = amount of surface runoff on a given day (mm)

For phosphorus (P), solution P (Psurf, kg ha^{-1}) lost via surface runoff is estimated as:

$$P_{surf} = \frac{P_{solution,surf} \times\ Q_{surf}}{\rho_b \times depth_{surf} \times\ k_{d,surf}}$$

Where $P_{solution,\ surf}$ = amount of P in solution in top 10 mm (kg ha^{-1})

$depth_{surf}$ = depth of surface layer (10 mm)

$k_{d,surf}$ = P soil partitioning coefficient (m^3 Mg^{-1}), which is the ratio of the soluble P concentration in the top 10 mm layer to the concentration in surface runoff.

The loss of sediment-bound organic P via runoff is calculated in the same way as described above for N, and in the case, loss mineral P that is bound to sediment is also considered.

Water, nutrients (N and P) and temperature can constrain crop growth in SWAT through modification to the user described canopy cover and potential yield. The crop module is therefore more sophisticated than Hydrus, but less so than a crop model such as APSIM and DSSAT.

An overview of the processes and parameters required are reviewed in the two tables below.

Table 11: Processes considered in Hydrus 1-D, APSIM and SWAT

Processes considered	**Hydrus-1D**	**APSIM**	**SWAT**
Runoff	If infiltration rate exceeded, surplus water assumed to be runoff	Yes USDA – curve number approach	Yes USDA – curve number approach / Green-Ampt method when hourly data available
Potential evapotranspiration	Yes	Yes	Yes
Actual evapotranspiration	Yes – Crop factor approach, water stress considered	Yes – including biomass and water stress	Yes – including biomass and water stress
Inorganic N/P runoff	No	No	Yes
Inorganic N/P leaching	Solute leaching considered, but not N and P cycling	Yes	Yes
Erosion	No	Yes	Yes
Organic, sediment-bound N/P + inorganic P runoff	No	No	Yes
Organic N/P leaching	No	No	No
Modified runoff conditions	No	Yes – residue, tillage	
Macropore flow	Yes	No	No
Lateral flow N/P export	No	No	Yes
Crop growth	No	Yes – mechanistic crop modules	General description of canopy development. Yield indicated by user, stress adjustments made by model
Plant stress	Water, salinity,	Water, temperature, nitrogen, phosphorus	Water, temperature, nitrogen, phosphorus
Detailed root growth	Yes	Yes	No
Dry/wet atmospheric N deposition	No	No	Yes

Table 12: Parameters needed in Hydrus 1-D, APSIM and SWAT

Soil parameter	Hydrus	APSIM	SWAT
SCS Curve number	No	Yes (CN2Bare)	
$k_{d,surf}$ = P soil partitioning coefficient	Adsorption coefficients and dynamics parameterisable	Estimated from other parameters	Yes
Bulk density (Mg m^{-3})	Yes	Yes	Yes
Nitrate leaching efficiency factor	Can be parameterised through defining mobile/immobile fractions	Yes – mixing factors, require calibration	Yes – 'mobile water' approach used
Organic N or P enrichment ratio ($\varepsilon_{N:sed}$)	No	No	Yes

4.1.2 Comparison of different water balance modelling approaches

As mentioned previously SWB, APSIM's SoilWat and SWAT use a cascading soil water balance approach, which is computationally efficient and stable, and therefore also attractive for basin scale modelling (Gandolfi, Facchi et al., 2006), while Hydrus and APSIM's SWIM3 are based on the more mechanistic and computationally intensive Richards' equation. All except Hydrus operate on a daily time-step by default and therefore require daily weather data, which is the most common format available. The models using the cascading approach also make use of a root-weighting factor or just consider root depth and available soil water in each layer.

In the case of the cascading approach models, flux will only occur when soil water contents are above field capacity, while for the Richards' equation models flux can still occur at water contents below field capacity. Using a cascading approach, may therefore estimate drainage to occur in pulses, as opposed to a smoother drainage curve with the latter models. This can potentially be improved in cascade models by including the number of layers simulated, and it has also been noted that when drainage is aggregated over longer periods the differences between modelling approaches decreases (Gandolfi, Facchi et al., 2006). The implications of this pulsing effect in cascading models on estimating solute fluxes are unknown.

Gandolfi, Facchi et al. (2006) observed that the influence of the lower boundary condition is only significant for shallow profiles and fine-textured soils. So if the groundwater is close to the surface, or if there is artificial drainage in place, it may be worth applying a Richards' equation-based model to investigate the system.

4.2 Conclusions

As stated by Jhorar, Smit et al. (2009), 'the problem is not the availability of models but much more the level of complexity desired to obtain reliable solutions'. Understanding the different approaches used in the models can assist researchers studying NPS nutrient pollution to best decide which to apply, and how to effectively parameterise the model to better understand their system and identify mitigation

measures. Hydrus and APSIM cannot be applied at the catchment to basin scale. Hydrus does not include a mechanistic crop module, but can account for a wide array of soil processes. APSIM includes a crop module that responds to stress in a way that represents what is happening in the field, and it can mechanistically represent important soil processes, but only at the plot scale, so it cannot link nutrient flows in the landscape.

The amount and type of input data differs between models according to what processes are simulated and the approaches used. Hydrus allows the detailed parameterisation of a specific soil, APSIM to a lesser degree, while SWAT allows for parameterisation of large areas with a variety of soil types, topographies and land uses, but with less user control over all the parameters it requires. Despite SWAT's capability to simulate larger areas, it includes many processes and often in detail. It may be challenging and cumbersome to set-up a simulation when only interested in investigating a particular cropping system, however.

Following the comparison of three commonly used but very different models that can be used to simulate NPS nutrient pollution, the following recommendations are made:

- Hydrus 1-D or 2D/3D is the only model suitable for simulation of very complex systems, such as fertigated orchards under drip or micro irrigation.
- Hydrus can be best applied to investigate complex soil hydrology at more detailed scales, for example, at the hillslope scale or to capture the impact of a wetland at the edge of a field.
- Shallow water tables or thin soils will likely be more accurately simulated by Richards' equation based models.
- APSIM (or SWB-Sci or DSSAT) is the best model to simulate responses to different in-field best management practices, for example, introducing split fertilizer applications, including more organic amendments in the fertilizer programme or using cover corps. This is because it combines mechanistic soil water, crop and nutrient modules. It can only be used to simulate at the plot scale.
- SWAT is the only model that can be applied at the sub-catchment to basin scale.
- Despite SWAT being intended for catchment scale applications, it contains many of the important processes involved in N and P pollution that are not even included in more detailed crop models. Its application for testing and validation against field scale data is therefore recommended, although it is acknowledge that this is difficult to set-up.
- SWAT has the most mechanistic runoff routine of all the models.
- In theory, hydrological models such as Hydrus and crop models such as APSIM and SWB-Sci can first be applied to test soil water dynamics, crop parameters and cropping pattern dynamics and so on, on a more local scale, and this information can then be used to more accurately parameterise and initialize the SWAT model at the HRU scale.

Ultimately it is not just about what processes are simulated, but the interaction between these processes as well as user parameterisation and calibration which enables the accurate representation of a system.

No model is considered ‘better’ than another, but is envisaged that this comparison can assist users to decide which model is best applied under different scenarios. It is envisaged that this work will be further developed into a journal paper.

4.3 References

BRANDI-DOHRN, F.M., HESS, M., SELKER, J.S., DICK, R.P. (1996) Field evaluation of passive capillary samplers. *Soil Science Society of America Journal*, 60: 1705-1713.

CORWIN, D., WAGGONER, B., RHOADES, J. (1991) A functional model of solute transport that accounts for bypass. *Journal of environmental quality*, 20: 647-658.

FLÜHLER, H., DURNER, W., FLURY, M. (1996) Lateral solute mixing processes − A key for understanding field-scale transport of water and solutes. *Geoderma*, 70: 165-183.

GANDOLFI, C., FACCHI, A., MAGGI, D. (2006) Comparison of 1D models of water flow in unsaturated soils. *Environmental Modelling & Software*, 21: 1759-1764.

JHORAR, R.K., SMIT, A., ROEST, C. (2009) Effect of model selection on computed water balance components. *Irrigation and Drainage: The journal of the International Commission on Irrigation and Drainage*, 58: 492-506.

MA, L., SCOTT, H., SHAFFER, M., AHUJA, L. (1998) RZWQM simulations of water and nitrate movement in a manured tall fescue field. *Soil science*, 163: 259-270.

MCELROY, A. (1976) *Loading functions for assessment of water pollution from nonpoint sources*, vol. 1. US Environmental Protection Agency, Office of Research and Development, [Office of Air, Land, and Water Use].

MENZEL, R. (1980) Enrichment ratios for water quality modeling. *CREAMS: A Field-Scale Model for Chemicals, Runoff, and Erosion from Agricultural Management Systems Conservation Research Report Number 26, May, 1980. p 486-492, 1 Fig, 2 Tab, 11 Ref.*

NEITSCH, S., ARNOLD, J., KINIRY, J.E.A., SRINIVASAN, R., WILLIAMS, J. (2002) Soil and water assessment tool user’s manual version 2000. *GSWRL report*, 202.

ŠIMŮNEK, J., VAN GENUCHTEN, M.T., ŠEJNA, M. (2008) Development and applications of the HYDRUS and STANMOD software packages and related codes. *Vadose Zone Journal*, 7: 587-600.

STIRZAKER, R. (2003) When to turn the water off: scheduling micro-irrigation with a wetting front detector. *Irrigation Science*, 22: 177-185.

VAN DER LAAN, M., STIRZAKER, R., ANNANDALE, J., BRISTOW, K., DU PREEZ, C. (2010) Monitoring and modelling draining and resident soil water nitrate concentrations to estimate leaching losses. *Agricultural Water Management*, 97: 1779-1786.

VAN DER LAAN, M., STIRZAKER, R.J., ANNANDALE, J.G., BRISTOW, K.L., DU PREEZ, C. (2011) Interpretation of electrical conductivity measurements from ceramic suction cups, wetting front detectors and ECH2O-TE sensors: short communications. *South African Journal of Plant and Soil*, 28: 244-247.

WEIHERMÜLLER, L., SIEMENS, J., DEURER, M., KNOBLAUCH, S., RUPP, H., GÖTTLEIN, A., PÜTZ, T. (2007) In situ soil water extraction: a review. *Journal of environmental quality*, 36: 1735-1748.

5 MODELLING VADOZE ZONE SOLUTE CONCENTRATIONS

M. van der Laan[1] and R.J. Stirzaker[1, 2]
[1]Department of Plant and Soil Sciences, University of Pretoria, Pretoria 0002, South Africa
[2]CSIRO Land and Water, P.O. Box 1666, ACT 2601, Australia

5.1 Introduction

Active soil water samplers such as ceramic suction cups and passive samplers such as pan lysimeters are commonly used to estimate soil nutrient or salinity status, for example, in solute leaching studies. Sometimes measured concentrations are combined with estimates of soil water fluxes, often estimated using numerical models, to predict leaching loads. Measurements from such devices have also played a role in soil solute dynamics understanding and the testing and refinement of models such Hydrus 1-D (Šimůnek, Van Genuchten et al., 2008) and RZWQM (Ma, Scott et al., 1998). Yet there remains large uncertainty related to what soil pore volume these devices are sampling, and how representative concentrations in the sampled water are of concentrations in the spectrum of soil pore sizes at the measurement depth. Further adding confusion are uncertainties regarding potential changes to the natural flow pattern imposed as a result of the device being installed in the soil, or from the suction being applied to the device in the case of active samplers. And is a possibility that certain organic and inorganic are sorbed by the suction cup material (Weihermüller, Siemens et al., 2007).

Suction cups can be operated in continuous mode (prolonged suction mimicking undisturbed surrounding soil), or in a discontinuous mode in which water collection is performed over short time intervals (Weihermüller, Siemens et al., 2007). But optimal operation and suction to apply are still not well understood. The amount of suction actually applied is influenced by soil type, antecedent soil water content and duration of applied suction, and the size of the sample needed must also be taken into account (Brandi-Dohrn, Hess et al., 1996; Weihermüller, Siemens et al., 2007).

Modelling can potentially improve understanding on what pore fraction these instruments are sampling and the related solute concentration as models do not create or destroy mass and therefore overcome issues with soil heterogeneity when sampling. Accounting for bypass flow or incomplete mixing between solutes in the draining water and those present in water in the smaller pore volumes has been observed as important (Corwin, Waggoner et al., 1991; Van der Laan, Stirzaker et al., 2010), but is challenging to get right or even to get the data to adequately test whether it is right.

Despite continued efforts we still have poor predictive power for field scale solute transport (Flühler, Durner et al., 1996). In this study, data from a large weighing lysimeter trial and modelled outputs from Hydrus 1-D were used to better understand what measured conservative tracer (chloride, Cl^-) from ceramic suction cups as well as passive samplers [wetting front detectors (WFDs)] represent. This included an investigation into the importance of accounting for bypass flow and incomplete solute mixing. Measurements of nitrate (NO_3^-) concentrations were also compared to estimate plant uptake concentrations.

5.2 Materials and methods

5.2.1 Weighing lysimeter set-up

A deep 1.8 m weighing lysimeter (surface area = 0.6 m^2) packed with a loam soil (21% clay, 18 silt, 61% sand) in a laboratory in Canberra, Australia. The lysimeter was continually weighed using loadcells linked to a logger. Ceramic suction cups, tensiometers and Watermark sensors were buried at 0.30, 0.60, 0.90, 1.20 and 1.50 m depths. Commercially available passive samplers called Wetting Front Detectors (WFDs) (Stirzaker, 2003; Van der Laan, Stirzaker et al., 2010) were installed at 0.15, 0.30. 0.45 and 0.60 m depths. Measurements were taken from June 2009 to April 2010. Sodium chloride (NaCl) was added to tap water to simulate irrigation water EC of 500 mS m^{-1} which was applied through drip emitters at the soil surface. Five Swiss chard plants (*Beta vulgaris* L.) were grown on the lysimeter and irrigated weekly. Irrigation was at first applied in excess of plant requirements in order to wet the profile to 1.50 m. From September 2009, irrigation was applied until the 30 cm WFD responded in an attempt to accumulate solutes between 0.30 and 0.60 m. Then starting middle December, large irrigation volumes were applied in an attempt to move the salt front past 0.60 m, resulting in the deeper WFDs at 0.45 and 0.60 m responding at this time.

5.2.2 Modelling

Hydrus 1-D was parameterised and initialised based on measured soil characteristic data and pedotransfer functions. Additional calibration was done using measured drainage from the bottom of the lysimeter over the trial period (Figure 19). For water flow, the Van Genuchten – Mualem single porosity hydraulic model was used and no hysteresis was assumed. Saturation = 0.39 m^3 m^{-3}, residual water content = 0.1 m^3 m^{-3}, alpha = 0.0059 (1 mm^{-1}) (parameter in soil water retention function), n =1.48 (parameter in soil water retention function), saturated hydraulic conductivity = 240 mm day^{-1}, and l = 0.5 (tortuosity parameter in conductivity function). For solute transport, the Crank-Nicholson time weighting scheme, and Galerkin finite elements space weighting scheme were used. A dual porosity (mobile-immobile water) solute transport model (physical non-equilibrium) was selected, and the immobile water fraction was set to 0.18 m^3 m^{-3}, bulk density was 1.5 Mg m^{-3}, and the Cl^- longitudinal dispersion parameter was 60 mm. The Feddes root water uptake model was used and no plant solute stress was simulated. Maximum root depth for the Swiss chard crop was set at 0.80 m. Bottom boundary condition was set to free drainage as the seepage face option in Hydrus 1-D as recommended for lysimeter set-ups such as ours did not simulate deep drainage satisfactorily.

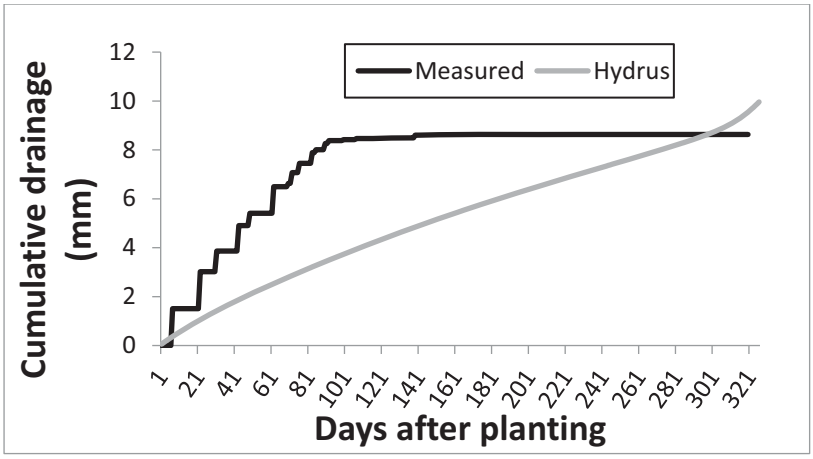

Figure 19: Measured and simulated cumulative drainage over the trial period

As daily evapotranspiration (ET) was measured by the weighing lysimeter, this value was used as input to run the model so as to reduce any error resulting from the inaccurate modelling of crop ET and to focus on soil water and solute flows. The crop model SWB-Sci (Van der Laan, Stirzaker et al., 2010) was run for the crop cycle and used to split weighing lysimeter measured ET into evaporation and transpiration based on the dynamic fractional interception of the crop canopy as estimated by SWB-Sci.

5.3 Results

5.3.1 Measured and simulated soil water potential

Soil water potential was relatively well simulated by Hydrus 1-D (Figure 20), although there was a general tendency for the model to simulate higher water potentials than those estimated by the sensors. This was potentially as a result of inaccurate soil hydraulic characteristic parameterisation in the model, a mismatch between simulated and actual root water uptake patterns, and/or any heterogeneity in irrigation distribution. Trends were extremely similar between measured and simulated values, and no further model calibration was done in an attempt to get a better fit between values.

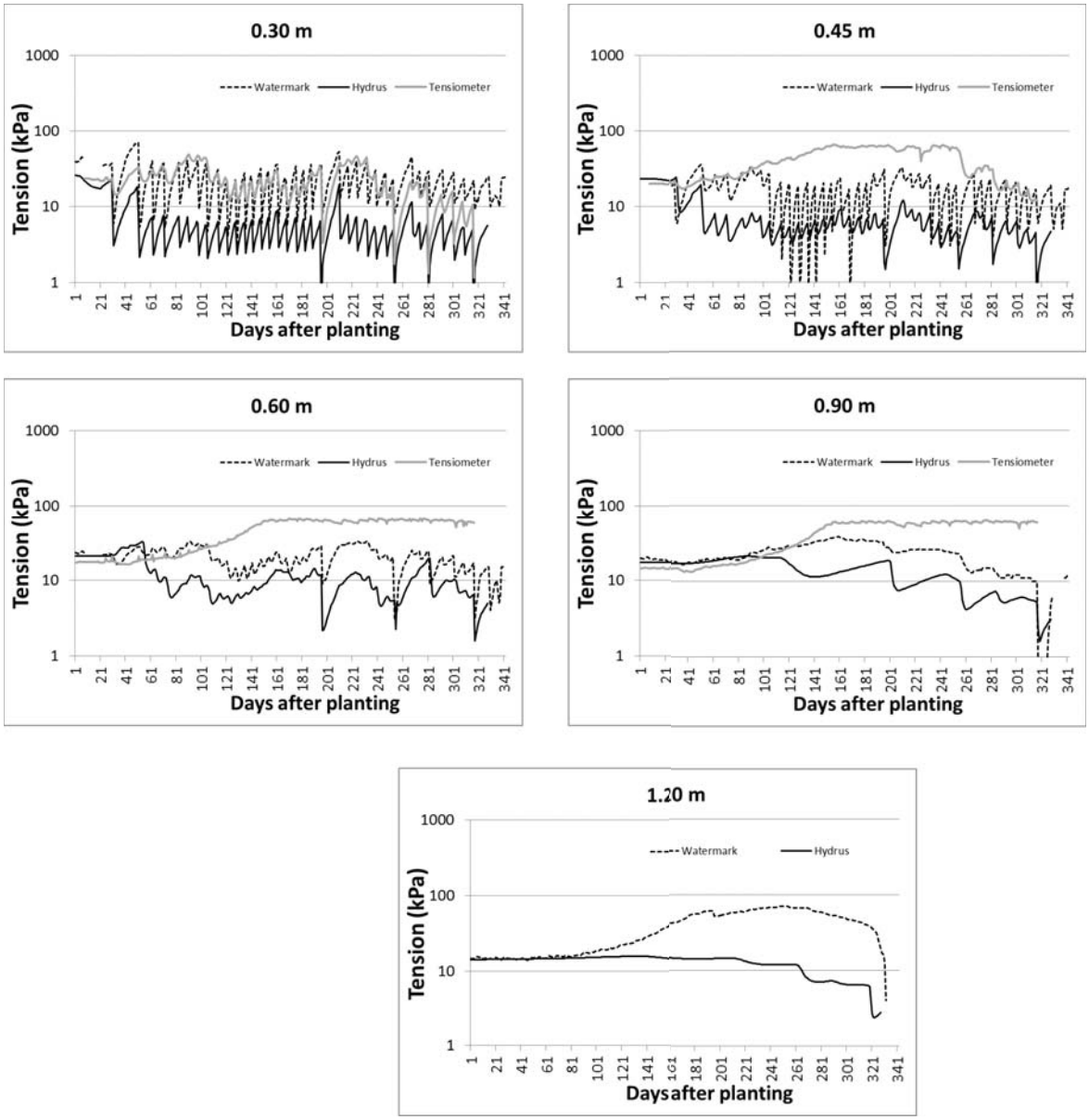

Figure 20: Measured and simulated soil water potential at different depths in the soil profile over the trial period

5.3.2 Measured and simulated Cl^- concentrations

As WFDs sample when the soil pores are full of water (1-3 kPa), compared to suction cups which are able to sample smaller pores when the soil is less wet (usually at suctions of 40-60 kPa), it was expected that solute concentrations would usually be lower in WFDs than suction cups, as has previously been observed by Van der Laan, Stirzaker et al. (2010) and Van der Laan, Stirzaker et al. (2011). This was generally observed at 0.30 m for this dataset (Figure 21), expect for the sampling events before 150 DAP when WFD concentrations were actually slightly higher than SC concentrations. Previously it has been hypothesised that this can occur due to the WFDs sampling mobilised salt at the beginning of a leaching event (Van der Laan, Stirzaker et al., 2011) colloquially termed 'snow-ploughing'. This could be because as the Cl^- was added with the irrigation water from the surface, we expect most of it to be moving downwards in the larger soil pores with faster flow velocities – which are more efficiently

sampled by the WFDs. Following 150 DAP, Cl^- concentrations measured in the SCs are consistently higher than those measured in the WFDs, potentially due to the migration of Cl^- into the smaller pores as driven by diffusion and advection. At the 0.45 and 0.60 m depths, SC and WFD Cl^- concentrations much more closely matched each other. We believe this is because these two types of samplers are actually sampling a similar pore water fraction at this depth. Although we may put 60-80 kPa of suction onto the cup, the largest pores drain first and perhaps the suction declines while this is happening. Furthermore, conductivity would be so low at 60 kPa that it is doubtful that water from smaller pores will continue to move into the cup. So, the whole suction cup sampling mechanism is most likely limited by unsaturated hydraulic conductivity to emptying a certain minimum pore size.

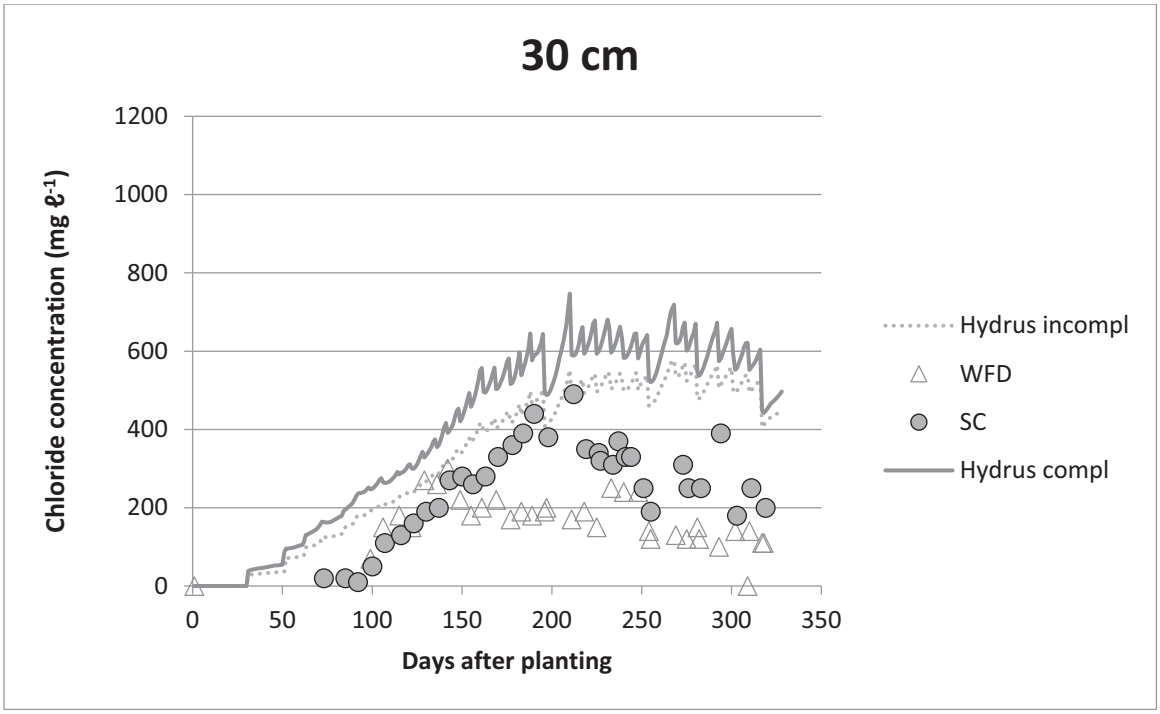
30 cm
Chloride concentration (mg ℓ-1)
1200
1000
800
600
400
200
0
0
50
100
150
200
250
300
350
Days after planting
Hydrus incompl
WFD
SC
Hydrus compl

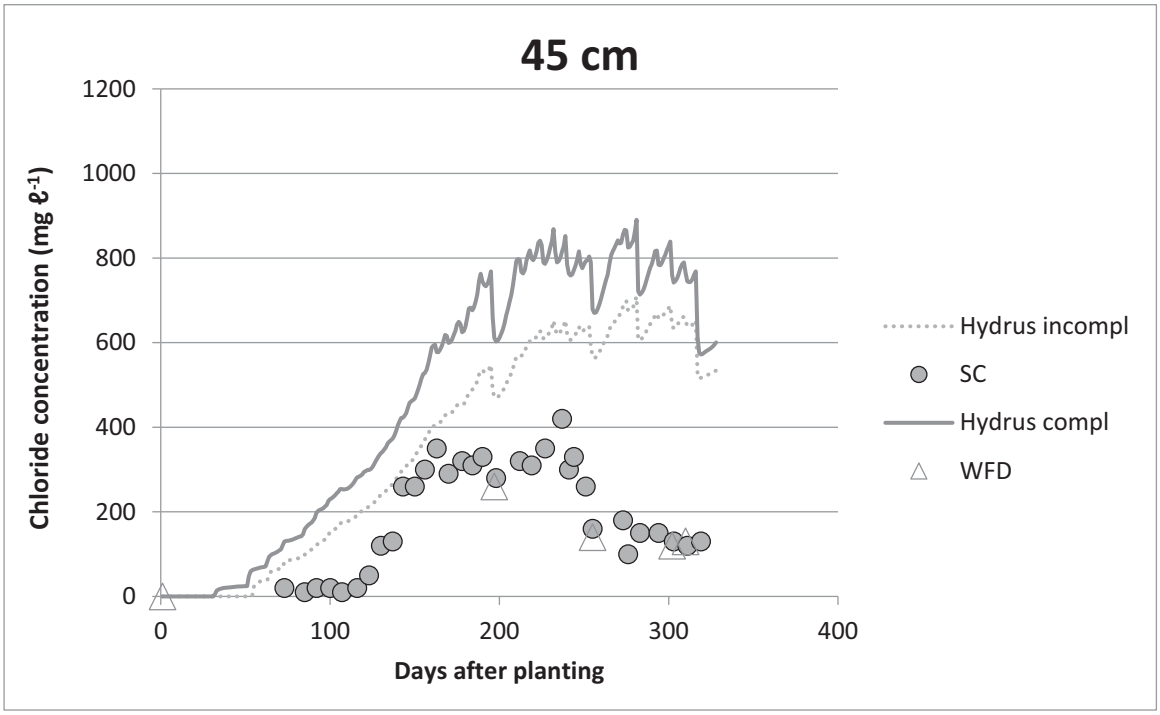
45 cm
Chloride concentration (mg ℓ-1)
1200
1000
800
600
400
200
0
0
100
200
300
400
Days after planting
Hydrus incompl
SC
Hydrus compl
WFD

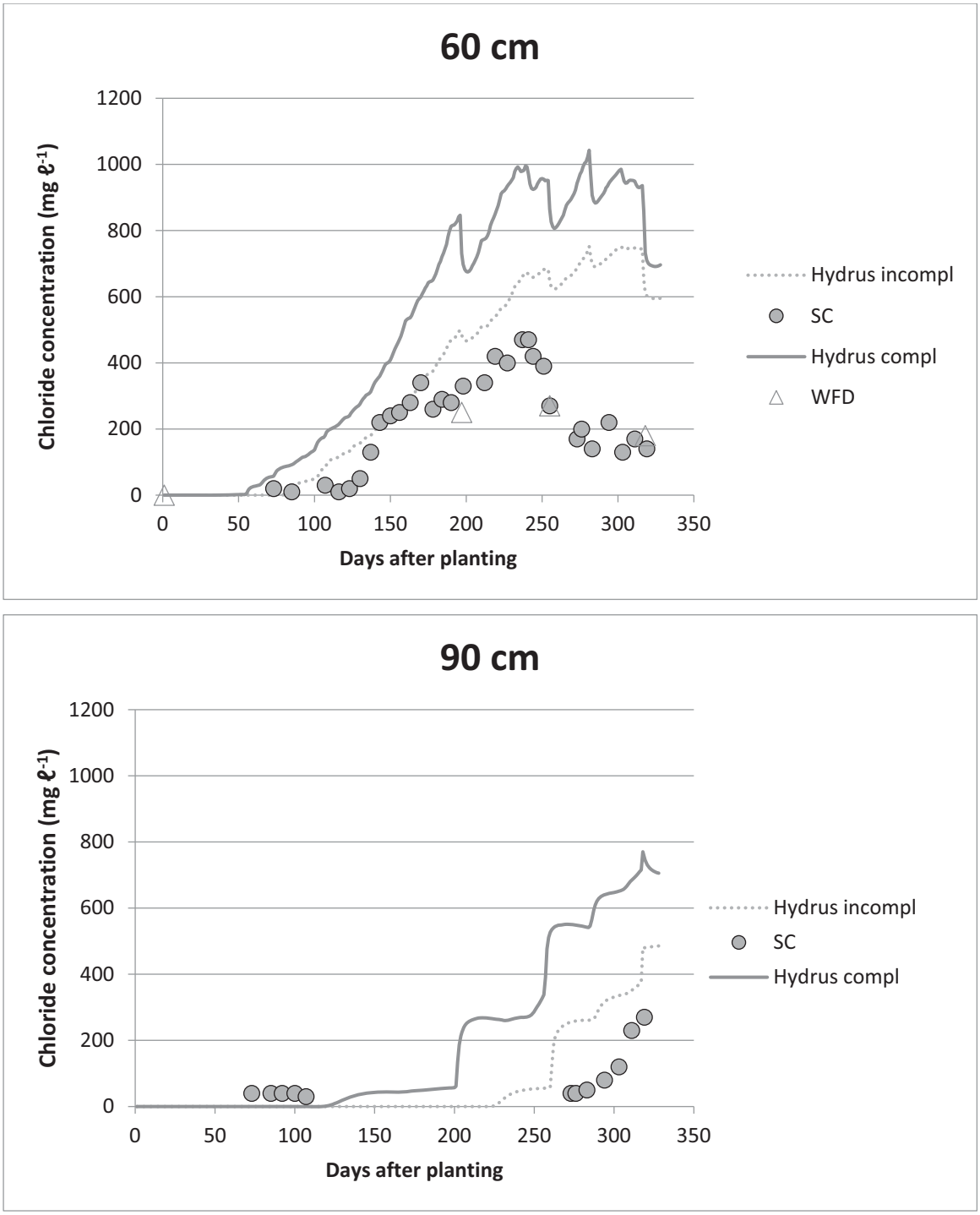

Figure 21: Measured and estimated soil water chloride (Cl-) concentrations at different depths

Compared to the irrigation concentration of 152 mg ℓ^{-1}, measured soil water Cl^- concentrations reached a peak of around 500 mg ℓ^{-1} at the 0.30, 0.45 and 0.60 m depths. The highest Cl^- concentration at 0.90 m was observed at the end of the trial at 270 mg ℓ^{-1}. By DAP 173, Hydrus-1D estimated that Cl^- added via irrigation water had reached a maximum depth of 1.075 m. Based on the mass of Cl^- added via the irrigation water up until DAP 173 (117 192 mg Cl^- m^{-2}) and tensiometer soil water potential converted to a volumetric water content for the 1.075 m depth, it was estimated that there would be an average Cl^- concentration of 703 mg ℓ^{-1} (Figure 22). The Hydrus-1D estimated concentrations were lower than this

average, with a peak Cl^- concentration of 643 mg ℓ^{-1} at the 0.53 m depth. Wetting front detector and SC concentrations were quite a bit lower, and peak concentration for the SC data was at the 0.30 m depth at 360 mg ℓ^{-1} (51% of mass balance value and 67% of Hydrus 1-D estimate for that depth). This mass balance calculation backs-up the findings with Hydrus-1D that SC and WFD concentrations are considerably lower than the concentrations expected at those depths. One reason for the difference between the mass balance estimated concentration and the Hydrus concentration could be inaccurate estimates of volumetric water content at the various depths. High water contents would have given lower concentration estimates closer to those of Hydrus.

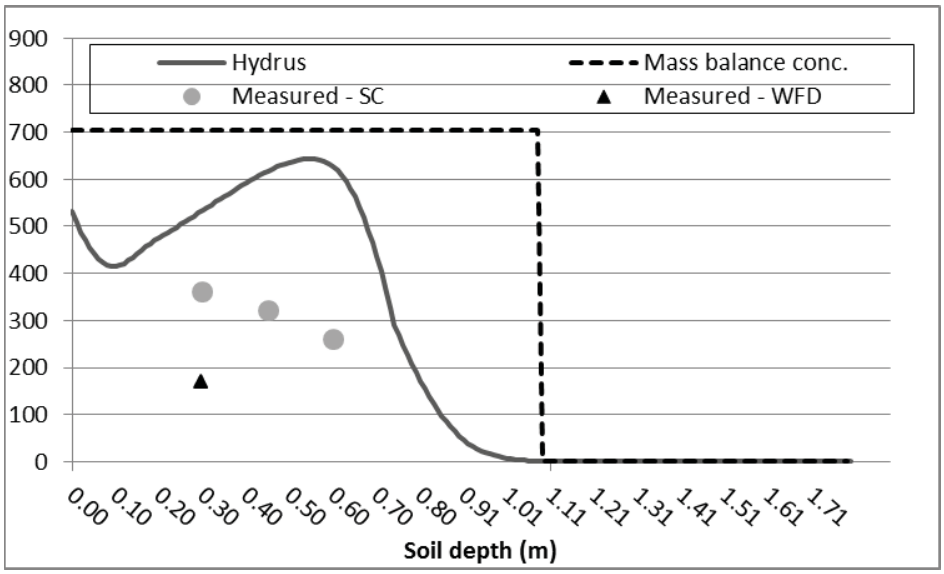

Figure 22: Mass balance and Hydrus-1D estimated chloride (Cl-) concentrations and measured values from soil water samplers [suction cups (SC) and wetting front detectors (WFD)] 173 days after planting

Simulating incomplete solute mixing in Hydrus 1-D resulted in Cl^- concentrations more closely matching what was measured, but simulated values were still consistently much higher than measured. Measured and simulated breakthrough of Cl^- into a specific soil layer were more closely correlated when incomplete solute mixing was simulated in Hydrus 1-D as opposed to complete mixing, potentially indicating the importance of this process in this soil. Inaccurate simulation of soil water content is not attributed to differences in measured and simulated Cl^- concentrations – Hydrus 1-D generally simulated higher water content than was measured by the sensors. Had these values been even more closely aligned then simulated concentrations would have been even higher in that case.

Considering the soil water tension threshold at which WFDs (approximately 3 kPa) and suction cups (somewhere around 40-70 kPa) sample, and the associated soil water content, it is clearer to understand how sampling is biased towards the larger, more dilute pore volumes (Figure 23). In addition to diffusion, root water uptake while excluding Cl^- will lead to a concentrating effect in the smaller pores which can occur until permanent wilting point (often associated with a soil water tension of 1500 kPa). Theoretical data for such concentrating of Cl^- in response to soil wetting followed by root extraction is shown in Figure 23. Assuming no change in the mass of Cl- present and instantaneous mixing of Cl^-

between all pores, a concentration under very wet conditions as sampled by a WFD could be 436 mg ℓ^{-1}, then increase to 641 mg ℓ^{-1} as the soil dries out to a tension of 60-70 kPa, and further increase to 908 mg ℓ^{-1} as the soil dries out to permanent wilting point (Figure 23). But this will depend on the history of the solute application, if coming from irrigation water via macropores above, higher initial concentrations in pore sampled by WFDs followed by SCs. If originating from smaller pores such as NO3 from SOM mineralisation, higher concentrations in micropores then those sampled by SCs followed by WFDs. This has implications on how data used – not just device but also the history of the solute application.

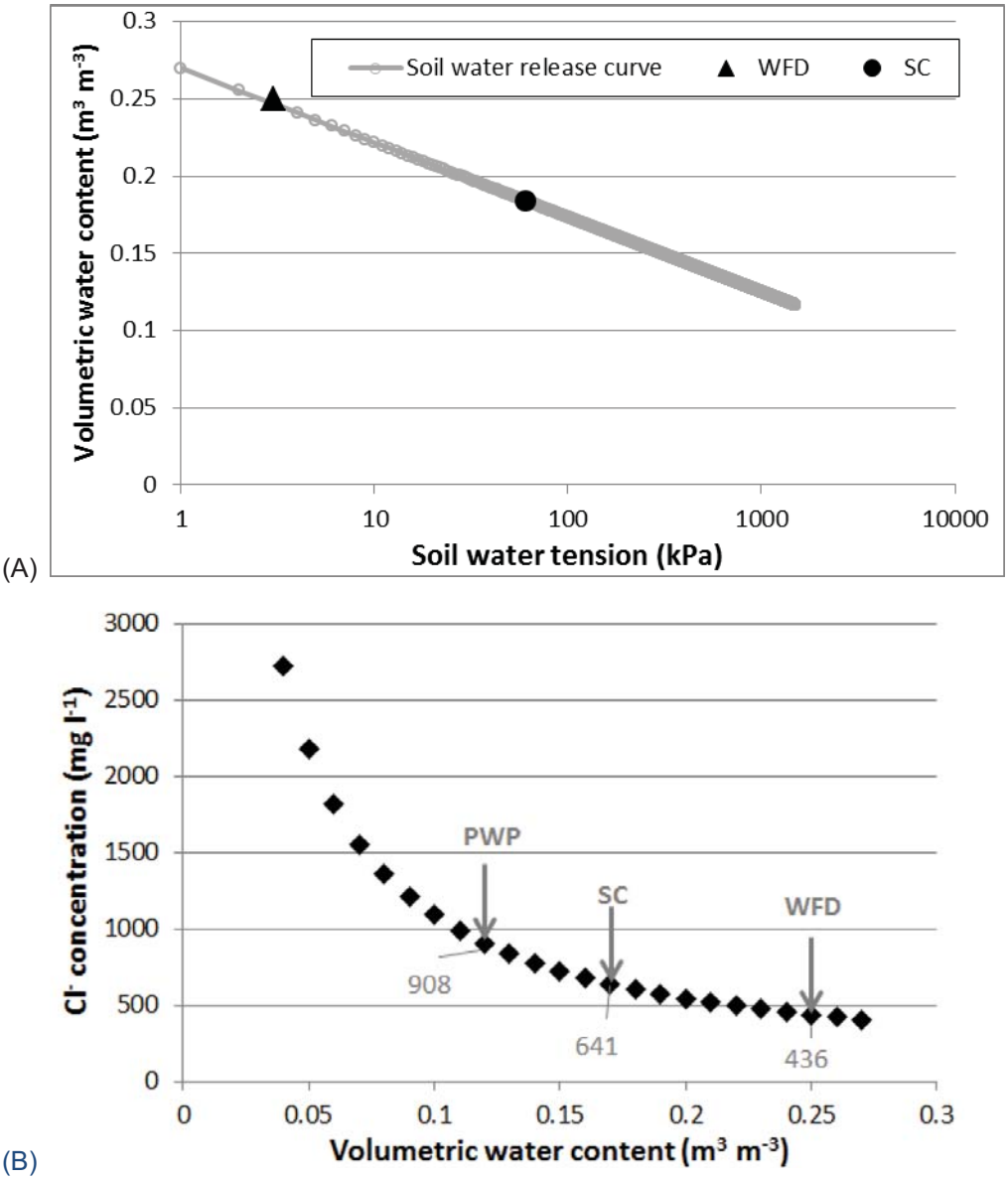

Figure 23: Soil water retention curve indicating at what volumetric water content suction cups (SC) and wetting front detectors (WFDs) are theoretically sampling, and (B) theoretical curve showing the expected chloride (Cl-) concentration at declining soil water

5.3.3 Estimated plant NO_3^- uptake and suction cup concentrations

Based on daily transpiration estimates and leaf N content at harvest events (data not shown), passive soil water NO_3^- uptake concentrations were estimated to be between 170-551 mg ℓ^{-1}, with an average of 300 mg ℓ^{-1}. These concentrations match suction cup concentrations over the same time periods for the 0.30 and 0.45 m depths, whereas for the 0.15 m depth, suction cup concentration were much lower than predicted passive uptake concentration.

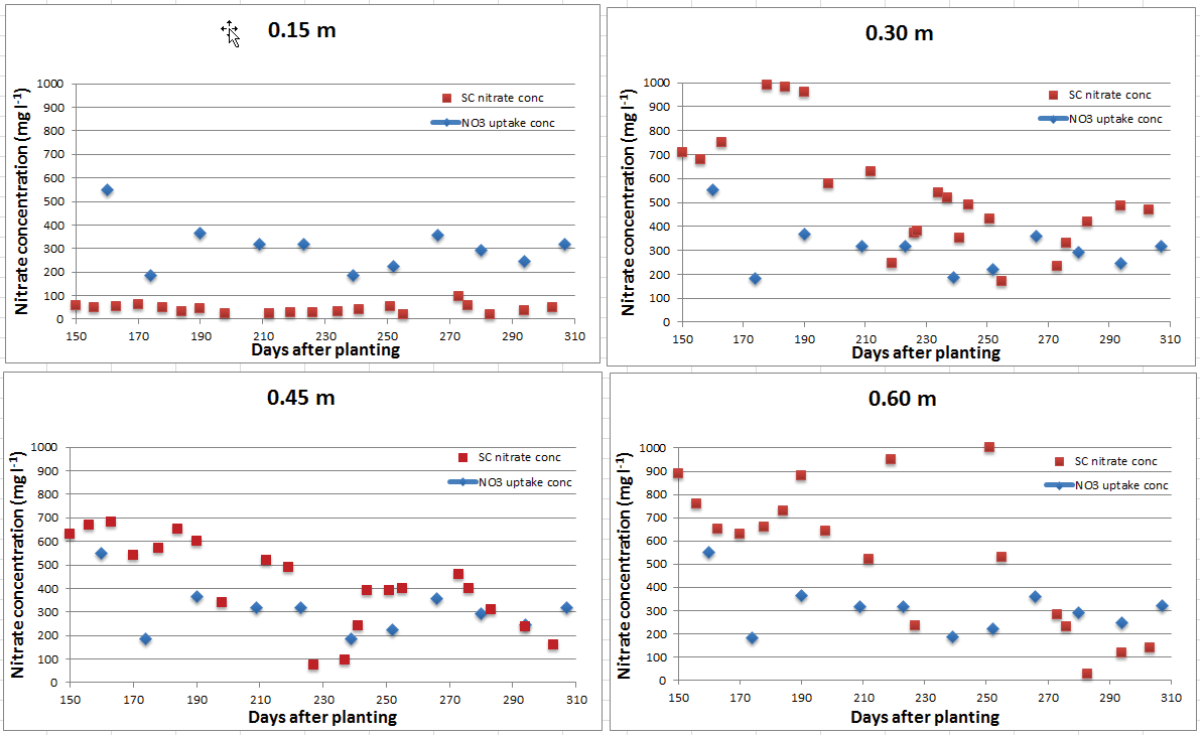

Figure 24: Comparison of estimated nitrate (NO_3^-) uptake concentration for Swiss chard and concentrations measured from suction cups at 0.15, 0.30, 0.45 and 0.60 m depths

5.4 Conclusions

In our study, soil water Cl^- concentrations in SC and WFDs were consistently lower than what was simulated by the model. The magnitude of differences for both Cl^- and NO_3^- measured in SCs versus WFDs changed over the experiment, and behaviour was also different for the two anions (small differences between SC and WFD Cl^-, but large differences between SC and WFD NO_3^- concentrations initially), which we attribute to the Cl^- being added from the top via the irrigation water, compared to the NO_3^- originating from newly mineralised soil organic matter in the smaller soil pores and slowly diffusing into the larger pores. In addition to uncertainty regarding the bias of samplers to sample certain soil pores, we also caution that the history of the wetting and solute addition pattern will influence concentrations sampled by such devices relative to the average concentration across all pore volumes.

5.5 References

BRANDI-DOHRN, F.M., HESS, M., SELKER, J.S. & DICK, R.P. (1996) Field evaluation of passive capillary samplers. Soil Science Society of America Journal 60(6), 1705-1713.

CORWIN, D., WAGGONER, B. & RHOADES, J. (1991) A functional model of solute transport that accounts for bypass. Journal of environmental quality 20(3), 647-658.

FLÜHLER, H., DURNER, W. & FLURY, M. (1996) Lateral solute mixing processes—A key for understanding field-scale transport of water and solutes. Geoderma 70(2-4), 165-183.

MA, L., SCOTT, H., SHAFFER, M. & AHUJA, L. (1998) RZWQM simulations of water and nitrate movement in a manured tall fescue field. Soil science 163(4), 259-270.

ŠIMŮNEK, J., VAN GENUCHTEN, M.T. & ŠEJNA, M. (2008) Development and applications of the HYDRUS and STANMOD software packages and related codes. Vadose Zone Journal 7(2), 587-600.

STIRZAKER, R. (2003) When to turn the water off: scheduling micro-irrigation with a wetting front detector. Irrigation Science 22(3-4), 177-185.

VAN DER LAAN, M., STIRZAKER, R., ANNANDALE, J., BRISTOW, K. & DU PREEZ, C. (2010) Monitoring and modelling draining and resident soil water nitrate concentrations to estimate leaching losses. Agricultural Water Management 97(11), 1779-1786.

VAN DER LAAN, M., STIRZAKER, R.J., ANNANDALE, J.G., BRISTOW, K.L. & DU PREEZ, C. (2011) Interpretation of electrical conductivity measurements from ceramic suction cups, wetting front detectors and ECH2O-TE sensors: short communications. South African Journal of Plant and Soil 28(4), 244-247.

WEIHERMÜLLER, L., SIEMENS, J., DEURER, M., KNOBLAUCH, S., RUPP, H., GÖTTLEIN, A. & PÜTZ, T. (2007) In situ soil water extraction: a review. Journal of environmental quality 36(6), 1735-1748.

6 MEASURING AND MODELLING NITROGEN USE EFFICIENCY AND LEACHING FROM WHEAT CROPPING SYSTEMS

T. Mangwende, M. van der Laan, G. Hall and J.G. Annandale
Department of Plant and Soil Sciences, University of Pretoria, Pretoria 0002, South Africa

6.1 Introduction

Nitrogen (N) is the most applied element in crop production (Raun and Johnson, 1999; Silgram and Shepherd, 1999; Smil, 1999). The cereal crops maize (*Zea mays* L.), wheat (*Triticum aestivum* L.) and rice (*Oryza sativa* L.) are the world's most produced crops and account for most of the applied N (Ladha et al., 2005). Although cultivars suited for high N rates have been bred, they still fail to recover and utilise all the applied N (Raun and Johnson, 1999; Smil, 1999). Hence, N losses have to be managed, as farming activities have often resulted in declining water quality and eutrophication, although it is still unclear on exactly how these activities contribute to non-point source (NPS) pollution to aquatic systems (Rossouw and Görgens, 2005; Görgens et al., 2012). Nitrogen from cultivated land is lost through runoff, leaching, volatilisation and denitrification. Considering all ways that N can be lost, N leaching is considered among the major pathways in which it is lost from the soil (Delgado et al., 2006; Sainju et al., 2016), and the main cause of groundwater pollution with nitrate (NO_3^-) (Gheysari et al., 2009). Therefore, leaching in cultivated lands has to be quantifiable, so as to find mitigatory measures.

Nitrogen leaching has been measured using various types of lysimeters, though with limited success. Martin et al. (2001) defined a lysimeter as any device used to measure and study water or solute movement in the soil profile. Commonly, two main types of lysimeters are used, which are: passive tension (for example, wetting front detectors) and active tension (for example, suction cups or wick tension lysimeters). Despite the various types of lysimeters that are in use, there is still no widely acceptable and reliable method used to quantify N leaching accurately (Van der Laan et al., 2009; Van der Laan et al., 2014). The major challenge is that to either estimate or calculate N leaching, N concentration and flux are required (Van der Laan et al., 2010), with flux being challenging to measure and high uncertainties surrounding the measured pore water NO_3^- concentrations. Previously, several studies conducted using suction cups failed to fully estimate solute flux accurately (Gee et al., 2009; Van der Laan et al., 2009).

Suction cups and weighing lysimeters are most commonly used in solute movement studies (Martin et al., 2001; Fisher, 2012; Yang et al., 2014). Field weighing lysimeters are usually expensive to install and maintain (Bowman et al., 2002), and they are bulky and permanently fixed which limit their application. Besides being flexible and portable, suction cups and wick tension lysimeters, like ceramic cups and commercial drain gauges (for example, Decagon G3 drain gauge), provide cheaper alternatives, as they can be used at several research sites to measure water drainage and estimate N leaching. A commercial drain gauge has now been designed to measure both the solute concentration

and flux, but its accuracy needs to be ascertained. Therefore, further testing of the equipment is essential.

Poor nitrogen (N) recovery, a ratio of N uptake versus N applied, in annual crops of 50% of the applied fertilizer is often reported in literature (Baligar et al., 2001; Fageria and Baligar, 2005; Foyer et al., 2016). Low N recoveries are linked to increasing N losses that will not only raise production costs, but also enhance the risk of N pollution. Therefore, ways to increase N recovery and reduce N losses to the environment must be devised. In commercial agriculture, N supply is usually dominated by applied N from fertilisers and often supplemented by soil organic matter mineralisation. If the contribution of both soil organic N mineralisation or the applied fertiliser can be precisely quantified, N recovery can be improved by adequately meeting the plant N demand in space and time which minimises excess N in the root zone.

Timing N applications to meet plant N demand and uptake will lead to better N management. But given the dynamic nature and behaviour of N in the soil, it makes the quantification of various N sources difficult to determine (Dobermann, 2005; Fageria and Baligar, 2005; Dawson et al., 2008; Edmonds et al., 2009), or even quantify the contribution of each source when calculating fertiliser N use efficiency (FNUE) (Moll et al., 1982). Despite considerable research directed to improve N management by minimising N losses in agro-ecosystems, the progress has been minimal (Gardner and Drinkwater, 2009).

In order to understand and quantify the contribution of various N sources, stable isotopes can be used to trace various N sources and their fate on various field crops (Bedard-Haughn et al., 2003). Therefore, ^{15}N natural abundance ($\delta^{15}N$) analysis account for the small differences of ^{14}N:^{15}N ratio between sources and sinks in the soil, water and plant, and can be calculated using Equation 3.1. The natural stable ^{15}N abundance has been used on several N studies (Awiti et al., 2008; Wei et al., 2013; Busari et al., 2016), yet $\delta^{15}N$ use is still limited compared to carbon (C) isotopes studies due to analytical problems and complexity of the N cycle (Hobbie et al., 2000; Adams and Grierson, 2001; Wienhold, 2007). The difference in $\delta^{15}N$ is caused by isotope fractionation in soil N processes which are influenced by soil microbes that prefer lighter ^{14}N to heavier ^{15}N in enzymatic regulated N transformations within the soil profile (Mordelet et al., 1996; Kriszan et al., 2007; Nakamura et al., 2012; Wei et al., 2013). Commonly, all the enzymes involved in the N transformation discriminate ^{15}N except for nitrogenase which is involved in N fixation and located in legume nodules (Adams and Grierson, 2001). As a result of ^{14}N preference, the soil $\delta^{15}N$ become enriched and leaves a signature in the soil (Handley and Raven, 1992), so it can provide a basis for monitoring ^{15}N abundance as a tracer of soil N processes and sources (Choi et al., 2003; Wei et al., 2013).

The purpose of this study was to evaluate and compare different techniques that measure or estimate NO_3-N leaching load. Several techniques that were evaluated include: lysimeters, stable isotopes, conservative tracers and modelling. The first objective was to evaluate the performance of a drain gauge in measuring drainage and NO_3-N leaching against a weighing lysimeter, and the second objective was to determine the fertiliser N use efficiency (FNUE) in a wheat (*Triticum aestivum* L.) cropping system.

Fertiliser-NUE determination was important because there was a need to quantify N uptake from applied fertiliser, and estimate the amount that would potentially leach out of the root zone. Third and fourth objective was to quantify the potential N leaching using conservative tracer, and to evaluate and validate the performance of APSIM after calibration.

6.2 EXPERIMENT 1: EVALUATING THE PERFORMANCE OF A COMMERCIAL DRAIN GAUGE AGAINST A FIELD WEIGHING LYSIMETER TO MEASURE DEEP DRAINAGE AND NITROGEN LEACHING

In this study, the performance of a commercial drain gauge (G3) in measuring drainage and nitrate-nitrogen (NO_3-N) leaching was compared against a weighing lysimeter by assessing drainage outputs under an irrigated winter wheat crop.

6.2.1 Materials and Methods

The experiment was conducted at the University of Pretoria Hatfield Experimental Farm (25°44'58.53'' S, 28°15'31.60''E, and elevation 1371 m). The trial site, measured 400 m^2 with several installed instruments. After repairing the weighing lysimeters, new equipment was installed consisting of: a rain gauge (Texas Electronic Inc., Dallas, Texas, USA) and a new load cell (Load Cell Services, South Africa), for each lysimeter. A commercial drain gauge (Decagon G3 drain gauge, Decagon Devices, Inc., Pullman, USA) was purchased in August 2015, and was installed five metres away and to the east of the field weighing lysimeters. The base of the drain gauge divergence control tube (DCT) was inserted into the soil in such a way that the measurement depth was at 0.9 m. The DCT was installed using the undisturbed soil core approach.

In addition, various sensors were also inserted in specific places within the lysimeter trial. Four MPS-6 Decagon soil water potential and temperature sensors, four GS3 soil water content, soil temperature and electrical conductivity sensors and four SPES20 suction cups (UMS Germany) were installed at depths of 0.15, 0.30, 0.50, 0.70 m in the two lysimeters. Similarly, suction cups and capacitance water content sensors were installed close to the drain gauge, two meters away and to the north from the weighing lysimeters. Fibre-glass side panels were installed on all sides surrounding the drain gauge to a depth of 0.30 m with 0.10 m left protruding out of the ground to prevent lateral flow and runoff.

The entire trial site, weighing lysimeter and drain gauge, had the same agronomic management practises. Before planting, soil samples were taken and analysed and used to formulate a fertiliser recommendation for the site. Optimum fertiliser was applied at a rate of 200 kg N ha^{-1} and 25 kg P ha^{-1} based on soil analysis results. Wheat cultivar PAN 3400 was planted on 30 June 2016. Plots were kept weed free by applying bromoxynil (3,5-Dibromo-4-hydroxybenzonitrile) at 1.0 ℓ ha^{-1}, MCPA (2-methyl-4-chlorophenoxyacetic acid) at 2.2 ℓ ha^{-1}, and pinoxaden (8-(2,6-diethyl-p-tolyl)-1,2,4,5-tetrahydro-7-oxo-7H-pyrazolo[1,2-d][1,4,5]oxadiazepin-9-yl 2,2-dimethylpropionate) at 0.8 ℓ ha^{-1} 43 days after planting (DAP), which were all tank mixed and applied at once. During the growing season and after scouting, the plots were also kept pest and disease free. Pyrinex 480 EC (chlorpyrifos) was applied at 2.0 ℓ ha^{-1} to control bollworms (*Helicoverpa armigera*) and aphids (*Diuraphis noxia*), and orius 250 EC

(1,3 dichloropropene) was applied at 0.75 L ha^{-1} to control powdery mildew (*Erysphe gramis f.sp tritici*). High density drip irrigation with lines and emitters spaced at 0.40 m was installed. The soil moisture sensors placed at 0.15 and 0.30 m were used to schedule irrigation, and 21 irrigation cycles were applied during the study. The crops were irrigated when plant available water was reduced to 50%. The frequency and amounts applied for each irrigation cycle are provided in Figure 25.

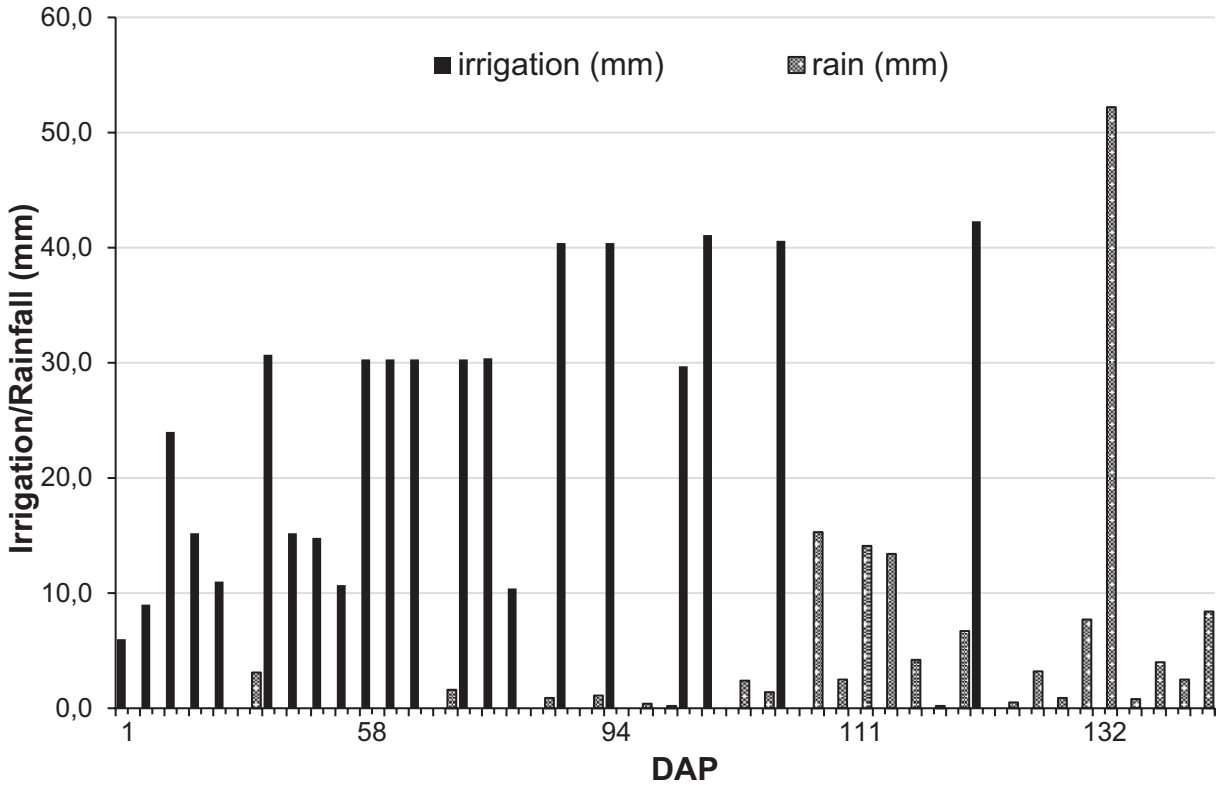

Figure 25: Irrigation applied and rainfall received (mm) on the lysimeter trial from 1 July to 18 November 2016 [1 to 141 days after planting (DAP)]

Weather data was collected using an automatic weather station (AWS) positioned at the University of Pretoria Experimental Farm, which was 50 m away from the trial site. The weather variables recorded were: maximum and minimum air temperature (°C), maximum and minimum relative humidity (%), average wind speed (m s^{-1}), solar radiation (MJ m^{-2}) and rainfall (mm). The weather data are summarised in Mangwende (2018).

Soil water samples were collected at regular intervals from the drainage gauge, lysimeter drainage and suction cups (approximately 24 hours after every irrigation cycle or rainfall event). The water samples were analysed for NO_3-N concentration using RQeasy Nitrat Reflectometer (Merck, Darmstadt, Germany).

6.2.2 Results

Daily drainage (mm) and soil water content ($m^3\ m^{-3}$), and NO_3-N levels (mg ℓ^{-1}) after irrigation are presented in Figure 26, and averaged weather data are presented in Table 13. Generally, the weather conditions were suitable for growing wheat, despite the relatively high maximum temperatures recorded in October, and the grain yield was not affected with the crop producing 8.2 t ha^{-1}.

Table 13: Monthly weather data from July to November 2016.

Month	Average Maximum Air Temp (°C)	Average Minimum Air Temp (°C)	Average Daily Wind Speed (m s^{-1})	Cumulative Solar Radiation (MJ m^{-2})	Cumulative ET_o[a] (mm)	Cumulative Rainfall (mm)	Average Daily VPD[b] (kPa)
Jul	20.6	4.2	1.5	339.8	84.7	3.1	1.0
Aug	25.1	6.6	1.5	427.4	115.1	0.0	1.5
Sep	27.8	12.3	2.1	425.8	143.7	3.6	1.9
Oct	30.1	14.3	2.3	526.1	177.4	60.8	2.1
Nov	28.7	15.6	2.1	478.4	148.5	105.6	1.6

[a]ET_o – evapotranspiration, [b]VPD – vapour pressure deficit

Figure 26 shows the daily drainage data from the drain gauge and lysimeters 1 and 2 with three distinct peaks. The drain gauge measured higher drainage than lysimeters 1 and 2, as shown by the three peaks, between 15 and 50 DAP. For the second drainage event, all the lysimeters had similar drainage, but lysimeter 1 measured slightly less drainage.

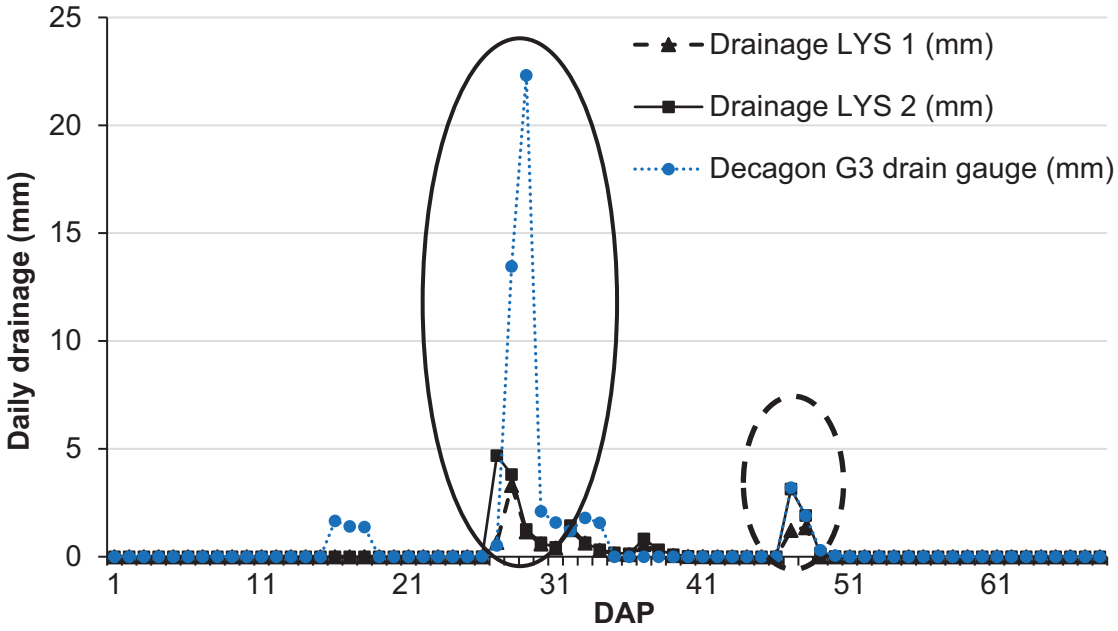

Figure 26: Daily drainage from lysimeter 1 and 2 (LYS 1 and 2) and the drain gauge measured from 1 to 70 days after planting (DAP). The big peak in the solid line ellipse is enlarged on Figure 27a, whereas another peak in the dashed line ellipse is enlarged on Figure 2.3b.

From 26 to 34 DAP, both lysimeters recorded drainage, but the drain gauge measured the highest draining volume, followed by lysimeter 2 as shown in Figure 26a. As can be seen in Figure 27b, from 46 to 51 DAP all the lysimeters drained, and the drainage patterns were similar from both lysimeters and the drain gauge. Related draining patterns can be attributed to all systems reaching saturation point thereby allowing both lysimeters and the drain gauge to drain. On all the draining days, the amounts that drained were not significantly different, except on 47 DAP. The reason for this difference is not known.

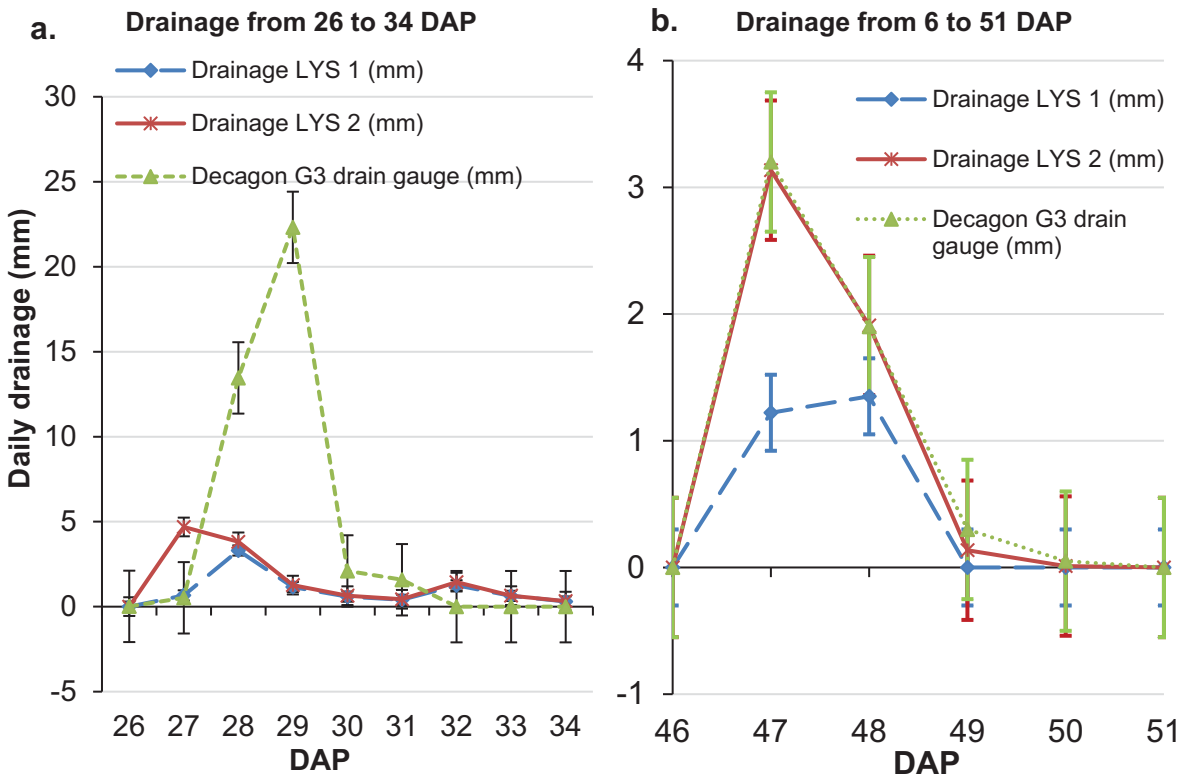

Figure 27: Daily drainage from lysimeters 1 and 2 and the drain gauge measured from (a) 26 to 34 days after planting (DAP) and (b) 46 to 51 DAP

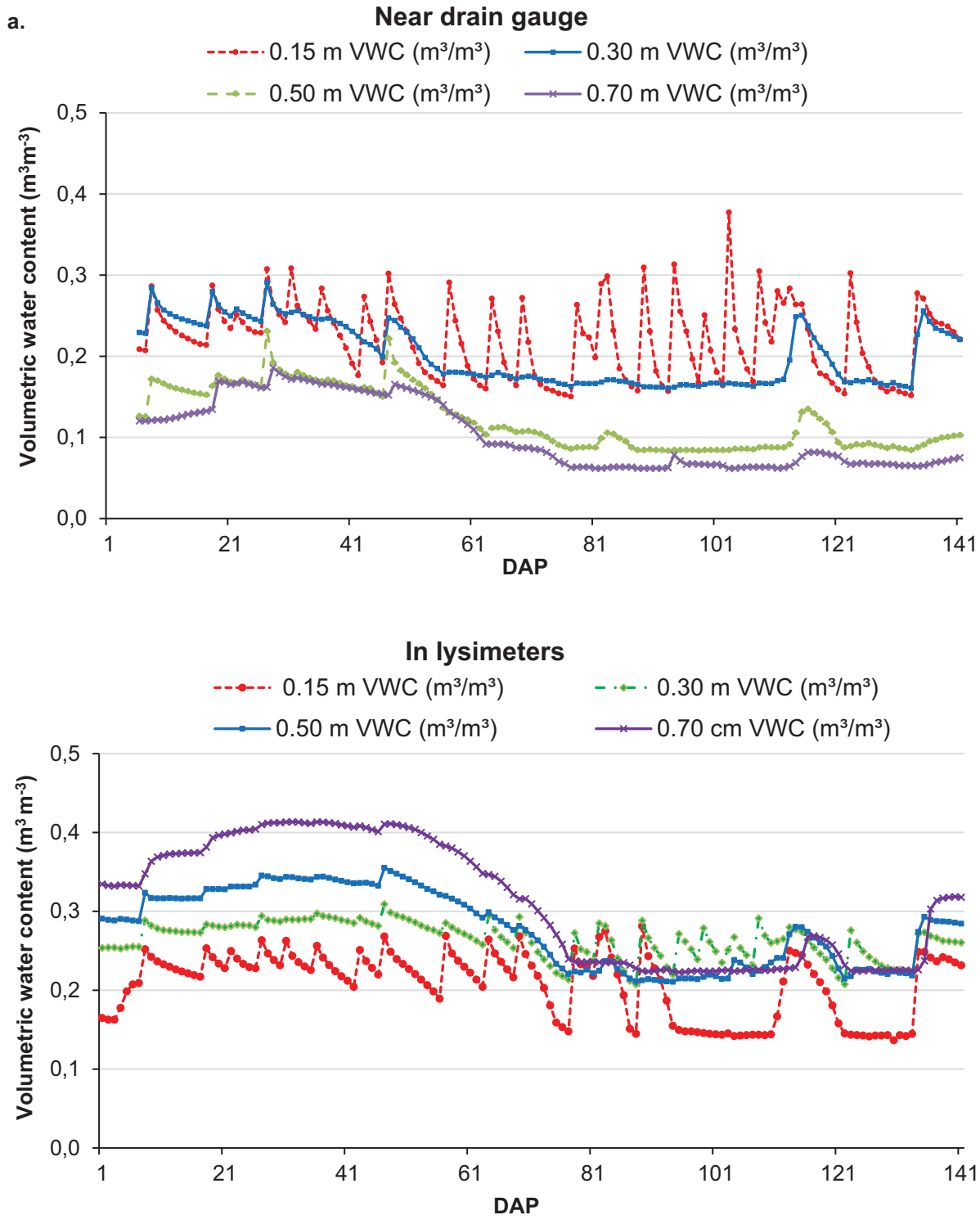

Figure 28: Daily volumetric water content ($m^3\ m^{-3}$) data collected using capacitance sensors installed at 0.15, 0.30, 0.50 and 0.70 m depths in the soil profile for (a) the drain gauge and (b) lysimeters 1 and 2 (averaged) from 1 to 141 days after planting (DAP)

Figure 27a shows volumetric water content data measured close to the drain gauge. At a depth of 0.15 m, water content was fluctuating rapidly because of irrigation and crop water uptake, but this layer remained the wettest. Deeper in the soil profile from 0.30 to 0.70 m, the soil content decreased with

depth. Whereas, water content recorded in the lysimeters at various depths (Figure 28b) is inverted when compared to Figure 28a (much wetter with depth). The soil water content inversion clearly shows that the bottom layer of the lysimeter needs to be saturated before drainage can occur. In the lysimeters, at 94 to 110 DAP and 122 to 133 DAP the sensor in the 0.15 m was unresponsive. Since the data was averaged for lysimeter 1 and 2, small changes could have been evened out by averaging and lost the actual response of the sensor. In addition, the unresponsiveness could have also been caused by very dry soil conditions.

The NO_3-N concentrations collected at all depths on 18 DAP (Figure 29a) shows a different flow pattern between the drain gauge and the lysimeters. Suction cups installed close to the drain gauge had free draining soil that showed highest NO_3-N concentrations at the 0.30 m depth, but were lower at 0.50 m and lowest concentrations were at 0.70 m. However, the NO_3-N concentration measured with the lysimeter SCs was highest in the 0.15 m layer and decreased to around 100 mg ℓ^{-1} in the 0.30 m zone, and then increased at 0.50 m to about 200 mg ℓ^{-1}, declining again at 0.70 m. Although the NO_3-N concentration measured in the drain gauge was 25 mg L^{-1}, the NO_3-N was undetectable from the draining lysimeters (the RQeasy Nitrat Reflectometer cannot measure NO_3-N concentrations of less than 1.1 mg ℓ^{-1}). Higher soil NO_3^-N concentrations 18 DAP are attributed to fertiliser application at planting and the mineralisation of the disturbed soil, but this is shown to be reduced intensely 48 DAP due to a bigger crop with deeper roots and increased plant N uptake. Generally, the NO_3-N was moving slower on the lysimeters compared to the drain gauge region.

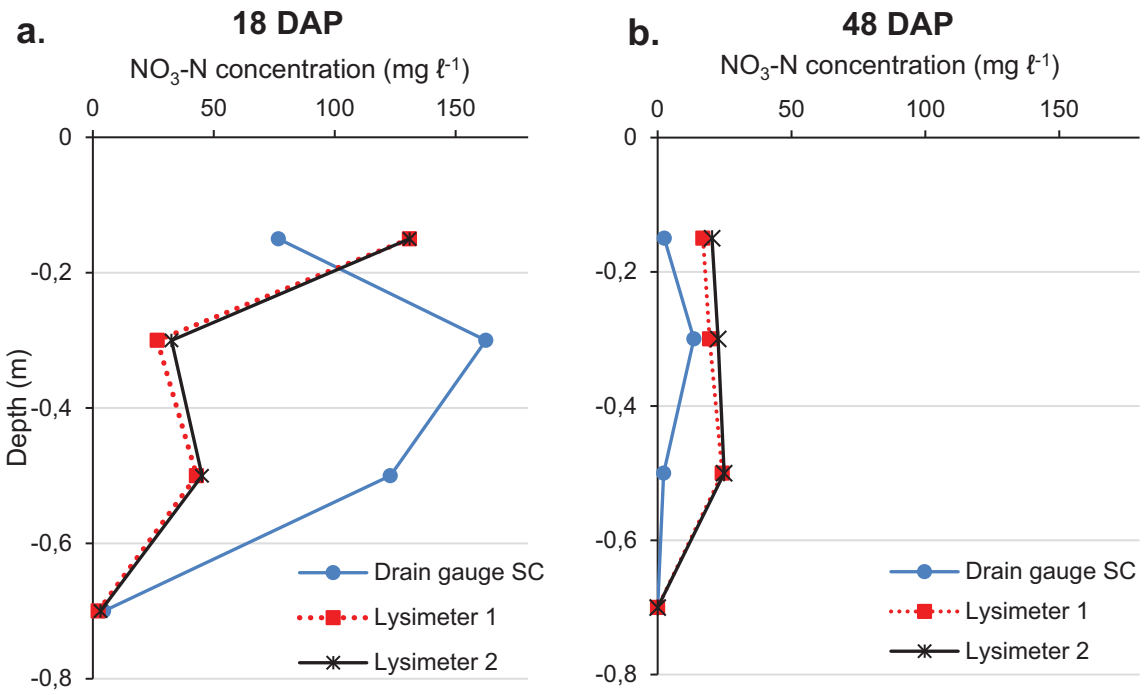

Figure 29: Suction cup nitrate (NO_3^-) concentrations measured at 0.15, 0.30, 0.50 and 0.70 m depths on (a) 18 days after planting (DAP) and b. 48 DAP.

In Figure 29b, the measured NO_3-N concentrations 48 DAP near the drain gauge were low, with all levels below 10 mg ℓ^{-1}, except for the 0.30 m depth which was a bit higher. The NO_3^-N concentration measured on the lysimeters was almost similar at all depths, except for 0.70 m at which NO_3-N was undetectable. However, the NO_3-N concentrations measured in the lysimeters at 0.15, 0.30 and 0.50 m were greater than those measured above the drain gauge at these depths.

Table 14: Total drainage and leached nitrate-nitrogen (NO_3-N) from the drain gauge and weighing lysimeters.

Drainage (mm)	Total drainage (mm)	Average NO_3-N concentration (mg ℓ^{-1})	Total NO_3-N leached (kg ha^{-1})
Lysimeter 1	12.0	<1.1	<0.1
Lysimeter 2	20.0	<1.1	<0.2
Drain gauge	54.1	46.1	24.9

The drain gauge measured a total NO_3-N load of 24.9 kg ha^{-1} being leached (Table 14). The high N leaching was caused by higher drainage with higher NO_3-N concentrations on the drain gauge compared to the weighing lysimeters.

6.3 Discussion

The drain gauge water content decreased with increasing soil depth, but the trend was reversed on the lysimeters. Nitrate concentration generally increased with depth but became lower again at very deep layers on the drain gauge and the lysimeters. Overall, the water content and NO_3-N concentration distribution seem to agree with the observed draining trends.

Early drainage was only observed from the drain gauge, but it was delayed on both lysimeters. The lag in draining on weighing lysimeters was because saturated lower soil layers first needed to form before drainage could take place, which was supported with the volumetric water content data above 0.4 m^3 m^{-3}. At a depth of 0.70 m, the soil was saturated from 1 to 60 DAP. Once saturation conditions are maintained, water could have been redistributed by capillary flow, thereby maintaining relatively higher water content at 0.30 and 0.50 m depths on the lysimeters. The saturated conditions created anaerobic conditions which may have limited the loss of NO_3-N leaching, but promoted gaseous N loss as nitrous oxide (N_2O), nitrogen oxide (NO_x) and dinitrogen gas (N_2) by denitrification process (Delgado et al., 2006; Cameron et al., 2013). Increased denitrification could have caused NO_3-N concentration to be below the detectable limit of 1.1 mg ℓ^{-1} in the lysimeters. Further research is required to confirm the processes that are occurring at the bottom of the lysimeter by installing redox potential sensors.

From 26 to 34 DAP, as irrigation was constantly being applied to support increasing crop growth, significantly higher drainage was measured on the drain gauge. Higher drainage recorded in the drain gauge compared to the lysimeter can also be attributed partly to the wick and diatomaceous earth (Gee et al., 2009; Decagon Devices Inc., 2015), which created a constant suction (11 kPa) resulting in a higher drained volume. A wick hastens water movement from the divergence control tube to be collected as drainage, as it can still sample in unsaturated conditions, which would restrict prolonged saturated conditions in the bottom layer (Landon et al., 1999; Czigány et al., 2005; Weihermüller et al., 2007).

The draining water and NO_3-N concentrations discrepancy on the lysimeters suggest occurrence of by-pass flow, which occurs in most structured soils (Cresswell et al., 1992; Nye and Tinker, 2000). Since lysimeters were refilled it could have created atypical conditions allowing quick flow of water to the bottom soil layers along the side walls, when compared to an undisturbed soil core in the drain gauge divergence control tube. Quick water flow (by-pass flow) without properly wetting the top soil layers was exhibited with higher soil water content in the lysimeter bottom soil profiles, while upper soil layers remained drier. By-pass flow has been reported on lysimeter studies (Reeder 1986; Young et al., 1996; Bowman et al., 2002), and was noted to cause fast wetting of the bottom layers before the top layers become saturated. Ordinarily, water is expected to flow in the soil following tipping bucket approach, where higher soil layer must be saturated to allow moisture to move to deeper layer.

There were a few limitations for this study, mainly related to the installation and design of the weighing lysimeter. Firstly, refilling the lysimeter disturbed the soil profile which created compacted layers as it settles over years, and it permitted by-pass flow that influenced NO_3-N movement and breakdown. Secondly, both weighing lysimeters have a small draining valve, which could have restricted free drainage. Meanwhile, restricted drainage resulted in little drainage that may have caused water redistribution by capillarity in the bottom soil layers on lysimeter. In addition, there is a need to monitor the drain gauge drainage against a weighing lysimeter over several seasons or multiple years to confidently verify the performance. However, the collected data set was adequate to prove that the drain gauge is useful, and it has a big potential to measure N leaching.

6.4 EXPERIMENT 2: DETERMINATION OF NITROGEN FERTILISER USE EFFICIENCY USING STABLE ISOTOPE ANALYSES

In this study, stable ^{15}N isotope abundance in the soil at different depths and in various plant parts was evaluated, so as to determine the fate of applied fertiliser N, and to quantify FNUE in an irrigated wheat crop. Alternatively, this work provided a preliminary study to understand soil-plant N relations that will be verified by running **A**gricultural **P**roductions **S**ystem s**IM**ulator (**APSIM**), and to find a plant part with $\delta^{15}N$ values that can be used to estimate plant N% and plant $\delta^{15}N$ values essential to calculate FNUE.

6.4.1 Materials and Methods

A field trial site consisting of six plots was used for this study. The dimensions of each plot were 2.0 x 2.0 m (length x width). Only three of the six plots were fertilised, but all the plots received similar cultural practices, and they were irrigated according to crop water requirements based on capacitance sensor

measurements inserted in the soil profile at a depth of 0.15 m. The crop was irrigated when the soil water content at 0.15 m measured by capacitance sensors had reached 0.20 m^{-3}, about 50% of plant available water. The irrigation volumes applied are given in detail on Mangwende (2017), which shows dates and amount of irrigation applied on the fertilised and unfertilised plots. Total irrigation water applied was 550 and 610 mm on the unfertilised and fertilised plots, respectively. High density drip irrigation was used with drip lines and emitters spaced at 0.40 m. Soil samples were taken and analysed before planting, and used as the basis for fertiliser application. The fertilised plots received 200 kg N ha^{-1} in four equal splits, on 1, 29, 41 and 70 days after planting (DAP), of 50 kg N ha^{-1}, and 25 kg P ha^{-1} was also applied to these plots in one application at planting. Lime ammonium nitrate (LAN) with 28%N was applied to supply N, and di-ammonium phosphate (DAP) supplied both P at 10.5% and N at 3.5%. Both LAN and DAP was supplied by Omnia Fertilisers, South Africa. Wheat cultivar PAN3400 was planted on the 30th of July 2016. The plots were kept weed, pest and disease free.

A soil baseline of natural ^{15}N abundance ($\delta^{15}N$) was established from the surface at 0.00 m up to a depth of 0.80 m before planting and after harvesting. Initially, the sampling depth interval was 0.05 m from soil surface to 0.20 m, and increased to 0.20 m between 0.20 and 0.80 m depths. Each soil sample was air dried after collection, and was split into two batches each of approximately 0.05 kg after mixing and grinding lightly. The first batch was acid washed with 1% hydrochloric acid (HCL), and they were left for 24 hours to remove any carbonates on the sediment. After washing with acid, the sediment was rinsed three times with distilled water, and placed in an oven to dry for 72 hours at 60°C. The second batch was filled into 5 ml micro test tubes to wait weighing. Following drying, 65-70 mg of sediment, both acid and non-acid washed, was weighed and placed in tin capsules that were pre-cleaned in toluene for isotopic analysis. Plant samples were dried and homogenized and aliquots of 1.0 to 1.1 mg were weighed for isotopic analysis. All isotopic results were referenced to Vienna Pee-Dee Belemnite for carbon (C) isotope values, and to air for N isotope values. A laboratory running standard (Merck Gel: $\delta^{13}C$ = -20.57‰, $\delta^{15}N$ = 6.8‰, C% = 43.83, N% = 14.64) and blank sample were run after every 5 unknown samples. The reproducibility of the results was 0.05‰ for both N and C. Stable isotopic analysis ($\delta^{15}N$ and $\delta^{13}C$) was carried out using a Flash EA (1112 Series) elemental analyser coupled to a Delta V Plus stable light isotope ratio mass spectrometer via a ConFlo IV system (all equipment supplied by Thermo Fischer, Bremen, Germany), housed at the Stable Isotope Laboratory, Mammal Research Institute, University of Pretoria.

Results were expressed in delta notation using a per mille scale as follows:

$$\delta X \text{‰} = \frac{\text{Rsample}}{\text{Rstandard}} \times 1000 \qquad (3.1)$$

where $\delta X = {}^{15}N$ or ^{13}C and
R represents $^{15}N/^{14}N$ or $^{13}C/^{12}C$ respectively

Initially, LAN and DAP were analysed for stable isotope abundance and had a $\delta^{15}N$ weight average of -2.1‰, and destructive plant sampling was done at tillering, flowering and physiological maturity. Plant material was separated into roots, senesced leaves, green leaves, flag leaves, and grains depending on sampling date and growth stage. Plant samples were ground, and a sample of 1.0-1.1 mg was

weighed for each of the six plots. The plant samples were also analysed for $\delta^{15}N$ using a mass spectrometer as described previously for soil. The data were analysed using student's t-test and the means were separated using standard errors at the 95% confidence interval. A regression analysis was also performed to establish correlations between $\delta^{15}N$ values and plant N%.

Plant N derived from fertiliser (Ndff) given in Equation 3.2 was calculated using plant stable isotopes $\delta^{15}N$ values (Vose, 2013).

$$\text{Ndff} = \frac{\text{Nu} - \text{Nt}}{\text{Nu} - \frac{\text{Nf}}{n}} \qquad (3.2)$$

Where: Nu = atom ^{15}N‰ in unfertilized plants

Nt = atom ^{15}N‰ in fertilized plants

Nf = atom ^{15}N‰ in the fertilizer

n = the plant discrimination factor between ^{14}N and ^{15}N.

Assuming no discrimination between ^{14}N and ^{15}N, then n = 1 (Vose, 2013).

Generally three assumptions at root-soil interface are considered which are a) negligible fractionation occurs on plant N uptake, b) no intra-plant $\delta^{15}N$ variation occurs among plants with similar treatment, and c) whole-plant $\delta^{15}N$ do not differ significantly from the source $\delta^{15}N$ value (Evans et al., 1996).

To calculate the FNUE, Equations 3.2 to 3.5 were used.

Total N uptake (kg ha^{-1}):

$$\text{N uptake} = \frac{[\text{Yield dry matter (kg ha}^{-1}) \times \text{plant N\%}]}{100} \qquad (3.3)$$

Fertiliser uptake (kg ha^{-1}):

$$\text{Fertiliser N yield (FNU)} = \frac{[\text{N uptake (kg ha}^{-1}) \text{ x \% Ndff }]}{100} \qquad (3.4)$$

Fertiliser N use efficiency (FNUE):

$$\%\text{FUE} = \frac{\text{Fertiliser N yield}}{\text{Applied N rate}} \times 100 \qquad (3.5)$$

6.4.2 Results

Figure 30a shows the $\delta^{15}N$ values in the soil profile increased from 0.00-0.05 m to 0.20-0.40 m for both fertilised and unfertilised plots and decreased for 0.40-0.60 m and 0.60-0.80 m. At tillering, $\delta^{15}N$ values were higher than at physiological maturity for both fertilised and unfertilised plots. An exception was observed for the 0.15-0.20 m and 0.20-0.40 m depths where the fertilised plots had slightly higher $\delta^{15}N$ than unfertilised plots, but for all the other depths the unfertilised plots $\delta^{15}N$ values were always greater.

Figure 30b shows $\delta^{15}N$ values increased from 0.00-0.05 m to 0.40-0.60 m in the soil profile after harvesting for both fertilised and unfertilised plots, and decreased slightly for 0.60-0.80 m. Although $\delta^{15}N$ values at 0.20 to 0.60 m were higher slightly than the deepest layer of 0.6-0.8 m, they were not significantly different for both fertilised and unfertilised plots. When comparing Figure 30a and Figure 30b for the 0.20-0.40 m depth, the $\delta^{15}N$ values before planting were higher than values obtained after harvesting for both fertilised and unfertilised plots. The peak $\delta^{15}N$ values were in the 0.20-0.40 m layer

before planting, but this peak shifted to 0.40-0.60 m layer after harvesting which potentially indicates movement of N to deeper soil layers, or microbial processes discriminating against ^{15}N at these depths.

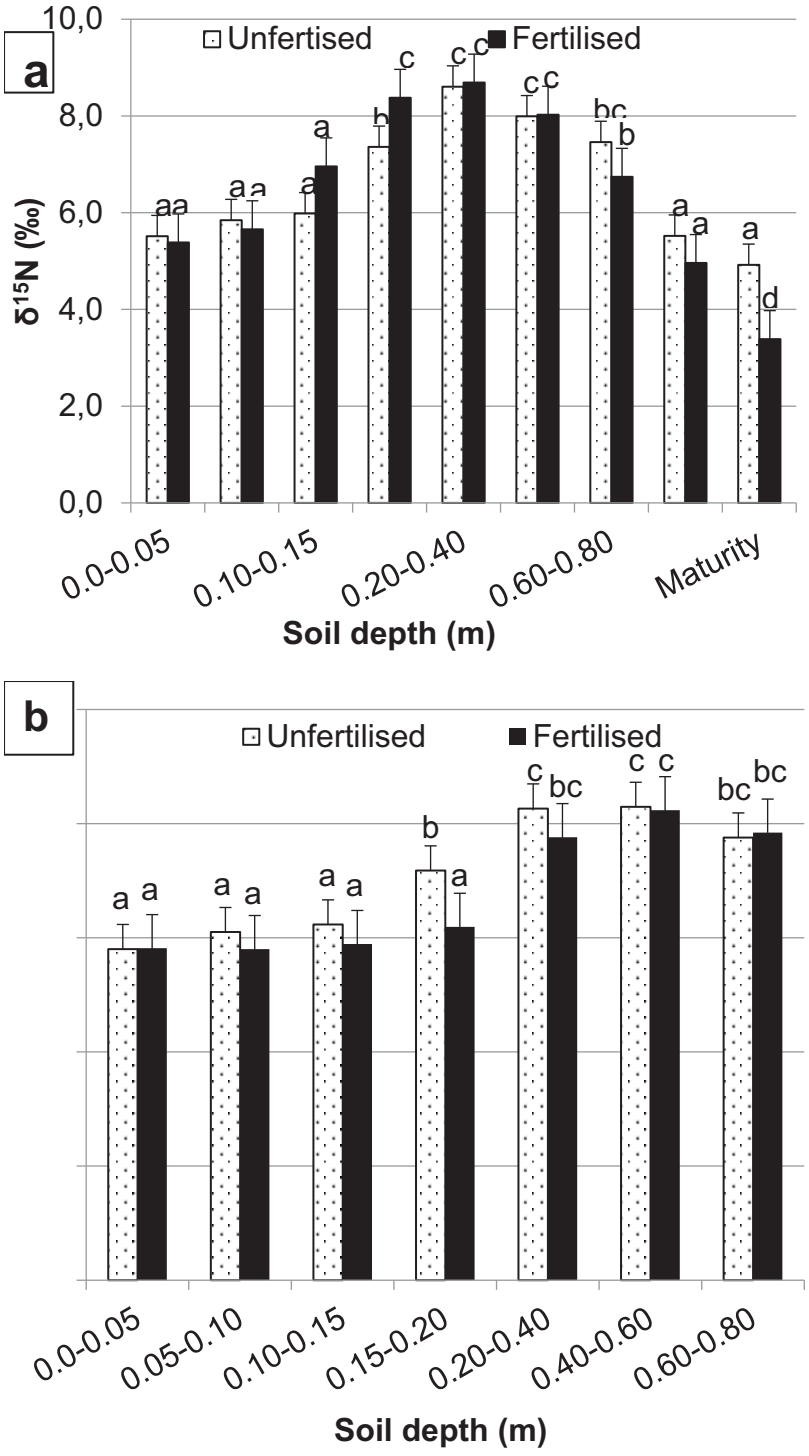

Figure 30: The $\delta^{15}N$ values for soil samples taken from fertilised and unfertilised plots a. before planting and b. after harvesting. Residual soil bound on plant roots after pulling out the plants at tillering and physiological maturity was also analysed and the values are shown on Figure 30a.

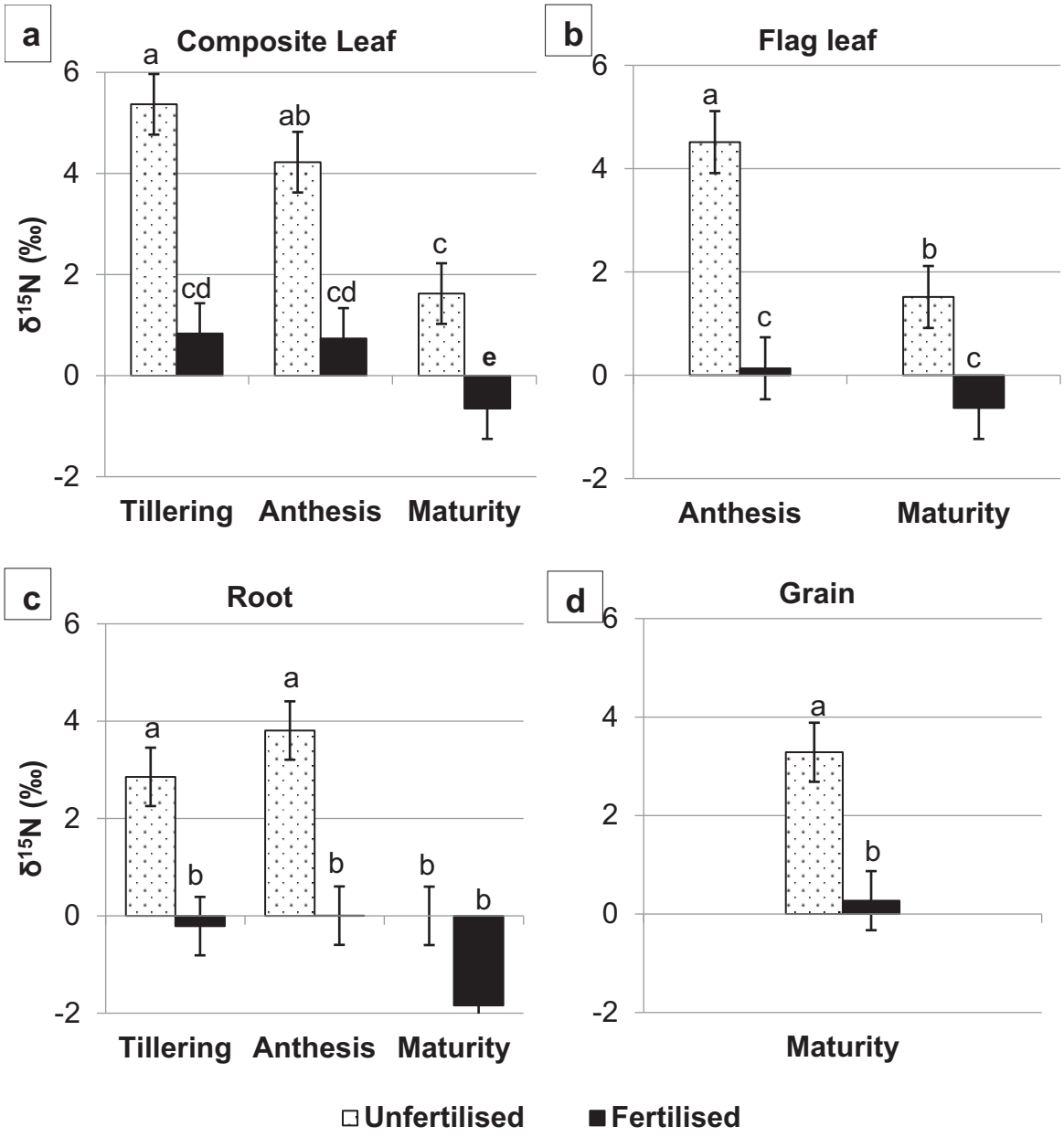

Figure 31: The $\delta^{15}N$ values for (a) composite leaf, (b) flag leaf, (c) root and (d) grain. The wheat was harvested at tillering, anthesis and maturity from the fertilised and unfertilised plots and separated into different plant parts before analysis.

In Figure 31 there was a clear distinction of $\delta^{15}N$ values on the fertilised and unfertilised plots. The $\delta^{15}N$ values on unfertilised plots were always enriched significantly higher than on fertilised plots for all the plant parts that were considered. The roots on the fertilised plots were depleted (low $\delta^{15}N$ values) than unfertilised plots and in all other plant parts. Figure 30a and Figure 30b shows $\delta^{15}N$ values decreasing as the plants gets old, however in the roots the trend of $\delta^{15}N$ values increases as the plants mature on unfertilised plots and more depleted on fertilised plots.

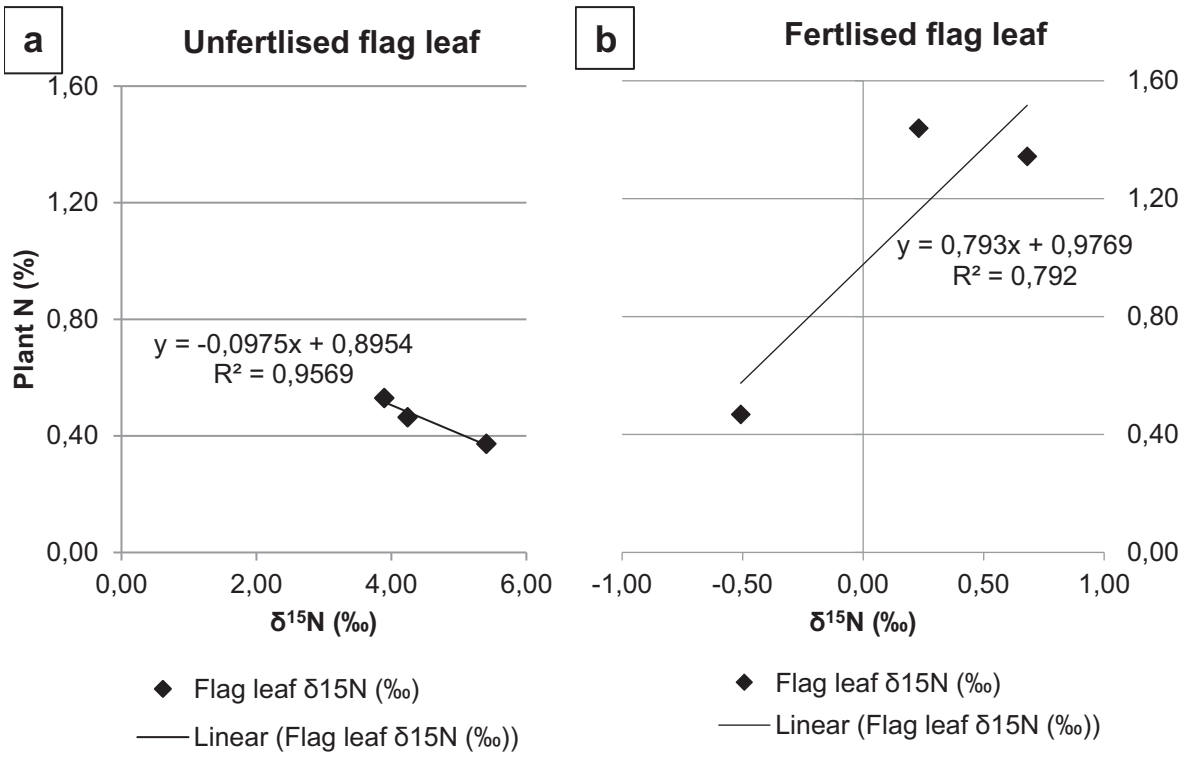

Figure 32: The correlation between the total plant nitrogen (N) and flag leaf $\delta^{15}N$ for (a) unfertilised plots and (b) fertilised plots at anthesis.

Figure 32 and Figure 33 shows the correlation between the flag leaf $\delta^{15}N$ values and plant N% at anthesis and physiological maturity. A positive correlation, $R^2 = 0.96$ and $R^2 = 0.79$, was observed between flag leaf $\delta^{15}N$ values and plant N% on both unfertilised and fertilised plots at anthesis. Flag leaf $\delta^{15}N$ values proved to be related to plant N source and plant N%. However, a decline of plant N% was observed on unfertilised plots with increasing flag leaf $\delta^{15}N$ values at anthesis, while plant N% increased as flag leaf $\delta^{15}N$ increased when fertilised. At physiological maturity (Figure 33), the correlation between flag leaf $\delta^{15}N$ and plant N% was strongly positive for both unfertilised ($R^2 = 0.99$) and fertilised plots ($R^2 = 0.91$).

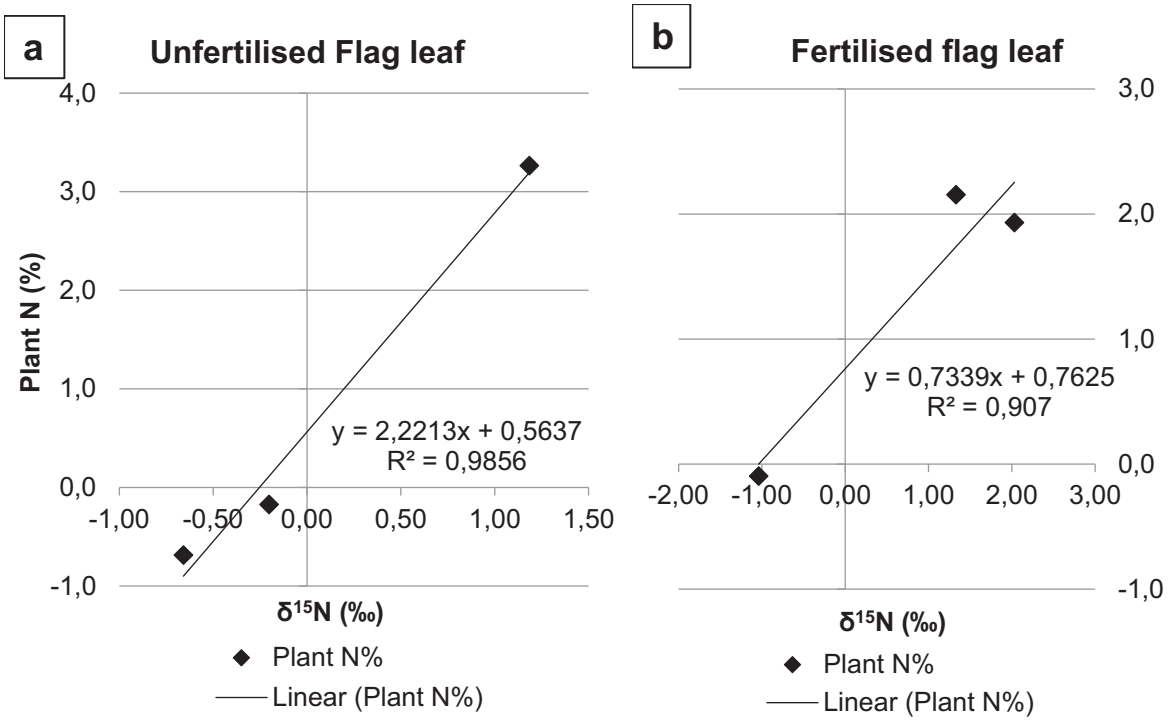

Figure 33: The correlation between flag leaf $\delta^{15}N$ and plant nitrogen (N) for (a) unfertilised plots and (b) fertilised plots at physiological maturity.

Table 15 shows the Ndff and FNUE values that are above 50% indicative of a well-managed agricultural system. Detailed information about the calculations is given by Equations 3.1 to 3.5, and further information is also given on Mangwende (2017).

Table 15: Calculated fertiliser use efficiency using depleted nitrogen fertiliser.

Parameter	Calculated Value
$\delta^{15}N$ in the fertilizer (‰)	-2.1
N derived from fertiliser (%)	61
Total above ground N uptake (kg ha^{-1}):	222.6
Fertiliser N yield (kg ha^{-1}):	135.5
Fertiliser N use efficiency (%)	68

6.5 EVALUATION OF APSIM TO SIMULATE WATER AND NITROGEN DYNAMICS IN WHEAT CROPPING SYSTEMS

The objective of this study was to establish the N leaching potential using Br^- as a conservative tracer for the Hutton sandy clay loam soil (Soil Classification Working Group, 1991). Another objective was to evaluate the performance of a parameterised and calibrated APSIM model, and to predict NO_3-N leaching from the soil profile using the model.

6.5.1 Materials and Methods

Both lysimeter and field trial sites were used for this study. The trial sites were located at the University of Pretoria Experimental Farm, and wheat was planted on the 30th of July 2016 and harvested on the 15th of November 2016. The soil is a sandy clay loam Hutton soil (Soil Classification Working Group, 1991), and a list of selected soil properties is summarised in Table 16.

Table 16: Selected soil properties of the lysimeter and field trial soil at the University of Pretoria Experimental Farm.

Parameter	UOM[a]	Lysimeter Trial			Field Trial		
		Depth (m)			Depth (m)		
		0.00-0.20	0.20-0.40	0.40-0.60	0.00-0.20	0.20-0.40	0.40-0.60
Organic carbon	%	1.12	0.70	0.54	0.63	0.61	0.51
Organic matter	% wt	1.7	1.9	2.2	1.5	1.5	1.5
pH (water)	log([H^+])	6.6	6.9	7.1	6.1	6.6	5.8
Total N	mg kg^{-1}	29.0	24.0	28.0	11.4	6.9	11.4
NO_3-N	mg kg^{-1}	13.0	11.0	9.0	7.7	5.1	9.5
NH_4-N	mg kg^{-1}	16.0	13.0	19.0	3.6	1.8	1.9
Sand	%	64.0	57.0	58.0	72.0	64.6	57.7
Silt	%	13.0	18.0	13.0	3.5	4.7	6.0
Clay	%	23.0	25.0	29.0	24.7	30.7	36.3
Texture	Class	SCL[b]	SCL	SCL	SCL	SCL	SC[c]

UOM[a] – unit of measurement, SCL[b] – sandy clay loam, SC[c] – sandy clay

The crop was kept weed, pest and disease free to obtain growth parameters under optimum conditions for the APSIM crop model. Recommended agronomic practices were followed, and tensiometers and volumetric soil water content (VWC) sensors inserted at 0.15 m were used to schedule irrigation. A total of 610 and 550 mm of irrigation were applied on the fertilised and unfertilised plots, respectively, and detailed irrigation schedules for the lysimeter and field trial are given in Figure 25 and Mangwende (2017), respectively. Saturated hydraulic conductivity was measured using a Decagon dual-head

infiltrometer (Decagon Devices Inc., Pullman WA, USA). Water potential sensors, wetting front detectors (WFDs), suction cups (SCs) and tensiometers, were also installed at selected depths depending on the trial site, see Table 17.

Table 17: Depth of insertion for various types of instruments in the lysimeter and field trial sites.

Depth (m)	Lysimeter Trial	Field Trial
0.15	MPS-6[a], SPES20[b], GS3[c]	CS[d]
0.25		WFD[e], SC[f], T[g], CS
0.30	MPS-6, SPES20, GS3	
0.50	MPS-6, SPES20, GS3	WFD, SC, T, CS
0.70	MPS-6, SPES20, GS3	

MPS-6[a] – soil water potential sensor, SPES20[b] – suction cup, GS[c] – volumetric water content sensor, and CS[d] – capacitance sensor (all supplied by Decagon Devices Inc., Pullman WA, USA), WFD[e] – wetting front detector (Agriplas, South Africa), SC[f] – suction cup (Soil Moisture Equipment Corp., Santa Barbara, CA, USA), and T[g] – tensiometer (Delta-T Devices, Cambridge, UK).

Phenological data that was collected during the wheat growing season included: days taken from sowing to germination, tillering, flowering, anthesis, and physiological maturity. Other data collected were: plant above ground dry matter accumulation, grain yield, ears per m^{-2} and stem, leaf and grain N concentration. Root depth was also measured by digging a pit close to the centre of the lysimeter trial site, and the roots were visually inspected. The leaf area index (LAI) was measured using an LI-3100C area meter (Li-Cor Inc., Lincoln, Nebraska, USA) and AccuPAR LP-80 ceptometer (Decagon Devices Inc., Pullman WA, USA). Destructive sampling was done at tillering, anthesis and physiological maturity, so plant material was oven dried for 72 hours at 60^{o}C. A moisture cup Mini GAC and GAC PLUS (DICKEY-john Corporation, Illinois, USA) was used to determine the grain moisture and adjust the oven dried grain moisture to 12.5%, the industry standard for maximum allowable moisture content of wheat grain.

The daily weather data required by the model was collected using an automatic weather station (AWS) positioned on the University of Pretoria Experimental Farm in close proximity to the trials. The parameters recorded were: maximum and minimum air temperature (°C), maximum and minimum relative humidity (%), average wind speed (m s^{-1}), solar radiation (MJ m^{-2}) and rainfall (mm). Evapotranspiration (ET_o) (mm) and average vapour pressure deficit (VPD) (kPa) were estimated and calculated using the weather data, and the ET_o and VPD for the growing season are shown in Figure 34: Daily evapotranspiration (ETo) (mm) and vapour pressure deficit (VPD) (kPa) variation during the growing season on the University of Pretoria Experimental Farm.

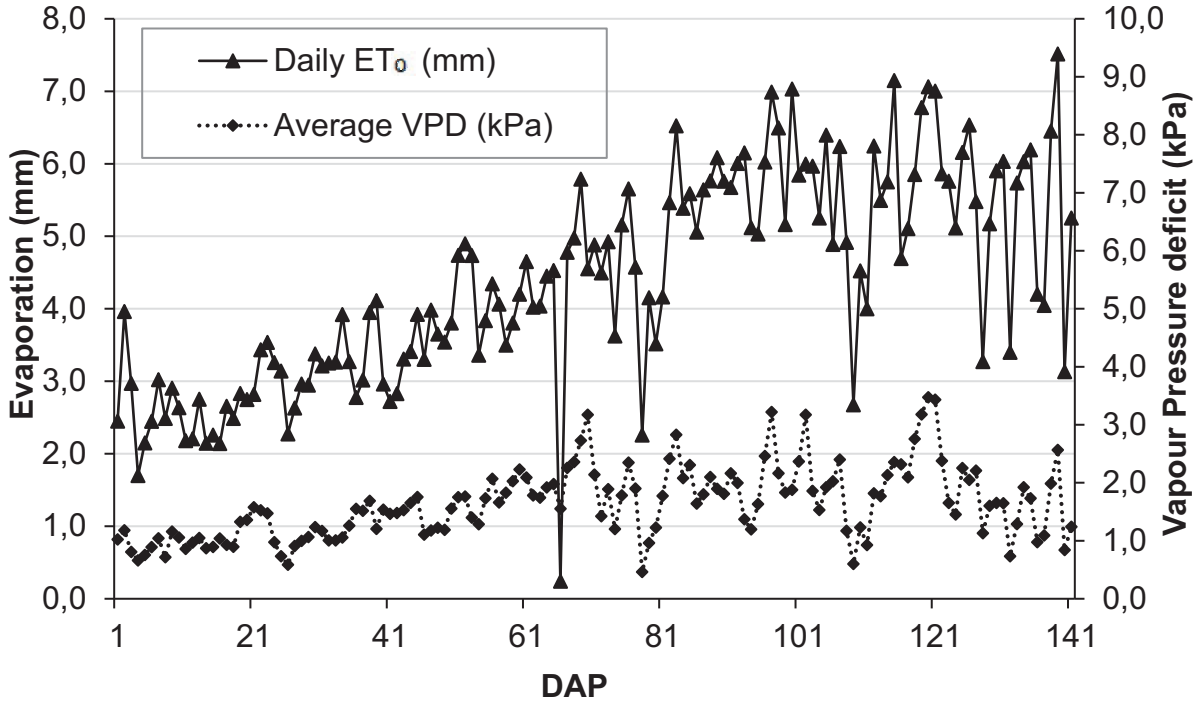

Figure 34: Daily evapotranspiration (ET_o) (mm) and vapour pressure deficit (VPD) (kPa) variation during the growing season on the University of Pretoria Experimental Farm

Bromide (Br^-), as a conservative tracer, was applied to the field trial (fertilised and unfertilised plots) 41 days after planting (DAP) at a rate of 0.020 kg m^{-2}. The Br^- was dissolved in 0.5 L of distilled water, and it was applied using a hand-held sprayer. Water samples were collected 24 hours after every irrigation cycle until physiological maturity. The water samples for Br^- analysis were collected at 0.25 and 0.50 m depths. Collected samples were put in a plastic container and stored in a cold room at 5°C until they were analysed. Samples were analysed for NO_3^- and selected samples for Br^- concentration due to high cost. Bromide was analysed using ion chromatography at the Agricultural Research Council (ARC) Climate and Soil, Pretoria, South Africa, while NO_3^- concentration was analysed using an RQEasy Nitrate Reflectometer (Merck, Germany).

6.5.2 APSIM model description

APSIM version 7.7 was used, and consists of several crop models, with APSIM-Wheat being applied for this simulation (McCown et al., 1996; Asseng et al., 1998; Asseng et al., 2002; Keating et al., 2003; Holzworth et al., 2014). Using SoilWat, soil N (SOILN) and residue modules, the APSIM-Wheat can simulate plant growth on a daily time step. The SoilWat module uses a multi-layer, cascading or tipping bucket approach to simulate water and solute movement, and a mixing factor is used to determine the fraction of solute that moves to the layer beneath (Van der Laan et al., 2014). The model requires a specified drained upper limit (DUL), saturation (SAT) and water lower limit (LL15), daily meteorological data and agronomic management practices (for example, planting, tillage, fertiliser, harvest) to simulate crop growth and development and soil processes. After calibrating APSIM using the lysimeter trial data, the model was tested using the field trial data, from fertilised and unfertilised plots.

Soil water content, soil inorganic N, LAI, total above ground dry matter (TDM) and grain yield were used to assess the performance of the model. The square of the correlation coefficient (R^2), mean absolute error (MAE), index of agreement (D), and root mean square error (RMSE) were the statistical tests used. When R^2 and D were above 0.8 and MAE% was below 20%, the model was considered to be performing well (De Jager, 1994). RMSE was evaluated on case-by-case basis, and usually must be less than 20% of standard deviation.

6.5.3 Results

Measured soil and growth parameters were results and used to calibrate the APSIM model. Saturated hydraulic conductivity was measured using a Decagon ring infiltrometer for lysimeter and field trial sites. The Soil-Plant-Air-Water (SPAW) software estimated values for soil hydraulic properties which are listed in Table 17 and Table 18. Cultivar specific parameters measured during the growing season are listed in Mangwende (2017), and all the parameters that were changed in the model are also provided.

Table 18: Measured and calibrated soil hydraulic properties for the field trial site.

Depth (m)	BD[a] (kg m^{-3})	LL15[b] (m^3 m^{-3})	DUL[c] (m^3 m^{-3})	SAT[d] (m^3 m^{-3})	K_s (cm day^{-1})
0.00-0.15	1540	0.14	0.24	0.35	500
0.15-0.30	1560	0.14	0.24	0.35	1000
0.30-0.60	1580	0.14	0.22	0.30	1000
0.60-0.90	1580	0.14	0.22	0.30	500
0.90-1.20	1580	0.14	0.22	0.30	500
1.20-1.50	1580	0.14	0.22	0.30	500
1.50-1.80	1580	0.14	0.22	0.30	500

[a]Estimated using SPAW pedo-transfer functions, [b-d]Derived from observed soil moisture content data collected by capacitance sensors.

6.5.3.1 Bromide concentrations

Bromide was applied 41 DAP, and according to APSIM peaked at 0.25 m at 168.4 kg Br ha^{-1} 51 DAP. It took 60 days for Br^- at 0.25 m depth to be less than 1 kg Br ha^{-1} after reaching the peak concentration, and the model simulated Br^- movement well because the r^2 and MAE% values were in the acceptable range, however, the D value was not in the range and RMSE value was high (Figure 35a and Table 19). At 0.50 m depth, the concentration peaked at 163.2 kg Br ha^{-1} 57 DAP, and, after peaking it took 70 days to reach less than 5 kg Br ha^{-1}. At 0.50 m depth, the r^2 and D values were in the acceptable range, whereas the MAE% was above the acceptable range by 53% and the RMSE value was high (Figure 35b and Table 19).

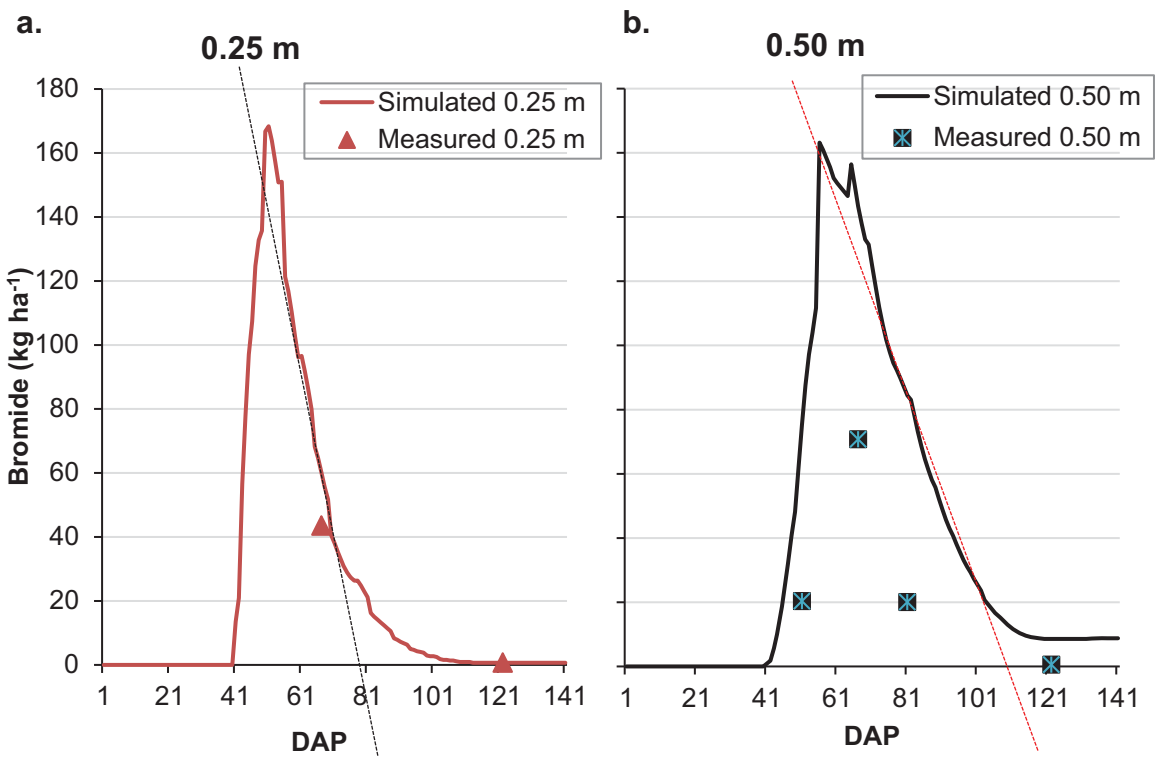

Figure 35: Measured and simulated bromide Br^- concentration at (a) 0.25 m and (b) 0.50 m. The rate of Br^- leaching was estimated using the declining concentration slope, with a dashed line touching many points on the declining slope.

The Br^- concentration was more dispersed (remained with higher concentration after peaking) at 0.50 m depth than at 0.25 m because of a lag of water movement. Water wets the topsoil first before moving to lower layers, delaying the movement of Br^-. The movement of Br^- was 7.2 kg Br ha^{-1} day^{-1} at 0.25 m, whereas at 0.50 m it was 2.9 kg Br ha^{-1} day^{-1}, and values for Br^- loss were calculated using the declining concentration slope, indicated with dashed slope on Figure 37. Using the model to simulate the possible Br^- leaching at 0.9 m it can be equated to 26.6 to 68.0 kg ha^{-1} $season^{-1}$, and the leaching range (minimum and maximum) was derived from the declining slope.

Table 19: Statistical evaluation of measured and simulated bromide (Br^-) concentration in fertilised and unfertilised plots.

Depth (m)	n	R^2	D	MAE%	RMSE (kg ha^{-1})
0.25	3	0.98	0.53	8.91	11.33
0.50	4	0.86	0.89	33.22	8.09

6.5.3.2 Volumetric water content

Figure 36 (a-c) and Figure 37 (a-c) shows the simulated and measured VWC at soil depths of 0.15, 0.30 and 0.50 m. APSIM was able to simulate VWC at the depths of 0.15 and 0.30 m well, as they had low MAE% values of less than 5% for both the fertilised and unfertilised plots. Although R^2 and D values at 0.15 and 0.30 m did not meet the criteria for a good simulation, the MAE% and RMSE values were in the acceptable range. However, the VWC simulation at 0.50 m in the fertilised plots was over estimated from 58 to 141 DAP, whereas in the unfertilised plots the VWC simulation only started to be over-estimated from 110 to 141 DAP. At 0.5 m, the MAE% and RMSE values met the criteria for a good simulation in fertilised and unfertilised plots, but they had poor D and R^2 values for all the simulations, except for unfertilised plots at 0.25 m which had a D value of 0.82 (Table 21 to Table 22)

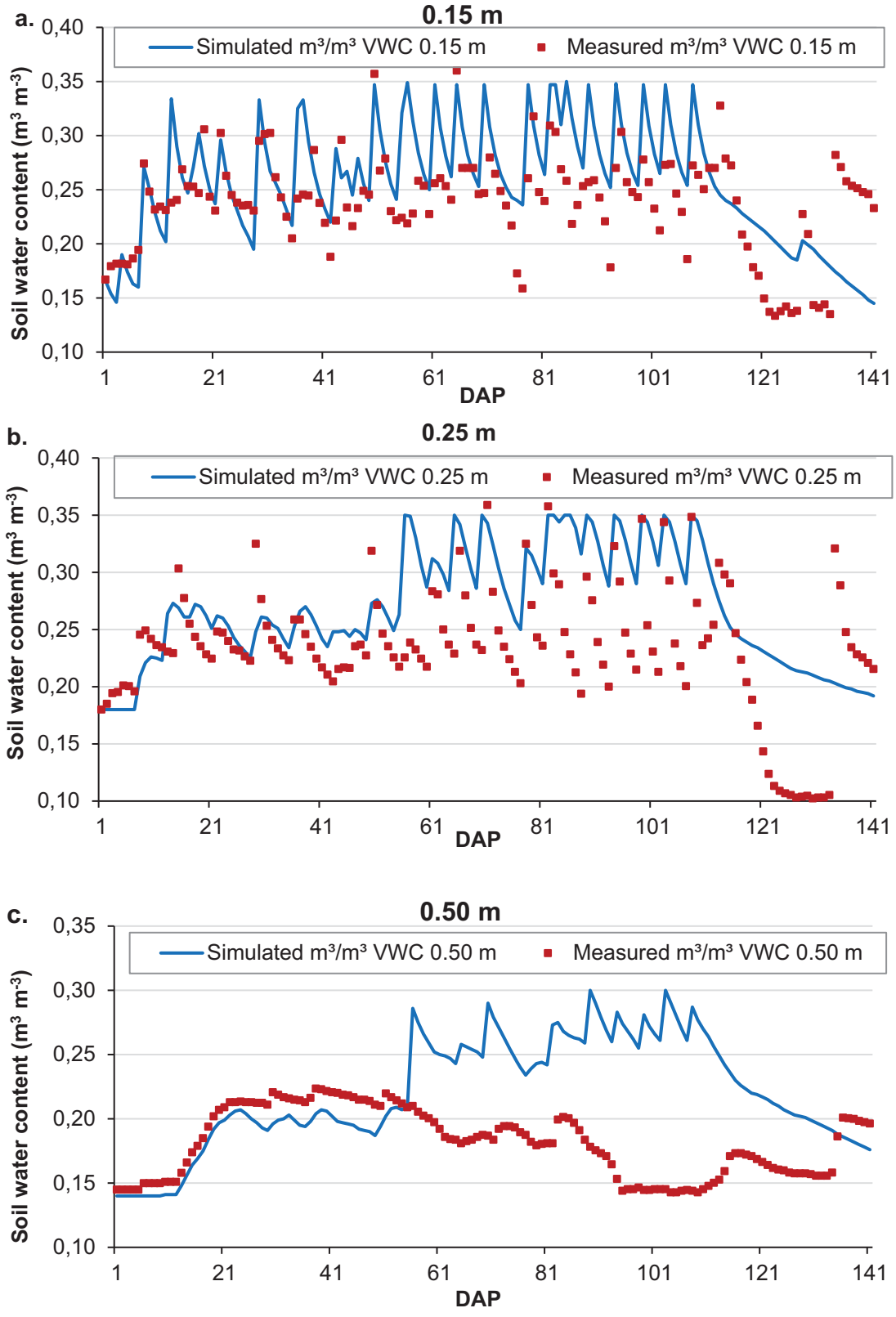

Figure 36: Measured and simulated volumetric water content (VWC) at (a) 0.15 m, (b) 0.30 m and (c) 0.50 m in fertilised plots.

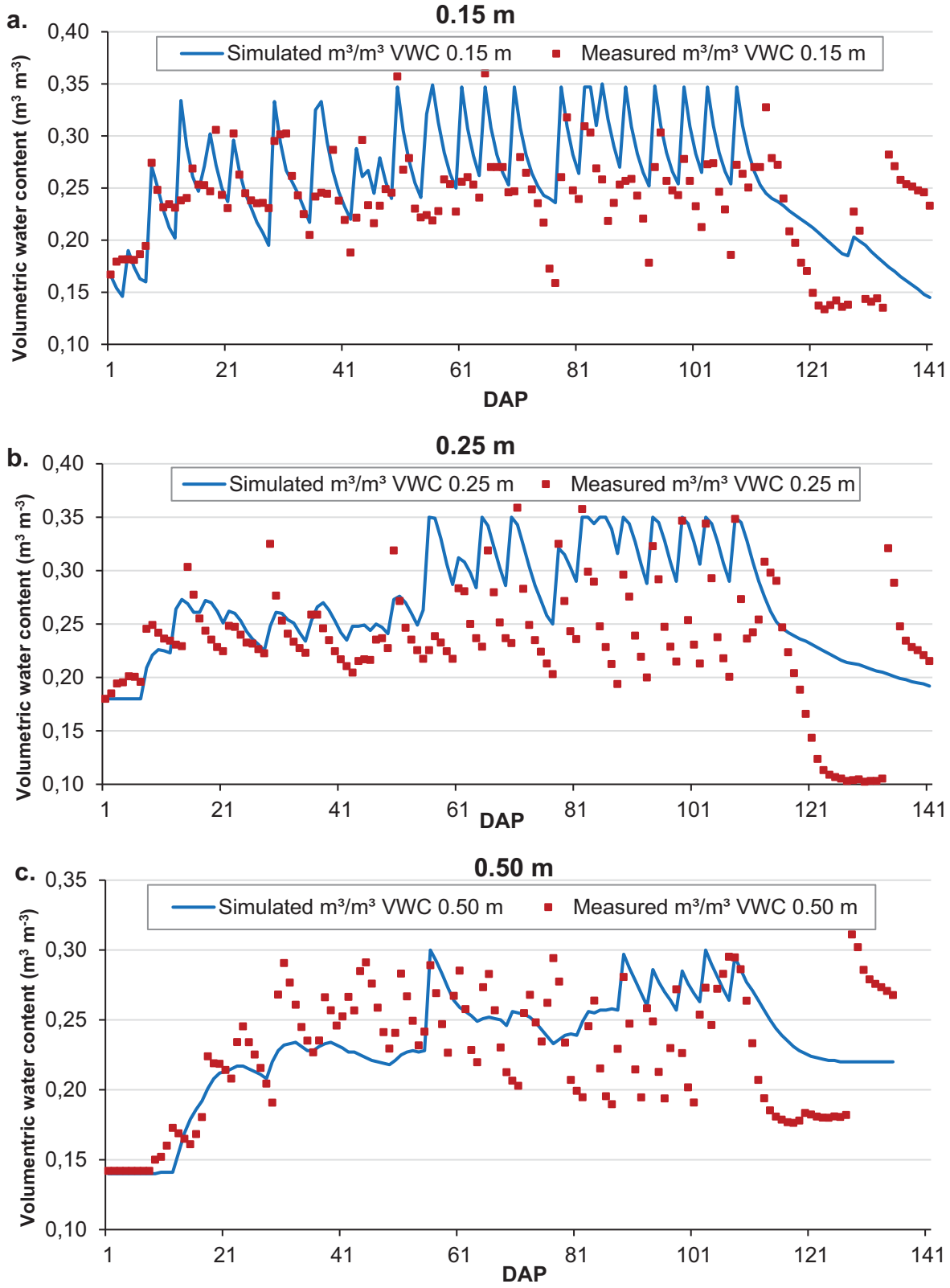

Figure 37: Measured and simulated volumetric water content (VWC) at (a) 0.15 m, (b) 0.30 m and (c) 0.50 m in unfertilised plots.

In all the plots, from 120 to 141 DAP the VWC sensor at all the depths were non-responsive and recorded low water content figures, which could have been caused by dry conditions of less than 0.1 m^3 m^{-3}. These dry conditions were experienced close to the physiological maturity as irrigation water is withdrawn to facilitate wheat drying off.

Table 20: Statistical evaluation of measured and simulated volumetric water content in fertilised plots.

Depth (m)	R^2	D	MAE%	RMSE (m^3 m^{-3})
15	0.34	0.52	4.0	0.05
25	0.31	0.51	4.9	0.06
50	0.01	0.41	5.1	0.07

Table 21: Statistical evaluation of measured and simulated volumetric water content in unfertilised plots.

Depth (m)	R^2	D	MAE%	RMSE (m^3 m^{-3})
15	0.01	0.48	9.2	0.11
25	0.31	0.82	2.3	0.03
50	0.33	0.71	3.1	0.04

6.5.3.3 Leaf area Index (LAI)

The model simulated the LAI for the fertilised plots well, but slightly over-estimated the LAI for fertilised plots, except at 85 DAP when it accurately simulated LAI. The model performed well to estimate the LAI in the fertilised and unfertilised plots as the R^2 and D values were greater than 0.8 and a low RMSE value although the D values were poor.

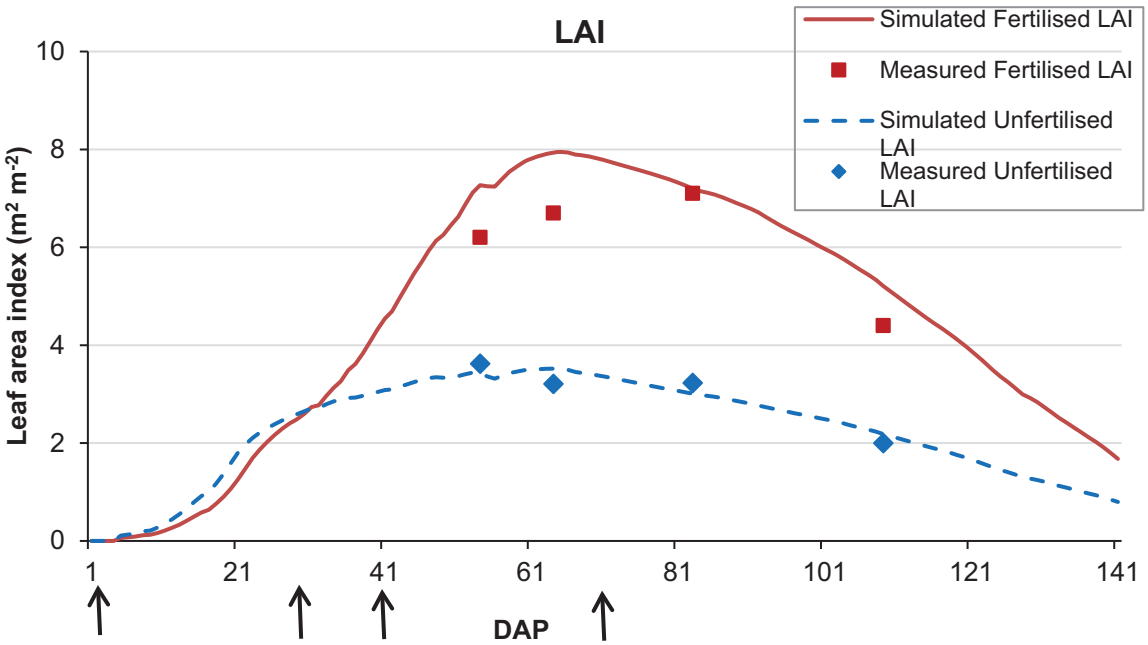

Figure 38: Measured and simulated leaf area index (LAI) in fertilised and unfertilised plots. The arrows indicate when fertiliser was applied to the fertilised plots (0, 29, 41 and 71 days after planting (DAP)).

The LAIs between the fertilised and unfertilised plots were initially similar, most likely due to access of mineralised N, but at 8 DAP there was a clear difference between the two treatments until 30 DAP. The high plant vigour may have been caused by mineralisation which supplied adequate N to ensure better LAI development. Mineralisation in fertilised plots and N applied at planting may have resulted in excess N in the root zone, which may have reduced LAI development, as excess N in the rhizosphere can inhibit root growth (Tian et al., 2008).

Table 22: Statistical evaluation of measured and simulated values for leaf area index (LAI) in fertilised and unfertilised plots.

Plot	r^2	D	MAE%	RMSE (m^2 m^{-2})
Fertilised	0.83	0.63	28.4	0.91
Unfertilised	0.86	0.97	22.8	0.23

6.5.3.4 *Total above-ground dry matter (TDM) production and grain yield*

The model was able to simulate the TDM and final grain yield well (Figure 39a) in fertilised plots. Although the TDM was overestimated in the early season and underestimated during the mid-season, all the model performance criteria were met (R^2, D, MAE% and RMSE), except for grain yield MAE% which was over by 9% (Table 24). On unfertilised plots, the TDM and grain yield was simulated well because the model performance criteria (R^2, D, MAE% and RMSE) were in the acceptable range, except for TDM MAE% which was above the threshold by 17% (Figure 39b and Table 24).

Table 23: Statistical evaluation of measured and simulated values for total aboveground dry matter (TDM) and grain yield on fertilised and unfertilised plots.

Plot	TDM				Grain yield			
	r^2	D	MAE%	RMSE (t ha^{-1})	r^2	D	MAE%	RMSE (t ha^{-1})
Fertilised	0.83	0.85	19.0	2.42	1.00	0.63	28.7	4.18
Unfertilised	1.00	0.95	36.9	0.38	1.00	0.98	7.7	0.11

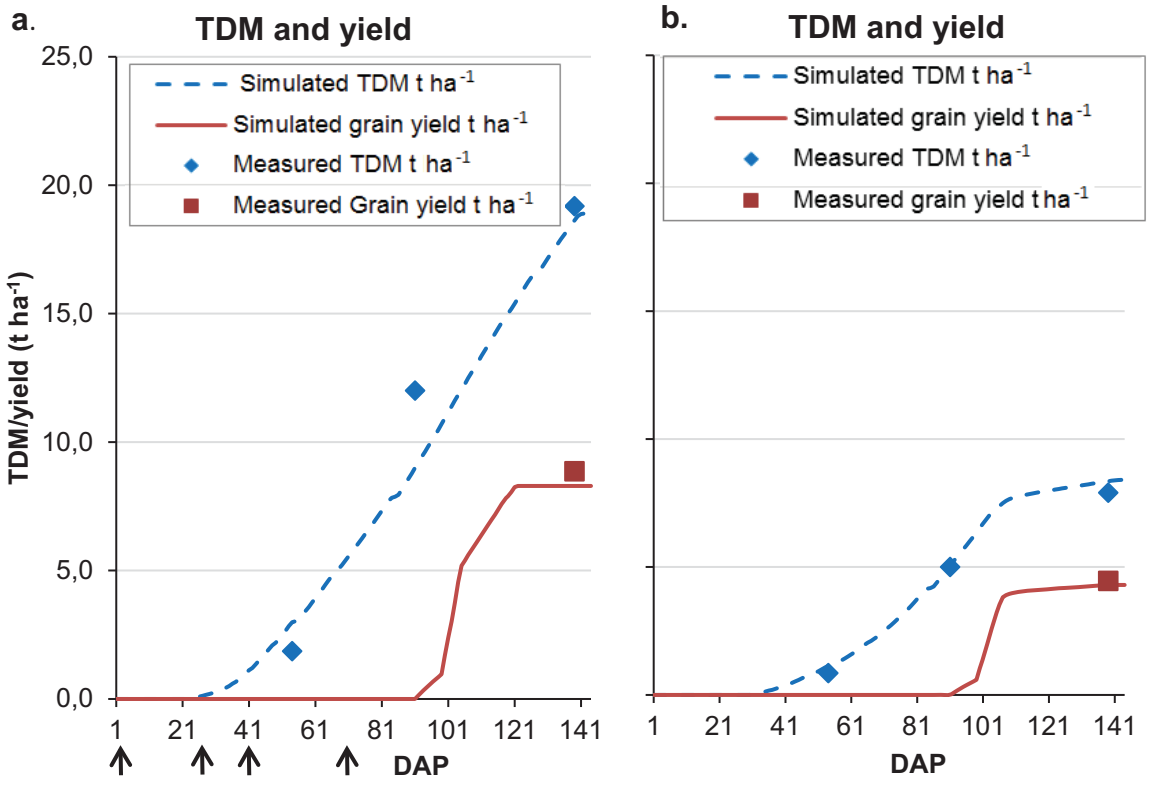

Figure 39: Measured and simulated total aboveground dry matter (TDM) and grain yield for the (a) fertilised and (b) unfertilised plots. Arrows indicate when the fertilised plots were fertilised at 0, 29, 41 and 71 days after planting (DAP).

6.5.3.5 Soil water nitrate-nitrogen concentrations

Figure 39 and Figure 40 shows the soil NO_3-N in fertilised and unfertilised plots at 0.25 m and 0.50 m depths. Soon after planting, the SC and WFD NO_3-N concentrations were underestimated by APSIM at 0.25 and 0.50 m depths in fertilised plots, but the simulations improved as the season progressed. At the 0.25 m depth in fertilised plots, the NO_3-N concentration in WFDs was simulated well, and this may be attributed to settling which minimised overestimation due to mineralisation. Since the SCs were installed just before planting, the overestimation of NO_3-N could be due to increased mineralisation as a result of soil disturbance during installation and during seedbed preparation. In unfertilised plots, the SCs also overestimated soil NO_3-N soon after planting just like in fertilised plots, but the WFD simulated the soil NO_3-N concentration well, probably because they had settled and the N pulse from increased mineralisation due to soil disturbance during seedbed preparation may not have been deep enough to be detected at 0.25 and 0.50 m depths. Generally, the measured WFD NO_3-N concentration was simulated well by APSIM in both fertilised and unfertilised plots, and the measured SC NO_3-N concentrations started to agree with the simulated values after 30 DAP until harvesting. Although the statistics show that the simulations were not Table 24can be seen that the APSIM simulation were able to give the same concentrations as WFDs. Suction cup concentrations were high soon after planting, but later into the growing season the concentrations reduced and were more closely simulated.

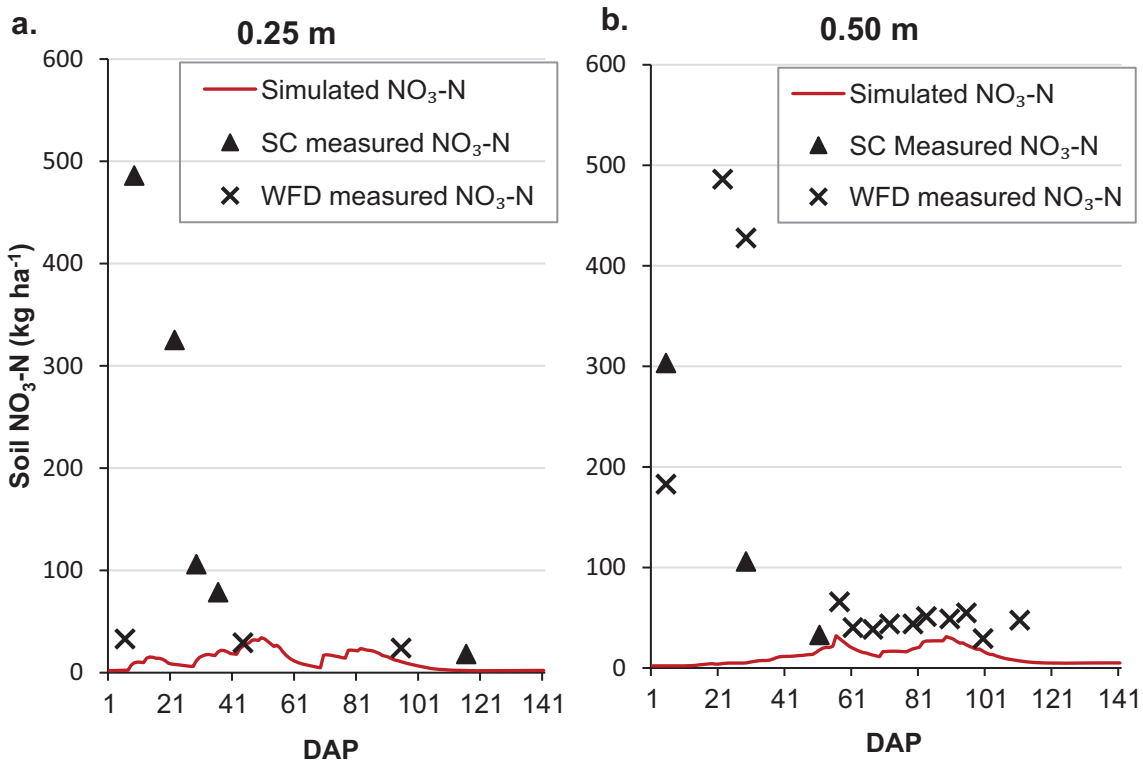

Figure 40: Simulated and measured soil water nitrate-nitrogen (NO_3-N) concentration in fertilised plots for (a) 0.25 m and (b) 0.50 m soil depth. Measured NO_3-N was collected by suction cups (SC) and wetting front detectors (WFD).

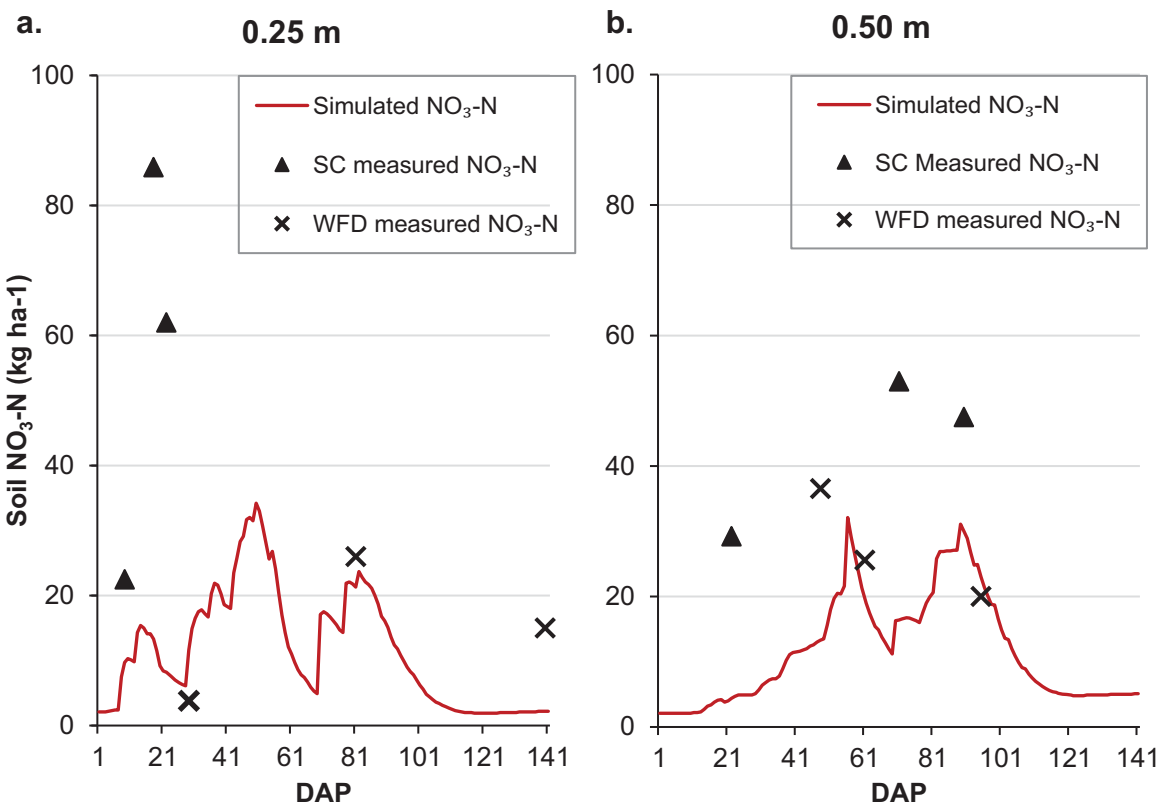

Figure 41: Simulated and measured soil water nitrate-nitrogen (NO_3-N) concentration in unfertilised plots for (a) 0.25 m and (b) 0.50 m soil depth. Measured NO_3-N was collected by suction cups (SC) and wetting front detectors (WFD).

Table 24: Statistical evaluation of measured and simulated nitrate-nitrogen (NO_3^-N) concentration in fertilised and unfertilised plots measured from suction cups (SC) and wetting front detectors (WFD).

Plot	Instrument	Depth (m)	r^2	D	MAE%	RMSE (kg ha^{-1})
Unfertilised	SC	0.25	0.33	0.50	46.4	30.42
Unfertilised	WFD	0.25	0.50	0.13	6.7	4.00
Unfertilised	SC	0.50	0.50	0.43	35.4	21.12
Unfertilised	WFD	0.50	0.50	0.31	21.1	16.50
Fertilised	SC	0.25	0.00	0.92	19.2	11.66
Fertilised	WFD	0.25	0.07	0.50	15.7	11.13
Fertilised	SC	0.50	0.68	0.90	33.9	26.01
Fertilised	WFD	0.50	0.30	0.82	32.2	38.97

6.5.3.6 Nitrate-nitrogen leaching

The cumulated leached NO_3-N was 22.7 kg ha^{-1} for the fertilised plots, whereas the daily leached NO_3-N reached a maximum of 1.6 kg ha^{-1} on 100 DAP (Figure 41) at the 0.9 m soil depth. In fertilised plots, the third split top dressing coincided with intensified NO_3-N leaching. In unfertilised plots, the cumulative leached NO_3-N was 4.5 kg ha^{-1}, and the daily leached NO_3-N peaked at 0.2 kg ha^{-1} 61 DAP. The leached NO_3-N peaked early in unfertilised plots, which suggested the loss of mineralised N from soil organic matter (SOM) in unfertilised plots.

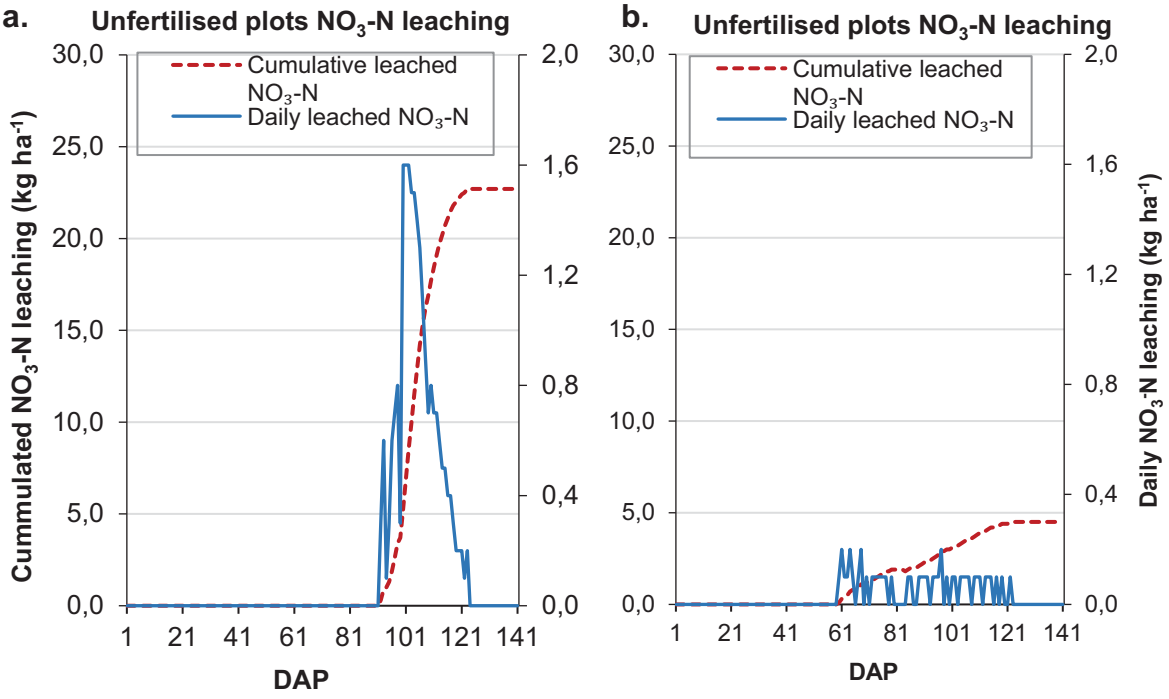

Figure 42: Simulated daily and cumulative nitrate-nitrogen (NO_3-N) leaching in (a) fertilised plots and (b) unfertilised plots at a soil depth of 0.9 m.

6.6 Discussion

Firstly, the drain gauge's performance was checked against a weighing lysimeter, by measuring the drainage and N leaching. More frequent drainage was measured using a drain gauge compared to weighing lysimeters. Drainage collected by a drain gauge was 54.1 mm, which was 338% more than the average drainage for the two weighing lysimeters. Even though all the lysimeters recorded some drainage, the NO_3-N concentration was undetectable in the draining water, whereas the drain gauge average season NO_3-N concentration was 46.1 mg ℓ^{-1}. As saturated soil conditions were created at the bottom of a weighing lysimeter, they caused anaerobic conditions that reduced NO_3-N loss through leaching but aggravated denitrification. The drain gauge maintained unsaturated conditions because of a wick that was put in the divergence control tube.

Drainage and NO_3-N concentration from the weighing lysimeter and drain gauge can be combined with stable isotopes to further explain the N dynamics. The lysimeters and drain gauge allows for the quantification of N leaching, but does not account for plants' uptake. Using the ^{15}N stable isotopes, the

NO_3-N taken up by the plant was 105.4 kg ha^{-1}. Stable isotopes at plot level provided the seasonal plant requirements, whereas the weighing lysimeters showed that denitrification was the main cause of N loss under saturated soil conditions, whereas NO_3-N leaching prevailed under unsaturated soil conditions. All techniques consolidated our understanding of N movement in the soil, so that N movement in the soil can be properly modelled.

The third and fourth objectives were combined, and APSIM was calibrated on wheat for the first time in South Africa. The objectives were to determine the potential leaching using bromide (Br^-) conservative tracer and validate the calibrated APSIM model. There were good APSIM simulations for leaf area index (LAI), grain yield, TDM and NO_3-N that warranted more confidence in the predicted NO_3-N leaching. The APSIM predicted leaching amount was agreeable with the NO_3-N measurement from a drain gauge, 22.7 and 24.9 kg ha^{-1} respectively. The leached NO_3-N was within the range that was stipulated with a Br^- tracer. Since APSIM simulated LAI, grain yield, TDM and water content on fertilised and unfertilised well, the model can be used for making decisions on N management in wheat cropping systems. Although the unfertilised plots had significantly lower leached NO_3-N (4.5 kg ha^{-1}), they had 44% lower grain yield compared to fertilised plots. Lower yield of this magnitude will not motivate farmers even if the plots had lower N leaching. An appropriate compromise can be set by running several model simulations to optimise the grain yield while minimising the N leaching losses.

Soil NO_3-N was monitored using suction cups (SC) and wetting front detectors (WFD). Soon after planting, high NO_3-N concentration in the top 0.0 to 0.3 m measured by SCs and WFDs indicated increased mineralisation. Such information from SC and WFD indicated the soil N movement in the soil profile, other than relying on NO_3-N concentrations measured at a single depth, which was the case for drain gauge and the weighing lysimeter. Initial soil water NO_3-N concentration was high irrespective of fertilisation, which suggested proper timing of N applications to avoid excess amounts in the root zone.

Overall, the objectives were met. The drain gauge managed to quantify the NO_3-N leaching, whereas the stable isotopes were used to calculate the FNUE. The calibrated APSIM performed well and was used to predict leached NO_3-N in wheat cropping system.

The APSIM model was able to simulate TDM and grain yield well, VWC and Br^- movement on fertilised and unfertilised plots. The good performance of the model increased certainty and confidence of the simulated NO_3-N leaching. The fertilised plots leached more N, and this can be reduced by determination of initial N available to crops and timing of split top dressings.

6.6.1 Bromide concentrations

The Br^- concentrations were found to be more dispersed at 0.50 m soil depth compared to 0.25 m depth. The increased Br^- dispersion was caused by diffusion process and hydrodynamic dispersion in a myriad of soil pore sizes and tortuosity in flow paths as the soil deepens (Tillman, 1991; Radcliffe and Šimůnek, 2010). Despite Br^- and NO_3^- being anions of almost similar molecular weight and charge, Clay et al. (2004) observed higher Br^- leaching rate when compared to NO_3-N because of different sorption characteristics. Bromide and NO_3^- have a sorption of 0.002 ± 0.036 mg kg^{-1} and 0.17 ± 0.03 mg kg^{-1} of soil, respectively, and converted Br^- leaching to NO_3-N leaching amount by reducing with 25%. The

faster movement of Br^- was also observed in this study. If observed Br^- leaching potential (2.9 to 7.4 kg Br ha^{-1} day^{-1}) of the Hutton soil is reduced by 25%, then 2.2 to 5.6 kg NO_3-N ha^{-1} day^{-1} (20.2 to 51.5 kg NO_3-N $season^{-1}$) would be expected, and the APSIM simulated maximum NO_3-N leaching concentration was in this range. Therefore, the Br^- was able to establish the upper leaching potential of a sand clay loam Hutton soil, and they have a high risk of heavy leaching.

6.6.2 Volumetric water content

APSIM simulated VWC well for all the depths. Typically, wheat is planted in winter in South Africa and relies on irrigation. In a study done in Asia using APSIM, the VWC of wheat varieties grown in India and China were simulated well, but the model was not able to simulate water content under water stressed conditions well (Gaydon et al., 2017). Simulating episodes of water stress when water content is less than 0.1 m^3 m^{-3} has also been reported in other crop models such as Soil Water Balance (SWB), where the model was not able to simulate low water levels in maize and wheat systems (Van der Laan et al., 2009; Van der Laan et al., 2010). Water stress did not negatively influence the results, as the crop was supplied with adequate water based on crop water requirements.

6.6.2.1 Leaf area Index (LAI)

Leaf area index (LAI) was simulated well. The unfertilised wheat LAI showed an early vigour for the first 30 DAP. Early vigour can be attributed to mineralisation that commenced during fallow period before planting, and due to disturbed soil and decomposed SOM after planting, which supplied adequate nutrients to the plants for the first 30 DAP. Limited N in the root zone can promote deeper roots (Jiang et al., 2017), which allows plants to have a large surface area to extract nutrients and limit the amount of N losses from the soil. Since better LAI was simulated on unfertilised plots, first N top dressing on wheat can, therefore, could target 30 DAP to support increased crop growth rates. Soil analysis results also indicated the availability of residual N fertiliser from the previous crop which could have benefited the establishing crop.

6.6.3 Total aboveground dry matter production and grain yield

The TDM and grain yield of wheat were simulated well, and the small discrepancies in observed and simulated values can be due to how radiation use efficiency (RUE) and temperature are simulated in the model. Typically, a sigmoidal growth curve is expected for crop growth, but this was not exhibited on fertilised plots because the RUE in the wheat module has a constant value which is not varied along the growing season (Zheng et al., 2014). Thus, when crops are fertilised the biomass accumulation is rapid in the early season and fail to exhibit the expected normal growth curve, whereas in unfertilised plots there is slow accumulation of biomass which allow the distinct sigmoid shape to be exhibited. In APSIM, the RUE has a default value of 1.24 g MJ^{-1} (Zheng et al., 2014), which was adjusted to 1.84 g MJ^{-1} during calibration to improve simulations.

On the other hand, the average temperature is calculated by taking an average of maximum and minimum air temperatures, but such an average may have a lower average when smaller time frames of an hour are considered, and, when seasons are changing from the cool to dry season (from July to August). Gaydon et al. (2017) also reported poor TDM and grain yield simulations for late-planted wheat

in India because of lower cardinal temperatures that are default in APSIM. As the wheat was planted in July, the average daily temperatures may not represent the shorter time frame temperature changes which can influence plant growth, and therefore simulated TDM was overestimated in the early season and underestimated mid-season. However, the variation between the measured and simulated values were small and did not affect the overall TDM and grain yield simulations, and therefore, N uptake was not compromised. Nitrogen uptake influences the amount of N that remains in the soil or leaches from the soil.

6.6.4 Soil water nitrate-nitrogen concentrations

Since the WFD was able to measure the simulated NO_3-N, it showed that the WFD can be a simple instrument that can be used to quantify the soil N status and monitor N leaching if they are allowed to settle. Van der Laan et al. (2010) reported conflicting results with this study, as they found that SC had higher NO_3-N concentrations compared to WFD, for they attributed WFD to be sampling from draining water that was by-passing the soil matrix. However, in this study water samples collected from settled WFD were simulated well with APSIM.

The measured SC NO_3-N concentration in fertilised plots was not simulated well. Since fertiliser was applied at planting, it may have contributed to increased NO_3-N movement that was detected at 0.25 and 0.50 m depths. The under-estimation can also be caused by APSIM's failure to simulate high mineralisation capacity of the trial soil, as Van der Laan et al. (2010) reported high NO_3-N in unfertilised plots because of mineralisation. Disturbing the soil also increase mineralisation (Courtaillac et al., 1998), for Kristensen et al. (2000) reported mineralisation to double in disturbed soils previously with a mono culture of maize and under no till system, and the increased mineralisation may have added to the soil NO_3-N and was detected and measured by the SCs.

6.6.5 Nitrate-nitrogen leaching

Nitrate-nitrogen leaching was 88% higher on the fertilised plots compared to unfertilised plots. The NO_3-N leaching peaked at 100 DAP in fertilised plots, which also coincided with the third N top dressing. High NO_3-N leaching was also reported in Hutton soils under sugarcane production (Van der Laan et al., 2011). They reported leaching losses of 31% of the applied fertilised on planted sugarcane field, whereas in this study it was 34% of the applied fertiliser. Considering the time taken to grow sugarcane compared to wheat, the intensity of leaching losses is higher under irrigated wheat systems as observed in this study. Although splitting the N fertiliser potentially helps in reducing the amount of NO_3-N leaching (Van der Laan et al., 2011), timing of the N top dressing can also help. From this study, the first N application at planting can be reduced or omitted, and the third top dressing can be applied earlier so that NO_3^-N leaching can be reduced. Such information from this study can be useful to farmers if N availability and mineralisation of the soil is known, otherwise, more work is required to evaluate how management practices may influence N availability and eventual fine tuning of fertiliser recommendations

N processes depend on soil temperature, but it is estimated using air temperature in APSIM. Such an approach has a tendency of over-estimating soil N process such as mineralisation, immobilisation,

nitrification and denitrification. Van der Laan et al. (2011) observed some significant differences in net mineralisation in sugarcane fields because of slight over-estimation of simulated soil temperature in winter, when they used Canegro-N model.

6.7 CONCLUSIONS AND RECOMMENDATIONS

The drain gauge performed well in measuring drainage and NO_3-N leaching. The wick in the drain gauge ensured unsaturated bottom boundary conditions, and represented the field conditions better than the case of saturated conditions created in the weighing lysimeter. The drain gauge can be used to quantify NO_3-N leaching, although further testing is still required on several crops and seasons to further check seasonal performance.

The stable isotopes natural abundance method distinguished between applied fertiliser N and soil-derived N taken up by the crop. There was a strong positive correlation between the flag leaf $\delta^{15}N$ values and plant N% on both the fertilised and unfertilised plots at physiological maturity, so flag leaf $\delta^{15}N$ values can be used to calculate FNUE instead of whole plant analysis. The FNUE was 68%, which meant that 32% of the applied fertiliser that was not used by the crop. Although stable isotopes analysis differentiated various N sources, it was not able to specify the main N transformation process occurring in the soil or plant. Hence, the use of labelled fertilisers is recommended to clarify when and how the N transformations occur. Since there is evidence of the crop failing to use all the applied fertiliser, crop sequences have to be carefully designed to cater for excess N leached into deep soil layers, as this can be achieved by planting deep rooted crops such as sunflowers.

The potential N leaching of the Hutton soil was estimated to range from 20.2 to 51.5 kg NO_3-N ha^{-1} $season^{-1}$ at a soil depth of 0.9 m. A calibrated APSIM model was able to simulate soil water content, TDM and grain yield well and was used to predict N leaching. The predicted season NO_3-N leaching agreed with the measured quantities from the drain gauge, which demonstrated that modelling and infield monitoring of NO_3-N movement can be used to understand N dynamics better. Such information is essential to refine fertiliser recommendations and reduce NO_3-N leaching.

Further research is required to evaluate the methods in different agro-ecological wheat growing regions in South Africa. The low leaching measured in the weighing lysimeter will require redox potential sensors to verify the mechanism of N transformation that occurs in saturated bottom layers. Further running of several APSIM simulations is also recommended to explore various N management options for various wheat growing regions in South Africa, so that the results can have a wide range of application.

The potential NO_3-N leaching potential of the Hutton soil has a range of 20.2 to 51.5 kg N ha^{-1} $season^{-1}$ at a soil depth of 0.9 m. APSIM was able to simulate VWC, TDM and grain yield well, and hence can be used to estimate N leaching. Well-timed fertiliser applications will reduce N leaching. Use of modelling and infield monitoring of NO_3-N movement can lead to better understanding of N dynamics, which will help to refine fertiliser recommendations and reduce NO_3-N leaching.

6.8 References

BOWMAN, M.S., CLUNE, T.S., SUTTON, B.G. (2002) A modified ceramic sampler and lysimeter design for improved monitoring of soil leachates. *Water Research*, 36: 799-804.

CAMERON, K.C., DI, H.J., MOIR, J.L. (2013) Nitrogen losses from the soil/plant system: *A Review Annals of Applied Biology*, 162: 145-173.

CRESSWELL, H.P., SMILES, D.E., WILLIAMS, J. (1992) Soil structure, soil hydraulic properties and the soil water balance*. Soil Research*, 30: 265-283.

CZIGÁNY, S., FLURY, M., HARSH, J.B., WILLIAMS, B.C., SHIRA, J.M. (2005) Suitability of fiberglass wicks to sample colloids from vadose zone pore water. *Vadose Zone Journal*, 4: 175-183.

DECAGON DEVICES INC. (2015) Drain gauge G3 operators manual. Available at http://www.decagon.com/en/hydrology/lysimeters/drain-gauge-g3-passive-capillary-lysimeter/ [accessed 24 April 2016].

DELGADO, J.A., ALVA, A.K., FARES, A., PARAMASIVAM, S., MATTOS, D., SAJWAN, K. (2006) Numerical modelling to study the fate of nitrogen in cropping systems and best management case studies. *Journal of Crop Improvement*, 15: 421-470.

FISHER, D.K. (2012) Simple weighing lysimeters for measuring evapotranspiration and developing crop coefficients. *International Journal of Agricultural and Biological Engineering*, 5: 35-43.

GEE, G.W., NEWMAN, B.D., GREEN, S.R., MEISSNER, R., RUPP, H., ZHANG, Z.F., KELLER, J.M., WAUGH, W.J., VAN DER VELDE, M., SALAZAR, J. (2009) Passive wick fluxmeters: Design considerations and field applications. *Water Resources Research*, 4: 45.

GHEYSARI, M., MIRLATIFI, S.M., HOMAEE, M., ASADI, M.E., HOOGENBOOM, G. (2009) Nitrate leaching in a silage maize field under different irrigation and nitrogen fertilizer rates*. Agricultural Water Management*, 96: 946-954.

GÖRGENS, A.H.M., LORENTZ, S.A., VAN DER LAAN, M., ANNANDALE, J.G., JOVANOVIC, N.Z., MATTHEWS, N.B.G., LE ROUX, J.J. (eds) (2012) Modelling agricultural NPS pollution and economic-environmental trade-offs of pollution control measures. A project overview. Water Research Commission, WRC Report No. TT 516/12.

LADHA, J.K., PATHAK, H., KRUPNIK, T.J., SIX, J., VAN KESSEL, C. (2005) Efficiency of fertilizer nitrogen in cereal production: Retrospects and prospects. *Advances in Agronomy*, 87: 85-156.

LANDON, M.K., DELIN, G.N., KOMOR, S.C., REGAN, C.P. (1999) Comparison of the stable-isotopic composition of soil water collected from suction lysimeters, wick samplers, and cores in a sandy unsaturated zone. *Journal of Hydrology*, 224: 45-54.

MARTIN, E.C., DE OLIVEIRA, A.S., FOLTA, A.D., PEGELOW, E.J., SLACK, D.C. (2001) Development and testing of a small weighable lysimeter system to assess water use by shallow-rooted crops. *Transactions of the American Society of Agricultural and Biological Engineers*, 44: 71-78.

NYE, P.H., TINKER, P.B. (2000) Solute movement in the rhizosphere. Oxford: Oxford University Press.

RAUN, W.R., JOHNSON, G.V. (1999) Improving nitrogen use efficiency for cereal production. *Agronomy Journal*, 91: 357-363.

REEDER, J.D. (1986) A nonweighing lysimeter design for field studies using nitrogen-15. *Soil Science Society of America Journal*, 50: 1224-1227.

ROSSOUW, J.N., GÖRGENS, A.H.M. (eds) (2005) Knowledge review of modelling nonpoint source pollution in agriculture from field to catchment scale. Water research commission. Water Research Commission Report, WRC Report No. 1467/1/05.

SAINJU, U.M., LENSSEN, A.W., ALLEN, B.L., STEVENS, W.B., JABRO, J.D. (2016) Nitrogen balance in response to dryland crop rotations and cultural practices. *Agriculture, Ecosystems and Environment*, 233: 25-32.

SILGRAM, M., SHEPHERD, M.A. (1999) The effects of cultivation on soil nitrogen mineralization. *Advances in Agronomy*, 65: 267-311.

SMIL, V. (1999) Nitrogen in crop production: An account of global flows. *Global Biogeochemical Cycles*, 13: 647-662.

VAN DER LAAN, M., ANNANDALE, J.G., BRISTOW, K.L., STIRZAKER, R.J., DU PREEZ, C.C., THORBURN, P.J. (2014) Modelling nitrogen leaching: Are we getting the right answer for the right reason? *Agricultural Water Management*, 133: 74-80.

VAN DER LAAN, M., DU PREEZ, C.C., BRISTOW, K.L., STIRZAKER, R.J., ANNANDALE, J.G. (2009) Development, testing and application of a crop nitrogen and phosphorus model to investigate leaching losses at the local scale. PhD Thesis, University of Pretoria, Pretoria.

VAN DER LAAN, M., STIRZAKER, R.J., ANNANDALE, J.G., BRISTOW, K.L., DU PREEZ, C.C. (2010) Monitoring and modelling draining and resident soil water nitrate concentrations to estimate leaching losses. *Agricultural Water Management*, 97: 1779-1786.

WEIHERMÜLLER, L., SIEMENS, J., DEURER, M., KNOBLAUCH, S., RUPP, H., GÖTTLEIN, A., PÜTZ, T. (2007) In situ soil water extraction: A review. *Journal of Environmental Quality*, 36: 1735-1748.

YANG, G., PU, R., ZHAO, C., XUE, X. (2014) Estimating high spatiotemporal resolution evapotranspiration over a winter wheat field using an IKONOS image based complementary relationship and lysimeter observations. *Agricultural Water Management,* 133: 34-43.

YOUNG, M.H., WIERENGA, P.J., MANCINO, C.F. (1996) Large weighing lysimeters for water use and deep percolation studies. *Soil Science*, 161: 491-501.

7 CROP COEFFICIENTS AND PHOTOSYNTHETIC ACTIVITY OF POTATO AND MAIZE AS ASSESSED WITH EDDY COVARIANCE TECHNIQUES

A.T.B. Machakaire and A.C. Franke
Department of Soil, Crop and Climate Sciences, University of the Free State, Private Bag 339
Bloemfontein 9300, South Africa

7.1 Introduction

Water is a limiting resource in crop production and farmers are faced with the challenge of optimizing its use. This is important for improved crop production, reduced nutrient loss through leaching and the future sustainability of agriculture. Crop growth is influenced by site-specific conditions, which include weather, soil types and crop management, and these vary across different locations and regions.

Recently, Eddy covariance (ECV) techniques have become more available and affordable for use in cropping systems, allowing direct and continuous measurements of crop evapotranspiration (ET_c). There are different types of systems using open or closed pathways for measurements, with the ECV using an open pathway. ECV techniques measure vertical fluxes of gasses over a surface with water and carbon dioxide (CO_2) being the most commonly measured gasses. The ECV technique measures the covariance between fluctuations in vertical wind velocity and CO_2 mixing ratio, thereby producing a direct measure of net CO_2 exchange across the plant canopy-atmosphere interface (Baldocchi, 2003). This technique, which encompasses infrared gas analysis, can be used to measure photosynthetic CO_2 uptake and simultaneously measure transpiration (Long et al., 1996). The ECV method has made it possible to measure ET over a short-term period and large area. ECV techniques have been found to accurately estimate water losses thereby allowing the assessment of water availability and crop water requirements. Usually estimates of evapotranspiration (ET) have been used in irrigation scheduling through calculations and use of crop coefficients. Reference evapotranspiration (ET_o) from pan's or grass surfaces is normally used but has some inaccuracies. Use of this equipment in South Africa has been limited so far due to costs and availability. It has however been used by Parent and Anctil (2012) under Canadian conditions to quantify ET of a rain-fed potato crop in South-Eastern Canada and by researchers on other crops to measure CO_2 fluxes, carbon budgets and respiration rates (Kustch et al., 2010; Gowda et al., 2011).

The energy balance is normally used to evaluate the accuracy of the ECV measurements. The energy exchange at the vegetation surface has an influence on the evaporation of water, which requires a huge amount of energy either in the form of sensible heat (H) or radiant energy. ET is therefore limited by the amount of available energy (Allen et al., 1988). An energy balance equation is normally used to check the degree of error when estimating ET using micro-meteorological equipment. The energy balance closure is a formulation of the first law of thermodynamics and it requires that the sum of the estimated latent energy (LE) and sensible heat flux (H) be equivalent to all other energy sinks and sources, net radiation (Rn) and soil heat flux (G) in the case of ECV measurements (Wilson et al., 2002). Energy balance measures the radiation exchange at the crop and soil surface and the closure should approach

1.0 for a good agreement. Imbalances have been observed and a number of reasons, such as homogenous terrain and sensor alignment problems have been reported in such situations.

There are various decision support systems that are available for use by farmers to schedule irrigation but estimates of ET_c and use of K_c are more popular for determining crop water requirements. The FAO-56 single crop coefficient procedure is being widely used to estimate crop irrigation requirements but some researchers have shown that this method is not accurate for various localities and can lead to inaccurate estimates (Facchi et al., 2013). K_c values have been found to depend on the environmental and management conditions under which they were obtained. K_c values for the same crop can vary significantly between locations due to differences in variety, soil properties, irrigation method and frequency, climate and crop management practices (Payero and Irmak, 2011). Consequently, it is preferable to derive K_c values for local conditions for more accurate crop water requirements. Determining the ET_c of a crop under optimal water conditions is crucial in estimating the irrigation requirements of the crop. In the procedure proposed in the FAO-56 paper, K_c is determined as the ratio between ET_c from a specific crop and condition to ET_o of a reference such as grass. ET_o is calculated using the Penman-Monteith formula with local climatic data for the reference crop. Four crop development stages are recognized (L_{ini}, L_{dev}, L_{mid}, L_{late}) with K_c values being presented for three of these stages (K_c-ini, K_c-mid, K_c-end) (Allen et al., 1988). Crop water use is influenced by many factors which are variable and interdependent on one another such as; the climate, type and size of the crop, the root system, soil characteristics, crop phenology and type of irrigation system.

Potato is a cool weather crop, which yields well in temperate environments with long day-lengths. Potato production in South Africa and other regions in the world is done in higher temperature environments with shorter day lengths and high evaporative demand. Assessing the photosynthetic efficiencies of potato crops grown in these sub-optimal conditions of intense radiation provides the opportunity to establish the interactions with radiation use efficiency (RUE), water use efficiency (WUE) as well as the relationship with ET. The performance or yield potential of potato crops depends on the genotype, as defined by the duration of its growth, the environment it is grown in, as defined by CO_2 availability, temperature, day length and solar radiation, and management of the crop. The potato crop duration is heat and water sensitive, with temperature being a main-determinant of yield (Kooman and Haverkort, 1995). Globally, potato is the most important food crop after maize, rice and wheat. Africa produces about 8% of the total global production (Food and Agricultural Organisation, 2015). In South Africa, potato production reached about 52 000 ha in 2011 (approximately 0.6% of the global production). It has been fluctuating over the years having reached a peak of 66 000 ha in 1991 (Potatoes South Africa, 2013). South Africa has sixteen different potato production regions that represent different climatic and soil conditions. This geographical dispersion enables South Africa to produce potatoes all year round, though the quality will vary according to the time of year. The largest potato production areas are in Limpopo, Western Free State, Eastern Free State and the Western Cape (the Sandveld) Provinces. SAF is an arid country with annual rainfall averaging 450 mm in comparison to the world average of 860 mm and the net rainfall is negative as evaporation exceeds rainfall (Harding, 2015).

The objectives of this study were to quantify the crop water use of potatoes using ECV techniques, investigate the interactions between environmental factors and crop growth parameters, assess net biomass growth rate and photosynthetic activity of potato and maize, assess how crop coefficients develop over the season and calibrate K_c for potato and maize grown under SA climatic conditions.

7.2 Methodology

7.2.1 Site description

Potato-maize rotations were selected on a commercial farm in the Western Free State nearby the village of Christiana. Two fields measuring 25 ha each under centre pivot irrigation systems using surface water from the Vaal River were selected. One field was planted to potato (Lat: 28° 4'38.87"S; Lon: 25° 6'28.98"E) and whilst the other had a rotational maize crop (Lat: 28° 3'47.53"S; Lon: 25° 5'53.62"E). The rotational maize crop was planted on 29 September 2016 and harvested on 16 February 2017 (140 days after plant) whilst the potato crop was planted on 3 November 2016 and harvested on 2 February 2017 (92 days after planting). The soils on the farm range from sandy to loamy sand with low organic matter (OM) content.

7.2.2 Crop management

7.2.2.1 Potato crop

Potato variety 'Mondial' was planted as seed tubers on rows that were 0.9 m apart at a target plant density of 35 000 plants per ha for the count 220 seed size planted.

Table 25: Input application to potato and maize: nutrients applied as mineral fertilizer (kg ha^{-1}) and irrigation water (mm)

Input	Maize	Potato
Nitrogen	103	290
Phosphorous	17	145
Potassium	11	248
Calcium	0	281
Irrigation water	243	395

7.2.2.2 Maize crop

Maize variety 'Monsanto 94-14' was planted in rows 1.0 m apart at a target density of 40,000 plants per ha. Fertilizer was applied as split applications throughout the growing season (Table 25). /

7.2.3 Sampling scheme

Within each potato field, 24 adjacent plots measuring 1.8 x 3.0 m (5.4 m^2) were demarcated. The experimental plots were randomized within blocks and replicated 4 times within the main plot. Six times during the growing season, plant growth measurements were taken. During each sampling event, 4 plots were destructively sampled. In each maize field, 24 adjacent plots of 4.0 x 3.0 m (12.0 m^2) were used for sampling. Each individual plot comprised of 4 rows of which the middle two rows measuring 2 x 3.0 m (6.0 m^2) were sampled for growth analysis and collection of crop data. The outer two rows per plot were considered as the border rows and no crop data was collected from them. As in the potato field, during each of the six samplings events during the growing season, four plots were destructively sampled.

7.2.4 Field measurements

7.2.4.1 Weather parameters

Precipitation and irrigation combined were measured using a tipping bucket rain gauge and the data recorded on a CR1000 data logger at 30-minute intervals. Reference evapotranspiration (ET_o) was calculated from weather data collected from the Agricultural Research Council's Jan Kempdorp weather station (Lat: 27°57'27.36"S.; Lon: 24°50'23.64"E, Altitude 1180 masl) using the Penman Monteith equations

7.2.4.2 Soil parameters

Soil samples were taken from the field at three different spots were the experimental plots were located at three different spots and three depths 0-0.3 m, 0.3-0.6 m and 0.6-1.0 m before planting of each crop and analyzed for total available N, NH_4^+-N, NO_3^--N (KCl extraction method), available P (Bray 1 method), organic matter (OM) content, pH (KCl), electrical conductivity (EC) and particle size. Three sub-samples at each depth made a composite sample.

7.2.4.3 H_2O and CO_2 fluxes measurements

The IRGASON integrated open-path CO_2/H_2O gas analyzer (eddy-covariance system – ECV) (Campbell Scientific) was used to measure the H_2O vapour density and CO_2 density above the crop canopy. The additional supporting sensors (sonic anemometer, fine wire thermocouple, NR-Lite net radiometer, silicon pyranometer, krypton hygrometer, CS616 reflectometer, Hukseflux heat flux plates) were sampled at a frequency of 10 Hz. The recorded 10 Hz data was processed using EddyPro 6.1.0 software (Li-COR Biosciences) and EasyFlux DL software (Campbell Scientific). The gas analyzer was installed as part of the ECV equipment on a tripod mast at a height of 2.0 m (potato) and 2.25 m (maize) above the soil surface, oriented towards the west as this was the predominant direction from which the wind blew from. The average fetch for the Irgason above the crop surface was about 150 m in either direction. Data was sampled, processed, recorded with a CR3000 data logger and downloaded from a 2 GB memory card.

7.2.4.4 Crop parameters

Plant biomass and dry matter were measured and recorded through destructive sampling in the season in four plots at each sampling event. The leaf area index (LAI) was measured using a ceptometer (AccuPAR LP-80, Decagon Devices) which derives LAI from the intercepted PAR data. The AccuPAR LP-80, which consists of a linear probe, was used to measure photosynthetic active radiation (PAR) above and below the crop canopy at each of the six sampling events from the four plots that were sampled. The ceptometer was placed between two potato rows with each end of the probe in the middle of each row and the external point sensor connected to it placed on a pole 1.2 m above the canopy. For the maize crop, the linear probe was placed across one row and the external point sensor held above the crop canopy. The LAI measurements with the AccuPAR LP-80 were calibrated through two destructive measurements done during the season. A sub-sample of the plant material harvested from each plot was used to measure leaf area with a LICOR LI-3100C.

The dry matter content of the roots, stems, leaves and tubers was determined using four sub-samples that were dried in an oven at 70°C to constant weight. The final tuber yield was measured at crop end, which was 91 days. The final grain yield was measured at crop end at 140 days. The fresh tuber yield, tuber dry matter yield and final grain yield were determined from the sample area harvested.

7.2.5 Data handling

Crop biomass production was calculated from the CO_2 flux data recorded by the ECV equipment. The 30 min interval data for g CO_2 m^{-2} was converted to net CO_2 flux for the season. Carbon (C) uptake by the crop was calculated from the net flux using the ratio of the molecular weight of C to that of CO_2 (0.27). To convert C uptake into glucose production, a C-glucose conversion factor of 2.5 was used. In the conversion of glucose to other structural DM there is a C condensation, which may result in more C per gram of biomass than glucose, and it was assumed that this C condensation was negligible. The calculated DM production based on CO_2 fluxes was compared to the actual measured DM production at crop maturity.

K_c was calculated as the ratio of the ECV measured crop evapotranspiration (ET_c) to the reference crop evapotranspiration (ET_o);

$$K_c = \frac{ET_c}{ET_o}$$

ET_o was calculated from the weather station measured climatic data using the FAO standardized Penman-Monteith equations (Allen et al., 2005);

$$ET_o = \frac{0.408\Delta(R_n - G) + [\frac{900\gamma}{T_a mean + 273}]\mu_2(e_s - e_a)}{\Delta + \gamma(1 + 0.34\mu_2)}$$

Where μ_2 is the wind velocity (m s^{-1}), Δ is slope of saturation vapor pressure curve (kPa $^oC^{-1}$), R_n is the net radiation (MJ m^{-1} day^{-1}), γ the psychometric constant (kPa $^oC^{-1}$), $T_a mean$ is the mean temperature, e_s

is the saturation vapor pressure (kPa) and e_a is the actual vapor pressure (kPa). The K_c values were calculated daily and then averaged for the specific growth stages as observed in the field sampling.

7.3 Results

7.3.1 Weather data

The season was hot and drier than normal in the early to mid-stages (October-December) with late rainfall of increased frequency and quantity received in early January 2017. Maximum temperatures occasionally exceeded 40°C (Figure 43).

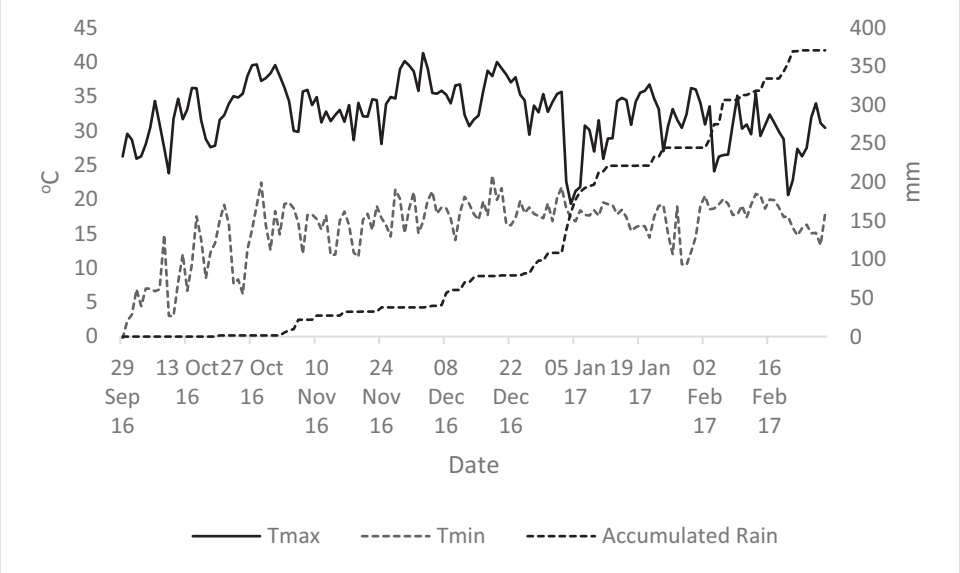

Figure 43: Actual weather data for the cropping season

7.3.2 Crop growth

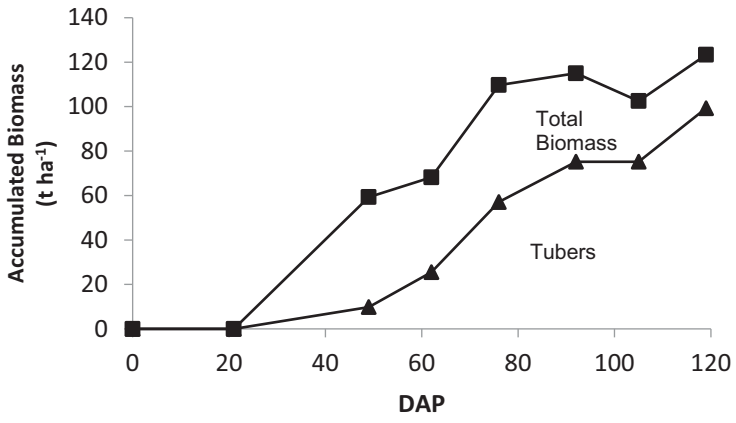

Figure 44: Observed potato crop biomass development

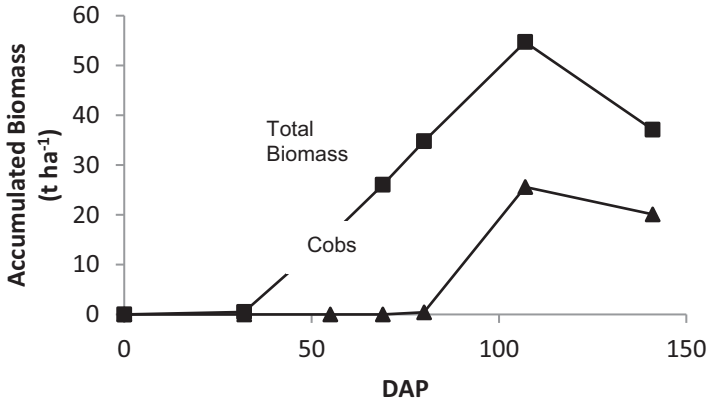

Figure 45: Observed maize crop biomass development

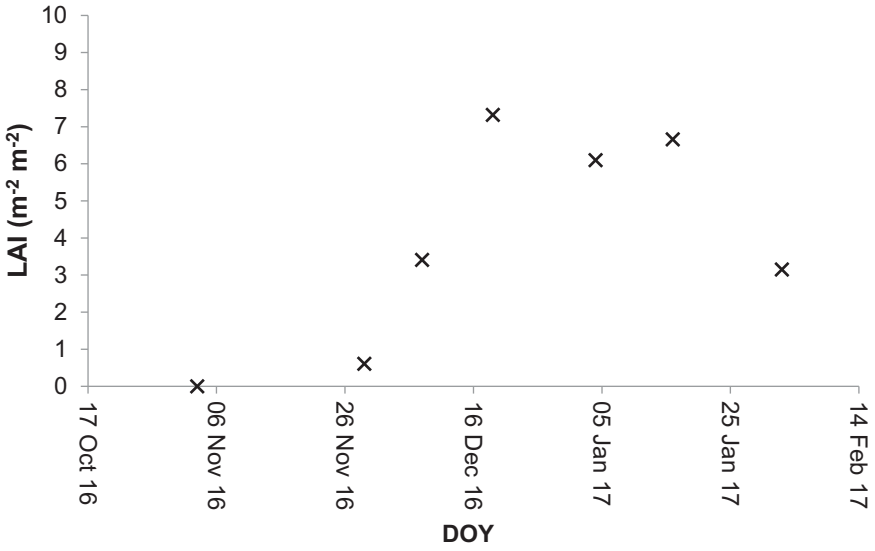

Figure 46: Observed leaf area index development for potato

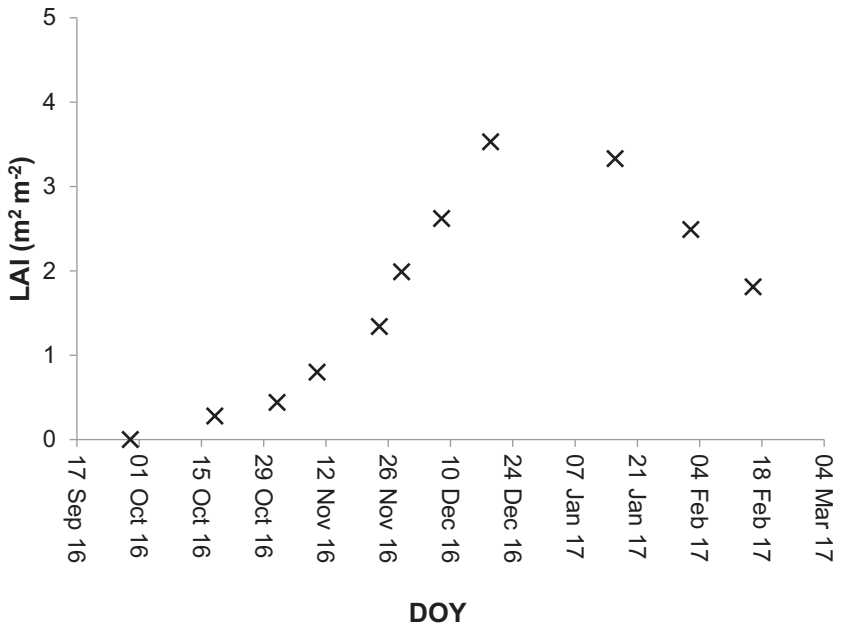

Figure 47: Observed leaf area index development for maize

Table 26: LAI measurements for AccuPAR LP-80 and Licor LI-3100C

Crop	LAI (m^{-2} m^{-2})			
	AccuPAR LP-80	Licor LI-3100C	AccuPAR LP-80	Licor LI-3100C
	Sample 1	Sample 1	Sample 2	Sample 2
Maize	2.60	2.61	3.30	2.47
Potato	3.40	1.21	6.66	3.80

7.3.3 Water and CO_2 Flux measurements

7.3.3.1 Potato crop

The net CO_2 flux was -0.46 g CO_2 m^{-2} 30 min^{-1} which is equivalent to 220.9 kg CO_2 day^{-1} ha^{-1} or 60.3 kg C day^{-1} ha^{-1}. When converted to glucose ($C_6H_{12}O_6$) using a conversion factor of 2.5, this represents 150.6 kg of glucose produced per day. Over the growing period of 91 days, the total DM production was 13.7 t ha^{-1}. The measured HI for this early harvested crop was 68% and the calculated DM production for the potato tubers was 9.3 t ha^{-1}. The measured DM production at harvest was 9.1 t ha^{-1}.

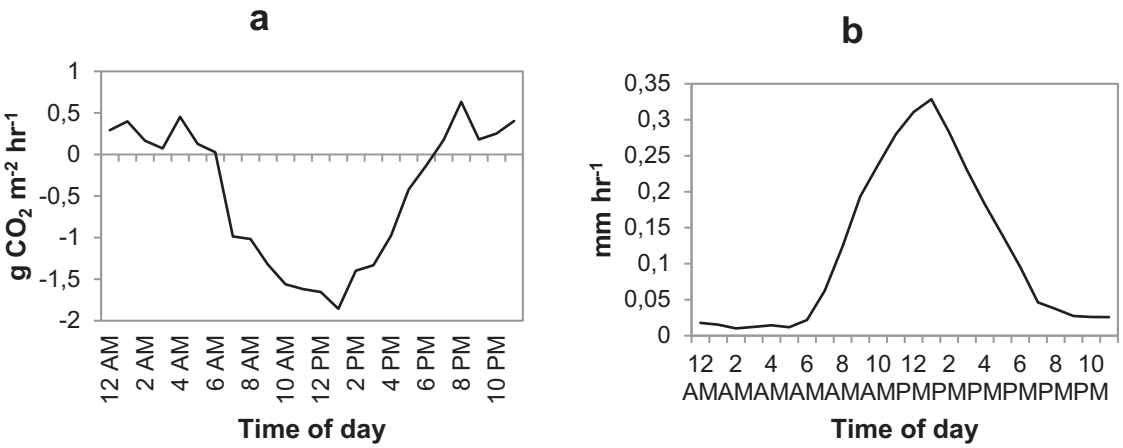

Figure 48: Average hourly fluxes for a) CO_2 and b) Water (Potato)

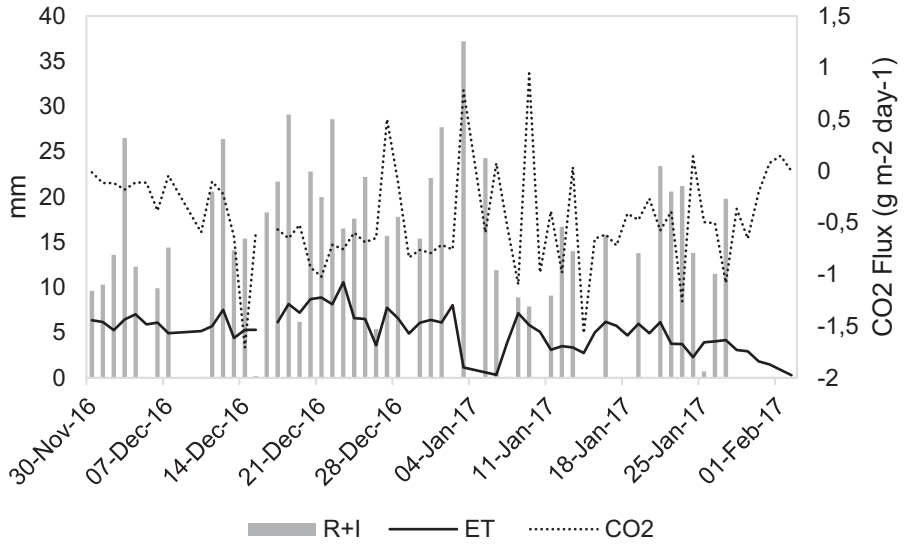

Figure 49: Average daily CO_2, H_2O fluxes and rainfall + irrigation for potato

Table 27: Crop coefficients for potato growth stages

Studies	Sprout development	Vegetative growth	Tuber initiation	Tuber bulking	Maturation	Study area
Doorenbos & Pruitt (1977)	0.50	0.80	-	1.10	0.72	
Allen et al. (1988)	0.80	0.98	-	1.15	0.75	USA
Kashyap & Panda (2001)	0.42	0.85	-	1.27	0.57	India
Allen & Wright (2002)	0.31	0.64	0.77	0.73	0.36	USA
US Bureau of Reclamation	0.46	0.78	0.88	0.93	0.70	USA
Parent and Anctil (2012)		0.63	0.91	0.81	0.78	Canada
This study: Christiana		**0.79**	**0.99**	**0.74**	**0.25**	**South Africa**

7.3.3.2 Maize crop

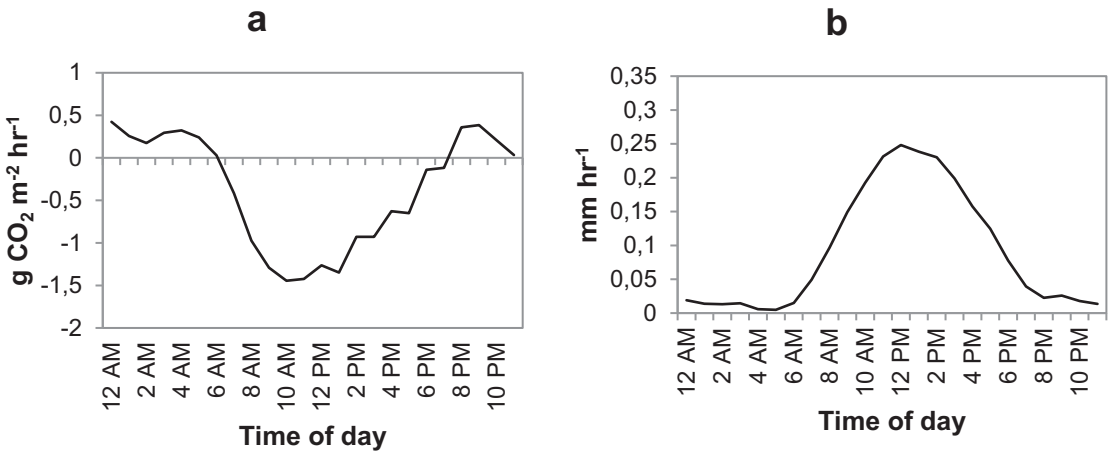

Figure 50: Average hourly fluxes for a) CO_2 and b) Water

The net CO_2 flux for the growing season was -0.38 g CO_2 m^{-2} 30 min^{-1} which is equivalent to 182.4 kg CO_2 day^{-1} ha^{-1} or 49.8 kg C day^{-1} ha^{-1}. When converted to glucose ($C_6H_{12}O_6$) using a conversion factor of 2.5, the calculated glucose production was 124.4 kg glucose day^{-1} ha^{-1}. For the 141 day growing season, calculated total glucose production was 17.5 t ha^{-1}. However, the glucose is converted into structural biomass in the plant. It was assumed that about 15% of the DM production was in the plant roots, and since the sampled plants were cut at the soil surface and harvested without the roots (which is also the norm under commercial field production), 14.9 t ha^{-1} of the glucose production was

considered which excluded the root component. The measured HI was 54% and the calculated DM production in the grain was 8.0 t ha^{-1}. The moisture content of the harvested grain was 13% and when this was added to the calculated DM production in the grain from the CO_2 flux, the estimated FM yield (grain) was 9.1 t ha^{-1}. The actual measured FM yield (grain) was 9.6 t ha^{-1}.

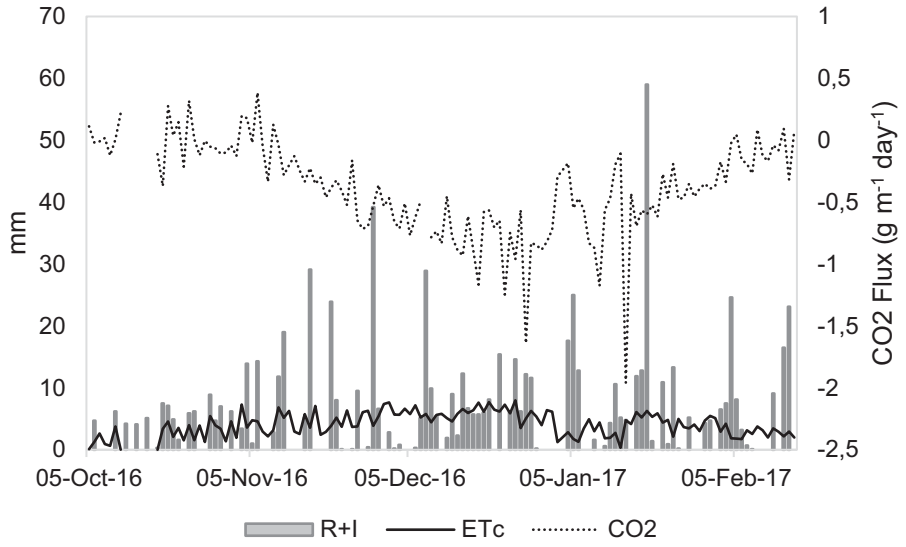

Figure 51: Average daily CO_2, H_2O fluxes and rainfall + irrigation for maize

Table 28: Comparison with Kc from literature

Studies	Initial stage	Development stage	Mid-stage	Late stage	Study Area
FAO			1.20	0.60	Sub-humid climate
Facchi et al. (2013)	0.33		0.99	0.35	Northern Italy
Govinda Bhandari (2012)	0.11	0.35	1.51	0.34	Nepal
Shahrokhnia & Sepaskhah (2013)	0.48		1.4	0.31	Iran
This study	**0.32**	**0.65**	**0.83**	**0.68**	**South Africa**

7.3.4 Energy balance

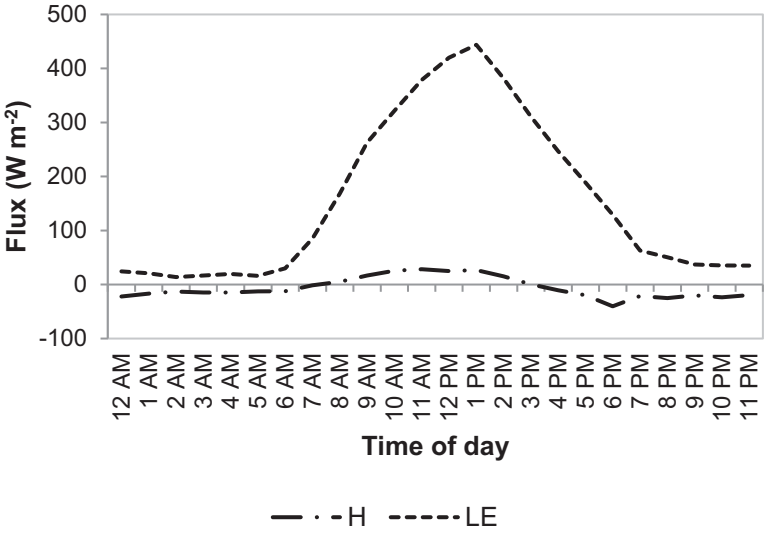

Figure 52: Energy balance components for Potato

H and LE were the energy balance components that were measured by the ECV on the potato field (Figure 52). Rn and G were not measured due to sensor malfunction.

7.4 Discussion

7.4.1 Crop growth

7.4.1.1 Potato

From emergence to tuber initiation, potato biomass was mainly made up of the aboveground plant parts (stems and leaves). As more dry matter was allocated from the leaves and stems into the tubers, the plant biomass part of the tubers increased. Later in the season as the tubers matured and the leaves senesced, the aboveground biomass declined (Figure 44). LAI gradually increased from planting reaching a maximum 7.32 m^2 m^{-2} (Figure 46). At LAI = 0 no radiation is intercepted, and close to 100% radiation is intercepted at LAI = 3 and above (Haverkort et al., 2015).

7.4.1.2 Maize

The development of maize crop followed a typical sigmoid pattern (Figure 45). LAI for maize reached a maximum of 3.5 m^2 m^{-2} (Figure 47) The LAI results from the AccuPAR LP-80 compared reasonably well with those from the Licor LI-3100C leaf area meter (Table 26).

7.4.2 Water and CO_2 fluxes

7.4.2.1 Potato crop

The CO_2 flux was generally positive (a net upward flux) from 7 pm to 6 am which was the night-time and negative (a net downward flux) during daytime (Figure 48). During the daytime, there was net photosynthesis as the crops take up CO_2 from the atmosphere and the net flux was negative. During the night-time, there is net respiration as the plants release CO_2 into the atmosphere and the flux was positive. Early in the season after the seed was planted, the net CO_2 flux was positive because there was no crop to absorb the CO_2 from the atmosphere. As the crop emerged and began to establish some CO_2 was absorbed but in small quantities (Figure 49). The flux became negative but was small. As the crop developed and used more CO_2 for photosynthesis, the net flux became more negative (Figure 49). However, there were few positive peaks within the development stages, these were observed to mostly coincide with periods with rainfall, creating conditions conducive for soil microbes to break down soil C releasing CO_2 in the process while photosynthesis rates are reduced due to reduced radiation and cold temperatures. Towards crop end as the crop matured and senesced, the net CO_2 flux became less negative and eventually positive again as photosynthesis ceased and dry matter was partitioned to the storage organs. The measured DM yield was 9.1 t ha^{-1} and it compared well to the DM production calculated based on net photosynthesis fluxes of 9.3 t ha^{-1}. The potato plants were observed to use more CO_2 for dry matter production than maize, reflecting potato's higher growth rate.

The average daily water flux was low during the night and reached a peak around midday when maximum ET_c occurs and solar radiation was close to its maximum (Figure 48). This confirms that ET_c is influenced by radiation and air temperature as ET_c was lowest at night when there was no radiation and temperatures were lower, gradually rising from sunrise to midday as temperature and solar radiation increased, after which it gradually declined as the temperature and radiation reduce. During the night-time, stomata are expected to be closed thereby restricting water loss by the plant.

Accumulated ET_c was 509 mm for the season. The highest daily ET_c measured for potato was 10.6 mm per day in the tuber initiation stage. The lowest ET_c was measured during the tuber bulking stage after a period of 4 days where 113 mm of rain and irrigation was received. It was cool during this period and radiation was low resulting in low ET_c. ET_c gradually dropped as the crop senesced, as less irrigation was applied to the crop in preparation for harvest. Other peaks and drops in ET_c during the season were a result of fluctuations in weather conditions, crop developmental stage, as well as irrigation events, which influenced the humidity of the air. Irrigation water applied to the crop during the season ranged from approximately 10-20 mm per irrigation cycle at 2-day intervals and for periods when high ETc was measured this amount may have not compensated for the evaporative losses.

There was a sensor malfunction on the ECV for the first 27 days after planting. However, flux data was recorded for the greater part of the growing season with some small gaps that occurred due to a possibility of the wind not being in the right direction for a proper recording.

7.4.2.2 Maize crop

The average daily water flux was low during the night and reached a peak around midday an indication that it was at that time when maximum ET_c occurred and solar radiation was close to its maximum (Figure 50). Throughout the season, there were upward and downward peaks which coincided with changes in radiation, air temperature, irrigation and rainfall events. There was a huge downward peak around 3-6 January 2017 as >100 mm rainfall was received in that 4-day period and radiation was low and humidity high. The general trend for ET_c was a gradual increase from planting until silking followed by a gradual decrease until maturation and harvest. The accumulated ET_c measured for the season was 567 mm.

Average hourly CO_2 fluxes peaked at -1.44 g CO_2 m^{-2} for the daytime and 0.42 g CO_2 m^{-2} for the night-time. As with potato, the net CO_2 flux is positive early in the season after planting before emergence, as there was no photosynthetic activity. As the plants emerged and began to develop, they absorbed CO_2 from the atmosphere to photosynthesize and the net flux was negative (Figure 51). There were some positive peaks earlier in the season and these could be a result of soil microbial decomposition of organic matter. As the maize crop developed and plant biomass increased, the plants utilized more CO2 and fluxes became more negative. Towards crop end, the net flux became positive as the crop matured and senesced. The estimated grain yield of 9.1 t ha^{-1} compared to the measured yield of 9.6 t ha^{-1} at harvest.

There were some gaps in the measured data due to system malfunction. The Irgason was installed one week after planting and there was no data collected for the initial period after planting.

7.4.3 Crop coefficients

7.4.3.1 Potato

K_c values gradually increased from emergence as the plants developed reaching a peak in the tuber initiation stage, beyond which they gradually declined as the crop matured. The calculated Kc values were relatively low in the tuber bulking and maturation stage (Table 27). This could be because of the weather conditions as the earlier planted potato crop matured in the summer months when radiation and temperature were high. In most other countries, potatoes are harvested in autumn when temperature is low, which is different from the early-planted crop in the study area. K_c in maturation stage was low because the crop was harvested at an earlier stage than it would normally be harvested, and irrigation had been stopped and the haulms had been destructed in preparation for harvest. The calculated K_c values for the vegetative and tuber initiation stages were comparable to those obtained from other research done in other parts of the world.

7.4.3.2 Maize

A comparison of the measured ET_c with results from other studies done in other parts of the world shows the wide variability of ET_c across different regions and hence the importance of determining site-specific values K_c values (Table 28). K_c vary from one area to another due to a number of factors. Planting density, crop variety and developmental stage also influences ET_c and hence K_c as crop height, ground cover and rooting characteristics may vary. The soil type will influence the soil water holding properties and ultimately ET. A poor crop nutritional status and health may limit development of the crop and reduce ET_c.

7.4.4 Energy balance

Due to sensor malfunction, not all energy balance components could be measured. However, the diurnal variations in the sensible heat and latent energy fluxes that were measured followed the expected trends (Figure 52).

7.5 Conclusions

The measured K_c values in the semi-arid areas of the Western Free State were different from those observed in the other parts of the world where measurements have been done. It is important to derive Kc values for local conditions in-order to ensure accurate determination of crop water requirements. The crop water requirement for potato based on ET measurements is around 550 mm for medium to late maturing varieties such as Mondial and water applications should be evenly distributed throughout the season. Maize, which is grown over a longer season, has a similar water requirement. However, the actual amount of water that needs to be applied is substantially more due to other evaporative losses, drainage and run-off.

Potato a C3 plant utilizes more CO_2 for photosynthesis and dry matter production in comparison to maize a C4 plant. However, maize is expected to be more efficient at photosynthesis in the hot, sunny conditions experienced in the study area.

7.6 References

ALLEN, R.G., PEREIRA, L.S., RAES, D. & SMITH, M. (1988) Crop evapotranspiration – Guidelines for computing crop water requirements. *FAO Irrigation & drainage paper 56*.

BALDOCCHI, D.D. (2003) Assessing the eddy covariance technique for evaluating carbon dioxide exchange rates of ecosystems: past, present and future. *Global Change Biology*, *9*(4), 479-492.

DOORENBOS, J., & PRUITT, W.O. (1977) Background and development of methods to predict reference crop evapotranspiration (ETo). *Guidelines for predicting crop water requirements*, (24), 108-119.

FACCHI, A., GHARSALLAH, O., CORBARI, C., MASSERONI. D., MANCINI, M. & GANDOLFI, C. (2013) Determination of maize crop coefficients in humid climatic regime using the eddy covariance technique. *Agricultural Water Management 130, 131-141*.

GOWDA, P. (2011) Lysimetric Evaluation of Eddy Covariance Fluxes over Irrigated Cotton in the Texas High Plains. *Assessment*, *194*, 8.

HARDING, W.R. (2015) Living with eutrophication in South Africa: a review of realities and challenges. *Transactions of the Royal Society of South Africa*, (ahead-of-print), 1-17.

HAVERKORT, A.J. & STRUIK, P.C. (2015) Yield levels of potato crops: Recent achievements and future prospects. *Field Crops Research 182*, 76-85.

KASHYAP, P.S. & PANDA, R.K. (2001) Evaluation of evapotranspiration estimation methods and development of crop-coefficients for potato crop in a sub-humid region. *Agricultural Water Management*, *50*(1), 9-25.

KOOMAN, P. & HAVERKORT, A.J. (1995) Modelling development and growth of the potato crop influenced by temperature and day length: LINTUL-POTATO. p. 41-59. *In:* Anonymous Potato ecology and modelling of crops under conditions limiting growth. Springer.

KUTSCH, W.L., MARC AUBINET, N. BUCHMANN, P. SMITH, B. OSBORNE, W. EUGSTER, M. WATTENBACH et al. (2010) "The net biome production of full crop rotations in Europe." *Agriculture, Ecosystems & Environment* 139, no. 3, 336-345.

LONG, S.P., FARAGE, P.K. & GARCIA, R.L. (1996) Measurement of leaf and canopy photosynthetic CO2 exchange in the field. *Journal of Experimental Botany*, *47*(11), 1629-1642.

PARENT, A. & ANCTIL, F. (2012) Quantifying evapotranspiration of a rainfed potato crop in South-eastern Canada using eddy covariance techniques. *Agricultural Water Management,* 113(0), pp. 45-56.

PAYERO, J.O. & IRMAK, S. (2011) Daily Crop Evapotranspiration, Crop Coefficient and Energy Balance Components of a Surface-Irrigated Maize Field. *IntechOpen*, DOI: 10.5772/18352.

SHAHROKHNIA, M.H. & SEPASKHAH, A.R. (2013) Single and dual crop coefficients and crop evapotranspiration for wheat and maize in a semi-arid region. *Theoretical Applied Climatology*, 114, 495-510.

WILSON, K., GOLDSTEIN, A., FALGE, E., AUBINET, M., BALDOCCHI, D., BERBIGIER, P. & VERMA, S. (2002) Energy balance closure at FLUXNET sites. *Agricultural and Forest Meteorology*, *113*(1), 223-243.

FOOD AND AGRICULTURAL ORGANISATION (2015% Crop production data. Available at http://faostat3.fao.org/download/Q/QC/E (Accessed 24 August 2015).

POTATOES SOUTH AFRICA (2013) Industry information. Available at www.potatoes.co.za/SiteResources/documents /Distrib%20crop.JPG (Accessed 24 August 2015).

8 NUTRIENT USE EFFICIENCIES AND LEACHING POTENTIALS OF IRRIGATED POTATO-MAIZE SYSTEMS IN CENTRAL SOUTH AFRICA

A.T.B. Machakaire[1,2], G.M. Ceronio[1], J.H. Barnard[1] and A.C. Franke[1]
[1]Department of Soil, Crop and Climate Sciences, University of the Free State, Private Bag 339 Bloemfontein 9300, South Africa
[2]McCain Foods SA, PO Box 1023, Delmas, 2210, South Africa

8.1 Introduction

Irrigated farming in South Africa faces a number of challenges which include scarcity of water as a resource, dependence and over use of fertilizers and chemicals, nutrient leaching and eutrophication. Most farming systems have become intensive and when poorly managed pose a risk to the environment and threaten the long-term productivity of land and water resources. Eutrophication is a reality in South Africa. It is a serious problem in a number of catchment areas and appears to have escalated over time with the root problem being nutrient enrichment in freshwater resources. Although the use of fertilizers in agriculture is beneficial in improving crop yields and quality, there are environmental implications associated with its use (Franke et al., 2011; Arauzo & Valladoid, 2013). Farmers tend to over-irrigate when they are unsure of when and how much to irrigate. The lack of use of decision support tools and systems for irrigation scheduling and management by some farmers worsens the problem. In sandy soils, the management of water and fertilizer inputs is especially a challenge because such soil types have a low water and nutrient holding capacity potentially leading to high drainage and nutrient leaching rates. Given the potato plant's shallow rooting system, nitrogen (N) and phosphorous (P) leaching potential is relatively high.

The continued use of inputs of fertilizer P in excess of crop requirements has also led to a build-up of soil P levels which are of an environmental concern particularly in intensive crop production areas such as those found in SAF (Sharpley et al., 1994; Ierna et al., 2011). The contribution of P originating from agricultural sources to non-point source (NPS) pollution of surface waters has been an environmental issue for a long time. P is relatively immobile in soils and therefore most research and NPS pollution control efforts have emphasized P losses by surface erosion and run-off and not through soil drainage. No published work from South Africa studying P leaching in drainage water from crop production systems has been found.

The fate of the nutrients removed by drainage from the root zone depends on the prevailing conditions (Van Rensburg et al., 2012). On soils that drain freely with no restricting soil layers or water table below the potential rooting depth of a crop, the nutrients will accumulate below the root zone and gradually precipitate or leach deeper into the substrata thereby contaminating the groundwater. The water leaching past the depth of the root zone tends to continue leaching down the soil profile and eventually enters the surficial aquifer, and thus, becoming a source of "non-point pollution" of the surficial aquifer (Alva, 2010). The groundwater is expected to flow laterally along the sloping topography at a steady rate and the leached nutrients from the root zone are mixed into this stream, eventually being removed from the system and ending up in an "unknown sink", such as river water. N leaching is directly related

to deep drainage processes. The aim to reduce and prevent water pollution caused by nitrate (NO_3^-) from agricultural sources in the European Union led to the guideline that both surface freshwater and groundwater are considered affected by NO_3^- pollution when they contain more than 50 mg ℓ^{-1} of NO_3^- (Arauzo and Valladolid, 2013). The permissible limits in South Africa are lower with a maximum of 10 mg ℓ^{-1} for NO_3^- and 0,025 mg ℓ^{-1} for phosphate.

Eutrophication is a process by which lakes, rivers and coastal waters become increasingly rich in plant biomass as a result of enhanced input of plant nutrients mainly N and P (Nyenje et al., 2010). Most of the nutrients causing eutrophication originate from agricultural and urban areas. Industrial and domestic activities also result in treated wastewater containing some of these nutrients being discharged into rivers. High nutrient concentration, stagnation for prolonged periods, with suitable temperature, oxygen concentration and high light intensity enhance eutrophication (Van Ginkel, 2011). South Africa is facing widespread eutrophication-related problems which are mostly associated with the larger metropolitan areas and the dams on which these areas rely for their water supplies such as the Vaal, Roodeplaat and Hartbeespoort dams in Gauteng and North West Provinces. There are 19 catchment management areas in South Africa and most of them are threatened by eutrophication. The Department of Water and Sanitation in its 2007/2008 annual report stated that 42% of the reservoirs that were subjected to water quality monitoring were eutrophic (Harding, 2015). There are five trophic categories; ultra-oligotrophic, oligotrophic, mesotrophic, eutrophic and hypertrophic. Each category is characterized by an average annual measured concentration of total P, chlorophyll-a, as well as maximum measured chlorophyll-a of water bodies using a Medium Resolution Imaging Spectrometer.

Globally, eutrophication is increasingly affecting surface waters and it directly influences the widespread increase in cyanobacterial blooms, whose effects are symptoms of increasing eutrophication, and many of their genera produce one or more of a range of cyanotoxins (Van Ginkel, 2011). Phosphate enriched waters therefore pose a risk of noxious cyanobacterial blooms. The presence of high nutrient concentrations in surface waters also supports the rapid growth of macrophytes. Excessive macrophyte biomass blocks waterways, impedes access to dams and rivers, clogs drainage systems and contributes to flooding and the destruction of canals. Eutrophication management options need to be developed to slow down the effects on surface water bodies in South Africa and the problem needs to be addressed at source. The most important management approach at farm level involves minimizing the influx of nutrients into fresh water systems. Production practices have been moving towards optimization of N, P and water usage, for optimized crop production and minimized N and P leaching risk. Maximizing the N and P use efficiencies on sandy soils is important for limiting groundwater and surface water contamination and improving the economic return on fertilizer applications (Ierna et al., 2011; Van der Laan et al., 2014, Hendricks et al., 2014). Collective management strategies to reduce nutrient enrichment of surface waters therefore need to be developed so that farmers can adopt them.

While definitions and aims of sustainable agricultural production vary, some consider the key aim of sustainable cropping to use inputs optimally, whilst maximizing crop production, quality and profitability with minimum negative effects on the environment (Alva et al., 2010; Ierna et al., 2011). Sustainability of irrigated agriculture depends primarily on the efficient management of irrigation water to enhance

crop productivity while minimizing salinification, drainage, nutrient leaching and eutrophication (Kayshap and Panda, 2001). The United Nations has sustainable consumption and production as one of its focus areas in its sustainable development goals, showing the importance of sustainable agricultural production. It will also ensure long-term productivity of land and water resources through reduced environmental pollution, increased resource use efficiencies and improved land management practices.

Potato in South Africa is produced in 16 climatically and edaphically distinct regions with the largest potato production areas found in Limpopo, the Western Free State, the Eastern Free State and the Western Cape (the Sandveld). Seed potato production mainly occurs in the Western Free State and North West Province in central South Africa under centre pivot irrigation. This area is semi-arid, receiving annual average rainfall of 554 mm per year and accurate estimates of crop water requirements are crucial because water resources for irrigation purposes are limited. Potato farmers in this area plant potatoes for both the seed and table markets. Typically, seed potato is planted in the first year of a crop rotation system, followed by maize, grass or a fallow period in the second year. Where grass follows a maize crop, it is usually planted in-between the maize crop and left to grow after the maize has been harvested. Onion is another crop planted in the rotation usually in the third year after the maize or a fallow period. Seed potato is re-planted in the rotation again after a period of 5 to 7 years from the last potato planting. Crop rotation is important in controlling soil-borne diseases as well as build-up of pests such as nematodes. Minimum amounts of fertilizers are used on the maize crop as it is expected to also use residual nutrients from the previous potato crop. Given the deep rooting characteristics of maize, a substantial part of the nutrient and water leached from the potato crop may be recovered by the maize. Following the subsequent maize crop, enables us to investigate if the residual nutrients lost below 1.2 m are available for use by a subsequent deeper rooting crop. Therefore, a cropping system approach is expected to give a better picture of the NPS pollution potential from potato-maize based systems than a focus on potato alone.

The objectives of this study were to determine nutrient and water use efficiencies of potato and maize crops grown in rotation, quantify the extent to which deep drainage water in potato-based cropping systems are likely to contribute to the eutrophication of water resources in central South Africa and recommend management strategies that optimize resource use and limit negative environmental impacts.

8.2 Methodology

8.2.1 Site description

Potato-maize rotations were selected on a commercial farm in the Western Free State nearby the village of Christiana. The area is in the Middle Vaal catchment area, downstream from the Bloemhof dam. The selected fields were under center pivot irrigation systems using surface water from the Vaal River. The fields in the study were ±3 km from the river bank. In Season 1, two potato fields on the same farm measuring 22 ha (Field A – Lat: 28° 4'41.80"S; Lon: 25° 5'42.28"E) and 25 ha (Field B – Lat: 28° 3'47.53"S; Lon: 25° 5'53.62"E), were used. Field A was planted on 20 January 2016, Field B on

25 January 2016 and both were harvested on 19 May 2016 (Field A was 121 days and Field B was 116 days after planting (DAP). In Season 2 Field B was planted to a rotational maize crop following the potato crop on 29 September 2016 and was harvested on 16 February 2017 and a new potato Field C (Lat: 28° 4'38.87"S; Lon: 25° 6'28.98"E) measuring 25 ha was planted on 3 November 2016 and harvested on 2 February 2017 (92 DAP). In Season 3 Field C was planted to a rotational maize crop following the potato crop on 19 September 2017 and was harvested on 20 February 2018 (154 DAP). A new potato Field D (Lat: 28° 4'49.63"S; Lon: 25° 6'47.26"E) measuring 25 ha was planted on 1 November 2017 and harvested on 20 February 2018 (112 DAP). The soils on the farm range from sandy to loamy sand with low organic matter (OM) content.

8.2.2 Crop Management

8.2.2.1 Potato crop

Potato variety 'Mondial' was planted as seed tubers on rows that were 0.9 m apart at a target plant density of 35 000 plants per ha for the count 220 seed size planted. Fertilisers were applied through four different methods: broadcasting, band placement, fertigation and spraying through a tractor mounted sprayer. The nutrients focused on in this study were N, P, potassium (K) and calcium (Ca). Other minor nutrients were also applied: magnesium, sulphur, zinc, manganese, iron, copper, boron and molybdenum. The nutrient levels applied were generally the same for both fields except for the N, P, K and Ca applied by fertigation which were higher on Field A than on Field B (Season 1) (Table 29). The input use is representative for other farmers in the area as confirmed by a survey (WRC Report, 2018).

Table 29: Input application to potato and maize, nutrients applied as mineral fertilizer (kg ha^{-1}) and irrigation water (mm)

Input	Field A Season 1 Potato	Field B Season 1 Potato	Field B Season 2 Maize	Field C Season 2 Potato	Field C Season 3 Maize	Field D Season 3 Potato
Nitrogen	325	295	103	290	100	214
Phosphorous	154	145	17	145	17	145
Potassium	245	229	11	248	11	217
Calcium	359	339	0	281	0	226
Irrigation water	186	280	243	395	325	717

8.2.2.2 Maize crop

Maize variety 'Monsanto 94-14' was planted in rows 1.0 m apart at a target density of 40 000 plants per ha. In Season 2 and 3, 103 and 100 kg ha^{-1} N was applied to the maize fields B & C respectively (Table 29) with 11 and 8 kg ha^{-1} applied with the planter at planting followed by 46 kg ha^{-1} at 2 weeks after planting and then repeated at 4 weeks after planting as urea (46% - N). All P was applied at planting

and placed in the band with the seed at a rate of 17 kg P ha^{-1}. P is relatively immobile in soils and hence usually applied prior to planting or at planting. All K was also applied at planting. No calcium was applied.

8.2.3 Sampling scheme

Within each potato field, 24 adjacent plots measuring 1.8 x 3.0 m (5.4 m^2) were demarcated. The experimental plots were randomized within blocks and replicated 4 times within the main plot. Six times during the growing season, plant growth measurements were taken. During each sampling event, 4 plots were destructively sampled. In each maize field, 24 adjacent plots of 4.0 x 3.0 m (12.0 m^2) were used for sampling. Each individual plot comprised of 4 rows of which the middle two rows measuring 2 x 3.0 m (6.0 m^2) were sampled for growth analysis and collection of crop data. The outer two rows per plot were considered as the border rows and no crop data was collected from them. As in the potato field, during each of the six samplings events during the growing season, four plots were destructively sampled.

8.2.4 Field measurements

8.2.4.1 Weather

Precipitation and irrigation combined were measured using a tipping bucket rain gauge and the data recorded on a CR1000 data logger at 30 minute intervals. Reference evapotranspiration (ET_o) was calculated from weather data collected from the Agricultural Research Council's Jan Kempdorp weather station (Lat: 27°57'27.36"S.; Lon: 24°50'23.64"E, Altitude 1180 masl) using the Penman Monteith equations.

8.2.4.2 Soil

Soil samples were taken from the field at three different spots were the experimental plots were located. Sampling was done at three depths: 0.0-0.3 m, 0.3-0.6 m and 0.6-1.0 m before planting of each crop and analyzed for total available N, NH_4^+-N, NO_3^--N (KCl extraction method), available P (Bray 1 method), organic matter (OM) content, pH (KCl), electrical conductivity (EC) and particle size. Three sub-samples at each depth made a composite sample. At each destructive sampling event, three samples were taken at 0-0.2 m, 0.2-0.4 m, and 0.4-0.6 m depths, from each of the four sampled plots, combined into composite samples and stored in a cooler box for approximately 24 hours prior to analysis for NO_3^--N and NH_4^+-N.

8.2.4.3 Water drainage and quality

Two drain gauge lysimeters (DG G3-Decagon devices) were installed on each field during the cropping season to monitor deep drainage and leaching below 1.2 m soil depth in Season 1 and 3, whilst in Season 2 the lysimeters monitored drainage below 1.8 m soil depth. The lysimeters in Season 2 were installed deeper in order to monitor drainage and nutrient leaching at different depths. Following the subsequent maize crop, which also has a deeper rooting system, enables us to investigate if the residual nutrients lost below 1.2 m are available for use by a subsequent deeper rooting crop.

The amount of deep drainage was directly measured from the drainage lysimeters at 4 intervals in Season 1 and 6 intervals in Season 2 and 3. Measurements (and sample collection) were recorded at each sampling interval. The DG G3 has a fiberglass wick below the divergence control tube (DCT) which generates suction and with gravitational pull results in water sample collection. Fiberglass wicks do not adsorb the NO_3^- and are normally used in N dynamics studies (Weihhemuller et al., 2007). The collected water sample settles in the tube below the DCT, and since the DCT's opening has a known surface area (506.7 cm), the drainage can be calculated by dividing volume collected and the surface area. A CTD-Drain Gauge sensor was installed at the bottom of the inside of the access tube. The sensor measures drainage at 30 min intervals by using a differential pressure transducer to measure the pressure being applied by the water column above the sensor. A direct relationship between pressure and water depth is used by the sensor to measure water depth and the known cross-sectional surface area of the water reservoir is used to calculate accumulated drainage.

Drainage water samples were analyzed for nutrient composition. Irrigation water samples were also analyzed during the seasons to determine the nutrient composition of the irrigation water from the Vaal River. Water samples were also taken from two boreholes on the farm at two different sampling intervals and the water quality was analyzed

8.2.4.4 Crop parameters

Plant biomass and dry matter were measured and recorded through destructive sampling in the season in four plots at each sampling event. The leaf area index (LAI) was measured using a ceptometer (AccuPAR LP-80, Decagon Devices) which derives LAI from the intercepted PAR data. The AccuPAR LP-80 which consists of a linear probe was used to measure photosynthetic active radiation (PAR) above and below the crop canopy at each of the six sampling events from the four plots that were sampled. The ceptometer was placed between two potato rows with each end of the probe in the middle of each row and the external point sensor connected to it placed on a pole 1.2 m above the canopy. For the maize crop, the linear probe was placed across one row and the external point sensor held above the crop canopy. The LAI measurements with the AccuPAR LP-80 were calibrated through two destructive measurements done during the season. A sub-sample of the plant material harvested from each plot was used to measure leaf area with a LICOR LI-3100C.

Leaf petioles (potato) and flag leaves (maize) were collected from the harvested plants at each sampling interval. Sub-samples collected from each plot were combined to make a composite sample for the field. Plant samples were analyzed for their nutrient composition using the ICP Perchloric acid digestion method. The dry matter content of the roots, stems, leaves and tubers was determined using sub-samples that were dried in an oven at 70°C to constant weight.

The final tuber yield for Field A, B, C and D was measured at crop end which was 115 days (Field A & B, Season 1), 91 days (Field C, Season 2) and 112 days (Field D, Season 3) after planting. The fresh tuber yield and tuber dry matter yield was determined from the sample area harvested. The final grain yield for Field B (Season 2) and Field C (Season 3) was measured at crop end at 140 days and 154 days after planting respectively. The crop had not completely dried naturally and the grain was sun-

dried before a 40 g composite sample collected from four sub-samples was oven dried at 130°C for 38 hours and the moisture content determined on a wet basis for yield determination.

The plant samples collected at final harvest were tested for nutrient composition after drying, using the ICP Perchloric acid digestion. The leaf, stem, root, grain and tuber samples used in the DM yield analysis were analyzed to determine the N and P in the different plant parts (N_{plant} and P_{plant}). The results were used to determine the amount of N and P removed in the plant parts. For potato plants, the above ground parts (leaves and stems) and tubers were tested separately, whilst for maize plants the grain and residual biomass (leaves, stems and husks) were also tested separately. The nutrient composition in the different plant parts was estimated from the amount of biomass harvested per plot and the measured concentration of the particular nutrient (N and P) in the plant parts. The calculated N_{plant} and P_{plant} values were then used in the N and P balance equations.

8.2.5 Data handling

WUE was calculated based on rain and irrigation (R+I) inputs. NUE, PUE, and KUE were calculated based on the total quantity of nitrogen, phosphorous and potassium applied to the crop as mineral fertilizer. The dry matter tuber yield obtained at the final harvest was used in the calculations. Growing degree days (GDD) were calculated using the maximum daily temperature (T_x) and minimum daily temperature (T_n) collected from the Agricultural Research Council's Jan Kempdorp station. A base temperature (T_{base}) of 2°C was used for potato, and 10°C for maize.

$$\mathrm{GDD} = \frac{(T_x + T_n)}{2} - T_{base}$$

The N and P balances were calculated using the following equations;

$$N_{bal} = N_{Ini} + N_{fert} - N_{drain} - N_{plant}$$

Where N_{bal} is the net gain or loss of the N input, N_{Ini} is the initial N considered from the preceding season deep drainage measured amount and soil incorporated residual matter, N_{fert} is the inorganic N added, N_{drain} is the N measured in deep drainage which may be available to follow-up crop and N_{plant} is N assimilated by the crop.

$$P_{bal} = P_{Ini} + P_{fert} - P_{drain} - P_{plant}$$

Where P_{bal} is the net gain or loss of the P input, P_{Ini} is the initial P considered from the preceding season deep drainage measured amount, P_{fert} is the inorganic P added, P_{drain} is the P measured in deep drainage and P_{plant} is P assimilated by the crop.

The water balance was calculated using the following equation:

$$D = R + I - ETo$$

Where R is the rainfall (mm); I is the irrigation (mm); ETo is the crop evapotranspiration (mm); and D is the drainage (mm). The calculated drainage was then compared to the measured drainage using the Drain gauge.

8.2.6 Statistical analyses

A one-way ANOVA was used to compare the mean yield from the three potato fields and the two maize fields at the 5% significance level based on the hypotheses that there were no yield differences. Differences between WUE, NUE and PUE calculated from the potato and maize fields were also tested for significance using a one-way ANOVA at the 95% confidence level.

8.2.7 Farmer survey

A survey was conducted in the Christiana area in 2018 to ascertain the farming practices of potato farmers. Six farmers were interviewed; VTV Farming (Lat:28^{o} 2’42.90S; Lon:25^{o} 7’30.36E), Aqua Farming (Lat:28^{o} 8’9.42S; Lon:25^{o} 2’42.30E), Belle River Farm (Lat:27^{o} 57’28.32S; Lon:25^{o} 7’34.44E), Laucob Farm (Lat:28^{o} 1’54.18S; Lon:25^{o} 8’23.16E), Anthorn Farming (Lat:28^{o} 7’33.60S; Lon:25^{o} 6’27.90E) and Agrivan Farm (Lat:28^{o} 5’54.08S; Lon:25^{o} 0’30.91E). A questionnaire was used in a face-to-face interview with the farmers. Questions asked related to farming practices, field characteristics, resource use and cropping information.

8.3 Results

8.3.1 Weather data

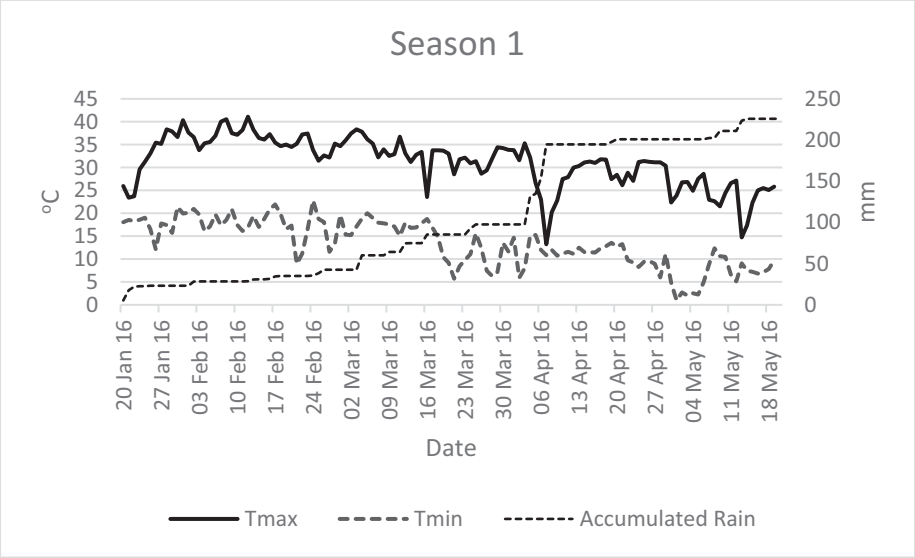

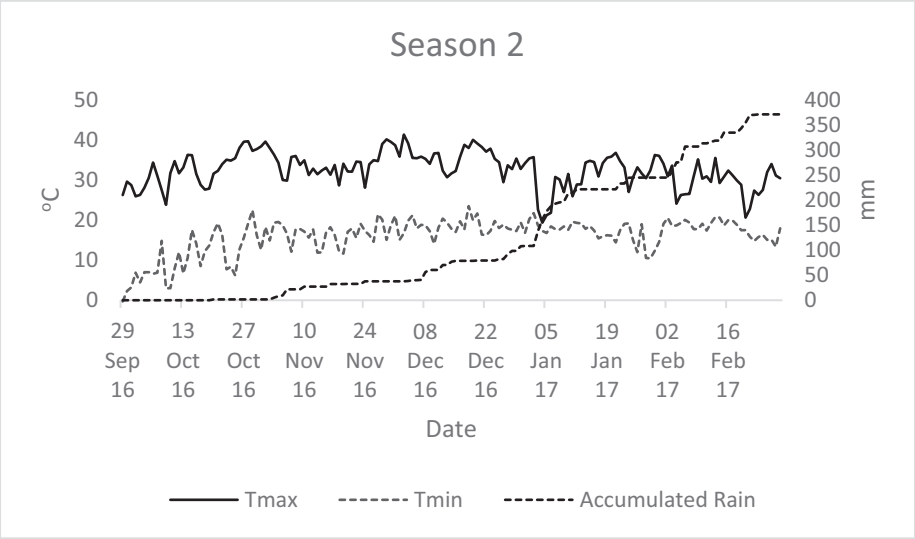

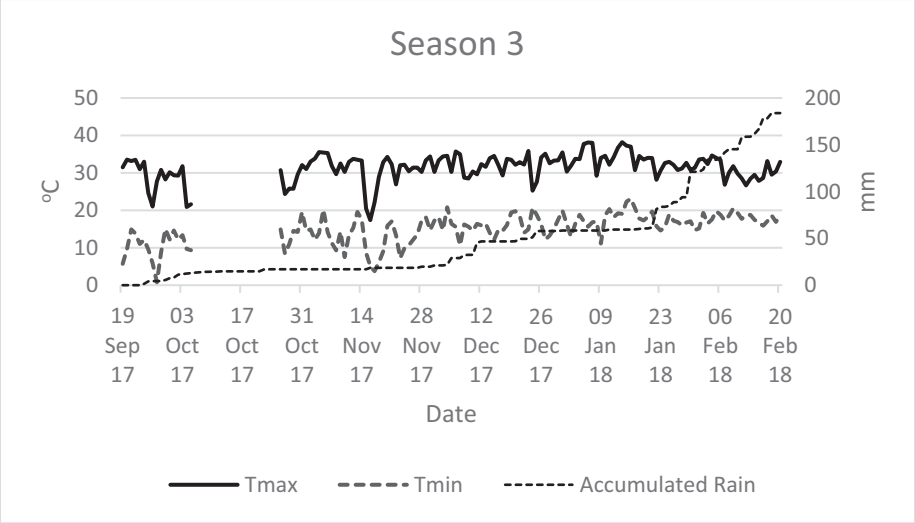

Figure 53: Temperatures and rainfall during Season 1, Season 2 and Season 3

8.3.2 Farmer survey

Total farm sizes range from 1500 to 11000 ha with 300 to 1000 ha irrigable yearly. Annual production of potatoes per farm ranges from 152 to 700 ha. Potatoes are planted in rotation with maize, onion and grass. The number of years potatoes are planted after the previous potato crop ranges from 5 to 7 years with one of the interviewed farmers practicing a 5-year rotation, whilst two are on a 6-year rotation and the rest on a 7-year rotation. In the year's in-between, the fields are planted to maize, onion and grass and then left fallow. Soils on the farms range from sandy to loamy sand with low OM content (<1.0%). Table 30 shows the level of inputs applied to the various crops that are planted in the area of the survey.

Table 30: Input application to potato, maize and onion crops as mineral fertilizer (kg ha-1) and irrigation water (mm)

Input	Potato	Maize	Onion
N	280-325	120-339	212-263
P	130-190	33-48	108-120
K	238-290	23-80	236-277
Ca	150-360	0-50	134-148
Irrigation water	350-600	0-700	500

Half of the farmers interviewed do not use soil moisture probes or irrigation software for irrigation scheduling and management. Irrigation water is mainly sourced from the Vaal River with some farmers supplementing with borehole water. The depth of the boreholes ranges 15 to 36 m. Planting density for potato seed tubers ranges between 40 000 to 45 000 per hectare with marketable yields of 55 to

76 t ha^{-1} achieved. The commonly planted varieties are Mondial, Sifra, Electra and Panamera. For the maize crop, plant density ranges from 28 000 to 78 000 per hectare with yields of 6 t ha^{-1} achieved for the low density planting and 16 t ha^{-1} for the high density planting. Marketable yields of up to 80 t ha^{-1} are harvested for the onion crop.

8.3.3 Resource use efficiency

The WUE was 3.3, 3.7, 1.0 and 1.9 g potato ℓ$^{-1}$ for potato Fields A, B, C and D respectively (Table 31). There were highly significant differences in average yield, WUE, NUE and PUE measured on the four fields at the 95% confidence interval.

Table 31: Input use and use efficiency of land (yield), water, N, P and K associated with potato

Resource	Field	Potato		Maize	
		Input rate	Use efficiency	Input rate	Use efficiency
Land (t potato tuber or maize grain DM ha^{-1})	Field A		13.2		
	Field B		18.6		9.6
	Field C		9.1		8.8
	Field D		16.3		
Water (mm and g tuber or grain DM ℓ$^{-1}$ water)	Field A	406	3.33		
	Field B	500	3.70	770	1.30
	Field C	939	0.98	516	1.70
	Field D	853	1.91		
Nitrogen (kg ha^{-1} and g tuber or grain DM g^{-1} N)	Field A	325	41		
	Field B	294	63	103	93
	Field C	290	32	100	88
	Field D	214	76		
Phosphorus (kg ha^{-1} and g tuber or grain DM g^{-1} P)	Field A	154	86		
	Field B	145	128	17	575
	Field C	145	63	17	517
	Field D	145	112		
Potassium (kg ha^{-1} and g tuber or grain DM g^{-1} K)	Field A	325	41		
	Field B	229	81	11	861
	Field C	249	37	11	798
	Field D	217	75		

There were no significant differences for use efficiencies for the maize crop at the 95% confidence interval.

Table 32: Potato petiole leaf nutrient concentrations (%) at different growth stages

Field	Nutrient	Vegetative	Growth stage			
			Tuber initiation	Tuber bulking	Maturity	Harvest
Field A	N	6.74	5.43	5.02	4.51	3.29
	P	0.49	0.32	0.21	0.27	0.20
Field B	N	6.13	6.06	4.62	5.06	3.40
	P	0.55	0.52	0.30	0.33	0.27
Field C	N	6.55	4.79	4.95	4.42	4.21
	P	0.85	0.55	0.44	0.42	0.54
Field D	N	6.37	4.39	5.42	5.03	3.65
	P	0.82	0.41	0.33	0.27	0.26

Table 33: Maize flag leaf nutrient concentrations (%) at different growth stages

Field	Nutrient	Growth stage					
		Seedling	Establishment	Tasseling	Silking	Yield Formation	Harvest
Field B	N	3.58	4.88	2.33	1.34	2.12	0.90
	P	0.48	0.46	0.39	0.29	0.18	0.07
Field C	N	3.65	2.63	3.01	1.98	2.21	1.76
	P	0.62	0.37	0.34	0.39	0.23	0.20

8.3.4 Deep drainage

There was deep drainage measured in Seasons 1 and 2, whilst no deep drainage was measured in Season 3 as shown in Table 34.

Table 34: Nutrient concentrations in river (irrigation) water, drainage water and nutrient losses

Source	Season 1		Season 2		Season 3	
	NO_3^-	P	NO_3^-	P	NO_3^-	P
Concentrations (mg l^{-1})						
Vaal River	1.2	0.2	<0.1	0.2	<0.01	<0.01
Field A	54.8-747.4	0.1-0.2	n/a	n/a	n/a	n/a
Field B	51.9-554.5	0.0-2.6	54.1-538.3	0.4-1.0	n/a	n/a
Field C	n/a	n/a	62.6	0.7	No drainage	No drainage
Field D	n/a	n/a	n/a	n/a	No drainage	No drainage
Contents (kg ha^{-1})						
Vaal River	**N**	**P**	**N**	**P**	**N**	**P**
Field A	0.6	0.3	n/a	n/a	n/a	n/a
Field B	0.8	0.5	0.0	0.4	n/a	n/a
Field C	n/a	n/a	0.0	0.7	0.0	0.0
Field D	n/a	n/a	n/a	n/a	0.0	0.1
Losses (kg ha^{-1})						
Field A	73	0	n/a	n/a	n/a	n/a
Field B	172	8	140	1	n/a	n/a
Field C	n/a	n/a	2	0	0	0
Field D	n/a	n/a	n/a	n/a	0	0

Table 35: Borehole water nutrient composition

Borehole reference	NO_3^- (mg ℓ^{-1})	P (mg ℓ^{-1})
A (1)	129.9	0.87
A (2)	125.2	<0.01
B	104.2	<0.01

Borehole A was 30 m deep and the samples A-1 and A-2 which were sampled at different times in the season showed similar results for NO_3^- (125.2 and 129.9 mg ℓ^{-1} NO_3^-) and variable results for P (Table 35). Borehole K was 60 m deep and next to a field were potato and maize crops are grown.

The calculated N and P losses through deep drainage for the two year potato-maize cropping system on Field B after Season 2 were 140 kg ha^{-1} N and 1 kg ha^{-1} P (Table 34). 32 kg ha^{-1} K and 109 kg ha^{-1} Ca were also lost in deep drainage. However, the actual measured losses for K and Ca (409 kg ha^{-1}) were actually higher since significant quantities of these nutrients were also being added through the irrigation water from the Vaal River.

Table 36: Values in brackets for potato represent nutrient balances when assuming nutrients in drainage water of potato is available to the subsequent crop. For maize, values in brackets represent nutrient balances after neglecting drainage of nutrients from the

Field	Season 1			Season 2			Season 3		
	Crop	N_{bal}	P_{bal}	Crop	N_{bal}	P_{bal}	Crop	N_{bal}	P_{bal}
A	Potato	17	116		n/a	n/a		n/a	n/a
		(90)	(117)						
B	Potato	-112	94	Maize	67	-4		n/a	n/a
		(60)	(96)		(-105)	(-6)			
C		n/a	n/a	Potato	101	108	Maize	20	-34
					(103)	(109)		(18)	(-34)
D		n/a	n/a		n/a	n/a	Potato	-65	86
								(-65)	(86)

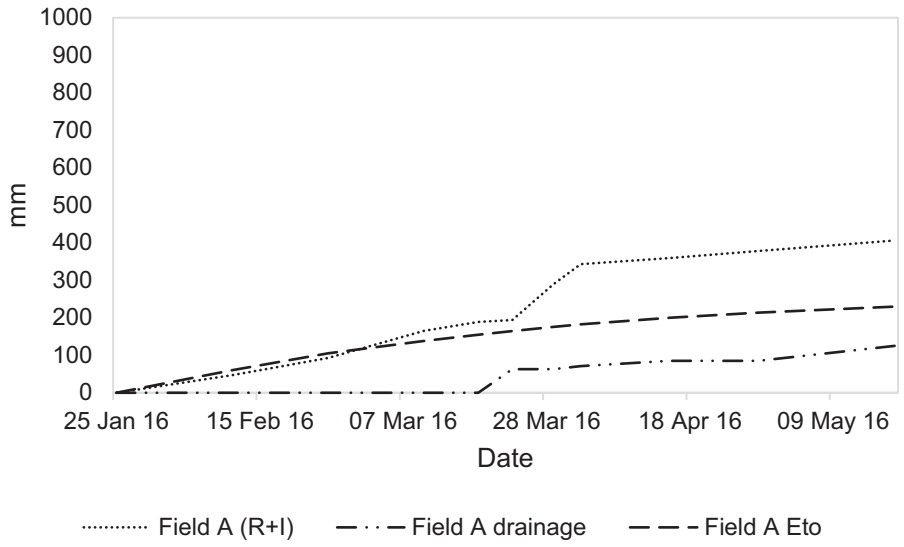

Figure 54: Rainfall + irrigation, reference evapotranspiration and drainage (mm) for potato Fields A (Season 1)

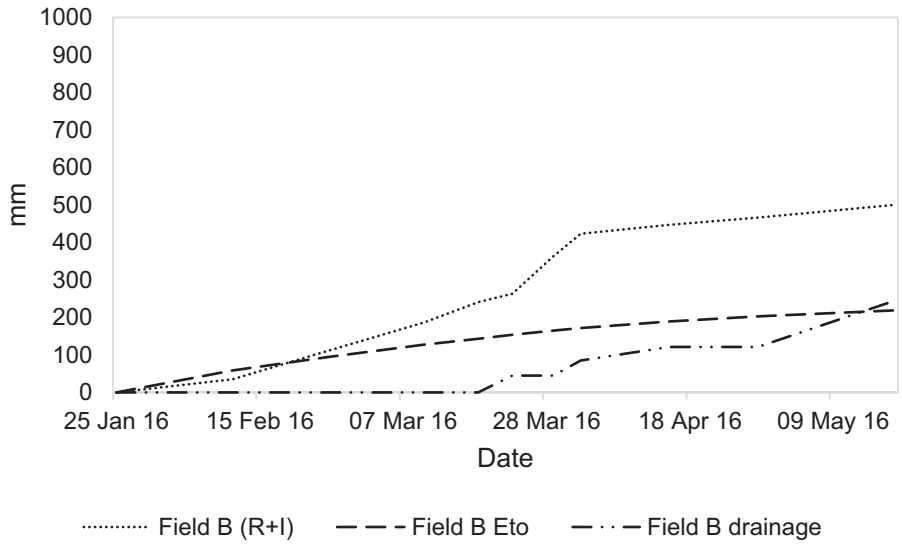

Figure 55: Rainfall + irrigation, reference evapotranspiration and drainage (mm) for potato Field B (Season 1)

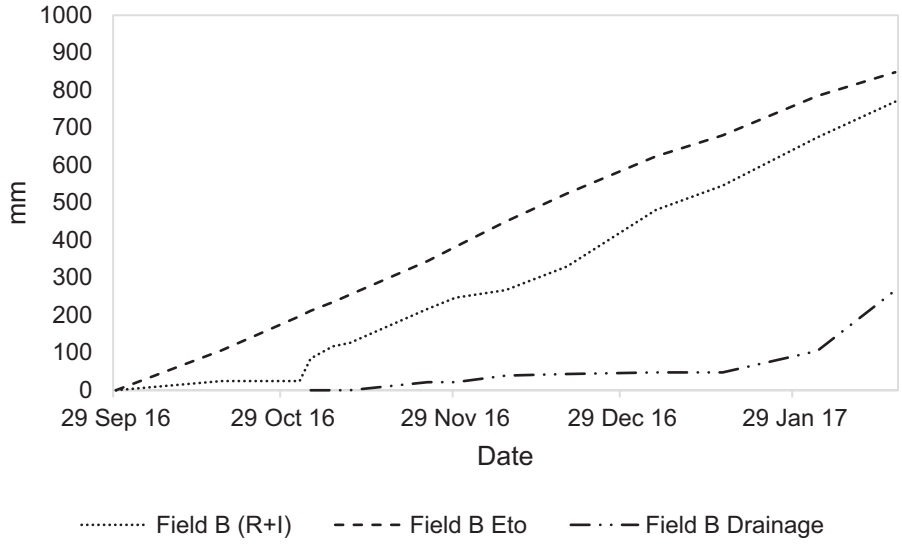

Figure 56: Rainfall + irrigation, reference evapotranspiration and drainage (mm) for maize Field B (Season 2)

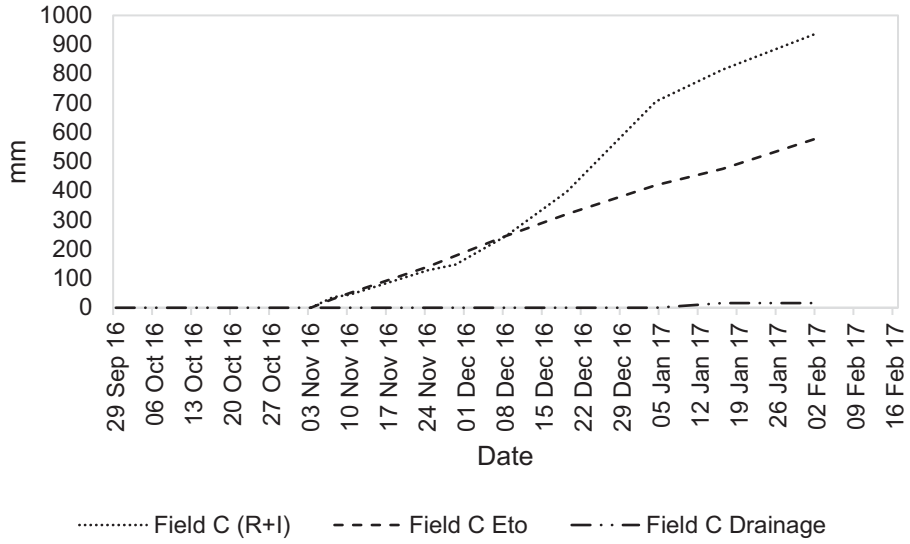

Figure 57: Rainfall + irrigation, reference evapotranspiration and drainage (mm) for potato Field C (Season 2)

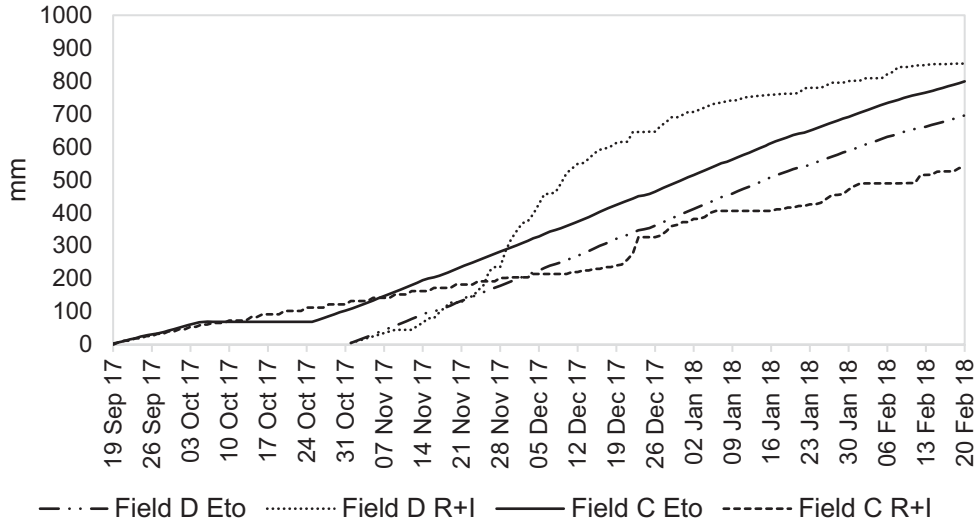

Figure 58: Rainfall + irrigation and reference evapotranspiration (mm) for maize Field C and potato Field D (Season 3)

Table 37: N and P application and plant uptake (kg ha-1) in potato and maize

Field – Crop	N_{fert}	N_{plant}	P_{fert}	P_{plant}
Field A – Potato (Season 1)	325	235	154	37
Field B – Potato (Season 1)	295	234	145	49
Field B – Maize (Season 2)	103	131	17	30
Field C – Potato (Season 2)	290	187	145	36
Field C – Maize (Season 3)	100	160	17	57
Field D – Potato (Season 3)	214	279	145	59

Table 38: Water balance inputs; Rainfall + Irrigation, reference evapotranspiration, calculated and measured drainage (mm)

Field	Crop	R+I	ETo	Water balance	Measured drainage
A	Potato	406	230	176	126
B	Potato	500	219	281	244
B	Maize	757	848	-91	263
C	Potato	814	580	234	16
C	Maize	536	799	-236	0
D	Potato	853	696	157	0

8.4 Discussion

8.4.1 Resource use efficiencies

The crop production systems assessed are intensive as demonstrated by the high input use. The results show that our farmer is a 'high-input user' leading to low efficiencies. The WUE results compare to those obtained by Franke et al. (2011) in the Sandveld region were values between 3 and 9 g potato ℓ^{-1} water were calculated based on rainfall and irrigation inputs. However, rainfall and irrigation measurements in Season 1 were done with a manual rain gauge and there could have been some biases due to blow-out and splash-out. An under-estimation of rainfall and irrigation inputs can result in higher WUE values. Allen et al. (2011) also reported that all tipping bucket rain gauges can on average lose one-half tip equivalent of rain between each wetting event through evaporation from the untipped bucket. The WUE for Field C was particularly low because the crop was grown over a short season of 92 days (2151 GDD) in comparison to 112 (2461 GDD), 116 (2355 GDD) and 121 (2458 GDD) days for the other potato fields. As a result, early harvest of the crop results in smaller tubers being harvested and lower yield. Crops in the higher yielding Fields B and D had a longer growing season which is expected to positively influence plant growth, development and yield.

The measured leaf petiole total N% regularly exceeded the sufficiency range for potato leaves. The results show excessive levels from planting till tuber bulking with the values dropping into the sufficiency range later in the tuber maturation and senescence stages. For Field C, petiole N was high at harvest

due to the early harvest of the crop 90 DAP (Table 32). The measured high N% in the leaf petioles are an indication of a possible over supply of N to the plant's requirement, indicating an opportunity for lowering the N application rates. The measured P% on Field A was within the sufficiency range whilst those on Field B and C were higher earlier in the season in the vegetative and tuber initiation stages but within acceptable range for the remainder of the season.

For the rotational maize crop, on Field B (Season 2), measured N was 3.6% in the seedling stage which was within range (4.0-5.0%). In the establishment stage it peaked to 4.9% and was above range (2.8-4.0%) possibly due to the plant's roots growing deeper and being able to absorb some of the residual N from the previous season's potato crop, or due to top dressing with urea fertilizer (46%-N). Maize roots were observed to be about 20 cm deep in the establishment stage. At tasseling and harvest, N had dropped to below sufficiency range (Table 33). The last N application in the form of urea was done at four weeks after emergence which was about four weeks before tasseling and could be the reason for the measured low N levels at tasseling. The measured P levels were within range up till the tasseling stage when level was above optimum. This could have been a result of the release of organic forms of P due to the mineralization of the soil organic matter. However, at harvest P was 0.07% which was low compared to the sufficiency level of 2.5-3.5%. Use efficiencies could have been improved had our farmer planted maize at a higher density as observed with other farmers in the area who plant up to 78 000 plants per ha and achieve yields of 16 t ha^{-1}.

8.4.2 Deep drainage

Measured deep drainage and nutrient losses recorded early in the season were low with the concentration increasing as the season progressed and gradually declining at the end of the season. Increase in deep drainage was observed to be related to high rainfall events in Seasons 1 and 2 which resulted in a sharp increase in the accumulated R+I (Figure 54 and Figure 55). During early crop development nutrients mostly reside in the upper soil layers and hence low nutrient concentrations are measured in drainage water. As the season progressed and the nutrients moved further down the soil profile, increasing levels in drainage water were measured. Later in the season the nutrient quantities in drainage water reduced since less irrigation water was applied to the crop as it matured and there was less drainage. The high losses of fertilizer N observed are a cause for concern not only for the environment but also result in economic losses for farmers.

The South African guideline of < 10 mg ℓ^{-1} and the European Union guideline of 50 mg ℓ^{-1} NO_3^- concentration being the risk levels for groundwater to NO_3^- pollution were exceeded in all the samples collected from the lysimeters throughout the growing seasons. On Field A, the soil in the divergence control tube was back-filled whilst on Fields B (Seasons 1 and 2). On Field C (Seasons 2 and 3) and Field D (Season 3) a less disturbed soil core was hammered in at the depth of the tube. Back-filling is expected to result in higher nutrient fluxes, but this was not the case under the conditions of the study as a high flux was also measured on the less disturbed soil cores. Nutrient losses on Field C were lower because the drain gauge was installed 1.2 m deeper. The quantity of NO_3^- measured in the borehole water samples was higher than that measured in the river water which supplies the irrigation water. It

is likely that leaching of nitrates results in a gradual build-up of nitrates in underground water. However, the study did not assess if the leached nutrients end up in the river water. Farmers need to regularly monitor the water quality of their boreholes so that they are able to identify any increases in nutrient levels and mitigate the risk of possible underground water pollution.

Although the potato crop received much more P input than taken up by the plant, P losses through drainage were small, indicating that the surplus P added to the soil P reserves. In Season 1 on Field B, high P concentrations were recorded mid-way in the season and this could have been after some of the fertilizer applied P had moved downward into the soil profile or mineralization of organic matter into P during the season as soil conditions became more suited for microbial activity due to consistently moist conditions. This period also coincides with the sharp increase in cumulative rainfall. Uptake of P by potato was between 36-59 kg ha^{-1} and it is recommended that farmers do not apply more than 100 kg ha^{-1} P. Even though higher applications contribute to the build-up of soil P reserves, farmers should not continuously apply high rates. The South African threshold for pollution risk is set at 0.025 mg L^{-1} and values greater than this limit were mostly observed throughout the growing seasons for the potato and maize crops.

These results confirm that sandy soils are vulnerable to leaching of water and soluble nutrients. They have a low retention capacity for water and nutrients which results in low crop recovery of nutrients. It is therefore important for farmers to optimize water and nutrient use in sandy soils in order to reduce nutrient losses. Increasing electricity prices which increase pumping costs should also provide an economic incentive for farmers to match irrigation applications to the crop water requirements. The extreme rainfall events experienced during Season 2 where more than 50 mm was received over a two-day period worsened the problem. Season 3 was a dry season in comparison to Seasons 1 and 2, and this could have been the reason why no drainage was measured. On the potato crop, 136 mm rainfall was received in Season 3 compared to 220 mm in season 1 and 544 mm in Season 2. In the absence of rainfall, farmers are probably able to minimise nutrient losses as shown by the lack of measured drainage in Season 3. Even though high drainage is related to high rainfall events, irrigation scheduling and management is recommended to ensure water application does not exceed the crop requirements. Farmers need to manage nutrient applications by splitting them so as to avoid leaching of nutrients with high intensity rainfall events. Applying more fertilizer through methods such as foliar feeds could help increase plant uptake and reduce soil nutrient losses. A combination of application methods will also minimize the risk and so will use of newer technologies for fertilizer production and application such as coated slow release fertilizers.

The nutrients added via the river water of which K and Ca are in greatest quantities are simply washed down through the soil profile and leached. There is possibly no uptake of these by the crop as they are unavailable for crop uptake. N and P applied via the river water were in small quantities. Farmers therefore tend to over-apply nutrients rather than apply the actual crop requirement, so as to avoid risk of any possible shortages in the growing season.

8.4.3 Water, N and P balances

Calculated drainage using the water balance of Field A and B in Season 1 was higher than the measured drainage (Table 38). Run-off was observed though not measured in the field during irrigation explaining this difference. Calculated drainage in maize on Field B (Season 2) was negative. However, a deep drainage of 263 mm was measured. The water balance of maize on Field C (Season 3) was also negative, while no drainage was measured. Drainage can be upward or downward and in this study it was assumed to be downward as there were no restricting soil layers observed or any shallow water tables. Accumulated ET_o exceeded R+I early in the season as the potato crop was still small and evaporative losses from bare soil were higher (Figure 54, Figure 55 and Figure 57). As potato crop growth progressed, cumulative R+I increased and exceeded ET_o for the rest of the season. For the maize crop cumulative ET_o exceeded cumulative R+I for the whole growth period in both seasons, an indication of the difference in water management compared to the potato crop (Figure 56 and Figure 58).

It is shown in Table 37 that more N was applied to the potato crop than taken up by the crop. There was a positive N balance (N_{bal}) on Field A in Season 1 of 17 kg N ha^{-1} in case drainage loss is neglected (Table 36). No rotational crop was planted on Field A in Season 2 and therefore drainage losses on this field from Season 1 were real losses (Table 34). Potato in Field B (Season 1) had a negative N_{bal} of 112 kg ha^{-1}. The negative N_{bal} of potato in Field B (Season 1) can be related to the large deep drainage measured of 245 mm in comparison to 126 mm for Field A. A rotational maize crop was planted on Field B (Season 2) and since maize plants have deeper roots, it is expected that maize will recover some of the N drainage loss from the previous season. If the measured N drainage loss of 172 kg ha^{-1} is considered as being lost from the potato crop but still being available for a subsequent deeper rooted crop like maize and not lost from the production system, then the N_{bal} for Field B (Season 1) becomes positive (60 kg ha^{-1}). At the end of the maize season the N_{bal} was positive with 67 kg ha^{-1} (Table 36). The residual biomass N and drainage N were considered as the initial N for the maize crop in Season 2 together with the inorganic fertilizer applied N, although only a small fraction of nutrients in plant material incorporated into the soil is available for plant uptake in the subsequent season. It was therefore assumed that there was in theory 339 kg ha^{-1} N potentially available for maize plant uptake in Season 2.

The calculated N plant uptake for the maize crop in Season 2 was 131 kg N ha^{-1} which does not match the 339 kg ha^{-1} that was potentially available for uptake (Table 37). The N uptake is expected to have come from the N_{fert} applied to Field B (Season 2), the organic N from the residual biomass of the previous potato plants on Field B in Season 1 (64 kg ha^{-1}) that was incorporated into the soil, as well as from the measured drainage loss from Season 1 of 172 kg ha^{-1}. The 64 kg ha^{-1} N in the residual biomass was estimated as follows: 236 kg ha^{-1} N was taken up by the potato crop in Season 1 and at harvest 191 kg N ha^{-1} was removed with the tubers (10% of which are assumed to be unmarketable and hence left on the field), whilst 45 kg N ha^{-1} was removed through the residual stems, leaves and roots. This residual biomass N together with the drainage N loss when assumed to be available in the soil before the rotational maize crop is planted on Field B (Season 2) result in approximately

236 kg ha^{-1} residual soil N from Season 1. However, not all of the 236 kg ha^{-1} is readily available for the rotational crop.

If the N in residual potato biomass (64 kg ha^{-1}) is ignored, since it is not readily available for plant uptake, and only the fertilizer and drainage N are considered (275 kg ha^{-1}), the maize plants took up 48% of the available N in Season 2. A reason for this could be that the deeper rooted maize plants do not fully recover the N lost in deep drainage in the previous potato season. This also shows that there is still high N leaching in the rotational maize crop at 180 cm soil depth, which could be an indication that there is substantial additional N coming from the soil. In contrast, if we neglect the nutrient drainage losses from the previous potato crop as not being available to the subsequent maize crop, then the N balance after the maize crop becomes negative (-105 kg ha^{-1}) (Table 36). The N balance on Potato Field C (Season 2) and Field D (Season 3) were 101 and -65 kg ha^{-1} respectively. The drainage on Field C in Season 2 was 16 mm which was lower than the 266 mm measured on Field B that had a maize crop in the same season. There was no drainage on Field D and the N_{bal} was negative primarily because the potato plants took up more N from the soil than what was applied through inorganic fertilizers. The field had been previously fallowed and the additional N could have come from organic sources in the soil.

There was a positive P balance on both Fields A and B in Season 1 and drainage losses were low (Table 36). The P balance on Field B (Season 2) includes the P from the residual biomass and drainage on the previous potato crop on Field B (Season 1) which was considered as being available for uptake by the subsequent maize crop. The P balances on all the fields cropped with potato were comparable.

N application and N removal are quite in balance in the entire potato-maize cropping system as the uptake by the rotational maize plants is more than the applied N, indicating that the deeper rooted maize is recovering some of the lost N from the shallowly rooted potato plants. There is nevertheless a substantial N loss through drainage due to N supply by the soil. Application of P on potato crop greatly exceeded uptake, and some of the applied P will be available for uptake by a following crop such as maize. The remaining excess P is likely to add to the soil P reserves which gradually build up. The P plant uptake which was higher than the fertilizer input on the rotational maize crop suggests that the crop utilized P reserves from the soil.

8.5 Conclusions

The possible over-supply of N to the potato plants' requirement presents an opportunity for farmers to lower N application rates. Application rates can be lowered to around 250 kg ha^{-1} for crop uptake as the highest NUE of 76 g potato g^{-1} P was measured at N application rate of 214 kg ha^{-1}. The high levels of NO_3^- measured in the drainage water show the risk of pollution of underground water sources and eutrophication of sub-surface water bodies by potato production in sandy soils. High NO_3^- levels measured in the boreholes, which exceeded levels measured in the river water, are also an indication of a gradual build-up of leached nutrients in underground water sources.

Planting a deep rooting crop such as maize following potato provides an option to recover some of the nutrients leached from the potato crop and is a good management strategy. Minimal nutrient

applications are used on the maize crop as the plants can make use of residual nutrients in the soil. Thus, maize as a rotational crop after potato plays an important role in recovering nutrients lost from the rooted zone of the potato crop. Some farmers plant the rotational maize at a higher density and this can potentially result in a higher recovery of nutrients as well as improving the farmers' harvestable yield, economic return and use efficiencies. Although the application of N through fertilizers is in balance with its crop uptake in the potato-maize cropping system, there is still high N leaching in the rotational maize crop indicating substantial additional N lost from the soil. The farmer survey showed that farmers also grow onions in rotation with potato. As onion is a shallowly rooting crop requiring high water and nutrient inputs, the environmental performance of a potato-onion rotation will be very different from a potato-maize system.

Given the high drainage rates observed in some of the cropping seasons, we expect there is potential for improving resource use efficiencies by optimizing application of input resources such as water and nutrients. However, it should be noted that the installation process for the drain gauge involved a lot of soil disturbance which could have led to altering of density, aeration and infiltration characteristics of the soil which could have resulted in an over-estimation of the drainage. It is recommended that for future studies machinery or tools that minimize soil disturbance need to be used. Performance of the drain gauge needs to be further tested in different soil types as it has shown potential to be used to quantify N leaching at various field locations.

8.6 References

Allen, R.G., Pereira, L.S., Howell, T.A. & Jensen, M.E. (2011) Evapotranspiration information reporting: 1. Factors governing measurement accuracy. *Agricultural Water Management, 98*, 899-920. DOI:10.1016/j.agwat.2010.12.015

Alva, A.K., Marcos, J., Stockle, C., Reddy, V.R. & Timlin, D. (2010) A crop simulation model for predicting yield and fate of nitrogen in irrigated potato rotation cropping system. *Journal of Crop Improvement*, *24*(2), 142-152.
DOI: 10.1080/15427520903581239

Arauzo, M. & Valladolid, M. (2013) Drainage and N-leaching in alluvial soils under agricultural land uses: implications for the implementation of the EU Nitrates Directive. *Agriculture, Ecosystems & Environment*, *179*, 94-107.
DOI: 10.1016/j.agee.2013.07.013

Franke, A., Steyn, J.M., Ranger, K. & Haverkort, A.J. (2011) Developing environmental principles, criteria, indicators and norms for potato production in South Africa through field surveys and modelling. *Agricultural Systems 104, 297-306*.
DOI: 10.1016/j.agsy.2010.12.001

Harding, W.R. (2015) Living with eutrophication in South Africa: a review of realities and challenges. *Transactions of the Royal Society of South Africa*, (ahead-of-print), 1-17.
DOI: 10.1080/0035919X.2015.1014878

Hendricks, G.S., Shukla, S., Obreza, T.A. & Harris, W.G. (2014) Measurement and modeling of phosphorous transport in shallow groundwater environments. *Journal of Contaminant Hydrology*, *164*, 125-137.
DOI: 10.1016/j.jconhyd.2014.05.003

Ierna, A., Pandino, G., Lombardo, S. & Mauromicale, G. (2011) Tuber yield, water and fertilizer productivity in early potato as affected by a combination of irrigation and fertilization. *Agricultural Water Management*, *101*(1), 35-41.
DOI:10.1016/j.agwat.2011.08.024

Kashyap, P.S. & Panda, R.K. (2001) Evaluation of evapotranspiration estimation methods and development of crop-coefficients for potato crop in a sub-humid region. *Agricultural Water Management*, *50*(1), 9-25.
DOI: 10.1016/S0378-3774(01)00102-0

Nyenje, P.M., Foppen, J.W., Uhlenbrook, S., Kulabako, R. & Muwanga, A. (2010) Eutrophication and nutrient release in urban areas of sub-Saharan Africa—a review. *Science of the Total Environment*, *408*(3), 447-455.
DOI:10.1016/j.scitotenv.2009.10.020

Sharpley, A.N., Chapra, S.C., Wedepohl, R., Sims, J.T., Daniel, T.C. & Reddy, K.R. (1994) Managing agricultural phosphorus for protection of surface waters: Issues and options. *Journal of Environmental Quality*, *23*(3), 437-451.
DOI: 10.1016/0925-8574(95)00027-5

Van der Laan, M., Annandale, J.G., Bristow, K.L., Stirzaker, R.J., Du Preez, C.C. & Thorburn, P.J. (2014) Modelling nitrogen leaching: Are we getting the right answer for the right reason? *Agricultural Water Management*, *133*, 74-80.
DOI: 10.1016/j.agwat.2013.10.017

Van Ginkel, C.E. (2011) Eutrophication: Present reality and future challenges for South Africa *Water SA Vol. 37 No. 5 WRC 40-Year Celebration Special Edition 2011, 694-701.*
DOI: 10.4314/wsa.v37i5.6

Van Rensburg, L.D., Barnard, J.H., Bennie, A.T.P., Sparrow, J.B. & Du Preez, C.C. (2012) Managing salinity associated with irrigation at Orange-Riet and Vaalharts Irrigation Schemes. *Water Research Commission Report*, (1647/1), 12.
DOI:

Weihermüller, L., Siemens, J., Deurer, M., Knoblauch, S., Rupp, H., Göttlein, A., Putz, T. (2007) In situ soil water extraction: A review. *Journal of Environmental Quality*, *36*, 1735-1748.
DOI: 10.2134/jeq2007.0218

9 Simulating nitrogen and water dynamics of potato-based cropping systems using APSIM

L.R. Fredericks and A.C. Franke
Department of Soil, Crop and Climate Sciences, University of the Free State, Private Bag 339
Bloemfontein 9300, South Africa

9.1 Introduction

The ability to manufacture mineral fertilizers has greatly increased plant production all over the world. Most notably is the Haber-Bosch process which produces mineral nitrogen (N). N dynamics in agricultural systems continue to be a highly researched topic due to its significance as an essential plant nutrient, but also as an environmental hazard. The latter has been the focus of research in recent decades, because losses of N applied to agricultural fields are a significant contributor to global N pollution. A surplus of fertilizer N has various fates in the soil including: immobilisation by soil organisms; gaseous emissions to the environment as NH_3 (via volatilisation), or N_2 and N_2O (via denitrification); leaching as NO_3; or carryover as mineral N to the next cropping season (Vos, 2009).

Potato cultivation in South Africa entails a high risk of N leaching, given the high N and water inputs to potato and the shallow rooting system of the potato. Farmers can minimize N leaching from potato-based systems by improving management practices, for example, by planting a deep-rooted crop like maize after potato which can mine leached N from deep soil layers. However, testing various management practices to reduce N leaching in the field is difficult, costly and time consuming. Therefore, the aim of the current work is to calibrate a computer simulation model with measured experimental data, to enable a feasible and more rapid way to evaluate N leaching and management options.

APSIM (Agricultural Productions Systems sIMulator) is a model that provides the user with a flexible structure for simulating biophysical processes in cropping systems (Holzworth, Huth et al., 2014) thus making it suitable for the project. APSIM's key features are its dynamic, daily time step biophysical and management modules which allow continuous simulation of soil water and nutrient dynamics in response to weather, management and crop uptake (Gaydon, 2014; Holzworth, Huth et al., 2014). The modules of high importance for this study are the potato and maize crop modules, the soil water (SoilWat), nitrogen (SoilN) and management module.

The aim of this computer simulation study is to estimate the amount and dynamics of nitrate leaching from a typical irrigated crop rotation (potato followed by maize) in the Western Free State of South Africa, using a modified version of APSIM. An additional aim is to assess mitigation strategies.

9.2 Methods and materials

9.2.1 Site Description

Field data were collected at experimental sites that are located nearby the village of Christiana alongside the Vaal River (situated at 28° 04.860'S; 25° 05.481'E and 28° 03.884'S; 25° 05.748'E), in South Africa (Figure 1). The climate of the area is semi-arid and receives on average 450-550 mm of rainfall annually, with the bulk of rain falling in the summer months (December to February). Summers are hot and winters cool, with frost occurring between mid-April and the end of August (Mamadi, 2013). The combination of a good water supply and deep productive soils allow for intensive crop production. Potato is popular crop chosen among other vegetables (onions), grains (maize) and trees (pecan nuts).

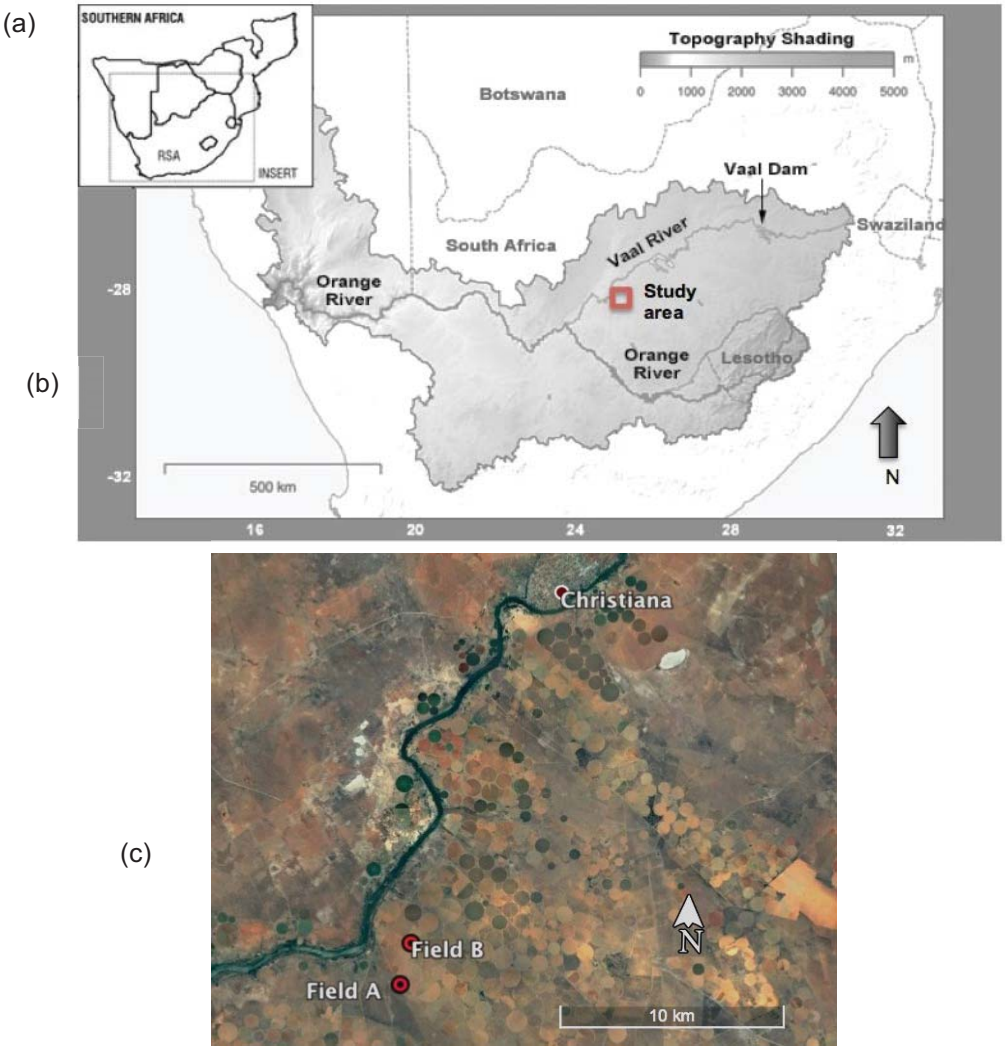

Figure 59: Aerial view of the study area: a) represents the map of South Africa and surrounding countries, b) showing the catchments of Orange River and Vaal River and, c) view of the two selected study areas where the Vaal River acts as a boundary between provinces.

Two fields (**Figure 59c**) with contrasting soil types, planted with seed potato followed by maize under centre pivot irrigation system, were selected for soil, crop and climatic parameter measurements starting with the 2015/2016 potato season (planted on 25 January 2016 and harvested on 19 May 2016). These experimental fields in the western Free State are about 3 km away from the banks of the Vaal River, from where irrigation water is supplied. The soils on this commercial farm range from loam to loamy sand and sandy loam. The soil types of the chosen fields represent sandy and sandy loam, respectively. All management events were carried out by the farmer and no additional treatments were introduced. The fields belonged to a commercial grower who followed the recommended agronomic practices as advised by agronomists. The grower normally plants maize after potato with the aim to mine surplus N, specifically from deeper soil layers, not used by the potato. After maize, the fallow period lasts at least several years, thus measuring equipment was moved to two different fields with similar soil conditions for data collection after each cropping cycle.

9.2.2 Model input parameters

The model needs data for parameterization. Unknown values may be determined by calibrating the model with measured values. Where measurements are unavailable, published data or expert knowledge can be employed. Gaydon (2014) appropriately describes the data requirements of the APSIM model by distinguishing the different levels of data needs, and organizing them into categories. The three categories of these data requirements are: i) basic biophysical data required to parameterise the model and allow it to run (includes basic climate soil and crop data); ii) the data needed to benchmark or validate the parameterised and calibrated model (primarily measured crop production, soil water and nutrient dynamics) and; iii) the data required to develop simulation scenarios (information on the farmers practices plus management practices which are to be evaluated like fertiliser management).

Daily weather data used to run the simulations were obtained from Agricultural Research Council Institute of Soil, Crop and Water (ARC-ISCW, 2017). The weather station (Vaalharts station, 30142) was located approximately 28 km from the study site. Hereafter data was converted to an APSIM format (.met) using Excel. Before using the file, it was necessary to insert the annual average temperature (TAV) and annual amplitude in mean monthly temperature (AMP) using software accessed from the APSIM website. The TAV and AMP values are used by the model to calculate the daily soil temperature for a site.

At the start of each cropping season soil samples were collected to a depth of 120 cm. Soil was sampled at 30, 60 and 120 cm and analysed in a lab for bulk density, particle size distribution and chemical properties (carbon content, pH, electrical conductivity, N content, plant available phosphorus (P), exchangeable calcium, magnesium and potassium (K) content). During crop growth, the soil was sampled biweekly at selected plots at a depth of 30, 60 and 120 cm to quantify the nutrient status of the soil.

Samples from the lysimeter were taken every two weeks. The lysimeter (Decagon Drain Gauge G3) was placed in the soil at the time of emergence at a depth of 60 cm for the 2015/2016 potato season

and 120 cm for the 2016/2017 maize season. This active-type lysimeter works by storing drained water in a reservoir until a sample is removed. The sample can be used to determine the amount of drainage since the last sample was taken. Together with a chemical analysis of the sample, the drainage rate and solute concentration allows one to calculate the chemical flux through the soil. One lysimeter in each field was installed. It was assumed that N leached below the depth of the lysimeter is eventually lost to groundwater. The nutrient concentrations in irrigation water was tested to quantify the nutrient input from irrigation.

Destructive crop samples were taken fortnightly. Before plant material was removed from the ground, the leaf area index (LAI) was measured with the LiCor Accupar Light Interception Meter. Hereafter plant material was cut at the base for lab analysis of fresh and dry matter biomass. Crop data used for model parametrisation and evaluation included aboveground biomass measurements, LAI and yield measurements.

The soil module requires water-related and chemical soil parameters that affect plant growth. There is an APSoil database with a repository of soils available. It is possible to either develop a soil from scratch or directly modify soil parameters within the APSoil database. The soil module has numerous parameters and thus it was decided to modify an existing soil instead of creating a new soil from scratch. The soil chosen from the database was the generic African soil “Sand_deep_LF (no. 914-Generic)” which is a deep sandy soil with low fertility.

Soil module coefficients and parameters were estimated from colour, texture and structure using the protocol developed by Dagliesh et al. (2016). The soil water holding parameters: crop lower limit (CLL), drained upper limit (DUL) and saturation were estimated using soil texture (Table 39).

Table 39: Key soil parameters

Depth	**BD**	***LL**	***DUL**	**PAWC**	**KL**	**Crop extractable water**	**OC**	**pH**
cm	**g cm^{-3}**	**vol vol^{-1}**	**vol vol^{-1}**	**mm**	**-**	**mm**	**%**	**1:5 H2O**
0-10	1.44	0.05	0.092	4.2	0.08	0.34	0.33	8.01
10-20	1.44	0.05	0.092	4.2	0.08	0.34	0.33	8.01
20-30	1.44	0.05	0.092	4.2	0.08	0.34	0.33	8.01
30-60	1.43	0.038	0.078	12	0.08	0.96	1.04	6.83
60-90	1.41	0.05	0.092	12.6	0.08	1.01	0.22	6.99
90-120	1.41	0.05	0.092	12.6	0.08	1.01	0.22	6.99

9.2.3 Calibration of the Model

Once the model is parameterized with the best available information, the next step is to run the simulation and check whether the results are in reasonable accuracy compared to the observed data (Ma et al., 2011). Most model parameters of validated models are assumed to be correct and don't need calibration. However, there are always a few other parameters that need calibration when applying the model under variable conditions. Due to the interaction of various modules the calibration process becomes iterative (Ma, Ahuja et al., 2011). Calibration of Cultivar specific parameters must be calibrated to meet observed yield or biomass under non-limiting conditions, i.e. no water or nutrient deficiencies (BOOTE, 1999).

After providing the initialisation data, measured data was incorporated into the APSIM platform to make use of the graphical tools. Then phenological parameters for the new cultivars were developed. With an iterative approach, several aspects of the system were evaluated in the order of: crop phenology, biomass production, biomass partitioning, yield and soil water dynamics. For the calibration process data from the 2016/17 seasons were used for both maize and potato.

9.2.4 Validation

The process of verification and validation is done to assess the value of the model for a given region. Model verification can be defined as ensuring that the computer model has been parameterised appropriately, while model validation determines if the model possess a satisfactory range of accuracy for the intended application of the model (Sargent, 2013).

Accuracy of the model can be expressed in terms of the criteria set out by De Jager (1994) (Table 40). "The square of the correlation coefficient (r^2) is used to evaluate the association between measured and predicted values, the mean absolute error (MAE) is an average of absolute errors" (Van der Laan, 2009) and Willmot's index of agreement (D) is used to measure the degree to which the model is error free. The index of agreement (D) varies between 0 (complete disagreement) and 1 (complete agreement between the measured and simulated data) (NAPE, 2011).

Table 40: Statistical criteria used to judge model performance (Van der Laan, 2009)

Statistical parameter abbreviation	Extended meaning of abbreviation	Reliability criteria
R^2	Square of the correlation coefficient	> 0.80
D	Wilmot (1982) index of agreement	> 0.80
MAE (%)	Mean absolute error (%)	< 20

Accuracy of the model can be expressed in terms of the variation explained (R^2) or correlation coefficient (r). The model performance can also be judged by using statistical criteria such as root mean square error (RMSE):

$$RMSE = \left(\frac{\Sigma(simulated\text{-}observed)^2}{number\ of\ observations}\right)^{1/2} \left(\frac{100}{mean\ observations}\right)$$

9.3 CALIBRATION RESULTS

9.3.1 APSIM-potato

9.3.1.1 Phenology

The dataset from the 2016/2017 potato season was used for model parameterization and calibration. A summary of the weather from planting to harvest in Table 41 shows that the temperatures in the potato season were high with a mean Tmax of 35°C. This season often had extremely high temperatures due to the ensuing El Niño conditions taking place. The initialisation data used in the manager module is listed in Table 42. After the model was parameterized and run, simulation results had little agreement with the measured data. The iterative method of calibrating first required the phenological parameters to be developed for the cultivars used in the trials because the phenology module drives many of the plant processes that have a strong impact on the water and N balances (Archountoulis, Miguez et al., 2014). According to Boote (1999) cultivar specific parameters must be calibrated under non-limiting conditions (potential yields). To simulate the potential yields the crop must be free of water and N stress.

Table 41: Weather data summary from planting to crop maturity for potato season 2016/2017

Parameter	Unit	2016/2017 Potato
Mean Tmax	°C	35
Mean Tmin	°C	17
Highest temperature	°C	41.8
Lowest temperature	°C	10.7
Accumulated GDD at maturity	°Cd	2212
Mean radiation	MJ m^{-2}	27
Total precipitation	mm	244

Table 42: Management parameters for potato 2016/2017

Variable	Potato
Year	2016/2017
Cultivar	Mondial
Planting dates	3-Nov-2016
Crop maturity date	2-Feb-2017
Crop duration	91 days
Foliage die off/ Crop end	Foliage killing
Irrigation	Yes
Double or Single rows	Double
Plant population	45000

After the first simulation, it was clear that the crop suffered from, water and nitrogen stress which impacted phenological development. To simulate potential yields the irrigation and fertilization modules were set up to apply sufficient amount of resources to avoid any stresses. Eliminating water stress was challenging as, according to the model, the sandy soil was not capable of providing sufficient quantities of water to satisfy the high water demand of the crop on hot days. After applying automatic irrigation at a rate of 710 mm per season the modelled crop still displayed moisture stress. However, no signs of water stress were observed in the field. It was decided to put place a cap on the soil water demand to overcome the deficiencies associated with the RUE/TE method. The parameter eo_crop_factor was changed to 1.2 as done by peake, Robertson et al. (2006). It was also decided to increase the fraction of water the crop can extract daily from the plant available water. The value of KL was increased from 0.08 to 0.4 for each soil layer.

After eliminating these stresses, the simulated crop development was delayed by the effect of temperature on phenology. In APSIM-potato (v 7.9) the only cultivar available is Russet Burbank which was validated extensively in New Zealand. The climate in New Zealand is cooler than in the current study region. Potato is a heat and drought sensitive crop, however different cultivars may respond to heat stress differently. In literature, there are various cardinal temperatures used in models for potato crop development. Table 41 shows the different threshold values used in various potato models. In general potato models have optimal temperatures ranging from 12-24°C. In this study, to ensure the crop performed well under the dry and hot climate typical for the western Free State in summer, in accordance with the field observations, the default cardinal temperatures were increased to 2°C, 28°C and 36°C for the base, optimal and maximum temperatures respectively (Figure 60). The optimum temperature values used in this study are higher compared to other models (Table 43). Hereafter, the

thermal time requirements for each phenological stage could be developed for the new cultivar (Table **44**). Although sprout growth rate also depends on temperature (mm $^{o}Cd^{-1}$), the interval from planting (sowing) to emergence can be adjusted by changing sowing depth (BROWN n.d.). Sowing depth is adjusted to obtain the correct emergence date because seed physiology, which affects emergence date, cannot be modelled yet. The vegetative, early tuber, late tuber and senesced phases each had a fixed thermal time requirement to commence to the next growth stage. Once the phenological development matched the observed data, crop canopy growth could be calibrated.

Table 43: Cardinal temperature values (mean temperature, °C) used in various potato models

Model	**T_{base} (ºC)**	**T_{opt} (ºC)**	**T_{max} (ºC)**	**Geographical location**	**Reference**
LINTUL-POTATO	2	16-24	35	Europe	Kooman and Haverkort (1995)
SWB	2	22	-	South Africa	Steyn et al. (1998)
APSIM-potato	2	12-24	34	New Zealand	Brown et al. (2011)
LINTUL-POTATO-DSS	3	15-20	28	Europe	Haverkort et al. (2015)
This study (APSIM-potato)	2	12-28	36	South Africa	-

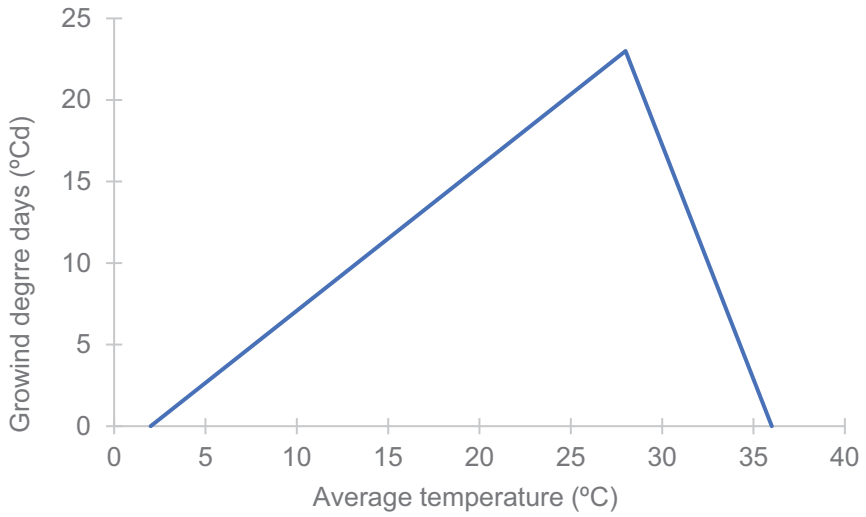

Figure 60: Thermal development based on daily average temperature

Table 44: Cultivar specific parameters used for potato in this study

Parameter name	Explanation	Unit	R. Burbank (default)	Mondial (new)
x_pp_emergence	Photoperiod required for emergence	daylight hours	12-18	12-18
y_tt_emergence	Thermal time duration before emergence	°Cd	280-280	180-180
tt_vegetative	thermal time duration vegetative phase	°Cd	20	400
tt_earlytuber	thermal time duration tuber initiation	°Cd	550	450
tt_senescing	thermal time duration tuber bulking	°Cd	850	500
tt_senesced	thermal time for completion of senescence	°Cd	5	5
tt_maturity	thermal time duration for maturity	°Cd	5	5

9.3.2 Canopy development and biomass production

The initially simulated leaf area index (LAI) was very low compared to the observed data. To improve growth predictions, the effect of temperature stress on RUE was diminished by increasing the threshold values to 2°C, 12-28°C and 36°C for minimum, optimum and maximum temperatures respectively (Figure 60). It was decided to also increase the leaf area parameters that could limit LAI growth by 50%. These parameters include: (i) leaf_growth_period; (ii) leaf_lag_period and (iii) leaf senesce period. The fourth leaf parameter, leaf_area_potential, was increased until it matched the observed data (Figure 61). The increases in these leaf area parameters were much larger than the initial values and perhaps it would be better to incorporate a parameter to change the number of main-stems (haulms) per tuber. Brown, Huth et al. (2011) says the number of stems is a constant but future developments will enable this to be modelled as a function of tuber size and treatment prior to planting. This feature was not yet available in APSIM version 7.9. The improved LAI simulations had a model fit (R^2) of 0.77 (Figure 61).

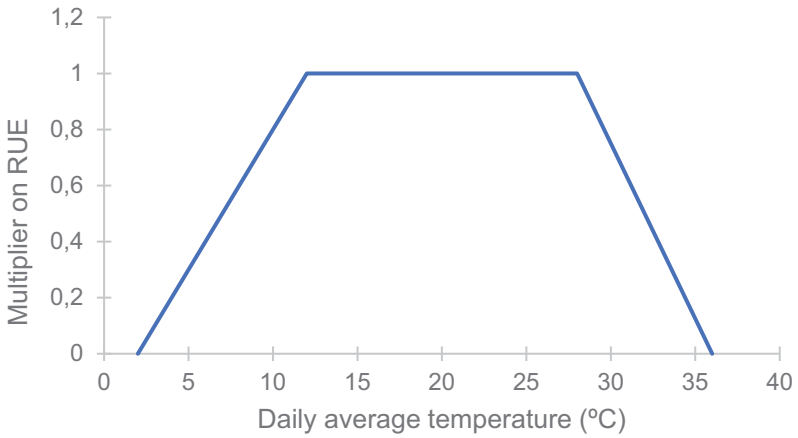

Figure 61: Effect of daily average temperature on the radiation use efficiency (RUE). Symbolised as the temperature stress factor (ft) in equation (2)

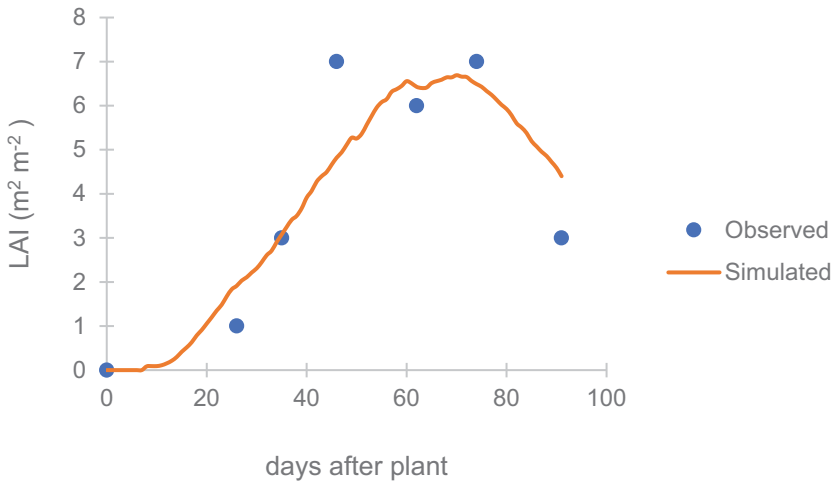

Figure 62: Progression of simulated and observed LAI for potato during the 2016/2017 season

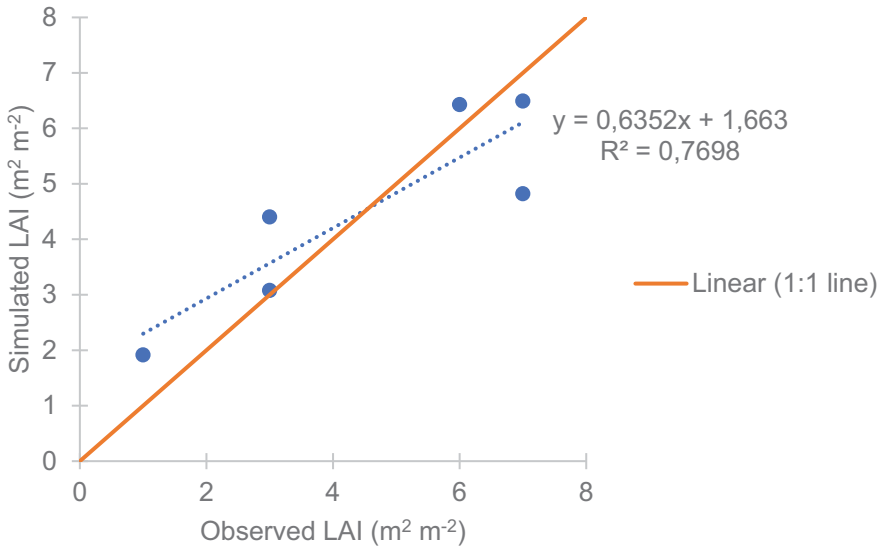

Figure 63: Observed versus simulated LAI for potato during the 2016/2017 season

The simulated final tuber dry matter (DM) yield matched well with that of the observed data (Figure 64). The model simulated the start of tuber growth earlier than observed.

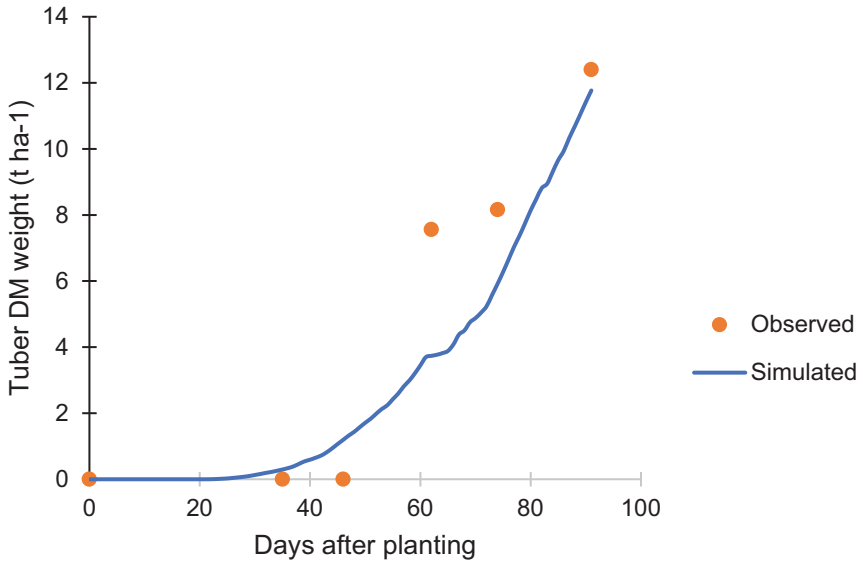

Figure 64: Observed and simulated dry matter tuber yield

9.3.3 Soil water dynamics

APSIM-potato simulates the evaporation from the soil and the transpiration from the plant separately. These two variables were summed to give the cumulative evapotranspiration of the season as simulated by the model. The potential reference evapotranspiration calculated from the weather data was changed to a crop specific potential evapotranspiration by multiplying it by the crop factor (Kc). A Kc value of 1.2 was used for the potato. The simulated and calculated evapotranspiration compared well (Figure 65).

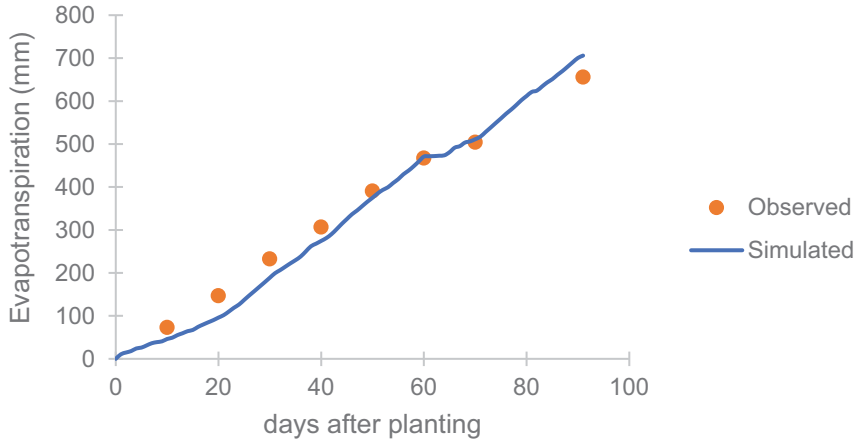

Figure 65: Observed and simulated accumulated evapotranspiration

9.4 APSIM-maize

9.4.1 Phenology

For calibration of the maize module, the 2016/17 dataset was used. A summary of the weather for this season is given in Table 45 and the management initialisation data shown in Table 46. As was done with the potato module, the first aim was to correctly simulate the phenological stages. As with potato, after the first simulation, it was clear that the parametrised soil was unable to supply the high water demand of the crop on hot days. It was decided to place a cap on the soil water demand to overcome the deficiencies associated with the RUE/TE method. The parameter eo_crop_factor was changed to 1.2 as done by Peake, Robertson et al. (2006). It was also decided to increase the fraction of plant available water the crop can extract daily from each soil layer. Kl was increased from 0.08 to 0.04 for each soil layer.

Table 45: Weather data summary from planting to maturity for maize season 2016/2017

Parameter	Unit	2016/2017 Maize
Mean Tmax	°C	34
Mean Tmin	°C	15
Highest temperature	°C	46
Lowest temperature	°C	-1
Accumulated GDD at maturity	°Cd	2318
Mean radiation	MJ m-2	26
Total precipitation	mm	334

Table 46: Management parameters used for maize 2016/2017

Variable	Maize
Year	2016/2017
Cultivar	Monsanto 94-14
Planting dates	29-Sep-2016
Crop harvest date	16-Feb-2017
Crop duration	140 days
Irrigation	Yes
Plant population	36000

The thermal time requirements for the newly developed cultivar are presented in Table 9. The thermal time between sowing and germination is dependent on soil moisture.

Table 47: Cultivar specific parameters used for maize in this study

Parameter name	Explanation	Unit	Hybred614 (default)	Monsanto 94-14 (new)
head_grain_no_max	Potential kernel number per ear	-	650	800
grain_growth_rate	Grain growth rate	g day^{-1}	10.5	10.5
tt_ermerg_to_endjuv	Thermal time from emergence to end of juvenile stage	°Cd	365	300
tt_endjuv_to_init	Thermal time end of juvenile to floral initiation	°Cd	0	0
tt_flag_to_flower	Thermal time from flag leaf to silking	°Cd	10	20
tt_flower_to_maturity	Thermal time from silking to physiological maturity	°Cd	740	900
tt_flower_to_start_grain	Thermal time from silking to start effective grain filling period	°Cd	70	150

9.4.2 Canopy development and biomass production

Figure 66 and Figure 67 give the observed and simulated development of leaf area index (LAI) of the 2016/2017 maize crop. The measured maximum LAI = 3.5 was on 81 days after planting (DAP) (Figure 66). The simulated maximum LAI = 3.2 was at 72 DAP. In Figure 67 it can be seen that the model tends to under-estimate the LAI. This may be due to the fact that field measurement of LAI does not separate the LAI of yellow leaves still attached to the plant whereas the model only accounts for the LAI of green leaves.

In Figure 68 it can be seen that the total aboveground biomass measured was 17.6 t ha^{-1} on 141 DAP. The simulated total aboveground biomass was higher at 20.7 t ha^{-1} on 141 DAP. Figure 69 compares the simulated and observed total aboveground biomass. The model simulates the biomass well for most of the season, but overestimates biomass towards the end of the growing season.

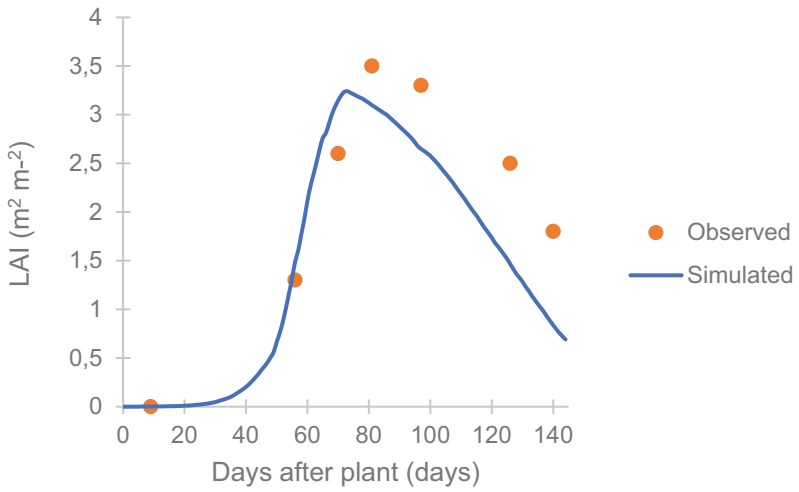

Figure 66: Progression of simulated and observed LAI for maize 2016/2017 season

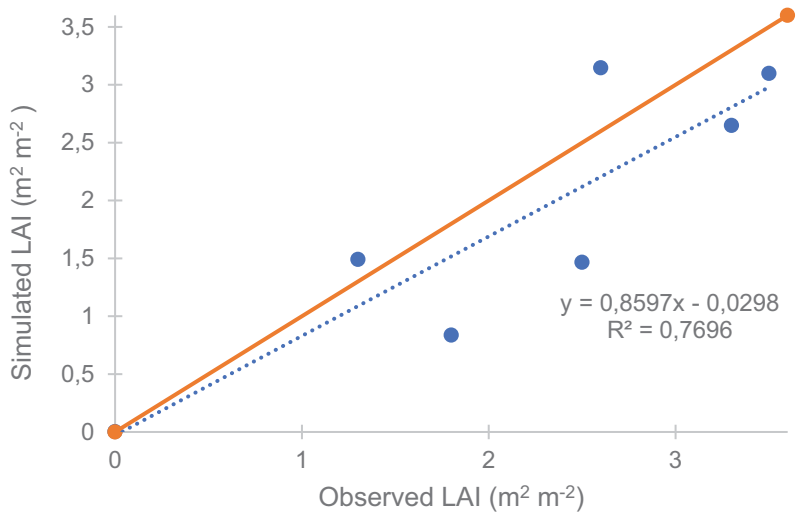

Figure 67: Simulated versus observed leaf area index (LAI) for maize in 2016/17 cropping season

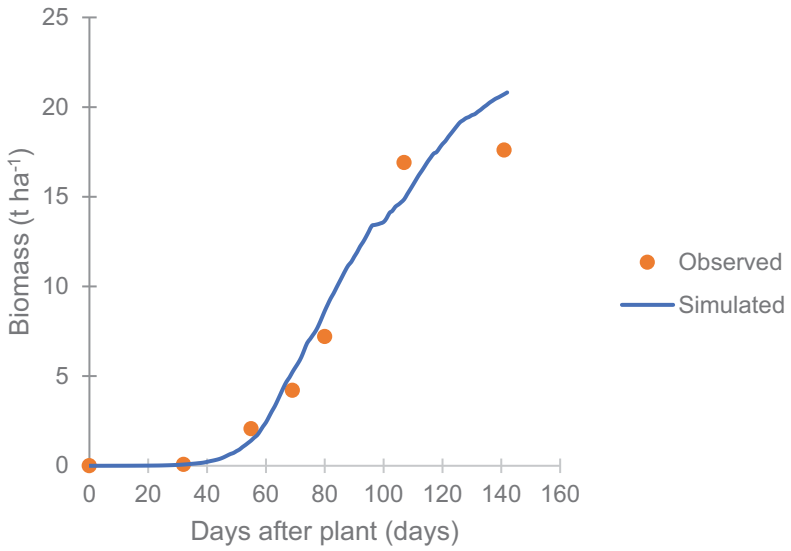

Figure 68: Progression of total aboveground dry biomass for maize in 2016/17 cropping season

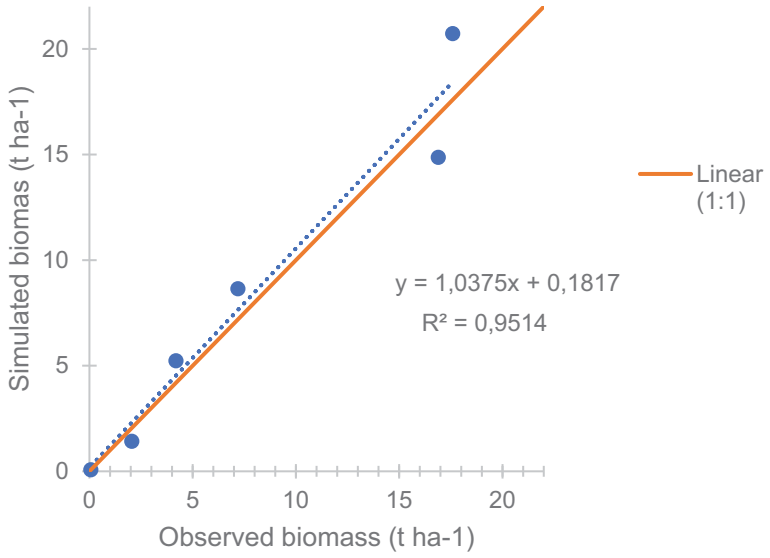

Figure 69: Simulated versus observed aboveground biomass for maize planted for 2016/17 cropping season

9.4.3 Soil water dynamics

APSIM-maize simulates the evaporation from the soil and the transpiration from the plant separately. These two variables were summed to give the cumulative evapotranspiration as simulated by the model. The potential reference evapotranspiration data from the weather file was changed to a crop specific evapotranspiration by multiplying it by the crop factor (Kc). A Kc value of 1.2 was used for the maize.

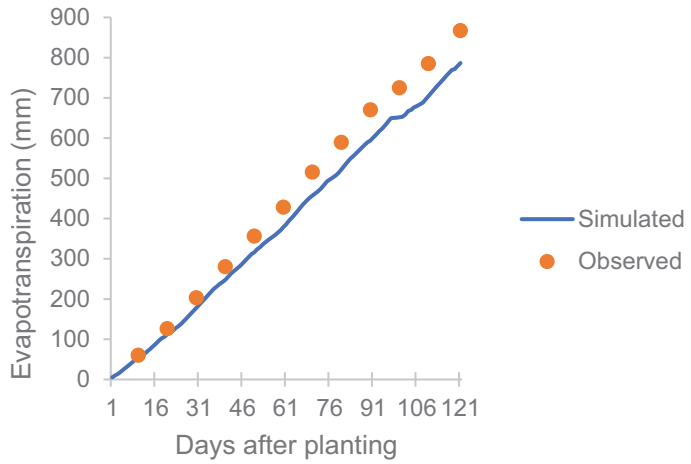

Figure 70: Cumulative calculated and simulated evapotranspiration

9.5 Validation

9.5.1 APSIM-Potato Validation

For validation of the modules the 2015/2016 data was used for the APSIM-potato and the 2017/2018 data used for APSIM-maize. Using the calibrated model, the data for the 2015/2016 potato season were inserted (Table 48) and the simulation run.

Table 48: Management parameters used for potato season 2015/2016

Variable	**Potato**
Year	2015/2016
Cultivar	Mondial
Planting dates	25-Jan-2016
Crop maturity date	19-May-2016
Crop duration	114 days
Foliage die off/ Crop end	Killed by manager
Irrigation	Yes
Double or Single rows	Double
Plant population	45000

The model simulated a large maximum LAI (LAI = 6.8 m^2 m^{-2}) compared to what was observed (LAI = 5.6 m^2 m^{-2}) (**Figure 59**).

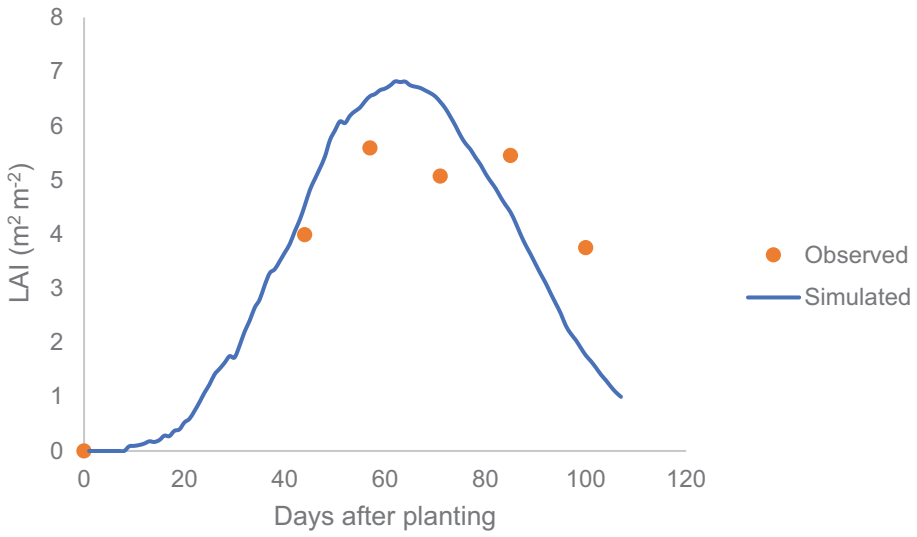

Figure 71: Course of simulated and observed leaf area index (LAI)

The model simulated tuber yields to be 11 t ha^{-1} while the observed tuber yield was 18.5 t ha^{-1}. Contrary to the over simulated LAI, the simulated dry tuber yield was well below what was observed (Figure 72). The air temperatures were hot this season leading to an earlier simulated crop maturity than observed. The WUE for the current simulation is 20.75 kg mm^{-1}.

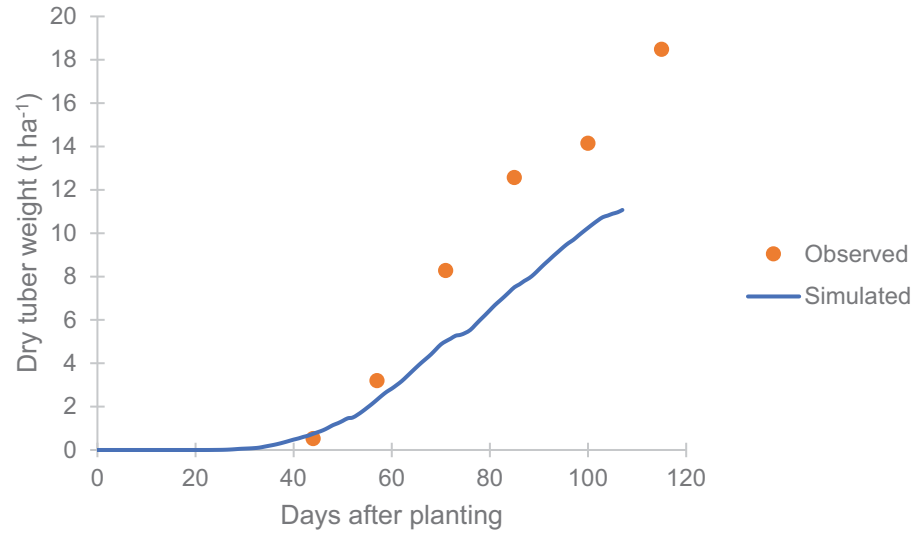

Figure 72: Observed versus simulated tuber dry matter yields

The model simulated a total drainage of 93.41 mm when irrigation was applied at a rate of 340 mm per season (Figure 73). However, the figure shows that most of the deep drainage took place from DAP 73-79 which coincided with days of heavy rainfall.

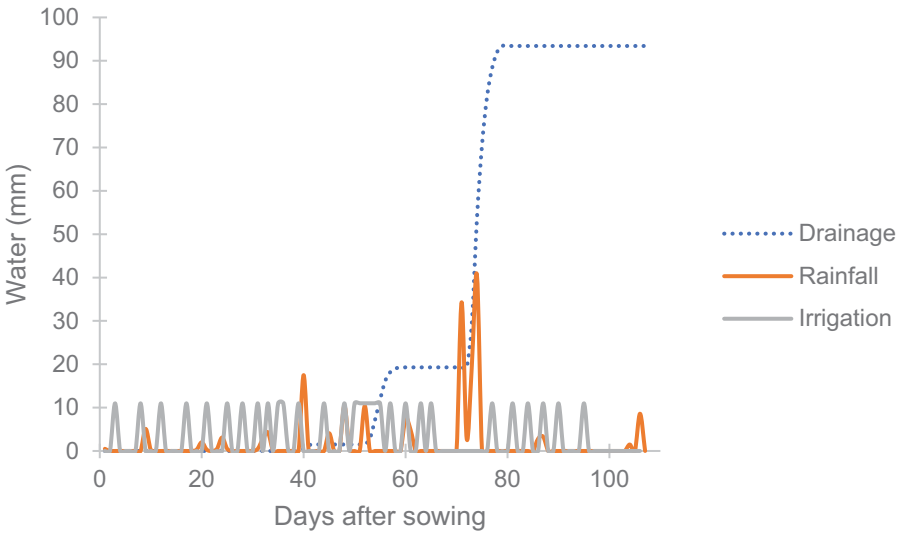

Figure 73: Comparison of rainfall, irrigation and drainage for potato season 2015/2016

9.5.2 Scenario exploration

In many parts of the world agricultural production is limited by an adequate water supply. In areas where there is a water source for irrigation, there should be judicious use of the resource to encourage sustainability in the ecosystem. Good irrigation scheduling practices as well as use of improved irrigation systems such as drip irrigation allow for more efficient use of the water resource. Water use efficiency (WUE, kg mm^{-1} H_2O) measure the total amount of product produced per unit of water.

The calibrated model allows for the quick testing of various management scenarios. A scenario that could possibly increase the productivity of a farm is to reduce the irrigation amounts. The irrigation amounts for APSIM-potato 2015/2016 season were reduced by 20% and the simulation run.

Reducing the irrigation by 20% resulted in a lower tuber yield (8 t ha^{-1}) compared to the full irrigation. The amount of deep drainage was also reduced to 56.52 mm for the season (Figure 16). Nonetheless, the majority of deep drainage still coincided with periods of high rainfall (days 73-79). The WUE after reducing the irrigation was 17.35 kg mm^{-1} H_2O. Thus, reducing the irrigation by 20% does reduce deep drainage but at the cost of efficiency (yield). Since nitrate moves with drainage water and deep drainage seems to be impacted most by rainfall intensity, reducing fertilizer rates may be more effective at reducing nitrate leaching

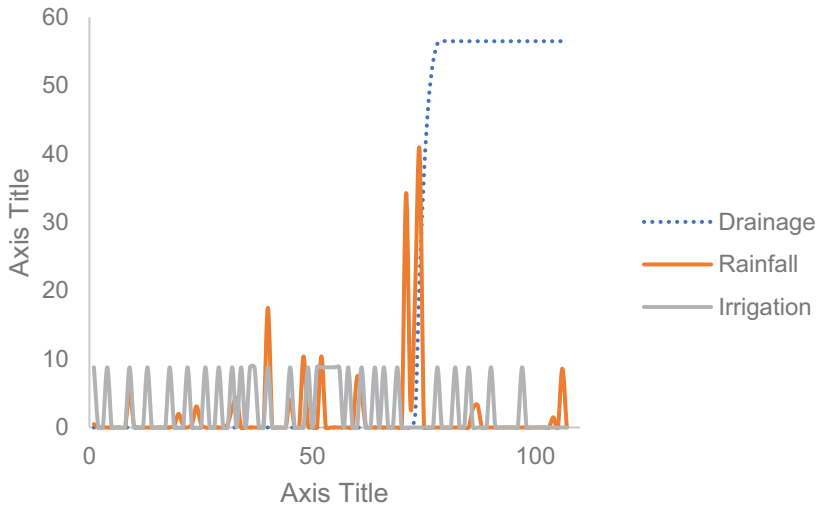

Figure 74: Comparison of drainage, rainfall and irrigation under 80% of full irrigation

Both the APSIM-potato and maize modules required rigorous calibration for the study region. The modified version of the model was able to simulate certain aspects of the agricultural system with accuracy.

The model suggests that most of the drainage and thus N leaching takes place during times of high rainfall. Reducing irrigation by 20% for the potato crop resulted in reduced yield, deep drainage and WUE. Thus, instead of reducing irrigation growers should try to avoid applying high amounts of N coinciding with periods of high rainfall.

More confidence can be placed in the model if it is validated with independent experimental data. To further refine the robustness of the crop modules future studies should test them in additional locations, years and management options.

9.6 References

ARC-ISCW (2017) Climate data supplied by Agricultural Research Council climate data bank. ARC-ISCW, Private Bag X79, Pretoria, 0001.

ARCHONTOULIS, S.V., MIGUEZ, F.E. and MOORE, K.J. (2014) Evaluating APSIM maize, soil water, soil nitrogen, manure, and soil temperature modules in the Midwestern United States. *Agronomy Journal* **106** (3) 1025-1040.

BOOTE, K.J. (1999) Concepts for calibrating crop growth models. in G Hoogenboom PW Wilkins and GY Tsuji (eds) *DSSAT Version 3. A Decision Support System for Agrotechnology Transfer, Vol. 4.* University of Hawaii, Honolulu, HI, pp.179-200.

BROWN, H.E., HUTH, N. and HOLZWORTH, D. (2011) A potato model built using the APSIM Plant.NET Framework. 19th Internatitonal Congress on Modelling and Simulation, Perth, Australia, pp. 961-967.

BROWN, H.E., HUTH, N.I. and HOLZWORTH, D. (n.d.) The APSIM potato model. Web Address: http://www.apsim.info/ApsimxFiles/Potato707.pdf

DALGLIESH, N., HOCHMAN, Z., HUTH, N. and HOLZWORTH,D. (2016) A protocol for the development of Apsoil parameter values for use in APSIM. Version 4. CSIRO.

DE JAGER, J.M. (1994) Accuracy of vegetation evaporation ratio formulae for estimating final wheat yield. *Water SA* **20** (1) 307-314.

GAYDON, D.S. (2014) The APSIM model – an overview, pp. 15-31.

HAVERKORT, A.J., FRANKE, A.C., STEYN, J.M., PRONK, A.A., CALIDZ, D.O., KOOMAN, P.L. (2015) A robust potato model: LINTUL-POTATO-DSS. *Potato Research* **58** 313-327.

HOLZWORTH, D.P., HUTH, N.I., ZURCHER, E.J., HERRMANN, N.I., MCLEAN, G., CHENU, K., VAN OOSTEROM, E.J., SNOW, V., MURPHY, C., MOORE, A.D. and BROWN, H. (2014) APSIM-evolution towards a new generation of agricultural systems simulation. *Environmental Modelling & Software* **62** (2014) 327-350.

KOOMAN, P.L., HAVERKORT, A.J. (1995) Modelling development and growth of the potato crop influenced by temperature and daylength: LINTUL-POTATO. in Haverkort AJ, MacKerron, DKL (eds.) Potato Ecology and Modelling of Crops under Conditions Limiting Growth. Current Issues in Production Ecology, vol. 3. Kluwer Acad. Publ., Dordrecht, pp. 41-59

MA, L., AHUJA, L.R., SASSEENDRAN, S.A., MALONE, R.W., GREEN, T.R., NOLAN, B.T., BARTLING, P.N.S., FLERCHINGER, G.N., BOOTE, K.J. and HOOGENBOOM, G. (2011) A protocol for parameterization and calibration of RZWQM2 in field research, pp. 1-64.

MAMADI, M.E. (2013) Comparative analysis of the soil carbon dioxide (CO2) concentration with different tillage systems – a case study in the Northwest Province. University of the Free State. Master of Science.

NAPE, K.M. (2011) Using seasonal rainfall with APSIM to improve maize production in the Modder River Catchement. MSc Disseration. University of the Free State, South Africa.

PEAKE, A.S., ROBERTSON, M.J. and BIDSTRUP, R. (2006) Optimising maize plant population and irrigation strategy on the Darling Downs: A simulation analysis. 6th Triennial Conference, Maize Association of Australia.

SARGENT, R.G. (2013) Verification and validation of simulation models. *Journal of Simulation* **7** 12-24.

STEYN, J.M., DU PLESSIS, H.F. and FOURIE, P. (1998) Response of potato genotypes to different irrigation water regimes. Water Research Commision (WRC) Report No. 389/1/98. Pretoria, South Africa.

VAN DER LAAN, M. (2009) Development, testing and application of a crop nitrogen and phosphorus model to investigate leaching losses at the local scale. PhD Thesis. University of Pretoria, South Africa.

VOS, J. (2009) Nitrogen responses and nitrogen management in potato. *Potato Research* **52** 305-317.

10 LONG-TERM EFFECTS OF MULCHING VERSUS BURNING AND INORGANIC FERTILIZATION ON SUGARCANE (*SACCHARUM OFFICINARUM L.*) YIELD, SOIL ORGANIC MATTER AND NITROGEN LEACHING

S. Maseko[1], M. van der Laan[1], R. van Antwerpen[2,3]
[1]Department of Plant and Soil Sciences, University of Pretoria, Pretoria 0002, South Africa
[2]South African Sugarcane Research Institute, Mount Edgecombe, 4300, South Africa
[3]Department of Soil, Crop and Climate Sciences, University of the Free State, Private Bag 339 Bloemfontein 9300, South Africa

10.1 INTRODUCTION

Sugarcane *(Saccharum officinarum* L.*)* is one of the most important agricultural crops in South Africa. Favorable soils and climate on the eastern parts of South Africa have seen the exclusive occurrence of sugarcane production in that region. In recent years, the South African sugar industry has been greatly concerned about decreasing sugarcane production (Jones and Singels, 2015). In 2011/2012, land under sugarcane production was reportedly 378 300 ha producing 16.8 million tonnes of cane, which is an indication of the gradual decrease in production when compared to 1999/2000 when a reported 421 600 ha of land was planted to sugarcane 23 million tonnes of cane stalks (SASA, 2014). This decrease can potentially harm the sugar industry through loss of revenue for commercial companies and individual farmers as well as reducing the availability of job opportunities. Sugarcane has been grown under monoculture for over a century in South Africa, Brazil, Australia, and elsewhere, as this has shown to be a viable production system for this crop (Meyer and Van Antwerpen, 2001). Monoculture production has proven to contribute to yield declines in other crops due to the absence of the beneficial effects that come with crop rotations, such as pest and disease control, and maintenance of soil fertility. To address such a potential decline in production, one of the major steps can be understanding the contribution of sugarcane monoculture to soil quality decline, which in the long-term, can contribute to decreasing yields.

Inorganic fertilization has been extensively used following World War II to enhance crop production by increasing soil fertility. Sugarcane can produce large quantities of biomass, often 70-90 t cane ha^{-1} yr^{-1} fresh weight, which usually requires significant amounts of fertilization (Shand, 2007). This means that inorganic fertilization represents a significant input cost in sugarcane production. Nitrogen (N) is the nutrient that most often limits plant growth as it is required in the highest proportion by crops. Sugarcane, like most agronomic crops, has a reportedly low nitrogen use efficiency (NUE), with only an estimated 35% of applied N being taken up by the crop (Meyer, Schumann et al., 2007). The other 65% remains in the soil or is lost to the environment through various pathways such as leaching, denitrification, volatilization, or runoff. This makes NUE an important aspect of production, and directly influencing the profitability and environmental sustainability of sugarcane production.

Sugarcane growers in South Africa commonly burn cane before harvest to make manual harvesting easier for the cane cutters. This residue management practice of burning rather than mulching crop

residues potentially reduces the organic matter returns to the soil, which in the long-term, can reduce the favorable physical, chemical and biological properties of the soil (Van Antwerpen, Meyer et al., 2001). Retaining residues can increase yields by conserving soil organic matter (SOM), reducing evaporation, and improving nutrient cycling. Pre-harvest burning is considered to be the cause of soil aggregate destabilization as a result of SOM loss leading to reduced microbial activities (Graham, Haynes et al., 2002). Optimal SOM levels can be maintained by balancing residues continually added to the soil and organic matter mineralization by micro-organisms. Retaining residues after harvest has been reported to improve SOM content compared to burning, as it allows the retention of a significant amount of residues at harvest containing about 42% carbon (C) (Vallis, Parton et al., 1996; Blair, 2000; Graham, Haynes et al., 2002; Thorburn, Meier et al., 2012).

Complex C and N dynamics of agroecosystems, such as in sugarcane cropping systems, can often be investigated better when combining physical measurements and mechanistic crop modelling. These crop models can be used as research tools to address specific hypotheses and explain trends that occur in the crop production cycles (Boote, Jones et al., 1996), but the robustness and accuracy of these models first need to be tested.

In this chapter, the aim was to assess the long-term impacts of residue burning versus mulching, with or without inorganic fertilization on sugarcane yields and soil quality by combining historical data and mechanistic modelling. Data from 1939-2016 was compared with simulated data from the APSIM model to test model performance and study the long-term trends.

10.2 MATERIALS AND METHODS

10.2.1 Experimental site

The long-term trial on which this study is based on was established in 1939 and is being maintained by the South African Sugarcane Research Institute (SASRI) in Mt Edgecombe, Durban, South Africa (29.04°S, 31.04°E, 123 m above sea level). The climate of the region is humid sub-tropical and characterized by predominantly summer rainfall with an annual average of 950 mm and an annual average temperature of 20.4°C (Graham et al., 2002). The site is located on a south-west facing slope of 13.5% and 18.5% for the upper and lower parts of the trial site respectively. The soil on the upper slope is classified as a Mayo form and on the lower slope as a Bonheim form (Soil Classification Working Group, 1991).

10.2.2 Experimental design and treatments

The trial covers an area of approximately 7200 m^2 (90 m × 80 m) consisting of 32 plots of 175 m^2 each with sugarcane planted in rows with a spacing of 1.4 m. The experiment is a split-plot factorial design arranged in a randomized complete block with four replicates for treatments burnt and eight replicates for treatments not burnt at harvest. The main plot treatments are (1) green cane harvesting with all residues mulched over the plot area (M), (2) cane burnt prior to harvesting with cane tops (unburnt top

green leaves) left scattered evenly over plot area covering two thirds of the surface area (BS), and (3) cane burnt prior to harvesting with all residues removed from the plots (BR). The split-plots consist of fertilized (F) and unfertilized (F0) treatments (Table 49). For this modelling study, data from 24 plots out of the 32 were selected to work with an even number of four replicates for all treatments

Table 49: Different treatments in the South African Research Institute (SASRI) BT-1 long-term sugarcane trial

No	Treatment	Code
1	Mulched, fertilized	MF
2	Mulched, not fertilized	MF0
3	Burnt with tops scattered, fertilized	BSF
4	Burnt with tops scattered, not fertilized	BSF0
5	Burnt with all residues removed, fertilized	BRF
6	Burnt with all residues removed, not fertilized	BRF0

The sugarcane crop was grown for an average of eight years per cycle, which equates to a planted crop and seven ratoons. Conventional tillage was used before planting for the first 30 years, but since then minimum tillage has been used (Graham, Haynes et al., 2002). Since 1939, fertilizer was applied as a 5:1:5 (46) nitrogen phosphorus and potassium (NPK) combination at 670 kg ha^{-1} on F plots, translating into a rate of 140 kg ha^{-1} N, 28 kg ha^{-1} P and 140 kg ha^{-1} K. Fertilizer was applied 40 days after harvesting the previous crop (Van Antwerpen, Meyer et al., 2001)

10.2.3 Measured data

10.2.3.1 Long-term yield and soil organic matter data

Five sugarcane varieties were grown on the site from 1939 to 2017. These were Co281 (1939-1947), Co301 (1948-1956), NCo376 (1957-1990), N16 (1991-2001), N27 (2002-2013) and currently N41 (2014-present) (Van Antwerpen et al., 2001, Mthimkhulu et al., 2018). Harvesting dates changed over the years with cane harvested every 24 months from 1930-1965, every 15 months from 1966-1986, and every 12 months from 1987 to present. Yield and SOM data for sugarcane treatments were retrieved from the SASRI trial records and published literature.

10.2.3.2 Soil data

Soil from strips between the experimental blocks have had grass growing on them for the duration of the experiment was previously sampled and considered to be a close representation of the initial soil conditions before the start of the trial (Graham, Haynes et al., 2002). This site has an unusually high SOM content compared to other South African soils. The virgin soil contains 4% OC, and this makes it to fall under a small proportion of South African soils that have more than 2% OC (representing only 4% of the South African soils) (FSSA, 2007). The average clay, sand, silt content of the soil was 43.4,

33.5 and 23.2% across all depths respectively (Mthimkhulu et al., 2016). Soil parameters used for modelling include drained upper limit (DUL), lower limit water content at 15 MPa (LL15), and saturation (SAT) estimated from soil texture using DSSAT software, bulk density (BD), organic C (%), and soil pH (H_2O) from measured data (Table 50). Soil hydraulic conductivity was measured using a dual-head infiltrometer (Decagon Devices, Inc. 2365 NE Hopkins Court Pullman WA 99163) during the 2016-2017 growing season.

Table 50: Bulk density (BD), saturation (SAT), drained upper limit (DUL), lower limit at 15 MPa (LL15), soil pH (H2O), and organic carbon (OC) for the BT-1 long-term trial at SASRI, Mt Edgecombe

Soil Layer (m)	BD (Mg m^{-3})	SAT (m^3 m^{-3})	DUL (m^3 m^{-3})	LL15 (m^3 m^{-3})	pH (H_2O)	OC (%)
0-0.05	1.25	0.48	0.37	0.22	6.6	6.0
0.05-0.15	1.15	0.48	0.37	0.22	7.0	4.0
0.15-0.30	1.15	0.48	0.37	0.22	6.9	2.0
0.30-0.45	1.15	0.48	0.37	0.22	6.9	1.0
0.45-0.65	1.15	0.48	0.37	0.22	6.9	1.0
0.65-0.85	1.15	0.48	0.37	0.22	6.9	1.0
0.85-1.00	1.15	0.48	0.37	0.22	6.9	1.0

DUL: represents field capacity
LL15: represents permanent wilting point

10.2.3.3 Daily weather data

Daily minimum and maximum temperature, precipitation and solar radiation data were used to create a long-term weather file from 1939-2017. Mount Edgecombe weather data was obtained from the SASRI WeatherWeb database (https://sasri.sasa.org.za/weatherweb/weatherweb.wwmenus.menu_frame?menuid=1). The annual average ambient temperature (TAV) and annual amplitude in monthly temperature (AMP) was calculated using the long-term daily minimum and maximum temperatures. These calculated values of TAV and AMP were inserted into the meteorological file by the tav_amp software programme (https://www.apsim.info/Products/Utilities.aspx).

10.2.3.4 APSIM model set-up

The model is influenced by soil, crop management, environmental and genetic variables (Keating, Robertson et al., 1999). The APSIM sugar module (Carberry and Abrecht, 1991), soil water module (SOILWAT), soil nitrogen (SOILN) and residue module (RESIDUE2) (Probert, Dimes et al., 1998) were already within APSIM to simulate the scenarios described in this chapter. These are one-dimensional modules, using a daily time step and influenced by weather conditions. The APSIM sugar module used default values of radiation use efficiency (RUE) for plant and ratoon crops (1.8 and 1.65 g of above-

ground dry matter production per MJ^{-1} of intercepted solar radiation, respectively) (Keating, Robertson et al., 1999). Root mass is calculated as a fraction of above-ground dry matter, and this fraction varies from 0.3 at emergence to 0.2 at flowering. The model partitions 70% of above-ground dry matter production to the stalk, and sucrose mass is calculated by partitioning a constant fraction of stalk mass increments to this pool after a given threshold of stalk matter has accumulated. The leaf sink demand and a stalk growth stress factor can adjust sucrose partitioning (Singels and Bezuidenhout, 2002).

10.2.4 Model application: Long-term simulations

Model calibration was done using the MF treatment (best management practice recommended by SASRI). Crop parameters for sugarcane were obtained from the APSIM sugar module. The variety used for the simulation was NCo376, a very popular variety in South Africa for about 30 years and one of the default varieties in the model. Planting was simulated on 1 November at a depth of 150 mm and there were four ratoons before another planting was done (APSIM model allows a maximum of four ratoons). Fertilizer was applied every year as ammonium nitrate at a rate of 140 kg ha^{-1} on 1 December on all fertilized treatments. Harvesting was done as per the intervals outlined in Section 10.2.3.1. For the mulched treatments (MF, MF0), all residues were simulated to be retained after harvest, while for the BS treatments 70% of residues were retained and for the BR treatments, all residues were simulated to be removed after harvest. The leaching of NO_3-N was estimated using the model for different residue management and fertilization treatments.

10.2.5 Low fertilizer application rates scenarios

The soil fertility decline and leaching of nutrients out of the root zone can be addressed using various management practices in sugarcane production. One of these management practices can be reducing the amount of N fertilizer applied, taking advantage of potential N mineralization from residues. After calibration and testing, the model was used to simulate low fertilization rate scenarios to investigate whether long-term N benefits from mulching can substitute a certain proportion of N fertilizer application and maintain high yields on lower fertilization rates. Scenarios of 40 kg ha^{-1} and 80 kg ha^{-1} N application on mulched treatment were simulated and compared to MF treatment. The same procedures outlined in 10.2.4 were used for the simulation, with only the low fertilizer rates for these scenarios used.

10.2.6 Testing model performance

Model evaluation was performed using long-term yields and SOM data from the MF, MF0, BSF and BSF0 plots from 1939, and from the BRF and BRF0 plots from 1980 (burning and removing cane tops started in 1980). Model performance was tested using the square of the correlation coefficient (R^2), the mean absolute error (MAE), root mean square error (RMSE), and the index of agreement (D) based on the criteria outlined in Maseko (submitted). The measured and simulated data were also graphically compared.

10.3 Results

10.3.1 Influence of long-term management practices on sugarcane yields

Sugarcane management practices (fertilized versus unfertilized and mulched versus burnt) had significant effects on yields. Fertilized treatments generally had higher yields compared to unfertilized treatments. Mulched treatments had higher yields than burnt treatments in either of the fertilizer regimes used. Decreasing trends in yields were evident for all treatments in both the measured and modelled data (Figure 75), although this is more closely related to the change in crop duration over the years (cutting age was 24 months at the beginning of the trial, changed to 15 months in 1966 and 12 months in 1987). Generally, the model yield estimations were robust, but there was a poor prediction in some years, such as overestimations in 1961 and 1964. In 1963 harvesting was done and another was done in 1964, thus resulting to low yields for that year in all treatments due to one-year crop duration instead of the normal two years for that period. Fertilized treatments yields were underestimated (difference between measured and simulated yields above RMSE) in the period between 1987 and 2009 when harvesting was done every 12 months. Unlike the fertilized treatments, unfertilized treatments were mostly overestimated by the model, more so in the early stages of the trial and becoming more accurately estimated in later years. The BRF0 treatment was generally underestimated, but the trends over time were similar.

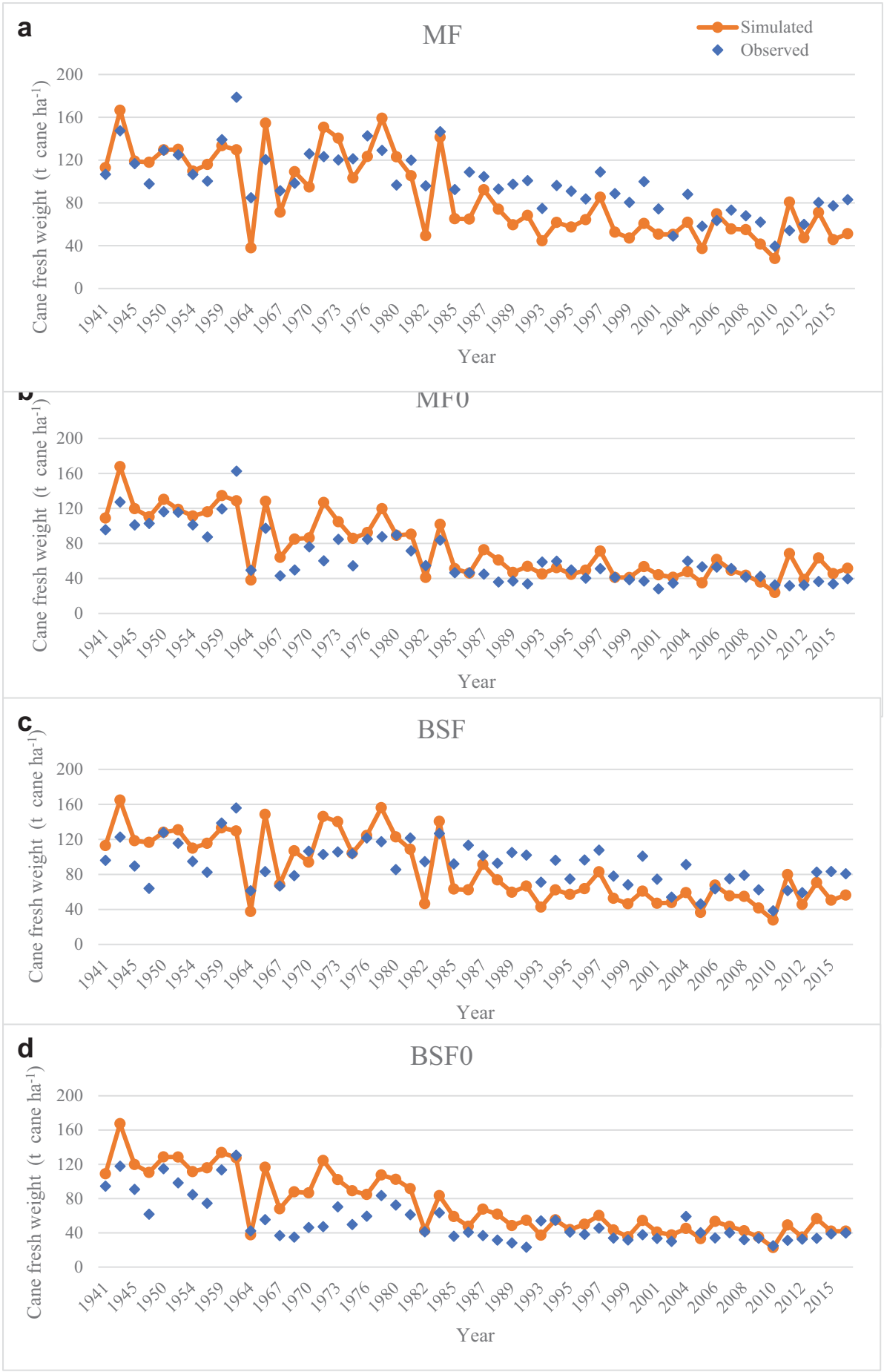
a
MF
Simulated
Observed
Cane fresh weight (t cane ha-1)
Year
b
MF0
c
BSF
d
BSF0

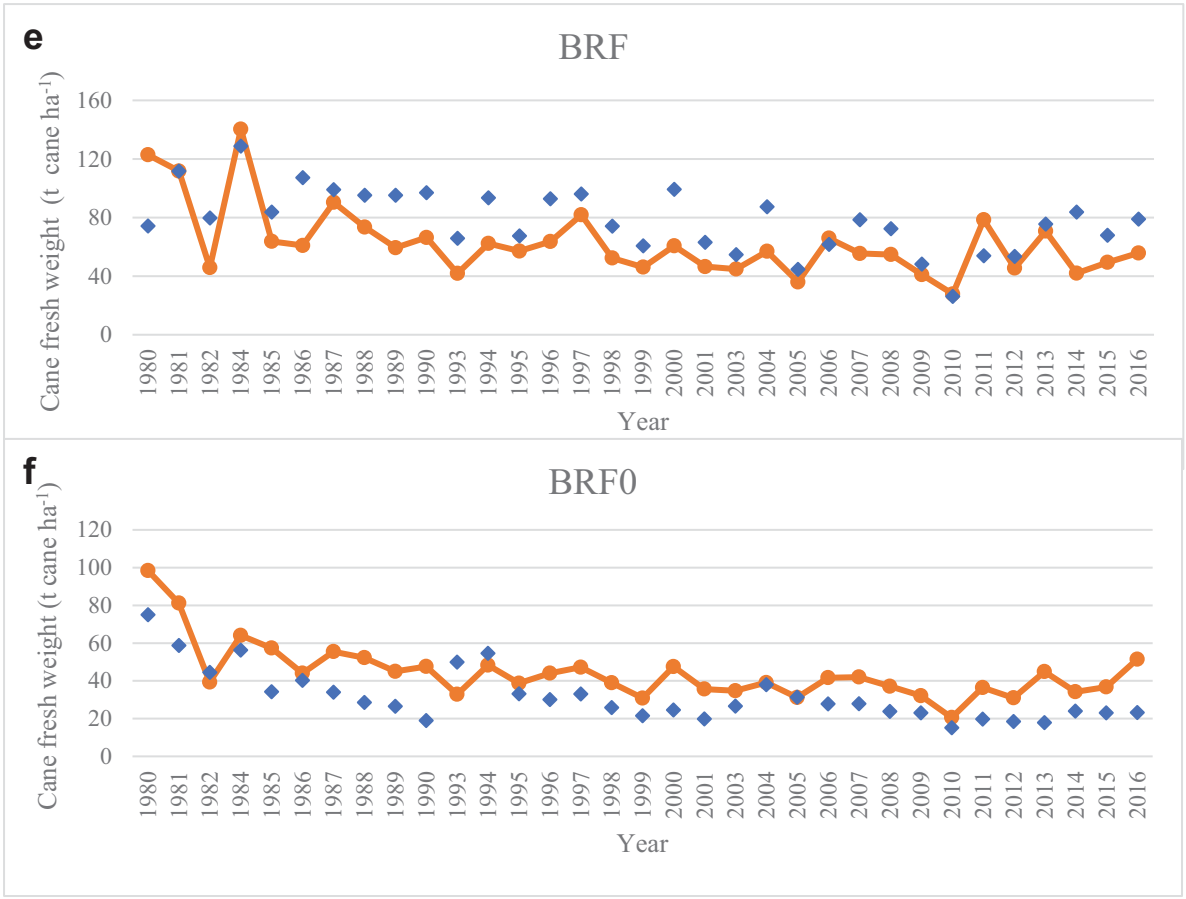

Figure 75: Observed and simulated cane fresh weight yields of fertilized versus unfertilized and burnt versus unburnt treatments from 1941 to 2016 for mulched (M) and burnt with tops scattered (BS) treatments, and 1980 to 2016 for BR treatments for (burning and r removal of residues started in 1980). a) MF: mulched and fertilized, b) MF0: mulched and unfertilized, c) BSF: burnt, cane tops removed and fertilized, d) BSF0: burnt, cane tops removed and unfertilized, e) BRF: burnt, residues removed and fertilized, f) BRF0: burnt, residues removed and unfertilized.

APSIM estimated yields well, meeting the statistical criteria in most instances (Table 51). Retaining residues after harvest proved to be beneficial to yield, as both measured and simulated data showed relatively higher yields on mulched than burnt treatments. The model was, therefore, able to simulate the relative effect of residue management and inorganic fertilization on sugarcane yields. Comparison of measured and simulated data resulted in MAE higher than the acceptable 20% in fertilized and unfertilized treatments, with only the MF0 treatment meeting the statistical criteria. The MF0 had an MAE of 18.8%, meeting the statistical criteria, and the BSF0 and BRF0 treatments had higher MAEs of 33.4% and 44.8%, respectively, indicating the least accurate simulation by the model for these two treatments. The RMSE was relatively higher in fertilized than unfertilized treatments. The D value met statistical criteria (D > 0.8) in the MF, MF0 and BSF0 treatments, and for all other treatments, the D value was above 0.73. The R^2 did not meet statistical criteria for any of the treatments indicating a poor correlation between measured and simulated cane yields.

Table 51: Statistical evaluation of measured versus simulated yields for the fertilized and unfertilized treatments

Treatment	R^2	D	MAE (%)	RMSE (t cane ha^{-1})
MF	0.65	0.84	22.5	25.7
BSF	0.44	0.77	29.1	27.1
BRF	0.43	0.74	26.5	24.6
MF0	0.74	0.92	18.8	16.3
BSF0	0.68	0.80	33.4	26.1
BRF0	0.54	0.73	44.8	16.4

10.3.2 Simulating long-term sugarcane management practices on soil quality

10.3.2.1 Soil organic matter

Simulation of SOM dynamics over the years (1939-2013) indicated a decline in SOM content across all treatments. Comparisons between observed and simulated SOM content of fertilized treatments are shown in Figure 76. Observed and simulated results showed a decline in SOM for all treatments regardless of mulching or residue burning and removal after harvest. The magnitude of SOM decline, however, differed with the management practices used between the treatments. The mulched treatments (MF and MF0) had relatively higher SOM levels than burnt treatments (BSF, BRF, BSF0, BRF0) over the 73 years of simulation, which clearly indicates the beneficial effects of retaining crop residues on SOM. This was consistent with a study by Luo, Wang et al. (2011) who reported that changes in SOM were highly correlated with the amount of residues retained in agricultural practices. The MF and MF0 treatments displayed SOM declines from 7% SOM in 1939 to 5.5% and 4.4% in 2013, respectively, with the BSF and BSF0 declining from 7% to 4.6% and 3.9% SOM respectively in 2013. The SOM content was not significantly influenced by the retention of cane tops (BS treatments) when compared with burning and removing all residues. The difference between SOM content was 0.2% in BSF versus BRF treatments, and 0.1% in BSF0 versus BRF0 treatments after 73 years of simulation. Fertilized treatments generally had higher SOM levels than their unfertilized partner treatments, which indicates that fertilization can slow down the decline of SOM content. A study by Beza and Assen (2016) reported high soil C loses after land has been converted to agriculture, which was stabilized with an increased duration of agricultural activities. In this trial, the SOM has not yet indicated that it has reached the stabilization phase, both observed and simulated SOM are showing a decline even in recent years.

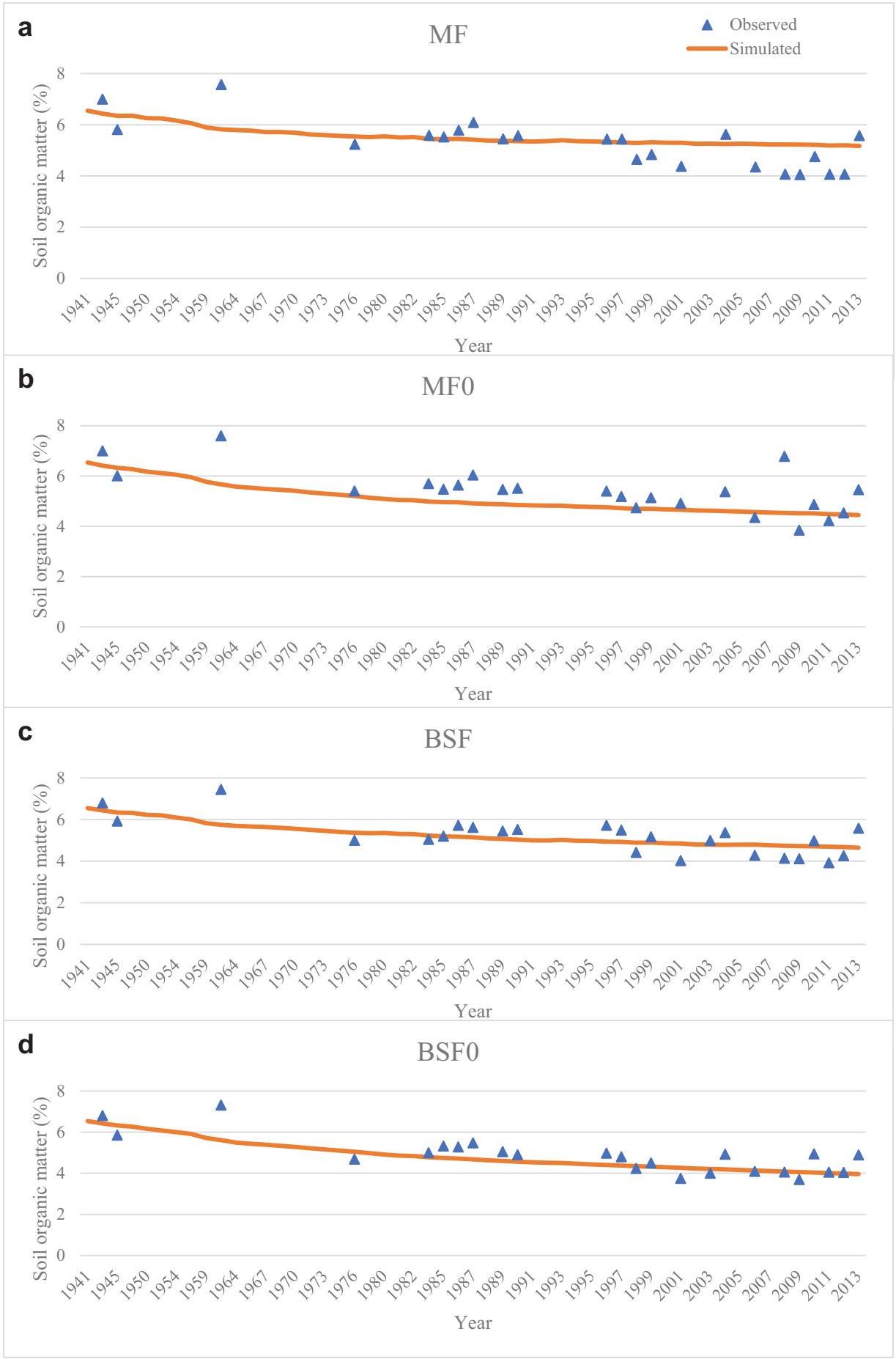
a
MF
Observed
Simulated
Soil organic matter (%)
Year
b
MF0
Soil organic matter (%)
Year
c
BSF
Soil organic matter (%)
Year
d
BSF0
Soil organic matter (%)
Year

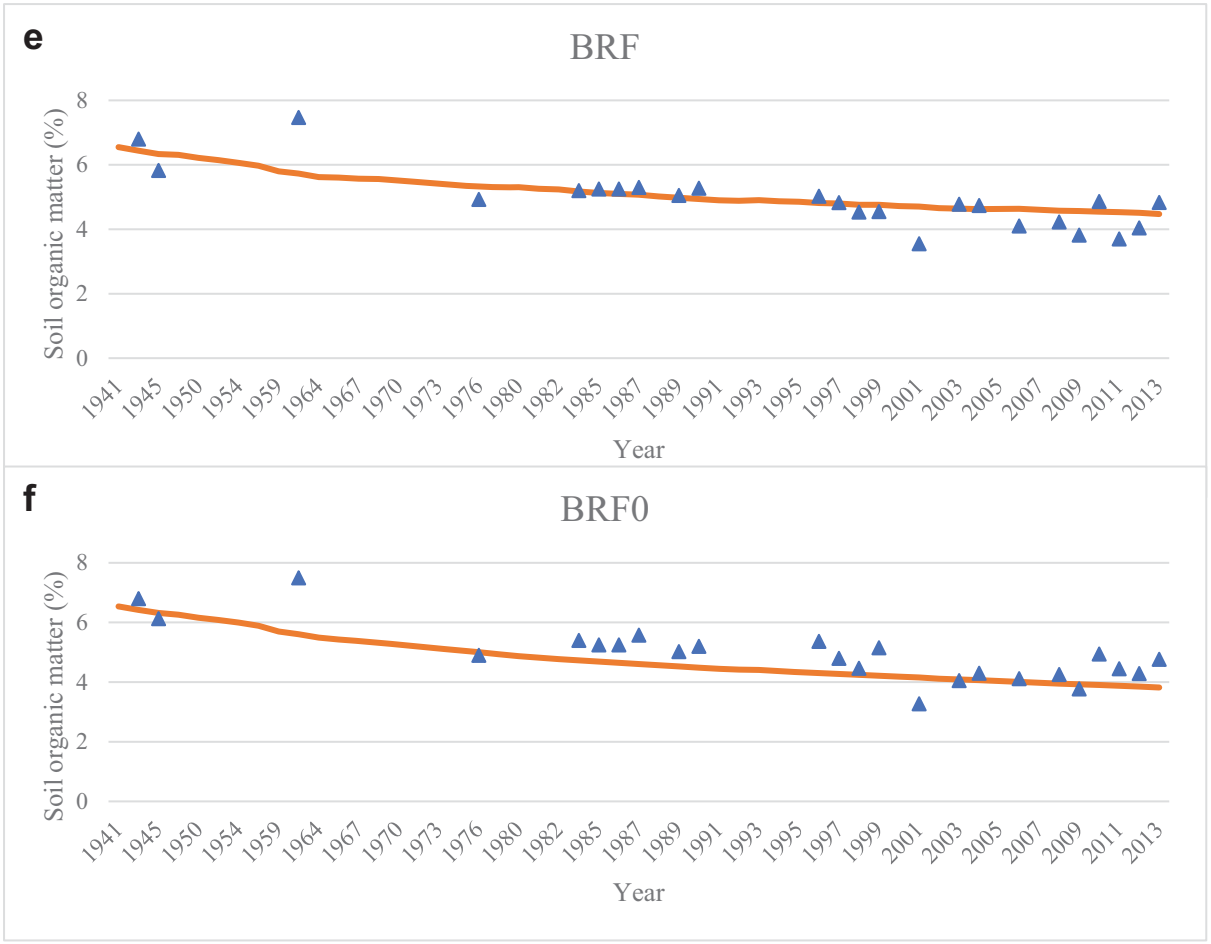

Figure 76: Observed and simulated soil organic matter content of the fertilized versus unfertilized treatments and mulched versus burnt treatments in the long-term sugar cane trial (comparison done at a depth of 0.2 m). a) MF: mulched and fertilized, b) MF0: mulched and unfertilized, c) BSF: burnt, cane tops removed and fertilized, d) BSF0: burnt, cane tops removed and unfertilized, e) BRF: burnt, residues removed and fertilized, f) BRF0: burnt, residues removed and unfertilized.

A summary of the statistical comparison between observed and simulated SOM is shown in Table 5.4. The model was able to predict SOM adequately as indicated by low MAE's (< 20%) and RMSE's across all treatments. Fertilized treatments had a higher RMSE than unfertilized treatments, indicating a higher degree of precision in unfertilized treatments. The D and R^2 values, however, did not meet the statistical criteria in any of the treatments. Despite the high error variance between the treatments (low R^2), the model performed fairly well in estimating SOM changes over the years.

Table 5.1 Statistical evaluation of measured and simulated soil organic matter content in fertilized versus unfertilized, and mulched versus burnt treatments.

Treatment	R^2	D	MAE (%)	RMSE (%)
MF	0.22	0.57	12.4	0.86
BSF	0.14	0.56	13.1	0.94
BRF	0.29	0.63	11.2	0.81
MF0	0.29	0.67	9.8	0.73
BSF0	0.31	0.66	11.4	0.76
BRF0	0.37	0.68	10.6	0.75

10.3.2.2 Deep drainage and nitrogen leaching dynamics

The total amount of water lost through deep drainage differed between the treatments, which would have also influenced the amount of N leaching between treatments. Modeled cumulative drainage indicated that mulched treatments (MF and MF0) had a higher volume of water lost through drainage over the simulated period of 76 years (Figure 77). The residue cover present in these treatments is known to influence soil water content through reducing evaporation (Vallis, Parton et al., 1996; Van Antwerpen, Thorburn et al., 2002). Residue burning reduced the amount of drainage as indicated but scattering of the cane tops after burning led to increased drainage compared to removal of tops (BR). The results showed that mulched treatments are estimated to have lost the highest volume of water through drainage over 76 years (MF and MF0 lost 13 209 mm and 15 164 mm respectively) and the burnt treatments with cane tops raked off losing the smallest amounts (BRF and BRF0 lost 10 701 mm and 12 908 mm respectively). This was also reported in a similar study by Cheong and Teeluck (2016) where sugarcane grown on fields with leaf residue cover lost more water through drainage than treatments with no residue cover in a water use efficiency study in Mauritius. The overall trend in the amount of cumulative drainage based on residue management observed on both fertilized and unfertilized treatments showed the following declining order: M > BS > BR. Less drainage was simulated for the fertilized treatments had low drainage compared to the unfertilized in all treatments. This can be a result of reduced aggregate stability where fertilizer was used leading to a higher probability of dispersion and therefore increased runoff (Van Antwerpen and Meyer, 1998).

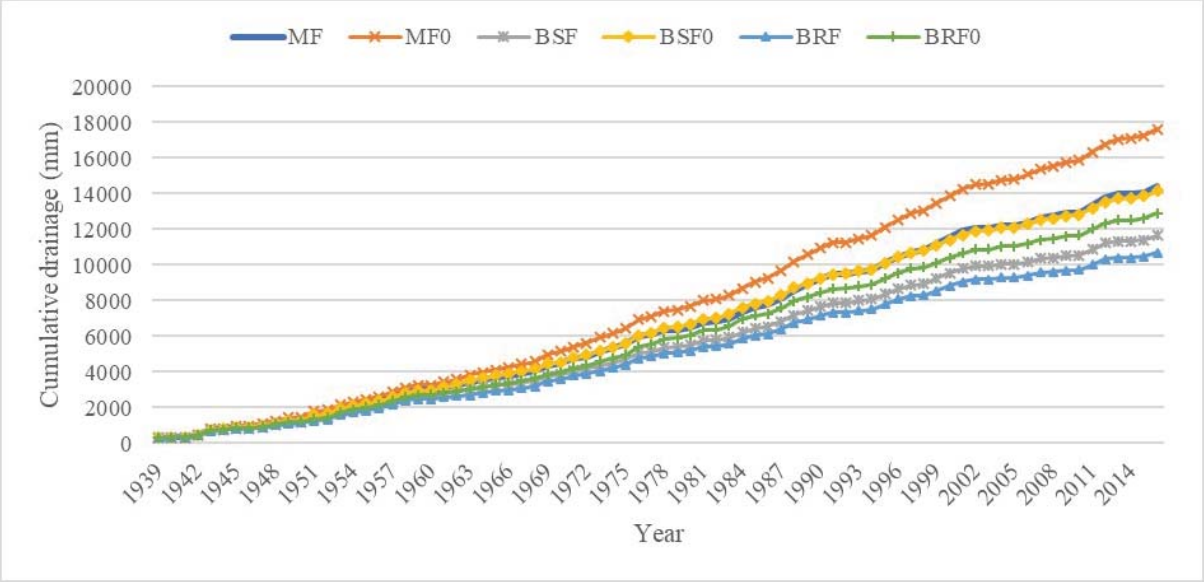

Figure 77: Cumulative deep drainage over the 76 year simulation period for different sugarcane management practices. MF: mulched and fertilized, MF0: mulched and unfertilized, BSF: burnt, cane tops removed and fertilized, BSF0: burnt, cane tops removed and unfertilized, BRF: burnt, residues removed and fertilized, BRF0: burnt, residues removed and unfertilized.

Annual N leaching proved to be highly variable for successive years as affected by rainfall, amount of deep drainage and fertilizer application strategy. Fertilized treatments (MF and BSF) generally had higher N leaching than unfertilized treatments. Leaching was also predicted for unfertilized treatments (MF0 and BSF0) which showed a declining trend in N leaching over the years (data not shown). In the last 20 years, NO_3-N leaching was below 20 kg N ha^{-1} per year. The differences in cumulative drainage also brought differences in cumulative leaching among the treatments. The simulation showed that fertilized treatments had higher N lost over the years, which could be expected as the result of seasonal inorganic N addition. At least 3 900 kg N ha^{-1} has been lost in each of the fertilized treatments since the experiment started in 1939. Residue burning reduced the amount NO_3-N leaching in the fertilized treatments (Figure 78) as shown by the MF having higher cumulative leaching than BRF and BSF. The MF had the highest cumulative leaching (1939-2016) estimated to have lost 4 526 kg ha^{-1} NO_3-N over the years (or about 59.6 kg NO_3-N ha^{-1} yr^{-1}). The burnt treatments (BSF and BRF) lost 3 909 kg ha^{-1} (or about 51.4 kg NO_3-N ha^{-1} yr^{-1}) and 3 914 kg ha^{-1} (or about 51.5 kg NO_3-N ha^{-1} yr^{-1}) respectively, showing an insignificant difference in NO_3-N leaching between the latter two treatments. The unfertilized treatments (MF0, BSF0, and BRF0) had relatively low leaching, that was almost identical. Unfertilized treatments showed no difference between burning or mulching treatments with regards to the amounts of N leached over the years, with about 700 kg ha^{-1} N over 76 years (or about 9.2 kg NO_3-N ha^{-1} yr^{-1}).

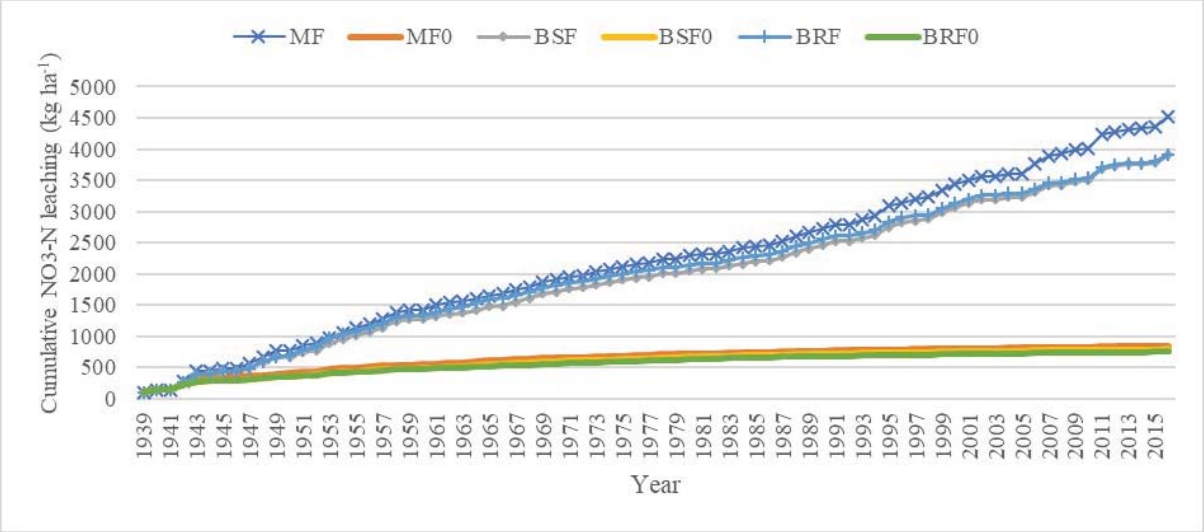

Figure 78: Cumulative nitrate-nitrogen (NO3-N) leaching over a 76-year simulation of fertilized versus unfertilized and mulched versus burnt treatments in sugarcane. MF: mulched and fertilized, MF0: mulched and unfertilized, BSF: burnt, cane tops removed and fertilized, BSF0: burnt, cane tops removed and unfertilized, BRF: burnt, residues removed and fertilized, BRF0: burnt, residues removed and unfertilized.

10.3.2.3 Fertilizer application scenario results

Sugarcane yields

Fresh cane weight yield on mulched treatments did not significantly differ with the reduction in N fertilization rate (Figure 79). For different fertilization rates scenarios, the model indicates that high (140 k ha^{-1} N application) fertilization on mulched treatments did not increase yields compared to lower rates (40 and 80 kg ha^{-1} N application). Yield differences can only be seen in high rainfall seasons whereby moisture was likely non-limiting (see period between 1970 and 1978 in Figure 79). Since harvesting was done every 12 months (1987 to present) the yields are almost the same across all fertilizer rates. The results indicate that under mulching there is a high possibility of over-fertilization if the benefits of NO_3-N released from the mineralization from microbial decomposition of residues is not considered in the fertilization programme.

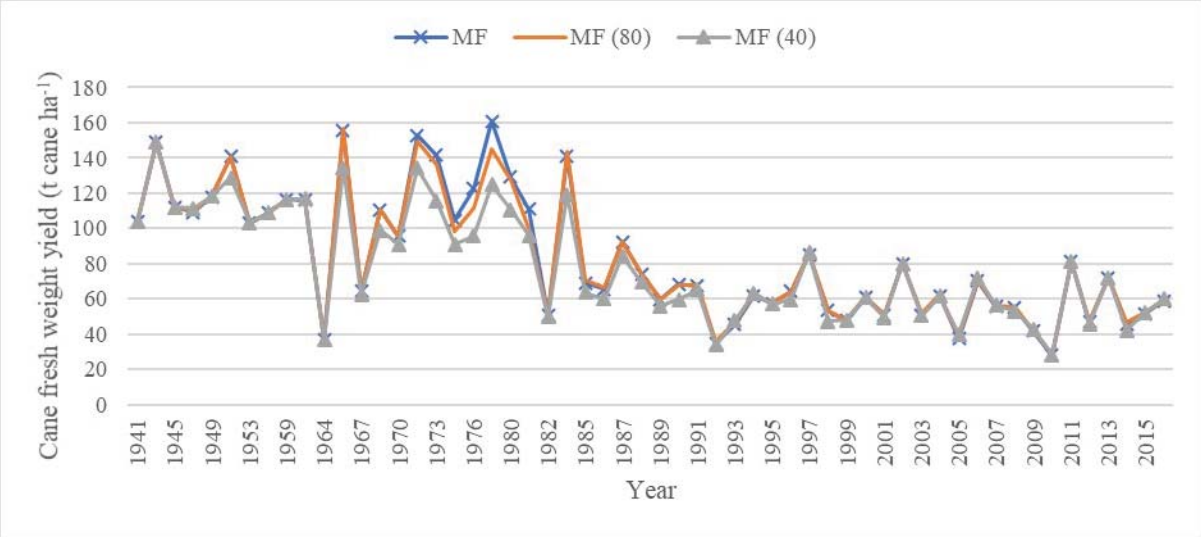

Figure 79: Simulated cane fresh weight of mulched and fertilized (MF) treatments on recommended rate (140 kg ha-1 N) used in the long-term sugarcane trial and lower rates fertilizer application scenarios (40 and 80 kg ha-1 N rates). MF: mulched and fertilized, MF (40): 40 kg ha^{-1} application rate, MF (80): 80 kg ha^{-1} application rate.

Nitrate leaching

As expected, simulated NO_3-N leaching in the mulched treatment was reduced by lower inorganic N fertilization rates (Figure 80). The cumulative leaching over 76 years was estimated to be reduced from 4 526 kg ha^{-1} for the 140 kg ha^{-1} fertilization rate to 1 313 kg ha^{-1} in the 40 kg ha^{-1} scenario (or about 17.3 kg NO_3-N ha^{-1} yr^{-1}), and 2 261 kg ha^{-1} in the 80 kg ha^{-1} scenario (or about 29.8 kg NO_3-N ha^{-1} yr^{-1}). This shows a 70% reduction in N leaching in the 40 kg ha^{-1} fertilizer rate with no significant effect on the cane fresh weight at harvest.

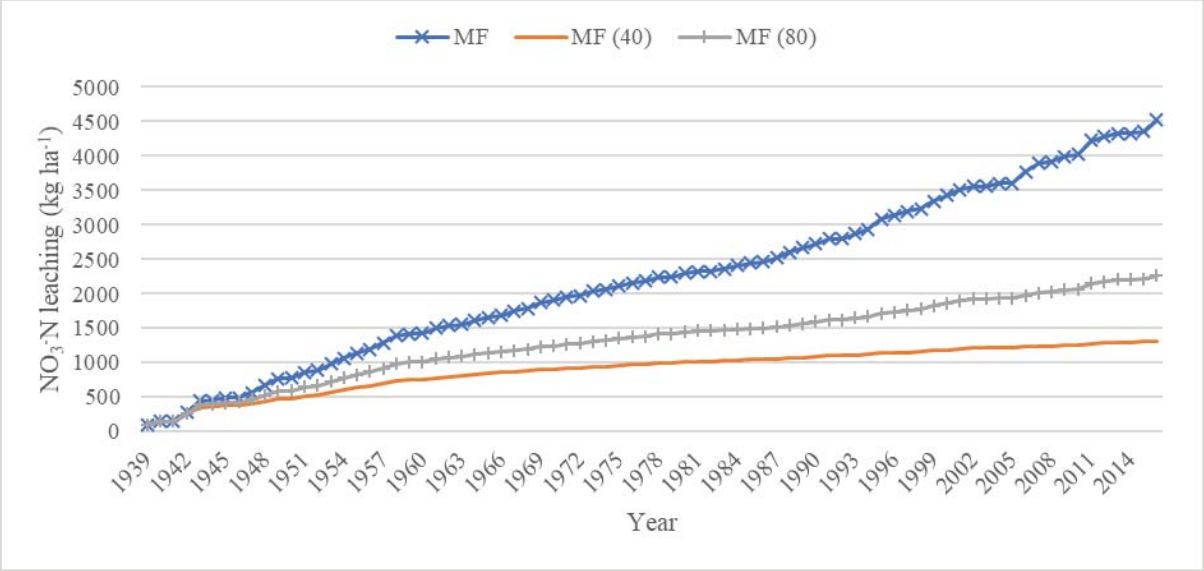

Figure 80: Cumulative nitrate-nitrogen (NO_3-N) leaching of mulched and fertilized treatments on recommended rate (140 kg ha^{-1} N) used in the long-term sugarcane trial and lower rates fertilizer application scenarios (40 and 80 kg ha-1 N application). MF: mulched and fertilized, MF (40): 40 kg ha^{-1} application rate, MF (80): 80 kg ha^{-1} application rate.

10.4 DISCUSSION

Simulating sugarcane yields

Observed and simulated results indicated that fertilizer application increased yields in sugarcane monoculture system. Non-fertilized treatments also produced relatively high yields, especially for the first two periods (1939-1960), and this can be attributed to the high nutrient storage capacity of the soil. Cation exchange capacity (CEC) ranged between 14.8 and 20.1 $cmol_c$ kg^{-1} in the 0-200 mm soil layer (Van Antwerpen and Meyer, 1998). The high soil fertility resulted in measured yields of fertilized and non-fertilized treatments not being significantly different over the first 18 years (Van Antwerpen et al., 2001). Residue retention led to consistently higher yields in the mulched treatments compared to the burnt, however, Van Antwerpen, Meyer et al. (2001) reported that the yields between the treatments over the years were not statistically significant. This agrees with a previous study by Vallis, Parton et al. (1996) on beneficial effects associated with residue retention, which included conserving moisture by reducing evaporation, reducing erosion, improving soil structure and increasing soil fertility when residues are decomposed, and all these factors have shown to be beneficial to long-term sugarcane yields. In some years, poor yield estimations were observed mostly in the form of overestimations by the model. This is probably a result of short-term extreme weather conditions at critical stages of the crop affecting growth, which the model cannot always account for. Temperature, water use, annual rainfall and incident solar radiation can be highly variable from one day, week, month and season to the next, thus causing variation in attainable yields. High temporal spatial variabilities due to short-term

weather patterns and extreme events not considered by the model can be a result of poor yield estimations in some years.

The different sugarcane varieties planted in the trial over the years can negatively influence the ability of the model to estimate yields. Changing varieties can have a significant influence on yields (Liu, Wang et al., 2010), thus affecting the long-term measured yields. The same cultivar was used throughout the simulation, therefore, yields from different varieties (measured versus simulated yields) were compared in some years. The model simulates cane growth as a function of weather, soil water and N inputs, with yields strongly influenced by radiation, temperature, crop phenology, physiology and architecture (Cheeroo-Nayamuth, Robertson et al., 2000). In the model, varieties may not be properly parameterized for local conditions and can negatively affect the robustness of the model predictions.

Harvested stalks and residue burning can contribute to substantial nutrient losses from the system if they are not adequately addressed in fertilizer programmes, thus negatively influencing the yields. A decline in P and K in long-term sugarcane mono-cropping system as a result of nutrient mining was reported in a study on the same trial (Van Antwerpen, Meyer et al., 2001). The N limited yields estimated by the model might be overlooking the beneficial or limiting effects of other nutrients that comes with NPK fertilizers which can lead to overestimations in unfertilized treatments (P and K limited yields) or underestimations in fertilized treatments (yields promoted by P and K additions) if the other factors are assumed to be non-limiting. Fertilizer application leads to higher biomass production and contributes to elevated SOM and lower the soil pH levels. The lowering of soil pH is mainly driven by the N-fertilizer and to a much lesser extend (not significant) by organic matter decomposition (Van Antwerpen et al., 2001). This acidification potential of inorganic fertilization can also negatively influence measured yields in fertilized treatments.

Simulating soil C dynamics

Soil cultivation has been highlighted to be the major reason of declining SOM trends in arable agriculture by burying crop residues and increasing soil microbial activities (West and Post, 2002; Ogle, Breidt et al., 2005). Measured and simulated results showed a decline over the years, with an initial steeper decline in the early compared to later years shown by simulated SOM content. The high SOM decline in the early years of land conversion to agriculture indicated by all management practices was a consistent observation that has also been reported in previous studies (Dominy, Haynes et al., 2002; Beza and Assen, 2016). After a rapid decline in the early years of cultivation, SOM is expected to reach a steady phase where the decline levels off (Swanepoel, Van der Laan et al., 2016), but in the simulation that period has not yet been reached since all management practices are still showing a decline.

Soil organic carbon is a product of the decomposition of organic matter and accumulation of C in the soil, thus making residue management crucial in determining long-term soil C stocks in cropping systems. The higher biomass production, as a result of fertilization, increases the amount of crop residue inputs into the soil, hence, higher SOM in fertilized than unfertilized treatments. The simulation clearly indicated the benefits of mulching on maintaining high SOM content is sugarcane monoculture

systems. In a study by Mthimkhulu, Miles et al. (2018) on the same trial, the residue retention benefits on SOC were only restricted to shallow depths regardless of the amount of residues retained. This was in agreement with the simulated results, as the model's robustness in estimating soil C dynamics was shown by high SOC in the top layer compared to other soil layers as a result of high residue returns and minimal soil disturbance in sugarcane cropping systems. According to Thorburn, Probert et al. (2001), sugarcane decomposition is a relatively slower process compared to other residues with similar biochemical composition. This keeps residues on the soil surface for a longer period allowing more time to be incorporated into the soil, thus contributing to soil C accumulation.

Burning the residues negatively affect soil C sequestration and the overall benefits of residue cover to soil properties that can be beneficial to the next crop. The results indicated a difference between long-term SOM content of mulched versus burnt treatments. However, despite burning residues for 73 years in BR treatments, the SOM content is still relatively high (soil organic carbon (SOC) > 3.5%, (Mthimkhulu et al., 2016) confirming that the magnitude of SOM loss with respect to management practices can be site specific. The underground roots that remain after burning in the BR treatments might still be adding considerable amounts of organic residues that slows down the decline of carbon over the years.

Simulating soil N dynamics

The simulation indicated that residue retention did not subsequently result in higher N benefits compared to burning or removal of residues in sugarcane monoculture system. Despite high residue returns and SOM content in mulched treatments, total N mineralization from residues and SOM pools was less than in burnt treatments since the trial commenced. The addition of residues increase soil microbial activities, but the high C:N ratio of the residues results to initial N immobilization, with a small amount of N mineralized (Robertson and Thorburn, 2007). Since 1939, an estimated 1 778 kg ha^{-1} N and 2 028 kg ha^{-1} N has been mineralized in the MF and MF0 treatments respectively, indicating more mineralization in unfertilized than fertilized treatment under mulching. Thorburn, Van Antwerpen et al. (2002) reported that many years of residue retention may be needed for soil C and N cycling to reach a new equilibrium for N immobilization to match mineralization, and further net N mineralization from residues. In this simulation that equilibrium has been reached under mulching in the long-term trial (not shown in results).

Nitrate leaching showed to be highly related to N application and the volume of water moving out of the root zone through drainage. The amount of nitrates and water lost through drainage differed among treatments, indicating that soil moisture and N leaching can be greatly influenced by management practices. The high drainage on the M treatments can be attributed to the benefits of the thrash blanket to SOM returns, reduced runoff and an increase of soil water content. In the short term, a thrash blanket can reduce soil evaporation which increases soil water content in top layers. About 90% ground cover is provided by sugarcane residues of mass greater than 3 t ha^{-1} (Thorburn, Probert et al., 2001). In the long term, it can increase the soil C stocks resulting in high SOM content which improves soil structure and increase microbial activities (Graham, Haynes et al., 2002). This increases water infiltration in

mulched compared to burnt treatments where the soil can be prone to surface crusting and increase runoff thus reducing the amount of water getting into the soil profile which will reduce overall drainage.

Nitrate leaching was estimated to be high on fertilized compared to unfertilized treatments. In a study by (Cameron, Di et al., 2013), it was stated that NO_3^-N leaching is highly dependent on NO_3^-N concentration in the soil solution and the amount of water lost through drainage over a certain period. This can be influenced by the ability of the soil to adsorb anions, as it can help retain NO_3^- making them available for plant uptake, enhancing soil nutrition in the process. The addition of N fertilizers increased the amount of N in the soil solution thus increasing the NO_3^-N prone to leaching. The results showed that MF treatment had the highest annual NO_3-N leaching compared to the other treatments. Van Antwerpen, Meyer et al. (2001) reported that an estimated 2 200 kg N ha^{-1} N input from mineralization in mulched and fertilized treatments, which was higher than the prediction of the current simulation (1 778 kg ha^{-1} N), with an additional 3 900 kg ha^{-1} from fertilizer application since the trial commenced. This proved that considerable amounts of NO_3^- are mineralized through the breakdown of organic residues, thus contributing to soil N and this is also the reason NO_3-N leaching also occurs in unfertilized treatments. This was also reported study by Mthimkhulu, Miles et al. (2018), where the N content of mulched treatments was reported to have increased significantly in both fertilized and unfertilized plots in the top 10 cm, indicating the benefits of retaining residues to increasing N content in both fertilized and unfertilized treatments.

Fertilization scenarios

The ability of the model to adequately simulate the long-term soil C and N dynamics of the BT 1 long-term trial allowed the application of the model to investigate a fertilizer application strategy that can minimize NO_3^- leaching. The results show that reducing the amount of fertilizer N applied can reduce NO_3^- N leaching without a significant reduction in yields on sugarcane cropping systems where all residues are retained after harvest. This has been previously reported in a study by Wiedenfeld (1995), where there was no yield response with increasing N application rates on rain-fed sugarcane production. This can be an indication of a significant contribution of potential N mineralization from SOM being able to satisfy a greater proportion of the crops N demand under mulching. Getting the same yields at different N rates indicates that increasing yields can only be achieved by exploring other factors rather than increased N application. Reducing fertilizer N can increase NUE and reduce N loss, but the high biomass production benefits that come with inorganic fertilization have to be maintained for high organic residue inputs to minimize SOM loss.

The cumulative NO_3-N loss increased with increases in fertilizer N application rate in the scenarios. This was an indication of over-fertilization regarding the fertilizer rate used in the trial. Reducing N export to the environment by accounting for mineralized N is an important management intervention required in the mulched and fertilized management practice. The balance between available N and crop N uptake is a key determinant of potential N loss from the soil system. Crop N uptake can be affected by soil characteristics, cultural practices as well as timing and method of N fertilizer application (Van der Laan, Jumman et al., 2015). These results are emphasizing the importance of a better understanding of the

fate of N in sugarcane production to improve fertilizer recommendations for improved NUE and reduce environmental losses. Small amounts of N mineralization can occur throughout the season, but this N may not be able to satisfy crop's demand at critical growth stages of high N demand. Timely N application to supplement mineralized N at these critical stages can be an important management intervention that can help reduce N leaching, though this might not be an easy exercise in large-scale sugarcane production.

10.5 Conclusion

Declining trends in long-term yields and soil quality in sugarcane monoculture systems requires new management practices to maintain high productivity without negatively affecting the quality of the soil and environment (offsite impacts). These gradual changes due to management practices are difficult to study in short-term experiments, therefore a combination of crop modelling and long-term monitoring data can be used to improve the understanding and evaluate long-term changes in yields and SOM under certain management practices as indicated by this study. Based on the results, the APSIM model was judged to adequately simulate long-term C and N dynamics in sugarcane cropping systems. The combination of mulching and fertilization was beneficial to long-term SOM content but needs N management strategies to reduce N leaching.

10.6 References

AZIZ, I., MAHMOOD, T., ISLAM, K.R. (2013) Effect of long term no-till and conventional tillage practices on soil quality. *Soil and Tillage Research*, 131: 28-35.

BELAY, A., CLAASSENS, A., WEHNER, F. (2002a) Effect of direct nitrogen and potassium and residual phosphorus fertilizers on soil chemical properties, microbial components and maize yield under long-term crop rotation. *Biology and Fertility of Soils*, 35: 420-427.

BELAY, A., CLAASSENS, A., WEHNER, F. (2002b) Soil nutrient contents, microbial properties and maize yield under long-term legume-based crop rotation and fertilization: A comparison of residual effect of manure and NPK fertilizers. *South African Journal of Plant and Soil*, 19: 104-110.

BELLO, A.Z. (2008) Effect of soil nutrient status on growth, reproductive development and yield components of maize in a long-term trial. *MSc Dissertation, University of Pretoria.*

CAMERON, K., DI, H.J., MOIR, J. (2013) Nitrogen losses from the soil/plant system: a review. *Annals of applied biology*, 162: 145-173.

CATES, A.M., RUARK, M.D., HEDTCKE, J.L., POSNER, J.L. (2016) Long-term tillage, rotation and perennialization effects on particulate and aggregate soil organic matter. *Soil and Tillage Research*, 155: 371-380.

DOMINY, C., HAYNES, R. (2002) Influence of agricultural land management on organic matter content, microbial activity and aggregate stability in the profiles of two Oxisols. *Biology and Fertility of Soils*, 36: 298-305.

DOMINY, C., HAYNES, R., VAN ANTWERPEN, R. (2002) Loss of soil organic matter and related soil properties under long-term sugarcane production on two contrasting soils. *Biology and Fertility of Soils*, 36: 350-356.

GALLOWAY, J.N., TOWNSEND, A.R., ERISMAN, J.W., BEKUNDA, M., CAI, Z., FRENEY, J.R., MARTINELLI, L.A., SEITZINGER, S.P., SUTTON, M.A. (2008) Transformation of the nitrogen cycle: recent trends, questions, and potential solutions. *Science*, 320: 889-892.

HERRICK, J.E. (2000) Soil quality: an indicator of sustainable land management? *Applied Soil Ecology*, 15: 75-83.

KAUR, T., BRAR, B., DHILLON, N. (2008) Soil organic matter dynamics as affected by long-term use of organic and inorganic fertilizers under maize – wheat cropping system. *Nutrient Cycling in Agroecosystems*, 81: 59-69.

KÖRSCHENS, M. (2006) The importance of long-term field experiments for soil science and environmental research – a review. *Plant Soil Environ*, 52: 1-8.

LIU, H., YANG, J., DRURY, C.A., REYNOLDS, W., TAN, C., BAI, Y., HE, P., JIN, J., HOOGENBOOM, G. (2011) Using the DSSAT-CERES-Maize model to simulate crop yield and nitrogen cycling in fields under long-term continuous maize production. *Nutrient Cycling in Agroecosystems*, 89: 313-328.

LIU, Y., WANG, E., YANG, X., WANG, J. (2010) Contributions of climatic and crop varietal changes to crop production in the North China Plain, since 1980s. *Global Change Biology*, 16: 2287-2299.

LUO, Z., WANG, E., SUN, O.J. (2010) Soil carbon change and its responses to agricultural practices in Australian agro-ecosystems: a review and synthesis. *Geoderma*, 155: 211-223.

LUO, Z., WANG, E., SUN, O.J., SMITH, C.J., PROBERT, M.E. (2011) Modeling long-term soil carbon dynamics and sequestration potential in semi-arid agro-ecosystems. *Agricultural and forest meteorology*, 151: 1529-1544.

MALHI, S., NYBORG, M., HARAPIAK, J., HEIER, K., FLORE, N. (1997) Increasing organic C and N in soil under bromegrass with long-term N fertilization. *Nutrient Cycling in Agroecosystems*, 49: 255-260.

MENG, L., DING, W., CAI, Z. (2005) Long-term application of organic manure and nitrogen fertilizer on N2O emissions, soil quality and crop production in a sandy loam soil. *Soil biology and biochemistry*, 37: 2037-2045.

MILLS, A., FEY, M. (2003) Declining soil quality in South Africa: effects of land use on soil organic matter and surface crusting. *South African Journal of Science*, 99: 429-436.

NARDI, S., MORARI, F., BERTI, A., TOSONI, M., GIARDINI, L. (2004) Soil organic matter properties after 40 years of different use of organic and mineral fertilisers. *European Journal of Agronomy*, 21: 357-367.

NEL, P., BARNARD, R., STEYNBERG, R., DE BEER, J., GROENEVELD, H. (1996) Trends in maize grain yields in a long-term fertilizer trial. *Field crops research*, 47: 53-64.

POULTON, P. (1995) The importance of long-term trials in understanding sustainable farming systems: the Rothamsted experience. *Australian Journal of Experimental Agriculture*, 35: 825-834.

REN, T., WANG, J., CHEN, Q., ZHANG, F., LU, S. (2014) The effects of manure and nitrogen fertilizer applications on soil organic carbon and nitrogen in a high-input cropping system. *PloS one*, 9: e97732.

SASEENDRAN, S.A., MA, L., NIELSEN, D., VIGIL, M., AHUJA, L. (2005) Simulating planting date effects on corn production using RZWQM and CERES-Maize models. *Agronomy Journal*, 97: 58-71.

SOLER, C.M.T., SENTELHAS, P.C., HOOGENBOOM, G. (2007) Application of the CSM-CERES-Maize model for planting date evaluation and yield forecasting for maize grown off-season in a subtropical environment. *European Journal of Agronomy*, 27: 165-177.

STEVENSON, F.J., COLE, M.A. (1999) *Cycles of soils: carbon, nitrogen, phosphorus, sulfur, micronutrients*. John Wiley & Sons.

SWANEPOEL, C., VAN DER LAAN, M., WEEPENER, H., DU PREEZ, C., ANNANDALE, J. (2016) Review and meta-analysis of organic matter in cultivated soils in southern Africa. *Nutrient Cycling in Agroecosystems*, 104: 107-123.

THORBURN, P.J., MEIER, E.A., PROBERT, M.E. (2005) Modelling nitrogen dynamics in sugarcane systems: Recent advances and applications. *Field crops research*, 92: 337-351.

VAN HEERDEN, P., CROSBY, C., GROVÉ, B., BENADÉ, N., THERON, E., SCHULZE, R., TEWOLDE, M. (2009) Integrating and updating of SAPWAT and PLANWAT to create a powerful and userfriendly irrigation planning tool. *Water Research Commission Report No. TT*, 391/09.

11 LONG-TERM EFFECTS OF INORGANIC FERTILIZER APPLICATION ON MAIZE *(ZEA MAYS L.)* YIELD, SOIL ORGANIC MATTER AND NITROGEN LEACHING

S. Maseko[1], M. van der Laan[1], R. van Antwerpen[2,3] and D. Marais[1]
[1]Department of Plant and Soil Sciences, University of Pretoria, Pretoria 0002, South Africa
[2]South African Sugarcane Research Institute, Mount Edgecombe, 4300, South Africa
[3]Department of Soil, Crop and Climate Sciences, University of the Free State, Private Bag 339 Bloemfontein 9300, South Africa

11.1 Introduction

Long-term experiments are important for understanding and evaluating the interactions between crops and the environment and have been essential in providing means of evaluating sustainable management systems in agriculture. Our present knowledge of soil fertility has had a significant contribution from long-term field experiments (Körschens, 2006). They are useful in developing beneficial management practices that can be able to economically produce high crop yields whilst maintaining soil quality at acceptable levels (Liu, Yang et al., 2011). Short-term studies may not reliably reveal certain soil processes, which can only be studied over a long period of time by looking at the trends. Long-term experiments are able to provide the best practical means of evaluating soil quality factors such as declining soil organic matter (SOM) levels and soil acidification on crop growth and soil properties (Poulton, 1995). These experiments have been used for several objectives, including determining optimal fertilizer requirements, testing the sustainability of a particular management system over a long period and determining changes that can improve productivity, and providing long-term data that can be used in validating crop models that can be used in the further evaluation of management practices.

Inorganic fertilizers are often used as the main source of nutrients needed to produce high yields in commercial agriculture. These fertilizers, however, can influence the soil chemical characteristics, affecting nutrient cycling and potentially resulting in negative environmental impacts (Galloway, Townsend et al., 2008). This has highlighted the importance of appropriate fertilizer management to maintain soil fertility and increase yields while minimizing negative impacts on the environment. There have been conflicting reports on the on the subject of long-term inorganic fertilizer usage, with some studies highlighting that it contributes to SOM loss (Belay, Claassens et al., 2002; Nardi, Morari et al., 2004), and others reporting beneficial effects of fertilization on SOM levels (Malhi, Nyborg et al., 1997; Meng, Ding et al., 2005).

Soil organic matter is often used as an indicator of soil quality and the sustainability of a cropping system due to its influence on soil physical, chemical and biological properties (Herrick, 2000; Mills and Fey, 2003; Aziz, Mahmood et al., 2013). It can be influenced by management practices especially fertilization and tillage practices, as has been reported by various studies on long-term experiments (Dominy and Haynes, 2002; Cates, Ruark et al., 2016). These management practices influence SOM by controlling the overall input of soil C and the rate at which it is decomposed (Kaur, Brar et al., 2008). To sustain

high yields and maintain soil quality over the long-term, a good understanding of the effects of management practices on crop production is required.

Data from a long-term experiment which started in 1939 at the University of Pretoria's Hillcrest Campus Experimental Farm (previously called the Hatfield Experimental Farm) can be valuable for studying the effects of management practices on yields and soil quality. In this chapter, the performance of the APSIM model in predicting long-term maize (*Zea mays* L.) yields and SOM changes under NPK fertilization. The model was then applied to evaluate the potential yield and SOM benefits of including manure in a fertilizer programme.

11.2 Materials and methods

11.2.1 Trial description

The long-term maize trial is described in Maseko (submitted). The specific treatments used for long-term simulation were the control (zero fertilization) and NPK treatment. The trial was initially established to determine fertilizer requirements of maize on the specific soil type. However, the objectives changed over the years, with more emphasis recently being placed on monitoring the performance of maize under different nutrient levels (balanced and imbalanced nutrients treatments) (Nel, Barnard et al., 1996). It was envisaged that this would help in evaluating the sustainability of the different inorganic nutrient applications and gain a better understanding of how basic production processes are affected by fertilizer treatment combinations.

11.2.2 Long-term measured data

11.2.2.1 Long-term yield and SOM data

Data from the experimental plots with zero and full fertilizer treatments was acquired from the trial records and published literature (Nel, Barnard et al., 1996; Belay, Claassens et al., 2002). Yield data from 1990-2017 for both treatments was acquired, but SOM data was more challenging to find as few previous publications focused on this variable in the long-term trial. Certain publications, however, did have data for percentage soil organic carbon (SOC) or total carbon (C) content in the soil (Nel et al., 1996; Belay et al., 2002; Bello, 2008). Data for total C content in 1990 and SOC in 1998, 2006, 2013 and 2017 were used to compare with model estimates. The factor of 1.724 (Stevenson and Cole, 1999) was used to convert SOC to SOM. Initial SOM content in 1950, which was the start of the simulation period, was estimated using analysis from samples from an undisturbed site adjacent to the trial at the end of 2016/2017 cropping season (-25º44'53"S, 28º15'36"E).

11.2.2.2 Long-term weather data

The minimum weather input required to run APSIM includes daily solar radiation (MJ m^{-2}), daily maximum and minimum temperature (ºC) and rainfall (mm). Hatfield daily weather data from 1950 to 1983 was obtained from a database developed by a team from the school of Bio-resources Engineering and Environmental Hydrology at University of KwaZulu-Natal using the South African Atlas of Climatology and Agro Hydrology (Van Heerden, Crosby et al., 2009). Pretoria automatic weather station provided 1984 to 2000 data, while data for 2001 to 2017 was obtained from the database of the South

African Weather Service (SAWS). Daily solar radiation was estimated using the minimum and maximum temperature, latitude and altitude [see Maseko (submitted)]. The annual average ambient temperature (TAV) and annual amplitude in monthly temperature (AMP) were calculated using the long-term daily minimum and maximum temperatures using the 'tav_amp' software provided by the APSIM platform. These calculated values of TAV and AMP were inserted to the met file automatically by the software.

11.2.3 Model application

11.2.3.1 Long-term maize simulation

The model requires inputs that describe field management, daily weather, soil profile characteristics, initial soil condition, and cultivar characteristics. The field management inputs include tillage date and type, planting date and density, irrigation, fertilizer application and residue management. The 'planting rule' was based on personal dialogue with the farm manager Mr. Burger Cillie on 11 November 2016. Tillage was done every year on 1st October to a depth of 0.3 m using a disc plough and 70% of the residues were assumed to be incorporated. The planting window period was from 1 October to 1 January every year, and sowing was done when a total of over 20 mm of rain occurred over five consecutive days. No sowing was allowed after 1 January as the growing season would then be too short for the crop to complete its life cycle. The maize variety calibrated in Section 3.2.4 was used for the simulation at a planting density of 50 000 plants ha^{-1}, although in reality a range of maize cultivars were planted over the years including Pretoria Potchefstroom Pearl (1939-1971), R200 (1972-1984), Pioneer 6431 (1985-2005) (Nel, Barnard et al., 1996) and Pioneer Phb 32W7, which is a short season variety planted in January 2006 after crop failure of initial planting due to birds attack (Bello, 2008). Fertilization was applied at sowing for the full fertilizer treatment (100 kg ha^{-1} N for the entire duration of the simulation). Soil profile characteristics, initial soil conditions, and cultivar characteristics are as described in Maskeo (submitted). Supplementary irrigation was simulated based on rainfall, with 15 mm irrigation being applied if rainfall over the previous 15 days was less than 5 mm.

11.2.3.2 Long-term manure application scenarios

Initially, manure (M) treatments were part of the long-term maize trial but were discontinued in 1990 after 50 seasons. A scenario of manure application (1950-2017) was simulated to assess the long-term beneficial effects of manure application and to what extent SOM levels could have been maintained. Historical data indicated that 9 tonnes ha^{-1} manure was applied (Nel, Barnard et al., 1996), hence the same amount was used in this scenarios. A manure only and NPK + manure treatments were simulated in the scenarios. An APSIM default manure was used, applied at sowing, and had C:N ratio of 12:1.

11.2.3.3 Testing model performance

Model evaluation was performed using long-term yields (1990 to 2017) and SOM (1950 to 2017) data control (zero fertilizer) and NPK treatments. Model performance was tested using the square of the correlation coefficient (R^2), the mean absolute error (MAE), root mean square error (RMSE) and the index of agreement (D) based on the criteria outlined in Maseko (submitted). The measured and simulated data were also graphically compared.

11.3 Results

11.3.1 Long-term fertilization effects on maize yields

The measured and simulated yields of the control and NPK treatments from 1990 to 2017 are shown in Figure 81. Measured and simulated yields were generally higher in the fertilized treatment than the control, clearly demonstrating the importance of fertilization on increasing yields over the years. There were yield over-estimations by the model in the NPK treatment in most seasons from 1990 to 2001, and after that period the yields were well estimated. The calibrated cultivar DKC 7374 BR, which was used for the simulation, was in reality first planted during the 2011 to 2012 season and this might explain the better estimations from 2011 to 2017. The control yields were poorly estimated, with a high variation of simulated yields in successive season from 1990 to 2010, but it was well estimated after 2011 when DKC 7374 BR was used for measured data. In some seasons the plots had erratic yields (plots of the same treatments recording very different yields), as reported in 1993 (Belay, Claassens et al., 2002), or the crop fails, reported in 2006 (Bello, 2008), which also contributes to inaccurately measured yields.

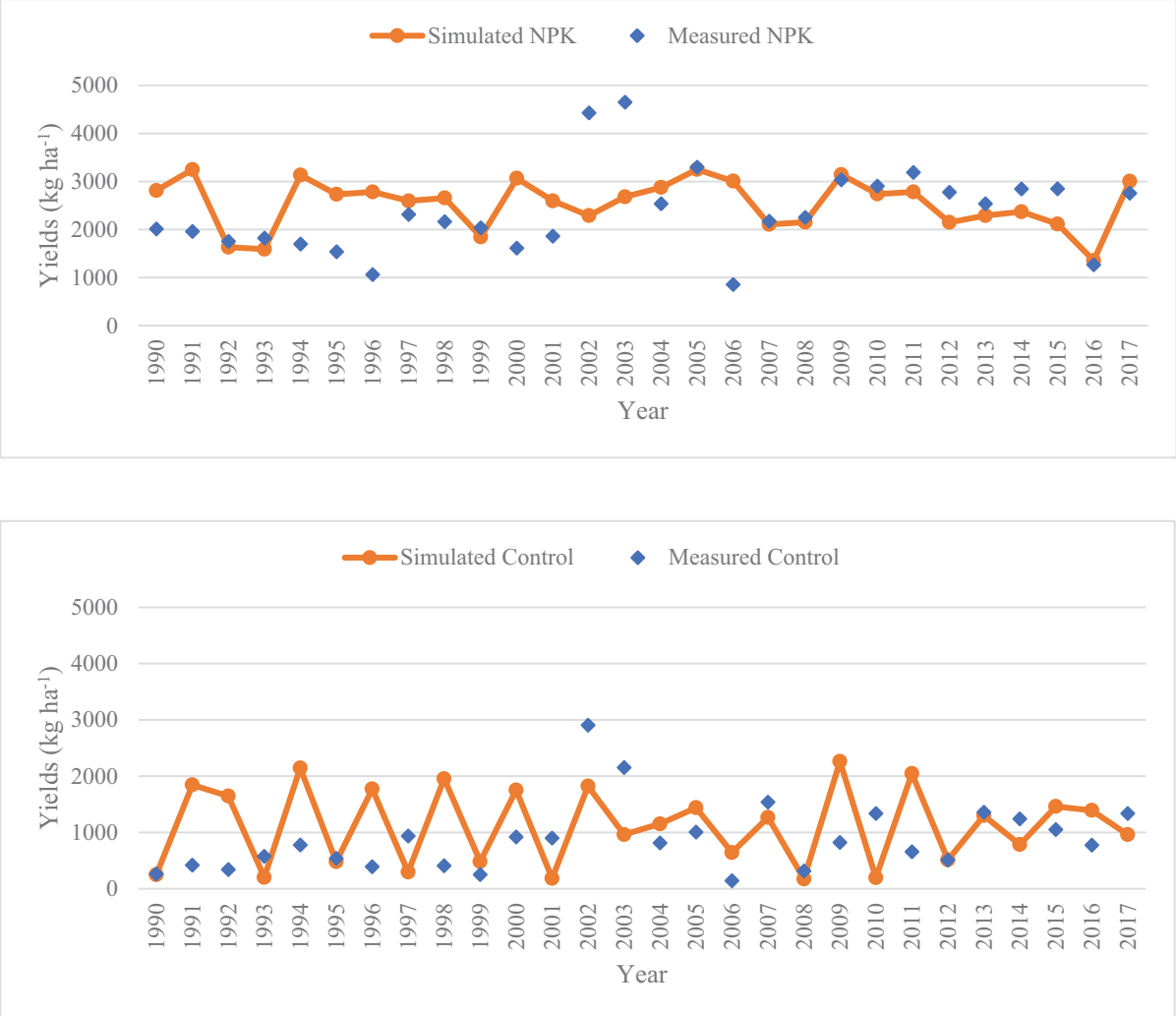

Figure 81: Measured and simulated maize grain yields for the NPK treatment and control treatments from 1990 to 2017

Despite MAE values being above 20% for both treatments, the NPK treatment was still judged to be generally well simulated (Table **52**). There was a low correlation on both treatments indicating a poor linear relationship between measured and simulated yields. This can be a result of outliers or inconsistent overestimations and underestimations deflating the linear relationship between the measured and simulated yields. These outliers can be caused by instances of high uncontrolled yield variance in some years due to possible inaccurate measurements.

Table 52: Statistical evaluation of measured and simulated yields in the control and NPK treatments

Treatment	R^2	D	MAE (%)	RMSE (kg ha^{-1})
NPK	0.1	0.44	30.0	991.5
Control	0.02	0.45	79.9	885.4

11.3.2 Long-term fertilization effects on soil organic matter content

Comparisons between observed and simulated SOM content of fertilized treatments are shown in Figure 82. Observed and simulated results showed a declining trend in SOM for both treatments, although the magnitude of SOM decline differed between the treatments. The results showed a higher long-term SOM loss in the control than NPK treatment. Similar results were reported by Luo, Wang et al. (2011), where there was a continuous C decline in fertilized wheat, though the N fertilization proved to slow down the decline. This demonstrates the beneficial effects of fertilization to SOM levels. Higher organic residue returns in fertilized plots in the trial were reported by Belay, Claassens et al. (2002), but it was also highlighted that the organic crop residues were mineralized at faster rates due to inorganic N applications enhancing the decomposition process. The simulated SOM (top 0.6 m) declined from 1.24% in 1950, to 0.96% and 0.86% in 2017 in the NPK and control treatments, respectively. Measured SOM data could only be sourced from a few previous publications due to less focus or omission of this variable in previous studies, with more focus directed to yields. Measured data also indicated the declining trend of SOM, with more decline in the control than the NPK treatment. The SOM has not yet reached the equilibrium stage after 66 years as shown by measured and simulated data.

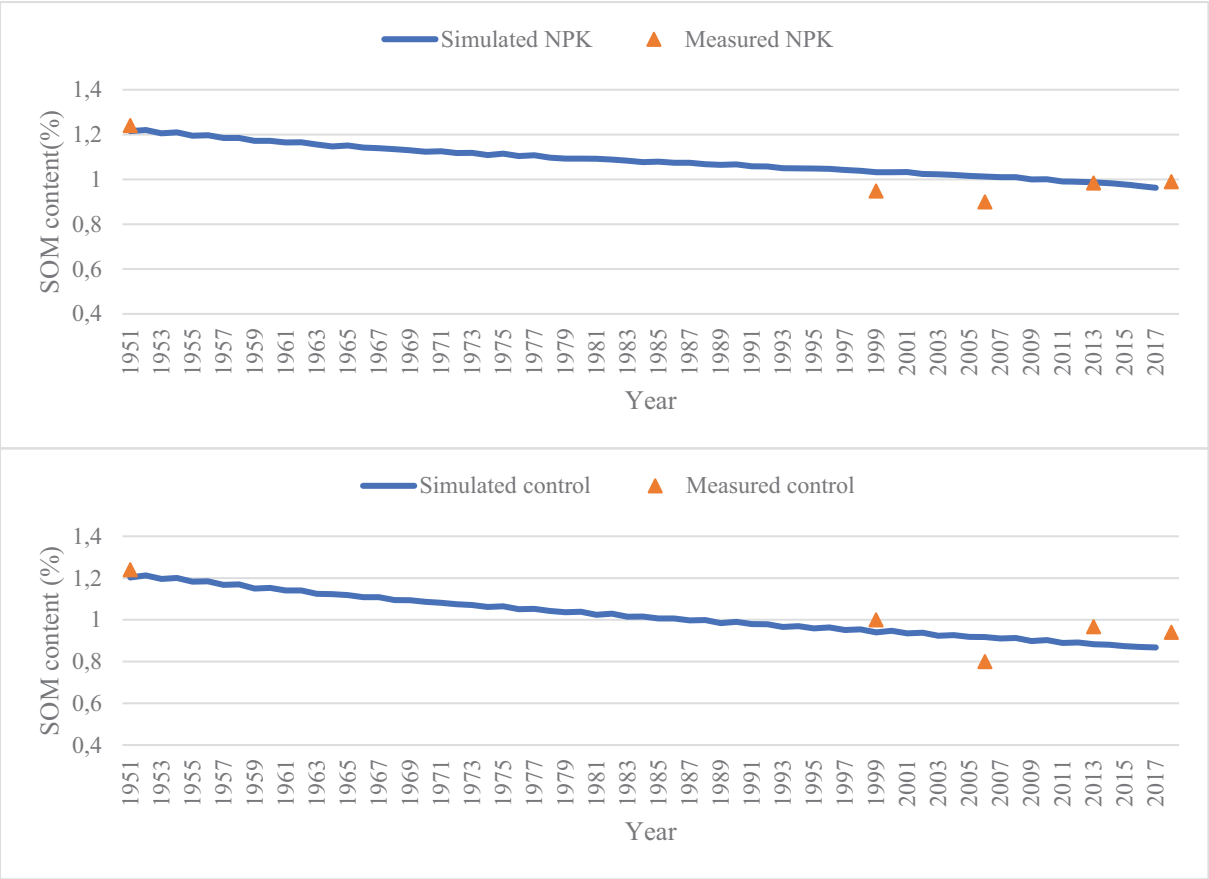

Figure 82: Observed and simulated soil organic matter content for the control and NPK treatments (soil depths measured to: 1950 = 0.6 m, 1999 = 0.2 m, 2006 = 0.2 m, 2013 = 0.6 m, 2017 = 0.6 m)

A statistical summary of the comparison between observed and simulated SOM is shown in Table 53. Despite simulated data being taken from the top 0.6 m and measured data from various soil depths, statistical criteria for a good simulation were met in terms of overall error (MAE). The D and R^2 did not meet the statistical criteria but were all above 0.62. The control was well estimated compared to the NPK treatment as indicated by higher R^2, D and lower MAE and RMSE.

Table 53: Statistical evaluation of measured and simulated soil organic matter content in the control and NPK treatments

Treatment	R^2	D	MAE (%)	RMSE (%)
NPK	0.62	0.87	6.5	0.10
Control	0.68	0.90	5.3	0.09

11.3.3 Long-term fertilization effects on deep drainage and nitrogen leaching.

Deep drainage volumes differed between the treatments, which influenced the amount of N lost through leaching. The control had a higher volume of water lost through drainage over the simulated period of 66 years (Figure 83). By 2016, the control was estimated to have lost a cumulative 11 984 mm of water compared to 7 110 mm in the NPK treatment. This was a result of fertilization promoting crop growth and water and increasing. These results were consistent with findings by Thorburn, Meier et al. (2005) who observed that poor crop growth due to low N fertilization reduced soil water uptake, resulting to increased water loss through drainage.

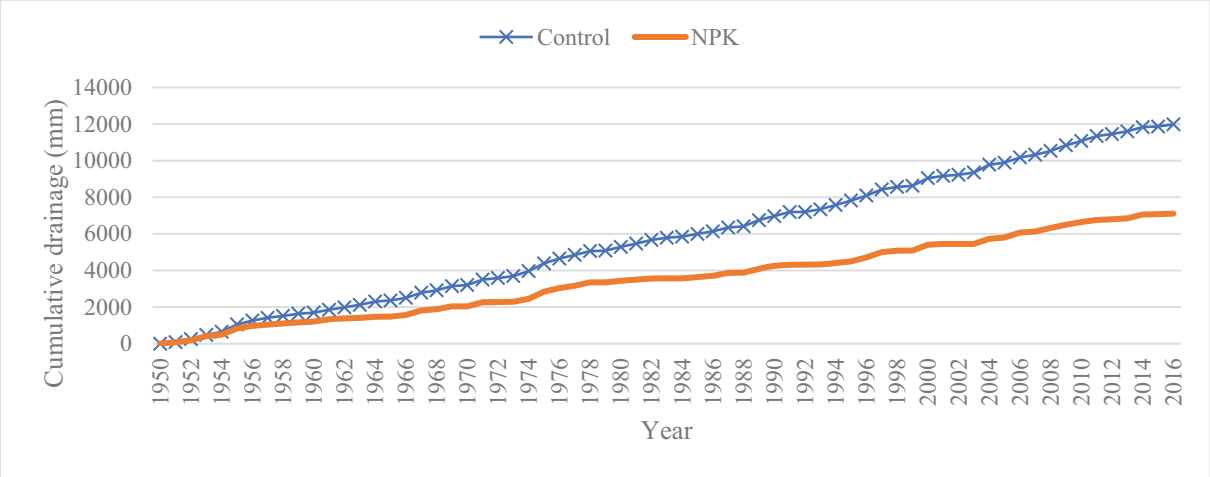

Figure 83: Cumulative deep drainage for the 1950 to 2016 simulation period for the control and NPK treatments

Nitrate leaching was highly between seasons and years closely linked to rainfall and was higher in the NPK treatment than the control due to the application of N fertilizer. In the 1950s, there was a relatively high loss of NO_3^- through leaching in both the control and NPK treatments, with the highest leaching recorded in 1953. The control had relatively low amounts of NO_3^- leaching, with some years with low rainfall even having no leaching estimated (Figure 84).

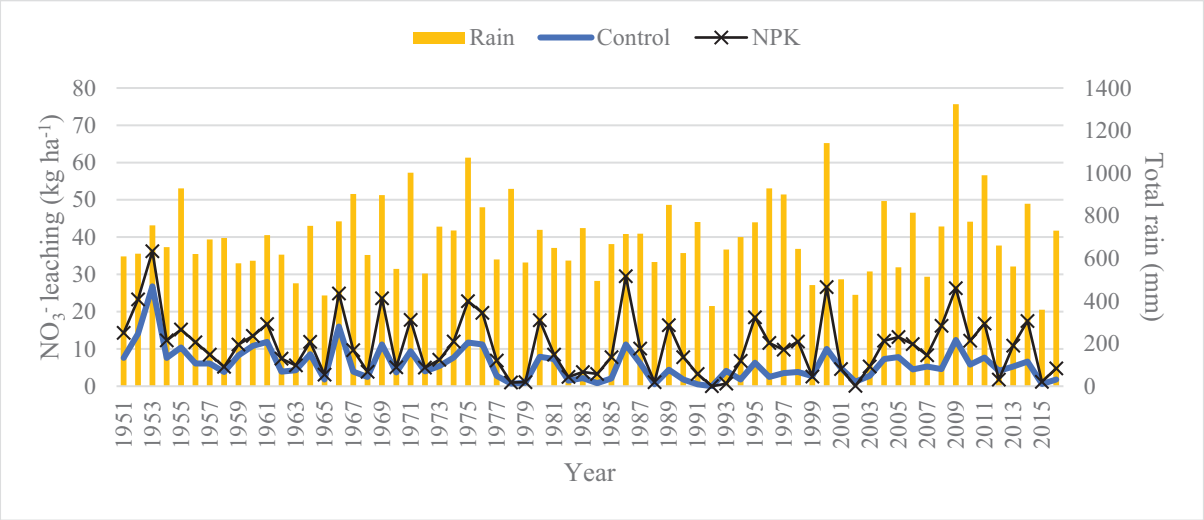

Figure 84: Total rainfall and estimated nitrate-nitrogen (NO3-N) leaching per year for the control and NPK treatment

Even when there was significant drainage in the control treatment, it did not necessarily result in high NO_3^- leaching (Figure 85). Since 1950, an estimated 4022 kg ha^{-1} N was estimated to have been lost through leaching in the NPK treatment, and this estimation is over 10 times higher than in control (387 kg ha^{-1}). This NO_3^- loss, however, cannot only be attributed to fertilizer N input, as a considerable amount would have come from SOM mineralization. This was the source of N leached from the control treatment which eventually reached a cumulative value of 387 kg ha^{-1} N over 66 years.

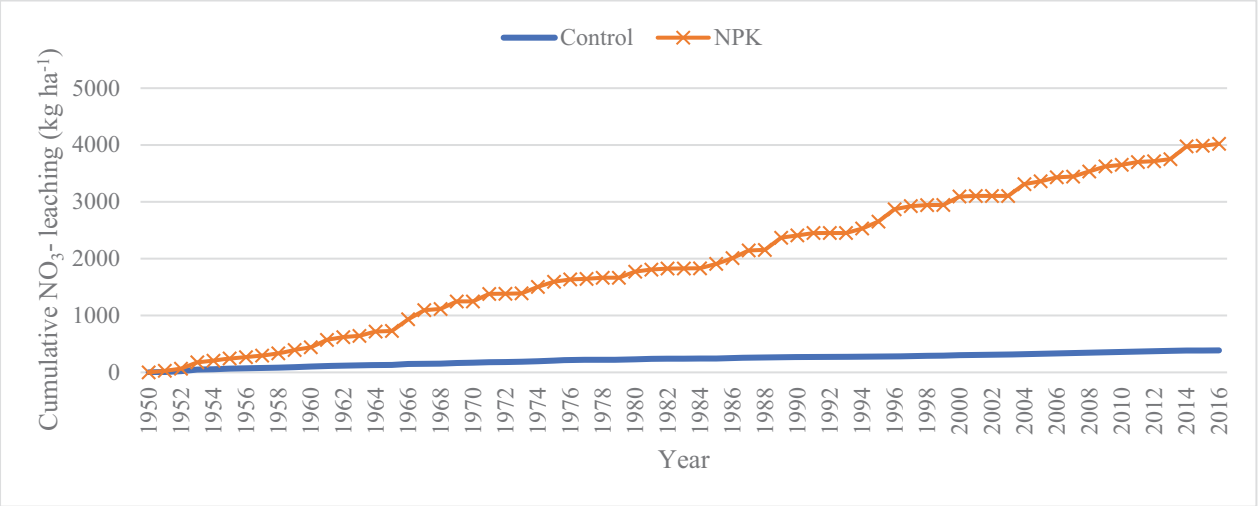

Figure 85: Cumulative nitrate-nitrogen (NO_3-N) leaching and deep drainage for the 1950 to 2016 simulation period of control and NPK treatments

11.3.4 Manure application scenario

11.3.4.1 Simulating long-term manure application effects on yields

Manure application was estimated to be beneficial to yields as indicated by the comparisons in Figure **86**. The yield differences were low in fertilized treatments, though NPK + manure treatment had slightly higher yields than NPK treatments with average yields of 2 778 kg ha^{-1} and 2 679 kg ha^{-1}, respectively, over 66 years, indicating low yield benefits of manure application over fertilized treatments in term of final yields in this long-term scenario. In unfertilized treatments, the final yield data of the 66-year simulation period was observed to be higher and more consistent for the manure treatment than control. The manure treatment achieved an average yield of 2 555 kg ha^{-1} compared to 1 463 kg ha^{-1} for the control, indicating significant yield benefits of manure application compared to the unfertilized control.

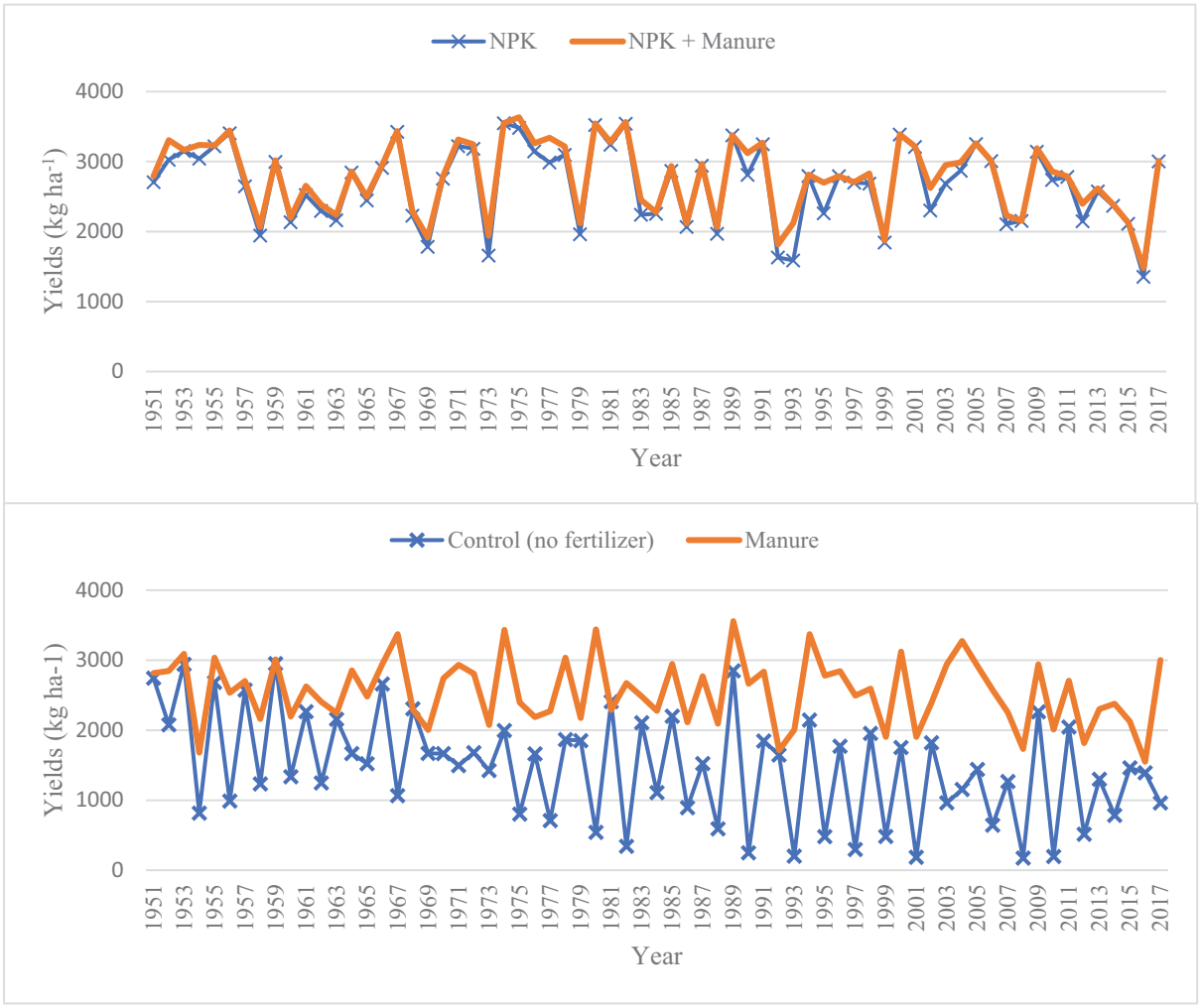

Figure 86: Seasonal yields over a 66 year simulation period for the NPK fertilizer, manure and control (zero fertilizer) scenarios

11.3.4.2 Simulating long-term manure application effects on soil quality

Soil organic matter

Manure application proved to be beneficial in maintaining SOM levels (Figure 87). The control treatment had the highest SOM loss, from 1.24% in 1950 to 0.87% in 2017 and the NPK and manure treatment

had the lowest decline having predicted to have 1.07% in 2017. The manure treatment had higher SOM than NPK treatment after 66 years, indicating that manure addition is beneficial to SOM content than fertilizer application. The addition of manure could not, however, maintain SOM at initial levels.

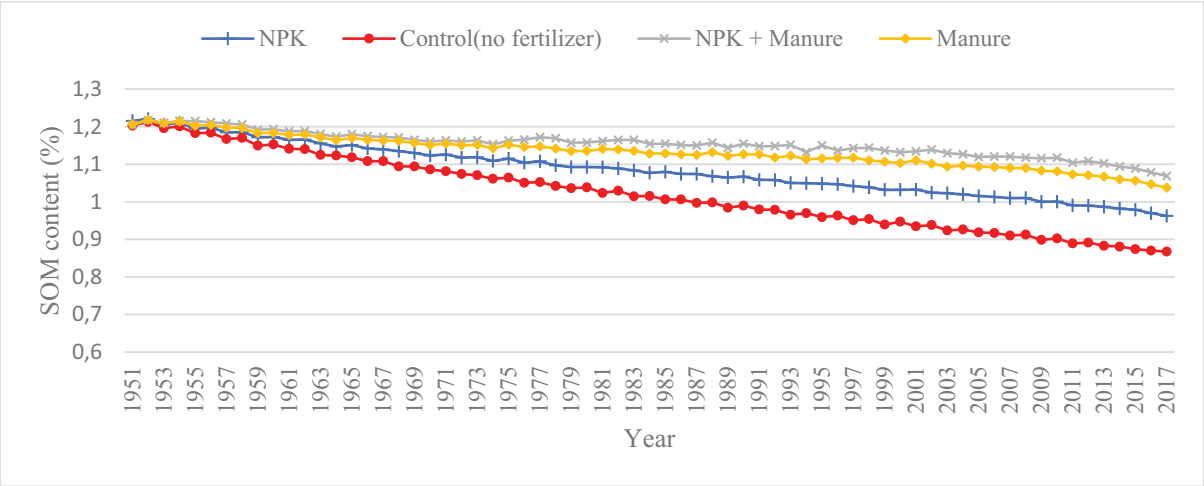

Figure 87: Seasonal soil organic matter content over a 66 year simulation period for the NPK fertilizer, manure and control (zero fertilizer) scenarios

Deep drainage

The simulation showed that unfertilized treatments (control and manure) had the highest volume of water lost through drainage over the 66 years simulation period (Figure 88). NPK treatment was estimated to have lost a cumulative 7 110 mm and NPK + manure lost 10 498 mm. This indicates that manure application increases deep drainage. This was further shown by manure treatment estimated to have lost a higher volume of water (12 332 mm) than the control (11 984 mm). This indicates that the beneficial effects of manure application on reducing surface crusting, hence reduced runoff thus increasing drainage.

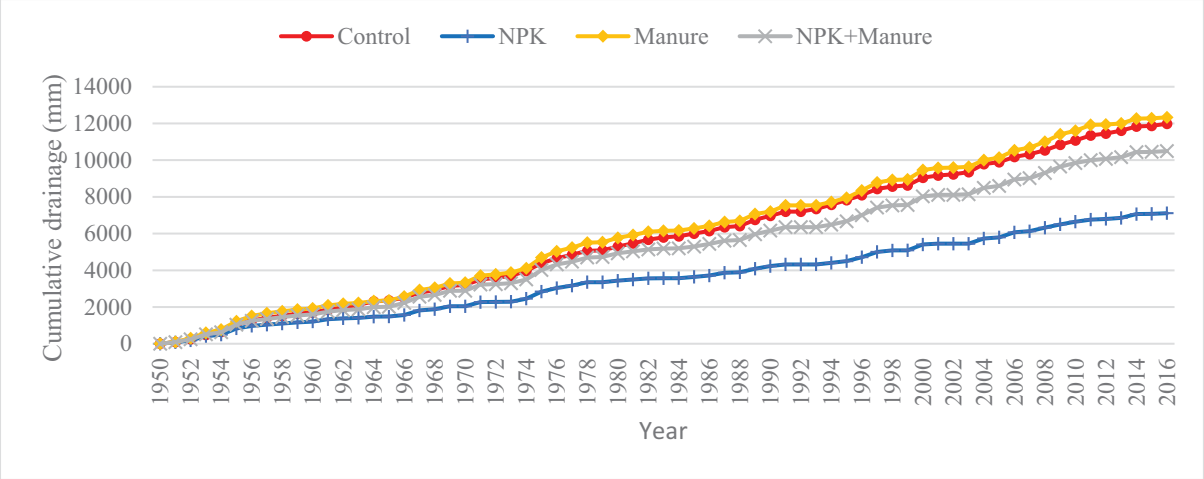

Figure 88: Cumulative deep drainage over a 66 year simulation period for the NPK fertilizer, manure and control (zero fertilizer) scenarios

Nitrate Leaching

Manure application was estimated to increase NO_3^- leaching due to the additional N mineralized from the applied manure (Figure 89). The NPK and manure treatment was estimated to have lost 7 312 kg ha^{-1} N since 1950. This indicated that as much as manure application can be beneficial to crop production, it can also increase N leaching if N is applied at rates greater than the crop demands.

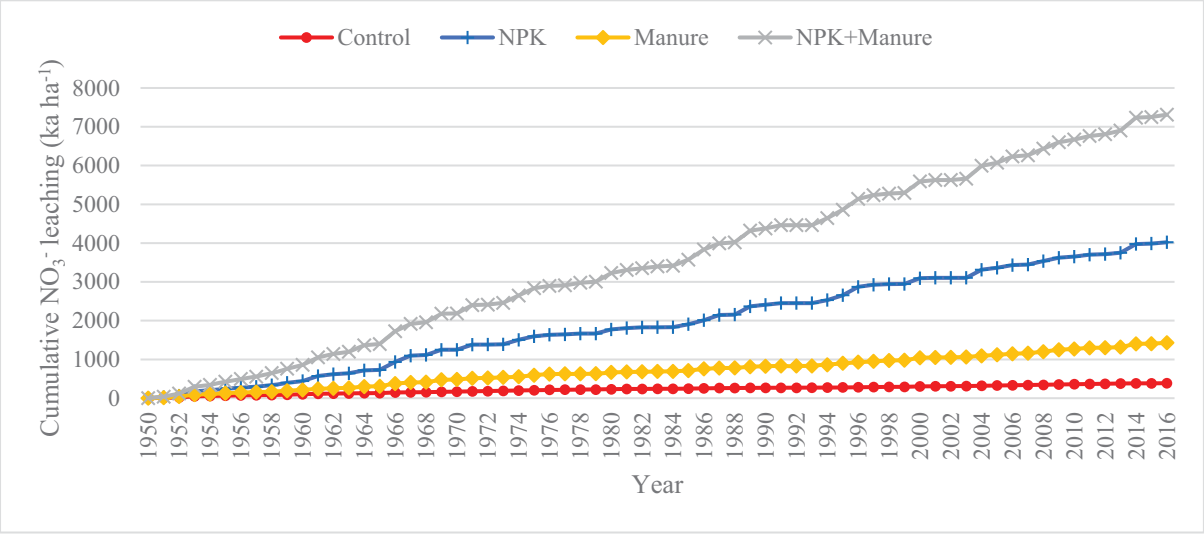

Figure 89: Simulated cumulative nitrate-nitrogen (NO3-N) leaching over a 66 year simulation period for the NPK fertilizer, manure and control (zero fertilizer) scenarios

11.4 Discussion

11.4.1 Maize yields

Yields of maize over the long-term maize are not easy to simulate. This was shown by seasonal yield variations in both treatments that proved to be difficult to predict. These variations can be brought about by extreme short-term duration environmental conditions such as high temperatures and moisture stress at critical periods, hail damage, high winds and possible attacks from pests, diseases or birds on the field influencing measured yields that the model did not consider. A similar study on long-term maize simulation also considered extreme short duration weather events not considered by the model the reason behind imprecise long-term maize simulation (Liu, Wang et al., 2010). Planting date is known to influence maize yield (Saseendran, Ma et al., 2005; Soler, Sentelhas et al., 2007), and in this simulation, the planting dates over the years were not known but only based on a management rule that initiated planting in a pre-defined planting window [see Maskeo (submitted)]. In reality, planting date can also be influenced by factors other than weather, for example, the availability of planting equipment and labour. For the NPK treatment, yield overestimations between 1990 and 2001 may be a result of cultivars planted in that period not being as vigorous as calibrated DKC 7374 BR which was used for the whole simulation. Another possible reason for erroneous yield estimation for the control would be the model reporting N and moisture limited yields yet in the measured yields there is also the contribution of the other factors not considered by the model. Over the years, yield measurements were done by different people, and this could possibly be another source of error in measured yields. All these factors show that in most cases the poor statistical results can be a result of inconsistencies in measured data rather than poor model performance.

11.4.2 Soil organic matter

Soil organic matter content was generally well simulated by APSIM as it proved to be robust by being able to estimate similar trends with measured data. In the simulation, the slow steady decline from the start of the simulation might be an indication that the decomposition of SOM of an uncultivated site is underestimated. It has been extensively reported that soil cultivation results to SOM loss in cropping systems, with high initial SOM loss when natural vegetation is replaced with cropping systems (Dominy, Haynes et al., 2002; Luo, Wang et al., 2010; Swanepoel, Van der Laan et al., 2016). Changes in SOM content are influenced by organic inputs and the rate of decomposition, which is highly influenced by management practices. In virgin soils, SOM is normally at equilibrium, which is a level where humus is formed and decomposed at the same rate. This equilibrium is then disturbed by human activities such as cultivation, which creates favourable conditions for oxidation that results in SOM decline and the ultimate decrease in plant nutrient reserves such as N, P and S which are integral parts of organic matter. Higher SOM in NPK than in the control treatment is attributed to higher C input as a result of fertilization increasing biomass production in NPK treatment. The decline in control is a result of soil cultivation and low C inputs from residues, yet for NPK, soil cultivation and N application can lead to high mineralization of organic inputs despite high C inputs. Belay, Claassens et al. (2002) reported a higher mineralization rate of organic inputs in NPK plots due to N fertilization enhancing the

decomposition process by increasing N availability required by microbes hence increasing their activity. As yields were not always accurately simulated, it is possible that biomass was not always accurately simulated, and this might have influenced the SOM level estimations.

11.4.3 Nitrate leaching

Higher cumulative drainage in the control treatment did not subsequently result in higher N leaching. Nitrate leaching is highly dependent on the amount of percolating water and the NO_3^- concentrations of the water moving out of the root zone. In rainfed agricultural systems, rainfall distribution and intensity can influence the amount of water lost through drainage. This is coupled with crop water use, where better crop growth in fertilized treatments increases ET, thus reducing deep drainage. In the simulation, fertilization was done at planting and this has the potential to increase N leaching in seasons with high rainfall events early in the season. Nitrates mineralized from SOM would have increased NO_3^- concentrations in percolating water. The contribution of mineralized N from the natural breakdown of SOM to overall soil N is often not accounted for in fertilizer recommendations used by farmers for different crops, and this can have a significant contribution to excess N loss in cropping systems. Nitrates are anions in nature and these characteristics make then not to be adsorbed in soils with a high cation exchange capacity (CEC). This makes it easy for these NO_3^- to be carried with percolating water making them more susceptible to leaching (Cameron, Di et al., 2013). In this simulation, fertilizer application was done only at planting, therefore, a split fertilizer application at critical growth stages of high N demand can reduce NO_3^- and increase nitrogen use efficiency. Planting a cover crop in the winter fallow period that can use NO_3^- mineralized during the winter season can also reduce the loss of NO_3^- through leaching in the event of heavy rains before the maize crop is planted.

11.4.4 Manure application scenario

With soil water and nitrogen often being the most limiting factor in crop production, additional nutrients received from manure are beneficial to biomass production, thus contributing to increased yields. Improved soil physical, chemical and biological properties following manure application allows roots to extend deeper into the soil profile, which increases water and nutrient access, thus contributing to higher yields. This is clearly demonstrated by the control and manure treatment, where both treatments receive equal amounts of moisture from rainfall and the yield differences can only be a result of the beneficial effects of manure application on soil properties. Manure can improve soil porosity hence increasing the water storage capacity, thus reducing potential water stress at critical crop growth stages that can negatively influence yields. This can explain the higher yield variations in the control compared to the manure treatment. In the NPK and NPK + manure treatments, the yields over the years are almost the same, with only small annual yield differences in some seasons. This can be brought about by a possible higher soil moisture content in NPK + manure treatment reducing moisture stress in seasons with poor rainfall distribution thus beneficial to the yields.

The scenario indicated that manure application can be a consistent method of slowing down long-term SOM decline. The direct C inputs by manure application as well as increased net biomass production are the reasons behind higher SOM levels in manured plots, and this was clearly shown in the control

versus manure plots. The simulated decline in SOM content across all treatments can be a result of organic C applied with manure and residue retention unable to compensate for soil C lost due to the conversion of natural soils to cultivated land or via different pathways over the season, but manure application proved to significantly lower the decline. Without manure application, the stable organic C declined resulting in reductions of C concentrations in the soil. Ren, Wang et al. (2014) reported that the ability of manure to enhance SOM depends on its C:N ratio, with a higher ratio enhancing SOM by reducing the mineralization of labile compounds.

Despite the beneficial effects of manure application on yields and SOM, this practice was shown to increase deep drainage. The depth of soil water fluctuates over time, with periods of rapid increase after rainfall or irrigation followed by periods of slow decline through evapotranspiration. However, if the rate of water loss is less than the amounts added during the same period, deep drainage occurs. Manure application improves soil structure and reduce surface crusting, hence decreasing runoff, and increasing infiltration rates allowing more water storage. The high drainage estimated in manure application treatments can be a result of a lower soil water deficit in manure treatments compared to other treatments between two periods of rainfall or irrigation events. The high infiltration rates can allow more water to fill remaining water deficit to saturation and excess water lost through drainage. In the NPK and control treatments without manure application, the water deficit might be larger than manure treatments and able to accommodate more water additions through rainfall or irrigation thus reducing drainage.

Deep drainage and NO_3^- concentration in the soil solution are the main drivers of NO_3^- leaching. Manure application can bring a lot of N into the plant/soil system depending on the type of manure used. For this reason, manure + NPK treatment was estimated to have the highest NO_3^- leaching. This indicates that manure application can be crucial in long-term sustainable crop production, but inappropriate use of manure can induce NO_3^- leaching in cropping systems. The amount of N in the soil solution can be controlled by mineralization and immobilization of N in SOC. This makes SOC improvement important in regulating N turnover due to the beneficial effects it has on increasing N immobilization, thus reducing N losses. For stable and sustainable crop production, rational fertilizer and manure applications rates that will account for mineralized N has to be identified to reduce leaching.

11.5 Conclusion

The long-term sustainability of agronomic management practices can be evaluated using the APSIM model for maize. Based on the results, long-term inorganic fertilization negatively affects soil quality. Model calibration, with sufficient data set, is essential for long-term simulations to increase the precision in estimating long-term trends. Long-term yields and SOM were not easy to accurately predict, but the model was useful in giving insights and a more representative estimate of long-term yields and SOM trends. Inorganic fertilization affected deep drainage and overall NO_3^- leaching, indicating the importance of carefully applying nutrients that the crops will remove to improve sustainable agricultural

production. Manure application can be beneficial to long-term productivity and maintenance of soil quality, but careful N management strategies are necessary to reduce N leaching.

11.6 References

BEZA, S.A., ASSEN, M.A. (2016) Soil carbon and nitrogen changes under a long period of sugarcane monoculture in the semi-arid East African Rift Valley, Ethiopia. *Journal of Arid Environments*, 132: 34-41.

BLAIR, N. (2000) Impact of cultivation and sugar-cane green trash management on carbon fractions and aggregate stability for a Chromic Luvisol in Queensland, Australia. *Soil and Tillage Research*, 55: 183-191.

BOOTE, K.J., JONES, J.W., PICKERING, N.B. (1996) Potential uses and limitations of crop models. *Agronomy Journal*, 88: 704-716.

CAMERON, K., DI, H.J., MOIR, J. (2013) Nitrogen losses from the soil/plant system: a review. *Annals of applied biology*, 162: 145-173.

CARBERRY, P., ABRECHT, D. (1991) Tailoring crop models to the semiarid tropics.

CHEEROO-NAYAMUTH, F., ROBERTSON, M., WEGENER, M., NAYAMUTH, A. (2000) Using a simulation model to assess potential and attainable sugar cane yield in Mauritius. *Field crops research*, 66: 225-243.

CHEONG, L.N., TEELUCK, M. (2016) The practice of green cane trash blanketing in the irrigated zone of Mauritius: effects on soil moisture and water use efficiency of sugarcane. *Sugar tech*, 18: 124-133.

DOMINY, C., HAYNES, R., VAN ANTWERPEN, R. (2002) Loss of soil organic matter and related soil properties under long-term sugarcane production on two contrasting soils. *Biology and Fertility of Soils*, 36: 350-356.

FSSA (Fertilizer Society of South Africa) (2007) Fertilizer handbook. The Fertilizer Society of South Africa. Lynwood Ridge, Pretoria.

GRAHAM, M., HAYNES, R., MEYER, J. (2002) Soil organic matter content and quality: effects of fertilizer applications, burning and trash retention on a long-term sugarcane experiment in South Africa. *Soil biology and biochemistry*, 34: 93-102.

JONES, M., SINGELS, A. (2015) Analysing yield trends in the South African sugar industry. *Agricultural systems*, 141: 24-35.

KEATING, B., ROBERTSON, M., MUCHOW, R., HUTH, N. (1999) Modelling sugarcane production systems I. Development and performance of the sugarcane module. *Field crops research*, 61: 253-271.

LIU, Y., WANG, E., YANG, X., WANG, J. (2010) Contributions of climatic and crop varietal changes to crop production in the North China Plain, since 1980s. *Global Change Biology*, 16: 2287-2299.

LUO, Z., WANG, E., SUN, O.J,, SMITH, C.J., PROBERT, M.E. (2011) Modeling long-term soil carbon dynamics and sequestration potential in semi-arid agro-ecosystems. *Agricultural and forest meteorology*, 151: 1529-1544.

MEYER, J., SCHUMANN, A., WOOD, R., NIXON, D., VAN DEN BERG, M. (2007) Recent advances to improve nitrogen use efficiency of sugarcane in the South African sugar industry. 238-246.

MEYER, J., VAN ANTWERPEN, R. (2001) Soil degradation as a factor in yield decline in the South African sugar industry *Proc Int Soc Sugar Cane Technol*, 26:8-15.

MTHIMKHULU, S., MILES, N., VAN ANTWERPEN, R., ELEPHANT, D. (2018) Effect of residue and fertiliser management on soil fertility in a long-term sugarcane trial in South Africa. *South African Journal of Plant and Soil*: 1-9.

MTHIMKHULU, S., PODWOJEWSKI, P., HUGHES, J., TITSHALLA, L. & VAN ANTWERPEN, R. (2016) The effect of 72 years of sugarcane residues and fertilizer management on soil physico-chemical properties. Agriculture, Ecosystems and Environment 225: 54-61.

OGLE, S.M., BREID, T.F.J., PAUSTIAN, K. (2005) Agricultural management impacts on soil organic carbon storage under moist and dry climatic conditions of temperate and tropical regions. *Biogeochemistry*, 72: 87-121.

PROBERT, M., DIMES, J., KEATING, B., DALAL, R., STRONG, W. (1998) APSIM's water and nitrogen modules and simulation of the dynamics of water and nitrogen in fallow systems. *Agricultural systems*, 56: 1-28.

ROBERTSON, F.A., THORBURN, P.J. (2007) Management of sugarcane harvest residues: consequences for soil carbon and nitrogen. *Soil Research*, 45: 13-23.

SHAND, C. (2007) Plant Nutrition for Food Security. A Guide for Integrated Nutrient Management. By RN Roy, A. Finck, GJ Blair and HLS Tandon. Rome: Food and Agriculture Organization of the United Nations (2006), pp. 348, US $70.00. ISBN 92-5-105490-8. *Experimental Agriculture*, 43: 132-132.

SINGELS, A., BEZUIDENHOUT, C. (2002) A new method of simulating dry matter partitioning in the Canegro sugarcane model. *Field crops research*, 78: 151-164.

SOIL CLASSIFICATION WORKING GROUP (1991) Soil classification: A taxanomic system of South Africa. Department of Agriculture and Development, Pretoria, South Africa

SWANEPOEL, C., VAN DER LAAN, M., WEEPENER, H., DU PREEZ, C., ANNANDALE, J. (2016) Review and meta-analysis of organic matter in cultivated soils in southern Africa. *Nutrient Cycling in Agroecosystems*, 104: 107-123.

THORBURN, P., VAN ANTWERPEN, R., MEYER, J., BEZUIDENHOUT, C. The impact of trash management on soil carbon and nitrogen: I Modelling long-term experimental results in the South African sugar industry*2002*. pp. 260-268.

THORBURN, P.J., MEIER, E.A., COLLINS, K., ROBERTSON, F.A. (2012) Changes in soil carbon sequestration, fractionation and soil fertility in response to sugarcane residue retention are site-specific. *Soil and Tillage Research*, 120: 99-111.

THORBURN, P.J., PROBERT, M.E., ROBERTSON, F.A. (2001) Modelling decomposition of sugar cane surface residues with APSIM-Residue. *Field crops research*, 70: 223-232.

VALLIS, I., PARTON, W., KEATING, B., WOOD, A. (1996) Simulation of the effects of trash and N fertilizer management on soil organic matter levels and yields of sugarcane. *Soil and Tillage Research*, 38: 115-132.

VAN ANTWERPEN, R., MEYER, J., TURNER, P. (2001) The effects of cane trash on yield and nutrition from the long-term field trial at Mount Edgecombe. *Proc S Afr Sug Technol Ass*, 75: 235-241.

VAN ANTWERPEN, R., THORBURN, P., HORAN, H., MEYER, J., BEZUIDENHOUT, C. (2002) The impact of trashing on soil carbon and nitrogen: ii: Implications for sugarcane production in South Africa. *Proc S Afr Sug Technol Ass*, 76: 269-280.

VAN DER LAAN, M., JUMMAN, A., PERRET, S. (2015) Environmental benefits of improved water and nitrogen management in irrigated sugar cane: A combined crop modelling and life cycle assessment approach. *Irrigation and drainage*, 64: 241-252.

WEST, T.O., POST, W.M. (2002) Soil organic carbon sequestration rates by tillage and crop rotation. *Soil Science Society of America Journal*, 66: 1930-1946.

WIEDENFELD, R.P. (1995) Effects of irrigation and N fertilizer application on sugarcane yield and quality. *Field Crops Research*, 43: 101-108.

12 USING CLIMATE FORECAST SYSTEM REANALYSIS (CFSR) DATA AS WEATHER INPUT TO SWAT IN A DATA POOR CATCHMENT

N. Mararakanye, J.J. Le Roux and A.C. Franke
Department of Soil, Crop and Climate Sciences, University of the Free State, Private Bag 339
Bloemfontein 9300, South Africa

12.1 Introduction

Globally, water covers 70% of the land resources, but yet freshwater is one of the scarcest resources on earth. Only a small fraction of about 2.5% of the total water on earth is freshwater and more than 97% is saltwater (Uitto, 2001). Even worse is that the supply of freshwater resource is unevenly distributed over time and space. The Southern African region is among the lowest runoff producing areas in the world. In South Africa (SA), water resource problems are compounded by the progressive increase in loads of harmful micro-organisms, nutrients, salts, metal ions, toxic chemicals, radionuclides and suspended sediments entering the country's river systems and reservoirs (Oberholster and Ashton, 2008). Predictions do not look good either, with reports estimating that by 2030, the country's freshwater resources will be fully depleted and unable to meet the needs of people, demands of agriculture, industry and conservational and ecosystem uses (Oberholster and Ashton, 2008; Ashton, 2010). It is therefore critical to manage this precious and finite resource.

Hydrological models are popular tools for efficient and effective water resource assessment and management at catchment scale (Srinivasan et al., 2010; Molina-Navarro et al., 2017). However, one of the challenges faced by hydrological modellers in Eastern and Southern Africa is the scarcity of quality weather data. This is largely because of gaps or missing values in weather records, low density of weather stations and short time span of weather observations. These limit the use of such data for long-term model simulations particularly in large catchments. Weather variables such as precipitation and temperatures are the key forcing variables in hydrologic modelling and have impact on various components of the water budget such as runoff, evaporation, and infiltration (Guo et al., 2004; Ji and Luo, 2013). Meanwhile, there is an increasing need for accurate and reliable weather products to overcome the problem of rain gauge observations. Satellite-based weather estimates were introduced as a way of augmenting conventional ground-based weather data for hydrological models and weather forecasting (Levizzani et al., 2001).

Satellite-based weather estimates are spatially and temporally continuous data that seamlessly capture weather variability across the globe (Abera et al., 2016). Their algorithms are based on a wide variety of infrared (IR) and combined visible (VIS) and IR radiances where precipitation is inferred from cloud top structure (Toté et al., 2015). Some of the global products using VIS and IR sensors include the Precipitation Estimation from Remotely Sensed Information using Artificial Neural Networks – Climate Data Record (PERSIANN-CDR) (Ashouri et al., 2015), and rainfall estimation from soil moisture using SM2RAIN algorithm (Brocca et al*.,* 2013). The use of passive and active microwave sensors with the ability to penetrate the cloud microphysical features is one of the major developments in the field of

meteorology. In this, precipitation is measured by scattering due to the large ice particles present in the clouds (Dembélé and Zwart, 2016). Examples of these products include the Tropical Rainfall Measuring Mission-Multisatellite Precipitation Analysis (TRMM-TMPA) (Huffman et al., 2007), the Climate Prediction Centre Morphing Technique (CMORPH) (Joyce et al., 2004) and the National Centres for Environmental Prediction (NCEP) Climate Forecast System Reanalysis (CFSR) (Saha et al., 2010a). Microwave sensors give more accurate estimates of weather variables than IR and VIS. Here, we chose CFSR because of its long-term data (i.e. 1979) availability, its public domain availability and its multiple weather variables data availability in SWAT format.

The CFSR is a suite of atmosphere, ocean, sea-ice and land models designed and executed in a coupled mode. The CFSR outputs are hourly generated by the NCEP Global Forecasts System (GFS) numerical weather prediction model. Atmospheric, ocean and sea-ice analysis is made every 6 h at 0000, 0600, 1200, and 1800 UTC, using a coupled 9-h guess forecast whereas land analysis is only made at 0000 UTC (Saha et al., 2010a). The GFS uses bias corrected radiance measurements from the National Oceanic and Atmospheric Administration (NOAA) polar-orbiting satellite which is directly assimilated into the system (Saha et al., 2010b). The NCEP CFSR was completed over a 36-year period from 1979 to mid-2014 and it will be extended as an operational, real time product into the future. The CFSR products are available at a high resolution of 0.25° near the equator, extending to 0.5° beyond the tropics. The CFSR provide detailed climate variables information including precipitation, wind, relative humidity and solar radiation. For details about the CFSR data assimilation methods, modelling components and coupling approaches, see Saha et al. (2010a).

Hydrological models are often used to gauge the performance of satellite-based weather estimates compared with the performance of observed weather stations data (Guo et al., 2004). Studies have shown that CFSR data is a viable alternative for use in hydrological models in case there is insufficient conventional weather gauge data. For example, Fuka et al. (2013) evaluated the utility of CFSR data versus the gauge weather data from two distinct hydro-climatic regions in the United States of America using the hydrological model Soil and Water Assessment Tool (SWAT). They found that CFSR data as weather input gave better simulation results than gauge weather data. Dile and Srinivasan (2014), however, found that the gauge weather data outperformed the CFSR data in a SWAT modelling study in the Upper Blue Nile catchment, Ethiopia. Nevertheless, their results for both models with different weather inputs were satisfactory, demonstrating that CFSR could be a valuable option in data scarce regions. On the contrary, Roth and Lemann (2016) found unsatisfactory performance of the SWAT model setup with CFSR data as weather input in the Ethiopian Highlands. Tolera et al. (2018) used the SWAT model to show that CFSR and gauge data gave a comparable simulated streamflow in an Ethiopian sub-catchment, while CFSR data performed better in another sub-catchment where gauge data was scarce. These studies demonstrate the variation of model performance using CFSR data from one place to the other. It is therefore necessary to assess the usefulness of the CFSR data in weather data scarce regions.

This study explores the utility of CFSR data for streamflow simulation in parts of the Lower Vaal River Catchment in SA, where irrigated arable cropping systems on sandy soils have been identified as potentially important sources of NPS agricultural nutrients pollution. This study involved (a) setting up SWAT models with CFSR weather data and with conventional gauge weather data, (b) a statistical performance evaluation of the SWAT models against the observed streamflow at multiple river gauge outlets, and (c) comparison of the relationships between rainfall estimates from CFSR data and rain gauge observations. A novelty of this study is the use of multiple river gauge outlets for performance evaluation. Usually, hydrologic models evaluation is conducted at the main catchment outlet. The problem with one catchment outlet evaluation is that models can have good performance measures at the main catchment outlet but poor performance measures at some internal sub-catchment outlets (Srinivasan et al., 2010). In this study, we also used multiple statistical metrics to avoid the weakness of individual statistic which is bias towards one type of error (Bennet et al., 2010). We used SWAT because it is regarded as one of the most effective continuous simulation models for estimating hydrological process at a variety of time and spatial scales with little or no calibration effort (Gassman *et al*., 2007; Srinivasan *et al*., 2010; Xiang et al., 2017). Calibration and validation of the SWAT model were outside the scope of this study.

12.2 Materials and methods

12.2.1 Study area

The study area is located in the lower reach of the Vaal River Catchment (Figure 90), the third longest river in SA. This includes the area downstream of Bloemhof dam until the main catchment outlet at Schmidts Drift Outspan farm, upstream of Douglas weir. It also includes the downstream catchment of the Harts River, a few kilometres south of the town of Taung, to the confluence with Vaal River. The total size of the study area is approximately 27 077 km^2. Numerous weirs within the study area serve to regulate water flow and the biggest of these include the Vaalharts and Spitskop dams.

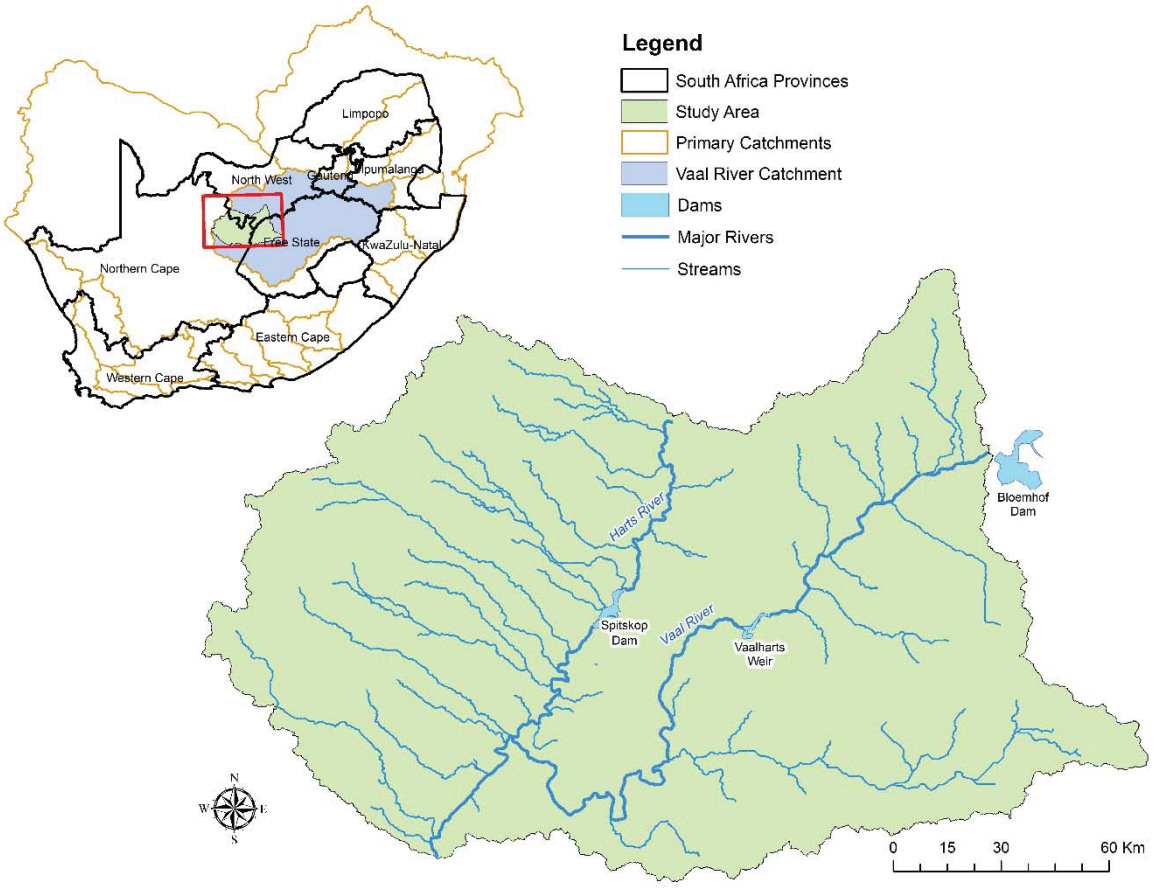

Figure 90: Location map of the study area in SA

The main underlying geological features of the region are shale and sandstone rocks. Several intrusive dykes and sills also occur as well as the Basalt, andesite, porphyry, tuff and clastic sediments (Council for Geosciences, 2007). The geology has given rise to sandy and freely drained red-yellow apedal soils with a depth exceeding 300 mm (Land Type Survey Staff, 1984). The study area mainly falls within the savannah biome. Vegetation types are predominantly thornveld, grasses and alluvial vegetation (Mucina and Rutherford, 2006). The climate is semi-arid, with the mean annual rainfall ranging from 200 to 600 mm, the majority of which is received in February (Schulze, 2010). The area is characterised by level plains with low to high hills or ridges in places (Land Type Survey Staff, 1984). Elevation ranges from 960 to 1840 m above sea level. The highest elevation points are along the catchment margin. Approximately 13% of the area is cultivated and roughly 8% of the cultivated fields are irrigated, usually through a centre pivot. Along the valley of Harts tributary is one of the oldest and largest irrigation system in South Africa known as the Vaalharts Irrigation Scheme (VIS). Irrigation water for the VIS is drawn from the Vaal River through a diversion of water into a network of open canals. Crops grown mainly include wheat, maize, cotton, grapes, potatoes, oats and lucerne, as well as a variety of fruits and nuts such as pecan nuts, peanuts, citrus and olives.

12.2.2 SWAT model

An ArcGIS-ArcView extension and graphical user input interface for SWAT version 2012, simply known as ArcSWAT 2012, was used for the simulation of flow. SWAT is a conceptual model developed by the United States Department of Agriculture-Agricultural Research Service (USDA-ARS) to simulate the impacts of land use, land management and climate change on water resource in large complex catchments (Arnold et al., 1998; 2012a). The application of SWAT has grown in regions outside the USA where the model was originally developed. SWAT operates on a daily time step, is capable of continuous simulation over long time periods, it is an open source and has been successfully applied in a wide range of scales and environmental conditions (Gassman et al., 2007; Arnold et al., 2012a; Xiang et al., 2017). SWAT allows for a simulation of a number of hydrological processes such as surface runoff, percolation, lateral flow and flow from shallow aquifers to streams, potential evapotranspiration, snowmelt, transmission losses from streams and water storage and losses from ponds (Neitsch et al., 2011). In all types of scenarios being modelled by SWAT, water balance is the driving force behind all processes.

12.2.2.1 SWAT data input

Data required to setup SWAT in this study included the Digital Elevation Model (DEM), land use, soil, slope, weather and streamflow gauge. We used the Shuttle Radar Topographic Mission (SRTM) 30 m resolution DEM acquired by the United States Geological Survey (USGS). The SRTM DEM is an open source data downloadable from the USGS Earth Explorer website (http://earthexplorer.usgs.gov/). The national land use/ cover data developed by GEOTERRAIMAGE (Pty) Ltd for the Department of Environmental Affairs (DEA) of South Africa was used. This land use / cover data was derived from 2013 to 2014 multi-seasonal Landsat 8 imagery using semi-automated modelling procedures and has a pixel resolution of 30 m (Geoterraimage, 2015). We append the cultivated field classes from field crop boundaries layer obtained from the Department of Agriculture, Forestry and Fisheries (DAFF). The field crop boundaries were digitised from SPOT 5 and 6 images of the period 2013 to 2015 (Crop Estimates Consortium, 2017a; 2017b, 2017c) and is considered to be a highly accurate representation of cultivated fields. Soil boundary layer was obtained from the 1: 250 000 scale landtype dataset of SA obtained from DAFF. Other soil physical and chemical properties required by SWAT were not readily available from the landtype data and were thus obtained from other sources or derived from criteria as illustrated in Table 54. Slope was directly extracted from the SRTM DEM and only a single slope class was used.

Table 54: Criteria used to assign soil physical and chemical properties required by SWAT

Soil properties	Soil properties definition	Information source or criteria used to assign the values
HYDGRP	Soil hydrologic group	The soil hydrological groups given in Schulze (2007) for each landtype was used.
SOL_ZMX	Maximum rooting depth of profile	Schulze (2007) depth of the topsoil layer (*DEPAHO*) for each landtype was used.
SOL_Z1	Depth to bottom of first soil layer (mm)	Schulze (2007) depth of the topsoil layer (*DEPAHO*) for each landtype was used.
SOL_BD1	Moist bulk density of first soil layer (Mg m^{-3})	Bulk density of the soil was obtained from Schulze (1995) approximations based on clay content as follows: 2-5% clay = 1.7, 6-15% clay = 1.6, 16-25% clay = 1.5, 26-32% clay = 1.4, 33-40% clay = 1.3
SOL_AWC1	Available water capacity of the first soil layer (mm H_2O mm^{-1} soil)	Schulze (2007) plant available water (*PAW*) given for each landtype was used.
SOL_K1	Saturated hydraulic conductivity of first soil layer (mm hr^{-1})	Estimation of SOL_K1 values was based on the soil texture classes of the dominant soil in the landtype, assuming 2.5% organic matter (OM) and no salinity, gravel or density adjustment (Saxton and Rawls, 2006) as follows: Sa = 108.1, L-Sa = 96.7, Sa-L = 50.3, L = 15.5, Si-L = 16.1, Si = 22, Sa-CL = 11.3, CL = 4.3, Si-C-L = 5.7, Si-C = 3.7, Sa-C = 1.4 and C = 1.1 Where Sa = sand; L = loam; Si = silt; C = clay.
SOL_CBN1	Organic carbon content of first soil layer (%)	Similar to Le Roux et al. (2015), an unpublished carbon map of SA derived from soil profile and landtype datasets was used to assign carbon values to each landtype in the study area.
CLAY1	Clay content of first soil layer (%)	The maximum value of clay percentages range given in a landtype memoir for the dominant soil was used (Land Type Survey Staff, 1984).
SILT1	Silt content of first soil layer (%)	Similar to Le Roux et al. (2015), silt content was assigned values between 10-22.5%, increasing with increase in clay as follows: percentage of landtype with <= 6% clay = 10% silt; 6.1-15% clay = 15% silt; 15.1-25% clay = 17.5% silt; 25.1-35% clay = 20% silt; 35.1-55% clay = 22.5% silt.

Soil properties	Soil properties definition	Information source or criteria used to assign the values
SAND1	Sand content of first soil layer (%)	Similar to Le Roux et al. (2015), sand content was estimated as follows: Sand = 100% – (%clay + %silt + %rock + %carbon).
ROCK1	Rock content of first soil layer (%)	The agricultural restriction/rock (MB) classes for each landtype was as follows: MB0=0%; MB1=20%; MB2=50%; MB3=20%; MB4=100% (no soil).
SOL_ALB1	Moist soil albedo	Moist soil albedo was assigned to the landtype based on texture of the dominant soil as follows: Sands = 0.25; clays = 0.7; remaining textures = 0.5 (Le Roux et al., 2015).
USLE_K1	USLE equation soil erodibility (K) factor	Erodibility was estimated using the Revised Universal Soil Loss Equation (RUSLE) (Le Roux et al., 2008).

Conventional weather gauge stations data including daily rainfall, temperature, wind speed, solar radiation and relative humidity were obtained from the Agricultural Research Council (ARC) and the South African Weather Services (SAWS). A total of 8 gauge stations (Figure 91) were used, which include two ARC weather stations and 6 SAWS stations. Missing values were filled using data from the nearest gauge stations including CFSR data in cases where both the gauge stations data have missing values. The daily CFSR weather data from 33 stations were downloaded from https://globalweather.tamu.edu/ website. Monthly weather statistics required by SWAT to generate weather files were calculated using SWAT Weather Database tool (Essenfelder, 2016). Observed daily streamflow data was obtained from the Department of Water and Sanitation's (DWS) central water quality database accessed from http://www.dwa.gov.za/iwqs/wms/data/. The DWS streamflow data has been collected since the early 1970s from the monitoring stations installed mostly in the rivers, tributaries, dams and canals.

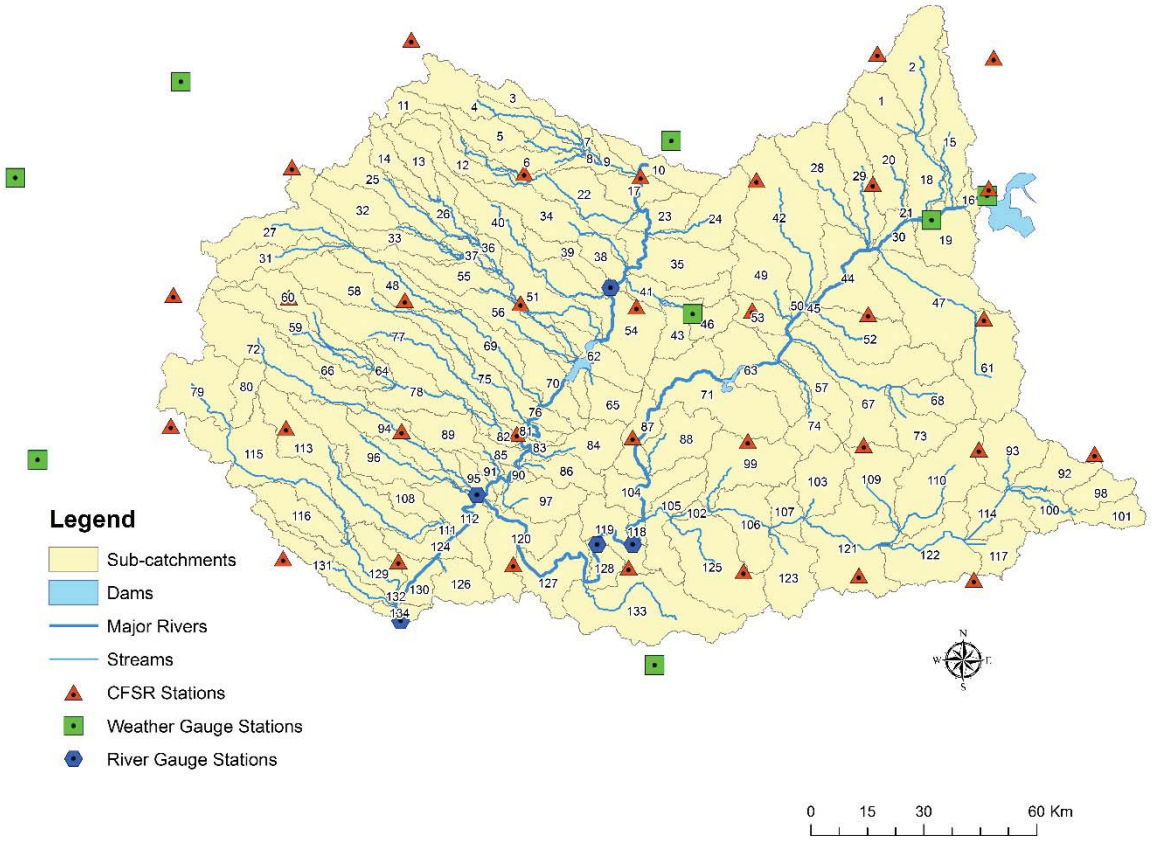

Figure 91: Map showing the location and distribution of weather gauge (SAWS and ARC), CFSR and river gauge stations overlying the sub-catchments boundary

12.2.2.2 SWAT model setup

A reliable hydrological model depends on critical decisions that should ensure proper representation of the hydrological system in the study area. The first major step required in setting up SWAT model is the delineation of watershed or sub-catchments boundary. This was accomplished using an SRTM DEM and stream network creation. Outlets were drawn automatically where streams adjoin each other and additional 5 outlets were added manually in locations where there is DWS streamflow gauge stations. We also defined one inlet at the outlet of Bloemhof dam to account for discharge from sub-catchments upstream of the study area. In addition, we included two major reservoirs (Vaalharts and Spitskop) along the Vaal and Harts Rivers respectively. A total of 134 sub-catchments were automatically delineated in accordance with the number of outlets points (Figure 91).

Sub-catchments boundaries were subdivided into 454 land parcels based on a unique combination of land use / cover, soil and slope classes called hydrological response units (HRUs). The model was setup and simulated with the gauge weather data first and then later with CFSR data. SWAT assigns to each sub-catchment the weather data of the nearest station based on the shortest distance from the weather station location to the centre point of a sub-catchment. After SWAT watershed delineation,

HRUs definition and weather data input, simulation was performed on a daily time step for a period of 14 years (2000 to 2013) for both the models with gauge data and CFSR data. The first three years, i.e. 2000 to 2002 were treated as a warm-up period, usually recommended in order to get the hydrological cycle fully operational (see Ji and Luo, 2013). SWAT simulates flow at HRUs level and then results are aggregated for the sub-catchments using a weighted average method. The initial simulation results with default parameters were not satisfactory. In order to improve the correlation between simulated and observed data, the Manning's roughness coefficient, "n", for channel flow was adjusted from the default value of 0.014 to 0.050 (Arnold et al., 2012b). The variables for two reservoirs, namely Vaalharts and Spitskop, were adjusted based on the information obtained from the South African Registers of large dams (http://www.sancold.org.za/index.php/about/about-dams/register-of-large-dams). The daily flow for the inlet catchment was populated based on the DWS river gauge data.

12.2.2.3 Model performance evaluation

The performance of the SWAT model was evaluated at five streamflow gauge outlets (i.e. sub-catchments 38, 95, 118, 119 and 134) where there is continuous data available for the simulation period (2000 to 2013). Evaluation was based on a visual assessment of the hydrographs and statistical metrics such as the coefficient of determination (R^2) and Nash-Sutcliffe Efficiency (NSE), Root Mean Square Error-observations (RMSE) standard deviation ratio (RSR) and Percent Bias (PBIAS). The R^2 describes the degree of collinearity between simulated and measured data whereas the NSE determines the relative magnitude of the residual variance ("noise") compared to the measured data variance ("information"). RSR is calculated as the ratio of the RMSE and the standard deviation of the observations. The PBIAS measures the average tendency of the simulated data to be larger or smaller than the observed data (Moriasi et al., 2007; Ayele et al., 2017). The statistics were calculated from the SWAT Calibration Uncertainties Program (SWAT-CUP) Sequential Uncertainty Fitting ver.2 (SUFI-2) algorithm after performing an initial calibration test with a parameter set to zero minimum and maximum values. The performance of the models against observed streamflow was compared. The interpretation of the model performance statistics, based on Moriasi et al. (2007) and Ayele et al. (2017), is given in Table 55.

Table 55: Model performance ratings for flow (Moriasi et al., 2007; Ayele et al., 2017)

Performance ratings	R^2	NSE	RSR	PBIAS
Very Good	>0.7-1	>0.75-1	≥0-0.5	<±10
Good	>0.6-0.7	>0.65-0.75	>0.5-0.6	±10-±15
Satisfactory	>0.5-0.6	>0.50-0.65	>0.6-0.7	±15-±25
Unsatisfactory	≤0.5	≤0.50	>0.7	≥±25

12.2.2.4 Comparison of CFSR precipitation and rain gauge data

Given the irregular distribution of the gauge stations, each of the eight weather stations from SAWS and ARC was spatially linked with the closest CFSR centroid point representing a grid cell of approximately 0.25° by 0.25°. Comparison was done on a monthly time step by adding together the cumulated daily rainfall amount for a given month for the period 2000 to 2013. The correlation between the cumulated monthly rainfall from gauge stations and CFSR grid was done using Pearson correlation coefficient which measures the degree of linear correlation between the two variables. We used the squared Pearson correlation coefficient which gives an idea of how much of the variability of a variable is explained by the other variable. Its value ranges from 0 to 1, where 0 indicates no linear relationship and 1 indicates a perfect linear relationship.

12.3 Results and discussion

12.3.1 SWAT model hydrographs

Figure 92 is the hydrographs illustrating the results of streamflow simulated using conventional weather gauge data and CFSR data compared with the observed streamflow at sub-catchments 38, 95, 118, 119 and 134. There is a good match between the observed and simulated streamflow using conventional weather data in all sub-catchments. The SWAT model using conventional weather data was well capable of simulating the major peak flow events, which is one of the most critical steps in water resource assessment and management. The model setup with CFSR data also performed well in the identification of peak flow events, except for sub-catchment 38 where the model underpredicted streamflow and the model failed to identify any peak flow event.

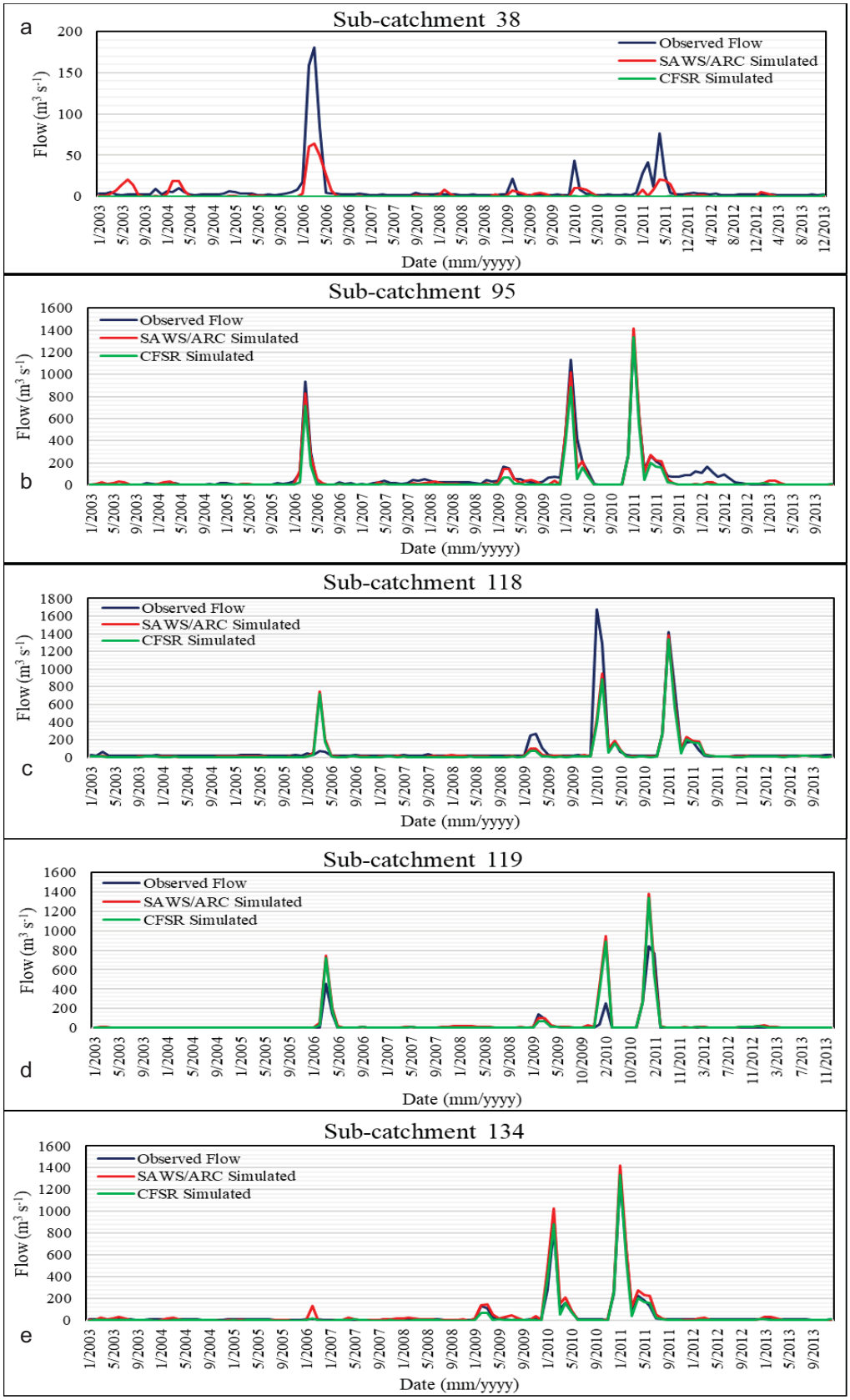

Figure 92: Comparison of the observed and simulated flows using SAWS/ARC weather gauge and CFSR weather datasets at a) sub-catchment 38, b) sub-catchment 95, c) sub-catchment 118, d) sub-catchment 119, and e) sub-catchment 134

12.3.2 SWAT model performances statistics

Table 56 shows the monthly model performance statistics for the SWAT streamflow simulated using CFSR data and conventional weather data at five river gauge locations. For the CFSR data, the poor graphical relationship between simulated streamflow and observed flow in sub-catchment 38 is confirmed by the poor statistical metrics. Both the R^2, NSE, PBIAS and RSR statistics were unsatisfactory with values of 0, -0.12, 99.40 and 1.06. In sub-catchment 95 and 118, the model performed well to very good in terms of the R^2, NSE and RSR statistics. The PBIAS values of 41 and 34.90 were unsatisfactory. In sub-catchment 119, the model only performed well in terms of the R^2 statistics. However, in sub-catchment 134, the CFSR data performed very well in all statistics where the R^2, NSE, RSR and PBIAS were 0.99, 0.99, 0.11 and 14.70 respectively. Overall, the PBIAS statistic was poor as confirmed by the model unsatisfactory performance in four of the five sub-catchments.

For the conventional weather gauge data, the R^2 values range from good (0.67) to very good (0.98) across all the five river gauge locations. On the contrary, the NSE values were unsatisfactory (0.34) to very good (0.95). The unsatisfactory NSE value was obtained in sub-catchment 119. In this sub-catchment, the PBIAS and RSR statistics were very poor compared to the rest of the sub-catchments. The PBIAS of -61.40 shows that the model had a tendency to overestimate flow in this sub-catchment. In other sub-catchments (38, 95, 118 and 134) the RSR statistics were satisfactory (0.69) to very good (0.22). Overall, the PBIAS statistics were only satisfactory in two of the five sub-catchments, i.e. sub-catchments 95 and 134.

Table 56: SWAT performance statistics for the model simulated with CFSR and conventional gauge weather data

Flow Gauge Sub-catchment no.	R^2		NSE		PBIAS		RSR	
	CFSR	Gauge	CFSR	Gauge	CFSR	Gauge	CFSR	Gauge
38	0	0.74	-0.12	0.52	99.40	51.70	1.06	0.69
95	0.94	0.96	0.90	0.95	41.00	19.70	0.32	0.22
118	0.66	0.67	0.64	0.66	34.90	25.60	0.60	0.58
119	0.79	0.80	0.44	0.34	-41.50	-61.40	0.75	0.81
134	0.99	0.98	0.99	0.95	-14.70	-20.40	0.11	0.22

SWAT simulations using conventional weather stations data outperformed those with CFSR data in three of the five sub-catchments. The CFSR data was superior over the conventional data in sub-catchments 119 and 134. Although the performance of both models was unsatisfactory in terms of the NSE, PBIAS and RSR statistics in sub-catchment 119, CFSR data gave better statistics compared to the conventional data. In sub-catchment 134, CFSR data outperformed the conventional data in all evaluation statistics, where the R^2, NSE, RSR and PBIAS were 0.99, 0.99, 0.11 and 14.70 respectively,

whereas for conventional data the values of 0.98, 0.95, 0.22 and -20.4 were obtained respectively. Although the overall comparison shows that conventional data produced a better match to the observed streamflow data than the CFSR data, this study showed that CFSR data can be a useful alternative in cases where there is insufficient or no gauge weather stations.

12.3.3 Rainfall comparison between gauge and CFSR data

Figure 93 shows the scatter plots of rain gauge data against the satellite based CFSR rainfall estimates at eight locations where rainfall was measured by the SAWS and ARC. Generally, the scatter plots in Figure 93 show a weaker relationship between the CFSR rainfall estimates and the gauge rainfall data, where the R^2 ranged from 0.05 to 0.15. Although further analysis of the data is not shown here, CFSR tend to overestimate the number of wet days compared to gauge data, however, the cumulative rainfall total tend to be lower for CFSR data. This is mainly because CFSR tend to underestimate rainfall peak amount during storm events.

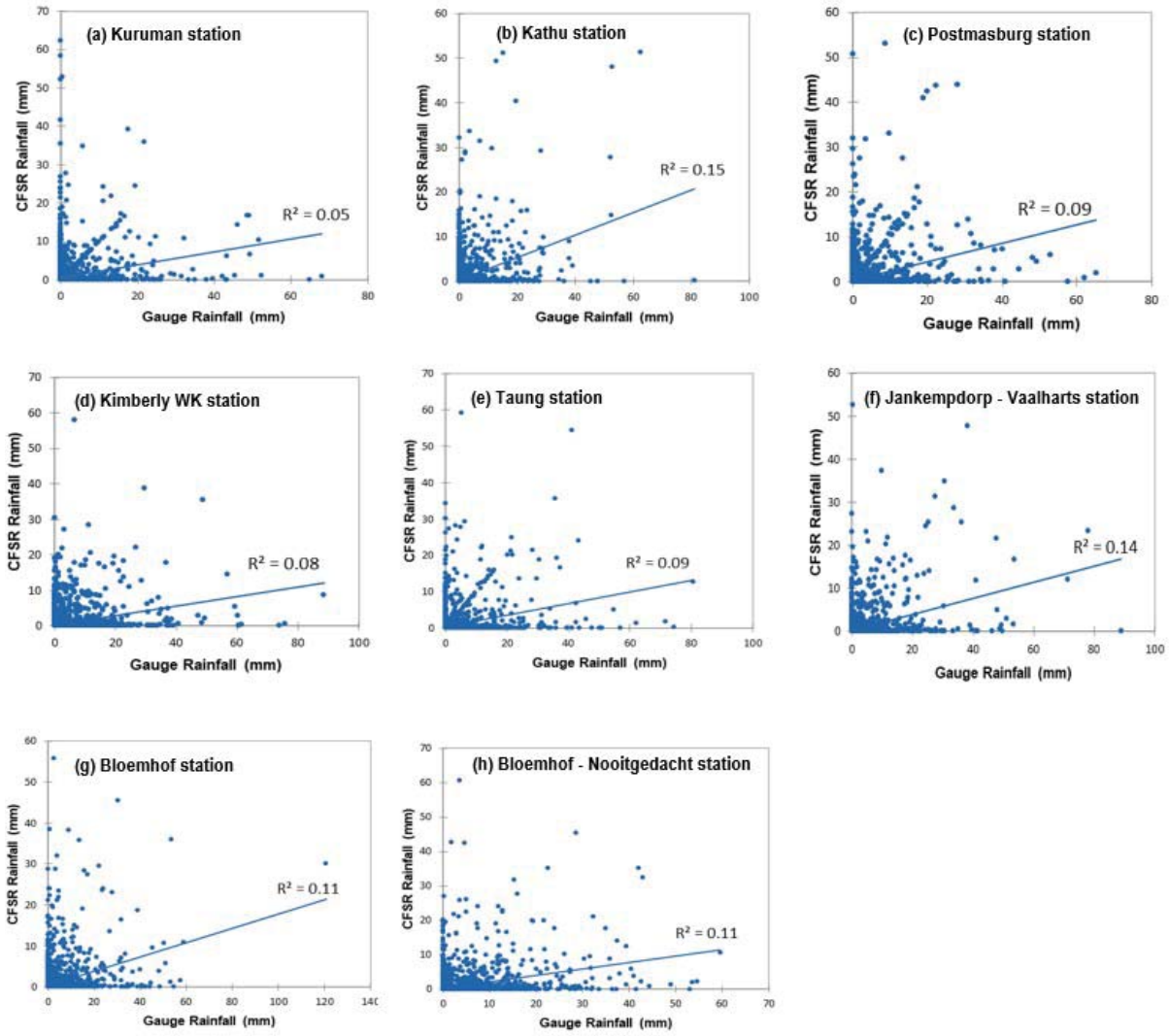

Figure 93: Scatter plots of monthly accumulated rainfall gauge stations data compared with the nearest CFSR rainfall estimates grid cell at (a) Kuruman, (b) Kathu, (c) Postmasburg, (d) Kimberly WK, (e) Taung, (f) Jan Kempdorp – Vaalharts, (g) Bloemhof and (h) Bloemhof

12.4 Discussion

Both models performed reasonably well in the identification of peak flow associated with extreme summer rainfall events. Corresponding high runoff volumes as a result of extreme runoff are a major contributor of water supply and flooding in the study area. Devkota and Gyawali (2015) indicated that peak flows can be essential information for flood control when designing a dam. Knowing the timing and magnitude of peak flows is important when dealing with the hydraulic structures such as the spillway of a dam to dispose the flood water and the embankments to contain the flood water within the river bed. These are critical information that may be useful for managers in the Lower Vaal River Catchment to make informed water resource management decisions.

The hydrographs show that the observed streamflow varies from 0 $m^3 s^{-1}$ in winter to 1 679 $m^3 s^{-1}$ in late summer months. The observed and simulated flows were generally low and intermittent most of the time, except for occasional extreme peak flow events that occurred in the year 2006, 2010 and 2011 mainly between January and March months. The bulk of surface runoff is in the Vaal River since streamflow observations at the Harts River had a maximum discharge of 180 $m^3 s^{-1}$. The low and intermittent flow suggests that the study area is within one of the water stressed region in the country. In addition to water losses as a result of hydrological processes, some of the water is lost due to the abstraction for irrigation, though the irrigation return flow partly compensates for this.

The CFSR performed better than the conventional weather gauge stations in sub-catchments 119 and 134 for various reasons. Foremost, the CFSR weather forecast model assimilate ground weather observations produced at various meteorological centres around the world (Saha et al., 2010a). Thus, more accurate conventional weather stations data steer the CFSR forecasts. Moreover, CFSR data represents weather averages over a large area, whereas gauge weather data represent observations made at a particular point (Fuka et al*., 2*013). Since weather can vary over a short distance due to the variation in topography, weather forecasts by CFSR better account for the heterogeneity of the landscape. Therefore, the relatively lower performance of gauge data compared to CFSR data in sub-catchment 134 could be attributed to the lack of weather stations nearby.

Generally, both models showed the tendency to underestimate streamflow. Simulated streamflows were consistently lower than the observed streamflow in sub-catchments 38, 95 and 118. The tendency of the model parameterized with CFSR data to underestimate precipitation and flow has been reported in previous studies (e.g. Monteiro et al., 2016; Nkiaka et al., 2017). This is mainly caused by a shortage of ground weather observation stations in many developing countries resulting in uncertainty in forecast model input (Nkiaka et al., 2017). Most striking is the underestimation of flow by the model setup with CFSR data in sub-catchment 38. Here, the effect of poor precipitation data is evident. Poor quality precipitation data often results in model prediction errors (Tuo et al., 2016).

This study has also shown a bias of statistics towards a certain type of error. In this study, multiple statistical measures were used to represent different aspects of the model error. The R^2, NSE and RSR evaluation statistics across the majority of sub-catchments indicated that both models performed

satisfactory to very good. The results of the R^2 and NSE are often biased due to the presence of data outliers and repeated data (Bennett et al., 2010; Ritter and Muñoz-Carpena, 2013) as also the case in this study, explaining the better performance ratings of these indicators compared to other metrics. Outliers in flow, probably caused by a persistent rainfall events, are known to have disproportionate effect on the slope of the regression line, causing the R^2 and NSE to be unreliable. To avoid the misinterpretation of R^2 and NSE values, Bennett et al. (2010) suggested that R^2 and NSE results should be interpreted in conjunction with PBIAS. In this study, the average magnitude of the differences between the simulated and observed streamflow (PBIAS) was within an unsatisfactory range (≥±25) most of the time in the majority of sub-catchments, besides the satisfactory (±15 to ±25) to good (±10 to ±15) performance at sub-catchments 95 and 134. The PBIAS also shows that flow was underestimated in the majority of sub-catchments except for the overestimation in sub-catchment 119 by both models and in sub-catchment 134 by the model simulated using conventional weather data. Satisfactory performance statistics in terms of the PBIAS can be obtained if a model is calibrated.

Although streamflow modelling using CFSR data is promising, this study found that CFSR data doesn't correlate well with gauge weather observations. The poor correlation between CFSR and gauge weather data could have been influenced by the analysis time step. Previous studies have shown that as the analysis time step increases from daily to monthly and monthly to yearly, the correlation between rainfall estimates and rain observations improves (e.g. Dembélé and Zwart, 2016; Kimani et al., 2017). It is also important to note that satellite rainfall estimates are inherently lower than rain gauge data due to the scale differences (Decker et al., 2012). CFSR data represents average rainfall estimates in a particular grid of 0.25° by 0.25°. The estimates are likely going to be affected by the high spatial and temporal variability of precipitation as well as the variation in topography due to the relatively larger area considered (Decker et al., 2012). Averaging rainfall is avoided on a point-based measurement used in gauge weather station observation. Surprisingly, CFSR performed reasonably well for streamflow simulation except in sub-catchment 38 where accurate representation of weather data seems to be the most defining model input parameter. Ignoring results from this sub-catchment lead to comparable performance by both the models simulated with CFSR and conventional gauge weather data. This suggests that CFSR can be useful for streamflow simulation where there is no sufficient gauge weather data. While the comparison of CFSR and gauge rainfall data was poor, the variation between CFSR and gauge rainfall datasets was probably within a reasonable statistical range to force SWAT streamflow model in a manner consistent with gauge weather data.

12.5 Conclusion and recommendations

This study focused on the usefulness of the CFSR data for streamflow modelling using SWAT in parts of the lower Vaal River catchment. The results of SWAT model forced with CFSR data were compared with the SWAT model executed with conventional weather stations data at five sub-catchments outlets. Multiple statistics including R^2, NS, RSR and PBIAS were used to assess the performance of both models. Both the models performed reasonably well in the majority of sub-catchments in terms of the R^2, NSE and RSR statistics except for poor performance of the CFSR data in sub-catchment 38. The

PBIAS was unsatisfactory in most of the sub-catchments except for sub-catchment 134 and satisfactory value for conventional weather stations data in sub-catchment 95. Overall, the conventional weather stations data performed better than the CFSR data in three of the five sub-catchments.

The study concluded that conventional weather data remains one of the most important data input to the SWAT model and is recommended for the lower Vaal River Catchment. However, CFSR has a huge potential in studying hydrological processes under data scarcity as demonstrated by satisfactory model performance in this study. CFSR data can be useful for improving gauge weather stations data in cases where there are gaps or missing values. It can also be used together with gauge weather stations data in places where there are insufficient gauge stations. Its main advantages over the conventional gauge weather data in our study is that, CFSR data provides a complete data at ±0.25º resolution, although this dataset has its own challenges. In our study area, CFSR precipitation do not correlate well with rain gauge data. Whether time step of analysis or scale played a role in the poor correlations of CFSR and gauge data remains one of the uncertainty issue which needs further investigation. Nevertheless, streamflow simulation with CFSR data was able to match streamflow simulation with gauge data even with a poor correlation of 0.05 to 0.15 between the two datasets, suggesting the importance of other input parameters. Future model applications should focus on the simulations of nutrients and sediments as well as the calibration of the model to minimize any model uncertainty.

12.6 References

ABERA, W., BROCCA, L., RIGON, R. (2016) Comparative evaluation of different satellite rainfall estimation products and bias correction in the Upper Blue Nile (UBN) basin. Atmos. Res. 178-179, 471-483. https://doi.org/10.1016/j.atmosres.2016.04.017

ARNOLD, J.G., KINIRY, J.R., SRINIVASAN, R., WILLIAMS, J.R., HANEY, E.B., NEITSCH, S.L. (2012b) Soil & Water Assessment Tool – input/output documentation.

ARNOLD, J.G., MORIASI, D.N., GASSMAN, P.W., ABBASPOUR, K.C., WHITE, M.J., SRINIVASAN, R., SANTHI, C., HARMEL, R.D., VAN GRIENSVEN, A., VAN LIEW, M.W., KANNAN, N., JHA, M.K. (2012a) SWAT: model use, calibration and validation. Trans. ASABE 55, 1491-1508.

ARNOLD, J.G., SRINIVASAN, R., MUTTIAH, R.S., WILLIAMS, J.R. (1998) Large area hydrologic modelling and assessment Part I: model development. J. Am. Water Resour. Assoc. 34, 73-89. https://doi.org/10.1111/j.1752-1688.1998.tb05961.x

ASHOURI, H., HSU, K.-L., SOROOSHIAN, S., BRAITHWAITE, D.K., KNAPP, K.R., CECIL, L.D., NELSON, B.R., PRAT, O.P. (2015) Daily precipitation climate data record from multisatellite observations for hydrological and climate studies. Am. Meteorol. Soc. 1, 69-84. https://doi.org/10.1175/BAMS-D-13-00068.1

ASHTON, P.J. (2010) A CSIR perspective on water in South Africa. Pretoria. https://doi.org/CSIR Report No. CSIR/NRE/PW/IR/2011/0012/A

AYELE, G.T., TESHALE, E.Z., YU, B., RUTHERFURD, I.D., JEONG, J. (2017) Streamflow and sediment yield prediction for watershed prioritization in the upper Blue Nile river basin, Ethiopia. Water (Switzerland) 9, 1-29. https://doi.org/10.3390/w9100782

BENNETT, N.D., CROKE, B.F.W., JAKEMAN, A.J., NEWHAM, L.T.H., NORTON, J.P. (2010) Performance evaluation of environmental models, in: 5th International Congress on Environmental Modelling and Software. Ottawa, Ontario, Canada, pp. 1-10.

BROCCA, L., MORAMARCO, T., MELONE, F., WAGNER, W. (2013) A new method for rainfall estimation through soil moisture observations. Geophys. Res. Lett. 40, 853-858. https://doi.org/10.1002/GRL.50173

COUNCIL FOR GEOSCIENCES (2007) Geological data: 1:250 000. Council for Geosciences, Pretoria.

CROP ESTIMATES CONSORTIUM (2017a) Field crop boundary data layer (Free State province), 2017. Department of Agriculture, Forestry and Fisheries. Pretoria.

CROP ESTIMATES CONSORTIUM, 2017b. Field crop boundary data layer (NC province), 2017. Department of Agriculture, Forestry and Fisheries. Pretoria.

CROP ESTIMATES CONSORTIUM (2017c) Field crop boundary data layer (NW province), 2017. Department of Agriculture, Forestry and Fisheries, Pretoria.

DECKER, M., BRUNKE, M.A., WANG, Z., SAKAGUCHI, K., ZENG, X., BOSILOVICH, M.G. (2012) Evaluation of the reanalysis products from GSFC, NCEP, and ECMWF using flux tower observations. J. Clim. 25, 1916-1944. https://doi.org/10.1175/JCLI-D-11-00004.1

DEMBÉLÉ, M., ZWART, S.J. (2016) Evaluation and comparison of satellite-based rainfall products in Burkina Faso, West Africa. Int. J. Remote Sens. 37, 3995-4014. https://doi.org/10.1080/01431161.2016.1207258

DEVKOTA, L.P., GYAWALI, D.R. (2015) Impacts of climate change on hydrological regime and water resources management of the Koshi River Basin, Nepal. J. Hydrol. Reg. Stud. 4, 502-515. https://doi.org/10.1016/j.ejrh.2015.06.023

DILE, Y.T., SRINIVASAN, R. (2014) Evaluation of CFSR climate data for hydrologic prediction in data-scarce watersheds: an application in the Blue Nile River Basin. J. Am. Water Resour. Assoc. 50, 1-16. https://doi.org/10.1111/jawr.12182

ESSENFELDER, A.H. (2016) SWAT weather database: A quick guide. Version: v.0.16.06. https://doi.org/10.13140/RG.2.1.4329.1927

FUKA, D.R., WALTER, M.T., MACALISTER, C., DEGAETANO, A.T., STEENHUIS, T.S., EASTON, Z.M. (2013) Using the Climate Forecast System Reanalysis as weather input data for watershed models. Hydrol. Process. 28, 5613-5623. https://doi.org/10.1002/hyp.10073

GASSMAN, P.W., REYES, M.R., GREEN, C.H., ARNOLD, J.G. (2007) The Soil and Water Assessment Tool: historical development, applications, and future research directions. Trans. ASABE 50, 1211-1250. https://doi.org/10.1.1.88.6554

GEOTERRAIMAGE (2015) 2013-2014 South African national land-cover dataset. GEOTERRAIMAGE Pty Ltd., Pretoria. Available on website: http://egis.environment.gov.za/national_land_cover_data_sa. Accessed: July 2017

GUO, J., LIANG, X., RUBY LEUNG, L. (2004) Impacts of different precipitation data sources on water budgets. J. Hydrol. 298, 311-334. https://doi.org/10.1016/j.jhydrol.2003.08.020

HUFFMAN, G.J., ADLER, R.F., BOLVIN, D.T., GU, G., NELKIN, E.J., BOWMAN, K.P., HONG, Y., STOCKER, E.F., WOLFF, D.B. (2007) The TRMM Multisatellite Precipitation Analysis (TMPA): Quasi-Global, Multiyear, Combined-Sensor Precipitation Estimates at fine scales. J. Hydrometeorol. 8, 38-55. https://doi.org/10.1175/JHM560.1

JI, X., LUO, Y. (2013) The influence of precipitation and temperature input schemes on hydrological simulations of a snow and glacier melt dominated basin in Northwest China. Hydrol. Earth Syst. Sci. Discuss. 10, 807-853. https://doi.org/10.5194/hessd-10-807-2013

JOYCE, R.J., JANOWIAK, J.E., ARKIN, P.A., XIE, P. (2004) CMORPH: A method that produces global precipitation estimates from passive microwave and infrared data at high spatial and temporal resolution. J. Hydrometeorol. 5, 487-503.

KIMANI, M.W., HOEDJES, J.C.B., SU, Z. (2017) An assessment of satellite-derived rainfall products relative to ground observations over East Africa. Remote Sens. 9, 1-21. https://doi.org/10.3390/rs9050430

LAND TYPE SURVEY STAFF (1984) Landtypes of South Africa: digital map (1:250 000 scale) and soil inventory databases. ARC-Institute for Soil, Climate and Water, Pretoria.

LE ROUX, J.J., BARKER, C.H., WEEPENER, H.L., VAN DEN BERG, E.C., PRETORIUS, S.N. (2015) Sediment yield modelling in the Mzimvubu River catchment. WRC Report No. 2243/1/15. Water Research Commission, Pretoria.

LE ROUX, J.J., MORGENTHAL, T.L., MALHERBE, J.D., SUMNER, P.D. (2008) Water erosion prediction at a national scale for South Africa. Water SA 34, 305-314.

LEMANN, T., ROTH, V., ZELEKE, G. (2017) Impact of precipitation and temperature changes on hydrological responses of small-scale catchments in the Ethiopian Highlands. Hydrol. Sci. J. 62, 270-282. https://doi.org/10.1080/02626667.2016.1217415

LEVIZZANI, V., SCHMETZ, J., LUTZ, H.J., KERKMANN, J., ALBERONI, P.P., CERVINO, M. (2001) Precipitation estimations from geostationary orbit and prospects for METEOSAT Second Generation. Meteorol. Appl. 8, 23-41.

MOLINA-NAVARRO, E., ANDERSEN, H.E., NIELSEN, A., THODSEN, H., TROLLE, D. (2017) The impact of the objective function in multi-site and multi-variable calibration of the SWAT model. Environ. Model. Softw. 93, 255-267. https://doi.org/10.1016/j.envsoft.2017.03.018

MONTEIRO, J.A.F., STRAUCH, M., SRINIVASAN, R., ABBASPOUR, K., GÜCKER, B. (2016) Accuracy of grid precipitation data for Brazil: Application in river discharge modelling of the Tocantins catchment. Hydrol. Process. 30, 1419-1430. https://doi.org/10.1002/hyp.10708

MORIASI, D.N., ARNOLD, J.G., VAN LIEW, M.W., BINGNER, R.L., HARMEL, R.D., VEITH, T.L. (2007) Model evaluation guidelines for systematic quantification of accuracy in watershed simulations. Trans. ASABE 50, 885-900. https://doi.org/10.13031/2013.23153

MUCINA, L. AND RUTHERFORD, M.C. (Eds.) (2006) The vegetation of South Africa, Lesotho and Swaziland. Strelitzia 19. South African National Biodiversity Institute (SANBI), Pretoria.

NEITSCH, S.., ARNOLD, J.., KINIRY, J.., WILLIAMS, J. (2011) Soil and Water Assessment Tool theoretical documentation version 2009, Texas Water Resources Institute Technical Report No. 406. Texas. https://doi.org/10.1016/j.scitotenv.2015.11.063

NKIAKA, E., NAWAZ, N.R., LOVETT, J.C. (2017) Evaluating global reanalysis precipitation datasets with rain gauge measurements in the Sudano-Sahel region: case study of the Logone catchment, Lake Chad Basin. Meteorol. Appl. 18, 9-18. https://doi.org/10.1002/met.1600

OBERHOLSTER, P.J., ASHTON, P.J. (2008) State of the nation report: An overview of the current status of water quality and eutrophication in South African rivers and reservoirs. State of the Nation Report.

RITTER, A., MUÑOZ-CARPENA, R. (2013) Performance evaluation of hydrological models: Statistical significance for reducing subjectivity in goodness-of-fit assessments. J. Hydrol. 480, 33-45. https://doi.org/10.1016/j.jhydrol.2012.12.004

ROTH, V., LEMANN, T. (2016) Comparing CFSR and conventional weather data for discharge and soil loss modelling with SWAT in small catchments in the Ethiopian Highlands. Hydrol. Earth Syst. Sci. 20, 921-934. https://doi.org/10.5194/hess-20-921-2016

SAHA, S., MOORTHI, S., PAN, H.L., WU, X., WANG, J., NADIGA, S., TRIPP, P., KISTLER, R., WOOLLEN, J., BEHRINGER, D., LIU, H., STOKES, D., GRUMBINE, R., GAYNO, G., WANG, J., HOU, Y.T., CHUANG, H.Y., JUANG, H.M.H., SELA, J., IREDELL, M., TREADON, R., KLEIST, D., VAN DELST, P., KEYSER, D., DERBER, J., EK, M., MENG, J., WEI, H., YANG, R., LORD, S., VAN DEN DOOL, H., KUMAR, A., WANG, W., LONG, C., CHELLIAH, M., XUE, Y., HUANG, B., SCHEMM, J.K., EBISUZAKI, W., LIN, R., XIE, P., CHEN, M., ZHOU, S., HIGGINS, W., ZOU, C.Z., LIU, Q., CHEN, Y., HAN, Y., CUCURULL, L., REYNOLDS, R.W., RUTLEDGE, G., GOLDBERG, M. (2010) Supplement to the NCEP Climate Forecast System Reanalysis. Bull. Am. Meteorol. Soc. 9-25. https://doi.org/10.1175/2010BAMS3001.2

SAHA, S., MOORTHI, S., PAN, H.L., WU, X., WANG, J., NADIGA, S., TRIPP, P., KISTLER, R., WOOLLEN, J., BEHRINGER, D., LIU, H., STOKES, D., GRUMBINE, R., GAYNO, G., WANG, J., HOU, Y.-T., CHUANG, H.-Y., JUANG, H.-M.H., SELA, J., IREDELL, M., TREADON, R., KLEIST, D., VAN DELST, P., KEYSER, D., DERBER, J., EK, M., MENG, J., WEI, H., YANG, R., LORD, S., VAN DEN DOOL, H., KUMAR, A., WANG, W., LONG, C., CHELLIAH, M., XUE, Y., HUANG, B., SCHEMM, J.-K., EBISUZAKI, W., LIN, R., XIE, P., CHEN, M., ZHOU, S., HIGGINS, W., ZOU, C.-Z., LIU, Q., CHEN, Y., HAN, Y., CUCURULL, L., REYNOLDS, R.W., RUTLEDGE, G., GOLDBERG, M. (2010) The NCEP climate forecast system reanalysis. Bull. Am. Meteorol. Soc. 91, 1015-1057. https://doi.org/10.1175/2010BAMS3001.1

SAXTON, K.E., RAWLS, W.J. (2006) Soil water characteristic estimates by texture and organic matter for hydrologic solutions. Soil Sci. Soc. Am. J. 70, 1569-1578. https://doi.org/10.2136/sssaj2005.0117

SCHULZE R.E. (2007) South African Atlas of Climatology and Agrohydrology. WRC Report No. 1489/1/06. Water Research Commission. Pretoria.

SCHULZE, R. E. (Ed.) (2010) Atlas of climate change and the South African agricultural sector: a 2010 perspective. Department of Agriculture, Forestry and Fisheries. Pretoria.

SCHULZE, R.E. (1995) Hydrology and agrohydrology: A text to accompany the ACRU 3.00 agrohydrological modelling system. WRC Report No. TT69/95. Water Research Commission. Pretoria.

SRINIVASAN, R., ZHANG, X., ARNOLD, J. (2010) SWAT ungauged: Hydrological budget and crop yield predictions in the upper Mississippi River Basin. Am. Soc. Agric. Biol. Eng. 53, 1533-1546. https://doi.org/10.13031/2013.34903

TOLERA, M.B., CHUNG, I.-M., CHANG, S.W. (2018) Evaluation of the Climate Forecast System Reanalysis weather data for watershed modelling in upper Awash Basin, Ethiopia. Water 10, 1-17. https://doi.org/10.3390/w10060725

TOTÉ, C., PATRICIO, D., BOOGAARD, H., VAN DER WIJNGAART, R., TARNAVSKY, E., FUNK, C. (2015) Evaluation of satellite rainfall estimates for drought and flood monitoring in Mozambique. Remote Sens. 7, 1758-1776. https://doi.org/10.3390/rs70201758

TUO, Y., DUAN, Z., DISSE, M., CHIOGNA, G. (2016) Evaluation of precipitation input for SWAT modelling in Alpine catchment: A case study in the Adige river basin (Italy). Sci. Total Environ. 573, 66-82. https://doi.org/10.1016/j.scitotenv.2016.08.034

UITTO, J. (2001) Global freshwater resources, in: Palo, M., Uusivuori, J., Mery, G. (Eds.), World Forests, Markets and Policies. Kluwer Academic Publishers, pp. 65-76. https://doi.org/10.1007/978-94-010-0664-4

XIANG, C., WANG, Y., LIU, H. (2017) A scientometrics review on nonpoint source pollution research. Ecol. Eng. 99, 400-408. https://doi.org/10.1016/j.ecoleng.2016.11.028

13 MODELLING NUTRIENT LOADS FROM IRRIGATED AGRICULTURE AT A SUB-CATCHMENT SCALE IN THE LOWER VAAL RIVER SYSTEM

N. Mararakanye, J.J. Le Roux and A.C. Franke
Department of Soil, Crop and Climate Sciences, University of the Free State, Private Bag 339
Bloemfontein 9300, South Africa

13.1 Introduction

Nonpoint source (NPS) nutrient pollution from agriculture is a major source of water quality problems in many parts of the world (Gao and Li, 2014). The two most important agricultural nutrients affecting water quality are nitrogen (N) and phosphorus (P). Progressive increase in nitrogen and phosphorus load in surface waterbodies contributes to a nutrient-rich environment (eutrophication) with adverse effects to the health of both humans and aquatic systems (Yang et al., 2008). The leaching of nutrients from catchments into streams, lakes, and groundwater is generally regarded as a natural part of nutrient cycling. However, it becomes of a serious concern when the natural balance of nutrient cycling is altered through fertilizers application, biodegradation of crop residues, agricultural and municipal wastes applied to land, and waste generated directly by animals (Bianchi and Harter, 2002). Our study focusses on the contribution of irrigated agriculture to nutrients pollution in the lower Vaal River system.

The lower Vaal River catchment is located in an intensively irrigated crop production region, which include the Vaalharts Irrigation Scheme, with high potential effects on sediment yield, phosphorus, and nitrogen pollution. Studies have shown that nutrient pollution is a serious problem in irrigated agricultural system as a result of leaching of nutrients from catchments into streams and lakes as well as nutrients transportation through groundwater discharge via baseflow and tile drainage (Bianchi and Harter, 2002; Jha et al., 2006). The challenge in the lower Vaal River catchment is that it is dominated by sandy soils which are prone to high leaching. The problem may worsen in the near future due to the intensification of irrigated crops in terms of new land development, crop production practices and a shift towards pecan nut production. Knowing these problems will assist water resource managers and other decision makers to effectively manage the catchment. Evidence suggest that the two large dams upstream and downstream (Taung and Spitskop respectively) of the Vaalharts Irrigation Scheme are currently in a eutrophic to hypertrophic state, with the possibility that cyanobacteria could reach a nuisance condition and negatively affect crops and irrigation infrastructure (Department of Water and Sanitation (DWS), 2014).

In the context of the above, the aim of this study is to apply the Soil and Water Assessment Tool (SWAT) model to study the effects of irrigated farming practices on nutrients (N and P) loadings in the lower Vaal River catchment. Due to the large size of the lower Vaal River catchment (greater than 27 000 km^2) and its natural complexity and spatial heterogeneity, insufficient systems knowledge and unfeasible data requirements at this scale, nutrients modelling was applied at smaller sub-catchment. Thus, part of the lower Vaal River catchment which incorporate the Vaalharts Irrigation Scheme was chosen for this study. The main objectives of this study were (a), to setup the hydrological model SWAT

in a smaller sub-catchment (b), manually calibrate the model for streamflow and nutrients load. The focus here is on calibrating ammonia nitrogen (NH_4-N), Total-P (TP) and Total-N (TN).

13.2 Study area

The delineated sub-catchment is part of the main lower Vaal River catchment (Figure 94). It has an area of approximately 1 343 km^2. The sub-catchment is located in the lower reaches of the Harts River and encompasses one of the oldest and largest irrigation system in South Africa known as the Vaalharts Irrigation Scheme. Irrigation water for the scheme is drawn from the Vaal River through a diversion of water into a network of open canals. Crops grown mainly include wheat, maize, cotton lucerne, and pecan nuts. Agricultural activities upstream and within the sub-catchment are placing high threat levels on the ecosystem and thus on the fitness for use of water to local and downstream users (Department of Water and Sanitation, 2014). The area is characterised by a low flow, with the mean annual runoff (MAR) of 147 million m^3 a^{-1} (Department of Water and Sanitation, 2014). The irrigation return flows from Vaalharts Irrigation Scheme generates a significant base flow. However, little flow reaches the Vaal River due to downstream releases from Spitskop Dam for irrigation along the river reach. Land cover is dominated by thornveld, grasses and alluvial vegetation (Mucina and Rutherford, 2006). The climate is semi-arid, with the mean annual rainfall ranging from 200 to 600 mm, the majority of which is received in February (Schulze, 2010). The spatial distribution of soil is diverse, with about 3 broad soil types. The majority of the soils are red and yellow well drained sandy soils found along the valley of Harts River where there is an irrigation scheme, and some soils with a marked clay accumulation in patches (Land Type Survey Staff, 1984).

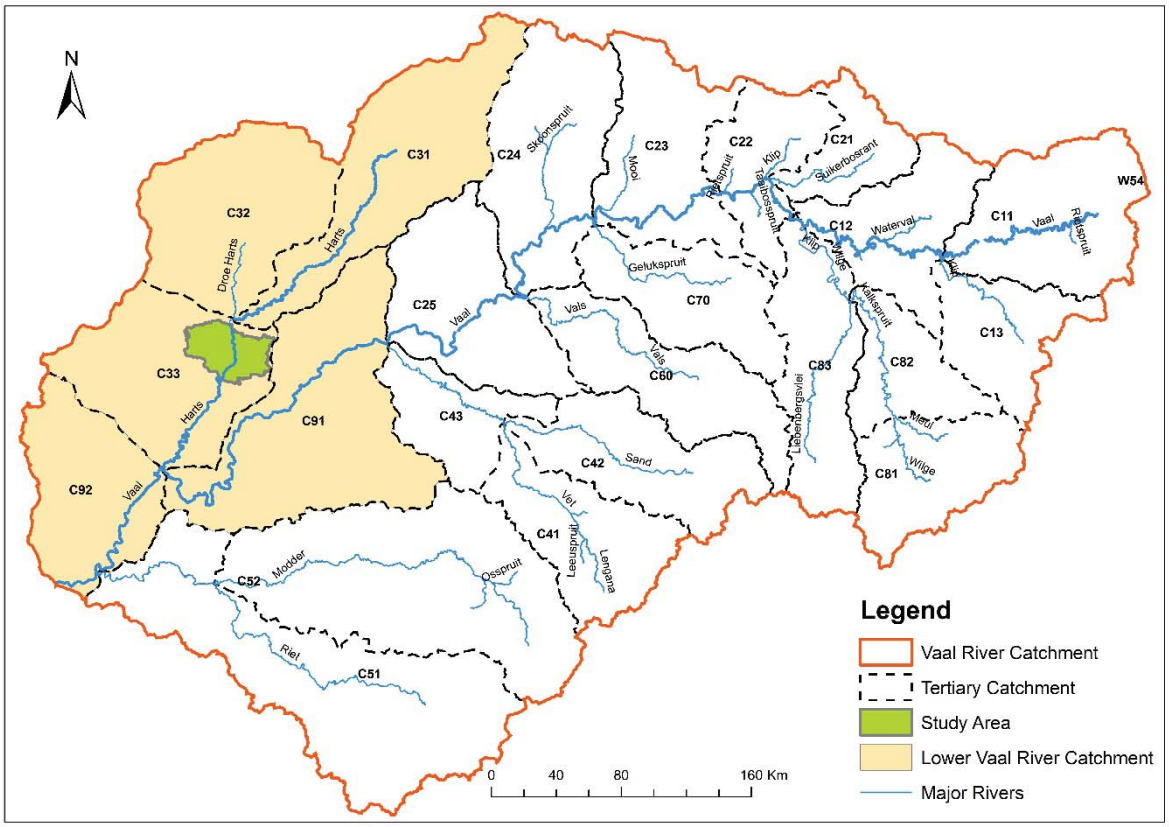

Figure 94: Location of the study area within the Vaal River system with tertiary catchments included

13.3 SWAT model application

13.3.1 Data input

SWAT requires several inputs datasets for watershed delineation, hydrological response units (HRUs) definition and simulating special features such as reservoirs and point sources. In this study, we used 25 x 25 m spacing Digital Elevation Model (DEM) data sourced by the National Geospatial Information (NGI) Chief Directorate (CD) of the Department of Rural Development and Land Reform (DRDLR) from a stereo pair of photogrammetric images and from contour data sets. The utilised DEM is freely available from the CD:NGI upon request. The land use/ cover, soil and slope derived from NGI DEM were used to delineate the HRUs. We used the national land use/ cover data developed by GEOTERRAIMAGE (Pty) Ltd for the Department of Environmental Affairs (DEA) of South Africa. This data was derived from 2013 to 2014 multi-seasonal Landsat 8 imagery using semi-automated modelling procedures and has a pixel resolution of 30 m (Geoterraimage, 2015). We appended the cultivated field classes from field crop boundaries layer obtained from the Department of Agriculture, Forestry and Fisheries (DAFF). The field crop boundaries were digitised from SPOT 5 and 6 images of the period 2013 to 2015 (Crop Estimates Consortium, 2017a; 2017b, 2017c) and is a highly accurate representation of cultivated fields. Soil boundary layer was obtained from the 1: 250 000 scale landtype

dataset of SA obtained from DAFF. Other soil physical and chemical properties required by SWAT were not readily available from the landtype data and were thus obtained from other sources or derived from criteria as illustrated in Table 57.

Table 57: Criteria used to assign soil physical and chemical properties required by SWAT

Soil properties	Soil properties definition	Information source or criteria used to assign the values
HYDGRP	Soil hydrologic group	The soil hydrological groups given in Schulze (2007) for each landtype was used.
SOL_ZMX	Maximum rooting depth of profile	Schulze (2007) depth of the topsoil layer (*DEPAHO*) for each landtype was used.
SOL_Z1	Depth to bottom of first soil layer (mm)	Schulze (2007) depth of the topsoil layer (*DEPAHO*) for each landtype was used.
SOL_BD1	Moist bulk density of first soil layer (Mg m^{-3})	Bulk density of the soil was obtained from Schulze (1995) approximations based on clay content as follows: 2-5% clay = 1.7, 6-15% clay = 1.6, 16-25% clay = 1.5, 26-32% clay = 1.4, 33-40% clay = 1.3
SOL_AWC1	Available water capacity of the first soil layer (mm H_2O mm^{-1} soil)	Schulze (2007) plant available water (*PAW*) given for each landtype was used.
SOL_K1	Saturated hydraulic conductivity of first soil layer (mm hr^{-1})	Estimation of SOL_K1 values was based on the soil texture classes of the dominant soil in the landtype, assuming 2.5% organic matter (OM) and no salinity, gravel or density adjustment (Saxton and Rawls, 2006) as follows: Sa = 108.1, L-Sa = 96.7, Sa-L = 50.3, L = 15.5, Si-L = 16.1, Si = 22, Sa-CL = 11.3, CL = 4.3, Si-C-L = 5.7, Si-C = 3.7, Sa-C = 1.4 and C = 1.1 Where Sa = sand; L = loam; Si = silt; C = clay.
SOL_CBN1	Organic carbon content of first soil layer (%)	Similar to Le Roux et al. (2015), an unpublished carbon map of SA derived from soil profile and landtype datasets was used to assign carbon values to each landtype in the study area.
CLAY1	Clay content of first soil layer (%)	The maximum value of clay percentages range given in a landtype memoir for the dominant soil was used (Land Type Survey Staff, 1984).

Soil properties	Soil properties definition	Information source or criteria used to assign the values
SILT1	Silt content of first soil layer (%)	Similar to Le Roux et al. (2015), silt content was assigned values between 10-22.5%, increasing with increase in clay as follows: percentage of landtype with <= 6% clay = 10% silt; 6.1-15% clay = 15% silt; 15.1-25% clay = 17.5% silt; 25.1-35% clay = 20% silt; 35.1-55% clay = 22.5% silt.
SAND1	Sand content of first soil layer (%)	Similar to Le Roux et al. (2015), sand content was estimated as follows: Sand = 100% – (%clay + %silt + %rock + %carbon).
ROCK1	Rock content of first soil layer (%)	The agricultural restriction/rock (MB) classes for each landtype was as follows: MB0=0%; MB1=20%; MB2=50%; MB3=20%; MB4=100% (no soil).
SOL_ALB1	Moist soil albedo	Moist soil albedo was assigned to the landtype based on texture of the dominant soil as follows: Sands = 0.25; clays = 0.7; remaining textures = 0.5 (Le Roux et al., 2015).
USLE_K1	USLE equation soil erodibility (K) factor	Erodibility was estimated using the Revised Universal Soil Loss Equation (RUSLE) (Le Roux et al., 2008).

Conventional weather gauge stations data including daily rainfall, temperature, wind speed, solar radiation and relative humidity were obtained from the Agricultural Research Council (ARC) and the South African Weather Services (SAWS). A total of 8 gauge stations were used, which include two ARC weather stations and 6 SAWS stations. Missing values were filled using data from the nearest gauge stations including National Centres for Environmental Prediction (NCEP) Climate Forecast System Reanalysis (CFSR) (Saha et al., 2010a) data. Monthly weather statistics required by SWAT to generate weather files were calculated using SWAT Weather Database tool (Essenfelder, 2016). Observed daily streamflow and nutrients data were obtained from the Department of Water and Sanitation's (DWS) central water quality database accessed from http://www.dwa.gov.za/iwqs/wms/data/. The DWS data has been collected since the early 1970s from the monitoring stations installed mostly in the rivers, tributaries, dams and canals. Nutrients concentration measurements were taken biweekly at best by the DWS with lots of intermittent data. As a result, concentrations of NH_4, TP and TN were determined on a monthly basis as an average of biweekly measurements from the DWS monitoring station located in the main sub-catchment outlet. We chose these variables because of the better quantity and quality of DWS data compared to other variables (e.g. NO_2, NO_3 and Mineral phosphorus) modelled in SWAT. Since nutrients data from DWS is measured in mg ℓ^{-1}, it was necessary to convert the measured nutrient concentrations (mg ℓ^{-1}) into nutrient loads (kg). To do this, monthly loads of NH_4, TP and TN were calculated as a product of monthly flow volume and nutrients concentrations in water (Abbaspour et al., 2007).

13.3.2 SWAT model setup

An ArcGIS-ArcView extension and graphical user input interface for SWAT version 2012, simply known as ArcSWAT 2012, was used to simulate streamflow, NH_4, TP and TN. The first major step undertaken was to delineate watershed or catchment into 34 sub-catchments using the NGI DEM. These sub-catchments were further subdivided into 459 hydrological response units (HRUs) based on a unique combination of land use / cover, soil and slope. The model was setup and simulated with the 8 gauge stations weather data obtained from the ARC and SAWS. Due to the lack of agricultural practices data for parameterization of the SWAT model in the study area, a generalization was made based on national crop growth and management statistics and information provided by the government official working in that area. A total of four major crops grown in the area were selected, including maize, wheat, lucerne and pecan nut. The crop growth and land management schedule adopted in this study is summarized in Table 58. A two-year crop rotation of maize and wheat under irrigation was defined. Crop management schedules for lucerne and pecan nut were also defined. SWAT auto-irrigation option was used, where irrigation is only applied when the soil moisture content drops below a threshold value. In addition, tile drainage management was defined with depth to subsurface drain of 1.8 m, time to drain soil to field capacity of 10 hours and drain tile lag time of 10 hours.

Table 58: Crop production and management schedules for maize, wheat, lucerne and pecan nuts (National Department of Agriculture, 2000; Food and Agriculture Organization of the United Nations, 2005; Department of Agriculture, Forestry and Fisheries, 2010; 2016)

Crops	Tillage date	Planting date	Fertilizer application (date and rate)	Harvest date
Maize (Year 1)	20 November	30 November	10 December, 150 kg N ha^{-1}, 150 kg P ha^{-1}	30 May
Wheat (Year 2)	05 June	10 June	10 June, 150 kg N ha^{-1}, 150 kg P ha^{-1}	30 November
Lucerne (Year 1)	10 March	20 March	20 March, 150 kg N ha^{-1}, 150 kg P ha^{-1}	20 August
Pecan nut (Year 1)	10 July	20 July	20 July (Year 2, 3, 4), 100 kg N ha^{-1}, 100 kg P ha^{-1}	20 May (Year 4-17)

Simulation was performed on a monthly time step for a period of 17 years (2000 to 2016). The first three years, i.e. 2000 to 2002 were treated as a warm-up period, usually recommended in order to get the hydrological cycle fully operational (see Ji and Luo, 2013). SWAT simulation was executed at HRUs level and results were then aggregated for the sub-catchments using a weighted average method.

13.3.3 Calibration and performance evaluation

Calibration of the SWAT model was performed using “trial and error method” of manual calibration approach, which involves manual tuning of the model input parameters until satisfactory results are achieved (Henriksen et al., 2003). First, we identified flow and nutrients load related parameters to be optimized based on their role and importance in runoff generation and nutrients transport. Here, various literature sources were also consulted in order to obtain parameters related to both streamflow and nutrients transport. Table **59** shows a list of parameters identified and their initial and final calibrated value in our study area. A total of 13 parameters were selected in the calibration phase. Three parameters are related to flow (CH_N2, CN2 and OV_N) whereas the rest are related to nutrients load.

Table 59: List of parameters adjusted during model calibration

Parameter	Description	Default value	Calibrated value
OV_N	Manning's "n" value for overland flow	0.15	0.05
CH_N2	Manning's roughness coefficient, "n", for channel flow	0.014	0.3
CN2	Initial SCS runoff curve number for moisture condition	69	90
SOL_NO3	Initial NO3 concentration in the soil layer	0	0.03
SOL_ORGN	Initial organic N concentration in the soil layer	0	0.03
SOL_LABP	Initial soluble P concentration in soil layer	0	0.03
SOL_ORGP	Initial organic P concentration in soil layer	0	0.03
RCN	Concentration of nitrogen in rainfall	0	0.5
CMN	Rate factor for humus mineralisation of active organic nitrogen	0.003	0.001
N_UPDIS	Nitrogen uptake distribution parameter	20	80
P_UPDIS	Phosphorus uptake distribution parameter	20	80
NPERCO	N percolation coefficient	0.2	1
PPERCO	P percolation coefficient	10	17.5

The results of the SWAT were loaded into the SUFI-2 algorithm of the SWAT-CUP software in order to assess the performance of the model calibration. We used three commonly used statistical measures to evaluate the performance of the model. This include the coefficient of determination (R^2), Nash-Sutcliffe efficiency (NS) and Percent Bias (PBIAS) statistical measures. The R^2 describes the degree of collinearity between simulated and measured data whereas the NS determines the relative magnitude of the residual variance ("noise") compared to the measured data variance ("information"). The PBIAS measures the average tendency of the simulated data to be larger or smaller than the observed data (Moriasi et al., 2007; Ayele et al., 2017). Generally, a value of R^2 and NS >0.5 is regarded as acceptable model performance, whereas a value <0.5 is interpreted as poor model performance. A PBIAS of <25

is regarded as satisfactory and >25 is interpreted as poor performance (Moriasi et al., 2007). Performance evaluation was carried out by comparing the flow and nutrients load simulation against the measured data for the period 2003 to 2010, whereas data for the period 2011 to 2016 was reserved for validation.

13.4 Results and discussion

13.4.1 Flow calibration results

The calibrated SWAT streamflow simulation was not too drastically different with the measured flow in terms of the graphical representations and the R^2 statistical measure (Figure 95). Most importantly, the major peak flow events were reasonably simulated, although peak flow values were too low. In addition, the pre-calibrated streamflow simulation generated peak flows that are inconsistent with the measured flows and the base flow was too low. Other statistical measures such as the NS and PBIAS suggest that the model performed poorly.

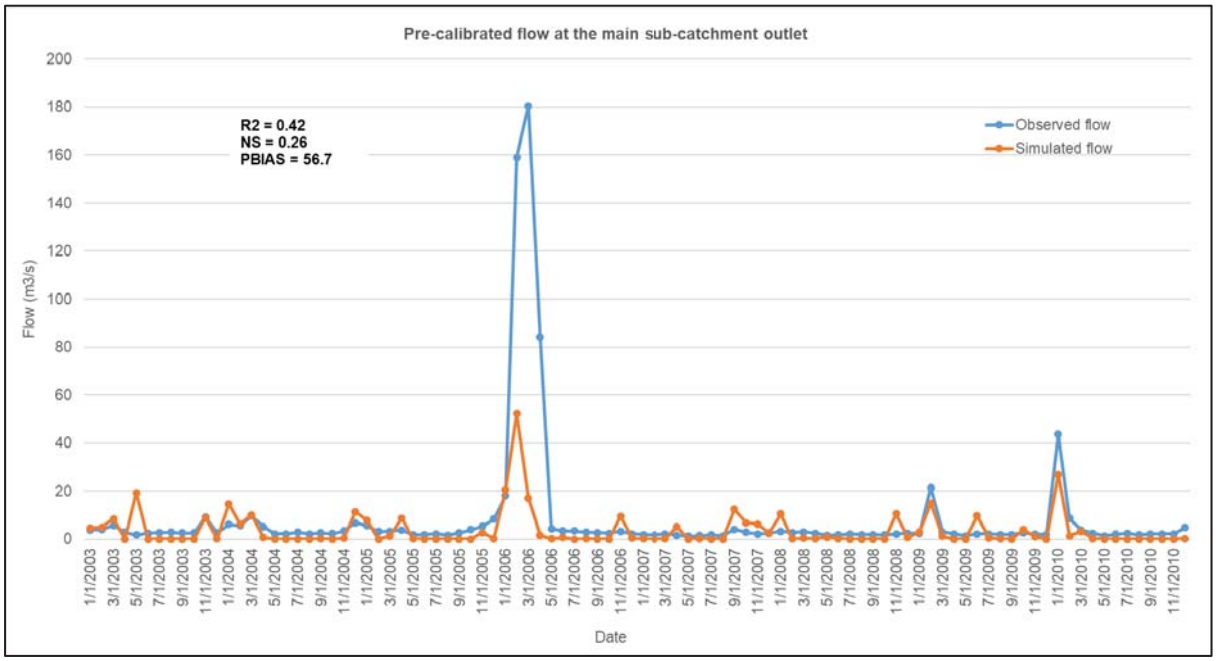

Figure 95: Measured and calibrated simulated flow at the main sub-catchment outlet with the values of R2 and NS statistical measures

13.4.2 Nutrients load calibration results

The nutrients load parameters calibrated in this study include the NH_4, TP and TN. Calibration of the model for nutrients load was a challenging task since the pre-calibrated simulation (not shown here) did not produce a reasonable match between the simulated and measured data in terms of the graphical representation and both the R^2 and NS statistical measures. The calibrated nutrient loads time series graphs for the NH_4, TP and TN at the main sub-catchment outlet are shown in Figure 96, Figure 97 and Figure 98. The NH_4 load simulation managed to reproduce some of the peak flow events discernible from the measured data, hence the R^2 and the NS values are slightly better than those of the TP and TN load simulation. Nevertheless, both the NH_4, TP and TN loads were underestimated most of the

time, except for some of the higher peaks generated during the simulation of TP. The general assumption made from other previous studies is that reasonable estimation of the flow is a prerequisite for sensible nutrient modelling (e.g. Lam et al., 2010; Jiang and Rode, 2012). Clearly, our study demonstrates that nutrients modelling has its own uncertainty issues that need to be addressed separately before any meaningful simulation and calibration is achieved.

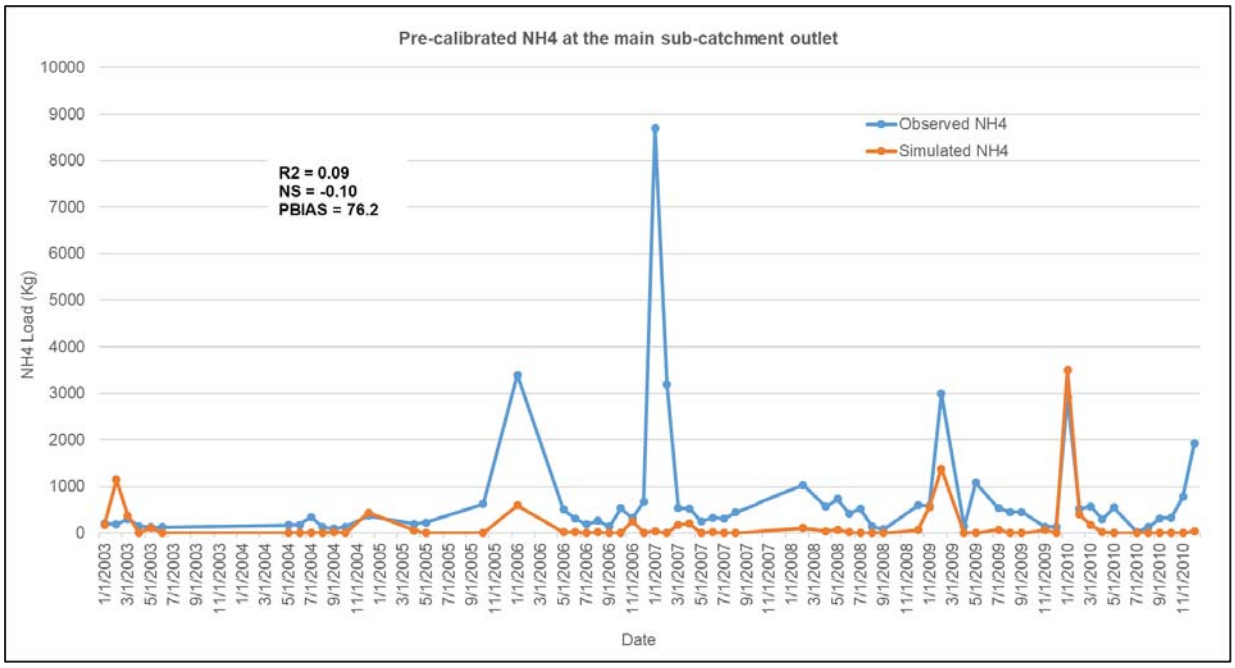

Figure 96: Measured and pre-calibrated simulated NH4 at the main sub-catchment outlet with the values of R2, NS and PBIAS statistical measures

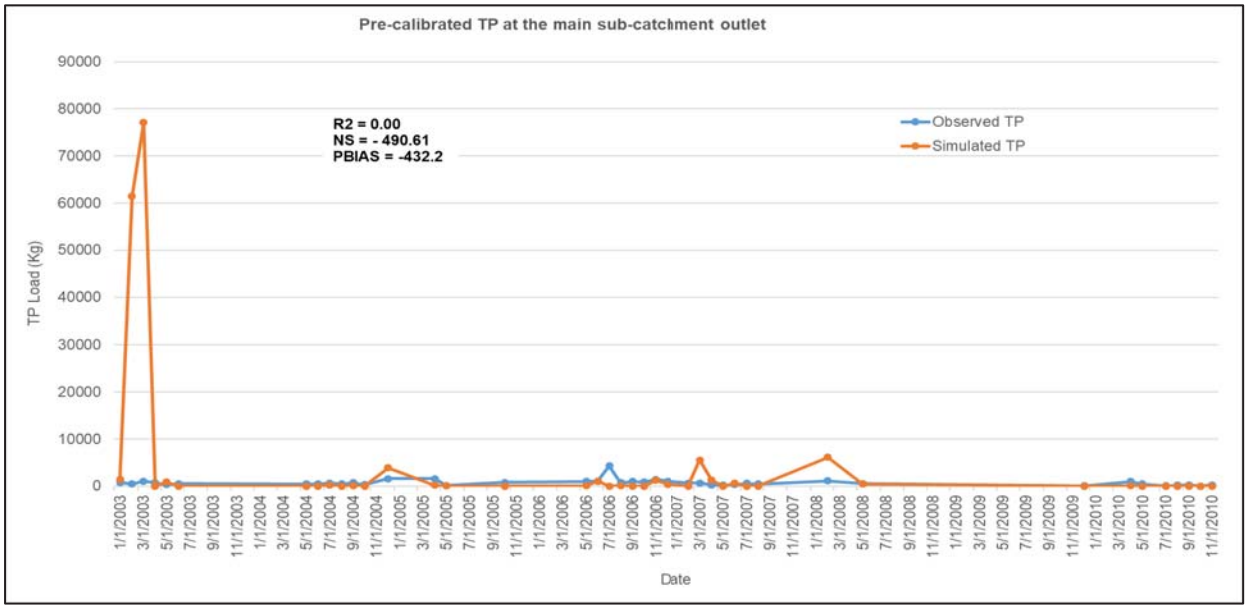

Figure 97: Measured and pre-calibrated simulated TP at the main sub-catchment outlet with the values of R2, NS and PBIAS statistical measures

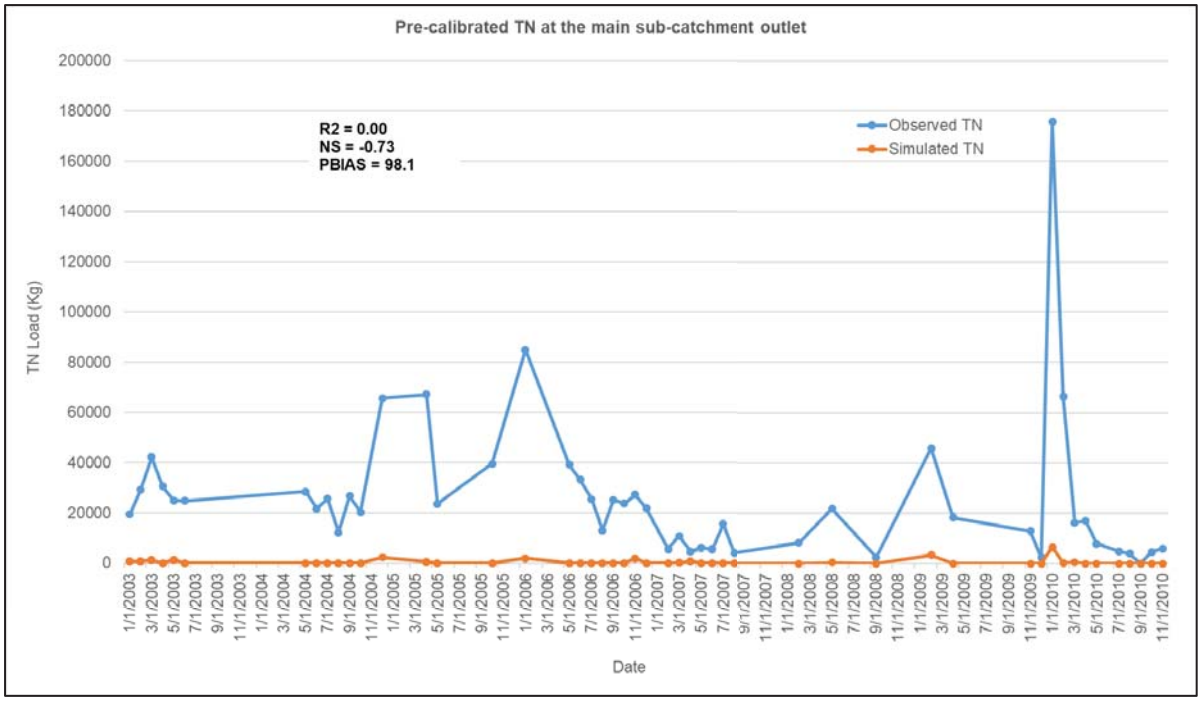

Figure 98: Measured and pre-calibrated simulated TN at the main sub-catchment outlet with the values of R2, NS and PBIAS statistical measures

Calibration of the model was made worse in our study due to the limited measured nutrients load data required to evaluate the model comprehensively. The accuracy of the model calibration depends critically on the quality of the calibration data used (Williams and Esteves, 2017). In our study, the available nutrients load data used was of poor quality due to gaps and missing values in the data. In addition, the nutrients data were obtained as concentration measurements, which was then converted into loads. As a result, the quality of nutrients load data is dependent on the quality of flow data.

13.4.3 Calibration uncertainty issues

Manual calibration of a hydrological model at catchment scale tend to suffer from a lot of uncertainty issues. These issues emanate from uncertainties over input parameters and their value range. For example, in this study, increasing CN2 resulted in the model increasing the smaller peaks in base flow. As a result, CN2 was subsequently reduced, to ensure satisfactory R^2 statistical measure. During auto-calibration, the parameters are adjusted in such a way that the behaviour of the model approximates, as closely and as consistently as possible, the observed response of the hydrologic system (Vrugt et al., 2005). Uncertainties in the model calibration procedure do not only comes from obtaining the accurate value estimates of the input parameter, but also emanate from measurement errors associated with the system input (forcing) and output, and from model structural errors arising from the aggregation of spatially distributed real-world processes into a mathematical model. Not properly accounting for these errors during model calibration, can result in model simulations and associated prediction uncertainty bounds, which do not consistently represent and bracket the measured system behaviour (Vrugt et al., 2005; Abbaspour et al., 2007; Abbaspour et al., 2015). Unlike in auto-calibration, manual

calibration requires in-depth knowledge of the catchment and is laborious in its approach. It is very important to account for uncertainties in the model during calibration since this can have a great impact on the model reliability.

13.5 Conclusion

In this study the hydrological model SWAT was applied to simulate streamflow, NH_4, TP and TN loads from irrigated cropping systems in the lower Vaal River catchment. Comparison of the field measurements data and the simulated results illustrated in the hydrographs and R^2 statistical measure suggests that streamflow prediction from SWAT was satisfactorily modelled. Therefore, we consider our modelled streamflow results a fair representation of the hydrological system in the lower Vaal River catchment because other statistical measures did not perform satisfactorily. However, SWAT model application failed to simulate the nutrients load satisfactorily in the study area. With better data and further adjustment of the model parameters, it is anticipated that simulation of the nutrients load can be substantially improved. Future research plan was to use the results of this study to extrapolate the SWAT simulation to a larger catchment. It is therefore suggested that, before any upscaling or extrapolation study is undertaken, the results for the smaller catchment need to be improved. Since manual calibration is laborious and time consuming and does not fully address most of the model uncertainty issues, it is proposed that calibration be continued using automated method such as the SUFI-2 algorithm of the SWAT-CUP software.

13.6 References

ABBASPOUR, K.C., ROUHOLAHNEJAD, E., VAGHEFI, S., SRINIVASAN, R., YANG, H., KLØVE, B. (2015) A continental-scale hydrology and water quality model for Europe: Calibration and uncertainty of a high-resolution large-scale SWAT model. J. Hydrol. 524, 733-752. https://doi.org/10.1016/j.jhydrol.2015.03.027

ABBASPOUR, K.C., YANG, J., MAXIMOV, I., SIBER, R., BOGNER, K., MIELEITNER, J., ZOBRIST, J., SRINIVASAN, R. (2007) Modelling hydrology and water quality in the pre-alpine/alpine Thur watershed using SWAT. J. Hydrol. 333, 413-430. https://doi.org/10.1016/j.jhydrol.2006.09.014

AYELE, G.T., TESHALE, E.Z., YU, B., RUTHERFURD, I.D., JEONG, J. (2017) Streamflow and sediment yield prediction for watershed prioritization in the upper Blue Nile river basin, Ethiopia. Water (Switzerland) 9, 1-29. https://doi.org/10.3390/w9100782

BIANCHI, M., HARTER, T. (2002) Nonpoint Sources of Pollution in Irrigated Agriculture. ANR Publ. 8055; Univ. California, Div. Agric. Nat. Resour. Calif. 1-8. https://doi.org/pr-9/02-WJC

CROP ESTIMATES CONSORTIUM (2017a) Field crop boundary data layer (Free State province), 2017. Department of Agriculture, Forestry and Fisheries. Pretoria.

CROP ESTIMATES CONSORTIUM (2017b) Field crop boundary data layer (NC province), 2017. Department of Agriculture, Forestry and Fisheries. Pretoria.

CROP ESTIMATES CONSORTIUM (2017c) Field crop boundary data layer (NW province), 2017. Department of Agriculture, Forestry and Fisheries, Pretoria.

DEPARTMENT OF AGRICULTURE FORESTRY AND FISHERIES (2016) Production guideline for wheat. Dep. Agric. For. Fish. Pretoria 1-25.

DEPARTMENT OF WATER AND SANITATION (DWS) (2014) Determination of Resource Quality Objectives in the Lower Vaal Water Management Area (WMA10): Resource Quality Objectives and Numerical Limits Report. Report No.: RDM/WMA10/00/CON/RQO/0214. Chief Directorate: Water Ecosystems. Study No.: WP10535. Pietermaritzburg, South Africa.

ESSENFELDER, A.H. (2016) SWAT weather database: A quick guide. https://doi.org/10.13140/RG.2.1.4329.1927

FOOD AND AGRICULTURE ORGANIZATION OF THE UNITED NATIONS (2005) Fertilizer use by crop in South Africa. FAO, Rome.

GAO, L., LI, D. (2014) A review of hydrological/water-quality models. Front. Agric. Sci. Eng. 1, 267. https://doi.org/10.15302/J-FASE-2014041

GEOTERRAIMAGE, 2015. 2013-2014 South African national land-cover dataset. GEOTERRAIMAGE Pty Ltd., Pretoria. Available on website: http://egis.environment.gov.za/national_land_cover_data_sa. Accessed: July 2017

HENRIKSEN, H.J., TROLDBORG, L., NYEGAARD, P., SONNENBORG, T.O., REFSGAARD, J.C., MADSEN, B. (2003) Methodology for construction, calibration and validation of a national hydrological model for Denmark. J. Hydrol. 280, 52-71. https://doi.org/10.1016/S0022-1694(03)00186-0

JHA, M.K., ARNOLD, J.G., GASSMAN, P.W. (2006) Water Quality Modeling for the Raccoon River Watershed Using SWAT. Ames.

JI, X., LUO, Y. (2013) The influence of precipitation and temperature input schemes on hydrological simulations of a snow and glacier melt dominated basin in Northwest China. Hydrol. Earth Syst. Sci. Discuss. 10, 807-853. https://doi.org/10.5194/hessd-10-807-2013

JIANG, S., RODE, M. (2012) Modeling water flow and nutrient losses (nitrogen, phosphorus) at a nested meso scale catchment, Germany, in: Seppelt, R., Voinov, A.A., Lange, S., Bankamp, D. (Eds.), 2012 International Congress on Environmental Modelling and Software Managing Resources of a Limited Planet, Sixth Biennial Meeting. International Environmental Modelling and Software Society (iEMSs), Leipzig, Germany.

LAM, Q.D., SCHMALZ, B., FOHRER, N. (2010) Modelling point and diffuse source pollution of nitrate in a rural lowland catchment using the SWAT model. Agric. Water Manag. 97, 317-325. https://doi.org/10.1016/j.agwat.2009.10.004

LAND TYPE SURVEY STAFF (1984) Landtypes of South Africa: digital map (1:250 000 scale) and soil inventory databases. ARC-Institute for Soil, Climate and Water, Pretoria.

LE ROUX, J.J., BARKER, C.H., WEEPENER, H.L., VAN DEN BERG, E.C., PRETORIUS, S.N. (2015) Sediment yield modelling in the Mzimvubu River catchment. WRC Report No. 2243/1/15. Water Research Commission, Pretoria.

LE ROUX, J.J., MORGENTHAL, T.L., MALHERBE, J., D.J., P., SUMNER, P.D. (2008) Water erosion prediction at a national scale for South Africa. Water SA 34, 305-314.

MORIASI, D.N., ARNOLD, J.G., VAN LIEW, M.W., BINGNER, R.L., HARMEL, R.D., VEITH, T.L. (2007. Model Evaluation Guidelines for Systematic Quantification of Accuracy in Watershed Simulations. Trans. ASABE 50, 885-900. https://doi.org/10.13031/2013.23153

MUCINA, L. AND RUTHERFORD, M.C. (Eds.) (2006) The vegetation of South Africa, Lesotho and Swaziland. Strelitzia 19. South African National Biodiversity Institute (SANBI), Pretoria.

NATIONAL DEPARTMENT OF AGRICULTURE (2000) Cultivating pecan nuts. Natl. Dep. Agric. Pretoria 1-10.

SAHA, S., MOORTHI, S., PAN, H.L., WU, X., WANG, J., NADIGA, S., TRIPP, P., KISTLER, R., WOOLLEN, J., BEHRINGER, D., LIU, H., STOKES, D., GRUMBINE, R., GAYNO, G., WANG, J., HOU, Y.T., CHUANG, H.Y., JUANG, H.M.H., SELA, J., IREDELL, M., TREADON, R., KLEIST, D., VAN DELST, P., KEYSER, D., DERBER, J., EK, M., MENG, J., WEI, H., YANG, R., LORD, S., VAN DEN DOOL, H., KUMAR, A., WANG, W., LONG, C., CHELLIAH, M., XUE, Y., HUANG, B., SCHEMM, J.K., EBISUZAKI, W., LIN, R., XIE, P., CHEN, M., ZHOU, S., HIGGINS, W., ZOU, C.Z., LIU, Q., CHEN, Y., HAN, Y., CUCURULL, L., REYNOLDS, R.W., RUTLEDGE, G., GOLDBERG, M. (2010) Supplement to the NCEP Climate Forecast System Reanalysis. Bull. Am. Meteorol. Soc. 9-25. https://doi.org/10.1175/2010BAMS3001.2

SAXTON, K.E., RAWLS, W.J. (2006) Soil Water Characteristic Estimates by Texture and Organic Matter for Hydrologic Solutions. Soil Sci. Soc. Am. J. 70, 1569-1578. https://doi.org/10.2136/sssaj2005.0117

SCHULZE R.E. (2007) South African Atlas of Climatology and Agrohydrology. WRC Report No. 1489/1/06. Water Research Commission. Pretoria.

SCHULZE, R.E. (Ed.) (2010) Atlas of climate change and the South African agricultural sector: a 2010 perspective. Department of Agriculture, Forestry and Fisheries. Pretoria.

SCHULZE, R.E. (1995) Hydrology and agrohydrology: A text to accompany the ACRU 3.00 agrohydrological modelling system. WRC Report No. TT69/95. Water Research Commission. Pretoria.

VRUGT, J.A., DIKS, C.G.H., GUPTA, H. V, BOUTEN, W., VERSTRATEN, J.M. (2005) Improved treatment of uncertainty in hydrologic modelling: Combining the strengths of global optimization and data assimilation. Water Resour. Res. 41, 1-17. https://doi.org/10.1029/2004WR003059

WILLIAMS, J.J., ESTEVES, L.S. (2017) Guidance on Setup, Calibration, and Validation of Hydrodynamic, Wave, and Sediment Models for Shelf Seas and Estuaries. Adv. Civ. Eng. 2017, 1-26. https://doi.org/https://doi.org/10.1155/2017/5251902

YANG, X., WU, X., HAO, H., HE, Z. (2008) Mechanisms and assessment of water eutrophication. J. Zhejiang Univ. Sci. B 9, 197-209. https://doi.org/10.1631/jzus.B0710626

14 INVESTIGATING NITROGEN AND PHOSPHOROUS POLLUTION IN THE MIDDLE OLIFANTS

L. Mudaly and M. van der Laan
Department of Plant and Soil Sciences, University of Pretoria, Pretoria 0002, South Africa

14.1 Introduction

South Africa is located in a predominantly semi-arid part of the world with an average rainfall of approximately 450 mm per annum for the country. This figure is well below the world average of 860 mm per annum. Water resources are already fully allocated in a number of catchments in South Africa. This intensive utilization has led to a degradation of river water quality and it is anticipated to deteriorate further due to the growing population and urbanisation in our country (Department of Water Affairs and Forestry, 2004). Eutrophication is a symptom of one of the major problems associated with degraded water quality.

Eutrophication is the process of nutrient enrichment and the associated excessive plant growth in water. Natural eutrophication is caused by the influx of nutrients from natural resources, such as rocks and soil, within a catchment area (Van Ginkel, 2011) as well as nitrogen (N) and phosphorus (P) loading from the domestic, agricultural and industrial sectors (Nel, 2013). Ideal conditions for eutrophication are high nutrient concentrations and water stagnation for long periods, coupled with suitable temperatures, oxygen concentrations and an appropriate light regime. These conditions result in the growth of algae, mycrophytes and other aquatic plants, which in turn results in severe blooms and eutrophication, negatively impacting water quality (Nel, 2013; Van Ginkel, 2011). Eutrophication is recognized as a major challenge to water security in our country (Nel, 2013). Nutrient pollution and the development of algal blooms associated with eutrophication are considered two of the largest threats to South Africa's freshwater resources (Dabrowski, 2014).

One of the major drivers of eutrophication is P as it is most often the limiting nutrient in freshwater systems. Point sources of P originate from mining activities and sewage treatment effluent. A source of non-point source (NPS) P export is from the removal of vegetation, exposing bare soil and weathering rock to erosion, resulting in potentially high losses of naturally occurring P. One of the most common sources of P pollution in freshwater resources originates from agricultural runoff (from fertilizers and manure) (Dabrowski, 2014). This study looked at N and P concentrations in water sources in the Middle Olifants catchment.

14.1.1 Study area

The Olifants Catchment (Figure 1) falls within three Provinces; Gauteng, Mpumalanga and Limpopo, and is shared by South Africa, Botswana, Zimbabwe and Mozambique. The river originates near Bethel on the Mpumalanga Highveld, flows through the Kruger National Park and finally into Mozambique. At the end of its journey it merges with the Limpopo River before discharging into the Indian Ocean. The catchment covers approximately 54550 km^2, and the main tributaries on the left bank are the Wilge, Elands and Ga-Selati Rivers, and on the right bank the main tributaries are the Steelpoort, Blyde,

Klaserie and Timbavati Rivers. There are distinct differences in climate from the cool Highveld in the South to subtropical conditions in the East. The mean annual rainfall ranges between 500-800 mm per year over most of the catchment (Department of Water Affairs, 2011b). The elevation in the Olifants Basin ranges from 300-2300 m and annual temperatures varying between -4 and 45°C (Udall, 2018).

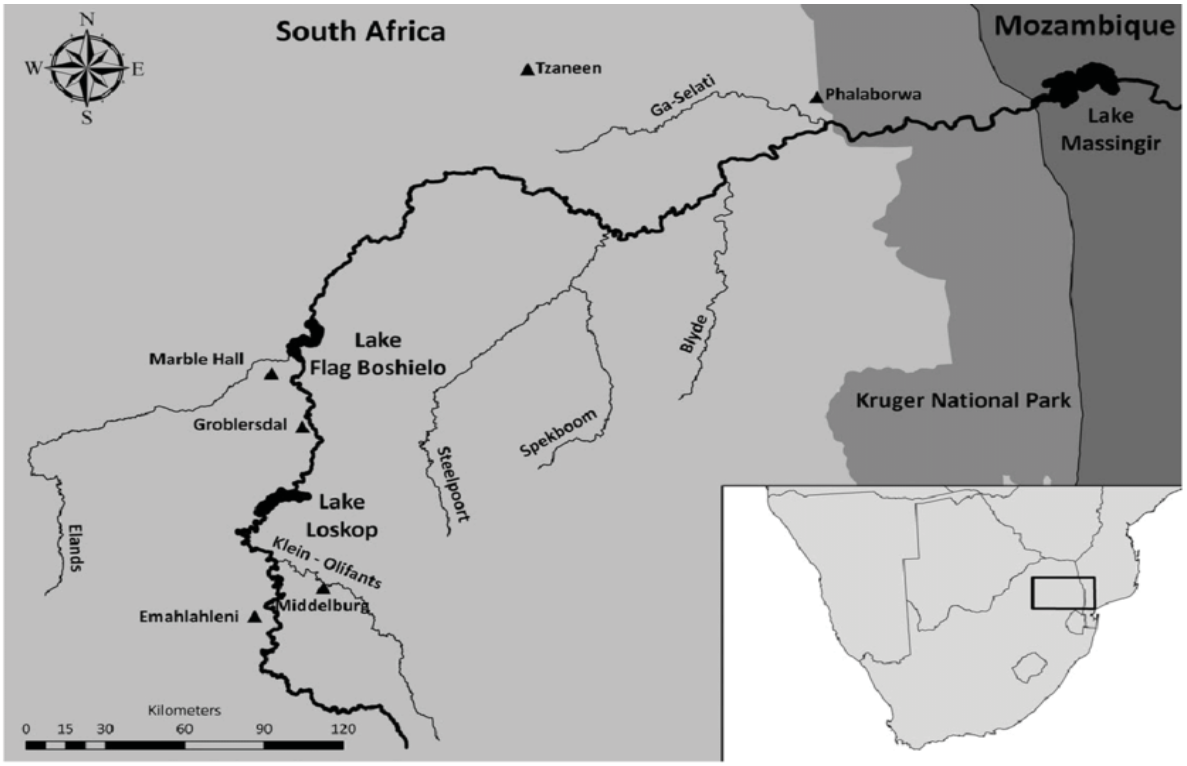

Figure 99: The Olifants River catchment in South Africa (Huchzermeyer et al., 2017)

Formal economic activity in this water management area (WMA) is highly diverse and characterized by commercial and subsistence agriculture (both irrigated and rain-fed), diverse mining activities, manufacturing, commerce and tourism. Land use in the Olifants WMA is just as varied and consists of irrigated and dryland cultivation, grazing, mining, industry, forestry, urban and rural settlements. The area also has many tourist destinations including the Blyde River Canyon and the Kruger National Park (Department of Water Affairs, 2011a). The Olifants can be divided into the Upper, Middle and Lower Olifants catchments (Figure 100).

The Upper Olifants is located upstream of Loskop Dam and includes the Wilge and Klein Olifants Rivers (Singh, 2001). The primary economic activities in this area come from the mining and industrial sectors situated in Witbank / Middleburg, Phalaborwa and Steelpoort. Some of the world's largest thermal power stations can be found in the Upper Olifants (Department of Water Affairs, 2011a). The Middle Olifants is located in the area between Loskop Dam and Penge and has four main tributaries, the Selons, Moses, Elands and Mohlapitse Rivers (Singh, 2001). Extensive irrigation is the main economic activity in this area. Platinum, chrome and vanadium mining is prominent (Department of Water Affairs, 2013). A large informal economy exists in the Middle Olifants with many resource-poor farmers dependent on ecosystem services (Department of Water Affairs, 2011a). The Lower Olifants lies between Penge and

the Mozambique border. The three main tributaries of the Lower Olifants are the Steelpoort, Selati and Blyde Rivers (Singh, 2001). Phosphate and copper mining is associated with the Lower Olifants (Department of Water Affairs, 2013).

Figure 100: The Upper, Middle and Lower Olifants (Biggs et al., 2017)

This study focuses on the Middle Olifants, where most of the agricultural activity occurs. Based on the hydrology, it is sub-divided into five tertiary catchments. The Middle Olifants is the third most water stressed basin in South Africa (Walter et al., 2011). It has an area of 22 550 km^2 and receives 500 mm of rainfall per annum. One of the main water users in this area are urban and rural households. The Middle Olifants has predominantly rural character with scattered formal and informal villages. The Middle Olifants is home to approximately 60% of the total Olifants basin population. Households in this area are historically disadvantaged with limited access to water. The other primary water users are the mining industry and large-scale agriculture (Walter et al., 2011).

Our study area in the Middle Olifants goes up to Flag Boshielo Dam. This area includes the towns of Marble Hall, Groblersdal and Roedtan. The economy is characterized by some intensive irrigated agriculture (particularly in Marble Hall and Groblersdal areas), commercial dryland agriculture (in the Springbok flats) and some subsistence agriculture. There is also platinum mining in this area. The population here is approximately 366 051 people (Department of Water Affairs, 2011a).

14.1.2 Mining in the Middle Olifants

Mining activities in the Middle Olifants is dominated by platinum – the Bushveld Igneous Complex is the largest and most valuable layered intrusion in the World. It holds half of the global reserve of platinum, chromium and vanadium. The ore reserves could last for hundreds of years into the future. There are significant reserves of tin, fluorite and copper as well. The Blue Ridge Platinum Mine (operated by Aquarius) is responsible for mining activities here. It is located 15 km from the Groblersdal town and produces about 992 kg of platinum annually (Department of Water Affairs, 2011a).

14.1.3 Agricultural activity in the Middle Olifants

The study area is heavily reliant on the agricultural sector (Department of Water Affairs, 2011a). There are several large-scale irrigation farmers who grow high value crops such as citrus and grapes, which require large volumes of water for their production (Department of Water Affairs, 2011a; Walter et al., 2011). Much of this produce is exported globally (Walter et al., 2011). The total area under agriculture is about 229 713 ha. Dryland agriculture accounts for 114 394 ha and irrigated agriculture 49 821 ha. Subsistence farming takes up about 65 499 ha. The dominant crops in the irrigation area are maize, citrus and wheat (Oberholster and Botha, 2011). Table 60 shows the irrigated crop profile in the Middle Olifants expressed as a percentage of the area it occupies as well as the irrigation season for the crops. Citrus, maize and wheat cover the largest areas with citrus and maize having equal coverages of 23.1% each. Tobacco and leafy vegetables also cover equal areas of 8% each. Irrigation in the Loskop area occurs throughout the year with some crops irrigated for all 12 months and others irrigated seasonally.

Table 60: Irrigated crop profile of the Loskop area (de Lange et al., 2016)

Crop	**Hectares**	**%**	**Irrigation season**
Citrus	5 879	23.1	12 months (with peaks in September/October & December to February
Maize	5 869	23.1	August-February
Wheat	5 070	20.0	May-Early October
Tobacco	2 112	8.3	October-March
Leafy vegetables	1 914	7.5	-
Peas	1 570	6.2	May-Early August
Cotton	1 209	4.8	October-April
Table grapes	942	3.7	12 months
Other	845	3.3	• Peas: May-Early August • Soybean: November-April • Groundnuts: October-March
Total	**25 410**	**100**	

14.1.4 Water quality problems in the Middle Olifants

The water quality problems in the Middle Olifants arise from salinity, eutrophication, toxicity and sediment. Poor agricultural practices resulting in overgrazing in rural areas is largely responsible for sedimentation. Sediment production in the Middle Olifants causes operational problems downstream. Salinity and eutrophication problems are a result of mining impacts, sewage treatment plant discharges and irrigation return flows, (Department of Water Affairs, 2011a). In South Africa, microalgae, especially *Cladophora glomerata*, is a significant problem in irrigation canals and potable water systems (Oberholster and Botha, 2011).

Filamentous green algae thrive under eutrophic condition. Although these algae do not pose a direct threat to crops, it affects the operational efficiency of irrigation systems and therefore the operation and maintenance costs of irrigation infrastructure (de Lange et al., 2016). Algae is a serious problem in the Olifants irrigation scheme (Department of Water Affairs, 2013). A study conducted by De Lange et al. (2016) looked at the economic impact of filamentous green algae on commercial agriculture. When the study commenced in the Loskop area it was found that the loads of filamentous green algae were so high that it decreased the volume and flow tempo of the main canal to the extent that the canal could not serve the weekly demand (de Lange et al., 2016). Besides decreasing the carrying capacity of the canals, detached algae continuously drift down the sediment channels, clogging the control gates and crop sprayers (Oberholster and Botha, 2011). On the other hand, canal structure has often flooded due to algae taking up volume and increasing the water level (Department of Water Affairs, 2013).

Algal mat formation does not occur uniformly throughout the canal and ward managers have to monitor their respective canal sections (consisting of 5 to 8 km) regularly and dose when necessary. This algae is controlled chemically with copper sulphate (de Lange et al., 2016). The Loskop Irrigation Scheme has radial gates along the canal structure to assist in the copper sulphate dosing for the reduction of algae (Department of Water Affairs, 2013). Each dosage affects approximately 5 to 6 km of canal and the canal is rarely dosed in entirety (de Lange et al., 2016). Dosing is conducted once every two months and sometimes the concentration is diluted and applied more often in order to prevent algae from causing water levels to rise and canals to overflow (Department of Water Affairs, 2013). Copper sulphate dosage is a sensitive issue because it is absorbed by plants and can negatively impact human and ecosystem health, therefore dosage levels are important (de Lange et al., 2016). Figure 101 is a photo taken of an irrigation canal during a sampling visit that was conducted after dosing of the canals. A blue-green colour was observed and a strong odour was emitted from the water.

A study by Oberholster and Botha (2011) showed evidence that the poor water quality in Loskop Dam, which contained high concentrations of phosphates, stimulated the growth of the nuisance algal *Cladophora glomerata* in the irrigation canals downstream (depicted in Figure 102). Water quality concerns in Loskop Dam besides eutrophication, and associated *Microcystis* blooms, include acid mine drainage related impacts and the pansteatitis disease in crocodiles and Mozambique tilapia (Dabrowski et al., 2014). The location of Flag Boshielo downstream of Loskop Dam means that it is susceptible to the same water quality impacts in the upper catchment. Pansteatitis was reported even further

downstream in the Olifants River in the Kruger National Park (Dabrowski et al., 2014). This further validates the urgency to improve water quality in the Middle Olifants catchment.

Figure 101: Water that was released from Loskop Dam into an irrigation canal after copper sulphate dosing

Figure 102: Filamentous green algae in the Loskop area (photo by PJ Oberholster) (Oberholster and Botha, 2011)

Once the water passes through the sluice gate at the take-off point, the algae becomes the farmer's responsibility. Algae obstructs and clogs strainers, intake valves and manifolds. It also places a higher load on impellers (rotors used to increase pressure and flow of fluids) and bearings of pumps, which decreases delivery rates resulting in a decrease in the volume pump per hour. Micro-jets and dripper lines also get clogged, resulting in uneven and sub-optimal moisture management in orchards. This could affect crop yield if not mitigated (de Lange et al., 2016).

The study by De Lange et al. (2016) conducted a survey with farmers in the area and it was revealed that participants were acutely aware of the problem and its effects on their profitability through an increase in operational and maintenance costs. There is a cost implication as increased mechanical and chemical cleaning of the system is required in order to maintain the operational efficiency of the irrigation systems. This cleaning includes a more frequent dosage of on-farm balancing dams with copper sulphate, more frequent cleaning of foot valves, intake manifolds, filter-banks, and the nozzles of micro-jets, center-pivot and drippers. Hydrogen peroxide is often used to clean the center-pivot system, although some farmers argue that peroxide shortens the life span of all plastic components by making them brittle (de Lange et al., 2016).

14.1.5 Water scarcity in the Middle Olifants

Irrigated agriculture is the largest water use in South Africa, accounting for more than 60% of water use nationally (Department of Water Affairs, 2013). The Olifants WMA is a highly utilized and regulated catchment. Like many other water management areas in South Africa, its water resources are becoming more stressed due to an accelerated rate of development and the scarcity of water resources (Department of Water Affairs, 2011a). Figure 103 shows a prediction that the Olifants is one of the few catchments that will experience a severe gap between existing supply and projected demand by the year 2030 (McKinsey and company, 2009).

The Middle Olifants is experiencing growing competition between water users, overuse of water resources and imbalanced water distribution. Over abstraction of groundwater resources has also led to the decrease of groundwater levels in this area. Water requirements (395 $Mm^3\ a^{-1}$) exceed availability (301 $Mm^3\ a^{-1}$) resulting in a deficit (Walter et al., 2011). The scheme is currently fully allocated with deficit irrigation fast becoming the norm (de Lange et al., 2016). It is therefore imperative to reduce water losses and improve irrigation water use efficiency in irrigation schemes to ensure a high economic return for the scheme area (Department of Water Affairs, 2013). Increasing water scarcity in South Africa requires optimal management of this resource (Van der Laan et al., 2012).

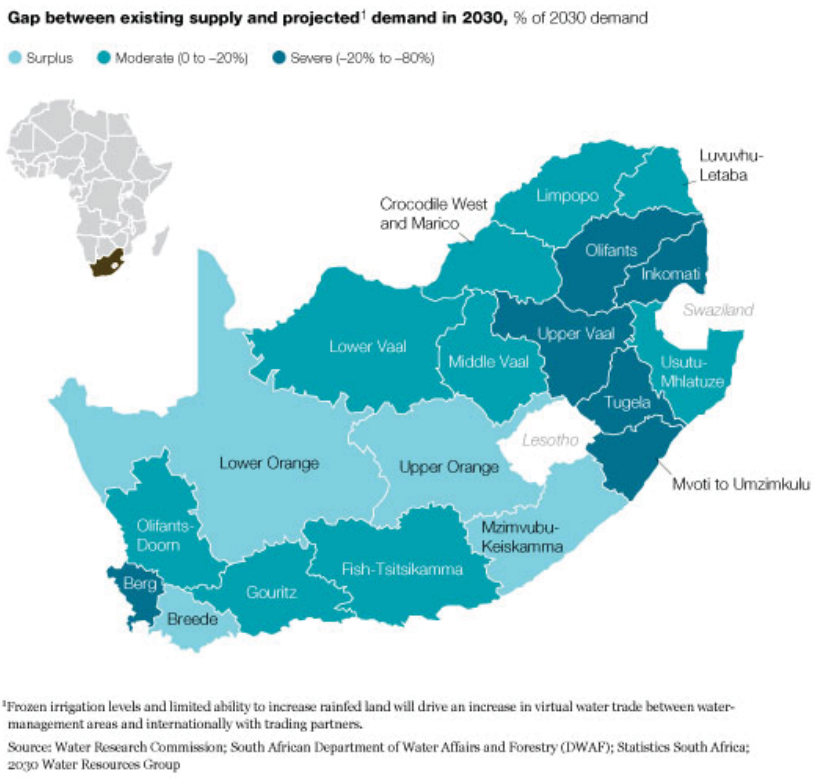

Figure 103: Predicted future gap between existing supply and projected demand (McKinsey and Company, 2009)

14.1.6 The Loskop Irrigation Scheme

In order to understand the influence of irrigated agriculture in the Middle Olifants catchment on water quality downstream, it is important to understand the Loskop Irrigation Scheme. Loskop irrigation scheme falls within drainage region B3H017 and therefore forms part of the Olifants WMA (de Lange et al., 2016). Loskop Dam (situated in Mpumalanga, South Africa) is fed by the Olifants River. The dam construction commenced in the mid-1930s and was completed in the early-1940s. The purpose of the dam was to supply water to the agricultural sector. The mean annual precipitation of this area is 683 mm and the mean annual runoff is 10 780 Mm^3 (Oberholster and Botha, 2011).

The Loskop irrigation scheme is the second largest in South Africa (Oberholster, 2011; Dabrowski, 2014). Infrastructure supplying the irrigation scheme consists of Loskop Dam, seven balancing dams, 135 km of concrete-lined main canal, and 345 km of service canals (de Lange et al., 2016). The irrigation scheme was constructed between 1933 and 1940. The scheme has an irrigation area of 25 600 ha and a total of approximately 480 km of irrigation canals. The water supply for the irrigation scheme is abstracted from the upper-hypolimnia of Loskop Dam and is transferred to crops through the use of two concrete canals. The distance of these two canals is approximately 46 km of short canal and 330 km of long canal (Oberholster and Botha, 2011). The canal structure is old and the concrete is deteriorating

in places. Some of the canal sections have shifted from their original positions due to age and soil conditions, resulting in cracks and possible leakages (Department of Water Affairs, 2013).

Water is managed via a demand-based approach. Demand scheduling is operated via eight wards and water users request their water from ward managers a week in advance. Water is supplied through 660 calibrated and registered sluice gates delivering 197 890 m^3 per take off per year. This represents an allocation of approximately 7 700 m^3 ha^{-1} yr^{-1} which is charges are R3 500 ha^{-1} yr^{-1} (de Lange et al., 2016).

14.2 Water quality monitoring study

Nitrogen and P concentrations were monitored from Loskop Dam downstream to Flag Boshielo Dam in order to study changes in and understand the current status of water quality downstream of the dense area of irrigated agriculture. Flag Boshielo Dam is located at the confluence of the Elands and Olifants Rivers, approximately 30 km from the town of Marble Hall in the Limpopo Province. The dam was built in 1987 for irrigation agriculture, to supply water to the town of Polokwane and to ensure dry season storage for mines in the area (Dabrowski et al., 2014). It is therefore imperative to understand water quality in the Middle Olifants as it impacts water quality received downstream.

The Department of Water and Sanitation (DWS), formerly the Department of Water Affairs (DWA), has accessible data that is extremely valuable to study water quality and long-term trends (Van der Laan et al., 2012). The water quality at any particular point in a river reflects the influence of basin lithology, climatic conditions, and atmospheric and anthropogenic inputs (Van der Laan et al., 2012). This water quality monitoring data is critical to improve our understanding of P contamination levels in our water. This data was used to validate our measured data.

14.3 Method and materials

14.3.1 Water sampling

Sampling was conducted over a period of 20 months commencing in March 2017. Selected monitoring points are displayed in Figure 104. Samples were initially taken from an area of the Moses River upstream, the Loskop and Flag Boshielo Dam walls and two irrigation canals (one close to Loskop Dam and another close to Flag Boshielo Dam). Later in the year, specific drainage canals in the area were then added to the monitoring points. These canals drain water from irrigated soils that would otherwise become water-logged.

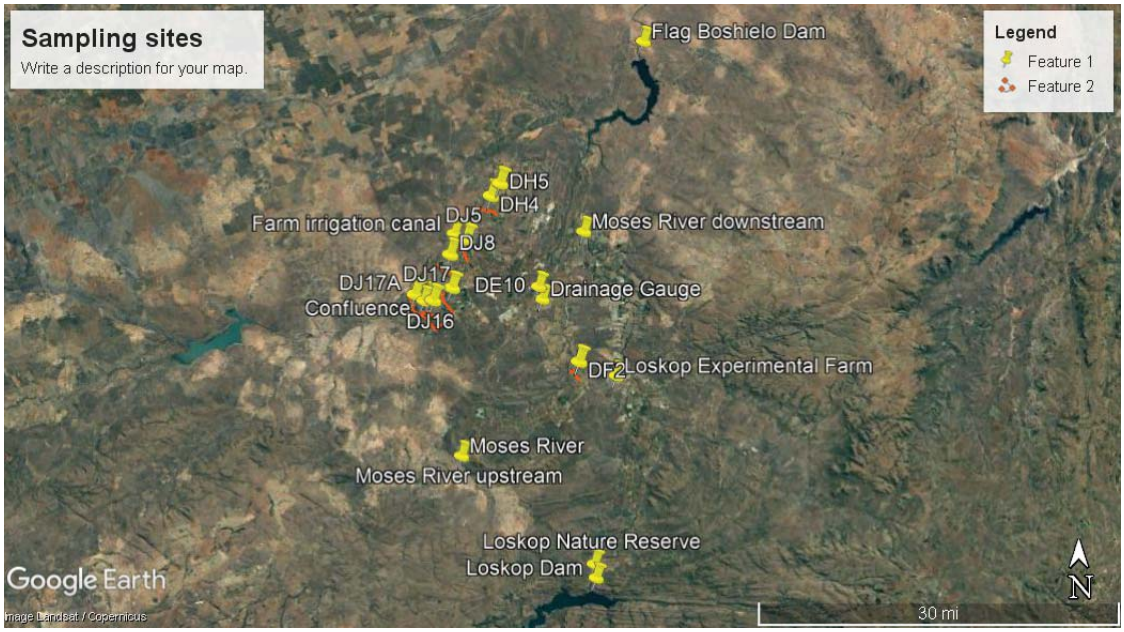

Figure 104: Sampling points between the Loskop and Flag Boshielo Dams

Each primary drainage canal is representative of approximately 400 ha of agricultural land (Pretorius, 2017). Irrigation canals were selected based on their proximity to intense agricultural activity and were also selected based on proximity to the Elands River, which is the closest freshwater resource to receive the exported nutrients. The drainage canal points can be seen in Figure 105, which is slightly zoomed in to more clearly indicate the agricultural activity in the areas in which these drainage canals are found. Initially there were more drainage canals included in our sampling, however, some of them were not in use, others were dry and some were in restricted areas with fencing preventing access.

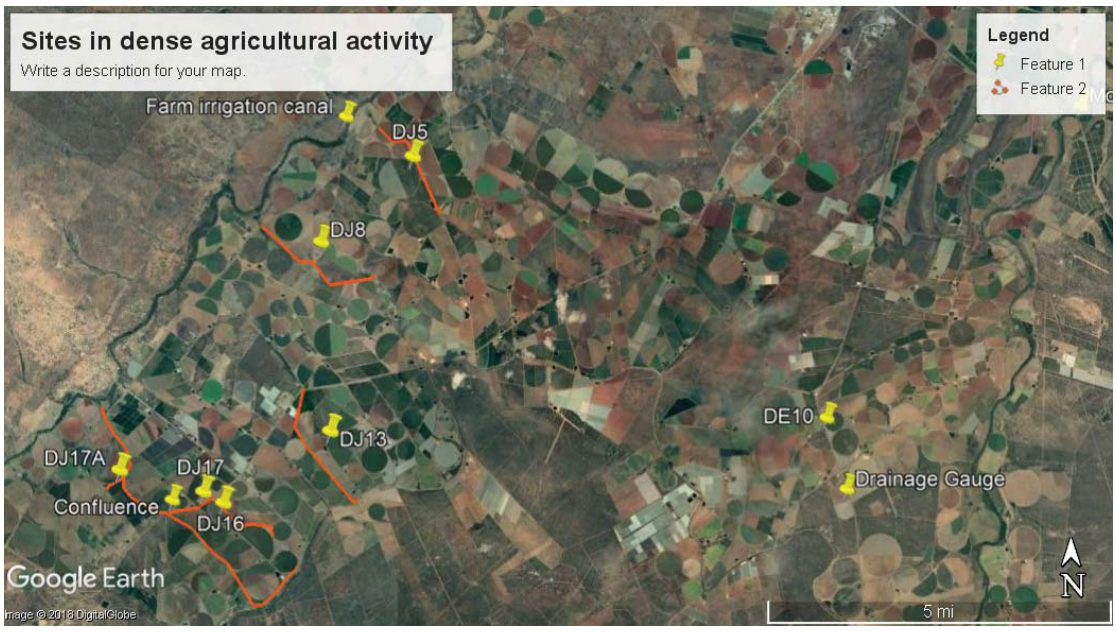

Figure 105: Irrigation canals selected in the area of intensively irrigated agriculture

There are several ways in which water enters the drainage canals from irrigated fields. In a few cases, drainage pipes feed directly from the fields into the drainage canals. In most instances water enters the drainage canals through seepage holes in the concrete panels of the irrigation canals as seen in Figure 106. Some irrigation canals discharge into the drainage canals, which is shown in Figure 107. Water can also enter via inlets for storm water runoff, depicted in Figure 107 and Figure 108 (de Waal, 2018).

Figure 106: Water entering drainage canal DE1 through seepage holes

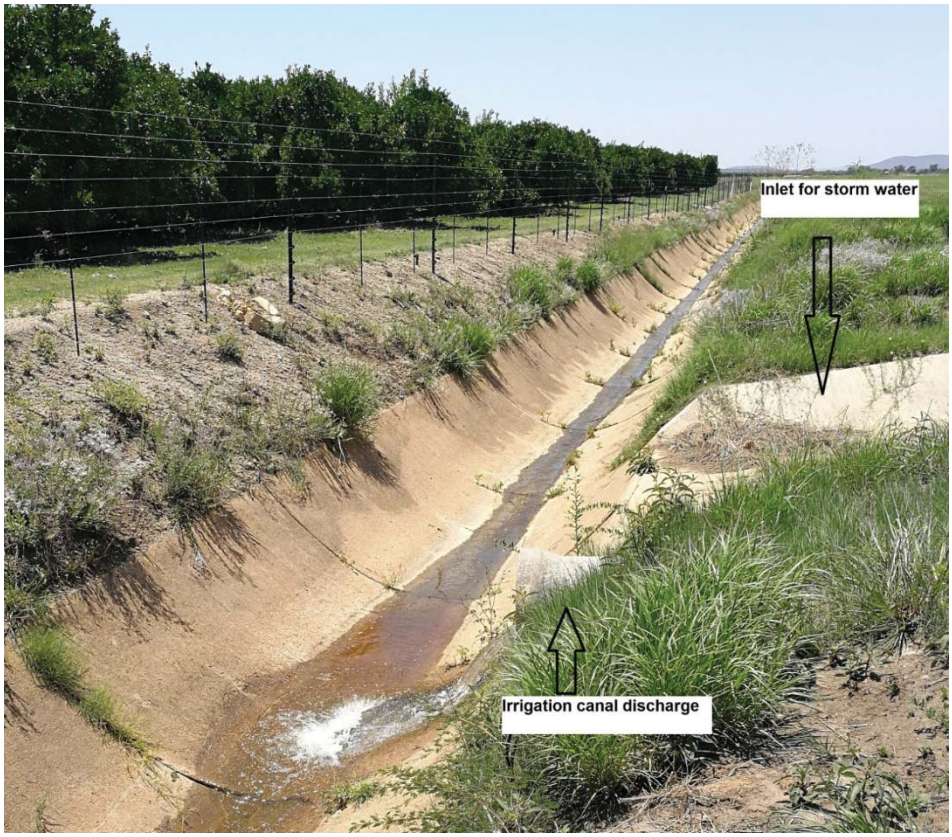

Figure 107: Irrigation canal discharge and inlet for storm water in drainage canal DJ17

Figure 108: Storm water inlet for water entering drainage canal DG4

An interesting observation that we found upon closer inspection of the Elands River in the Google Earth images was the visible eutrophication. The luminous green colour of the river close to the area of intensive irrigation is indicative of algal blooms. This can been seen in Figure 109 and a zoomed in image of the algal blooms is in Figure 110.

Figure 109: Luminous green colour of the Elands River, indicative of algal blooms, close to our drainage canal sampling

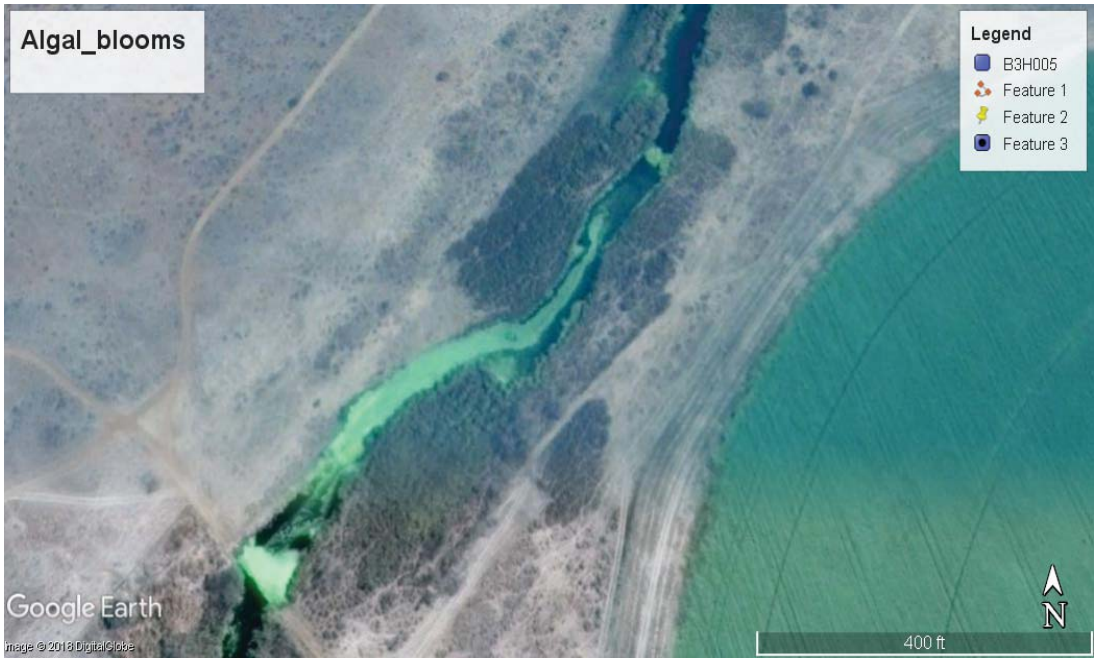

Figure 110: Zoomed in image of algal blooms in the Elands River

14.3.2 Sampling locations

The dams sampled during the study were the Loskop Dam, Flag Boshielo Dam and the farm storage dam at the ARC-Loskop Research Farm. The rivers sampled in this study were the Moses River (upstream and downstream) and the Elands River (the sampling point was just upstream of Flag Boshielo Dam). The irrigation canals sampled were the Loskop Nature Reserve irrigation canal, which is located closest to Loskop Dam, the ARC-Loskop Research Farm irrigation canal, DH5 irrigation canal, which is located closest to Flag Boshielo Dam and Farm irrigation canal located in between Loskop Dam and Flag Boshielo Dam.

There were several drainage canals sampled in the area. Drainage canals DJ16, DJ17 and DJ17a were a confluence of canals located close to farms producing mostly citrus and wheat. The DJ5 drainage canal was at a site where mostly citrus was produced. The site where DJ13 is located is close to what is perceived to be citrus production. Drainage canal DE10 had citrus, wheat and potato production close by. At the farm close to DF2 it was unsure what was being grown, however, this location had livestock nearby in a relatively small fenced off area. The area where DJ8 is located had citrus and wheat. All of the canals showed sedimentation that has settled at the bottom of the canal. Access was often restricted on these sites. The drainage canal samples represent activity of the ±400 ha of land that each one represents. Photographs of all sampling locations can be seen in Appendix A.

In addition to the drainage canals, a drainage gauge was installed in a grape orchard in order to monitor root zone leaching. Samples could only be analysed when there was adequate water collected to be pumped out of the drainage gauge. Permission was granted to install this drainage gauge at the start of 2018.

14.3.3 Water analysis

Grab samples were taken at each site and analysed at the University of Pretoria for phosphate (converted to phosphate-P), nitrate (converted to nitrate-N), pH and EC. Phosphate was analysed using a Hanna phosphate low range photometer. Nitrate was analysed using a Nitrate Test RQeasy by Merck. The analysis of pH was conducted using a laboratory calibrated pH meter. Electrical conductivity (EC) was tested using a Eutech Thermofisher Waterproof EC Scan High Meter (Singapore).

For phosphate analysis, a reagent was added to the water sample inducing a colour reaction between the phosphate in the water and the reagent used. A sample containing phosphate turns a blue hue. The higher the concentration, the deeper the blue colour. The intensity of the colour is measured with the photometer, which provides a measured phosphate value in mg ℓ^{-1} (ppm). The colour change is colorimetrically analysed using the Beer-Lambert Law. This principle states that light is absorbed by a complementary colour, and the emitted radiation is dependent on the concentration. The range of the photometer is 0.00-2.50 mg ℓ^{-1}. For low levels of phosphate, a narrow band interference filter at 610 nm permits only orange light to be detected by the silicon photometer. It omits all other visible light emitted from the tungsten lamp and therefore prevents their detection. Absorbance of the specific wavelength of light increases as the colour change of the reacted sample increases, while transmittance decreases simultaneously. Standards were used for calibration and performance verification (Hanna Instruments Inc., Rhode Island, United States of America).

For the nitrate analysis, test strips were dipped in the sample analysed using the instrument. The analysis system is based on reflectometry. The light reflected from the test strip is proportional to the nitrate level in the sample. Test strips are calibrated batch-wise during manufacture and therefore user calibration is not necessary. The measuring range is 5-250 mg ℓ^{-1} (Merck, 2012).

14.4 Results and discussion

From the analysis of the results it could be deduced whether or not the tested parameters were in line with water quality guidelines for the prevention of eutrophication (in the case of PO_4^{3-} and NO_3^-) and fell within the acceptable parameters for good water quality (in the case of EC and pH) according to the RWQOs (Receiving Water Quality Objectives) set out by the Department of Water and Sanitation (Department of Water Affairs, 2011b). These threshold values are given in their respective results sections that follow. Gaps in sampling are indicative of when drainage and irrigation canals were dry. This was at times due to maintenance of the canals.

14.4.1 Phosphate concentrations in dams, river, irrigation canals and drainage canals

The upper limit threshold for PO_4^{3-}-P concentration before it reaches a level that causes eutrophication is 0.025 mg ℓ^{-1} (red line in Figure 111) (de Villiers, 2007; Department of Water Affairs, 2011b) (red line in Figure 111). At the start of the sampling period, all dams had elevated levels of phosphate. After September 2017, however, the concentrations decreased to below the eutrophication threshold for all except the Flag Boshielo Dam sample collected in June 2018. The phosphate concentration in Flag

Boshielo Dam $PO4^{3-}$ concentration was always higher than or equal to Loskop Dam, except in February 2018. The ARC-Loskop Research Farm storage dam had phosphate concentrations that remained above the eutrophication threshold until April 2018. After April the concentration went back up to 0.025 mg ℓ^{-1} in October 2018.

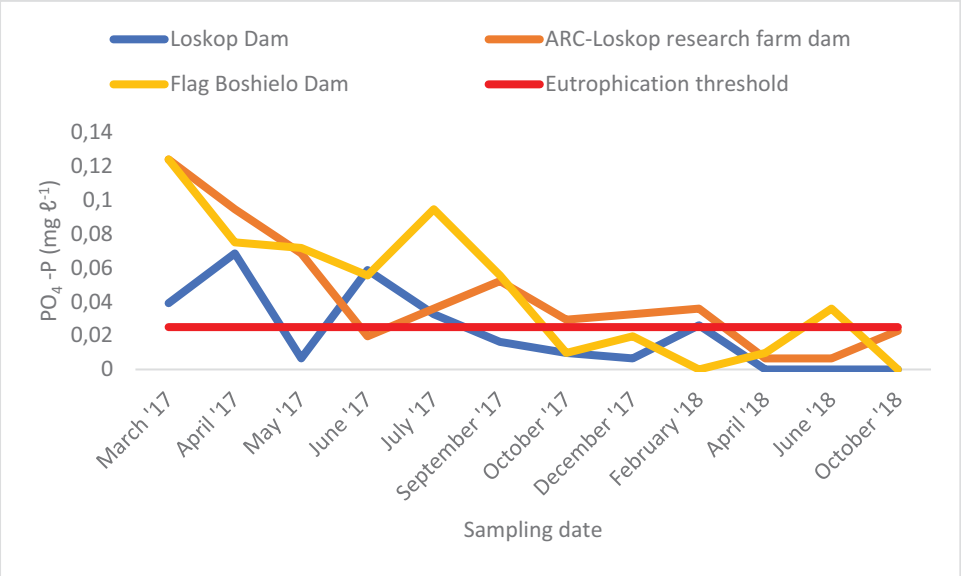

Figure 111: Phosphate-P concentrations in the dams

The Moses River downstream and the Elands River sampling began a few months after the Moses River upstream was started. The general trend observed from the results in Figure 111 is that phosphate concentrations were elevated in the summer months and lower in the winter months. This is contrary to what is commonly expected, where diluted nutrient concentrations are more likely in the wetter summer months. The higher concentrations observed can potentially be explained by increased surface runoff during the high summer rainfall months. Another possibility is that during the winter months, with low rainfall, there are periods of stagnation which allows filamentous algae to deplete the phosphorous in the water bodies (McDowell, 2012).

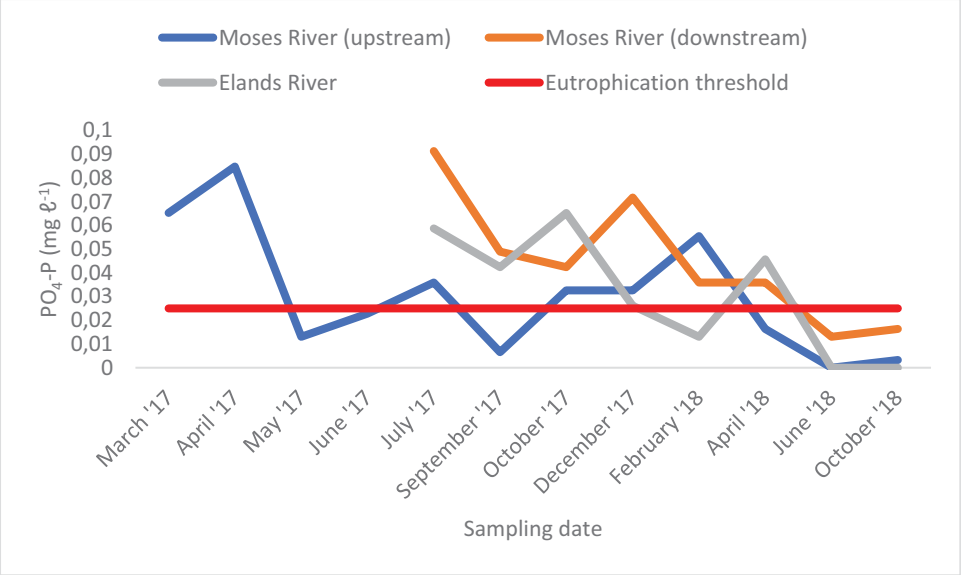

Figure 112: Phosphate-P concentrations in the rivers

Results from Figure 112 show that the 'Farm' irrigation canal and the ARC-Loskop Research farm irrigation canal were the only two that had PO_4-P concentrations higher than the eutrophication threshold, however, this was only at the start of the sampling period. After that point, all samples remained below the eutrophication threshold (including all samples that started off below the eutrophication threshold). This corresponds to the water the irrigation canals received from Loskop Dam, which had PO_4-P concentrations below the eutrophication threshold for this period. What was unexpected was that the phosphate concentration in DH5 was at times lower than the Farm irrigation canal. Sedimentation had been observed at some canals and it is possible that surface runoff containing elevated phosphate concentration entered DH5.

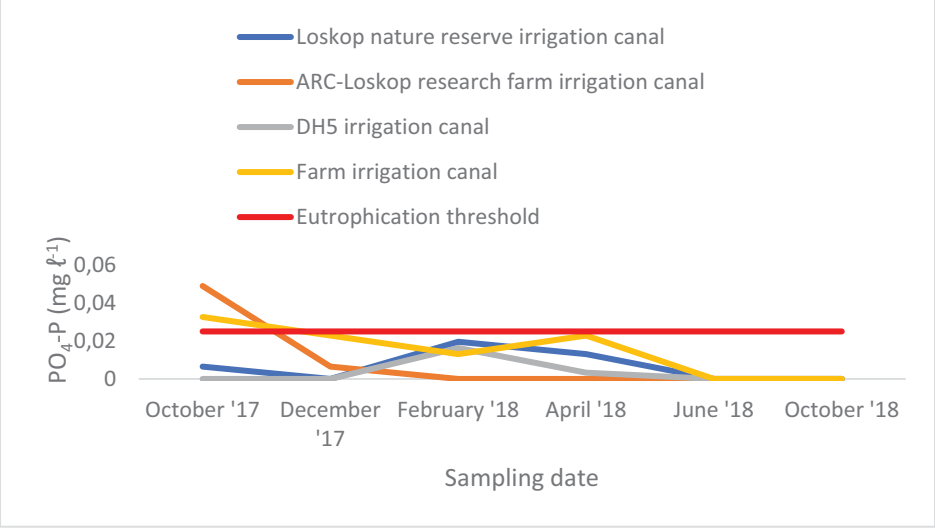

Figure 113: Phosphate-P concentrations in irrigation canals

Figure 114 shows the PO_4-P coming out of the drainage canals in the area. Drainage canal DJ13 appears to be the anomalous sample and the graph is eclipsed by this particular drainage canal. Since October 2017, these concentrations were much higher than any of the other drainage canals in the study area. The drainage canal is situated outside what appears to be a citrus processing plant on a citrus farm. Phosphates have known use in the processing and preservation of fruits and to protect the colour of fresh fruits and vegetables that are to be directly consumed (Soceanu et al., 2009).

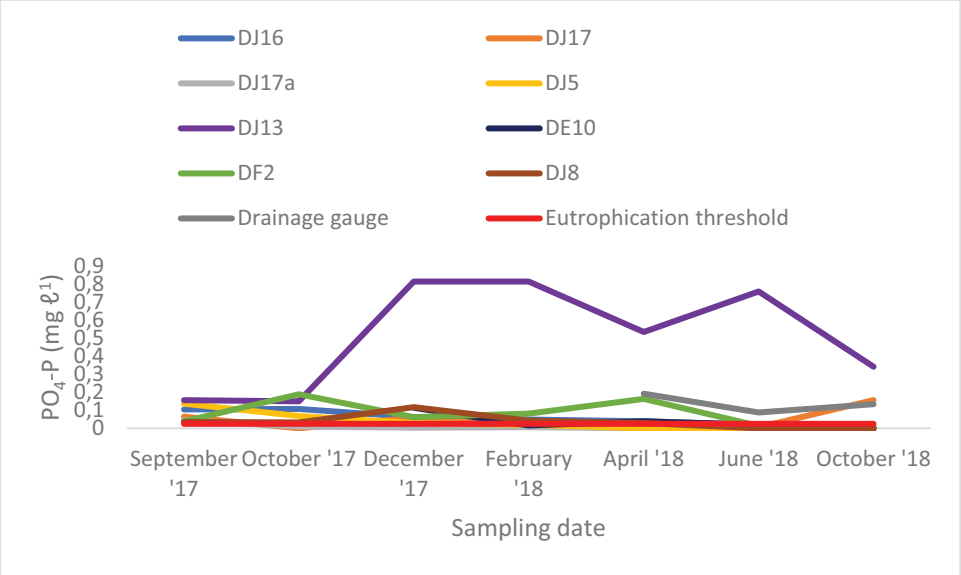

Figure 114: Phosphate-P concentrations in drainage canals

Figure 115 shows the same results as Figure 114 but with DJ13 being omitted. The highest concentration on this graph is now represented by the drainage gauge. This high concentration was expected as there was no dilution from any other source of water other than the irrigation and rainfall at that localized point. The drainage gauge is located close to DE10, which showed lower phosphate concentrations even though the concentrations were above the eutrophication threshold at times. The phosphate was therefore diluted before it reached the drainage canal. It was observed that when the phosphate concentration of the drainage gauge decreased in June 2018, the same was observed at DE10.

The phosphate concentration of DF2, although not as high as DJ13, was also considerably higher than the other drainage canals. A small amount of livestock was observed in a fenced off area close to this drainage canal. The concentrated manure where the livestock are held could have influenced the PO_4^{3-} concentration in any runoff that was exported from this area to DF2. Another possibility is that these animals could have been allowed to graze near the canal, resulting in exposed soil surfaces or defecation directly into the drainage canal. Other drainage canals that showed phosphate concentrations higher than the eutrophication threshold for the majority of the sampling period was DJ16, which is part of the confluence of canals, and DJ8, which is close to where citrus and wheat is produced. The general trend observed was that higher phosphate concentrations were observed in the

summer rainfall months than the drier winter months. Due to low flow, load was not measured and it is acknowledged that concentrations do not translate directly to loads. It is however important to note the high and potentially problematic concentrations of P being lost from these drainage canals.

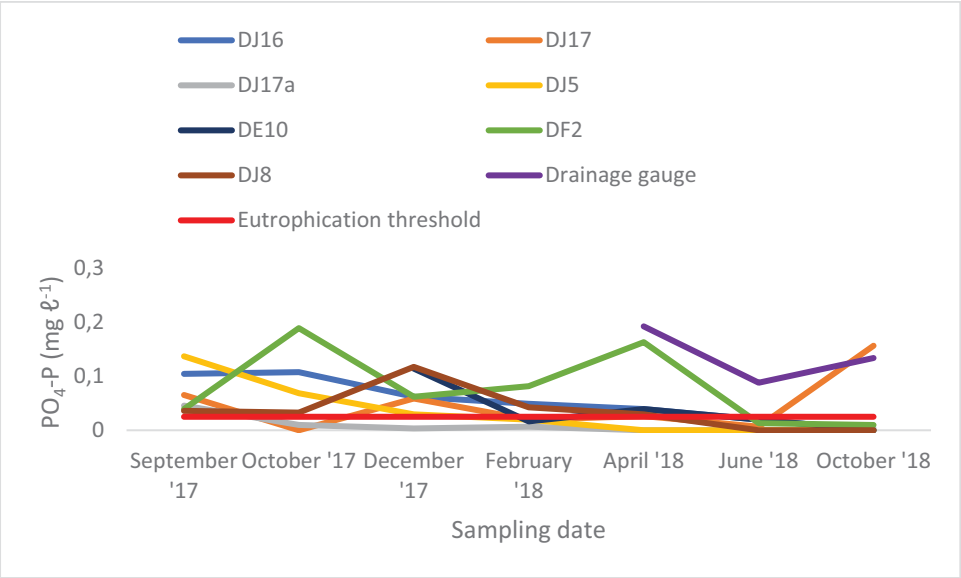

Figure 115: Phosphate-phosphorus concentrations in irrigation canals excluding DJ13

14.4.2 Nitrate concentrations in dams, river, irrigation canals and drainage canals

According to the water quality guidelines set by the Department of Water and Sanitation, the threshold for NO_3^--N concentration before it reaches levels where it could contribute to eutrophication is 6 mg ℓ^{-1} (Department of Water Affairs, 2011b). This is indicated by the red line on Figure 116, which shows the nitrate concentrations of the dams in the study area. All samples remained below the eutrophication threshold throughout the sampling period. Results for the Loskop and Flag Boshielo Dams were similar and showed negligible nitrate concentrations for the best part of the sampling period. There was a slight lag between the increased nitrate concentration seen at Loskop Dam (April 2018) and Flag Boshielo Dam (June 2018). The ARC-Loskop Research Farm storage dam showed higher concentrations than Loskop and Flag Boshielo Dams, but even at its highest concentration it was still below the eutrophication threshold. This could be due to water already present in the storage dam having elevated nitrate concentrations.

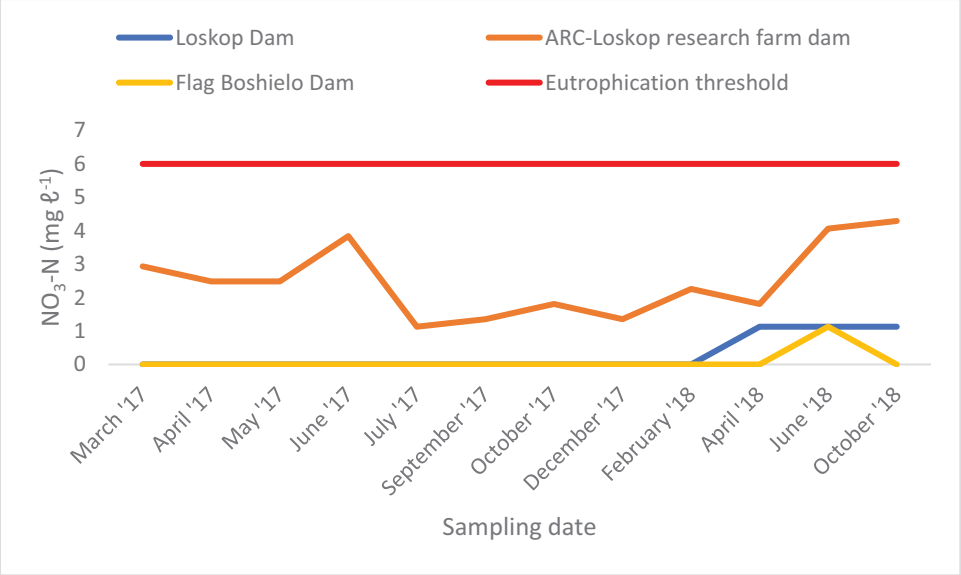

Figure 116: Nitrate-nitrogen concentrations in dams

The results for all the rivers sampled, as shown in Figure 117, indicate that all samples remained below the eutrophication threshold for the entire sampling period. The Elands River, sampled close to Flag Boshielo Dam, had no measurable nitrate throughout the study. The Moses River downstream section showed the same increases and decreases in nitrate concentration as its upstream counterpart. A similar lag in these concentrations could be seen to that of the Loskop and Flag Boshielo Dams. The Blue Ridge Platinum Mine is situated 30 km south-east of Groblersdal. The mine is situated in close proximity to Loskop Dam and uses water from the dam (Smith, 2010). Morin and Hutt (2009) cited a study conducted in British Columbia in which results show that some of the nitrogen in the explosives used during blasting are leached by drainage. Nitrate constituted the largest form of the nitrogen species (Morin and Hutt, 2009). It is possible that this, along with irrigated agriculture, could be sources of nitrate in the rivers.

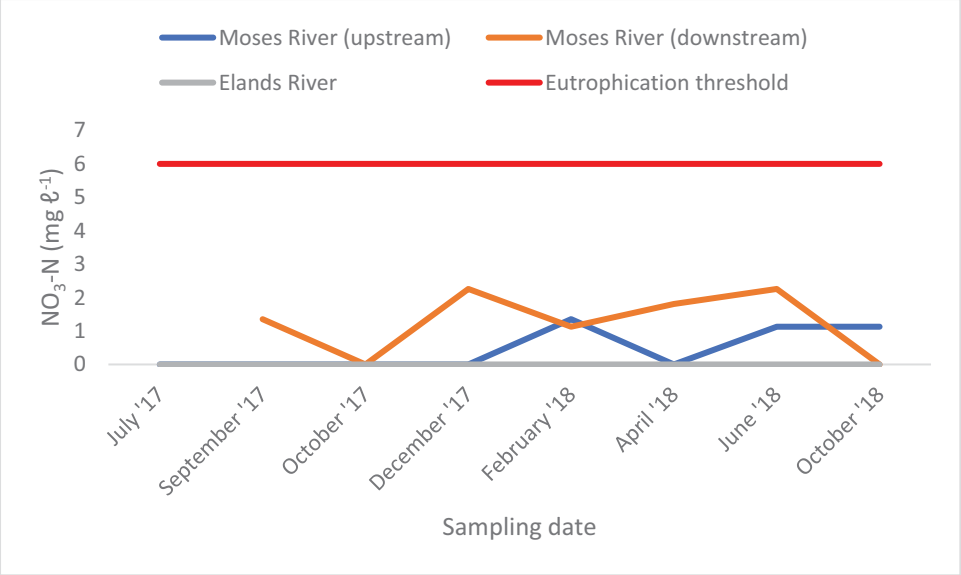

Figure 117: Nitrate-nitrogen concentrations in rivers

Figure 118 shows the results for nitrate concentrations in the irrigation canals. All sample concentrations stayed below the eutrophication threshold through the sampling period. The only samples that showed measurable nitrate concentrations were the DH5 and 'Farm' irrigation canals but these always remained below 2 mg ℓ^{-1}. The irrigation canal on the ARC-Loskop Research Farm only reached that concentration in October 2018. The ARC-Loskop Research Farm storage dam showed the same trend as the Loskop Dam. The DH5 irrigation canal showed higher nitrate concentrations in the summer months, which were not measured up in Loskop Dam. The Farm irrigation canal stayed constant for almost the entire sampling period with a dip in concentration in February 2018. It is therefore possible that nitrate containing water could be entering the irrigation canals via surface runoff during rainfall events. It is also possible that when there are deteriorations in the canal structures drainage water from the farms can enter the irrigation canals.

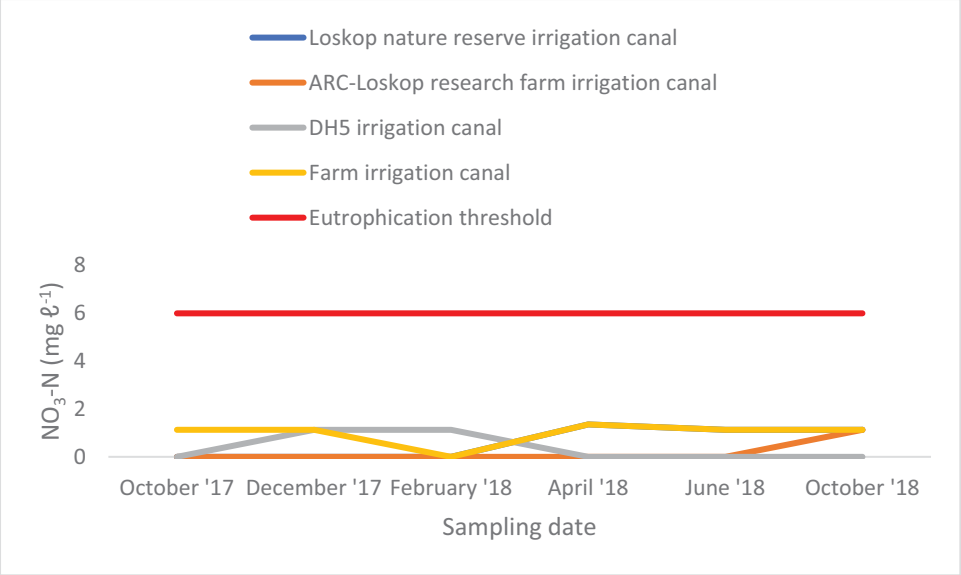

Figure 118: Nitrate concentrations in irrigation canals

The results for the concentrations of the samples from the drainage canals (Figure 119) showed two clear spikes above the eutrophication threshold. The first spike, indicating the highest nitrate concentrations occurred in December 2017 and was likely due to a flush of nutrients with summer rainfall after the summer crops had been fertilized. The second, less pronounced, spike occurred in June and was most likely caused by the loss of nutrients through irrigation water after the winter crops had been fertilized.

Interesting to note is that DJ13, which exhibited very high phosphate concentrations stayed below the eutrophication threshold for the entire sampling period except for October 2018. The highest concentration was in DJ8, where citrus and wheat is found close by, in December. The second highest concentration was DF2, which displayed both concentration spikes. The N export here was likely from the nearby livestock. The drainage canal DJ16 also showed concentration spikes in December and June. It is unknown what the exact crop constitution is where the water drains from, but citrus and wheat was visible in this area. Although these nitrate concentrations were high in these samples, it did not appear to influence river water quality to a large extent since the nitrate concentrations of the rivers were always below the eutrophication threshold.

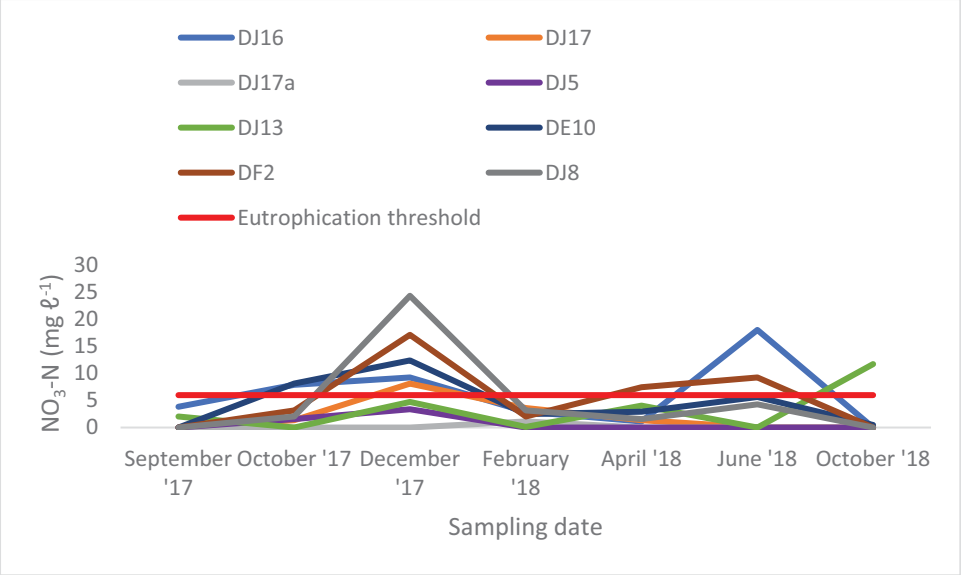

Figure 119: Nitrate-nitrogen concentrations in drainage canals

The drainage gauge data was not added to the graph due to its very high nitrate concentrations and is represented in Table 61. The sample in April measured above 250 mg ℓ^{-1}, which is the upper detection limit of the instrument. There was not enough sample for a dilution to be made. The concentration was very high in April and June but decreased by October 2018. This does not follow the trend of concentrations being higher in summer.

Table 61: Nitrate-nitrogen (NO_3-N) concentrations from the drainage gauge

Date	April 2018	June 2018	October 2018
NO_3-N (mg ℓ^{-1})	>250	70.0	8.58

14.4.3 Measured pH in dams, river, irrigation canals and drainage canals

Many chemical processes are largely controlled by pH, including the solubility and toxicity of elements in water. It is therefore vital to keep pH within an acceptable range. According to water quality guidelines set out by DWS, the ideal surface water pH is ≥ 6.5 and ≤ 8.0. A pH of < 6.5 or > 8.4 is unacceptable (Department of Water Affairs, 2011b). An elevated pH also poses a threat for eutrophication as alkalinity has a direct impact on P release from sediment. A higher pH leads to more P released in water (Li, 2013). The pH of water is very important in sediments where P retention depends on iron (Fe). As the pH increases, the P binding capacity of the oxygenated sediment layer decreases. This arises from the competition between hydroxyl ions and P ions. In the sediment of eutrophic water bodies, photosynthetically elevated pH can result in more P. This is loosely sorbed to Fe and increases release rates (Søndergaard et al., 2003).

The pH of the dams (Figure 120) stay within acceptable limits for most of the sampling period (for the entire period in the case of the ARC-Loskop Research Farm storage dam). The pH of Loskop dam started slightly higher than the upper pH limit but then fell within the acceptable range. There was a drop in pH observed in June 2018 for Loskop Dam and the same was observed, to a lesser extent, for Flag Boshielo Dam. It is possible that acidic water from mining activities upstream could have caused this decrease in pH. Both dams were within the acceptable range by October 2018. The pH of the rivers all stayed within acceptable limits (Figure 121). The only sample that dropped below the lower limit was Moses River upstream, which is consistent with what was observed at Loskop and Flag Boshielo Dams.

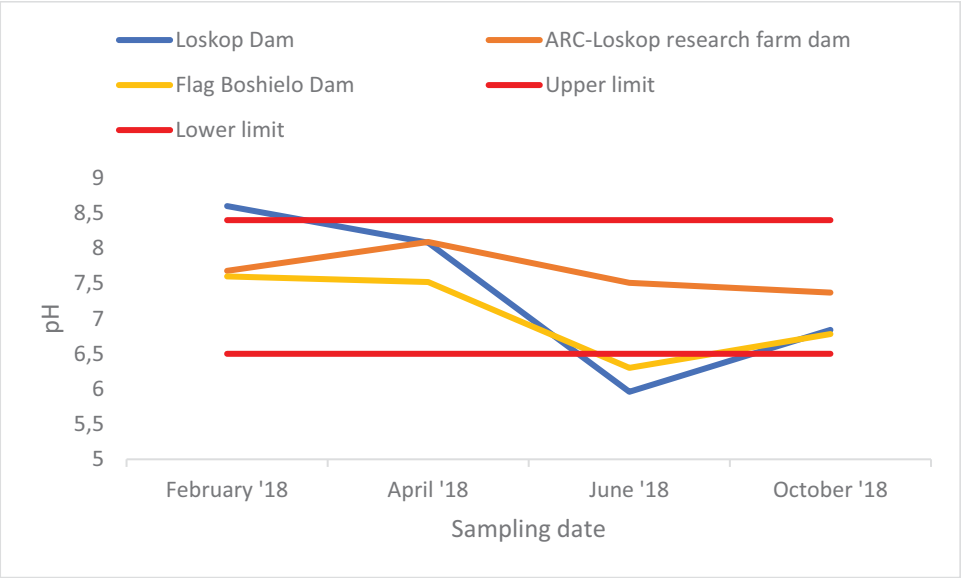

Figure 120: Measured pH in dams

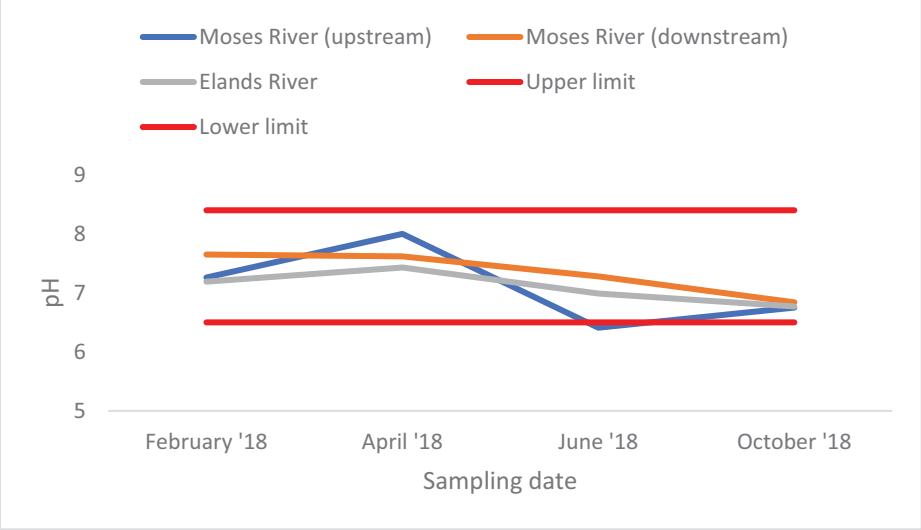

Figure 121: Measured pH in rivers

Figure 122 shows the pH of the irrigation canals which stayed within acceptable limits apart from DH5 which dropped slightly below the lower limit in October 2018. All irrigation canals showed a decrease in pH in October 2018. It is possible this is due to the decreased pH of Loskop Dam in June 2018, however there was a lag in the decrease observed in the source and the irrigation canal water. Figure 123 shows the pH of the drainage canals. Most of the drainage canals stayed within acceptable limits for the sampling period. The only sample that showed a high pH for the majority of the sampling period was DJ17. Drainage canal DJ16 and, to a lesser extent, DJ 17a, showed pH levels above the upper limit in April 2018. These three make up the confluence of canals that was sampled. A possible reason for this increased pH here could be due to liming. Although the pH is high for the samples, the pH of the river samples remain within the acceptable limits.

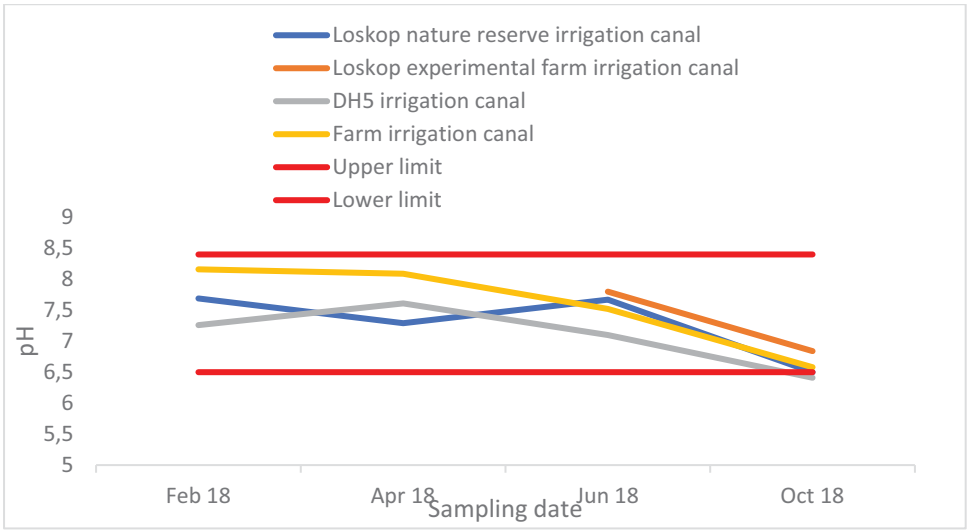

Figure 122: Measured pH in irrigation canals

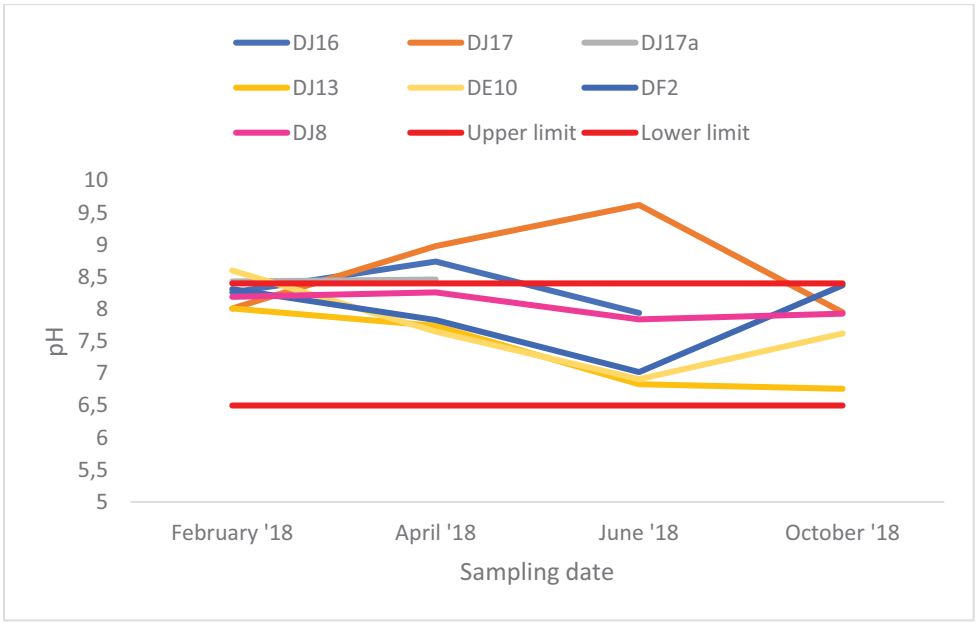

Figure 123: Measured pH in drainage canals

14.4.4 Electrical conductivity (EC) in dams, river, irrigation canals and drainage canals

Electrical conductivity (EC) provides a measure of salinization. It is also proportional to the total dissolved solids (TDS) concentration in water. The TDS concentration can be used as an indicator of the overall presence of soluble chemical contaminants. Sources of contamination include industrial and domestic wastewater and leaching of soil contaminants (Department of Water Affairs, 2011b). The EC of water should ideally be ≤ 30 mS m^{-1}, acceptable ranges from > 30 and ≤ 50 mS m^{-1}, tolerable ranges from > 50 and ≤ 85 mS m^{-1}, unacceptable EC levels are > 85 mS m^{-1} (Department of Water Affairs, 2011b). Irrigating with water high in salts can significantly reduce yields especially when soil drainage is poor (Van der Laan et al., 2012).

Figure 124 shows the results of the EC measured in the dams. All samples had levels below the tolerable but above the ideal threshold range. The storage dam at the ARC-Loskop Research farm was the only sample that deviated from this in June 2018 and continued to be high in October 2018. The anomaly of this dam is consistent with the results for other parameters for this dam. It appears there is another source of water in this dam apart from the water from Loskop Dam. The EC measured in the rivers were also all below the tolerable limit (Figure 125). The EC of the irrigation canal samples (Figure 126) were well below the tolerable limit, even falling below the acceptable limit in many cases. This is in accordance with the water the canals receive from Loskop Dam.

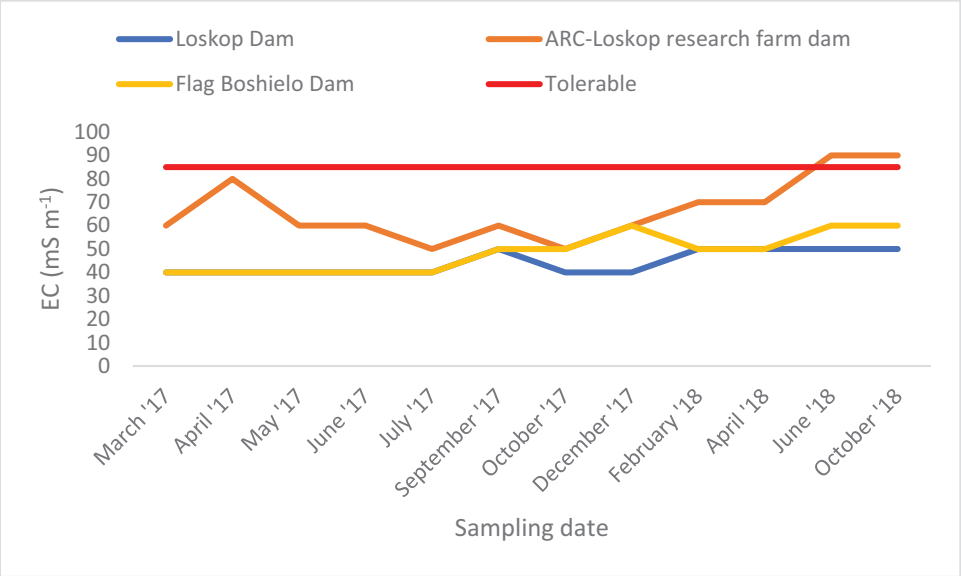

Figure 124: Measured electrical conductivity (EC) of dams

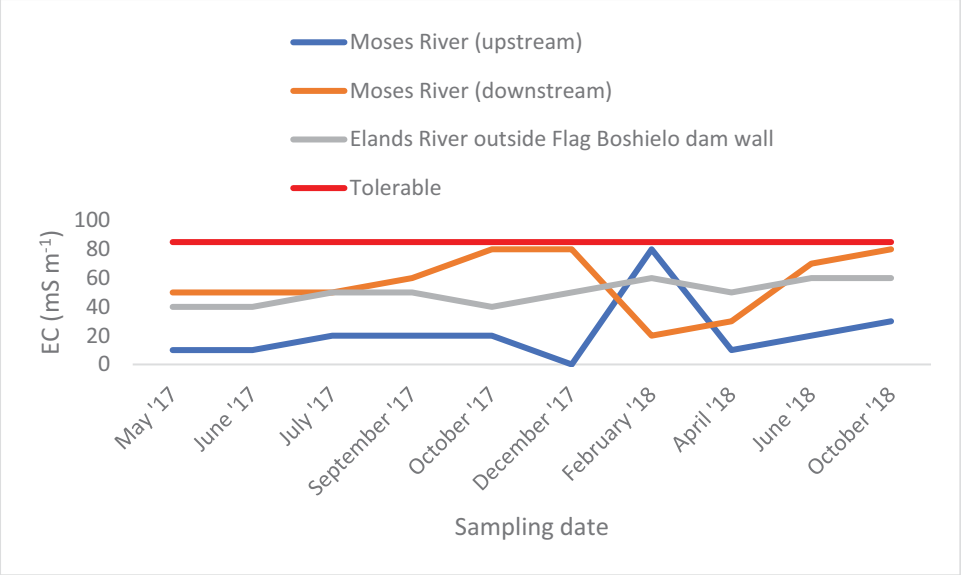

Figure 125: Measured electrical conductivity (EC) of rivers

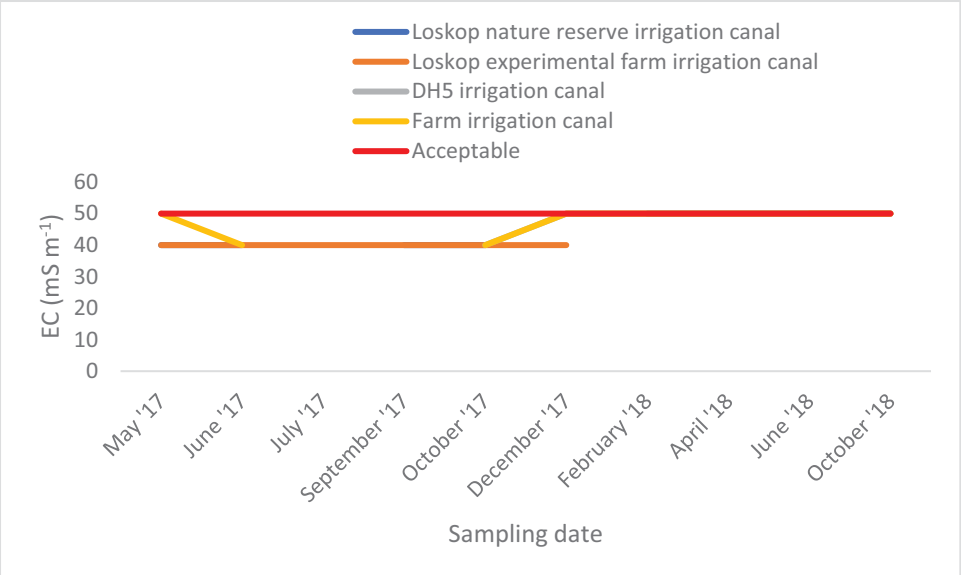

Figure 126: Measured electrical conductivity (EC) of irrigation canals

The results for the EC levels in the drainage canals were above the tolerable limit. Only DJ17a and DF2 were below the tolerable limit for a large part of the sampling period. It is interesting to note that EC level spikes (in December and June) corresponded to the nitrate concentration spikes, which may be explained by the application of chemical fertilizers, which are salts, and their subsequent export into the drainage canals. This high EC was not seen in the rivers sampled, which have EC levels below the tolerable limit.

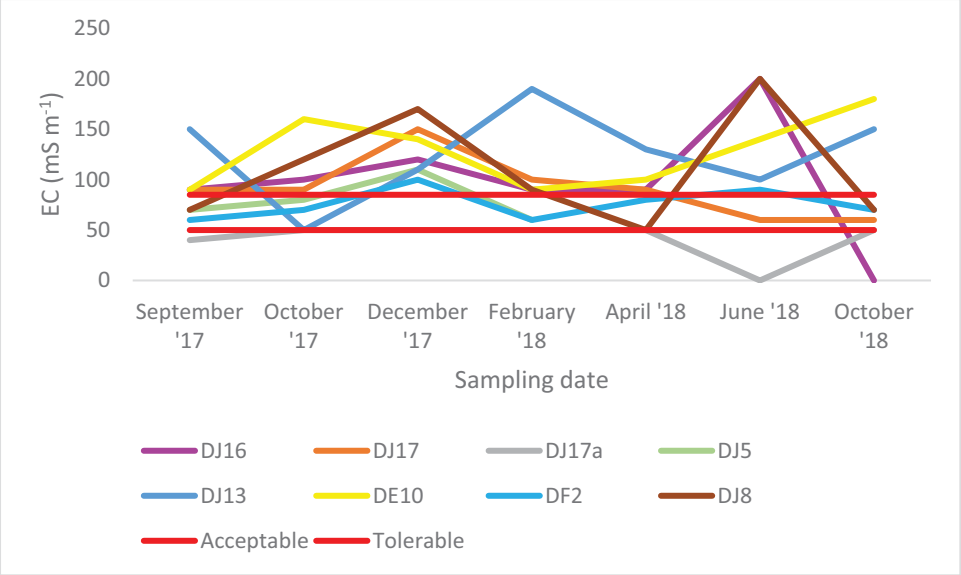

Figure 127: Measured electrical conductivity (EC) of drainage canals

14.4.5 Comparison of measured data with DWS Data

Results obtained from our study were compared to DWS data close to Loskop Dam, Flag Boshielo Dam, Moses River upstream and downstream, DF2 and DH5. Unfortunately, only Loskop and Flag Boshielo Dam phosphate and nitrate concentrations were analysed regularly. The rest of the monitoring stations only had two or three analyses for phosphate and nitrate in the last eight years. Comparisons are therefore only shown for Loskop and Flag Boshielo Dams, with EC comparisons also shown for these dams. The pH levels could not be compared as this was tested from the start of 2018 and there was no DWS data available for 2018. For Loskop Dam, samples could only be compared until October 2017 because there was no available DWS data after October 2017. Flag Boshielo Dam had available data until February 2018.

Results for the phosphate concentration comparison for Loskop Dam is seen in Figure 128. The data appeared to be almost the inverse of each other. Apart from April and October, our measured values were higher than DWS values. It was also observed that our measured values were mostly above the eutrophication threshold, whereas DWS concentrations were consistently lower than the eutrophication threshold for all but one sampling event. The phosphate concentration comparison for Flag Boshielo Dam (Figure 129) showed a better relationship between both sets of data, however, similar to Loskop Dam, with our measured values almost always higher and above the eutrophication threshold compared to the DWS data, which was mostly below the eutrophication threshold.

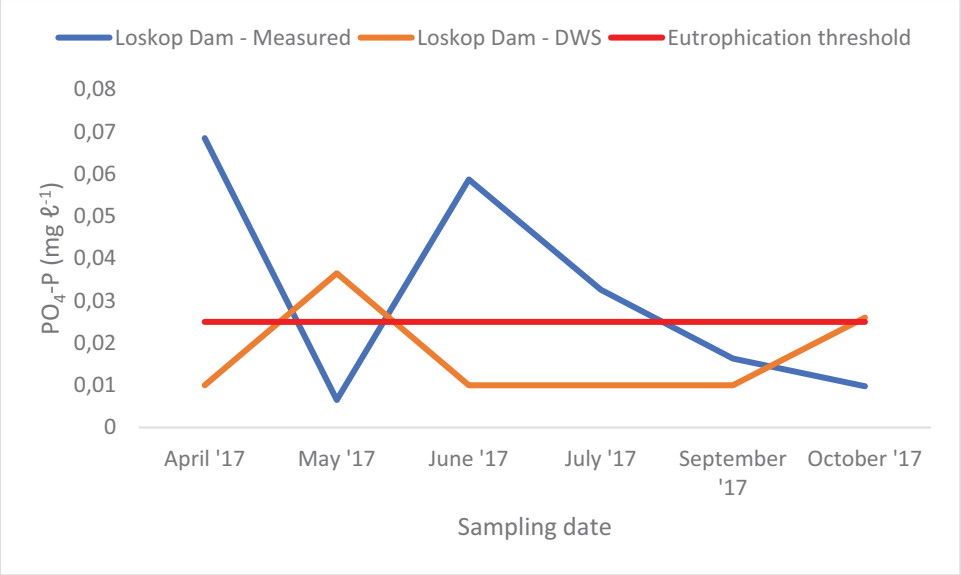

Figure 128: Comparison of phosphate concentrations in Loskop Dam between our measured data and Department of Water and Sanitation data

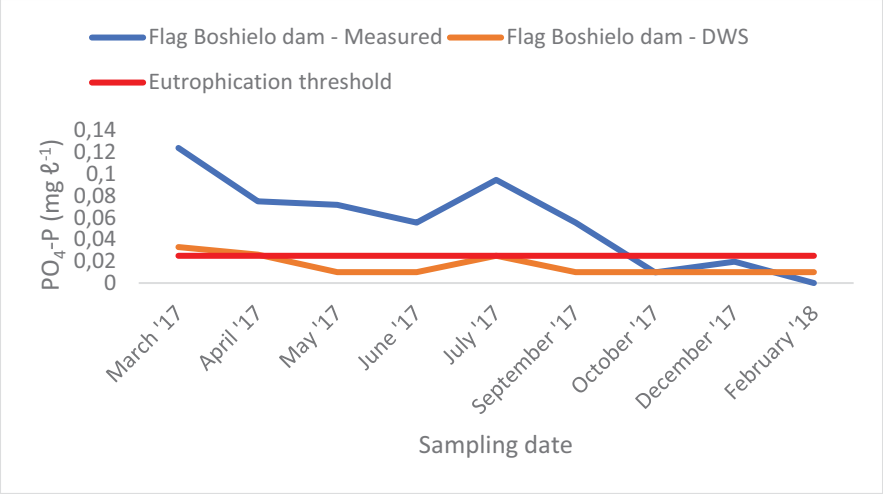

Figure 129: Comparison of phosphate concentrations in Flag Boshielo Dam between our measured data and Department of Water and Sanitation data

Results for the nitrate concentration comparison for Loskop Dam is displayed in Figure 130 and for Flag Boshielo Dam in Figure 131. The eutrophication threshold was omitted from the graphs since they were all well below this limit. The opposite phenomenon was seen to that of the phosphate comparison, as DWS values were now higher than our measured ones. Nitrate was picked up in the Loskop Dam by DWS data but laboratory analyses showed no measurable nitrate. The measured and DWS values are closer in the comparison for Flag Boshielo Dam but there is a spike in concentration in July (same seen in June for Loskop Dam so there is a lag in concentration change) that was not picked up in our measured data. The possible reason that DWS data was higher than measured data is possibly because DWS measures Nitrate- and nitrite-N while our measured values were only nitrate-N. Since

nitrite is not very stable and is an intermediate species between nitrate and ammonium, it was thought that it would be present in negligible concentrations, but it is possible that it is present and measureable in these water samples. Samples were sent to commercial laboratories and tested for nitrite. The results obtained from Lab 2 indicate negligible (<0.05) nitrite concentrations in the samples. This warrants further investigation.

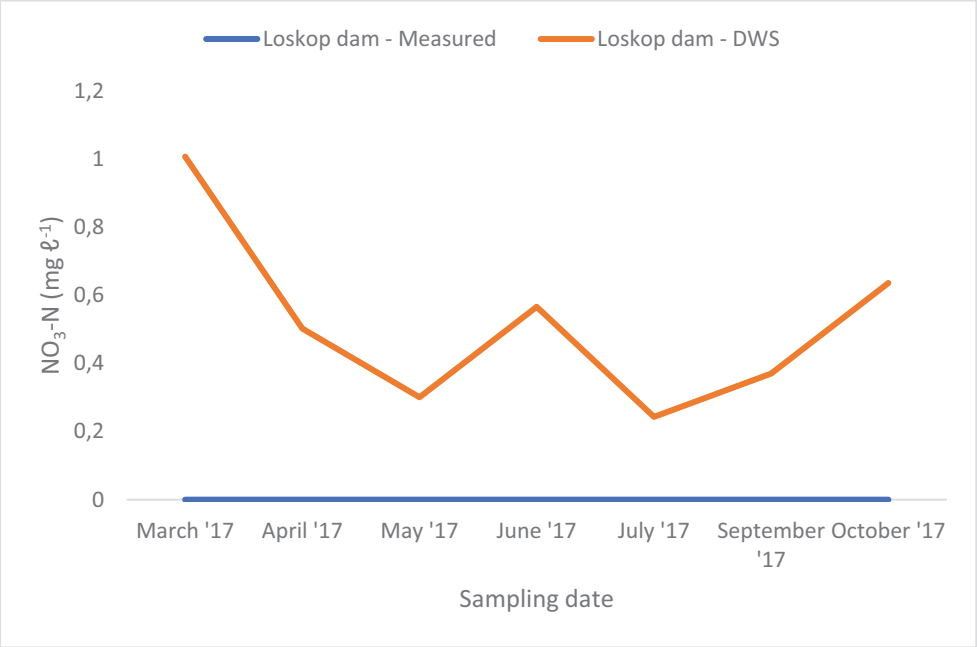

Figure 130: Comparison of nitrate-nitrogen concentrations in Loskop Dam between measured data and Department of Water and Sanitation data

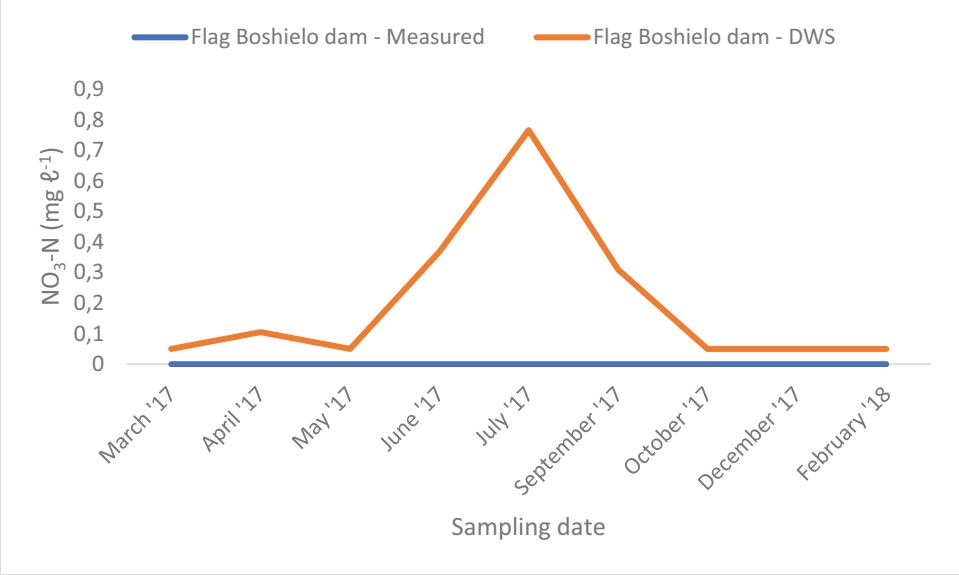

Figure 131: Comparison of nitrate concentrations in Flag Boshielo Dam between measured data and Department of Water and Sanitation data

The comparison of EC in Loskop Dam (Figure 132) and Flag Boshielo Dam (Figure 133) was similar to nitrate, in that DWS values were higher than our measured ones. For Loskop Dam, spikes in EC were seen at two different times (May for DWS data and September for measured data). The DWS data for Flag Boshielo Dam had lower EC levels than measured data on the first date of sampling and after that the values were higher (and the same in December).

Sebastian or someone else will argue that DWS data is also measured – not sure if there is time to change though

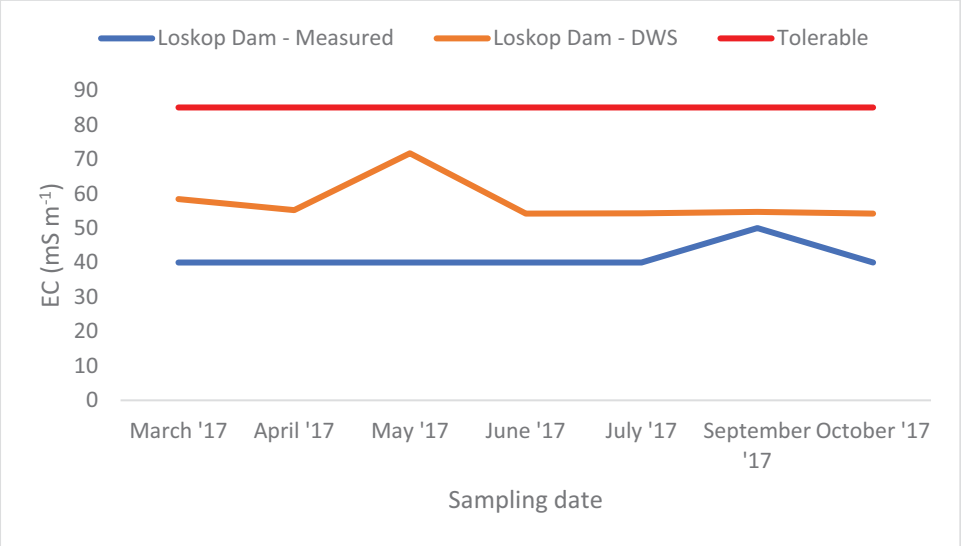

Figure 132: Comparison of EC in Loskop Dam between measured data and DWS data

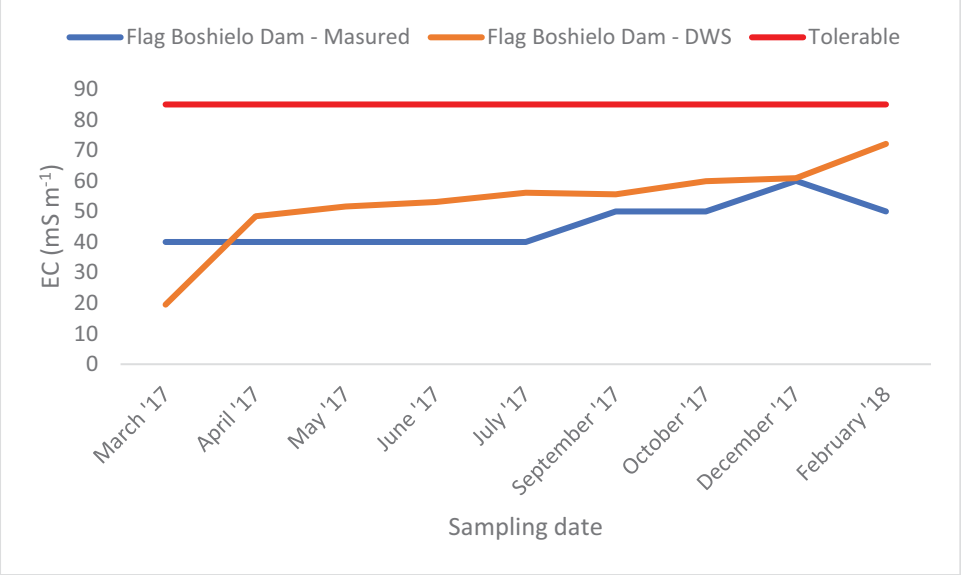

Figure 133: Comparison of electrical conductivity (EC) in Flag Boshielo Dam between measured data and Department of Water and Sanitation data

14.4.6 Laboratory validation of measured results

Samples were sent to two commercial laboratories to compare with our measured results. Blank cells indicate analyses that are still outstanding from external labs. Light green indicates results that are similar. Dark green indicates that results are 'accurate' due to being above or below the detection limit of nitrate. Most of our measured values were close to the commercial laboratory values. The remaining results are necessary to further validate measured values with the laboratories. Results from the other commercial lab is still outstanding. This higher nitrate levels measured by DWS are therefore not explained by the presence of nitrite.

Table 62: Comparison of measured values with commercial laboratories

		NO_3-N				PO_4-P		
		Lab 1	**Lab 2**	**Measured**		**Lab 1**	**Lab 2**	**Measured**
Sample	**Month**	**mg ℓ^{-1}**	**mg ℓ^{-1}**	**mg ℓ^{-1}**		**mg ℓ^{-1}**	**mg ℓ^{-1}**	**mg ℓ^{-1}**
	Apr-18							
Drain Gauge		86.90	89.00	>56.5		0.13	0.20	0.19
DE 10		2.06	2.10	2.94		0.02	<0.10	0.04
DF 2		8.10	7.70	7.45		0.17	0.10	0.16
DJ13		4.92	3.40	4.07		0.98	1.10	0.53
DJ8			4.20	1.58			<0.10	0.03
	Jun-18							
Drain Gauge			69.00	70.0			0.20	0.09
DE 10			3.60	5.65			<0.1	0.02
DF 2			7.30	9.26			<0.1	0.01
DJ13			0.10	0.00			1.50	0.76
DJ8			3.70	4.29			<0.10	0.00
	Oct-18							
Drain Gauge			7.00	8.58			0.20	0.13
DE 10				0.47				0
DF 2			0.80	0.00			<0.1	0.01
DJ13			10.0	11.7			0.50	0.34
DJ8			0.70	0.00			0.10	0.00

14.5 Summary and Conclusions

The general observation from this study was that P pollution appears to be a larger issue than N pollution in the Middle Olifants catchment. Drainage canal data, which represents losses from irrigated agriculture, showed elevated amounts of P (and N seasonally) from agriculture, but deeper investigations are required to determine how significant nutrient pollutant loads from agriculture are. Nutrient concentrations were often higher in the summer rainfall months compared to the drier winter months. The rivers sampled in this study showed a similar trend to the drainage canals with higher phosphate concentrations in the summer months, and with concentrations being higher than the eutrophication threshold for the majority of the sampling period.

The irrigation canal water quality does not always reflect the water that it receives from Loskop Dam. This suggests that there is possible contamination from surface runoff or seepage when the concrete canals deteriorate. Although the irrigation canals that receive water from Loskop Dam have 'acceptable' N and P levels, farmers should take into account the N and P they are adding with the irrigation water when designing a fertilizer programme. Future work for this study involves calculating N and P masses added with the irrigation water. This would help farmers save cost by reducing fertilizer application.

Most of the commercial laboratory results corresponded well our measured values. The PO_4-P measured values were higher than DWS data, however, NO_3-N showed the opposite phenomenon. This may be due to the fact that DWS data measures nitrite- and nitrate-N combined and our measured values were only nitrate-N, however, preliminary results from commercial laboratory analyses found negligible nitrite concentrations. Department of Water and Sanitation historical data is a major national asset for use, for example in catchment scale modelling, but the apparent decrease in water quality sampling frequency and water chemistry data quality is a concern.

The results appear to confirm that the impact of activities upstream of Flag Boshielo Dam impacts the water quality of this reservoir. The phosphate concentration of Flag Boshielo Dam was consistently higher than that of Loskop Dam for the majority of the sampling period, indicating a concentrating P effect downstream. This is problematic to the farms downstream who receive this impaired water quality as irrigation water. It also affects the communities in the area who rely on this water for domestic use. It is acknowledged that there are impacts from point sources in this catchment. It also acknowledged that the drainage canals have low flow and the concentrations measured do not translate directly to load. The results however do suggest that agriculture is a contributor to the nutrient pollution problem in the Olifants catchment. Catchment scale modelling can help quantify these losses.

14.6 References

BIGGS, H.C., CLIFFORD-HOLMES, J.K., FREITAG, S., VENTER, F.J. and VENTER, J. (2017) Cross-scale governance and ecosystem service delivery: A case narrative from the Olifants River in North-Eastern South Africa. *Ecosystem Services* 2017: 173-184. https:doi.org.10.1016/j.ecoser.2017.03.008.

DABROWSKI, J., OBERHOLSTER, P.J. and DABROWSKI, J.M. (2104) Water quality of Flag Boshielo Dam, Olifants River, South Africa: Historical trends and the impact of drought. *Water SA* 40 (2): 345-358.

DE LANGE, W.J., BOTHA, A.M. and OBERHOLSTER, P.J. (2016) Monetary value of the impacts of filamentous green algae on commercial agriculture: Results from two geographically different case studies. *Water SA* 42 (3): 449-255. http://dx.doi.org/10.4314/wsa.v42i3.10.

DE VILLIERS, S. and THIART, C. (2007) The nutrient status of South African rivers: concentrations trends and fluxes from the 1970s to 2005. *South African Journal of Science* 103: 343-349.

DE WAAL, L. (2018) Personal communication, 11 November 2018. Mr Leon de Waal, Loskop Irrigation Board, Groblersdal, Limpopo, South Africa.

DEPARTMENT OF WATER AFFAIRS, SOUTH AFRICA (2011b) Directorate Water Resource Planning Systems: Water Quality Planning. Resource Directed Management of Water Quality. Planning Level Review of Water Quality in South Africa. Sub-series No. WQP 2.0. Pretoria, South Africa. http://www.dwaf.gov.za/Documents/Other/Water%20Resources/DWA%20WQ%20Planning%20Report%20_Final_Version_06-July-2011.PDF.

DEPARTMENT OF WATER AFFAIRS AND FORESTRY (2002) National Eutrophication Monitoring Programme.
http://www.dwaf.gov.za/iwqs/eutrophication/NEMP/EutrophicationMonitoringProgramme.pdf

DEPARTMENT OF WATER AFFAIRS, SOUTH AFRICA (2011a) Classification of Significant Water Resources in the Olifants Water Management Area (WMA 4): Management Classes of the Olifants WMA. Report No: RDM/WMA04/00/CON/CLA/0213 Prepared by: Golder Associates Africa, Prime Africa and Retha Stassen. http://www.dwa.gov.za/rdm/WRCS/doc/Olifants%20Classification_Management%20Classes_Report_Feb_2013_Final_Draft.pdf.

DEPARTMENT OF WATER AFFAIRS, SOUTH AFRICA (2013) Development and implementation of irrigation water management plans to improve water use efficiency in the Agricultural Sector. Loskop Irrigation Board Water Management Plan Final Report. Project No: WP 10276: Directorate Water Use Efficiency. http://www.dwa.gov.za/Projects/WUE/Documents/Loskop_WMP_Final.pdf.

HANNA INSTRUMENTS INC. (2018) HI 96713 Phosphate low range photometer. https://hannainst.com/hi96713-phosphate-low-range-porTable-photometer.html. (Accessed 11 November 2018).

HUCHZEMEYER, K.D.A., WOODBORNE, S., OSTHOFF, G., HUGO, A., HOFFMAN, A.C., KAISER, H., STEYL, J.C.A. and MYBURGH, J.G. (2017) Pansteatitis in polluted Olifants River impoundments: nutritional perspectives on fish in a eutrophic lake, Lake Loskop, South Africa. *Journal of Fish Diseases* doi: 10.1111/jfd.12633

LI, H., LIU, L., LI, M. and ZHANG, X. (2013) Effects of pH, temperature, dissolved oxygen, and flow rate on phosphorus release processes at the sediment and water interface in storm sewer. *Journal of Analytical Methods in Chemistry* doi 10.1155/2013/104316.

McDOWELL, R. (2012) Minimising phosphorus losses from the soil matrix. *Current Opinion in Biotechnology*, 23 6(): 860-865. doi:10.1016/j.copbio.2012.03.006.

McKINSEY & COMPANY (2009) Charting our water future: Economic frameworks to inform decision-making. Water Resources Group, 2030; McKinsey & Company. https://www.mckinsey.com/business-functions/sustainability-and-resource-productivity/our-insights/confronting-south-africas-water-challenge (Accessed 08 November 2018).

MERCK (2012) Rapid on-site determination of nitrate in vegetables with Reflectoquant RQeasy nitrate and RQflex. file:///C:/Users/u12108597/Downloads/64794_NL_RQeasy_Nitrat_120907_eng_2012.pdf. (Accessed 11 November 2018).

MORIN, K.A. and HUTT, N.M. (2009) Mine water leaching of nitrogen species from explosive residues. *Geohalifax* 1549-1553 URL: http://citeseerx.ist.psu.edu/viewdoc/download?doi=10.1.1.520.5390&rep=rep1&type=pdf (Accessed 30 August 2018).

NEL, J., COLVIN, C., LE MAITRE, D., SMITH, J. & HAINES, I. (2013) South Africa's Strategic Water Source Areas. CSIR Report No CSIR/NRE/ECOS/ER/2013/0031/A. http://www.fewlbnexus.uct.ac.za/sites/default/files/image_tool/images/91/CSIR%20Nel%20et%20al.%20Report%20on%20Strategic%20Water%20Source%20Areas_FINAL.pdf.

OBERHOLSTER, P.J. and BOTHA, A-M. (2011) Dynamics of phytoplankton and phytobenthos in Lake Loskop (South Africa) and downstream irrigation canals. *Fundamental and Applied Limnology* 179 (3): 169-178. DOI: 10.1127/1863-9135/2011/0179-0169.

PRETORIUS, P. (2017) Personal communication, 28 September 2017. Mr Pieter Pretorius, Loskop Irrigation Board, Groblersdal, Limpopo, South Africa.

RASHLEIGH, B., HARDWICK, D. and ROUX, D. (2009) Fish assemblage patterns as a tool to aid conservation in the Olifants River Catchment (East), South Africa. *Water SA* 35 (4) 517-524. http://dx.doi.org/10.4314/wsa.v35i4.76811.

SINGH, A. and VAN VEELEN, M. (2001) Ecological Reserve Report. Olifants River Ecological Water Requirements Assessment. Project number: P9104. DWAF report number: PB-000-00-5299. https://www.environment.gov.za/sites/default/files/docs/olifant_ecological_reserve_report.pdf.

SMITH, C. (2010) Blue Ridge Mine, South Africa. URL: http://www.miningweekly.com/print-version/blue-ridge-mine-2010-10-22 (Accessed 30 August 2018).

SOCEANU, A., DOBRINAS, S., BIRGHILA, S., POPESCU, V. and MAGEARU, V. (2009) Levels of phosphorus in citrus fruits. *Ovidius University Annals of chemistry* 20 (1): 87-90.

SØNDERGAARD, M., JENSEN, J.P. and JEPPESEN, E. (2003) Role of sediment and internal loading of phosphorus in shallow lakes. *Hyrobiologia* 506-509: 135-145.

UDALL, B. (2018) 21st Century Climate Change Impacts on Olifants River Flows, South Africa. URL: https://cer.org.za/wp-content/uploads/2018/05/Udall-Olifants-River-Analysis-FINAL.pdf (Accessed 25 November 2018).

VAN DER LAAN, M., VAN ANTWERPEN, R. and BRISTOW, K.L. (2012) River water quality in the Northern sugarcane-producing regions of South Africa and implications for irrigation: A scoping study. Water SA 38 (1): 87-96. http://dx.doi.org/10.4314/wsa.v38i1.11.

VAN GINKEL, C.E. (2011) Eutrophication: Present reality and future challenges for South Africa. *Water SA* 37 (5) 693-702. http://dx.doi.org/10.4314/wsa.v37i5.6.

WALTER, T., KLOOS, J. and TSEGAI, D. (2011) Options for improving water use efficiency under worsening scarcity: Evidence from the Middle Olifants sub-basin in South Africa. *Water SA* 37 (3): 357-370. http://dx.doi.org/10.4314/wsa.v37i3.68487.

WALTER, T., KLOOS, J. and TSEGAI, D. (2011) Options for improving water use efficiency under worsening scarcity: Evidence from the Middle Olifants sub-basin in South Africa. *Water SA* 37 (3): 357-370.

15 MODELLING OF THE CONTRIBUTION OF IRRIGATED AGRICULTURE TO RIVER NITROGEN AND PHOSPHORUS LOADS IN THE MIDDLE OLIFANTS

L. Mudaly[1], M. van der Laan[1], J.M. Dabrowski[2] and J.J. le Roux[3]
[1]Department of Plant Production and Soil Sciences, University of Pretoria, Pretoria 0002, South Africa
[2]Confluent Environmental, South Africa
[3]Department of Geography, University of the Free State, Bloemfontein, South Africa

15.1 Introduction

Demographic and land use changes, as well as other external factors, add increasing pressure on local national and regional water supplies. This valuable resource is necessary for energy production, industrial uses, domestic use and irrigation (Abbaspour et al., 2015). Irrigation accounts for about 70% of global water use (Salmon et al., 2015). Irrigated agriculture is a critical contributor towards global food supply and security (Chen et al., 2018) by producing between 33 to 40% of global food production (Salmon et al., 2015). In irrigated agricultural systems, irrigated return flows are the major non-point source of pollution of surface and groundwater bodies (Dechmi et al., 2012).

The growing global population has resulted in a need to increase food production to meet the demands. Nutrient inputs are the most important for increased agricultural production (Timsina, 2018). The excessive land application of fertilizers leads to increased concentrations of nutrients in nearby and downstream, freshwater resources and impairment of these resources (Singh et al., 2014). As the uncertainty of meeting future water demands increases and water scarcity is on the rise, societies become more vulnerable to the risks associated with inadequate water quantity and quality (Abbaspour et al., 2015).

South Africa is faced with finding new and innovative ways to improve water quality and quantity (Nel, 2013). Hydrological water quality models have been increasingly used in order to simulate the impact of land use activities on flow as well as point and non-point source pollution in large catchments (Dabrowski, 2014). They are important tools in the planning of the sustainable use of water resources to meet the demand (Abbaspour et al., 2015). In tandem with monitoring programmes, hydrological models can identify critical source areas of non-point source pollution (Singh et al., 2014). Once these models have been calibrated and validated, they can be used effectively to evaluate the efficiency of proposed management plans or practices (Dabrowski, 2014).

The model chosen for the catchment scale study was the Soil and Water Assessment Tool (SWAT). The SWAT model is a physically based, continuous time, river basin scale model. It has the capability to model the entire hydrological cycle, which includes evapotranspiration, shallow infiltration, percolation to deep aquifers and lateral flow processes (Olivera et al., 2006). The SWAT model contributes to the understanding of water quality by predicting the impact of weather, soils, land use and land management practices on nonpoint source pollution. It is a comprehensive catchment scale model developed to evaluate the effects that alternative management decisions have on water resources as well as NPS pollution in large river basins (Arnold *et al*., 2012). It quantifies the impact of

land management practices on flows, sediment loads and chemical yields (Olivera et al., 2006). The SWAT model was developed in the United States but has been successfully used globally. It is used mainly to simulate hydrology but also sediment, nutrient and pesticide loading in catchments. The model is able to simulate nutrient concentrations in large reservoirs, making it ideal to link nutrient loading with trophic status (Dabrowski, 2014).

In this study the model is applied to the Middle Olifants catchment, which is an intensively irrigated watershed. A canal water distribution system is used in the area. A wide variety of canal water distribution procedures exist globally, however, a daily schedule of water delivered to each field for irrigation is scarce or unavailable for use to model and simulate irrigation systems. Modelling the volume and delivery of irrigation water, especially in large canal systems, is very complex and difficult (Kannan et al., 2011). The Loskop irrigation scheme is the second largest in South Africa (Oberholster and Botha, 2011). The study aimed to determine if SWAT could model the hydrology and quantify nutrient loss from irrigated agricultural activity adequately.

15.2 Study Area

This study area is the Middle Olifants catchment (Figure 134: The Upper, Middle and Lower Olifants (Biggs et al., 2017)). It is part of the Olifants Basin which is split into the Upper, Middle and Lower Olifants. The Middle Olifants is where most of the agricultural activity occurs and is the third most water stressed basin in South Africa. It has an area of 22 550 km^2 and receives 500 mm of rainfall per annum. One of the primary water users in this area is large scale irrigated agriculture (Walter et al., 2011).

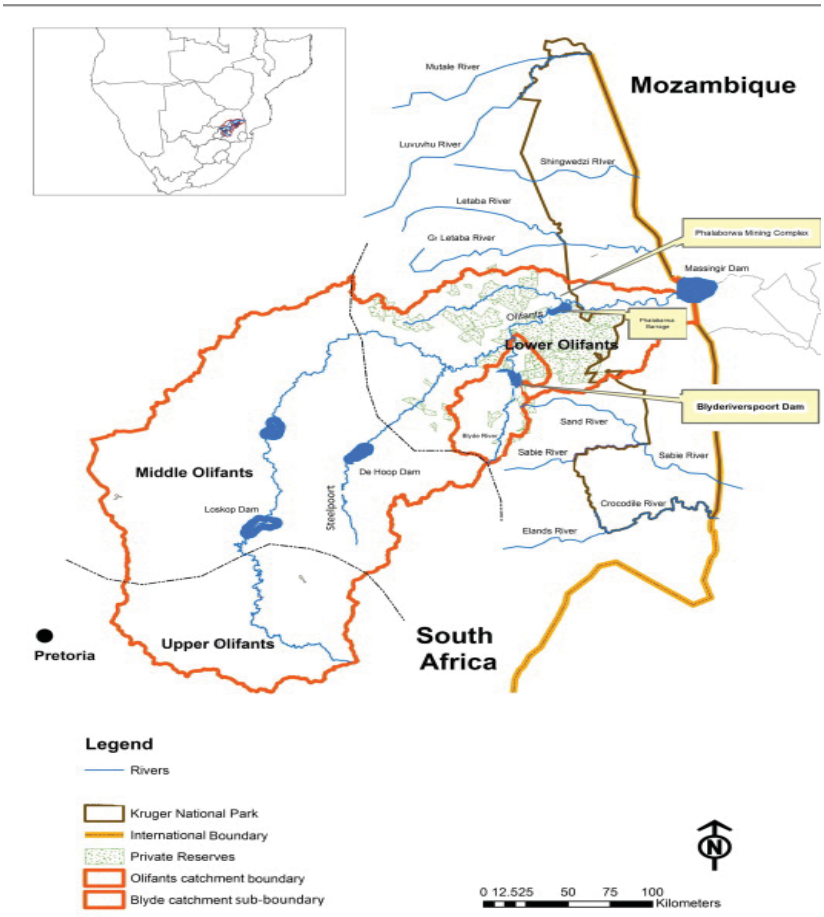

Figure 134: The Upper, Middle and Lower Olifants (Biggs et al., 2017)

The Middle Olifants is heavily reliant on the agricultural sector (Department of Water Affairs, 2011). There are several large-scale irrigation farmers in the area who grow high value crops such as citrus and grapes, which require large volumes of water for their production (Department of Water Affairs, 2011; Walter et al., 2011). Much of this produce is exported globally (Walter et al., 2011). The total area under agriculture is about 22 9713 ha. Dryland agriculture accounts for 114394 ha and irrigated agriculture for 49821 ha. Subsistence farming takes up about 65 499 ha. Pasture is the prominent crop type (10876 ha) followed by maize (5080 ha) (Department of Water Affairs, 2011). The dominant crops in the irrigation area are maize, citrus and wheat (Oberholster and Botha, 2011). Irrigation in the Loskop area occurs throughout the year with some crops irrigated for all 12 months and other irrigated seasonally (de Lange et al., 2016).

15.3 Method and Materials

15.3.1 Setting up the SWAT model

15.3.1.1 Programme selection

The programme selected to run the SWAT model for this study was ArcGIS version 10.4. Input data for SWAT requires spatial data. There are GIS tools for extracting information from spatial data for SWAT that have been developed. ArcGIS-SWAT was developed for the ArcGIS platform. This has the ability to store SWAT geographic, numeric and text input data and results. An important feature of ArcGIS-SWAT is that it geo-references hydrologic response units (HRUs). Hydrologic response units are units of similar land uses, soils and slope within a sub-basin (Kalcic et al., 2015). This allows a more accurate calculation of the model parameters because values are not averaged over the sub-basins (Olivera, 2006).

15.3.1.2 Input for SWAT

The use of a highly parameterized model such as the SWAT requires initial data preparation of a large and multi-disciplinary database. The use of SWAT in countries that do not have well-developed databases makes this process slightly more challenging (Bouslihim et al., 2016). The first step that needs to be taken for data preparation is the selection of a GIS interface in which to run SWAT. Thereafter a digital elevation map (DEM) of the catchment area, a land cover map and a soil map of the catchment area needs to be acquired. These maps then need to be projected. The ArcSWAT spatial datasets may be created in any projection. The only requirement is that the same projection is used for all maps (Winchell et al., 2010). The projection selected for all maps used for the model was the Africa Albers Equal projection. Re-projections were done using the re-project tool in ArcGIS 10.3.1.

15.3.2 Digital elevation model

The digital elevation map (DEM) used was a 20 m digital terrain model of South Africa (ASTER/GDEM, 2009). The DEM was clipped to cover the Middle Olifants catchment. Figure 135 below represents the DEM of the catchment.

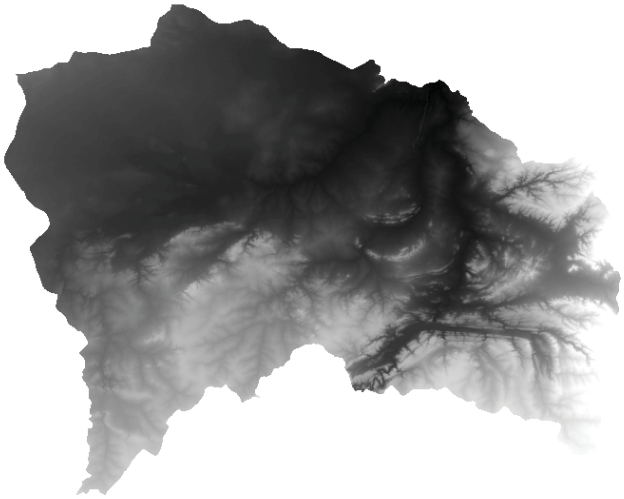

Figure 135: DEM of the middle Olifants catchment

15.3.3 Land cover map

The land use map chosen for the model was the National Land Cover map developed by SANBI (SANBI, 2009). Figure 136 below shows that the majority of catchment area is uncultivated (55%), with agricultural activity occupying 29% of the study area. Residential areas make up 5% of the land use and industrial activities account for less than 1%.

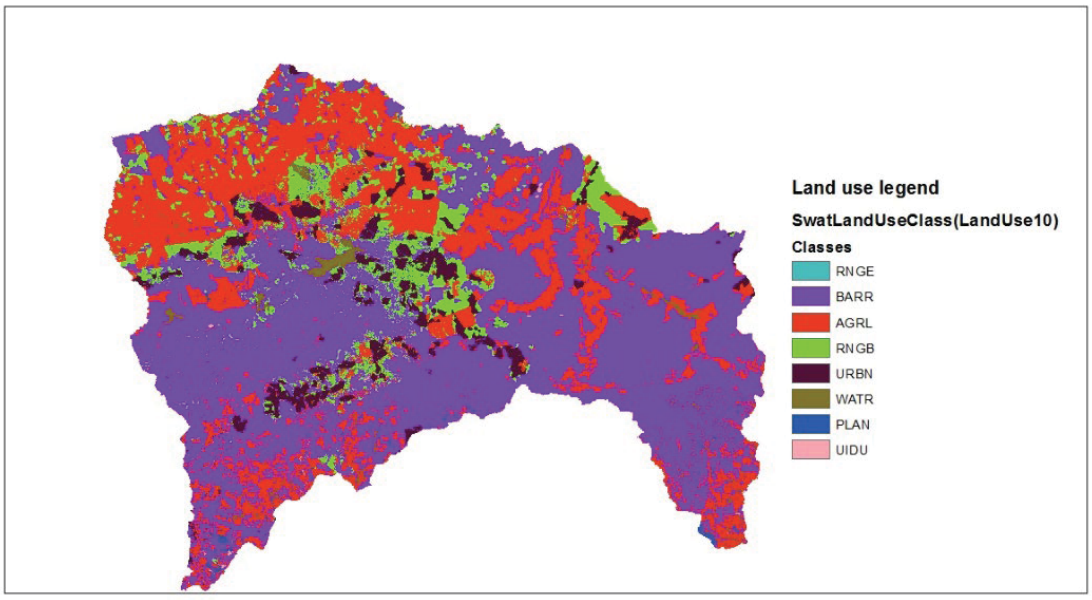

Figure 136: Land use map of the Middle Olifants catchment

15.3.4 Soil map

The soil map used was from land type survey staff (1984), seen in Figure 137: Map representing soil classes. A fair amount of soils data was associated with this map, however there were patches in the data that needed to be supplemented by other sources. One of the sources used was the land type memoirs generated by the land type survey staff (1984) and the other was the Schulze (2007) map. Another source used was SPAW (Soil-Plant-Air-Water). This model simulates daily hydrologic water budgets (Saxton et al., 2006). The use of SPAW was necessitated where data required by the SWAT was not identified in the Schulze (2007) and land type survey staff (1984) maps. Table 63 provides a breakdown of how the soil parameters were identified for use in the model.

Table 63: Method used to assign value to required SWAT soil characteristics

SWAT soil parameter	Description	Method used to obtain value
SNAM	Soil name	Used the name as given in the land type memoirs (Land type survey staff, 1984)
NLAYERS	Number of layers in soil profile	Always used a value of 1 (only wanted one depth)
HYDGRP	Soil hydrologic group	Taken from Schulze (2007)
SOL_ZMX	Maximum rooting depth of soil profile (mm)	Taken from Schulze (2007)
ANION_EXCL	Fraction of porosity from which anions are excluded	Could not obtain values
SOL_CRK	Potential or maximum crack volume of the soil profile expressed as a fraction of total soil volume	Could not obtain values
TEXTURE	Texture of soil layer	Given in the land type memoirs (Land type survey staff, 1984)
Soil Layer	Soil layer	Always used a value of 1 (only wanted one depth)
SOL_Z (mm)	Depth to bottom of soil layer (mm)	Taken from Schulze (2007)

SWAT soil parameter	Description	Method used to obtain value
SOL_BD (g/cm^3)	Moist bulk density of soil layer (Mg/m3)	Derived from SPAW
SOL_AWC (mm/mm)	Available water capacity of soil layer (mm/mm)	Taken from Schulze (2007)
SOL_CBN (% wt.)	Organic carbon content of soil layer (%)	Similar to Le Roux et al. (2015), an unpublished carbon map of SA derived from soil profile and landtype datasets was used to assign carbon values to each landtype in the study area.
SOL_K (mm/hr)	Saturated hydraulic conductivity of soil layer (mm/hr)	Derived from SPAW
CLAY (% wt.)	Clay content of soil layer (%)	Values were provided in the land type memoirs (Land type survey staff, 1984). The average of the range of values provided was used.
SILT (% wt.)	Silt content of soil layer (%)	Similar to Le Roux et al. (2015), silt content was assigned values between 10-22.5%, increasing with increase in clay as follows: percentage of landtype with <= 6% clay = 10% silt; 6.1-15% clay = 15% silt; 15.1-25% clay = 17.5% silt; 25.1-35% clay = 20% silt; 35.1-55% clay = 22.5% silt.
SAND (% wt.)	Sand content of soil layer (%)	Similar to Le Roux et al. (2015), sand content was estimated as follows: Sand = 100% – (%clay + %silt + %rock + %carbon).
ROCK (% wt.)	Rock content of soil layer (%)	Similar to Le Roux et al. (2015), the agricultural restriction/rock (MB) classes in for each landtype was as follows: MB0=0%; MB1=20%; MB2=50%; MB3=20%; MB4=100% (no soil).
SOL_ALB (fraction)	Moist soil albedo of soil layer	Similar to Le Roux et al. (2015), moist soil albedo was assigned to the landtype based on texture of the dominant soil as follows: Sands = 0.25; clays = 0.7; remaining textures = 0.5.
USLE_K	USLE equation soil erodibility (K) factor	Taken from Schulze (2007)
SOL_EC (dS/m)	Electrical conductivity of soil layer (dS/m)	Could not obtain values

SWAT soil parameter	Description	Method used to obtain value
SOL_CAL (%)	Calcium carbonate content, (%)	Could not obtain values
SOL_PH	Soil pH	Could not obtain values

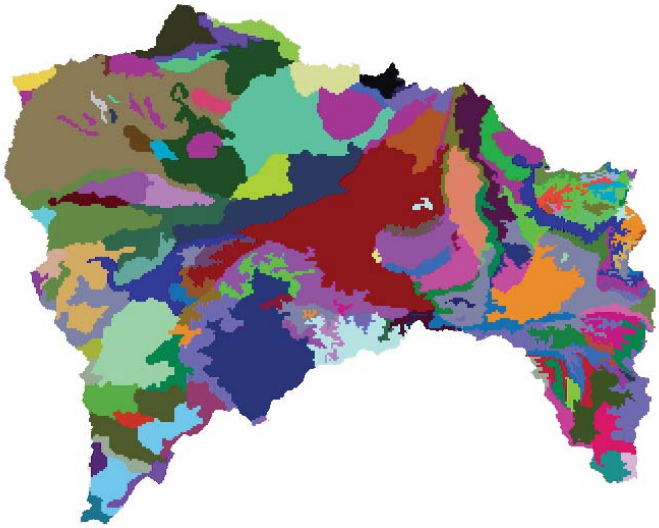

Figure 137: Map representing soil classes

15.3.5 Sub-basins and HRUs

A SWAT model simulation begins by separating subunits that will be defined within a watershed. The first division is the sub-basin. Sub-basins are geographically positioned in the watershed in such a way that they are spatially related to each other. In this way, the outflow of one particular sub-basin is the inflow of another. A sub-basin contains a minimum of one HRU, a tributary channel and a main channel or reach (Arnold et al., 2012). The below image (Figure 138) illustrates the sub-basins that make up the Middle Olifants catchment. There are 58 sub-basins in the catchment.

The land area in the sub-basins can be partitioned into HRUs (Arnold et al., 2012). These are areas of the landscape that have similar land uses, soils and slope within a sub-basin (Kalcic et al., 2015). An HRU does not correspond to a field but rather represents the total area with unique land use, soil and management characteristics. Individual fields within these specific afore-mentioned characteristics are combined to form one HRU. It is often impractical to simulate individual fields and SWAT simplifies this process by creating HRUs (Arnold, 2012).

The SWAT model assumes that there is no interaction between HRUs in a particular sub-basin. Loadings, such as runoff with sediment and nutrients transported by runoff, are calculated separately for each HRU. The separate loadings are then added to determine the total loadings from that sub-basin. The benefit of an HRU is the accuracy that it adds to the prediction of loadings from sub-basins.

It does this by taking into account the diversity of plant cover within a sub-basin. This makes the calculation of net runoff entering a main channel/reach from the sub-basin more accurate (Arnold, 2012).

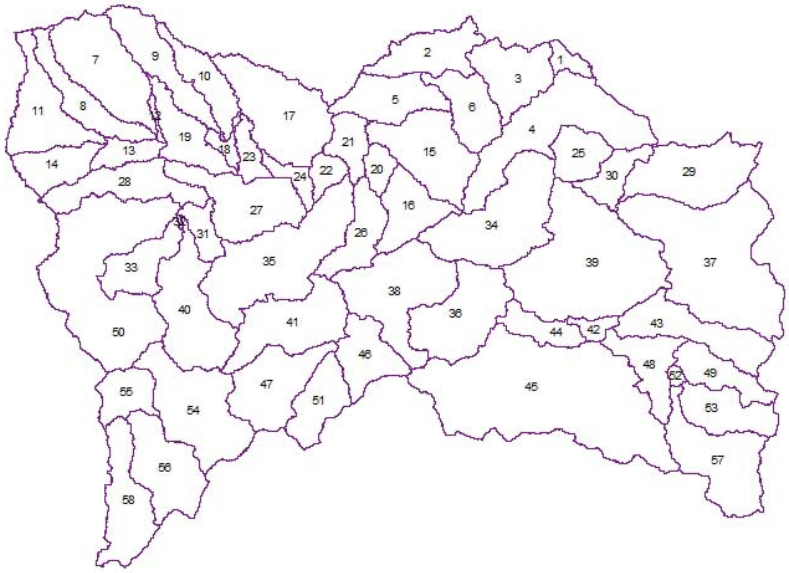

Figure 138: Sub-basins the make up the Middle Olifants catchment

15.3.6 Main channels / reach

Each sub-basin is associated with one main channel or reach. Loadings from the sub-basin and outflow from the upstream reach segments enter the channel network of the catchment in the associated reach segment (Arnold, 2012). Figure 139 below illustrates the main channel associated with each sub-basin for the Middle Olifants catchment.

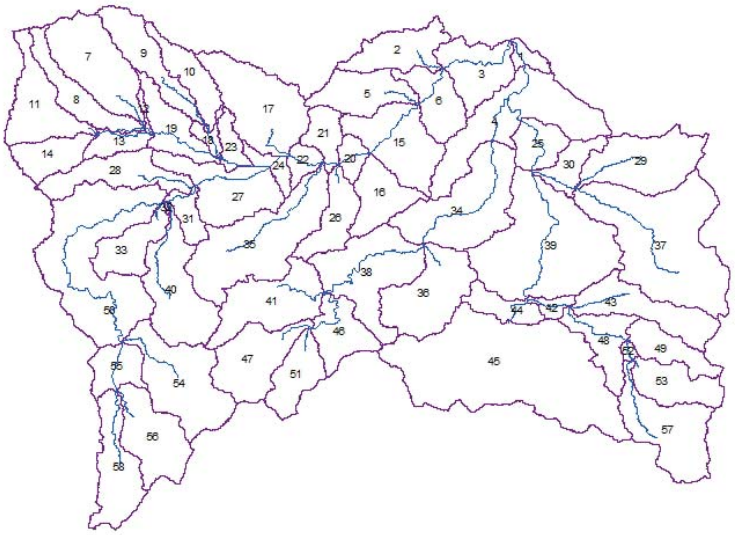

Figure 139: Main channels associated with each sub-basin

15.3.7 Writing Input tables

This Write Input Tables option is the next step once the watershed has been configured. This is the process of building database files that contain the necessary information that is required to generate default input for the SWAT model (Winchell et al., 2013). The first step is to define the weather data. The two most important parameters of the weather data are air temperature and precipitation. Solar radiation, relative humidity and wind speed are good parameters to include but are optional for the model.

15.3.8 Weather data

The climate data for the Middle Olifants catchment was obtained from the Agricultural Research Council's Institute for Soil, Climate and Water (ARC ISCW) as well as the South African Weather Services (SAWS). The period that had the least patchy weather data, and coincided with good Department of Water Sanitation (DWS) data for calibration, was 1984 till 2001. This was therefore used to run the model.

15.3.9 Creation of input

In order for the SWAT model to run, the initial watershed input values need to be defined. These values are set automatically based on the watershed delineation and the characterization of the land use, soil and slope. Input tables need to be written for the specific catchment characteristics. There is an option to create and populate all the tables with default values. This can later be re-written with data specific to the catchment of interest. Once all of the default inputs have been created, a SWAT run can be made from the SWAT simulation (Winchell, 2013).

The reservoir file was edited to accommodate the Loskop dam and the release data, which was supplied by DWS. The management file was changed in order to reflect the land use of the catchment in order to accommodate the agricultural land covered by intensively irrigated horticulture and agricultural land covered by maize. An auto-irrigation operation (based on plant-water demand) was added to the management of the HRU's with agricultural land use with the source of the irrigation water being Loskop Dam.

The auto-irrigation function in SWAT is based on a water stress identifier of either 1) plant water demand or 2) soil water content. The plant-water demand option applies irrigation water whenever a user-defined decrease in plant growth occurs due to water stress. The soil water content option triggers irrigation when a user-defined soil water deficit threshold is exceeded (Chen et al., 2018). If no value is provided, SWAT assigns a default irrigation amount of 25.4 mm (Chen et al., 2017). The soil water deficit is calculated as the difference between field capacity and soil water content (Chen et al., 2018).

Actual field irrigation is commonly scheduled according to soil water content fluctuations in the plant rooting zone (Chen et al., 2017), however, recent studies have concluded that limitation of the soil water content method could result in inadequate simulation of irrigation from reduced system capacities related to center-pivot travel times. A study also found that SWAT auto-irrigation triggered by the soil water content method resulted in actual irrigation amounts that varied greatly from what was observed in the field, even though the simulation of evapotranspiration was reasonable (Chen et al., 2018).

15.3.10 Calibration of flow

The model was calibrated using DWS flow data. The monitoring point chosen at the outlet was B3H001. This gauge is called Olifants River North of Loskop Dam and the coordinates are 24°55'36.0"S, 29°23'21.9"E. This monitoring point is located in sub-basin 4 in the SWAT catchment A calibration period was used from 1984 until 1991. Calibration is the procedure of adjusting parameter values to optimize model performance according to a set of pre-defined criteria (Jajarmizadeh et al., 2017). Validation is necessary in order to assess the accuracy of the calibration. A local sensitivity analysis was performed initially to look at sensitive parameters. The model output was thereafter put into Soil Water Assessment Tool – Calibration and Uncertainty Procedures (SWAT-CUP) for automatic calibration. This is a stand-alone programme that was developed for SWAT calibration (Abbaspour et al., 2015). The SWAT-CUP programme links Sequential Uncertainty Fitting ver. 2 (SUFI-2), Particle Swarm Optimization (PSO), Generalized Likelihood Uncertainty Estimation (GLUE), Parameter Solution (ParaSol) and Markov Chain Monte Carlo (MCMC) algorithms to the SWAT model (Khalid et al., 2016). The algorithm used for this calibration was SUFI-2. This is efficient to use for time-consuming large-scale models (Abbaspour et al., 2015).

In SUFI-2, a P-factor is used to quantify the degree of all uncertainties. This is the percentage of measured data bracketed by the 95% prediction uncertainty (95PPU). The R-factor is also used in order to quantify the strength of a calibration/uncertainty analysis. This is the average thickness of the 95PPU band divided by the standard deviation of the measured data. The algorithm of SUFI-2 brackets most of the measured data with the smallest possible uncertainty band. The 95PPU is calculated at the 2.5%

and 97.5% levels of the cumulative distribution of an output variable that is obtained through Latin Square hypercube sampling (a statistical method for generating a near-random sample of parameter values from a multi-dimensional distribution), while disallowing 5% of the very bad simulations. A P-factor of 1 and an R-factor of 0 is a simulation that corresponds exactly to measured data (Khalid et al., 2016).

Model simulation can be judged as 'satisfactory' if the Nash Sutcliffe efficiency (NSE) > 0.5 and RMSE (root mean square error) – observations standard deviation ratio (RSR) ≤ 0.70 and if Percentage bias (PBIAS) is ± 25% for streamflow. The NSE is a normalized statistic that determines the relative magnitude of the residual variance ('noise') compared to measured data variance ('information'). An NSE of '1' is the optimal value. Percentage bias measures the average tendency of simulated data to be greater or less than the observed counterparts and is expressed as a percentage. The optimal value is '0' indicating an accurate model. Positive values indicate model underestimation bias, and negative values indicate model overestimation bias. (Moriasi et al., 2007).

15.4 Results and Discussion

15.4.1 Model calibration

The initial relationship between the observed and simulated data can be seen in Figure 140. The first simulation showed that there were some extremely high peaks that could not be explained by rainfall events. Upon investigating the source of the peaks it was observed that extremely high flow values corresponded to missing weather data. A value of -99.0 is inserted where weather data is unavailable and SWAT recognizes this as missing data and generates data for that day (in this case precipitation). The results in Figure 141 show that the missing data in the weather file was patched by using data from another weather station in the same area. This resulted in more accurate precipitation, lower flows and a closer relationship between observed and simulated peaks. This indicates that SWAT did not generate accurate precipitation data for the missing values. In Figure 141, the period 1984 to 1986 shows low observed flow compared to simulated flow due to a drought period that SWAT did not pick up.

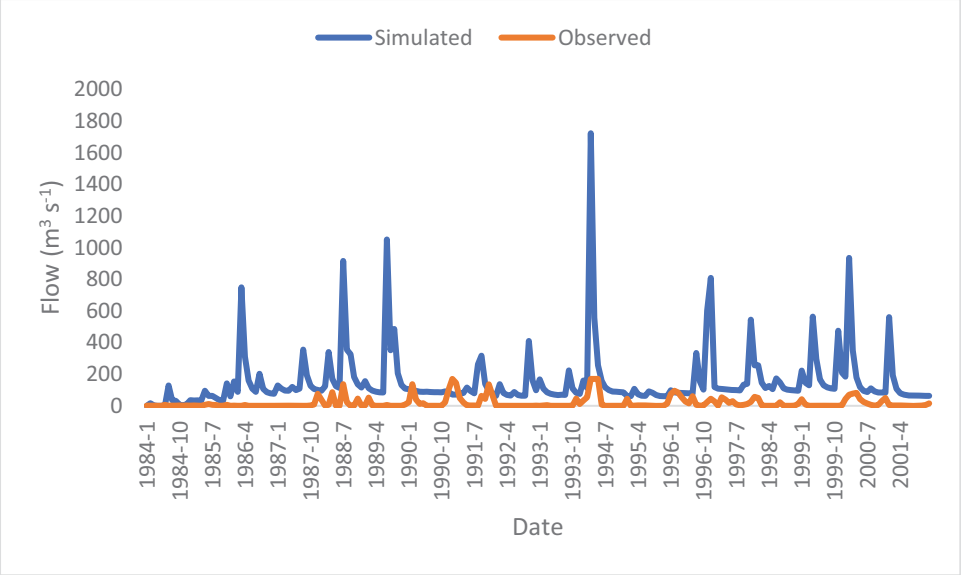

Figure 140: Simulated vs observed flow after model run

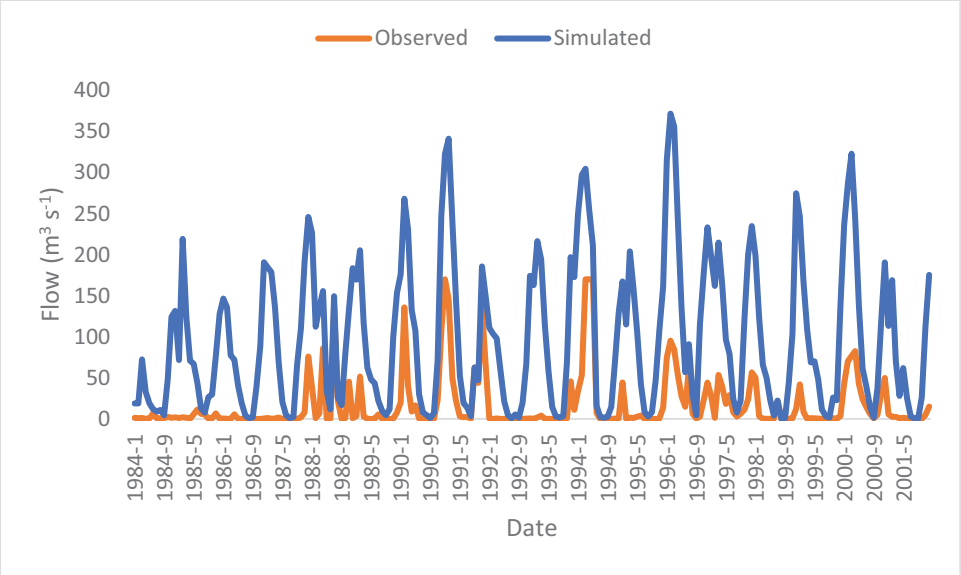

Figure 141: Simulated vs observed flow after weather data patching

The patching of the weather data removed the very high peaks however the simulated flow was still overestimated. A manual local sensitivity analysis was performed to find the sensitive parameters to reduce the peak flow of the simulated data to better fit the observed data. The first parameter that was changed was CH_N2, which is Manning's n value, used to estimate channel flow (Me et al., 2015). The results shows that there was no observable difference in the model output, and therefore the model was not very sensitive to this parameter. The CN2 (curve number) was then lowered to see if this would reduce peak flow. According to Abbaspour et al. (2015), when the peak flow is too high, the CN2 should be reduced. The CN2 was adjusted to a value of 25 and lower peak flows were obtained, as illustrated in Figure 142.

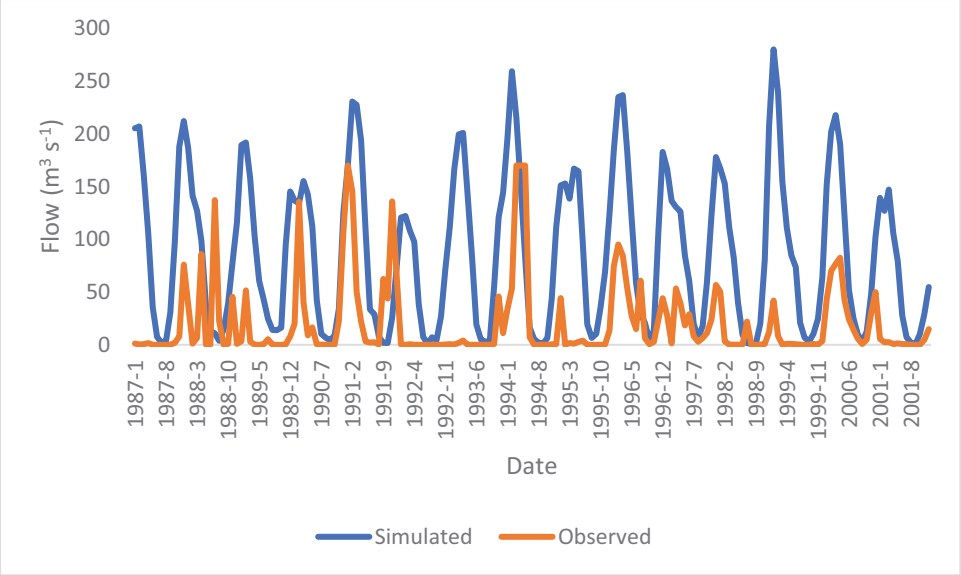

Figure 142: Simulated vs observed flow after changing CN2

Once the peaks matched well, the model was automatically calibrated with SWAT-CUP using the SUFI-2 algorithm. The period 1984 until 1987 was used as a 3 year warm up period. A warm up period is necessary in order to minimize the effects of the estimated initial state variables such as soil water content and surface residue (Singh et al., 2014). Parameters used for calibration were selected according to the ones which affect flow. The first calibration was conducted using the first six parameters as shown in Table 64 and 1000 iterations were run. The results are seen in Figure 143. The calibration was redone using all of the parameters in Table 64 with 100 iterations and the results are in Figure 144. The model performance statistics are provided in Table 65. The calibration with more parameters influenced flow calibration to a larger extent and resulted in more accurate model performance statistics. All statistics improved when all of the parameters that influence flow were used for calibration.

Table 64: Parameters used for calibration

	Parameter code	Description
1	CN2	Initial SCS runoff curve number for moisture condition II
2	ALPHA_BF	Baseflow alpha factor
3	GW_DELAY	Groundwater delay
4	GWQMN	Threshold depth of water in the shallow aquifer for 'revap' to occur
5	ESCO	Soil evaporation compensation factor
6	SOL_AWC	Available water capacity of the soil layer
7	GWREVAP	Groundwater 'revap' coefficient
8	CH_N2	Manning's 'n' value for the main channel
9	CH_K2	Effective hydraulic conductivity in the mail alluvium
10	ALPHA_BNK	Baseflow alpha factor for bank storage
11	SOL_K	Saturated hydraulic conductivity of soil layer
12	SOL_BD	Moist bulk density of soil layer

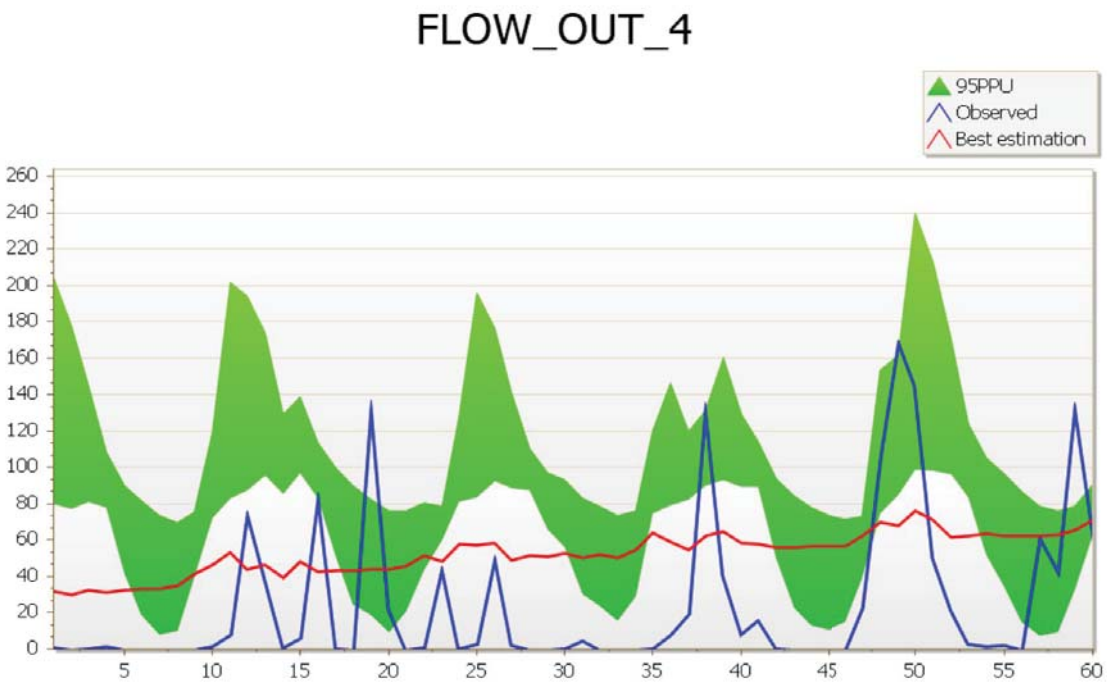

Figure 143: SWAT-CUP calibration with 6 parameters

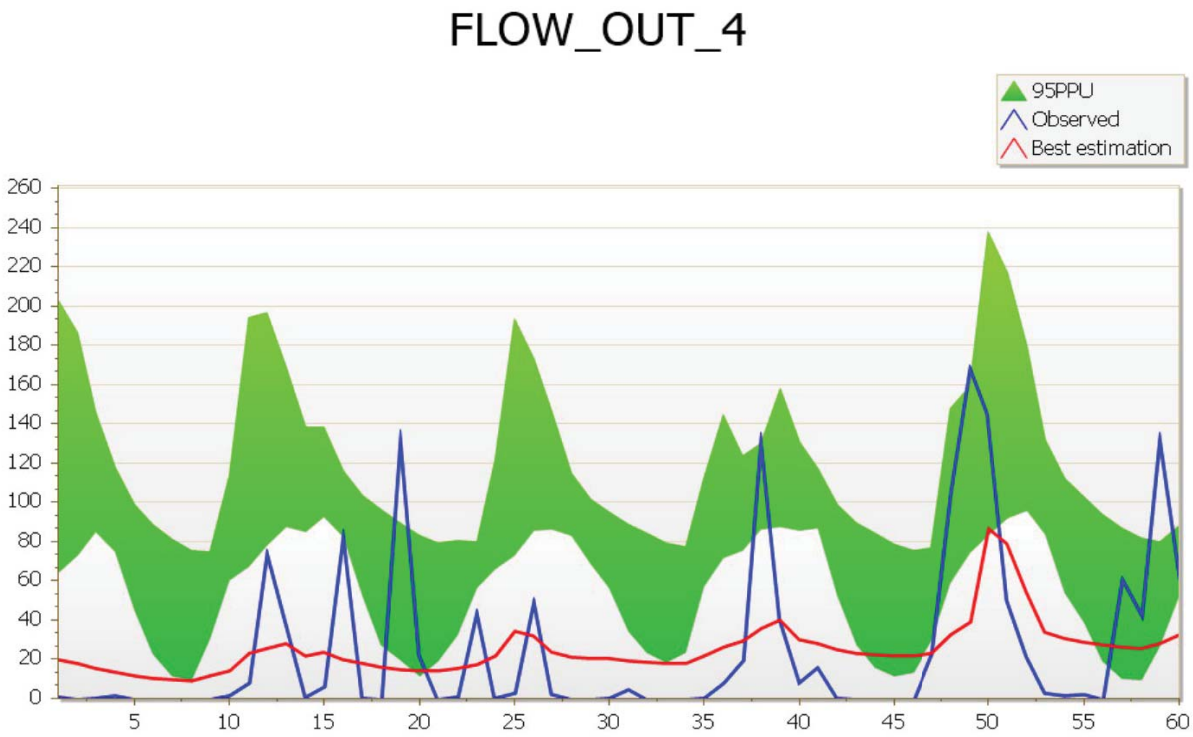

Figure 144: SWAT-CUP calibration with all parameters

Table 65: Model performance statistics

No. of parameters used for calibration	R^2	NS	PBIAS
6 parameters	0.17	-0.24	-104.4
All parameters	0.22	0.2	1.3

Sensitivity of one parameter often depends on the value of another parameter therefore a global sensitivity analysis was performed in SWAT-CUP in order to see which parameters are most sensitive during calibration (Arnold et al., 2012). The P-value and t-stat are important to look at here. The larger the absolute t-stat value and the smaller the P-value, the more sensitive the parameter. From Table 66 it can be seen that SOL_K followed by ALPHA_BNK, SOL_BD and lastly ALPHA_BF were the most sensitive parameters (Figure 144). This is contrary to the parameters that flow is usually most sensitive to, which are GWQMN, CN2 and GWREVAP. This will be checked again when improving calibration. These parameters will have to be improved to optimize the calibration.

Table 66: Global sensitivity analysis

Parameter Name	t-Stat	P-Value
4:V__GWQMN.gw	-0.07	0.94
5:V__ESCO.hru	0.12	0.90
1:R__CN2.mgt	0.39	0.69
7:V__GW_REVAP.gw	0.45	0.65
8:V__CH_N2.rte	-0.74	0.46
3:V__GW_DELAY.gw	0.79	0.43
6:R__SOL_AWC(..).sol	1.28	0.20
9:V__CH_K2.rte	-5.92	0.00
2:V__ALPHA_BF.gw	6.72	0.00
12:R__SOL_BD(..).sol	8.17	0.00
10:V__ALPHA_BNK.rte	8.74	0.00
11:R__SOL_K(..).sol	14.60	0.00

The results that were obtained thus far correspond to several studies in irrigated watersheds with similar results. Studies of the use of SWAT in intensive irrigation systems, where irrigation return flows are the major component of the hydrologic balance, could not produce total stream flow adequately due to limitations in applying maximum irrigation doses in an irrigation event, especially when the irrigation source is outside the watershed (Dechmi et al., 2012). In this study the irrigation source, Loskop Dam, was within the watershed, however inadequate flow was produced by the model. Studies have also reported that the default auto-irrigation function was unable to adequately represent the hydrological processes in intensively irrigated watersheds. An example is the continuation of irrigation events after crop harvesting when using the soil water content method (Chen et al., 2018). It is therefore imperative to get as much information on irrigation scheduling in the Middle Olifants before calibration continues.

15.5 Preliminary P export results

A rough estimation of P losses was looked at from the SWAT model output as it stands. It is important to note that this is taking into account that there was no data from wastewater treatment works to add to the model and importantly that model is not fully calibrated. We are currently trying to obtain wastewater treatment works data but this is a sensitive issue. We expect to have achieved significant improvements in Middle Olifants simulations by the time we submit the final report.

The SWAT output in the reach file indicated mineral P and sediment P in surface runoff. Mineral P is a measure of dissolved reactive P (orthophosphate) concentrations, which is an indication of the waterbody's ability to support the growth of algal blooms. These were used to represent a trend to look at which land use activities contributed the most to the loads with respect to these two parameters. Intensively irrigated horticulture is found in sub-basins 3, 4, 6, 15, 25 and 34. Table 67 indicates the

highest loads of mineral P from these sub-basins. Loads are sorted in descending order and the 10 highest concentrations are represented. The loads highlighted in yellow in indicate the sub-basins with intensively irrigated horticulture.

Table 67: Highest mineral P loads

Sub-basin	Mineral P (kg for simulation period)	kg P ha^{-1} exported (kg for simulation period)
3	1081	0.013
1	972	0.011
6	932	0.011
4	923	0.011
34	833	0.010
15	769	0.009
38	644	0.008
20	424	0.005
41	342	0.004
21	305	0.004

From table 67 it can be seen that the highest P loads come from the sub-basins with intensive horticulture. P loads in surface runoff are also highest from the area of intensive horticulture. This is likely due to the increased fertilizer required for horticulture production and resulting loss due to rainfall and/or irrigation. A calculation of the percentage of the P in runoff that is orthophosphate is provided in table 68. From this it can be seen that the majority of the P lost is in the form of phosphate, which is the primary limiting factor for eutrophication. In most cases it accounts for over 70% of the P in the surface runoff. The results provide an idea that irrigated agriculture, horticulture in particular, contributes to P losses in the Middle Olifants catchment. Most of this P is in the form of phosphate, which is the major driver of eutrophication. This trend need to be quantified accurately once the model has been calibrated and validated.

Table 68: Percentage of P in the form of phosphate in surface runoff

Sub-basin	Total P in surface runoff (kg for simulation period)	Mineral P (kg)	Percentage of orthophosphate in the runoff P (kg)
15	1359	769	56.6
6	1331	932	70.0
3	1306	1081	82.8
34	1100	833	75.7
4	1088	923	84.9
16	746	769	103

15.5.1 Recommendations for future research

Proper calibration and validation of models with the use of observed data is required to meaningfully evaluate outputs and its subsequent use in decision-making (Chen et al., 2017). The model calibration has to be further refined and validated to accurately evaluate nutrient loads and quantify agricultural contributions to nutrient pollution in the Middle Olifants catchment. It would be useful to adjust the irrigation input according to irrigation scheduling information for the study area. A study by Kannan et al. (2011) showed that irrigation systems need to be understood well and represented adequately in watershed models in order to accurately capture irrigation return flows when modelling the hydrology of the irrigated watersheds.

In agricultural watersheds, a continuous monitoring of drainage water in terms of quantity and quality is invaluable to improve the understanding of pollutant dynamics (Dechmi et al., 2012). This is being implemented in parts of Europe. The monitoring studies permit the identification of actual trophic status of freshwater bodies and assess the effectiveness of post-implementation of best management practices (Dechmi et al., 2012). This could be implemented in the Middle Olifants to improve the simulation of accurate nutrient losses.

15.6 Summary and conclusions

A model was created to simulate flow and nutrient loss in the Middle Olifants catchment, where the main economic activity is irrigated agriculture. A reasonable relationship between simulated and observed flow data was reached and SWAT-CUP was used for flow calibration to determine the best parameter values to fit the model. The work done up until this point has unfortunately yielded unacceptable statistics. The results from the last calibration are promising, however, and with further refinement of the calibration it is believed that statistically acceptable results will be obtained.

Conclusions and recommendations with regards to agricultural contributions to nutrient losses were not made as the calibration is incomplete.

15.7 References

ABBASPOUR, K.C., ROUHOLAHNEJAD, E., VAGHEFI, S., SRINIVASAN, R., YANG, H. and KLØVE, B. (2015) A continental-scale hydrology and water quality model for Europe: Calibration and uncertainty of a high-resolution large-scale SWAT model. *Journal of Hydrology* 524: 733-752.

ARNOLD, J.G., MORIASI, D.N., GASSMAN, P.W., ABBASPOUR, K.C., WHITE, M.J., SRINIVASAN, R., SANTHI. C., HARMEL. R.D., VAN GRIENSVEN, A., VAN LIEW, M.W., KANNAN, N. and JHA, M.K. (2012) SWAT: Model use, calibration, and validation. *American Society of Agricultural and Biological Engineers* Vol. 55 (4): 1491-1508.

ASTER – Advanced Spaceborne Thermal Emission and Reflection Radiometer/GDEM – Global Digital Elevation Model: Courtesy of the Ministry of Economy, Trade and Industry (METI) of Japan and the United States National Aeronautics and Space Administration (NASA). https://ssl.jspacesystems.or.jp/ersdac/GDEM/E/4.html

BIGGS, H.C., CLIFFORD-HOLMES, J.K., FREITAG, S., VENTER, F.J. and VENTER, J. (2017) Cross-scale governance and ecosystem service delivery: A case narrative from the Olifants River in North-Eastern South Africa. *Ecosystem Services* https:doi.org.10.1016/j.ecoser.2017.03.008.

BOUSLIHIM, Y., KACIMI, I., BRIRHET, H., KHATATI, M., ROCHDI, A., PAZZA, N.E.A., MIFTAH, A. and YASLO, Z. (2016) Hydrologic modelling using SWAT and GIS, Application to subwatershed Bab-Merzouka (Sebou, Morocco). Journal of Geographic Information System **8** 20-27.

CHEN, Y., MAREK, G.W., MAREK, T.H., BRAUER, D.K. and SRINIVASAN, R. (2017) Assessing the Efficacy of the SWAT Auto-Irrigation Function to Simulate Irrigation, Evapotranspiration, and Crop Response to Management Strategies of the Texas High Plains. *Water* 9 (50): 509. doi:10.3390/w9070509.

CHEN, Y., MAREK, G.W., MAREK, T.H., BRAUER, D.K. and SRINIVASAN, R. (2018) Improving SWAT auto-irrigation functions for simulating agricultural irrigation management using long-term lysimeter field data. *Environmental Modelling & Software* 99: 25-38. https://doi.org/10.1016/j.envsoft.2017.09.013.

DABROWSKI, J., OBERHOLSTER, P.J. and DABROWSKI, J.M. (2104) Water quality of Flag Boshielo Dam, Olifants River, South Africa: Historical trends and the impact of drought. *Water SA* 40 (2): 345-358.

DE LANGE, W.J., BOTHA, A.M. and OBERHOLSTER, P.J. (2016) Monetary value of the impacts of filamentous green algae on commercial agriculture: Results from two geographically different case studies. *Water SA* 42 (3): 449-255. http://dx.doi.org/10.4314/wsa.v42i3.10.

DECHMI, F., BURGUETE, J. and SKHIRI, A. (2012) SWAT application in intensive irrigation systems: Model modification, calibration and validation. *Journal of Hydrology* (470-471): 227-238. http://dx.doi.org/10.1016/j.jhydrol.2012.08.055.

DEPARTMENT OF WATER AFFAIRS, SOUTH AFRICA (2011) Classification of Significant Water Resources in the Olifants Water Management Area (WMA 4): Management Classes of the Olifants WMA. Report No: RDM/WMA04/00/CON/CLA/0213 Prepared by: Golder Associates Africa, Prime Africa and Retha Stassen. http://www.dwa.gov.za/rdm/WRCS/doc/Olifants%20Classification_Management%20Classes_Report_Feb_2013_Final_Draft.pdf.

JAJARMIZADEH, M., SIDEK, L.M., SOBRI HARUN, S. and MOHSEN SALARPOUR (2017) Optimal Calibration and Uncertainty Analysis of SWAT for an Arid Climate. *Air, Soil and Water Research* 10: 1-14.

KALCIC, M.M., CHAUBEY, I. and FRANKENBERGER, J. (2015) Defining Soil and Water Assessment Tool (SWAT) hydrologic response units (HRUs) by field boundaries*. Int J Agric & Biol Eng*, 8 (3) 69-80.

KANNAN, N., JEONG, J. and SRINIVASAN, R. (2011) Hydrologic Modeling of a Canal-Irrigated Agricultural Watershed with Irrigation Best Management Practices: Case Study. *Journal of Hydraulic Engineering* 2011: 746-757. DOI: 10.1061/(ASCE)HE.1943-5584.0000364.

KHALID, K., ALI, M.F., RAHMAN, N.F.A., MISPAN, M.R., HARON, S.H., OTHMAN, Z. and BACHOK, M.F. (2016) Sensitivity analysis in watershed model using SUFI-2 algorithm. *Procedia Engineering* 162 (2016)
441-447. doi: 10.1016/j.proeng.2016.11.086.

LAND TYPE SURVEY STAFF (1984) *Land types of South Africa: digital map (1:250 000 scale) and soil inventory databases.* ARC-Institute for Soil, Climate and Water, Pretoria.

LE ROUX, J.J., BARKER, C.H., WEEPENER, H.L., VAN DEN BERG, E.C. and PRETORIUS, S.N. (2015) *Sediment Yield Modelling in the Mzimvubu River Catchment. Report to the Water Research Commission*. Water Research Commission, Pretoria. WRC Report No. 2243/1/15.

ME, W., ABELL, J.M. and HAMILTON, D.P. (2015) Effects of hydrologic conditions on SWAT model

MORIASI, D.N., ARNOLD, J.G., VAN LIEW, BINGNER, R.L., HARMEL, M.W.R.D. and VEITH, T.L. (2007) Model evaluation of guidelines for systematic quantification of accuracy in watershed simulations. *American Society of Agricultural and Biological Engineers* Vol. 50(3): 885-900.

NEL, J., COLVIN, C., LE MAITRE, D., SMITH, J. and HAINES, I. (2013) South Africa's Strategic Water Source Areas. CSIR Report No CSIR/NRE/ECOS/ER/2013/0031/A.

OBERHOLSTER, P.J. and BOTHA, A-M. (2011) Dynamics of phytoplankton and phytobenthos in Lake Loskop (South Africa) and downstream irrigation canals. *Fundamental and Applied Limnology* 179 (3): 169-178. DOI: 10.1127/1863-9135/2011/0179-0169.

OLIVERA, F., VALENZUELA, M., SRINIVASAN, R., CHOI, J., CHO, H., KOKA, S. and AGRAWAL, A. (2006) ArcGIS-SWAT: A geodata model and GIS interface for SWAT. *Journal of the American Water Resource Association* 04087 295-309.

SALMON, J.M., FRIEDL, M.A., FROLKING, S., WISSER and DOUGLAS, E.M. (2015) Global rain-fed, irrigated, and paddy croplands: A new high resolution map derived from remote sensing, crop inventories and climate data. *International Journal of Applied Earth Observation and Geoinformation* 38: 321-334.

SANBI – South African National Biodiversity Institute: National Land Cover (2009) http://bgis.sanbi.org/landcover/project.asp

SAXTON, K.E., WILLEY, P.W. and RAWLS, W.J. (2006) Field and pond hydrologic analyses with the SPAW model. In: *ASABE Annual International Meeting*, 9-12 July 2006, Portland, Oregon.

SCHULZE, R.E. (2007) *South African Atlas of Climatology and Agrohydrology, WRC Report 1489/1/06*. Water Research Commission: Pretoria, South Africa.

SINGH, A., IMTIYAZ, M., ISAAC, R.K. and DENIS, D.M. (2014) Assessing the performance and uncertainty analysis of the SWAT and RBNN models for simulation of sediment yield in the Nagwa watershed, India. *Hydrological Sciences Journal* 59 (2): 351-364. DOI: 10.1080/02626667.2013.872787.

TIMSINA, J. (2018) Can organic sources of nutrients increase crop yields to meet global food demand? *Agronomy* 8 (2014) 1-30.

WALTER, T., KLOOS, J. and TSEGAI, D. (2011) Options for improving water use efficiency under worsening scarcity: Evidence from the Middle Olifants sub-basin in South Africa. *Water SA* **37** (3) 357-370.

WINCHELL, M., SRINIVASAN, R., DI LUZIO, M. and ARNOLD, J. (2010) ArcSWAT interface for SWAT2009 – User's guide.

16 CONCLUSIONS AND RECOMMENDATIONS

The very nature of agricultural non-point source (NPS) nutrient pollution makes it extremely difficult to quantify or even estimate. Work done in the United States of America, Europe and Australia has shown that agriculture can contribute significantly to river and ocean nitrogen (N) and phosphorus (P) loads, and that it is very challenging to mitigate this type of pollution. This project has helped us take a step closer towards better understanding NPS N and P pollution in South Africa and refining the means to study and manage it.

A scoping study done as part of this research has listed a number of water bodies which are potentially impacted on by NPS pollution from irrigated crop production. Addressing and reducing agriculture's contribution is only a small part of the problem, however. The ineffective management of sewerage in South Africa means that untreated or partially treated wastewater is often returned directly to waterways, and this is most likely the dominant source of N and P pollution. Informal settlements which do not have sanitation infrastructure can also potentially contribute significant amounts of N and P to watercourses.

Research has now been completed on the use of soil water samplers, drainage lysimeters, drain gauges and stable isotope approaches together with mechanistic modelling to better understand the fate of N and P in our agroecosystems. Drain gauges have been used for the first time in South Africa to the best of our knowledge, and show excellent potential for quantifying deep drainage and studying solute leaching. When compared to a large drainage lysimeter, a drain gauge was observed to perform better in representing natural soil drainage conditions. This is due to a fibreglass wicking device at the bottom of the drain gauge that is not present in a traditional drainage lysimeter that improves continuation of flow to the bottom collection device without fully saturated conditions first needing to occur for the release of water at the bottom boundary. Devices such as wetting front detectors and suction cups, when compared with mechanistic modelling using Hydrus, were observed to be very biased to sampling large pore volumes. While this is expected in theory, it remains very important in the interpretation and application of measured solute concentrations collected with these devices in estimating NPS N and P pollution.

The use of stable isotope analysis shows excellent potential in determining nitrogen use efficiencies (NUEs) of crops, without the burden of trying to measure several components of the soil water and nitrogen balances. It cannot, however, fully inform on the fate of applied nutrients not taken up by the crop, for example, how much N not taken up was leached, immobilised or lost in gaseous form. Using a stable isotope approach, we estimated fertiliser NUE to be 68% for a very carefully managed wheat crop.

In a field trial with potatoes in the western Free State, data indicates that there is a high risk for N leaching and the pollution of under-ground water surfaces in South Africa. However, a maize crop following potato in a rotation can recover ('mop-up') some of the residual (previously fertilised) nutrients left behind by the potato crop, thereby minimizing the risk. We conclude that potato production on sandy

soils entails a high risk for N leaching but a minor risk of P leaching, and does represent a potential NPS for nutrient pollution of water bodies. Potato and maize production in sandy soils can gradually lead to nutrient enrichment of underground water and ultimately eutrophication of surface water bodies. Given the high drainage rates observed, we expect there is potential for improving resource use efficiencies by optimizing application of input resources and by rotating shallowly rooted crops such as potato with deep rooting crops such as maize fertilized at moderate rates.

In the catchment-scale modelling of NPS pollution with SWAT, a need to assess the usefulness and reliability of satellite-based weather estimates for accurate water resource assessment was identified. The utility of Climate Forecast System Reanalysis (CFSR) data for streamflow simulation in parts of the Lower Vaal River Catchment was assessed. We setup two SWAT 'models', first with conventional gauge weather data obtained from the South African Weather Services (SAWS) and the Agricultural Research Council (ARC), second with CFSR data. The conventional gauge weather data had eight stations and CFSR weather data had 33 stations. The performance of the two models was compared against the observed flow at five stream gauge locations. We also compared CFSR precipitation against rain gauge measurements for CFSR stations in close proximity with the eight gauge stations. Overall, both the models simulated flow reasonably well in terms of the R^2, NSE and RSR statistics except for the notably poor performance of a model simulated with CFSR data in one sub-catchment where accurate representation of weather data was the most defining model input parameter. The streamflow simulations using conventional weather data outperformed the simulations using CFSR data in three of the five sub-catchments. A poor relationship between CFSR precipitation and rain gauge data was observed, where the R^2 ranged from 0.05 to 0.15. While conventional gauge data remain the most accurate and reliable dataset, CFSR can play a role as an alternative data input where there is insufficient gauge data. CFSR can be used to fill gaps where values are missing and can be used together with gauge data where there are insufficient weather stations.

SWAT was applied to estimate N and P loads in part of the Lower Vaal River catchment, covering an area of approximately 1 343 km^2. We manually calibrated the model for streamflow, ammonia (NH_4), Total-P (TP) and Total-N loads. SWAT performed satisfactorily for flow, based on the R^2 whereas other statistical measures performed poorly. Nutrients load calibration was very poor, but due in part to insufficient calibration. This was probably because of model uncertainties such as input parameters and their value range which cannot be approximated as consistently as in auto-calibration. Future research work should focus on applying auto-calibration procedures such as those offered by the SUFI-2 algorithm of the SWAT-CUP software.

The SWAT model was also used to model the hydrology and water quality, in particular P losses, from agricultural activity, of the Middle Olifants Catchment, which is the second largest irrigation scheme in South Africa and a very intensively irrigated watershed. It has an area of 22 550 km^2 and receives on average 500 mm of rainfall per annum. The SWAT-CUP program was used for automatic calibration. Global sensitivity analysis revealed that the most sensitive parameters for calibration are saturated hydraulic conductivity, the baseflow alpha factor for bank storage, the moist soil bulk density and the

baseflow alpha factor. Calibration of flow and nutrient concentrations is ongoing, but it was noted that streamflow was often over-estimated by the model. Work is underway to better represent the irrigation systems within the catchment to improve streamflow simulation. Highest P pollution loads were estimated to come from sub-basins with intensive horticulture, but relatively low exports were predicted for irrigated agriculture, ranging from 0.004 to 0.013 kg P ha^{-1}.

So how do we go about reducing NPS N and P pollution from agriculture in South Africa? While farmers are encouraged to adopt best management practices that match (temporally and spatially) N and P supplied as fertiliser with crop demand as closely as possible, practical and economical challenges often make this difficult, and this together with the nature of agroecosystems results in some nutrient loss always being inevitable.

In long-term simulation studies guided by historical data, it was shown that sugarcane systems may have been generally over-fertilised with N in the past. Modelling the application of reduced fertilizer application rates did not result in a marked reduction in yield, indicating that mineralized N from SOM can be able to satisfy a proportion of crop N demand, so fertilizer application recommendations should also account for mineralized N to minimize N losses. This can be one way of improving N management in sugarcane cropping systems, thus reducing inputs, increasing profits and minimizing losses that can lead to environmental pollution. But ultimately organic N cannot be relied on as a net source of N, and it is about matching supply and demand both in terms of time and space. For a long-term maize trial which was also simulated, SOM was observed to decline more rapidly in the control treatment receiving zero fertiliser compared to a fully fertilised treatment. APSIM estimated higher drainage in the zero fertilizer but higher N leaching in the fertilized NPK treatment. A manure application scenario proved to be more sustainable for long-term maize production to maintain SOM levels, although it requires a good inorganic N fertilizer management programme to minimize the over-supply of N and subsequent leaching losses.

Further research and incentives to improve farmer nutrient management is required. In this study, research was focussed on more commonly encountered wheat, maize and potato cropping systems in South Africa. But sustainable intensification, including conservation agriculture may have a huge role to play in addressing this problem. ‘Rotational diversity’ or ‘rotational complexity’ (Robertson et al., 2014), which involves rotations with legumes and cover or catch crops, can, for example, play a major role in reducing nutrient export from farmer fields. Cover crops scavenge nutrients from the soil profile, preventing leaching losses and making them available to subsequent crops through recycling. They can also reduce erosion. In some cases, but not always, including rotational complexity may come at the cost of short-term profitability. Multiple other benefits may result however, including decreased pressure from pests and diseases. Greater understanding is needed on who can and should carry these costs.

Some of the NO_3^- that has been exported from cultivated soils can be captured by adjacent riparian vegetation, or chemically altered streamside or in transit to more reduced forms of N, and wetlands can immobilise significant fractions as organic N (Robertson et al., 2014). Restoring, maintaining and/or

constructing wetlands, and the inclusion of appropriate buffer strips of natural vegetation between cultivated lands and fresh watercourses is important to reduce nutrient exports from cultivated land.

Switching from conventional tillage to minimum- or no-till can play an important role, primarily through improved nutrient cycling and the reduction of sediment, SOM and nutrient losses via surface runoff, but also because improved soil structure in no-till systems allows percolating water to move through via bypass flow avoiding equilibration with microsites which may have higher NO_3^- concentrations (Strudley et al., 2008; Robertson et al., 2014). But such systems may also lead to relatively higher deep drainage due to the reduced evaporation, so N fertiliser programmes need to be adjusted accordingly to prevent increased N leaching.

Catchment scale modelling using a model such as SWAT is an arduous exercise. It requires good GIS skills, and there are often many issues in the set-up and calibration phases that need to be overcome. One such example is collecting all the spatial data needed and overlaying it in SWAT in a compatible way. This project has built up significant capacity in this type of modelling in South Africa. The further application of the calibrated models that have been set-up for the Lower Vaal and Middle Olifants for studying NPS pollution, as well as issues such as algal blooms and climate change, would add much value to the work already done over the four years of this project.

Recommendations for future research are:

- Continue to calibrate, refine and apply the SWAT models for the Lower Vaal and Middle Catchments.
- Investigate ways to best communicate findings on NPS pollution to various stakeholders within the catchments and to policy makers.
- Better quantify the contributions of wastewater treatment works to river N and P loads.
- Find ways to incentivise farmers to reduce the application of nutrients to their lands.
- Quantify the contribution of wind erosion to NPS N and P pollution, especially in wind erosion-prone areas such as the Free State.
- Create a platform with all the necessary GIS layers for the whole of South Africa so that new users can get the model up and running for their catchment faster.
- Further investigate the ‘hotspots’ identified in this study.

17 APPENDIX

Appendix A – Capacity Building

Tapera Mangwende

Tapera received his MSc(Agric) Agronomy degree in the University of Pretoria's Department of Plant and Soil Sciences. His dissertation was titled 'Quantifying nitrogen leaching in wheat (Triticum aestivum) using lysimeters, stable isotopes, conservative tracer and modelling techniques'. Tapera now works in Mozambique as an agronomist in the sugar industry.

Leushantha Mudaly

Leushantha is a lecturer at the University of Pretoria in the Department of Plant and Soil Sciences, Faculty of Natural and Agricultural Sciences. Leushantha is currently doing a PhD on monitoring and modelling nutrient pollution of fresh-water resources, in particular non-point source pollution and the role that phosphorous plays. Her study looks at the impact of agricultural phosphorous losses on water quality at field and catchment scale. This Water Research Commission project has provided her the opportunity to pursue her postgraduate studies and continue her role as an early career academic.

Leushantha attended a two day intensive ArcSWAT workshop in Sardegna, Italy in June 2015. The purpose of the workshop was to provide basic training on how to use the SWAT model using ArcGIS as the interface. The workshop covered the following topics:

- An introduction to the SWAT model and its applications
- Watershed delineation
- Land use and soil overlay
- HRU delineation
- Weather and remaining inputs to develop the SWAT model
- Review of summary outputs

This training was essential to get acquainted with the model and how to use it with ArcGIS. While there for the workshop, Leushantha attended the SWAT conference. This included relevant topics to the project such as large-scale applications of SWAT and modelling nutrient loadings using SWAT.

In 2018 Leushantha also attended an Advanced SWAT workshop – SWAT-CUP and a conference in Brussels, Belgium. SWAT-CUP is an auto-calibration tool that was developed for SWAT and is a stand-alone programme. The workshop consisted of two-day intensive training in the use of SWAT-CUP and was presented by the Karim Abbaspour who is the developer. Topics of the training included:

- Sensitivity and calibration/validation (theory)
- Model application

- Uncertainty analysis
- Example of calibration and validation using SWAT-CUP

After the training was completed, Leushantha attended a SWAT conference where relevant topics were being presented. During the conference I was able to interact with developers and experts in the field.

Leushantha has also been involved with the co-supervision of a BSc(Hon) Environmental Soil Science student at the University of Pretoria, Keketso Mokhothu.

Ndifelani Mararakanye

Ndifelani has been studying towards his PhD degree in the Department of Geography of the University of the Free State. His topic is 'Quantification of agricultural nonpoint source nutrient pollution dynamics from field to catchment scale'. Ndifelani works for the Department of Agriculture, Rural Development, Land and Environmental Affairs as a researcher involved in developing and managing the implementation of advanced innovative GISc technology and applications, and providing strategic direction in the organization.

Keketso Mokhothu

Keketso completed his BSc(Hons) Environmental Soil Science degree in the University of Pretoria's Department of Plant and Soil Sciences in 2017. The title of his honours report was 'Estimating the contribution of cultivated land to the Middle Olifants River catchment phosphorous load'. Keketso is now busy with his MSc(Agric) Soil Science degree in the same department.

Allan Machakaire

Allan is currently busy with his PhD degree in the University of the Free State's Department of Soil, Crop and Climate Sciences. The topic of this PhD degree is 'Measuring and modelling water, nitrogen and phosphorous use efficiencies in potato under pivot irrigation in South Africa'. Allan works fulltime as an agronomist for McCain Foods. Allan attended a course on the APSIM crop model in Brisbane during October 2017 and a course on Eddy Covariance systems in Pietermaritzburg in June 2017. Allan has also presented his work at multiple local conferences.

Corrie Swanepoel

Corrie completed her PhD thesis titled 'Assessment of the potential of conservation agriculture management practices to sequester organic carbon in South African soils' in August 2017. Corrie has attended multiple local conferences and workshops as part of her work. Corrie works as a soil researcher at the Agricultural Research Council – Soil, Climate and Water.

Lucian Fredericks

Lucian is studying to obtain an MSc in Agrometeorology Interdisciplinary at the University of the Free State. The focus of his topic is using agricultural simulation models (APSIM) to analyse water and nitrogen dynamics of potato cropping systems, as well as develop and test management strategies that mitigate nitrogen fertilizer pollution. Lucian is in his second year of study and his dissertation is expected to be completed in the first quarter of 2019. During the course of his studies, Lucian has attended a number of workshops offered by University of the Free State's Postgraduate Department. Most of the workshops attended were to develop academic writing skills. After the completion of his studies, Lucian intends to work in the agricultural advisory industry as a consultant.

Simphiwe Maseko

Simphiwe completed his BSc(Hons) Crop Science in the University of Pretoria's Department of Plant and Soil Sciences in 2015 as part of this project. He then continued with his MSc(Agric) Agronomy degree and has just submitted his dissertation titled 'Modelling long-term carbon and nitrogen dynamics in maize (Zea mays l.) and sugarcane (Saccharum officinarum l.) cropping systems in South Africa'.

Appendix B – Project research outputs

Peer-review journal papers

Van der Laan, M., Bristow, K.L., Stirzaker, R.J. & J.G. Annandale (2017) Towards ecologically sustainable crop production: A South African perspective. *Agriculture, Ecosystems & Environment*, *236*, pp.108-119.

Swanepoel, CM; Van der Laan, M; Weepener, HL; du Preez, CC; & Annandale, JG (2016). Review and meta-analysis of organic matter in cultivated soils in southern Africa. *Nutrient Cycling in Agroecosystems*, *104*, 107-123.

Swanepoel, CM; Rötter, RP; Van der Laan, M; Annandale, JG; Beukes, DJ; du Preez, CC; Swanepoel, LH; Van der Merwe, A & Hoffmann, MP (2018) The benefits of conservation agriculture on soil organic carbon and yield in southern Africa are site-specific. *Soil and Tillage Research*, 183, 72-82.

Conference papers

Swanepoel, CM; Van der Laan, M; Weepener, HL; du Preez, CC & Annandale, JG. Quantifying soil organic matter loss due to cultivation in southern Africa. Combined Congress, 23-26 January 2017, ATKV Klein Kariba.

Mudaly L and Van der Laan, M. Understanding the contribution of irrigated agriculture to river nitrogen and phosphorous levels in the Middle Olifants. South African National Committee on Irrigation and Drainage (SANCID) Symposium in White River, Mpumalanga, November 2018.

Mararakanye et al., Using CFSR data as weather input to SWAT in the lower Vaal River Catchment, South Africa. 19th WaterNEt/WARFSA/GWP-SA Symposium, 31 October-02 November 2018, Avani Resort, Zambia, Title:

Appendix C

№	Median Chl a µg/L	n	Median TP mg/L	n	Name (click on name to zoom to site in Google Earth)		Plot Chl a TP	Plot all chem	Secchi disk	T oC	O2 mg/L
1	29.5	13	0.258	11	A2R004Q01 Rietvlei Dam on Hennops River: near Dam Wall			chem	Secchi	T	O
7			0.149	13	A2H013Q01 Scheerpoort 477 JQ Magalies River at Scheerpoort		90165	chem	-	T	-
9			0.875	10	A2H012Q01 Kalkheuwel 493 JQ on Crocodile River		90164	chem	-	T	-
10			0.929	13	A2H014 Schurveberg 488 JQ at Skurweberg on Hennopsrivier		90166	chem	-	-	-
11			0.487	11	A2H083Q01 Hartbeespoort Dam on Crocodile River: Down Stream Weir		90214	chem	-	-	-
12	150.3	24	0.484	23	A2R001Q01 Hartbeespoort Dam on Crocodile River: near Dam Wall			chem	Secchi	T	O
13			0.437	11	A2H048 Krokodilpoort 418 JO /Thaba Moya on Krokodilrivier		90192	chem	-	-	-
14			0.496	11	A2H081Q01 Hartbeespoort Dam on Crocodile River: Left Canal		90212	chem	-	-	-
17			0.146	11	A2H019Q01 Roodekopjes Dam on Crocodile River: downstream Weir		90167	chem	-	-	-
18			0.051	1	A2H113Q01 Roodekopjes Dam on Crocodile River: Left Canal		90231	chem	-	-	-
21	60.4	12	0.115	11	A2R015Q01 Roodekopjes 203 JQ - Roodekopjes Dam on Krokodilrivier: near Dam Wall			chem	Secchi	T	O
22			0.060	6	A2H096 Lindleyspoort 220 JP on Right Canal from Lindley S Poort Dam			chem	-	-	-
28	16.9	11	0.062	9	A2R003 Olifantsnek Dam at Commissiesdrift 327 JQ on Hexrivier near Dam Wall			chem	Secchi	T	O
29			0.010	6	A2H038 Rietvalei 314 JO on Waterkloofspruit Lower Site		90184	chem	-	-	-
30	29.0	12	0.537	9	A2R006 Bospoort Dam at Tweedepoort 283 JQ on Hexrivier near Dam Wall			chem	Secchi	T	O
32			0.056	13	A2H111Q01 Vaalkop Dam on Elands River: downstream Weir		90230	chem	-	-	-
34			2.204	9	A2H027Q01 Pienaars River at Baviaanspoort		90174	chem	-	T	-
36	46.1	22	0.206	23	A2R009Q01 Roodeplaat Dam on Pienaars River: near Dam Wall			chem	Secchi	T	O
37			0.173	11	A2H006Q01 Pienaarsrivier 90 JR at Klipdrift on Pienaars River		90160	chem	-	-	-
38			0.339	1	A2H100Q01 Roodeplaat Dam on Pienaars River: Left Canal		90223	chem	-	-	-
39			0.237	11	A2H102Q01 Roodeplaat Dam on Pienaars River: Down Stream Weir		90225	chem	-	-	-
40			0.201	9	A2H056Q01 Steenoond Spruit at Belle Ombre Station/Apies Confluence		90200	chem	-	-	-
41			0.205	10	A2H057Q01 Skinner Spruit at Daspoort Pretoria/Bantule		90201	chem	-	-	-
42			0.100	11	A2H062Q01 Walker Spruit at Sunnyside Pretoria/Loftus Versveld		90206	chem	-	-	-
43			0.066	9	A2H063Q01 Wonderboom Spruit at Mayville Pretoria		90207	chem	-	-	-
44			0.147	9	A2H085Q01 Bon Accord Dam on Apies River: Right Canal		90216	chem	-	-	-
45	33.2	13	0.113	11	A2R002Q01 Bon Accord Dam on Apies River: near Dam Wall			chem	Secchi	T	O
46	38.6	12	1.222	8	A2R016Q01 Leeukraal Dam on Apies River: near Dam Wall			chem	Secchi	T	O
48			0.714	9	A2H106Q01 Klipvoor Dam on Pienaars River: Down Stream Weir		90227	chem	-	-	-
49	142.9	12	0.759	8	A2R012Q01 Klipvoor Dam on Pienaars River: near Dam Wall			chem	Secchi	T	O
51	7.2	4	0.071	8	A3R002 Klein-Maricopoort Dam at Kalkdam 241 JP near Dam Wall			chem	Secchi	T	O
57	1.9	5	0.086	5	A8R004Q01 Mutshedzi Dam on Mutshedzi River: near Dam Wall			chem	Secchi	-	-
60	3.5	7	0.062	9	A8R002Q01 Luphephe Dam on Luphephe River: near Dam Wall			chem	Secchi	-	-
62	1.8	5	0.050	2	A9R001Q01 Albasini Dam on Luvuvhu River: near Dam Wall			chem	Secchi	T	O
65			0.148	2	B1H005Q01 Olifants River at Wolvekrans			chem	-	-	-
66			0.148	6	B1H019 Naauwpoort 335 JS on Noupoortspruit			chem	-	-	-
74			0.059	5	B2H004Q01 Os Spruit at Boschkop		90434	chem	-	-	-
75			0.208	6	B2H010Q01 Bronkhorstspruit Dam on Bronkh. Spr: Return to Ri		90440	chem	-	-	-
76	15.4	12	0.093	9	B2R001Q01 Bronkhorstspruit Dam on Bronkhorstspruit near Wall			chem	Secchi	T	O
77			0.076	6	B2H003Q01 at Bronkhorstspruit on Bronkhorstspruit		90433	chem	-	-	-
78	7.5	12	0.047	7	B3R001Q01 Kliprand 76 JR - Rust de Winter Dam on Elandsrivier: near Dam Wall			chem	Secchi	T	O
81			0.068	4	B3H015Q01 Loskop Dam on Olifants River: Left Canal			chem	-	-	-
93			0.060	4	B7H007Q01 at Oxford on Olifants River			chem	-	-	-
105	5.0	8	0.082	4	B8R009 Nsami at Nsami Dam near Dam Wall			chem	Secchi	-	-
					B8R005Q01 Tzaneen Dam on Groot Letaba: near dam wall						
108			0.346	18	C1H006 Rietvley 488 IS on Blesbokspruit		90588	chem	-	-	-
109			0.119	17	C1H007Q01 Vaal River at Goedgeluk/Bloukop		90589	chem	-	-	-
110			0.102	12	C1H005 Welbedacht 382 IS on Leeuspruit		90587	chem	-	-	-
112			0.077	5	C1H019Q01 Grootdraai Dam on Vaal River: downstream Weir		90599	chem	-	-	-
113			0.071	8	C1H020Q01 Grootdraai Dam on Vaal River: Right Canal to Saso		90600	chem	-	-	-
114			1.058	17	C1H008Q01 Elandslaagte on Waterval River		90591	chem	-	-	-
115			0.151	14	C1H012Q01 Vaal River at Nooitgedacht/Gladdedrift		90595	chem	-	-	-
117	6.6	12	0.078	14	C1R001Q01 Vaalbank 476 IR - Vaal Dam on Vaalrivier: near Dam Wall			chem	Secchi	T	O
118	11.4	11	0.106	10	Inlet to Homestead from Blaaupan Lake at Benoni			chem	-	-	-
120	26.9	11	0.084	11	Inlet to Civic Lake at Benoni			chem	-	-	-
121	60.4	11	0.107	9	Outlet Kleinfontein at Benoni			chem	-	-	-
122	10.8	11	0.048	11	Roodepoort Bothasfontein 408 JR - at Florida Lake Outlet			chem	-	-	-
124			0.100	1	C2H122Q01 Vaal Dam on Vaal River: Down Stream Weir		90678	chem	-	-	-
125			0.355	11	C2H140Q01 Vaal River at Woodlands/Goose Bay Canyon		90688	chem	-	-	-
128			0.314	18	C2H069Q01 Mooirivierloop (River) at Blaauwbank		90652	chem	-	-	-
133			0.297	7	C2H061 Palmietfontein 250 - at Klipplaatdrift on Vaal River			chem	-	-	-
138			0.099	13	C3H007 Espagsdrif Seoding 25 Bridge at the Weir on Harts River			chem	-	-	-
139			0.108	12	C3R002Q01 Farm 92 - Spitskop Dam on Hartsrivier: near Dam Wall			chem	Secchi	T	O
140	0.3	2	0.174	3	C4R002Q01 Corannakraal 87 - Erfenis Dam on Vet River near Dam Wall			chem	Secchi	T	O
141	66.2	2	0.489	10	C4R001Q01 Willem Pretorius Wildtuin - Allemanskraaldam on Sandrivier: near Dam Wall			chem	Secchi	T	O
142			0.076	16	C5R002Q01 Kalkfontein Nature Reserve - Kalkfontein Dam on Rietrivier: near Dam Wall			chem	Secchi	T	O
144			0.147	11	C5R004Q01 Uitvlugt West 2810 - Krugersdrifdam on Modderrivier: near Dam Wall		90841	chem	-	T	O
145			0.097	6	C7R001Q01 Fischer 58 - Koppies Dam on Renosterrivier: near Dam Wall			chem	Secchi	T	O
148			0.045	3	C8H032Q01 at Sterkfonteindam on Nuwejaar Spruit		90886	chem	-	-	-
150			0.109	7	C8H023Q01 at the Willows on Meul River		90880	chem	-	-	-
151			0.166	9	C8H027Q01 at Ballingtomp on Wilge River		90884	chem	-	-	-
152			0.090	8	C8H026Q01 at Frederiksdal on Liebenbergsvlei River		90883	chem	-	-	-
153			0.130	8	C8H001Q01 Wilge River at Frankfort		90859	chem	-	-	-
155	4.7	2	0.057	3	C9R002Q01 Bloemhofdam Nature Reserve - Bloemhofdam on Vaalrivier: near Dam Wall			chem	Secchi	T	O
156	16.9	6	0.075	12	C9R001Q01 at Vaalharts Barrage on Vaalrivier: near Barrage Wall			chem	Secchi	T	-
166	27.8	3	0.309	3	D4H026Q01 Cooke S Lake (Molopo River) at Mafikeng			chem	Secchi	-	-
167	43.5	3	0.458	3	D4H037Q01 Lotlamoreng Dam on Molopo River: near Dam Wall			chem	Secchi	-	-
168	7.8	3	0.048	8	D4R003Q01 Disaneng Dam on Molopo River: near Dam Wall			chem	Secchi	T	-
169	53.4	2	0.321	9	D4R004Q01 Molopo (Ratshidi) - Modimola Dam (Aka Setumo Montshiwa) on Molopo River: near Dam Wall			chem	Secchi	T	-
171			0.083	1	Volgraafsig Balancing Dam	See Hartswater Irrigation scheme		chem	-	-	-
182			0.159	6	G1H036Q01 at Vleesbank Hermon Bridge on Berg River		101939	chem	-	-	-
183			0.059	5	G1H008Q01 Nieuwkloof 198 - on Klein Berg River		101917	chem	-	-	-
185			0.048	2	G1H066 Gouda Nieuwkloof - on Inlet Canal from Klein Berg River to Voelvlei Dam		101955	chem	-	-	-
189			0.716	6	G1H034Q01 Moorreesburg Spruit at Holle River		101937	chem	-	-	-
190			0.334	1	G1H035Q01 at Matjiesfontein on Matjiesriver		101938	chem	-	-	-
191			0.136	6	G1H059Q01 Canal (Right) from Leeu River at de Hoek Estates		101951	chem	-	-	-
193			0.107	6	G1H031Q01 at Misverstand Die Brug on Berg River		101935	chem	-	-	-
204			0.497	3	R2H010 135 K.W.T. Q. 2.25 U/S James Mcintyre Bridge on Buffalo River		102514	chem	-	-	-
205			0.339	5	R2H015 Fort Murray North Outspan on Yellowwoods River		102517	chem	-	-	-
207			0.183	3	R2H017Q01 Laing Dam on Buffalo River: Pipe to Purification		102519	chem	-	-	-
209			0.094	5	R2R003Q01 Bridle Dam Nature Reserve - Bridle Drift Dam on Buffalo River: near Dam Wall			chem	Secchi	T	-
210	chem	-	0.069	3	R3H001Q01 Gqunube River at Outspan						
211			0.083	3	R3R001Q01 Farm 305 - Nahoon Dam on Nahoon River: near Dam Wall			chem	Secchi	T	O
256			0.078	2	V1H040Q01 Tuva Canal at Woodstock		102720	chem	-	-	-
257	1.0	1	0.054	1	V1R003Q02 Woodstock Dam on Tugela River: Point in Dam			chem	-	-	-
261			0.056	6	V3R001Q01 Ntshingwayo (Chelmsford) Dam on Ngagane: near Wall			chem	Secchi	T	O
269			0.126	7	W2H030Q01 Klipfontein Dam on White Mfolozi River: D/S Weir			chem	-	-	-
270			0.196	2	W2R001Q01 Klipfontein Dam on White Mfolozi River: near Dam			chem	Secchi	T	O

Appendix D – Photographs from the Middle Olifants

Figure A1: Loskop Dam wall

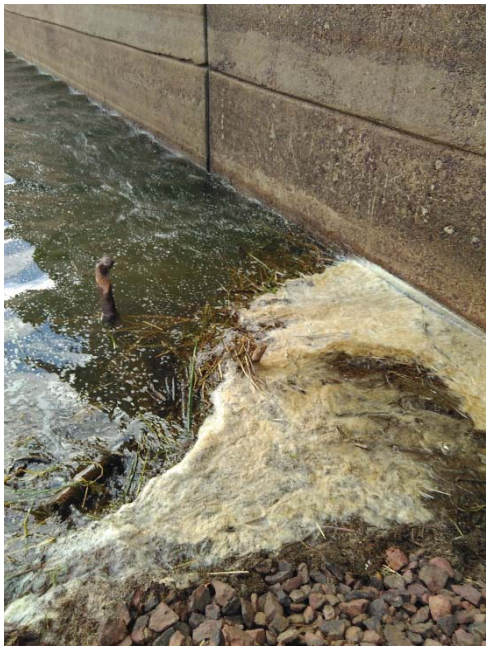

Figure A2: Loskop Dam

Figure A3: Sampling at Flag Boshielo Dam wall

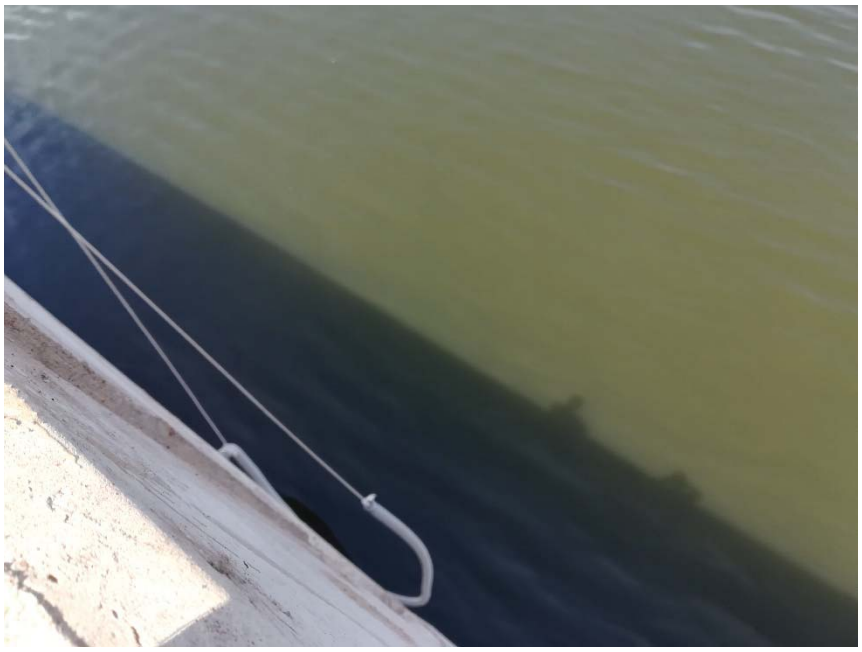

Figure A4: Water at Flag Boshielo Dam wall

Figure A5: ARC-Loskop Research Farm storage dam

Figure A6: Moses River upstream

Figure A7: Moses River downstream

Figure A8: Elands River

Figure A9: Loskop Nature Reserve irrigation canal

Figure A10: ARC-Loskop Research Farm irrigation canal

Figure A11: DH5 irrigation canal

Figure A12: Farm irrigation canal with construction conducted when this photo was taken

Figure A13: Confluence of drainage canals consisting of DJ16, DJ17 and DJ17a

Figure A14: Drainage canal DJ5

Figure A15: Drainage canal DJ13

Figure A16: Drainage canal DE10

Figure A17: Drainage canal DF2

Figure A18: Drainage canal DJ8

Figure A19: Drainage gauge

Proposal for archiving of data

The data for this project will be archived at the following institutions:

- Department of Plant and Soil Sciences, University of Pretoria, South Africa
- Department of Soil, Crop and Climate Sciences, University of the Free State, Bloemfontein, South Africa

Prof Michael van der Laan (michael.vanderlaan@up.ac.za) can be contacted in this regard.